MTA Doktori Értekezés

A REPRODUKCIÓT SZABÁLYOZÓ HIPOTALAMIKUS NEURONHÁLÓZAT MORFOLÓGIAI ÉS FUNKCIONÁLIS JELLEMZÉSE

Dr. Hrabovszky Erik

MTA
Kísérleti Orvostudományi Kutatóintézet
Endokrin Neurobiológia Csoport

Budapest

2010

dc_27_10

TARTALOMJEGYZÉK

RÖVIDÍTÉSEK JEGYZÉKE

2-AG	2-arachidonoyl-glycerol
ARC	nucleus arcuatus hypothalami
CB1, CB2	1. és 2. típusú kannabinoid receptor
cDNS	komplementer dezoxiribonukleinsav
CRH	corticotropin-releasing hormone
cRNS	komplementer ribonukleinsav
DAB	diaminobenzidin
DBH	dopamin-β-hidroxiláz
EM	eminentia mediana
ER-α	"α" ösztrogén receptor
ER-β	"β" ösztrogén receptor
E2	17β-ösztradiol
FSH	follikulus stimuláló hormon
GABA	gamma-amino vajsav
GFP	zöld fluoreszcens protein
GHRH	growth hormone-releasing hormone
GnRH	gonadotropin-releasing hormone
GPR54	G-protein kapcsolt receptor 54
IR	immunreaktív
LH	luteinizáló hormon
MPOA	mediális preoptikus area
mRNS	messenger ribonukleinsav
Ni-DAB	nikkel-diaminobenzidin
NK3	neurokinin-3 receptor
NPY	neuropeptide Y
OT	oxitocin
OVLT	organum vasculosum laminae terminalis
PCR	polimeráz láncreakció
PVN	nucleus paraventricularis hypothalami
RP3V	A III. agykamra rosztrális periventrikuláris területe
RT-qPCR	Valós-idejű kvantitatív PCR
SON	nucleus supraopticus hypothalami
SSC	„standard saline citrate solution" (1XSSC=0,15 M NaCl/15 mM Na-citrát; pH 7,0)
THC	Δ9-tetrahidrokannabinol
TRH	thyrotropin-releasing hormone
VGLUT1-3	1-3. típusú vezikuláris glutamát transzporterek
VP	vazopresszin

I. BEVEZETÉS

I/1. A gonádműködés szabályozása emlősökben

Valamennyi emlős faj szaporodásában meghatározó szerepet játszik a reproduktív tengely hierarchikusan egymásra épülő három fő szintje, a hipotalamusz, az adenohipofízis és a gonádok közt működő összetett kölcsönhatás. A hipotalamusz kimeneti jelét az adenohipofízis számára a gonadotropin-releasing hormone (GnRH) - másik elfogadott nevén: luteinizing hormone-releasing hormone (LHRH) - neuroszekretoros rendszer biztosítja, mely neurohormon tartalmát 30-90 percenként jelentkező szekréciós pulzusok formájában üríti a hipofízis portális keringési rendszerébe (Krsmanovic *et al.*, ; Knobil, 1980; Krsmanovic *et al.*, 1996; Terasawa, 1998; Moenter *et al.*, 2003). A GnRH hatására az adenohipofízisből elválasztott két gonadotrop hormon, a follikulus stimuláló hormon (FSH) és a luteinizáló hormon (LH) a gonádok gametogenezisét illetve szteroid hormon termelését irányítja. A reproduktív tengely működésének egy lényeges vonása, hogy a gonádokban folyó szteroid hormon termelés és gametogenezis szabályozottságát a hipotalamusz és a hipofízis szintjén ható visszacsatolási mechanizmusok biztosítják (Karsch & Foster, 1975; Knobil, 1980; Herbison, 1998). A gonádokban termelt szteroid hormonok - specifikus hormon receptoraik közvetítésével – egyúttal számos fontos élettani hatást gyakorolnak csaknem valamennyi szerv, köztük a központi idegrendszer működésére.

I/2. A gonadotropin-releasing hormone (GnRH) neuronrendszer anatómiai felépítése

A GnRH idegsejtek az orrplakodból fejlődnek. Egérben a prenatális 11. napon kezdik meg vándorlásukat az orrsövény mentén a bazális előagy felé (Wray *et al.*, 1989; Schwanzel-Fukuda & Pfaff, 1990). A fejlődő szaglórendszerrel alkotott szoros kapcsolat miatt, a migrációs folyamat zavarai anozmiával járó hipogonadotrop hipogonadizmust okozhatnak, melyet a hipotalamikus GnRH idegsejtek hiánya jellemez. A különböző genetikai hátterű humán kórképek gyűjtőneve Kallmann szindróma (Seminara *et al.*, 2000).

Születés idejére a GnRH idegsejtek perikaryonjai megérkeznek a preoptikus/hipotalamikus területekre. A rendkívül kisszámú (1000-1500) GnRH neuron egérben és patkányban laza csoportokban, főképp a Broca-féle diagonális köteg, a mediális septum, a mediális preoptikus area (MPOA), az organum vasculosum laminae terminalis (OVLT) és a medián preoptikus mag területén helyezkedik el (Merchenthaler *et al.*, 1980). Emberben megoszlásuk még kevésbé kompakt. Jelentős számú sejttest található a hátsó hipotalamusz, így a nucleus infundibularis (=arcuatus; ARC) területén is (Rance *et al.*, 1994). A meglehetősen diffúz megoszlás miatt, a GnRH perikaryonok topográfiai viszonyaira történő hivatkozáskor egyszerűsített anatómiai nómenklatúrát használunk.

A GnRH neuronok fő projekciós helyeit az OVLT, továbbá az eminentia mediana (EM) külső zónájának vér-agy gát-mentes területei jelentik (Wray *et al.*, 1989; Schwanzel-Fukuda & Pfaff, 1990). Az EM egyúttal a hipofízis portális keringési rendszerébe történő GnRH neuroszekréció fő helye. A kevésbé tanulmányozott, extrahipotalamikus axonvetületek ugyanakkor elérik a középagyi periakveduktális szürkeállományt és a mediális amygdalát (Liposits & Setalo, 1980; Merchenthaler *et al.*, 1989).

Az alaktanilag bipoláris, emberben kisebb részben multipoláris (Rance *et al.*, 1994) GnRH idegsejtek anatómiai és funkcionális hálózatot alkotnak. Köztük kommunikáció jöhet létre valódi szinaptikus kapcsolatok útján (Witkin & Silverman, 1985). A GnRH-t szekretáló, immortalizált GT1-7 sejtek szinaptoid valamint tight junction típusú kapcsolatokat létesítenek egymással (Liposits *et al.*, 1991), egyúttal termelnek gap junction fehérjéket is (Matesic *et al.*, 1993). A GnRH idegsejtek közt megfigyelt egyik érdekes kapcsolati típust olyan folytonos citoplazma hidak jelentik, melyekből a GnRH idegsejteket elválasztó sejtmembrán hiányzik (Witkin, 1999). Végül a GnRH neuronok axonjai az OVLT és az EM területén

szinaptikus specializáció nélküli kötegeket hoznak létre, ezáltal a terminálisok közötti parakrin kommunikáció anatómiai alapjait teremtve meg (Lehman & Silverman, 1988).

A GnRH idegsejtek egymással alkotott kapcsolatai mellett, a szinkronizált szekréciós működés szabályozásában kulcsfontosságú szerepet játszanak a számos forrásból érkező szinaptikus bemenetek is (Herbison, 1998), melyeket az I/7. fejezetben, külön tárgyalunk.

I/3. A GnRH „pulzus generátor" és szabályozása

A fent vázolt kapcsolatrendszer „GnRH pulzus generátorként" működik (Knobil, 1990), mely az EM vér-agy gát-mentes külső zónájában végződő GnRH axonvetületek 30-90 percenként jelentkező, koordinált szekréciós aktivitását eredményezi. A szinkronizált neuroszekréció hátterében az egyedi GnRH idegsejtek kálcium tranzienseinek egyidejű megjelenése áll (Terasawa, 1998). A pulzatilis GnRH elválasztás a hipofízis gonadotrop sejtjeinek pulzatilis aktiválását és ezáltal, pulzusokban történő LH és FSH termelését illetve szekrécióját hozza létre. Egyúttal meggátolja a hipofízis GnRH receptorainak deszenzitizációját, mely ligandum folyamatos jelenlétében következne be (Belchetz *et al.*, 1978; Catt *et al.*, 1985; Limonta *et al.*, 2001). A GnRH szekréciós pulzusok mintázata fontos kódot hordoz az adenohipofízis gonadotrop sejtjei számára. A ciklus follikuláris fázisára jellemző, alacsony frekvenciájú GnRH elválasztás elsősorban az FSHβ alegység átírását és az FSH szekrécióját stimulálja. A preovulatórikus GnRH hiperszekréció („surge") idején jellemző, frekvensebb pulzusok ezzel szemben az LHβ alegység átírását fokozzák és előidézik az ovulációt közvetlenül kiváltó LH hiperszekréciót („LH surge") (Wildt *et al.*, 1981; Dalkin *et al.*, 1989; Marshall & Griffin, 1993; Burger *et al.*, 2002; Counis *et al.*, 2005).

A GnRH pulzatilis szekréciója már olyan egyszerű modellrendszerben is megfigyelhető, mint a GnRH-t szekretáló, immortalizált GT1-7 sejtvonal (Wetsel *et al.*, 1992). *In vivo* azonban a pulzus generátor működése jóval bonyolultabb, és a végső szekréciós mintázat kialakításához számos tényező hozzájárul. A szervezetnek a környezetével alkotott kapcsolatát és belső állapotát tükröző endokrin-, metabolikus-, cirkadián-, szezonális-, stressz- és egyéb szignálok a pulzatilis GnRH szekréció megváltoztatásával befolyásolják a fertilitást. Ezért a GnRH pulzus generátor szabályozásának megértése a reproduktív neuroendokrinológia egyik fontos feladata.

I/4. Negatív és pozitív ösztrogén visszacsatolás hatása a GnRH pulzus generátor működésére

Hím állatokban a herében termelt tesztoszteron és az abból aromatizációval keletkező 17β-ösztradiol (E2), androgén ill. ösztrogén receptorokon hatva, folyamatos gátló hatást gyakorol a GnRH pulzus generátor működésére. Nőstényekben a petefészekből származó ösztrogének (elsősorban az E2) negatív visszacsatolása szintén fékezi a GnRH pulzus generátort és az LH szekréciót az ovariális ciklus nagy részében. Ezt spontán ovuláló fajokban a ciklus közepén (laboratóriumi rágcsálókban a proösztrusz délutánján) jelentkező, pozitív ösztrogén visszacsatolás szakítja meg (Moenter *et al.*, 2009), mikor a GnRH szekréciós pulzusok frekvenciája és az időegység alatt ürülő GnRH mennyisége egyaránt megnő („GnRH surge") (Sarkar *et al.*, 1976; Moenter *et al.*, 1990; Pau *et al.*, 1993). Ezzel párhuzamosan, az adenohipofízis gonadotrop sejtjeinek válaszkészsége GnRH-ra szintén fokozódik (Aiyer *et al.*, 1974; Adams *et al.*, 1981). A magas E2 szint hatására bekövetkező GnRH surge - a portális keringési rendszer közvetítésével - a hipofízisben LH surge-öt okoz, ami a petefészekben kiváltja az ovuláció.

Az E2 központi idegrendszeri hatásainak közvetítésében fontos szerepet tölt be a két ösztrogén receptor típus (ER-α és ER-β), melyek ligand-függő transzkripciós faktorokként, promoter régiók ösztrogén-válasz eleméhez kötve befolyásolják az ösztrogén-függő gének átírását. A fenti, klasszikus genomiális hatáson kívül, újabban az érdeklődés homlokterébe

kerültek az ösztrogének nem-genomiális, gyors hatásai is (Genazzani *et al.*, 2005). Az ösztrogén hormonok a GnRH idegsejt működésének számos aspektusát befolyásolják. Ilyen a GnRH bioszintézise és lebontása, a GnRH neuronok galanin termelése, elektromos aktivitása vagy pulzatilis GnRH szekréciója (Herbison, 1998; Christian *et al.*, 2008; Moenter *et al.*, 2009).

Mióta Shivers és mtsai 1983-ban publikálták, hogy a GnRH idegsejtek a tríciummal megjelölt E2-t nem képesek felvenni (Shivers *et al.*, 1983), széles körben elfogadott az a nézet, miszerint az ösztrogén visszacsatolás GnRH idegsejtek felé kizárólag E2-érzékeny interneuronok közvetítésével jöhet létre. Három évtizedes kutatómunka eredményeképp mára körvonalazódott (Herbison, 2008), hogy a pozitív ösztrogén visszacsatolás szempontjából rágcsálókban kitűntetett jelentőséggel bír a III. agykamra rosztrális periventrikuláris területe (RP3V). Az RP3V kisspeptint termelő sejtcsoportja tartalmazza az ER-α-t (Franceschini *et al.*, 2006), beidegzi a GnRH idegsejteket (Clarkson & Herbison, 2006), aktiválódik az LH surge idején (Irwig *et al.*, 2004) és kisspeptin termelése E2 hatására nő (Oakley *et al.*, 2009). A negatív ösztrogén visszacsatolás egyik régóta feltételezett helye rágcsálókban az ARC (Herbison, 1998). Egy ARC-ban található, és kisspeptint termelő sejtcsoport szintén tartalmaz ER-α-t (Franceschini *et al.*, 2006). Az RP3V kisspeptin sejtjeitől eltérően, az ARC kisspeptin expressziója negatív ösztrogén szabályozás alatt áll (Oakley *et al.*, 2009). Főemlősökben az RP3V-vel analóg magot még nem sikerült megfigyelni. A jelenleg elfogadott nézet szerint, mind a pozitív, mind a negatív ösztrogén visszacsatolásban a nucleus infundibularis (=ARC) játssza a fő szerepet (Knobil, 1980).

I/5. A pulzatilis GnRH szekréciót befolyásoló egyéb tényezők

Az ösztrogén-függőség mellett, a GnRH szekréciót a cirkadián ritmus (Christian *et al.*, 2005) is jellemzi. Ennek következménye, hogy patkányban és egérben a preovulatórikus LH surge mindig a proösztrusz délutánján, a nappali fény megszűnése előtti órákban jelentkezik. A cirkadián hatás közvetítésében szerepet játszó, egyik több-neuronos pálya magában foglalja a retino-hipotalamikus köteget, a nucleus suprachiasmaticus vazopresszin (VP) idegsejtjeit, valamint az RP3V GnRH idegsejteket beidegző kisspeptin neuronjait (Vida *et al.*, 2010).

A napszakok hosszának eltolódása a melatonin termelésén keresztül képes szabályozni a reprodukció éves ciklusát szezonális szaporodást mutató fajokban (Revel *et al.*, 2009).

Elégtelen táplálékfelvétel (Sullivan *et al.*, 2003) vagy túlhajtott sport (De Cree, 1998) miatt bekövetkező leptin hiány a pulzatilis GnRH és LH szekréciót megszünteti. A metabolikus eredetű anovuláció jellemző klinikai példája az anorexia nervosa (Miller & Golden). A metabolikus hatások közvetítésében fontos szerepe lehet az ARC leptin receptort tartalmazó idegsejtjeinek. A neuropeptide Y (NPY)-t és agouti-related protein (AGRP)-t termelő, ARC-ból eredő, leptin-érzékeny pálya hozzájárulását a GnRH idegsejtek gátló szabályozásához egyik tanulmányunk vizsgálja (**5**).

Az endokrin rendszer és az anyagcsere egyéb rendellenességeivel, mint a stresszel (Berga & Loucks, 2005)-, a pajzsmirigyműködés zavaraival (Koutras, 1997)- vagy a diabetes mellitussal (Livshits & Seidman, 2009) kapcsolatos infertilitás a pulzus generátor sérülékenységét jelzi. A kórképek részletezése az értekezés témakörét meghaladná.

I/6. Ösztrogén receptor-β szerepe a hipotalamikus működésekben

Kuiper és mtsai 1996-ban klónozták az ER-β receptor típust prosztatából (Kuiper *et al.*, 1996). Az ER-β topográfiai megoszlása rágcsálók agyában a klasszikus ER-α receptorétól feltűnően eltért (Shughrue *et al.*, 1996; Shughrue *et al.*, 1997). A második ösztrogén receptor típus felfedezésével részben már megmagyarázhatóvá vált a nucleus paraventricularis (PVN) és a nucleus supraopticus (SON) magnocelluláris neuroszekretoros idegsejtjeinek E2 általi

szabályozása is. Ezek a neuronok patkányban ER-α-t nem tartalmaznak (Simerly *et al.*, 1990), miközben a hipotalamikus oxitocin (OT) és VP messenger ribonukleinsav (mRNS) expresszió (Van Tol *et al.*, 1988) és peptid szint (Jirikowski *et al.*, 1988), a szérum (Skowsky *et al.*, 1979) és a hipofízis (Van Tol *et al.*, 1988) OT és VP tartalma, a dendritikus OT ürítés (Wang *et al.*, 1995), vagy az OT idegsejtek elektromos aktivitása (Negoro *et al.*, 1973) ismert ösztrogén-függést mutatnak. Immuncitokémiát és *in situ* hibridizációt ötvöző korábbi munkánkban valóban sikerült is igazolni az ER-β előfordulását az OT-t és VP-t termelő hipotalamikus neuronok egyes populációiban (Hrabovszky *et al.*, 1998). Mivel a receptor expresszió egyenetlenül oszlott meg az anatómiailag és funkcionálisan is heterogén sejtcsoportok között, az értekezésben szereplő egyik munkánk az ER-β tartalmú hipotalamikus OT és VP idegsejtek finomabb topográfiai analízisét tűzte ki célul (**6**). Ugyanezen tanulmányban vizsgáltuk a kolokalizációs jelenséget a humán hipotalamusz OT és VP sejtjeinek vonatkozásában is (**6**).

A GnRH idegsejtekre gyakorolt pozitív és negatív ösztrogén visszacsatolás (Herbison, 1998) lényegének megértése kezdettől fogva a reproduktív neuroendokrinológia központi kérdése. Mióta Shivers és munkatársai megfigyelték a tríciummal megjelölt E2 *in vivo* felvételének hiányát patkány GnRH neuronjaiban (Shivers *et al.*, 1983), majd ezt követően mások az ER-α hiányát immuncitokémiával is alátámasztották (Herbison & Theodosis, 1992; Lehman & Karsch, 1993), a kutatások középpontjába az E2 hatásait közvetítő, ösztrogén-érzékeny interneuronok azonosítása került. Értekezésem egy része az ilyen indirekt ösztrogén hatásokban szerepet játszó rendszerekkel (hisztamin, kisspeptin, neurokinin B) foglalkozik (**1, 21**). Az ER-β felfedezését és hipotalamikus megoszlásának leírását követően azonban ismét felmerült a GnRH idegsejtek direkt E2 érzékenységének kérdése. Ösztrogén visszacsatolással kapcsolatos, értekezésben szereplő vizsgálataink az ER-β-n keresztül gyakorolt, közvetlen ösztrogén visszacsatolás lehetőségét is vizsgálják rágcsálókban és emberben (**2, 3, 15, 18**).

I/7. Neurotranszmitterek/neuromodulátorok jelentősége a GnRH neuronműködés afferens szabályozásában

A GnRH pulzus generátor működését módosító hatások (**I/4**. és **I/5**. fejezetek) jelentős része idegi afferensek útján éri a GnRH idegsejteket (Herbison, 1998). Alább ezek jelentősebb átvivőanyagait tárgyaljuk röviden.

A gamma-amino vajsav (GABA) a GnRH idegsejtek afferenseinek legfontosabb átvivőanyaga. A GnRH idegsejteken kimutatható szinaptikus végződések jelentős része GABAerg (Leranth *et al.*, 1985). A GnRH idegsejtek mind $GABA_A$ (Petersen & McCrone, 1994), mind $GABA_B$ (Zhang *et al.*, 2009) receptorokkal rendelkeznek. A GnRH neuronok sajátos klorid homeosztázisának tudható be, hogy a GABA a GnRH idegsejteket $GABA_A$ receptorokon keresztül depolarizálja (DeFazio *et al.*, 2002). Elektrofiziológiai munkákból ismert, hogy a GABAerg afferens szabályozás egyaránt fontos a metabolikus (Sullivan *et al.*, 2003)-, ösztrogén (Christian *et al.*, 2005)-, és cirkadián (Christian *et al.*, 2005) szignálok közvetítésében. Mivel a GnRH neuronokat a glutamáton kívül a GABA is serkenti (DeFazio *et al.*, 2002), a serkentő GABAerg bemenetek endokannabinoid érzékenységének különös jelentősége lehet a GnRH neuronhálózat gátló szabályozásában. Ezt az értekezés keretein belül vizsgáljuk (**23**).

A fő serkentő neurotranszmitter, az L-glutamát is megtalálható a GnRH idegsejteket beidegző axonokban (Kiss *et al.*, 2003). Mivel a szinapszisok többsége nagy valószínűséggel a GnRH dendritfa szómától távoli elágazódásaira érkezik, a glutamáterg bemenet jelentőségét az afferens szabályozásban whole-cell patch-clamp elektrofiziológiai vizsgálatokkal nehéz megítélni. Míg $GABA_A$ receptor-mediált miniatűr posztszinaptikus áramokat valamennyi GnRH idegsejtben ki lehet mutatni, excitatórikus poszt-szinaptikus áramok a neuronok 25-

30%-ában nem mérhetőek (Christian *et al.*, 2009). A reproduktív tengely alsóbb szintjein ható, nem-szinaptikus glutamáterg hatások vizsgálata az értekezés célkitűzései között szerepel (**7-12, 14, 17, 20**). Ezeket a bevezetés külön pontjában (**1.8**) vesszük sorra.

Az agytörzsi noradrenalin is fontos szerepet tölt be a GnRH neuronok fiziológiás szabályozásában. Ennek megfelelően, patkányokban az LH surge létrejötte α-adrenerg antagonistákkal vagy a felszálló katekolaminerg pályák átmetszésével meggátolható (Clifton & Sawyer, 1979; Coen & Coombs, 1983). Közvetlenül a surge-öt megelőzően, az agytörzsi A2 noradrenerg sejtcsoportban megjelenik az aktivitást jelző c-Fos (Jennes *et al.*, 1992). Nem ismert ugyanakkor, hogy a GnRH idegsejtek direkt noradrenerg beidegzése milyen mértékű. Az értekezés egy részében a neuropeptide Y (NPY)-t is tartalmazó, felszálló noradrenerg/adrenerg pályák GnRH neuronokkal képzett direkt kapcsolatát vizsgáljuk (**5**).

A GnRH pulzus generátor működésére ható további klasszikus idegi átvivőanyag és neuropeptidek közül (dopamin, opioid peptidek, neurotenzin, P anyag, dinorfin, stb.) (Herbison, 1998) a továbbiakban csak az értekezésben szereplőket tárgyaljuk.

Hisztamin (**1**)

A reproduktív neuroendokrinológia egyik legizgalmasabb kérdését az E2 pozitív és negatív visszacsatolásának mechanizmusai jelentik. Az E2 indirekt hatásait közvetítő idegsejtek ösztrogén receptorral rendelkeznek, GnRH neuronokkal idegi kapcsolatban állnak és szelektív transzmitter receptorokon keresztül kommunikálnak (Herbison, 1998; Petersen *et al.*, 2003). A hisztamin ösztrogén visszacsatolásban játszott szerepe számos korábbi tanulmány alapján felvethető. Igy, az E2 hisztamin elválasztást képes kiváltani hipotalamikus szöveti blokkból *in vitro* (Ohtsuka *et al.*, 1989), hisztaminerg axonok bőségesen beidegzik a GnRH idegsejteket is tartalmazó proptikus areat (Panula *et al.*, 1989), az agykamrába juttatott hisztamin nyulakban ovulációt vált ki (Sawyer, 1955), és a GnRH-t szekretáló GT1 sejtvonal H1 hisztamin receptort expresszál (Noris *et al.*, 1995). Több nyitott kérdés maradt azonban a hisztamin szerepével kapcsolatban. Tisztázatlan, hogy a tuberomammilláris mag hisztaminerg neuronjai rendelkeznek-e ösztrogén receptorral, innerválják-e közvetlenül a GnRH idegsejteket, továbbá részt vesznek-e, és mely hisztamin receptor közvetítésével, a pozitív ösztrogén visszacsatolásban.

NPY (**5**)

A 36 aminosavból álló NPY a hipofízis és a központi idegrendszer területén hatva egyaránt fontos szerepet játszik a gonadális tengely befolyásolásában (Kalra & Crowley, 1992). Az NPY egyik központi idegrendszeri támadáspontja az OVLT és az MPOA. Az itt található, GnRH-t termelő idegsejtek perikaryonja expresszálja az Y5 receptor típust (Campbell *et al.*, 2001), és bőséges NPY-immunreaktív (IR) beidegzést nyer (Tsuruo *et al.*, 1990). Az innervációban résztvevő, NPY tartalmú axonok egyik valószínű forrása az ARC. Ennek megfelelően, az ARC léziója az MPOA NPY-IR rostjainak jelentős számbeli csökkenését okozza (Broberger *et al.*, 1998). Anterográd jelölőanyag bejuttatása az ARC területére valóban igazolja is egy ARC-ból eredő, GnRH neuronokat beidegző NPY tartalmú pálya létezését (Li *et al.*, 1999). Ennek ösztrogén visszacsatolásban játszott szerepére utalhat, hogy az ARC NPY neuronjainak 10%-a tartalmaz ösztrogén receptort (Kalra & Crowley, 1992), és a mag NPY mRNS tartalma a proösztrusz délutánján bekövetkező LH surge idején megnő (Bauer-Dantoin *et al.*, 1992). Az ARC NPY idegsejtjei leptin receptort is tartalmaznak (Baskin *et al.*, 1999), és fontos metabolikus hatásokat közvetíthetnek a reproduktív tengely felé. Az ARC NPY neuronjainak közel 100%-a tartalmaz egy másik peptidet, AGRP-t is (Broberger *et al.*, 1998). Az NPY-hoz hasonlóan, táplálékfelvételt fokozó hatású AGRP kizárólag az ARC-ban szintetizálódik. Így, immunfluoreszcens megjelenítése NPY-IR idegrostokban azok ARC-beli eredetét is jelzi. A GnRH idegsejtek beidegzésében résztvevő NPY idegrostok egy további valószínű forrása az agytörzs, ahol az NPY noradrenerg és adrenerg idegsejtekben fordul elő (Everitt *et al.*, 1984; Sawchenko *et al.*, 1985). A felszálló

agytörzsi NPY vetületek így a noradrenerg marker enzim, a dopamin-β-hidroxiláz (DBH) jelenlétével jellemezhetőek. A fenti két fő NPY rendszeren kívül, NPY tartalmú idegsejtek számos egyéb anatómiai lokalizációban, így a hipotalamusz dorzomediális magjában, a stria terminalis magjában, a laterális preoptikus area-ban, a dorzális hipotalamikus area-ban, a középagy központi szürkeállományában és a commissura anterior körül is megfigyelhetőek (Chronwall *et al.*, 1985). Nem tudott, hogy az anatómiailag és funkcionálisan heterogén NPY idegsejtek milyen mértékben járulnak hozzá a GnRH neuronrendszer beidegzéséhez.

Acetilkolin (**16**)

Míg az acetilkolin önmagában az adenohipofízis szintjén nem hat a gonadotrop hormon szekrécióra (Simonovic *et al.*, 1974), a központi idegrendszer területén a reprodukció számos aspektusát képes befolyásolni (Everett, 1964). Így, a muszkarinerg receptor antagonista atropin gátolja mind a spontán, mind a reflexes ovulációt (Everett, 1964). A patkány laterális hipotalamuszába ültetett atropin implantátum megnyújtja az ovariális ciklus diösztrusz fázisát (Benedetti *et al.*, 1969). Ezentúl, a mediobazális hipotalamuszból acetilkolinnal GnRH szekréció váltható ki *in vitro*, mely gátolható a nikotinerg receptor antagonista hexamethoniummal (Richardson *et al.*, 1982). Irodalmi adat a GnRH idegsejtek közvetlen kolinerg beidegzésére vonatkozó nem áll rendelkezésre.

Kisspeptin (**21**)

Reproduktív neuroendokrinológia területén az utóbbi évtizedek kétségtelenül legnagyobb jelentőségű felismerése a kisspeptin/G-protein kapcsolt receptor 54 (GPR54) szignalizációs rendszer szerepére vonatkozott. A GPR54 gén inaktiváló mutációi emberben hipogonadotrop hipogonadizmust (de Roux *et al.*, 2003; Seminara *et al.*, 2003; Semple *et al.*, 2005), míg aktiváló mutációi centrális eredetű pubertas praecoxot okoznak (Teles *et al.*, 2008). A receptor természetes liganduma az (emberben) 54 aminosavas kisspeptin-54 (másik nevén metastin), mely a *KISS1* gén terméke. Különböző emlős fajokban a kisspeptinek – a kisspeptin-54 és rövidebb, biológiailag ugyancsak aktív C-terminális fragmentumai - erőteljesen serkentik az LH szekrécióját *in vivo*. A kisspeptin támadáspontja centrális, és hatása GnRH antagonista előkezeléssel kivédhető (Gottsch *et al.*, 2004; Shahab *et al.*, 2005). A kisspeptint termelő neuronok GnRH idegsejtekre gyakorolt közvetlen hatását mutatja kisspeptin-IR kontaktusok jelenléte GnRH-IR sejttesteken és dendriteken (Kinoshita *et al.*, 2005; Clarkson & Herbison, 2006), a GPR54 mRNS expresszió GnRH neuronokban (Irwig *et al.*, 2004; Han *et al.*, 2005), c-Fos immunreaktivitás megjelenése kisspeptin adását követően GnRH idegsejtek magjában (Irwig *et al.*, 2004), valamint a GnRH-GFP idegsejtek kisspeptin okozta depolarizációja akut szelet-preparátumban (Dumalska *et al.*, 2008; Pielecka-Fortuna *et al.*, 2008). A kisspeptin rendszer neuroanatómiai viszonyaira vonatkozó ismereteink főképp rágcsálókon tett megfigyeléseken alapulnak. Rágcsáló fajokban a kisspeptint két jól elkülönülő sejtcsoport termeli, a III. agykamra rosztrális periventrikuláris területén (RP3V), valamint az ARC-ban (Clarkson & Herbison, 2006). Az előbbi terület kisspeptin neuronjainak száma nőstény egérben és patkányban jelentősen meghaladja a hímekben megfigyelhető sejtszámot (Clarkson & Herbison, 2006; Kauffman *et al.*, 2007). Egyre elfogadottabb, hogy rágcsáló fajokban az RP3V szexuálisan dimorf és ösztrogén érzékeny kisspeptin idegsejtcsoportja lényegesen hozzájárul a GnRH idegsejtek beidegzéséhez és nőstényekben a pozitív ösztrogén visszacsatolás kiváltásához (Herbison, 2008). Főemlősökben viszont analóg, szexuálisan dimorf idegmag ezen az agyterületen nem ismert, és kisspeptin termelő neuront nagyobb számban csupán a nucleus infundibularisban (ARC) figyeltek meg (Rometo *et al.*, 2007; Ramaswamy *et al.*, 2008). A ma is elfogadott nézet szerint (Knobil, 1980), a nucleus infundibularis mind a negatív, mind a pozitív ösztrogén visszacsatolási mechanizmusokért felelős lehet. További érdekes faji különbségre utalhat, hogy míg rágcsálók kisspeptin idegsejtjei axo-szomatikus és axo-dendritikus kapcsolatok útján kommunikálnak GnRH idegsejtekkel (Kinoshita *et al.*, 2005; Clarkson &

Herbison, 2006), Ramaswamy és mtsai majomban elsősorban axo-axonális kapcsolatokat figyeltek meg az EM területén (Ramaswamy *et al.*, 2008).

Emberben nem ismert a hipotalamikus kisspeptin neuronrendszer felépítése. Nem áll rendelkezésre nemi dimorfizmusára és GnRH idegsejtekkel alkotott kapcsolatainak típusára vonatkozó irodalmi adat sem.

Neurokinin B (**21**)

A tachykinin peptidek szerepe meglehetősen sokrétű és a reprodukció vonatkozásában a kisspeptinénél kevésbé specifikus. A csoportba tartozó neurokinin B és receptora, a neurokinin-3 receptor (NK3) csupán az elmúlt évben került az érdeklődés homlokterébe, mióta kiderült, hogy a neurokinin B-t vagy az NK3-t kódoló gének mutációi emberben hipogonadotrop hipogonadizmust okoznak (Guran *et al.*, 2009; Topaloglu *et al.*, 2009). Rágcsálókban a neurokinin B a hipotalamusz szintjén, GnRH idegsejtek közvetítésével hat, a kisspeptinhez hasonló módon. Úgy tűnik azonban, támadáspontja nem a GnRH idegsejtek perikaryonjait és dendritjeit tartalmazó preoptikus area, hanem az EM. A GnRH idegsejtek EM-re vetülő axonjai NK3 immunreaktivitást mutatnak (Krajewski *et al.*, 2005) és axo-axonális kontaktusokat létesítenek neurokinin B-IR axonokkal (Ciofi *et al.*, 2006). A neurokinin B-IR axonok forrása az ARC egy olyan sejtcsoportja, mely birkában és egérben kisspeptint, neurokinin B-t, NK3-t és dinorfint egyaránt termel (Goodman *et al.*, 2007; Navarro *et al.*, 2009). Egy újonnan kibontakozó koncepció szerint, ezek a neuronok kiemelkedő jelentőséggel bírnak mind a pulzatilitás GnRH szekréció (Navarro *et al.*, 2009) mind a negatív ösztrogén visszacsatolás (Smith *et al.*, 2006) szabályozásában. Ezzel szemben, az RP3V kisspeptin idegsejtjei nem tartalmaznak neurokinin B-t. Ugyanakkor fontos szerepet játszanak a pozitív ösztrogén visszacsatolásban (Herbison, 2008).

Emberi hipotalamuszban a neurokinin B-t termelő idegsejtek megoszlása, valamint a neurokinin B és kisspeptin kolokalizációja nem ismert.

Endokannabinoidok (**23**)

Az endokannabinoid szignalizációs rendszer bioaktív lipid mediátorokat használ, melyek két legismertebb képviselője az anandamid (Devane *et al.*, 1992) és a 2-arachidonoyl-glycerol (2-AG) (Mechoulam *et al.*, 1995). Az anandamid és a 2-AG kannabinoid receptorokhoz (CB1, CB2) kötve fejti ki hatását. A receptorok közül a központi idegrendszerben a CB1 izoforma dominál (Pagotto *et al.*, 2006). A preterminális axonokban működő CB1 a központi idegrendszer legbővebb G-protein kapcsolt receptora (Herkenham *et al.*, 1991; Katona *et al.*, 1999; Katona *et al.*, 2001). Aktiválása gátolja számos neurotranszmitter, köztük a GABA, a glutamát, a noradrenalin és az acetilkolin ürülését a CB1 receptort tartalmazó axonvégződésekből (Hoffman & Lupica, 2000; Gerdeman & Lovinger, 2001; Vizi *et al.*, 2001; Degroot *et al.*, 2006). Az endogén kannabinoidok mellett, ugyancsak kannabinoid receptorokon hat az indiai kender (cannabis sativa) fő hatóanyaga, a Δ9-tetrahidrokannabinol (THC).

A THC endokrin funkciók egész sorát, így a reprodukciót is befolyásolja, gátolva az LH szekrécióját (Smith *et al.*, 1978; Asch *et al.*, 1981). A gátlást GnRH neuronok közvetítik, mivelhogy *in vitro* a THC nem csökkenti az adenohipofízis LH elválasztását (Dalterio *et al.*, 1987; Wenger *et al.*, 1987), GnRH-val a szisztémásan adott kannabinoidok ovulációt gátló hatása kivédhető (Ayalon *et al.*, 1977; Smith *et al.*, 1978; Wenger *et al.*, 1987), és az agykamrába injektált THC - az LH szekréció fokozása mellett - megnöveli a mediobazális hipotalamusz GnRH tartalmát is (Wenger *et al.*, 1987).

A GnRH idegsejtek fő bemenetét GABAerg idegrostok jelentik. A más neuronrendszereken megfigyelhető gátló hatással ellentétben, a GABA a GnRH idegsejteket $GABA_A$ receptorokon át serkenti (DeFazio *et al.*, 2002). Ezért feltételezhető, hogy a reproduktív tengely THC okozta gátlásában kulcs szerepe lehet a serkentő GABAerg bemenetek CB1 receptor által közvetített kannabinoid érzékenységének. A CB1 receptorok hipotalamikus megoszlására és GnRH idegsejtekkel alkotott kapcsolatára vonatkozóan morfológiai adatok jelenleg még nem állnak rendelkezésre. Nem

ismert továbbá, hogy a kannabinoid rendszer farmakológiai befolyásolása miképp hat a GnRH idegsejtek és GABAerg afferenseik elektromos aktivitására.

I/8. Glutamáterg hatások a reproduktív tengely különböző szintjein

A hipotalamusz fő serkentő neurotranszmittere az L-glutamát (van den Pol *et al.*, 1990). Ionotrop és metabotrop receptorain hatva, szerepet játszik valamennyi endokrin tengely, így a reproduktív folyamatok szabályozásában is (Brann, 1995). Ismert, hogy a glutamát receptor agonista N-metil-DL-aszpartát *iv.* infúziójával patkányban pubertas praecox váltható ki (Urbanski & Ojeda, 1987). Ionotrop glutamát receptorok aktivációja egyaránt szerepet játszik a GnRH szekréció pulzatilis (Bourguignon *et al.*, 1989) valamint surge (Ping *et al.*, 1997) mintázatának kialakításában is. A glutamát hatásai a reproduktív tengely különböző szabályozási szintjein érvényesülnek.

A centrális támadáspontok egyike a preoptikus area, ahol a GnRH surge idején a glutamát ürítése fokozódik (Ping *et al.*, 1994; Jarry *et al.*, 1995). A terület GnRH neuronjai glutamáterg szinaptikus beidegzést nyernek (Kiss *et al.*, 2003) és ionotrop glutamát receptorokat tartalmaznak (Eyigor & Jennes, 2000).

A GnRH idegsejtek neuroendokrin végződéseit tartalmazó mediobazális hipotalamusz a GnRH rendszert érő, centrális glutamát hatások egy további megjelenési helye. *In vitro* kísérletekben a területből készített explantátumok GnRH szekrécióját az N-metil-D-aszpartát fokozza (Bourguignon *et al.*, 1989; Arias *et al.*, 1993; Kawakami *et al.*, 1998a). A hatások valószínű keletkezési helye az EM külső zónája, ahol a perikapilláris térségben végződő GnRH axonok több ionotrop glutamát receptor alegységet is tartalmaznak (Kawakami *et al.*, 1998b). Az EM GnRH axonvégződéseire fiziológiás viszonyok közt ható glutamát eredete azonban nem ismert. A három vezikuláris glutamát transzporter izoforma (VGLUT1-3) felfedezésével és immuncitokémiai markerként történő alkalmazásával, csupán az utóbbi években nyílt lehetőség a glutamátot átvivőanyagként használó, valódi excitatórikus idegsejtek megkülönböztetésére a glutamátot csupán metabolikus folyamatokban használó, egyéb sejtektől. A hipotalamusz serkentő neuronjai a glutamát szinaptikus vezikulába csomagolásáért felelős enzimek közül a VGLUT2 izoformát termelik (Herzog *et al.*, 2001; Lin *et al.*, 2003). Az EM külső zónájának gazdag VGLUT2-IR beidegzése (Lin *et al.*, 2003) felveti, hogy a GnRH terminálisokra ható glutamát egy eddig ismeretlen neuroszekretoros idegsejt populációból származhat. Másrészt, mivel a hipofízis szabályozásában ismert szerepű hipotalamikus régiók közül több is (OVLT, MPOA, PVN, nucleus periventricularis) expresszál VGLUT2 mRNS-t (Herzog *et al.*, 2001; Lin *et al.*, 2003), felmerül az a lehetőség is, hogy a glutamáterg aminosav fenotípus (VGLUT2 immunreaktivitás) az ismert, klasszikus neuroendokrin rendszerek, így a GnRH neuronok egy endogén sajátossága. Korábbi munkákból tudjuk, hogy a hipotalamusz neuroszekretoros rendszerei közül a growth hormone-releasing hormone (GHRH) termelő neuronok (Meister & Hokfelt, 1988), a tuberoinfundibuláris dopaminerg idegsejtek (Meister & Hokfelt, 1988), valamint a corticotropin-releasing hormone (CRH) termelő idegsejtek egy kis csoportja (Meister *et al.*, 1988) γ-amino vajsavat (GABA-t) tartalmaz. A további neuroendokrin rendszerek, köztük a GnRH idegsejtek aminosav neurotranszmitter fenotípusa azonban nem ismert. Glutamáterg jellegük felvetné, hogy a neuroendokrin terminálisokat szabályozó glutamát (Bourguignon *et al.*, 1989; Arias *et al.*, 1993; Kawakami *et al.*, 1998a) forrása endogén. A GnRH és a glutamát feltételezett ko-szekréciója új típusú autokrin/parakrin szabályozási mechanizmusok alapját jelentheti. A GnRH idegsejtek és további neuroendokrin sejttípusok glutamáterg aminosav fenotípusát több, értekezésben foglalt munkánkban is vizsgáljuk (**7-10, 12, 14, 17**).

Az adenohipofízis szintjén működő, további glutamáterg mechanizmusokra utal ionotrop és metabotrop glutamát receptorok előfordulása különböző hormontermelő sejttípusokon (Kiyama *et al.*, 1993; Bhat *et al.*, 1995). A receptorokon ható glutamát eredete azonban

kérdéses. Származhat egyrészt a portális keringésből, ahová az EM-t innerváló VGLUT2-IR terminálisokból ürülhet. Ennél valószínűbb a glutamát adenohipofízisben történő, helyi képződése és részvétele olyan lokális autokrin/parakrin glutamáterg szabályozási mechanizmusokban, melyekhez hasonlót a hasnyálmirigy Langerhans szigeteiben már megfigyeltek (Hayashi *et al.*, 2003). Az adenohipofízis feltételezett „glutamáterg" sejttípusait a VGLUT1 és VGLUT2 marker enzimek immunhisztokémiai vizsgálatával kíséreltük meg azonosítani (**11, 14, 17, 20**).

A VGLUT1 és VGLUT2 enzim izoformák termelése a központi idegrendszerben regulált. Ahol az enzimek a szinaptikus jelátvitelben játszanak szerepet, változó bioszintézisük a kvantális méret és az excitatórikus poszt-szinaptikus áramok szabályozásának fontos eszköze (Wojcik *et al.*, 2004; Erickson *et al.*, 2006). Az EM-ben a VGLUT2-IR terminálisokból ürülő glutamát feltételezett autokrin/parakrin szerepe új szabályozási mechanizmust jelent a GnRH és további neuroszekretoros rendszerek nem-szinaptikus, lokális szabályozásában. Az a kérdés, hogy neuroszekréció/szekréció helyén működő VGLUT2 enzim expressziója endokrin állapotok függvényében szabályozott-e, a VGLUT2-t termelő sejtek elhelyezkedésének ismeretében, kvantitatív *in situ* hibridizációval vizsgálhatóvá válik. Az értekezésben foglalt munkáink három különböző endokrin modellben vetik fel a VGLUT2 expresszió szabályozottságát (**10, 11**).

I/9. Agyi ösztrogén szignalizáció élettana és változásai menopauzában

Fentiekben az ösztrogén visszacsatolásnak a reprodukció szabályozásában játszott szerepével foglalkoztunk. A gonadális ösztrogének azonban jóval általánosabb élettani hatást is gyakorolnak a központi idegrendszer, így az agykéreg működésére, melyek egy része genomiális, más része gyors, nem-genomiális mechanizmusú (Genazzani *et al.*, 2005).

Emberben az életkor előrehaladtával csökken a petefészek tüszőinek száma. A menopauza beálltával - működőképes tüszők híján - az E2 termelése megszűnik. Az E2 célszerveiben, így a központi idegrendszerben számos működési zavar jelentkezik (Morrison *et al.*, 2006). A hőhullámok, verejtékezés, elhízás, magas vérnyomás, szorongás, depresszió, fejfájás és álmatlanság olyan gyakori panaszok, melyek összefüggésbe hozhatók a hipotalamusz, hippokampusz és limbikus struktúrák megváltozott működésével (Keenan *et al.*, 2001; Adams & Morrison, 2003; Genazzani *et al.*, 2005). A prefrontális agykéreg kitüntetett szerepet játszik több olyan kognitív, érzelmi, figyelmi, motivációs és tanulási folyamatban, melyek a menopauzát követő ösztrogén hiányos állapotban károsodhatnak (Keenan *et al.*, 2001; Adams & Morrison, 2003; Genazzani *et al.*, 2005). A kellő időben elkezdett hormonpótlás a funkciók romlását mérsékelni vagy megelőzni képes (Bohacek & Daniel, 2010; Sherwin, 2003). Menopauzában mélyreható változások érintik a noradrenerg-, dopaminerg-, szerotoninerg-, kolinerg- és peptiderg neurotranszmissziót (Genazzani et al., 2005). Nem ismert azonban, hogy az alacsony E2 szint milyen transzkripciós változásokat idéz elő, és melyek játszhatnak szerepet a fenti funkciók hanyatlásában.

Az értekezésben szereplő egyik tanulmányunk az aggyal mint a gonadális tengely célszervével foglalkozik. Az E2 frontális agykéregre gyakorolt genomiális hatásait vizsgáljuk a teljes transzkriptom szintjén, ovariektomizált nőstény patkányokon, microarray megközelítéssel (**19**).

Öregedő rágcsálókban a reproduktív funkciók fokozatos megszűnését nem a tüszők eltűnése, hanem a tengely megváltozott működése okozza, mely igen hosszan tartó folyamat. Ezt a 8-18. hónap közötti életkort sokkal inkább az E2 szintek változatossága, mintsem alacsony szintje jellemzi. Az emberi menopauza hormonális viszonyait is hűen tükröző rágcsáló modellek előállítása ezért nehézségbe ütközik (Acosta *et al.*, 2010). Egyik tanulmányunk a humán menopauza modelljeként középkorú ovariektomizált patkányokat

alkalmaz. A krónikus hormonpótlás frontális agykérgi génexpresszióra gyakorolt hatásait egy négyhetes E2 infúziót követően, microarray megközelítésel vizsgáljuk (**22**).

II. CÉLKITŰZÉSEK

Az értekezésben tárgyalt munkák a reproduktív tengely működésének központi idegrendszeri mechanizmusait vizsgálták. A GnRH neuronrendszerre vonatkozó egyes megfigyelések szélesebb összefüggéseit további neuroszekretoros rendszereken is tanulmányoztuk. Az alábbi konkrét kérdéskörök megértését céloztuk meg:

II/1. GnRH neuronok afferens szabályozását végző neurotranszmitter rendszerek azonosítása

- Hisztaminerg afferentáció szerepének vizsgálata a pozitív ösztrogén visszacsatolásban (**1**)
- Az NPY tartalmú afferensek eredetének feltárása (**5**)
- Kolinerg afferensek azonosítása (**16**)
- A humán hipotalamikus kisspeptin rendszer anatómiai viszonyainak tisztázása (**21**)
- Neurokinin B és kisspeptin idegsejtek kapcsolatának vizsgálata emberben (**21**)
- Endokannabinoid szignalizáció tanulmányozása GnRH idegsejtek GABAerg afferens kapcsolataiban (**13**, **23**)

II/2. Direkt ösztrogén visszacsatolás igazolása GnRH neuronokban: A "β" típusú ösztrogén receptor szerepe

- *In situ* hibridizációs eljárás kidolgozása alacsony kópiaszámú mRNS-ek hisztokémiai kimutatására (**4**)
- ER-β mRNS expresszió igazolása patkány GnRH neuronjaiban (**2**)
- Ösztrogén receptor ligandum kötésének megjelenítése patkány GnRH neuronjaiban (**2**)
- Nukleáris ER-β fehérje detektálása immuncitokémiával patkány GnRH neuronjaiban (**3**)
- Az ER-β immuncitokémiai kimutatása emberi hipotalamusz minták GnRH idegsejtjeiben (**15**)
- E2-regulált gének és szignalizációs útvonalak azonosítása a GnRH-t termelő GT1-7 sejtvonalban microarray módszerrel (**18**)
- ER-β megoszlásának leírása OT-t és VP-t termelő hipotalamikus neuronok csoportjaiban patkányban és emberben (**6**)

II/3. Glutamáterg (VGLUT2) fenotípus megjelenítése GnRH neuronokban és további neuroszekretoros rendszerekben

- Glutamáterg (VGLUT2 fenotípusú) neuroszekretoros idegsejtek lokalizálása (**12**)
- VGLUT2 termelés *in situ* hibridizációs és immuncitokémiai kimutatása GnRH neuronokban (**7**)
- Egyéb neuroszekretoros rendszerek aminosav fenotípusának azonosítása (**8-10**)
- Glutamáterg markerek vizsgálata az adenohipofízis egyes hormon termelő sejttípusaiban (**11, 20**)
- Szabályozott VGLUT2 expresszió bemutatása endokrin állatmodelleken (**10, 116**)

II/4. 17β-ösztradiol E2 kötését követő transzkripciós válaszok azonosítása a frontális agykéregben

- A frontális agykéreg E2-regulált génjeinek és szignalizációs útvonalainak azonosítása ovariektomizált patkánymodellben (**19**)

- Krónikus ösztrogén pótlás génexpresszióra gyakorolt hatásainak kimutatása ösztrogén-hiányos középkorú nőstény patkány frontális agykérgében (**22**)

III. MÓDSZEREK

Az alábbiakban rövid áttekintést adunk a felhasznált módszerekről, a rövid (tézises) értekezés formai sajátosságainak megfelelően. A módszerek részletes leírása az eredeti közleményekben (Melléklet, VIII.fejezet) található meg, melyekre a zárójelbe tett sorszámokkal utalunk.

III/1. KÍSÉRLETI ÁLLATOK

Állatkísérleteinket az MTA Kísérleti Orvostudományi Kutatóintézet Állatkísérleti Etikai Bizottsága és a Budapest Fővárosi Állategészségügyi és Élelmiszer Ellenőrző Állomás engedélyével végeztük (A5769-01), összhangban az „Állatok védelméről és kíméletéről" szóló, 1998. évi XXVIII. tv. 32. § (3) rendelkezéseivel. Az állatokat standard állatházi körülmények között tartottuk (világítás 06:00-18:00 h között, hőmérséklet 22±1°C, rágcsálótáp és víz folyamatosan rendelkezésre állt). Az eredmények reprodukálhatósága érdekében, a morfológiai tanulmányokat állandó hormonszintek mellett, intakt hím vagy ovariektomizált nőstény rágcsáló modellekben végeztük el. Főképp 200-500g súlyú, felnőtt Wistar és Sprague-Dawley patkányok (**1-4, 6-12, 14, 17, 19, 20**), az időskori E2-hiányos agyi állapot modellezésére (**22**), tenyészetből kivont 1-1,5 éves Harlan-Wistar anyaállatok kerültek felhasználásra. Egyes vizsgálatokban CD1 és C57/Bl6 törzsekből származó, vadtípusú egerek (**13**), CB1-génkiütött (**13, 23**) és VGLUT1-génkiütött (**20**) egerek, valamint a GnRH promoter irányítása alatt zöld fluoreszcens proteint expresszáló, GnRH-GFP transzgenikus egerek (**5, 23**) szerepeltek.

III/2. MŰTÉTEK, KEZELÉSEK

*Ovariektómia, ösztrogén kezelések (**1, 2, 3, 6, 11, 19, 22**)*

Ösztrogén-hiányos állapot előidézésére felnőtt nőstény patkányok és egerek kétoldali ovariektómiáját végeztük el, általános érzéstelenítésben (25 mg/kg ketamine, 5 mg/kg xylavet és 2,5 mg/kg pipolphen, *ip.*). Exogén hormonpótlásra 7-14 nappal a műtétet követően került sor, a következő kezelési eljárások egyikével: E2 egyszeri olajos injekciója *sc.* (**1, 11, 19**), E2 olajos oldatát tartalmazó szilikon kapszula *sc.* beültetése 1-7 napra (**2, 3**), vagy propilén glikolban feloldott E2 folyamatos *sc.* infúziója Alzet ozmotikus minipumpával 4 héten keresztül (**22**). Az E2 hiányos kontroll csoport kezelése valamennyi esetben vivőanyaggal történt.

*Neonatális nátrium glutamát kezelés (**5**)*

A mediobazális hipotalamusz NPY/AGRP fenotípusú neuronjainak elpusztítására használt kezelés során, az 1. és 3. posztnatális napokon nátrium glutamát 8%-os vizes oldatát 4 mg/g dózisban, majd az 5., 7. és 9. napon 8 mg/g dózisban injektáltuk újszülött egerek bőre alá. Felnőtt állatokból nyert, krezilibolyával megfestett, hipotalamikus metszeteken az ARC neuronális elemeinek hiánya jelezte a kezelés eredményességét. Immuncitokémiai vizsgálatokban jellemző volt az AGRP immunreaktivitást mutató idegrostok számának nagyfokú csökkenése is, melyek kizárólagos forrása az ARC (Broberger *et al.*, 1998).

*Hypo- és hyperthyreoid patkánymodellek előállítása (**11**)*

Felnőtt, hím, Wistar patkányokat hypothyreoiddá 0,02%-os methimazole oldat 3 hétig tartó itatásával tettünk. Hyperthyreoid állapotot 10µg/diem tyroxin 10 napon keresztül végzett, *ip.* injekciójával hoztunk létre.

*„Sóterhelés" magnocelluláris vazopresszin neuronok krónikus stimulációjára (**10**)*

A sóterhelt állatok ivóvíz helyett 7 napig 2%-os konyhasóoldatot kaptak.

*Kolhicin kezelés perikaryonok immuncitokémiai láthatóvá tételére (**1**)*

A hisztaminerg perikaryonok immuncitokémiai megjelölése kolhicin előkezelést (50-150 mg/100g, *icv*.) igényelt. A kolhicint sztereotaxiás készülék és Hamilton fecskendő segítségével juttattuk a patkányok oldalsó agykamrájába a szövetgyűjtést 24-48 órával megelőzően.

In vivo ^{125}*I [ösztrogén] kötési vizsgálat (**2**)*

Ösztrogén *in vivo* kötésének bemutatásához 200µl vivőanyagban (50% DMSO/50% foszfát puffer) 2µg/kg 17α iodovinyl-11β-methoxyestradiolt (^{125}I-ösztrogén) injektáltunk ovariektomizált patkányok bőre alá. Az állatok agyát 4-6 órával később, transzkardiális perfúzióval (4%-os paraformaldehid oldat) rögzítettük.

III/3. SZÖVETTANI METSZETEK

Hisztológiai vizsgálatokban (immuncitokémia és *in situ* hibridizáció) többféle szövettani rögzítési és metszetkészítési eljárást alkalmaztunk.

In situ hibridizációs mRNS kimutatást általában tárgylemezre szárított, 12µm vastag, frontális síkú metszeteken végeztünk. A metszeteket kriosztát berendezéssel készítettük előzőleg porított szárazjégen lefagyasztott agyszöveti blokkokból, és zselatinnal vagy 3-amino-propil-trietoxi-szilánnal előkezelt lemezekre rögzítettük. A rövid szöveti fixálást (5-30 perc) a prehibridizációs munkafolyamat első lépéseként, 4%-os paraformaldehid oldattal végeztük el (**2-4, 6-10**).

Fénymikroszkópos immuncitokémia (**5, 7-13, 16, 19, 20, 23**) végzésére, továbbá *in situ* hibridizációs és immuncitokémiai eljárások együttes alkalmazására (**12**) 4%-os paraformaldehid oldattal transzkardiálisan perfundált állatok szöveteit használtuk, melyekből fagyasztó mikrotómmal készítettünk 20-30 µm vastagságú, frontális síkú, „úsztatva kezelt" metszeteket. Egyes antigének immuncitokémiai kimutatására 4% akroleint és 2% paraformaldehidet tartalmazó rögzítőkeveréket alkalmaztunk (**3, 6**). Az immuncitokémiát megelőzően, az akrolein feleslegét a metszetek nátrium borohidrid (0,5-1%; 30 perc) előkezelésével semlegesítettük. A hisztaminerg idegelemek immuncitokémiai megjelenítése 4%-os 1-ethyl-3(3-dimethylaminopropyl)-carbodiimide oldattal elvégzett, egyedi szövetrögzítési eljárást igényelt (**1**).

Humán szövettani vizsgálatokhoz (**1, 6, 15, 21**) boncolásból származó hipotalamikus mintákat használtunk, melyeket a Budapesti Regionális Tudományos Etikai Tanács engedélye (TUKEB 49/1999) alapján, a Semmelweis Egyetem Igazságügyi Orvostani Intézetével kollaborációban gyűjtöttünk. A hipotalamikus blokkokat immerziós módszerrel fixáltuk 4%-os paraformaldehid oldatban vagy 4% akroleint és 2% paraformaldehidet tartalmazó rögzítőszer keverékben (1-3 hét), majd 20-30%-os szaharóz oldattal infiltráltuk (24-168 h). Végül fagyasztó mikrotómmal 20-30 µm vastag, úsztatva kezelt szövettani metszeteket készítettünk. Az akrolein feleslegét 1%-os nátrium borohidrid oldattal semlegesítettük (30 perc).

Elektronmikroszkópos vizsgálatok céljára glutáraldehid- vagy akrolein tartalmú rögzítőszerrel perfundált rágcsáló szöveteket használtunk, melyekből vibratom metszőberendezéssel, fagyasztás nélkül készítettünk 30-40 µm vastagságú, frontális síkú metszeteket (**5, 6, 12, 13, 16, 23**). Az immuncitokémiai lépéseket megelőzően a fixálószerek maradékát 1%-os nátrium borohidrid oldattal semlegesítettük (30 perc).

III/4. FÉNY- ÉS ELEKTRONMIKROSZKÓPOS IMMUNCITOKÉMIA

Immuncitokémiai módszerek alkalmazása előtt a metszeteket 20 percig 0,2%-os Triton X-100 oldattal előkezeltük a reagensek penetrációjának elősegítésére. Elektronmikroszkópia végzésekor a szövetek átjárhatóságát folyékony nitrogénnel végzett, fagyasztásos feltárással biztosítottuk (**5, 6, 12, 13, 16, 23**). A szöveti peroxidáz aktivitást 0,5%-os H_2O_2 oldat használatával (30 perc) csökkentettük.

A fénymikroszkópos vizsgálatok többségében immunperoxidáz kimutatási módszert alkalmaztunk, primér antitest (48 h, 4°C), biotinnel jelölt másodlagos antitest (1 h, szobahőn), majd avidin peroxidáz-komplex (ABC Elite kit, Vector; 1 h, szobahőn) egymás utáni alkalmazását követően. A peroxidáz reakció megjelenítését diaminobenzidin (DAB) vagy nikkel-diaminobenzidin (Ni-DAB) kromogént tartalmazó hívóoldattal végeztük.

Kettős-immunperoxidáz alapú vizsgálatokban, melyek célja egy nukleáris és egy citoplazmatikus antigén egy neuronon belüli kolokalizációja (**1, 3, 6, 15**) vagy két különböző neuron fenotípus közti afferens kapcsolat fénymikroszkópos kimutatása (**1, 5, 16, 21, 23**) volt, a fekete színű, ezüst-amplifikált (Liposits *et al.*, 1984) Ni-DAB kromogént a barna színű DAB kromogénnel kombinálva alkalmaztuk.

Immunfluoreszcens módszert kettős- és hármas-jelöléshez használtunk. Különböző fajokban termelt, specifikus elsődleges antitestek alkalmazása után, az antigéneket fluorokrómhoz konjugált másodlagos antitestekkel mutattuk ki. Egyes antigének esetében biotinhez kötött másodlagos antitestet, majd fluoreszcein izotiocianáttal vagy indokarbocianinnal konjugált avidint alkalmaztunk. Több esetben használtuk a biotin-tyramid jelerősítési rendszert is. A humán hipotalamikus mintákon végzett immunfluoreszcens vizsgálatokat megelőzően a metszeteket acetonnal delipidáltuk és szudán fekete lipidfestővel kezeltük **(19, 21, 22**), a lipofuszcin depozitumokból eredő autofluoreszcencia csökkentésére. A fluorokrómokkal megjelölt preparátumokat végül Zeiss epifluoreszcens mikroszkóppal (**5**) és Bio-Rad Radiance 2000 konfokális mikroszkóppal (**7-12, 20, 21, 23**) vizsgáltuk.

Ultrastrukturális vizsgálatokra preembedding immuncitokémiát alkalmaztunk (**5, 6, 12, 13, 16, 23**). Az antigének kimutatásához immunarannyal jelölt másodlagos antitesteket, peroxidáz enzimreakciót, vagy e kettő kombinációját használtuk. Az egyes- és kettős-immunjelölésen átesett metszeteket Durcupan epoxy műgyantába ágyaztuk. Az ultramikrotómmal készített, ultravékony metszeteket Formvar hártyával borított rézgridekre vettük fel, ólom citráttal kontrasztoztuk, végül Hitachi 7100 elektronmikroszkóppal vizsgáltuk.

III/5. *IN SITU* HIBRIDIZÁCIÓ

Komplementer ribonukleinsav (cRNS) próbák gyártása

Az „antiszensz” (komplementer ribonukleinsav; cRNS) próbák *in vitro* előállításához komplementer dezoxiribonukleinsav (cDNS) templátokat használtunk. Ezek többségét - kereskedelmi forgalomban kapható - klónozó kitek („PGEM T”, Promega; „TOPO TA”, Invitrogen) alkalmazásával magunk készítettük (**2-4, 6, 7, 9, 19**). Elsőként a kimutatni kívánt mRNS-t bőven tartalmazó agyterületekből teljes RNS-t izoláltunk. Ebből oligo-dezoxitimidin „primer” és reverz transzkripció használatával cDNS könyvtárat készítettünk. Ezután már a vizsgálandó mRNS-re specifikus primer párokat alkalmazva, polimeráz láncreakcióban (PCR) a cDNS könyvtárból egy 250-1500 bázispár hosszúságú szakaszt sokszorosítottunk, melyet klónozó vektorba ligáltunk. A transzformációval E. coli baktériumba (DH5α törzs) bejuttatott plazmidot LB táptalajban 100μg/ml ampicillin jelenlétében szaporítottuk, majd a Qiagen Maxi Prep kittel izoláltuk. Az inszertumok bázis sorrendjét valamennyi esetben szekvenáltatással ellenőriztük. A detektálandó mRNS-re nézve komplementer bázissorrendű, antiszensz RNS szekvenciák *in vitro* átírását megelőzően, a cirkuláris plazmid vektort restrikciós endonukleázzal felnyitottuk, majd fenol-kloroform-izoamil alkohol extrakció és NaCl/ethanol kicsapás segítségével tisztítottuk. Az RNS átírását - az inszertum irányultságától függően - T7 vagy SP6 RNS polimerázzal végeztük el. Izotópos hibridizáció céljára a reakciót ^{35}S-UTP (**2-4, 6-12, 19**), nem-izotópos módszer használatához digoxigenin-11-UTP (**2, 3, 6-10**) vagy fluoreszcein-12-UTP (**6, 10**) jelenlétében hajtottuk végre.

Hibridizációs oldat készítése

A hibridizációs oldatot közvetlenül használat előtt kevertük össze „hibridizációs puffer"-ből (50% formamid, 2X citrát /„SSC"/ puffer, 20% dextrán szulfát, 1X „Denhardt oldat", 500 µg/ml élesztő transzfer ribonukleinsav, 500 µg/ml Na-heparin), 50-1000 mM ditiotreitolból, valamint a cRNS hibridizációs próbá(k)ból. Alacsony kópiaszámú mRNS-ek kimutatásakor (**2-4, 6-12**) az anatómiai munkák sikere a hibridizációs oldat ditiotreitol, próba és dextrán szulfát tartalmának növelésén alapult, mely módszertani eredményként az értekezés **IV/2.** fejezetének részét képezi (**4**).

In situ hibridizáció tárgylemezre felhúzott metszeteken

A tárgylemezekre rögzített metszeteket tárgylemeztartó dobozokban -80 °C-on tároltuk felhasználásig. Felmelegítést követően, az irodalomban elterjedt prehibridizációs lépéseket alkalmaztuk, ribonukleáz-mentes oldatokat és laboratóriumi eszközöket használva: 5-30 perc szöveti rögzítés 4%-os paraformaldehid oldattal, acetilálás 0,25%-os ecetsav anhidriddel (10 perc), dehidrálás alkoholsorban (2-2 perc), delipidálás kloroformmal (5 perc) és részleges rehidrálás 100%-os, majd 96%-os etanollal (2-2 perc). Ezt követően, a metszetekre hibridizációs oldatot pipettáztunk és csipesszel üveg fedőlemezt helyeztünk. A hibridizációt 52 °C-on, 12-40 óráig, nedves kamrában hajtottuk végre. Az aspecifikus próbakötést poszthibridizációs kezelésekkel csökkentettük (20µg/ml ribonukleáz A oldat, 30 perc, 37 ^{o}C; 0,1X citrát /"SSC"/ puffer, 62^{o}C, 60 perc). Izotóppal jelölt próbák használatát követően, a tárgylemezeket 70%-os etanol oldatban részlegesen dehidráltuk, majd megszárítottuk. Nem-izotópos próbákat használva, szárítás előtt végeztük el a digoxigenin (vagy fluoreszcein) immuncitokémiai kimutatását. Kettős- vagy hármas-*in situ* hibridizáció végzésekor ezt követte az izotóppal jelölt próba autoradiográfiás megjelenítése (**2, 3, 6-10**).

In situ hibridizáció úsztatva kezelt metszeteken

A módosított prehibridizációs kezelések a metszetek acetilálásából (0,25%-os ecetsav anhidrid; 10 perc) és részleges delipidálásából (50%-os, 70%-os és 50%-os aceton használata; 5-5 perc) álltak. A hibridizációt PCR csövekben végeztük el. Ezt a felhúzott metszetek kezelésénél már részetezett poszthibridizációs lépések követték, majd a nem-izotópos próbába épített markerek (digoxigenin, fluoreszcein) vagy endogén szöveti antigének immuncitokémiai kimutatását hajtottuk végre. A metszeteket végül tárgylemezre rögzítettük, megszárítottuk, majd a radioizotóppal jelölt próbák autoradiográfiás detektálását végeztük el. Egyes antigének kimutathatósága a hibridizációs kezelések során sérült. Ilyen esetben először az immuncitokémiai jelet detektáltuk oly módon, hogy a szöveti mRNS-ek lebomlását az antitest oldatokhoz és egyéb reagensekhez hozzáadott Na-heparinnal (1000U/ml) gátoltuk (**12**)

Nem-izotópos hibridizációs jelek kimutatása

A nem-izotópos hibridizáció jel kimutatására többféle megközelítést alkalmaztunk. A cRNS próbába beépített digoxigeninhez először többnyire tormagyökér peroxidázzal konjugált anti-digoxigenin antitestet kötöttünk, majd a peroxidáz reakció erősítésére biotin-tyramid szignál amplifikációt alkalmaztunk. A lerakódott biotin detektálására ezt követően peroxidáz alapú vagy fluoreszcens módszert választottunk (**2, 3, 6-10**). Hasonló érzékenységű megközelítésnek bizonyult az alkalikus foszfatázzal konjugált anti-digoxigenin antitest használata, a jel végső kimutatását az 5-bromo-4-chloro-3-indolyl phosphate/nitro blue tetrazolium kromogén rendszerrel végezve el (**6, 10**).

Autoradiográfia

A ^{35}S-UTP-vel megjelölt próbákból származó autoradiográfiás jelet regionális analízis céljára röntgen filmen, egy-sejt elemzés céljára Kodak fotoemulzión rögzítettük, 1-6 hetes expozíciós időt használva (4°C). Alacsony jel expresszió esetén, egyedi neuronok láthatóvá tételéhez további módszer optimalizálást is végeztünk (**4**).

Kvantitatív képelemzés

A röntgen filmen megjelenített, különböző kezelési csoportokból származó hibridizációs képek összehasonlító elemzésére (**11**) a digitalizált autoradiogrammok denzitometriás elemzését végeztük el, az analizált területek átlag szürkeség értékének („mean grey value") meghatározásával (Image J programcsomag; http://rsb.info.nih.gov/ij/download/src/). Egyedi idegsejtek autoradiográfiás képeit digitális felvételeken elemeztük, a jel intenzitását az ezüstszemcsék által borított pixelek számával jellemezve (**10**). Csoportok összehasonlítására egy- vagy többutas varianciaanalízist alkalmaztunk.

III/6. MICROARRAY VIZSGÁLATOK

A microarray vizsgálatok egy részében a GnRH-t termelő és szekretáló, GT1-7 neuronális sejtvonal (Mellon *et al.*, 1990) transzkriptomjának E2-függő regulációját tanulmányoztuk (**18**). Az E2-t 10^{-8} M koncentrációban, 0,5h, 2h, 8h, 24h és 48h kezelési idővel alkalmaztuk az ösztrogén-mentes tápoldatban. A tenyészetekből izolált RNS minták (RNeasy Lipid Tissue Mini Kit, Qiagen) feldolgozását az Affymetrix cég technikai útmutatásai alapján végeztük el. A megjelölt cRNS-eket az "Affymetrix murine MG-U74Av2" chipen hibridizáltuk. A Hewlett-Packard G2500A Gene Array Scanner-rel rögzített képek elemzését az ArrayAssist programcsomaggal (Stratagene, ArrayAssist® Expression Software) végeztük el.

Az E2 frontális agykérgi transzkriptomjára gyakorolt hatásait is microarray metodikával vizsgáltuk (**19, 22**). E2-kezelt és ovariektomizált kontroll állatok agyait 10%-os RNAlater oldat transzkardiális perfúziójával rögzítettük. Az azonos módon kimetszett, prefrontális, motoros és szenzoros kérgi területeket magukban foglaló, frontális lebeny blokkokból teljes RNS-t izoláltunk (RNeasy Lipid Tissue Mini Kit, Qiagen), melynek minőségét Bioanalyzer berendezéssel (Agilent, Santa Clara, CA) ellenőriztük. A minták további feldolgozását Affymetrix protokollok alapján, a teljes transzkriptom analízisét biztosító Affymetrix Rat 230 2.0 Array használatával végeztük el. A phycoerythrinnel megfestett array-ek fluoreszcens képét GCS 3000 confocal laser scanner-rel (Affymetrix) digitalizáltuk. Ezt követően, a fluoreszcens intenzitásokat a GCOS program (Affymetrix) alkalmazásával határoztuk meg.

III/7. RT-qPCR ÉS TAQMAN ARRAY MÓDSZEREK

A microarray vizsgálatok eredményeit válogatott esetekben valós-idejű kvantitatív PCR (RT-qPCR) módszerrel is megerősítettük. Az egyedi RNS mintákból először cDNS-eket készítettünk, melyeket egyedi PCR reakciókban (**18**) vagy az Applied Biosystems (Santa Clara, CA) „TLDA microfluidic card" megközelítésével vizsgáltuk. Az utóbbi módszer 96 cDNS mintapár párhuzamos kvantitatív elemzését biztosította (**19, 22**). A metodika további technikai részletei az eredeti közleményekben megtalálhatók (**18, 19, 22**).

III/8. *IN VITRO* SZELET ELEKTROFIZIOLÓGIA

Elektrofiziológiai vizsgálatok céljára GnRH-GFP transzgenikus egerek mediális szeptumából és preoptikus területéről 250μm vastagságú, akut szeleteket készítettünk vibratome metszőberendezéssel. Az elektrofiziológiai kísérletek részletes technikai leírása az eredeti közleményben olvasható (**23**).

A CB1 agonista WIN55,212 (1 μM) GnRH idegsejtek tüzelésére gyakorolt hatását loose-patch-clamp vizsgálatokkal tanulmányoztuk. A neuron aktivitásra gyakorolt hatás kivédését ionotrop glutamát receptor antagonista (2 mM kinurénsav) vagy $GABA_A$ receptor antagonista (20 μM bikukullin-methiodide) szerekkel kíséreltük meg.

Whole-cell patch-clamp kísérletekben CB1 receptoron ható szerek $GABA_A$ receptor mediálta hatásait vizsgáltuk. Az akciós potenciál-függő áramokat 750nM tetrodotoxinnal gátoltuk. A különböző vizsgálatokban CB1/CB2 agonista WIN55,212 (1μM) és CB1 antagonista AM251 (1μM) GABAerg miniatűr posztszinaptikus áramokra gyakorolt hatásait

elemeztük. A GnRH neuronok 2-AG termelésének gátlására használt tetrahydrolipstatin (10 μM) az intracelluláris oldatban került alkalmazásra.

IV. EREDMÉNYEK

Az eredmények részletesebb leírása és megbeszélése a VI/2. fejezetben felsorolt és VIII. fejezetben teljes terjedelemben is mellékelt, eredeti közleményekben található. A zárójelbe tett sorszámokkal ezekre hivatkozunk.

IV/1. GnRH neuronok afferens szabályozását végző neurotranszmitterek rendszerek azonosítása

Hisztaminerg afferentáció szerepének vizsgálata a pozitív ösztrogén visszacsatolásban (**1**)

A hisztaminerg idegelemek immuncitokémiai megjelenítése igényelte, hogy az antigéngyártáskor a hisztamin konjugációjára használt speciális rögzítőszer jelen legyen a szöveti fixálóban is (Panula *et al.*, 1984). Kolhicinnel kezelt, ovariektomizált nőstény patkányokon elvégzett kettős-immuncitokémiai vizsgálataink kimutatták, hogy a tuberomammilláris mag valamennyi alegységében (E1-E5) a hisztamin-IR idegsejtek többségének (66-81%) magja tartalmazza az ER-α-t (**1/1. ábra**).

Patkányból származó és humán hipotalamikus szöveteken egyaránt megvizsgáltuk, hogy a hisztaminerg neuronrendszer beidegzi-e a GnRH neuronokat. A hisztaminerg axonok mindkét fajban számos axo-szomatikus és axo-dendritikus kapcsolatot létesítettek GnRH idegsejtekkel. Patkányban a GnRH-IR idegsejtek 40±2.3%-án, humánban 51±3.0%-án figyeltük meg hisztamin-IR axonok kontaktusait (**1/3. ábra**).

Dr. Clive Coen londoni munkacsoportjával kollaborációban megvizsgáltuk, hogy az általunk feltárt, ösztrogén-érzékeny hisztaminerg pálya részt vesz-e a pozitív ösztrogén visszacsatolásban, és ha igen, melyik hisztamin receptoron keresztül. A kísérletek során ovariektomizált patkányok ösztradiol benzoát kezelésével (50μg/0,2 ml olajos *sc*. injekció) LH surge-öt váltottunk ki az injekció másnapján, melynek bekövetkeztét a szérum LH szintek radioimmunoassay vizsgálatával igazoltuk, fél óránként gyűjtött mintákból. Az oldalsó agykamrába infúzióval bejuttatott H2 receptor antagonista, ranitidin (0,5 ml/min) nem befolyásolta az LH surge normál lefolyását. Ezzel szemben, a H1 receptor antagonista mepyramin infúziója meggátolta az ösztrogénnel kiváltható LH surge jelentkezését (**1/4. ábra**).

Az NPY tartalmú afferensek eredetének feltárása (**5**)

A hím GnRH-GFP transzgenikus egereken elvégzett vizsgálataink megmutatták, hogy az ARC neuronjainak pusztulását okozó, újszülöttkori nátrium glutamát kezelés következtében felnőttkorban a preoptikus area-t beidegző NPY idegrostok száma jól látható mértékben lecsökken (**5/1C-D ábrák**). A csökkenést az ARC NPY-t és AGRP-t egyaránt termelő neuronjainak pusztulása okozta, mint azt a hipotalamikus AGRP immunreaktivitás csaknem teljes eltűnése jelezte (**5/1E-F ábrák**). A kezelés hatására a GnRH neuronok perikaryonján és proximális dendritjén észlelt NPY-IR kontaktusok száma 63.7±5.0%-os csökkenést mutatott, igazolva, hogy az ARC a GnRH idegsejtek NPY bemenetének legjelentősebb forrása. A kvantitatív elemzés finomítására hármas-fluoreszcens vizsgálatokat végeztünk. A GnRH-GFP neuronok kimutatására a GFP fluoreszcenciáját használtuk, kombinálva azt kettős immunfluoreszcens módszerrel. Megállapítottuk, hogy a GnRH idegsejtekkel kapcsolatban álló NPY-IR axon varikozitások fele (49.1 ±7.3%) tartalmaz ARC-beli eredetre utaló AGRP immunreaktivitást is (**5/4D-F ábrák**). A rostok további egynegyede (25.4 ±3.3%) az agytörzsi katekolaminerg rendszer marker enzimjét, a DBH-t tartalmazta (**5/4J-L ábrák**), míg a rostok maradék egynegyede egyik topográfiai marker antigént sem hordozta. Az

AGRP/NPY rendszer GnRH neuronokkal alkotott kapcsolatát ultrastrukturális szinten is tanulmányoztuk, immunarany és DAB jelölőanyagok kombinációjával. Az AGRP-IR axonok valódi axo-szomatikus és axo-dendritikus szinapszist képeztek GnRH neuronokkal. A szinaptikus specializációk karaktere minden esetben – GABAerg kapcsolatokra jellemzően - szimmetrikus volt (**5/3B ábra**).

Kolinerg afferensek azonosítása (**16**)

A GnRH neuronrendszer kolinerg beidegzését hím patkányokon, fény- és elektronmikroszkópos immuncitokémiai vizsgálatokkal vetettük fel. A kolinerg idegelemek megjelenítését két marker enzim, a vezikuláris acetilkolin transzporter és a kolin-acetiltranszferáz immuncitokémiai kimutatásával végeztük el.

A GnRH idegsejtek fő megoszlási területein (OVLT és MPOA) nagy számban figyeltünk meg kolin-acetiltranszferáz- és vezikuláris acetilkolin transzporter-IR idegrostokat. Jelölt kolinerg sejttestek laterálisabb elhelyezkedésben, a Broca-féle diagonális köteg horizontális magjában tűntek elő (**16/1A és B ábrák**). A GnRH idegsejtek megoszlási területén vastag és vékony kolinerg idegrostok egyaránt előfordultak. Az utóbbiak gyakorta axo-szomatikus és axo-dendritikus kontaktust képeztek GnRH idegsejtekkel (**16/1C-E**). Elektronmikroszkóppal vizsgálva a kolinerg rostokat (**16/2. ábra**), azok számos, asztroglia közbeékelődéstől mentes appozíciót képeztek GnRH neuronokkal. Valódi szinapszis viszonylag ritkán volt megfigyelhető a preoptikus területen és specifikusan, GnRH idegsejteken. Ezen ritka szinapszisok aszimmetrikus specializációt mutattak (**16/2E és F ábrák**).

A humán hipotalamikus kisspeptin rendszer anatómiai viszonyainak tisztázása (**21**)

Magánforrásból származó anti-mouse kisspeptin-10 és anti-humán kisspeptin-54 antitestek használata immuncitokémiára hasonló kisspeptin-IR axon megoszlási mintázatot tárt fel a *post mortem* női agyakból származó mintákban. Míg a hipotalamusz III. agykamrához közeli, mediális területei bőségesen tartalmaztak kisspeptin-IR axon varikozitásokat, jelölt rostok csak elvétve jelentek meg a laterálisabb hipotalamusz régiókban. Különösen gazdag rostozat volt megfigyelhető a periventrikuláris, paraventrikuláris és infundibuláris magokban (**21/1-3. ábrák**). A rágcsálóagy viszonyaitól eltérően, gazdag perikapilláris rostfonat jelent meg az EM portális kapillárisai körül is (**21/1F ábra**), felvetve a kisspeptin neuroszekréció lehetőségét a humán hipofízis portális keringésébe. A kisspeptint termelő neuronok perikaryonja az anti-humán kisspeptin-54 antitest használatával vált láthatóvá (**21/3. ábra**). A neuronok zöme a nucleus infundibularisban jelent meg (**21/3D ábra**). Egy kevésbé intenzív festődésű, ám számbelileg jelentős további sejtcsoport a rosztrális periventrikuláris területen is megfigyelhető volt, a kis- és nagysejtes paraventrikuláris idegmagvakkal átfedő anatómiai megoszlásban (**21/3A és B ábrák**). Topográfiai helyzete alapján, ez a neuron populáció megfelelhet a rágcsálókban azonosított RP3V pozitív ösztrogén visszacsatolásért felelős (Herbison, 2008) kisspeptin sejtcsoportjának.

A humán hipotalamikus kisspeptin neuronrendszer - rágcsálókból nyert adatok alapján megjósolt - szexuális dimorfizmusát férfiakból és nőkből származó szövetminták párhuzamos immuncitokémiai vizsgálatával vetettük fel (**21/4. ábra**). A férfiakból származó minták többsége igen kevés kisspeptin-IR idegrostot tartalmazott. A női és férfi minták közti különbség kvantitatív elemzése (0,0625 mm^2 területre vonatkoztatott rost számok összehasonlítása) igazolta, hogy azonos területen a női minták 4-7-szer több idegrostot tartalmaznak, mint a férfiakból származó hipotalamusz metszetek (nucleus infundibularis: $F1,7 = 9,42$, $P = 0,018$; nucleus periventricularis: $F1,8 = 14,87$, $P = 0,005$; ANOVA). Hasonlóan robusztus volt a nemek különbsége, amikor a nucleus infundibularis 0,25 mm^2–nyi területein a kisspeptin-IR perikaryonok számát vetettük össze, ami a női mintákban 6-7-szer volt nagyobb ($F1,7 = 35,72$, $P = 0,0006$; ANOVA). A megfigyelés érdekessége, hogy a

nucleus infundibularissal analóg ARC kisspeptin rendszerének rágcsálókban nincs jól látható nemi dimorfizmusa (Clarkson & Herbison, 2006). Az RP3V területén kisspeptin-IR sejttestek kizárólag nőkből származó mintákban voltak láthatóak. A megfigyelés rámutat, hogy emberben is létezik egy rágcsálók RP3V-beli kisspeptin neuronjaival analóg sejtcsoport, ami a rágcsálókéval azonos irányú, jelentős mérvű nemi dimorfizmust mutat.

Immuncitokémiai kettős-festésen alapuló vizsgálataink a kisspeptin és GnRH neuronrendszerek közti kontaktusok helyeit és számát vizsgálták (**21/4. ábra**). A GnRH-IR sejttesteken női mintákban 0,7 ± 0,5 (átlag±SEM), férfiakból származó mintákban 0,12 ± 0,05 kontaktus volt látható. Női mintákban a GnRH idegsejtek 25,8 ± 15,0%-ának, férfi mintákban 8,3 ± 3,6%-ának felszínén volt kisspeptin-IR axon kontaktus megfigyelhető. Hasonlóan, axo-dendritikus kapcsolatok is jelen voltak mindkét nemben, és az EM területén vékony kaliberű kisspeptin-IR axonok gyakori axo-axonális kontaktust is képeztek GnRH-IR axonokkal (**21/4I ábra**).

Neurokinin B és kisspeptin idegsejtek kapcsolatának vizsgálata humán hipotalamuszban (**21**)

Női hipotalamikus szövetmintákon elvégzett immunfluoreszcens vizsgálataink a kisspeptin és neurokinin B feltételezett kolokalizációját vizsgálták egy új, anti-humán preproneurokinin B antitest használatával. Először egyes-jelölés és peroxidáz-alapú immuncitokémia alkalmazásával feltérképeztük a humán hipotalamikus neurokinin B rendszert (**21/5. ábra**), mely kiterjedtebb rost és sejttest megoszlást mutatott, mint a kisspeptin neuronrendszer. Nagyszámú perikaryon volt látható a stria terminalis magjában, a Broca-féle diagonális köteg mentén és a nucleus infundibularisban, de elszórt immunpozitív sejtek a nucleus periventricularisban is megjelentek. A kettős-immunfluoreszcens vizsgálatok megmutatták, hogy a nucleus infundibularis kisspeptin- és neurokinin B-IR perikaryonjai többségükben azonosak (**21/6A-C ábrák**). A kisspeptin-IR axonoknak egy régió függvényében változó hányadában szintén megjeleníthető volt a neurokinin B immunjel (**21/6D-I ábrák**). Ez az arány a nucleus infundibularisban 56,5 ± 7,8%, a nucleus periventricularisban 13,6 ± 7,9% volt, míg neurokinin B nem volt jelen kisspeptin neuronok extrahipotalamikus rostvetületeiben a laterális szeptumban. Az eltérő kolokalizációs arányok arra utalnak, hogy a különböző kisspeptin sejtpopulációk nem azonos mértékben járulnak hozzá a vizsgált területek beidegzéséhez. Az RP3V-vel analóg terület kisspeptin sejttestjeinek immunfluoreszcens vizsgálata technikai okokból nem volt lehetséges. Rágcsálókban és birkában tett észleletek (Goodman *et al.*, 2007; Navarro *et al.*, 2009) azonban azt valószínűsítik, hogy emberben is ezek a neuronok jelenthetik a neurokinin B-t nem tartalmazó kisspeptin idegrostok forrását.

Endokannabinoid szignalizáció tanulmányozása GnRH idegsejtek GABAerg afferenseiben (**13, 23**)

Vizsgálataink egyik célja a hipotalamusz CB1-IR beidegzésének tanulmányozása volt, fény- és elektronmikroszkópos immuncitokémia alkalmazásával. Egy további morfológiai és elektrofiziológiai kísérletsorozatban a GnRH neuronrendszer GABAerg afferenseit befolyásoló endokannabinoid szignalizációt vizsgáltuk.

Immuncitokémiai eredményeinket egy új CB1 antiszérum használatával nyertük (Fukudome *et al.*, 2004). Fénymikroszkópos megfigyeléseink alapján (**13/1. és 2. ábrák**), a hipotalamikus magok többsége meglepően bő CB1-IR beidegzést nyert, melyet korábbi tanulmányok nem tudtak megjeleníteni. Különösen dús innervációt kapott az elülső hipotalamikus area, az MPOA, a PVN, a nucleus dorsomedialis, a nucleus ventromedialis és a nucleus supramammillaris. A CB1-IR rostok ugyanakkor alacsony számban jelentek csak meg az SON, a nucleus suprachiasmaticus és a nucleus mammillaris lateralis területén. Az immuncitokémiai jel specificitását CB1-génkiütött egér agyszövet - mint negatív kontroll -

használatával igazoltuk (**13/2K ábra**). Ultrastrukturális szinten a legintenzívebb CB1 immunjelet a jelölt axonok preterminális/terminális szegmentumában figyeltük meg (**13/3 és 13/4 ábrák**). A CB1-IR terminálisok PVN területén elvégzett elemzése 50 szinapszis közül 28 esetében a glutamáterg fenotípusra jellemző aszimmetrikus, míg 22 esetében a GABAerg fenotípusra jellemző szimmetrikus morfológiát igazolt. Hasonló számarányokat találtunk az ARC területén is.

GnRH-GFP idegsejtek elektrofiziológiai vizsgálata során a CB1 agonista WIN55,212 csökkentette a GnRH idegsejtek spontán tüzelési frekvenciáját (**23/1A ábra**). Ez a hatás ionotrop glutamát receptorok gátlása (2 mM kinurénsav) mellett is kimutatható volt, de a $GABA_A$ receptorokat blokkoló bikukullin (20μM) szelethez adását követően megszűnt (**23/1C ábra**), a GABA közvetítő szerepét igazolva. Morfológiai vizsgálatokkal valóban sikerült is kimutatni GnRH idegsejtekkel szinapszist képező CB1-IR axon végződéseket, melyek egy része - a GABAerg transzmisszióra jellemző - szimmetrikus morfológiát mutatott (**23/3. ábra**). Whole-cell patch-clamp vizsgálatokkal megállapítottuk, hogy a GnRH idegsejtekre érkező GABAerg miniatűr posztszinaptikus áramok frekvenciáját a CB1 agonista WIN55,212 lecsökkenti (**23/4 B, D ábrák**). A CB1 antagonista AM251 (1μM) önmagában alkalmazva növelte a frekvenciát, mely egy GABAerg bemeneteket gátló endokannabinoid tónus fennállására utalt (**23/5 ábra**). A 2-AG szintézist gátló tetrahydrolipstatin jelenléte az intracelluláris oldatban a gátló tónust megszüntette, jelezve, hogy a preszinaptikus CB1-en ható ligandum forrása maga a GnRH idegsejt (**23/5 ábra**).

Megbeszélés

A reprodukció szabályozásában a központi idegrendszer kimeneti jelét a hipofízis felé a GnRH pulzatilis szekréciója jelenti. A keringő ösztrogén és androgén hormonok szintje, metabolikus-, cirkadián- és stressz szignálok, szezonális szaporodású fajoknál a napszakok hosszának változása mind a pulzatilis GnRH szekréció mintázatát módosítva hat az adenohipofízis és a gonádok működésére. A GnRH idegsejtek összehangolt szekréciós aktivitásán alapuló pulzatilitást afferens bemenetek szabályozzák. Az afferensekben működő átvivőanyagok némelyike obligát a GnRH pulzus generátor pubertás kori beindításához vagy a fertilitás fenntartásához. Igy a kisspeptin/GPR54 (Seminara *et al.*, 2003) vagy a neurokinin B/NK3 (Topaloglu *et al.*, 2009) jelátvitel hiánya nem kompenzálható, hipogonadotrop hipogonadizmussal jár. Patológiás körülmények közt hasonlóan hatékonynak mutatkozhat az NPY által közvetített gátló szabályzás is. A leptin-deficiens *ob/ob* egerek infertilisek (Mounzih *et al.*, 1997), ám reproduktív fenotípusuk jelentősen javítható az NPY-génkiütött egerekkel való keresztezéssel (Erickson *et al.*, 1996), rámutatva, hogy *ob/ob* egérben a reproduktív tengely gátlásában a megnövekedett NPY tónusnak kitüntetett szerepe van. A felszálló noradrenerg pályarendszerek átmetszésével patkányban ugyancsak megelőzhető az LH surge jelentkezése, ám ez esetben 3 hét elteltével az ép funkció noradrenerg szabályozás hiányában is visszatér (Clifton & Sawyer, 1979), a kiesést kompenzáló plaszticitást jelezve. A GnRH idegsejtekkel kommunikáló afferens rendszerek feltárása elengedhetetlen a GnRH pulzus generátor szabályozásának megértéséhez. E fejezetben szereplő munkáinkban morfológiai és farmakológiai megközelítésekkel igazoltuk a hisztaminerg rendszer részvételét a pozitív ösztrogén visszacsatolásban (**1**). Bizonyítottuk, hogy a GnRH idegsejteket beidegző NPY-IR afferensek fele az ARC-ból ered, AGRP-t tartalmaz, és szimmetrikus szinapszisokat képez. Noradrenerg marker enzimet tartalmazó NPY tartalmú afferensek is jelentős arányban (25%) járulnak hozzá a GnRH idegsejteken megfigyelhető NPY-IR kontaktusok képzéséhez (**5**). Számos kolinerg appozíciót is megfigyeltünk GnRH idegsejteken (**16**), melyekben a szinaptikus specializáció gyakori hiánya a nem-szinaptikus jelátviteli mechanizmusra (Vizi & Kiss, 1998) utalt. A humán kisspeptin neuronrendszer tanulmányozása során elsőként figyeltünk meg egy rágcsálók RP3V területével analóg, szexuálisan dimorf idegmagot és

kisspeptin sejtcsoportot. Az észlelet alapján felvethető, hogy a jelenleg elfogadott nézettel szemben (Knobil, 1980), a pozitív ösztrogén visszacsatolás emberben nem teljes egészében az infundibuláris magban játszódik. A humán nucleus infundibularis (ARC) kisspeptin idegsejtjeinek általunk megfigyelt, igen nagyfokú szexuális dimorfizmusa rágcsálókban nem volt ismert. Ugyancsak rágcsálóktól eltérően, humánban a portális erek körül is megfigyeltünk kisspeptin-IR rostokat, továbbá a kisspeptin rostok axo-axonális kontaktusokat létesítettek GnRH terminálisokkal az EM-ben (**21**). Az utóbbi kapcsolat típus megmagyarázza a kisspeptinek LH szekréciót fokozó hatását *iv*. injekciót követően (Shahab *et al.*, 2005). Egyúttal előrejelzi, hogy GPR54-en ható, új terápiás készítmények a GnRH szekréciót a vér-agy gáton kívül hatva is képesek lesznek befolyásolni. A neurokinin B kimutatása a humán nucleus infundibularis kisspeptin neuronjaiban (**21**) a rágcsálóban és juhban tett korábbi megfigyelésekkel (Goodman *et al.*, 2007; Navarro *et al.*, 2009) analóg jelenséget takar. Mivel a GnRH idegsejteket a glutamáton kívül a GABA is serkenti (DeFazio *et al.*, 2002), a GABAerg terminálisokon - részben tónusosan ható – retrográd endokannabinoid szignalizáció, melyet kombinált morfológiai, farmakológiai és elektrofiziológiai megközelítésekkel tártunk fel, különösen fontos élettani mechanizmust képviselhet a GnRH idegsejt működésének gátló szabályozásában (**23**). A gátló mechanizmus jelentőségét a metabolikus-, szteroid hormone-, és cirkadian jelek átvitelében további vizsgálatok hivatottak feltárni. Az értekezés keretein belül vizsgált afferens rendszereket az **I. Ábra** foglalja össze.

IV/2. Direkt ösztrogén visszacsatolás igazolása GnRH neuronokban: A "β" típusú ösztrogén receptor szerepe

A GnRH idegsejtekre gyakorolt pozitív és negatív ösztrogén visszacsatolás (Herbison, 1998) mechanizmusa kezdetektől fogva a reproduktív neuroendokrinológia központi kérdése volt. Mióta Shivers és munkatársai leírták a tríciummal megjelölt E2 *in vivo* kötésének hiányát patkány GnRH neuronjaiban (Shivers *et al.*, 1983), a kutatások középpontjában az E2 hatást közvetítő interneuronok keresése állt. Az ER-β felfedezésével (Kuiper *et al.*, 1996) izgalmas lehetőségként ismét felmerült a GnRH idegsejtek direkt, ER-β közvetítette E2 érzékenysége. ER-β antitestek hiányában, első kolokalizációs vizsgálatainkat *in situ* hibridizációs kettős-jelöléssel végeztük.

Az alacsony kópiaszámú ER-β mRNS egy-sejt szintű kimutatása metodikai kihívást is jelentett. Alábbiakban ezért egy érzékenyített izotópos hibridizációs módszertan kidolgozását is leírjuk, melyet kettős-jelöléshez adaptálva, sikerrel vizsgáltuk ER-β megjelenését GnRH idegsejtekben.

A GnRH idegsejtek direkt ösztrogén-érzékenységét ligandum kötési vizsgálatokkal is elemeztük, majd a közben kifejlesztett ER-β antitestek használatával, immuncitokémiával is felvetettük, mind patkányban mind emberben.

A továbbiakban az E2 genomikus hatásainak kimutatására microarray vizsgálatokat végeztünk a - GnRH neuronok egy *in vitro* modelljét jelentő - GT1-7 sejtvonalon.

Egy korábbi munkánkban kimutattuk az ER-β előfordulását a PVN és az SON OT és VP neuronjaiban (Hrabovszky *et al.*, 1998). A megfigyelés igazolta, hogy a magnocelluláris neuronok direkt módon is ösztrogén-érzékenyek.

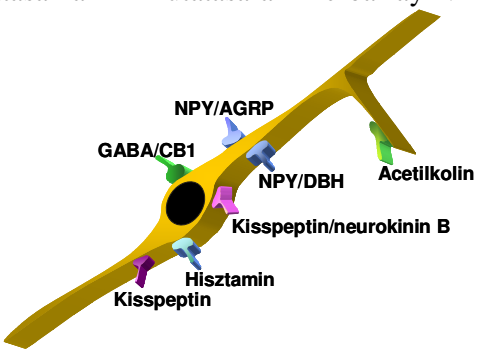

I. Ábra. GnRH neuronok újonnan feltárt afferensei

A receptor expresszió ugyanakkor egyenetlenül oszlott meg az OT és VP neuronok anatómiailag és funkcionálisan is igen heterogén csoportjai között. Ezért az értekezésben szereplő egyik munkánk az ER-β tartalmú hipotalamikus OT és VP idegsejtek finomabb topográfiai analízisét tűzte ki célul (**6**). E tanulmányunkban megvizsgáltuk a kolokalizációs jelenséget a humán hipotalamusz OT és VP sejtjeire vonatkozóan is (**6**).

Új *in situ* hibridizációs eljárás kidolgozása alacsony kópiaszámú mRNS-ek hisztokémiai kimutatására (**4**)

A kénizotóppal (^{35}S) jelölt hibridizációs próbák eredményes alkalmazásának egy gyakori korlátja a magas aspecifikus háttér képződése, mely ditiotreitol (DTT; 10-100 mM) hibridizációs pufferhez adásával mérsékelhető. A hibridizációs módszertan javítását célzó teszt vizsgálatainkban a szokásosnál egy nagyságrenddel magasabb koncentrációjú (750-1000 mM) DTT jelenléte további háttércsökkenést és javuló jel/háttér arányt eredményezett (**4/1. ábra**). Ilyen pufferben a megszokottnál jóval több izotóppal jelölt próba hozzáadása sem okoz háttér képződést (**4/2. ábra**). A próba koncentráció többszörösére emelésekor (**4/3. ábra**) a jel meglepő mértékű erősödést mutatott. Az észlelettel bizonyítottuk, hogy a háttér megfelelő kontrollja mellett (1000 mM DTT használata) a hibridizációs jel erőssége a próba mennyiség emelésével javítható. A továbbiakban igazoltuk, hogy magas próbakoncentráció, ennek alternatívájaként, a hibridizációs pufferben megemelt dextrán szulfát koncentráció (20-30%, szemben a rutin módszertanokban használt 10%-kal), vagy e kettő kombinációja, jelentősen javítja a hibridizációs jel erősségét (**4/3. ábra**). A jelölt neuronok egy-sejt szintű kimutathatósága ennek eredményeképp autoradiográfiás emulzión oly mértékben javulhat, hogy lehetővé teszi alacsony kópiaszámú mRNS-ek megjelenítését is (**4/4. ábra**). Igazoltuk, hogy további jelnövekedés érhető el a hibridizációs idő megnövelésével is (40 h, a rutin 12-16 h hibridizációs idővel szemben; **4/7. ábra**). A magas DTT, dextrán szulfát és próba koncentráció, továbbá a megnyújtott hibridizációs idő a következőkben tárgyalt kettős-*in situ* hibridizációs vizsgálatokban a sikeres kolokalizáció kulcsa volt (**2, 3, 6-11**).

ER-β mRNS expresszió igazolása patkány GnRH neuronjaiban (**2, 3**)

Kettős-*in situ* hibridizációval mRNS szinten is megerősítettük mások immuncitokémiai eredményeit, melyek szerint a patkány GnRH neuronjai jelentős mennyiségű ER-α-t nem termelnek (Herbison & Theodosis, 1992) (**2/a-c ábrák**). Laflamme és mtsai korábban publikált megfigyelésével szemben, mely az ER-β mRNS expresszió hiányát mutatta GnRH neuronokban (Laflamme *et al.*, 1998), javított hibridizációs módszertanunkkal a GnRH idegsejtek többségében sikerült megjeleníteni az ER-β mRNS termelődését (**2/d-i ábrák**). A kolokalizáció aránya ovariektomizált (67,2±1,8%) és ovariektomizált majd E2-vel szubsztituált (73,8±4,2%) patkányokban, továbbá hím és nőstény patkányokban (**3/1. ábra**) nem mutatott szignifikáns eltérést.

Ösztrogén receptor ligandum kötésének megjelenítése patkány GnRH neuronjaiban (**2**)

Az ER-β altípust kódoló mRNS szelektív jelenlétének kimutatása után célunk funkcionális ösztrogén receptor fehérje termelődésének igazolása volt a GnRH idegsejtekben. Shivers és mtsai 1983-ban tríciummal jelölt E2-t használtak az ösztrogén felvétel hiányának kimutatására (Shivers *et al.*, 1983). Ennél érzékenyebb megközelítésre törekedve, az *in vivo* ligandum kötés megjelenítésére mi rövidebb féléletidejű radioizotópot alkalmaztunk. A felvett izotop autoradiográfiás megjelenítését a GnRH immuncitokémiai kimutatásával ötvöztük. A preoptikus terület GnRH idegsejtjeinek 8,8%-ában sikerült kimutatni 17α-iodovinil-11β-metoxiösztradiol (^{125}I-ösztrogén) *in vivo* felvételét (**2/l. ábra**). A kötés specificitását igazolta, hogy jelöletlen E2 előzetes injekciójával a ^{125}I-ösztrogén felvétele teljesen kiküszöbölhető volt.

Nukleáris ER-β fehérje megjelenítése immuncitokémiával patkány GnRH neuronjaiban (**3**)

Az ER-β megbízható immuncitokémiai kimutatását GnRH idegsejtekben sokáig késleltette a jó minőségű, specifikus antitestek hiánya. A Zymed cég nyúlban termelt poliklonális antiszéruma (Z8P) az ER-β immunreaktivitás megoszlását az *in situ* hibridizációs kísérletekből is ismert területeken mutatta, a nukleáris receptorokra jelemző sejtmagi lokalizációban (Shughrue & Merchenthaler, 2001).

Fekete színű, ezüst-amplifikált Ni-DAB és barna színű DAB kromogén kombinációt használva kettős-immuncitokémiai vizsgálatainkban, a nukleáris ER-β immunreaktivitást ovariektomizált patkányok GnRH idegsejtjeinek 87,8±2,3%-ában sikerült kimutatnunk. Hasonlóan magas kolokalizációs arányt figyeltünk meg E2-szubsztituált ovariektomizált nőstény (74,9±3,2%) és intakt hím (85,0±4,7 %) patkányokban (**3/1. ábra**).

Az ER-β immuncitokémiai kimutatása emberi hipotalamusz minták GnRH idegsejtjeiben (**15**)

Egy magánforrásból származó, korábban karakterizált poliklonális anti-humán ER-β antitest (Saunders *et al.*, 2000) használata lehetővé tette, hogy immuncitokémiával felvessük a patkányokon tett megfigyelések emberi relevanciáját. A Semmelweis Egyetem Igazságügyi Orvostani Intézetével kollaborációban elvégzett, kettős-immuncitokémiai vizsgálatok férfi kadáverekből származó hipotalamusz minták GnRH neuronjainak 10,8-28,0%-ában kimutatták a nukleáris ER-β jelenlétét. Az ER-α hiányát mutató korábbi vizsgálatokkal együtt (Rance *et al.*, 1990), eredményeink megmutatták, hogy rágcsálókhoz hasonlóan, a humán GnRH idegsejtek is szelektíven expresszálják az ER-β receptor izoformát. Így az ER-β emberi GnRH idegsejteken is egy közvetlen ösztrogén visszacsatolási mechanizmus molekuláris alapját jelentheti.

E2-regulált gének és szignalizációs útvonalak azonosítása a GnRH-t termelő GT1-7 sejtvonalban microarray módszerrel (**18**)

Microarray vizsgálatainkban a GT1-7 sejtek mintegy 1000 génje mutatott az E2 kezelés hatására megváltozott expressziót. A változásokat különböző időbeli lefutás jellemezte (**18/3. ábra**). A legkorábban jelentkező válaszok már 0,5-2 órával a kezelést követően látszottak, míg a késői válaszok a 24-48 órás kezelési csoportokban mutatkoztak. Az E2 kezelés következményeképp aktivált gének közt számos transzkripciós faktort, neurotranszmittert, neuromodulátort, azok receptorait, ion csatornát és transzportert azonosítottunk (**18/36. táblázatok**). A változások egy részét RT-qPCR-rel erősítettük meg.

ER-β megoszlásának leírása OT-t és VP-t termelő hipotalamikus neuronok csoportjaiban patkányban és emberben (**6**)

Egy korábbi, immuncitokémiát és *in situ* hibridizációt ötvöző tanulmányunkban már kimutattuk, hogy az ER-β mRNS megjelenik a patkány - ER-α-t nem tartalmazó - OT és VP idegsejtjeinek egyes csoportjaiban (Hrabovszky *et al.*, 1998). A jelenség finomabb anatómiai analízisét patkány és humán hipotalamuszban immuncitokémiával folytattuk. A patkányra vonatkozó megfigyeléseket hármas-*in situ* hibridizációs vizsgálatokkal is kiegészítettük.

Az ER-β immuncitokémiai kimutatását követő topográfiai elemzés a legintenzívebb ER-β festődést a PVN egyes vegetatív almagjaiban mutatta ki. Ezek a mediális parvicelluláris almag ventrális és dorzális alegységei, továbbá a laterális parvicelluláris almag voltak (**6/1. ábra**), melyekben az intenzív magfestődés OT-IR neuronokban jelent meg (**6/2J és K ábrák**). A második legerősebb ER-β jelet az SON magnocelluláris vazopresszin idegsejtjeiben, valamint a PVN hátsó magnocelluláris almagjának vazopresszin idegsejtjeiben észleltük (**6/1. és 6/2F, L és O ábrák**). Mivel az OT és VP neuronok szinte valamennyi

csoportja magas százalékban tartalmazta az ER-β-t, a jel-intenzitást a százalékos megjelenési aránynál jellemzőbb paraméternek ítéltük, és négyes-skálán, táblázatos formában, almagonként értékeltük. Kiemelendő a magnocelluláris OT neuronok jellemzően gyenge vagy közepes szintű ER-β immunfestődése, szemben a magnocelluláris VP neuronok intenzív jelölődésével (**6/1. táblázat; 6/2E ábra**).

A Z8P antitesttel tett fenti megfigyeléseket kiegészítettük és megerősítettük egy általunk kidolgozott, hármas-*in situ* hibridizációs módszerrel. Digoxigeninnel, fluoreszceinnel és kénizotóppal (^{35}S) jelölt cRNS próbák együttes kimutatását alkalmazva, magas kolokalizációs százalékot és differenciált ER-β expressziót tártunk fel a hipotalamusz OT és VP idegsejtjeinek különböző funkcionális alcsoportjaiban (**6/4. ábra**).

A humán kolokalizációs viszonyok tisztázására a Semmelweis Egyetem Igazságügyi Orvostani Intézetével kollaborációban végeztünk immuncitokémiai vizsgálatokat. Mind OT, mind VP neuronok csoportjaiban sikerrel mutattuk ki az ER-β immunreaktivitást az SON és a PVN területén (**6/5. ábra**).

Megbeszélés

Megfelelő jel/háttér arány esetén, röntgen filmen az alacsony expressziójú mRNS-ek is vizsgálhatóak hosszú autoradiográfiás expozíciós idő megválasztásával. Gyakori tapasztalat azonban az, hogy ugyanezekben a metszetekben az adott mRNS-t expresszáló egyedi idegsejtek megjelenítése fotóemulzión sikertelen marad. Ez a probléma az autoradiográfiás ezüst szemcsék túlságosan gyenge, jelként nem értékelhető csoportosulásaként, vagy alacsony jel/háttér arányként jelentkezik. Technikai megoldás keresésekor azt a nézetet vizsgáltuk felül, miszerint a rutin izotópos hibridizációs módszerek biztosítják a maximális hibridizációs jelerősséget és a szöveti mRNS molekulák „telítéséhez" szükséges feltételeket. Az általunk javasolt gyakorlati megoldások, mint a megemelt DTT, dextrán szulfát és próba koncentráció, továbbá a megnyújtott hibridizációs idő alkalmazása, az értekezésben tárgyalt kettős-*in situ* hibridizációs vizsgálatokban az eredményes kolokalizáció kulcsa volt (**2, 3, 6-11**). Elvi szempontból is fontos volt cáfolni azt az elterjedt hiedelmet, hogy rutin hibridizációs módszerekkel telíteni lehet a szöveti mRNS molekulákat. Egyik elméleti következtetésünk, hogy az *in situ* hibridizáció sebessége nem csupán a detektált mRNS molekulák szöveti mennyiségétől, hanem a próba koncentrációtól is függ. Ennek megfelelően, a reakcó kinetikája nem elsőrendű, mint azt *in vitro* hibridizációs reakciók vizsgálata alapján korábban feltételezték. Fixált szövetben a próba diffúzió lassúsága és az mRNS korlátozott hozzáférhetősége magyarázhatja megfigyeléseinket (**4**).

Az ER-β mRNS és immunreaktivitás valamint az *in vivo* ^{125}I-ösztrogén kötés kimutatása GnRH idegsejtekben cáfolt egy régi dogmát, mely szerint a GnRH idegsejtek közvetlenül nem képesek az E2 szintek érzékelésére (Shivers *et al.*, 1983). A vizsgálataink óta azonosított, valószínűleg ER-β közvetítette, direkt (részben gyors, részben magreceptorok által mediált) ösztrogén hatások közt szerepel a cAMP response element-binding protein foszforilációja (Abraham *et al.*, 2003), intracelluláris kálcium oszcillációk stimulációja (Temple *et al.*, 2004), galanin génexpresszió indukciója (Merchenthaler, 2005) és a GnRH-GFP neuronok ingerlékenységének fokozása (DeFazio & Moenter, 2002). A

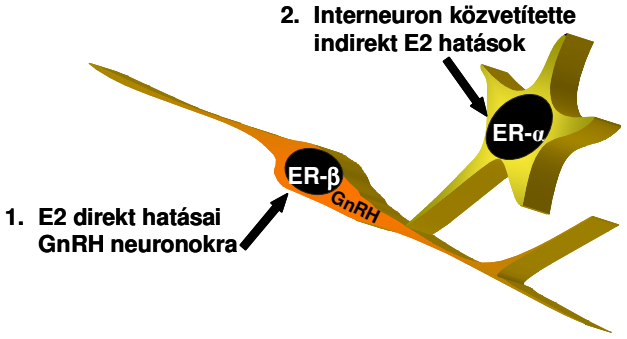

II. Ábra. Ösztrogén visszacsatolás direkt és indirekt útja

GnRH neuronok *in vitro* modelljét jelentő GT1-7 sejteken elvégzett microarray kísérletek eredményei részleges betekintést nyújthatnak azon genomikus változásokba is, melyeket az E2 GnRH neuronokban *in vivo* indukálhat. A direkt hatások mellett azonban az ER-α tartalmú interneuronok által közvetített indirekt hatások is fontos szerepet játszanak a reprodukció szabályozásában. Ezt támasztja alá az ER-α-génkiütött egerek infertilitása (Korach *et al.*, 1996). Az ösztrogén visszacsatolás ER-β által közvetített direkt, és nagyrészt ER-α által közvetített, indirekt útjait a **II. Ábra** vázolja sémásan. Az ER-β receptor altípus szelektív előfordulása GnRH idegsejtekben felveti annak jövőbeli lehetőségét, hogy a GnRH pulzus generátort ER-β-szelektív ligandumokkal is befolyásolni lehet. A leírt jelenség humán relevanciájának megerősítése egyik munkánkban (**15**) ezért különös jelentőségű.

Saját korábbi, immuncitokémiát és *in situ* hibridizációt ötvöző munkánk igazolta az ER-α-t nem expresszáló (Simerly *et al.*, 1990) hipotalamikus OT és VP idegsejtek ER-β tartalmát (Hrabovszky *et al.*, 1998), magyarázatot kínálva a két rendszer működésének régóta ismert ösztrogén érzékenységére (Van Tol *et al.*, 1988; Jirikowski *et al.*, 1988; Skowsky *et al.*, 1979; Van Tol *et al.*, 1988; Wang *et al.*, 1995; Negoro *et al.*, 1973). Az OT és VP fenotípusú hipotalamikus neuronok szerepe azonban rendkívül szerteágazó. ER-β tartalmuk részletes elemzésével (**6**) pontos képet adtunk arról, hogy mely funkcionális alcsoportok, és milyen mértékben ösztrogén érzékenyek. Érdekes módon, a magnocelluláris neuronok közül a VP-t termelők mutattak lényegesen erősebb ER-β jelet. A legintenzívebb receptor festődés a PVN vegetatív almagjainak OT neuronjait jellemezte. A vizsgálat egy további fontos eredménye volt a kolokalizációs jelenség humán relevanciájának igazolása (**6**).

IV/3. Glutamáterg (VGLUT2) fenotípus megjelenítése GnRH neuronokban és további neuroszekretoros rendszerekben

Glutamáterg (VGLUT2) fenotípusú neuroszekretoros idegsejtek lokalizálása (**12**)

Az első vizsgálatok célja az EM külső, vér-agy gát mentes zónáját és a neurohipofízist beidegző VGLUT2-IR idegrostok (Lin *et al.*, 2003) forrásának azonosítása volt. Hím patkányokon elvégzett kísérleteinkben FluoroGoldot juttattunk a szisztémás vérkeringésbe (*ip.* injekció), a vér-agy gát mentes területekre vetítő neuronok, köztük a hipotalamusz neuroendokrin sejtjeinek szelektív megjelölésére. Ezt követően, a perikaryonokban felhalmozódó FluoroGold immunfluoreszcens kimutatását ötvöztük a VGLUT2 mRNS *in situ* hibridizációs megjelenítésével. További immuncitokémiai kísérletek a VGLUT2 immunreaktivitás axonokon belüli, szubcelluláris megoszlását vizsgálták az EM külső zónájában és a - magnocelluláris neuroszekretoros idegvégződéseket tartalmazó - hátsó hipofízislebeny területén.

Eredményeink FluoroGold immunreaktivitás és VGLUT2 mRNS expresszió együttes előfordulását az OVLT, a PVN (kis- és nagysejtes alegységek), a nucleus periventricularis és az SON területén mutatták. Ezzel szemben, az ARC FluoroGold-pozitív neuronjai VGLUT2 hibridizációs jelet nem tartalmaztak (**12/1A-K ábrák**).

A neuroendokrin axonok mindkét végződési területén, az EM külső zónájában és a hátsó hipofízislebenyben, a mikrovezikula marker, SV2 és a VGLUT2 immunreaktivitás egyaránt kimutatható volt, egymással átfedő megoszlásban. Az SV2 és a VGLUT2 immunfluoreszcens jelek a perikapilláris térség közvetlen környezetében voltak legerősebbek (**12/1L-W ábrák**). Az immunarany módszerrel kimutatott VGLUT2 immunreaktivitás elektronmikroszkópos vizsgálata igazolta, hogy a VGLUT2 mindig szinaptikus vezikulák környezetében jelenik meg a kis- és nagysejtes neuroszekretoros rendszerekben. A jelölt mikrovezikula csoportok legjellemzőbben a perikapilláris térség szomszédságában fordultak elő, míg peptideket tartalmazó „dense-core" granulumok folytonos eloszlást mutattak a neuroendokrin axonvetületek mentén (**12/2. és 3. ábrák**).

VGLUT2 termelésének *in situ* hibridizációs és immuncitokémiai kimutatása GnRH neuronokban (**7**)

Az orrplakodban születő GnRH idegsejtek vándorlásuk során - tranziens módon - GABAerg fenotípusúak. Születéskor az előagyba megérkezett GnRH neuronokból a GABA már nem mutatható ki (Tobet *et al.*, 1996). A VGLUT2 mRNS GnRH neuronokéval átfedő megoszlása, a VGLUT2 és a GnRH immunreaktivitás együttes megjelenése az EM külső zónájában (Lin *et al.*, 2003), és neuroendokrin karaktert mutató (vérkeringésbe juttatott FluoroGold-dal megjelölhető; **12**) VGLUT2 idegsejtek előfordulása az OVLT és az MPOA területén felvetették, hogy a felnőtt patkányok GnRH neuronjai glutamáterg fenotípusúak lehetnek.

In situ hibridizációs kettős-jelölés alkalmazásával felnőtt, hím patkányok GnRH neuronjainak közel 100%-ában igazolni tudtuk a VGLUT2 mRNS expresszióját (**7/1A és B ábrák**).

Konfokális mikroszkóppal vizsgálva az EM külső, paliszád zónáját és az OVLT-t, a GnRH-IR axonokban sikerült a VGLUT2 immunreaktivitást is kimutatni (**7/1D-G ábrák**). A VGLUT2 szubcelluláris megoszlása az EM-ben (**12/2. ábra**) valószínűsítette, hogy a VGLUT2 a GnRH axonokban is mikrovezikuláihoz asszociált, melyek legnagyob számban a valódi axonvégződésekben fordultak elő.

Egyéb neuroszekretoros rendszerek aminosav fenotípusának azonosítása (**8-10**)

A fenti tanulmányban használthoz hasonló, kettős- és hármas-*in situ* hibridizációs megközelítést használtunk a többi klasszikus neuroendokrin rendszer aminosav neurotranszmitter fenotípusának vizsgálatára is.

Ezen tanulmányokban bebizonyítottuk, hogy VGLUT2 mRNS termelődik a PVN kissejtes CRH és TRH neuronjaiban (**8/2A-L ábrák**), a PVN és a nucleus periventricularis kissejtes szomatosztatin termelő idegsejtjeiben (**9/1B ábra**), továbbá az SON és a PVN nagysejtes OT és VP neuronjaiban (**10/2. ábra**). Ezzel ellentétben, VGLUT2 hibridizációs jel nem volt látható az ARC GHRH idegsejtjeiben (**9/1A ábra**). Az EM metszetein elvégzett kettős-immunfluoreszcens vizsgálatok megerősítették, hogy a CRH-t, TRH-t és szomatosztatint tartalmazó neuroendokrin terminálisok tartalmazzák a VGLUT2 fehérjét (**8/2M és N, 9/1E ábrák)**. A glutamáterg markert nem expresszáló GHRH idegsejtek axonjaiban ugyanakkor kimutattuk a GABAerg marker, vezikuláris GABA transzporter jelenlétét (**9/1B ábra**), igazolva Meister és mtsai hasonló, korábbi következtetéseinek helyességét (Meister & Hokfelt, 1988).

Glutamáterg markerek vizsgálata az adenohipofízis egyes hormontermelő sejttípusaiban (**11, 20**)

A neurohipofízis VGLUT2 immunreaktivitását vizsgálva (**10**), a mellső lebenyi endokrin sejtek egy csoportja is mutatta a glutamáterg idegsejtekre jellemző VGLUT2 immunreaktivitást. Az immuncitokémiai jel több antitesttel is megfigyelhető volt (**11/1A-C ábrák**). A VGLUT2 mRNS *in situ* hibridizációs kimutatásával igazoltuk, hogy az adenohipofízis valóban VGLUT2 molekulát termel (**11/1D és E ábrák**). Későbbi vizsgálataink a VGLUT1 immunreaktivitást is megjelenítették az adenohipofízisben (**20/1A-C ábrák**). VGLUT1-génkiütött egerek használatával és további kontroll megközelítésekkel a VGLUT1 jel specificitását is alátámasztottuk (**20/2-4 ábrák**).

A két VGLUT izoformát expresszáló, nem-neuronális adenohipofízis sejtek hormontermelő fenotípusát kettős-immunfluoreszcens vizsgálatsorozatban azonosítottuk. A VGLUT2 szelektíven fordult elő az LH-t termelő sejtek közel 93%-ában, az FSH-t termelő sejtek 45%-ában és a thyreoidea-stimuláló hormont termelő sejtek 70%-ában (**11/2 G-I és**

11/3 ábrák). A VGLUT1 az adrenokortikotrop hormont termelő sejtek 46%-ában és az LH-t termelő sejtek 8%-ában jelent meg (**20/5A-C, 5I, és 6. ábrák**).

Szabályozott VGLUT2 expresszió bemutatása endokrin állatmodelleken (**10, 11**)

Kvantitatív *in situ* hibridizációval megvizsgáltuk azt a kérdést, hogy a neuroendokrin/endokrin sejttípusokban megjelenő VGLUT2 expressziója az endokrin állapotoktól függően szabályozott-e.

Az SON magnocelluláris vazopresszin neuronjainak krónikus stimulációjára sóterhelést alkalmaztunk, 2% konyhasó 7 napig tartó itatásával. A kettős-*in situ* hibridizációs vizsgálatokat egy új megközelítéssel végeztük el. Ennek során a digoxigeninnel jelölt VP próba immunfluoreszcens kimutatását az izotóppal jelölt VGLUT2 próba autoradiográfiás megjelenítésével ötvöztük. A két interferencia-mentes jel mikroszkópos képét digitalizáltuk és Adobe Photoshop (PSD) file-ok külön rétegeiben, egymásra vetítve kezeltük. A módszer lehetővé tette a VGLUT2 hibridizációs jel kvantitatív elemzését (ezüst szemcsével fedett pixelek számának meghatározása) az egyedi vazopresszin sejtek felett (**10/2E ábra**). A VGLUT2 immunreaktivitás sóterhelést követő megváltozását szintén megvizsgáltuk a neurohipofízisben, a DAB kromogén denzitometriás elemzésével (átlagos szürkeség érték meghatározása).

Az elvégzett kvantitatív képelemzés eredményei alapján megállapítottuk, hogy sóterhelés hatására az SON vazopresszin sejtjeiben a VGLUT2 expresszió jelentős növekedést mutat (**10/3. ábra**). Evvel egyidőben, a neurohipofízis VGLUT2 immunreaktivitása is megnövekszik (**10/3. ábra**).

Az adenohipofízisben a VGLUT2 mRNS főképp a gonadotrop hormonokat termelő sejtekben jelent meg (**11**), melyek ösztrogén-érzékenyek (Mitchner *et al.*, 1998). Ezért felvetettük, hogy ovariektomizált patkányok E2 kezelése hat-e, és miként, a VGLUT2 expresszióra.

A röntgen filmen rögzített hibridizációs jelek denzitometriás elemzésével megállapítottuk, hogy E2 egyszeri *sc.* injekciója szignifikánsan megnöveli az adenohipofízisben a VGLUT2 mRNS expresszióját (**11/4. ábra**).

A VGLUT2 mRNS az adenohipofízis thyreoidea-stimuláló hormont termelő sejtjeiben is jelen volt (**11**), melyek hypothyreoidismusban aktiválódnak. Kísérleteinkben a VGLUT2 expresszióját euthyreoid kontroll, methimazole oldat itatásával hypothyreoiddá tett, valamint napi tyroxin injekciókkal hyperthyreoiddá tett patkányok adenohipofízisében vizsgáltuk meg. A röntgen filmen rögzített hibridizációs jelek összehasonlító elemzését az előző kísérletben leírtakhoz hasonlóan végeztük el.

Euthyreoid és hyperthyreoid állatok VGLUT2 expressziója az adenohipofízisben nem különbözött. Ezzel szemben, hypothyreoidismusban a hibridizációs jel szignifikáns növekedését figyeltük meg (**11/5. ábra**), melyet az immuncitokémiával kimutatható VGLUT2 és thyreoidea-stimuláló hormon (β alegység) immunjelek - fokozott szekrécióra utaló - csökkenése kísért (**11/6. ábra**).

Megbeszélés (**14, 17**)

A perifériás vérből felvett FluoroGold és a VGLUT2 mRNS együttes megjelenítésével feltérképeztük a vér-agy gát-mentes területeket beidegző, glutamáterg neuronok megoszlását (**12**). Mivel az így nyert kép több klasszikus peptiderg neuroszekretoros rendszer perikaryonjainak ismert elhelyezkedésével átfedett, a továbbiakban a GnRH idegsejtekben és további klasszikus neuroendokrin sejttípusokban vizsgáltuk meg - az endogén glutamát használatára utaló - VGLUT2 előfordulását.

A VGLUT2 sikeres kimutatása GnRH neuronokban az endogén glutamát és a GnRH koszekréciójára utal az EM külső zónájában. Mivel glutamáterg agonista szerek serkentik a

GnRH ürülését az EM axonterminálisaiból (Bourguignon *et al.*, 1989; Arias *et al.*, 1993; Kawakami *et al.*, 1998a), feltételezhető, hogy élettani körülmények között az endogén forrásból származó glutamát is hasonlóan képes fokozni a GnRH szekrécióját.

A glutamát receptort hordozó, helyi célsejtek egyrészt lehetnek maguk a neuroendokrin GnRH terminálisok, ami az EM szintjén működő autokrin/parakrin hatásmechanizmusok alapját teremtheti meg. Valóban, a GnRH-IR axonok tartalmaznak is glutamát receptor alegységeket (N-metil-D-aszpartát R1 és a kainát 2)(Kawakami *et al.*, 1998a; Yin *et al.*, 2007). A III. agykamrát határoló tanycyták ugyancsak expresszálnak többféle AMPA és kainát receptor alegységet (Diano *et al.*, 1998; Eyigor & Jennes, 1998; Kawakami, 2000). Így szintén a neuroendokrin terminálisokból ürülő glutamát célsejtjei lehetnek. Végül, a GnRH neuronokból ürülő glutamát hathat a portális érrendszer falát alkotó sejtekre is. Ismert, hogy agyi mikroerek mind ionotrop, mind metabotrop glutamát receptorokat expresszálhatnak (Krizbai *et al.*, 1998; Gillard *et al.*, 2003).

Funkció tekintetében tudott, hogy a glutamát vagy ionotrop glutamát receptor agonista szerek kálcium-függő GnRH szekréciót váltanak ki az EM *in vitro* preparátumából (Kawakami *et al.*, 1998a). Az EM szintjén ható glutamáterg mechanizmusok szerepet játszanak a pulzatilis GnRH szekréció kialakításában (Bourguignon *et al.*, 1989; Matagne *et al.*, 2005). Eredményeink arra utalnak, hogy az EM-ben a GnRH szekréciót fokozó glutamát legalább részben endogén forrásból, magukból a GnRH terminálisokból származik. Ez autokrin/parakrin mechanizmus révén lehetőséget nyújthat az egyedi GnRH axonok szinkronizált szekréciójának megteremtésére. A részleteiben még nem értett, glutamát kiváltotta folyamatok egyéb hírvivő molekulákat is használhatnak (Bhat *et al.*, 1998; Prevot *et al.*, 2000). Ilyen lehet a nitrogén-oxid, mely az EM-ben főképp endotheliális eredetű és kulcs szerepet játszik a pulzatilitás GnRH szekréció kialakításában (Prevot *et al.*, 2000).

Noha több idegi átvivőanyag előfordulása egyazon neuronban mint kivételes érdekesség került először leírásra (Hokfelt *et al.*, 1977), mára a klasszikus neurotranszmitterek és neuromodulátor peptidek együttes jelenléte idegsejtekben általánosnak tekintett jelenség (Hokfelt *et al.*, 2000). Eredményeink alapján, a szabály alól egyik klasszikus peptiderg neuroszekretoros rendszer sem kivétel. Saját megfigyeléseink (**7-10, 12**) és mások korábbi észleletei (Meister & Hokfelt, 1988) nyomán kirajzolódott a teljes kép a klasszikus neuroendokrin rendszerek aminosav neurotranszmitter fenotípusát illetően (**III. Ábra**). Az endogén glutamát több rendszerben (GnRH, CRH, TRH, szomatosztatin, OT) hasonló, de részleteiben még nem ismert mechanizmussal járulhat hozzá a pulzatilis szekréciós mintázatok kialakításához. A glutamát további hatásai befolyásolhatják glia sejtek (tanycyták, pituicyták) morfológiai és kémiai plaszticitását, továbbá szabályozhatják a portális erek átmérőjét a neuroszekréció helyén (**14, 17**). A jövőbeli vizsgálatok egyik további iránya a VGLUT2 termelés szabályozottsága (**10, 11**) lesz. Az endogén glutamát jelentőségének megértéséhez a laboratóriumunkban előállított GnRH sejttípus-függő VGLUT2-génkiütött állatmodell nyújthat segítséget, melynek jellemzését megkezdtük.

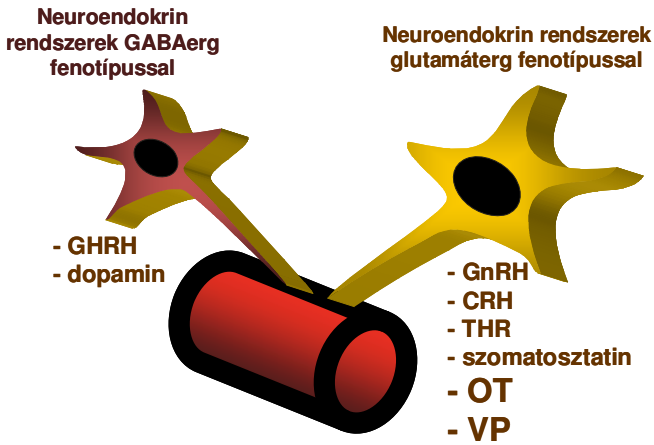

III. Ábra. Aminosav transzmitterek neuroszekretoros idegsejtekben

IV/4. 17β-ösztradiol kötését követő transzkripciós válaszok azonosítása a frontális agykéregben

A frontális agykéreg, mint ösztrogén célszerv teljes transzkriptomra kiterjedő microarray vizsgálatával az E2 által kiváltott génexpressziós válaszokat tanulmányoztuk. Először az egyszeri E2 injekció hatásait elemeztük ovariektomizált fiatal nőstény patkányokban (**19**). A humán menopauzát több szempontból is jobban közelítő állatmodellként, ezután bevezettük a középkorú ovariektomizált patkányok használatát. A kísérletben a krónikus hormonpótlási terápiát modellező, négyhetes infúziós E2 kezelés genomikus hatásait azonosítottuk (**22**).

Immuncitokémiai eredményeink szerint, mindkét nukleáris ösztrogén receptor altípus kimutatható a prefrontális agykéreg III-V. rétegeiben (**19/1. ábra**), jelezve, hogy az ösztrogének részben direkt módon hatnak a terület funkcióira.

Fiatal, ovariektomizált nőstény patkányok egyszeri E2 kezelését 24 órával követően, microarray vizsgálatainkban a frontális kérgi szövetblokk 136 génje mutatott a vivőanyaggal megkezelt állatokétól eltérő expressziót (szűrési feltételek: $P<0,05$; fold-change>1,5). 46 transzkriptum mennyisége nőtt a kezelés hatására. A megváltozott expressziójú gének közt (**19/1. és 2.** táblázatok) több neuropeptidet kódoló is előfordult (neurotenzin, cocaine- and amphetamine-regulated transcript, preproenkephalin). Az expressziós különbségeket válogatott esetekben RT-qPCR-rel is megerősítettük (**19/3. táblázat).** Több génválasz érintette a dopaminerg jelátvitelt (dopamin 1a receptor; adenozin A_{2A} receptor, „Regulator of G-protein signaling-9"), valamint a Ca^{++} szignalizáció elemeit (**19/3. ábra**). A változó gének közül a cocaine- and amphetamine-regulated transcript kérgi megoszlását *in situ* hibridizációval is megvizsgáltuk. A legintenzívebb hibridizációs jel a szomatoszenzoros kéreg IV. rétegében volt látható (**19/3. ábra**).

Az ovariektomizált, középkorú nőstény patkánymodell bevezetésével a tartósan alacsony ösztrogén szintnek kitett posztmenopauzális agy állapotát kívántuk pontosabban modellezni. A pótlásra használt E2 4-hetes *ip.* infúziója egyúttal a krónikus hormon pótlási terápia pontosabb modellezését is szolgálta. A krónikus kezelésre változást mutató transzkriptumok között ismét megjelentek neuropeptideket kódolók (neurotenzin, cocaine- and amphetamine-regulated transcript), valamint a dopaminerg jelátvitel molekuláris elemei (dopamin 1a és dopamin 2 receptorok, adenozin A2A receptor, „Regulator of G-protein signaling-9"; **22/2. táblázat**). Szembetűnő expressziós változást mutatott számos immunválasszal összefüggő gén, köztük a klasszikus komplement aktiválódási út egyes komponenseit (C3 and C4b), Fc receptorokat (Fcgr2a és Fcgr2b), és MHC class I és class II antigéneket kódolók **(22/2. táblázat**).

Megbeszélés

A menopauzát követő E2 szint csökkenés agykérgi és limbikus funkciók zavarához vezet (Keenan *et al.*, 2001; Adams & Morrison, 2003; Genazzani *et al.*, 2005; Morrison *et al.*, 2006). Számos kognitív, emocionális, figyelmi, motivációs és tanulási folyamat hanyatlását azon genomikus változások okozzák, melyek az agyszövet ösztrogén hiányos állapotában jelentkeznek. A fiatal, ovariektomizált nőstény patkányok egyszeri E2 kezelését használó génexpressziós tanulmányunk a frontális agykéreg E2-függő génjeit azonosította. A vizsgálat általában kismérvű, de igen nagyszámú ösztrogén-függő génválaszt mutatott ki (**19**). A microarray módszerrel azonosított transzkriptumok finomabb molekuláris és neuroanatómiai vizsgálata laboratóriumunkban folyamatban van.

A posztmenopauzális E2-hiányos agyi állapot pontosabb modellezésére a középkorú ovariektomizált patkánymodellt használtuk, melyben a 4-hetes *sc.* E2 infúzió transzkriptomra gyakorolt hatásait elemeztük. Remélhető, hogy a vizsgálatban azonosított génválaszok közelebb visznek az ösztrogén-hiányos agyi állapottal társuló funkciózavarok jobb megértéséhez, elősegítik egyes kóros állapotokat jelző biomarkerek azonosítását valamint

sikeres hormonpótlási stratégiák (Bohacek & Daniel, Sherwin, 2003) kidolgozását. Rágcsálókban az agykéregre gyakorolt genomiális hatásokért a domináns ER-β magreceptor típus lehet a felelős (Shughrue *et al.*, 1996; Shughrue *et al.*, 1997), felvetve annak lehetőségét, hogy a jótékony kérgi ösztrogén hatások ER-β szelektív agonista ligandumokkal is kiválthatóak. Távlatilag ilyen ER-β szelektív szerek használata hormonpótlásra kiküszöbölheti az ösztrogének - ER-α receptor által közvetített - proliferatív hatásait a méh és az emlő szöveteire, mely a hagyományos hormonpótlási stratégiák elterjedésének gátja (Nelson *et al.*, 2002; Beral, 2003).

V. ÖSSZEFOGLALÁS

Legfontosabb eredményeink összefoglalva:

A GnRH neuronok afferens szabályozására vonatkozóan, a következő új észleleteket tettük:

- Leírtuk ösztrogén receptor-α jelenlétét a tuberoinfundibuláris magkomplexum hisztaminerg sejtcsoportjaiban patkányban. Patkány és ember GnRH neuronjainak sejttestjén és dendritjein hisztaminerg idegvégződéseket azonosítottunk. Megmutattuk, hogy patkányban H1 receptor antagonistával kivédhető az exogén ösztrogén adással kiváltott LH surge. A vizsgálatsorozattal igazoltuk a centrális hisztaminerg rendszer részvételét a pozitív ösztrogén visszacsatolás mechanizmusában.
- Patkány GnRH idegsejtjein kolinerg idegvégződéseket mutattunk ki, melyek a nem-szinaptikus jelátvitelre jellemző, szinaptikus specializáció nélküli direkt kontaktusokat képeztek.
- Megállapítottuk, hogy a GnRH idegsejtek NPY tartalmú afferenseinek fele a nucleus arcuatusból származik, AGRP neuropeptidet tartalmaz, és GABAerg jelátvitelre utaló szimmetrikus szinapszist képez GnRH idegsejtekkel. A kontaktusokat létrehozó NPY tartamú rostok egynegyede az agytörzsi katekolaminerg rendszerekből származik és a noradrenerg rendszer marker enzimjét hordozza.
- Leírtuk a humán hipotalamusz kisspeptin neuronrendszerét, annak jelentős nemi dimorfizmusát, neurokinin B tartalmát és GnRH idegsejtekkel alkotott axo-szomatikus, axo-dendritikus és axo-axonális kapcsolatait. Azonosítottunk egy szexuálisan dimorf kisspeptin sejtcsoportot, mely csupán női hipotalamusz mintákban volt jelen, és elhelyezkedésében a rágcsálók - pozitív ösztrogén visszacsatolásában résztvevő - „RP3V"-beli kisspeptin sejtcsoportjával analóg.
- Morfológiai és elektrofiziológiai megközelítésekkel feltártunk egy GABAerg afferenseket gátló, retrográd endokannabinoid szignalizációs mechanizmust, mely szerepet játszik a GnRH idegsejt aktivitás fiziológiás gátló szabályozásában.

A "β" típusú ösztrogén receptor szerepét vizsgáló tanulmányok fontosabb új eredményei az alábbiak:

- Új *in situ* hibridizációs eljárást dolgoztunk ki, mely alkalmas alacsony kópiaszámú mRNS-ek igen érzékeny hisztokémiai kimutatására.
- ER-β mRNS, ösztrogén receptor ligandum kötés és nukleáris ER-β immunreaktivitás kimutatásával bizonyítottuk egy GnRH neuronokat direkt módon is befolyásolni képes ösztrogén visszacsatolási út létezését.
- Immuncitokémiai bizonyítékot szolgáltattunk az ER-β által közvetített, direkt ösztrogén visszacsatolás létezésére emberben.
- A GnRH-t termelő GT1-7 sejtvonalban microarray módszerrel számos 17β-ösztradiol által szabályozott gént és szignalizációs útvonalat azonosítottunk.

- Részletes anatómiai leírást adtunk az ER-β-t tartalmazó hipotalamikus oxitocin és vazopresszin idegsejt populációkról patkányban. Kimutattuk az ER-β jelenlétét a humán hipotalamusz magnocelluláris neuronjaiban is.

Új típusú glutamáterg mechanizmusok tanulmányozása az alábbi ismereteket hozta:

- Megállapítottuk, hogy a hipotalamusz glutamáterg (VGLUT2 fenotípusú) neuronjainak egy csoportja az eminentia mediana és a neurohipofízis vér-agy gát-mentes területeire vetít. Ilyen neuroendokrin glutamáterg idegsejtek főképp a PVN, az SON, a nucleus periventricularis, az OVLT és az MPOA területén találhatóak.
- Kettős-*in situ* hibridizáció és immuncitokémia használatával kimutattuk GnRH idegsejtekben a glutamáterg fenotípust bizonyító VGLUT2 jelenlétét.
- Leírtuk, hogy a GnRH idegsejtekéhez hasonló glutamáterg (VGLUT2) fenotípus jellemzi a hipofiziotrop TRH, CRH és szomatosztatin rendszereket, továbbá a magnocelluláris oxitocin és vazopresszin neuronokat is, míg a nucleus arcuatus GHRH idegsejtjei GABAergek.
- Kimutattuk, hogy az endokrin tengelyekre ható, nem-szinaptikus mechanizmusú glutamáterg hatások egy további helye az adenohipofízis, ahol a gonadotrop és tirotrop sejtek VGLUT2-t, míg a kortikotrop sejtek egy része VGLUT1-t tartalmaz.
- Igazoltuk, hogy a neuroszekretoros/szekretoros sejtek VGLUT2 expressziója több endokrin modellben is regulált. Sóterhelés a nucleus supraopticus vazopresszin neuronjaiban, míg a hypothyreoid állapot vagy a magas ösztrogén szint az adenohipofízisben fokozza a VGLUT2 mRNS expresszióját.

Az agykérgi ösztrogén szignalizáció élettanának és menopauzában jelentkező zavarainak megértését célzó microarray vizsgálataink eredményei a következők:

- Egyszeri E2 injekció frontális agykérgi transzkriptomra gyakorolt hatását ovariektomizált fiatal nőstény patkánymodellen vizsgálva, azonosítottunk számos ösztrogén-függő gént és jelátviteli utat. Kimutattuk több neuropeptidet kódoló, a dopaminerg jelátvitellel, valamint a kálcium szignalizációval összefüggő gén megváltozott expresszióját. A változások egy részét RT-qPCR módszerrel is megerősítettük.
- A humán menopauza rágcsáló modelljeként középkorú ovariektomizált patkányokat használtunk. A krónikus hormonpótlási terápiát négyhetes, *sc.* E2 infúzióval modelleztük. Megmutattuk, hogy a krónikus E2 kezelés hatására tartósan megváltozik több dopaminerg jelátvitellel összefüggő, immunrendszerrel kapcsolatos, és neuropeptidet kódoló gén expresszió.

VI. IRODALOM

VI/1 AZ ÉRTEKEZÉS ÁLTALÁNOS IRODALOMJEGYZÉKE

Abraham, I.M., Han, S.K., Todman, M.G., Korach, K.S. & Herbison, A.E. (2003) Estrogen receptor beta mediates rapid estrogen actions on gonadotropin-releasing hormone neurons in vivo. *J Neurosci*, **23**, 5771-5777.

Acosta, J.I., Mayer, L.P., Braden, B.B., Nonnenmacher, S., Mennenga, S.E. & Bimonte-Nelson, H.A. (2010) The cognitive effects of conjugated equine estrogens depend on whether menopause etiology is transitional or surgical. Endocrinology, 151, 3795-3804.

Adams, M.M. & Morrison, J.H. (2003) Estrogen and the aging hippocampal synapse. *Cereb Cortex*, **13**, 1271-1275.

Adams, T.E., Norman, R.L. & Spies, H.G. (1981) Gonadotropin-releasing hormone receptor binding and pituitary responsiveness in estradiol-primed monkeys. *Science*, **213**, 1388-1390.

Aiyer, M.S., Fink, G. & Greig, F. (1974) Changes in the sensitivity of the pituitary gland to luteinizing hormone releasing factor during the oestrous cycle of the rat. *J Endocrinol*, **60**, 47-64.

Arias, P., Jarry, H., Leonhardt, S., Moguilevsky, J.A. & Wuttke, W. (1993) Estradiol modulates the LH release response to N-methyl-D-aspartate in adult female rats: studies on hypothalamic luteinizing hormone-releasing hormone and neurotransmitter release. *Neuroendocrinology*, **57**, 710-715.

Asch, R.H., Smith, C.G., Siler-Khodr, T.M. & Pauerstein, C.J. (1981) Effects of delta 9-tetrahydrocannabinol during the follicular phase of the rhesus monkey (Macaca mulatta). *J Clin Endocrinol Metab*, **52**, 50-55.

Ayalon, D., Nir, I., Cordova, T., Bauminger, S., Puder, M., Naor, Z., Kashi, R., Zor, U., Harell, A. & Lindner, H.R. (1977) Acute effect of delta1-tetrahydrocannabinol on the hypothalamo-pituitary-ovarian axis in the rat. *Neuroendocrinology*, **23**, 31-42.

Baskin, D.G., Breininger, J.F. & Schwartz, M.W. (1999) Leptin receptor mRNA identifies a subpopulation of neuropeptide Y neurons activated by fasting in rat hypothalamus. *Diabetes*, **48**, 828-833.

Bauer-Dantoin, A.C., Urban, J.H. & Levine, J.E. (1992) Neuropeptide Y gene expression in the arcuate nucleus is increased during preovulatory luteinizing hormone surges. *Endocrinology*, **131**, 2953-2958.

Belchetz, P.E., Plant, T.M., Nakai, Y., Keogh, E.J. & Knobil, E. (1978) Hypophysial responses to continuous and intermittent delivery of hypopthalamic gonadotropin-releasing hormone. *Science*, **202**, 631-633.

Benedetti, W.L., Lozdziejsky, R., Sala, M.A., Monti, J.M. & Grino, E. (1969) Blockade of ovulation after atropine implants in the lateral hypothalamus of the rat. *Experientia*, **25**, 1158-1159.

Beral, V. (2003) Breast cancer and hormone-replacement therapy in the Million Women Study. *Lancet*, **362**, 419-427.

Berga, S.L. & Loucks, T.L. (2005) The diagnosis and treatment of stress-induced anovulation. *Minerva Ginecol*, **57**, 45-54.

Bhat, G.K., Mahesh, V.B., Chu, Z.W., Chorich, L.P., Zamorano, P.L. & Brann, D.W. (1995) Localization of the N-methyl-D-aspartate R1 receptor subunit in specific anterior pituitary hormone cell types of the female rat. *Neuroendocrinology*, **62**, 178-186.

Bhat, G.K., Mahesh, V.B., Ping, L., Chorich, L., Wiedmeier, V.T. & Brann, D.W. (1998) Opioid-glutamate-nitric oxide connection in the regulation of luteinizing hormone secretion in the rat. *Endocrinology*, **139**, 955-960.

Bohacek, J. & Daniel, J.M. The beneficial effects of estradiol on attentional processes are dependent on timing of treatment initiation following ovariectomy in middle-aged rats. *Psychoneuroendocrinology*, **35**, 694-705.

Bourguignon, J.P., Gerard, A., Mathieu, J., Simons, J. & Franchimont, P. (1989) Pulsatile release of gonadotropin-releasing hormone from hypothalamic explants is restrained by blockade of N-methyl-D,L-aspartate receptors. *Endocrinology*, **125**, 1090-1096.

Brann, D.W. (1995) Glutamate: a major excitatory transmitter in neuroendocrine regulation. *Neuroendocrinology*, **61**, 213-225.

Broberger, C., Johansen, J., Johansson, C., Schalling, M. & Hokfelt, T. (1998) The neuropeptide Y/agouti gene-related protein (AGRP) brain circuitry in normal, anorectic, and monosodium glutamate-treated mice. *Proc Natl Acad Sci U S A*, **95**, 15043-15048.

Burger, L.L., Dalkin, A.C., Aylor, K.W., Haisenleder, D.J. & Marshall, J.C. (2002) GnRH pulse frequency modulation of gonadotropin subunit gene transcription in normal gonadotropes-assessment by primary transcript assay provides evidence for roles of GnRH and follistatin. *Endocrinology*, **143**, 3243-3249.

Campbell, R.E., ffrench-Mullen, J.M., Cowley, M.A., Smith, M.S. & Grove, K.L. (2001) Hypothalamic circuitry of neuropeptide Y regulation of neuroendocrine function and food intake via the Y5 receptor subtype. *Neuroendocrinology*, **74**, 106-119.

Catt, K.J., Loumaye, E., Wynn, P.C., Iwashita, M., Hirota, K., Morgan, R.O. & Chang, J.P. (1985) GnRH receptors and actions in the control of reproductive function. *J Steroid Biochem*, **23**, 677-689.

Christian, C.A., Glidewell-Kenney, C., Jameson, J.L. & Moenter, S.M. (2008) Classical estrogen receptor alpha signaling mediates negative and positive feedback on gonadotropin-releasing hormone neuron firing. *Endocrinology*, **149**, 5328-5334.

Christian, C.A., Mobley, J.L. & Moenter, S.M. (2005) Diurnal and estradiol-dependent changes in gonadotropin-releasing hormone neuron firing activity. *Proc Natl Acad Sci U S A*, **102**, 15682-15687.

Christian, C.A., Pielecka-Fortuna, J. & Moenter, S.M. (2009) Estradiol suppresses glutamatergic transmission to gonadotropin-releasing hormone neurons in a model of negative feedback in mice. *Biol Reprod*, **80**, 1128-1135.

Chronwall, B.M., DiMaggio, D.A., Massari, V.J., Pickel, V.M., Ruggiero, D.A. & O'Donohue, T.L. (1985) The anatomy of neuropeptide-Y-containing neurons in rat brain. *Neuroscience*, **15**, 1159-1181.

Ciofi, P., Leroy, D. & Tramu, G. (2006) Sexual dimorphism in the organization of the rat hypothalamic infundibular area. *Neuroscience*, **141**, 1731-1745.

Clarkson, J. & Herbison, A.E. (2006) Postnatal development of kisspeptin neurons in mouse hypothalamus; sexual dimorphism and projections to gonadotropin-releasing hormone neurons. *Endocrinology*, **147**, 5817-5825.

Clifton, D.K. & Sawyer, C.H. (1979) LH release and ovulation in the rat following depletion of hypothalamic norepinephrine: chronic vs. acute effects. *Neuroendocrinology*, **28**, 442-449.

Coen, C.W. & Coombs, M.C. (1983) Effects of manipulating catecholamines on the incidence of the preovulatory surge of of luteinizing hormone and ovulation in the rat: evidence for a necessary involvement of hypothalamic adrenaline in the normal or 'midnight' surge. *Neuroscience*, **10**, 187-206.

Counis, R., Laverriere, J.N., Garrel, G., Bleux, C., Cohen-Tannoudji, J., Lerrant, Y., Kottler, M.L. & Magre, S. (2005) Gonadotropin-releasing hormone and the control of gonadotrope function. *Reproduction, nutrition, development*, **45**, 243-254.

Dalkin, A.C., Haisenleder, D.J., Ortolano, G.A., Ellis, T.R. & Marshall, J.C. (1989) The frequency of gonadotropin-releasing-hormone stimulation differentially regulates gonadotropin subunit messenger ribonucleic acid expression. *Endocrinology*, **125**, 917-924.

Dalterio, S., Steger, R., Peluso, J. & de Paolo, L. (1987) Acute delta 9-tetrahydrocannabinol exposure: effects on hypothalamic-pituitary-testicular activity in mice. *Pharmacol Biochem Behav*, **26**, 533-537.

De Cree, C. (1998) Sex steroid metabolism and menstrual irregularities in the exercising female. A review. *Sports Med*, **25**, 369-406.

de Roux, N., Genin, E., Carel, J.C., Matsuda, F., Chaussain, J.L. & Milgrom, E. (2003) Hypogonadotropic hypogonadism due to loss of function of the KiSS1-derived peptide receptor GPR54. *Proc Natl Acad Sci U S A*, **100**, 10972-10976.

DeFazio, R.A., Heger, S., Ojeda, S.R. & Moenter, S.M. (2002) Activation of A-type gamma-aminobutyric acid receptors excites gonadotropin-releasing hormone neurons. Mol Endocrinol, 16, 2872-2891.

DeFazio, R.A. & Moenter, S.M. (2002) Estradiol feedback alters potassium currents and firing properties of gonadotropin-releasing hormone neurons. *Mol Endocrinol*, **16**, 2255-2265.

Degroot, A., Kofalvi, A., Wade, M.R., Davis, R.J., Rodrigues, R.J., Rebola, N., Cunha, R.A. & Nomikos, G.G. (2006) CB1 receptor antagonism increases hippocampal acetylcholine release: site and mechanism of action. *Mol Pharmacol*, **70**, 1236-1245.

Devane, W.A., Hanus, L., Breuer, A., Pertwee, R.G., Stevenson, L.A., Griffin, G., Gibson, D., Mandelbaum, A., Etinger, A. & Mechoulam, R. (1992) Isolation and structure of a brain constituent that binds to the cannabinoid receptor. *Science*, **258**, 1946-1949.

Diano, S., Naftolin, F. & Horvath, T.L. (1998) Kainate glutamate receptors (GluR5-7) in the rat arcuate nucleus: relationship to tanycytes, astrocytes, neurons and gonadal steroid receptors. *J Neuroendocrinol*, **10**, 239-247.

Dumalska, I., Wu, M., Morozova, E., Liu, R., van den Pol, A. & Alreja, M. (2008) Excitatory effects of the puberty-initiating peptide kisspeptin and group I metabotropic glutamate receptor agonists differentiate two distinct subpopulations of gonadotropin-releasing hormone neurons. *J Neurosci*, **28**, 8003-8013.

Erickson, J.C., Hollopeter, G. & Palmiter, R.D. (1996) Attenuation of the obesity syndrome of ob/ob mice by the loss of neuropeptide Y. *Science*, **274**, 1704-1707.

Erickson, J.D., De Gois, S., Varoqui, H., Schafer, M.K. & Weihe, E. (2006) Activity-dependent regulation of vesicular glutamate and GABA transporters: a means to scale quantal size. *Neurochem Int*, **48**, 643-649.

Everett, J.W. (1964) Central Neural Control of Reproductive Functions of the Adenohypophysis. *Physiol Rev*, **44**, 373-431.

Everitt, B.J., Hokfelt, T., Terenius, L., Tatemoto, K., Mutt, V. & Goldstein, M. (1984) Differential co-existence of neuropeptide Y (NPY)-like immunoreactivity with catecholamines in the central nervous system of the rat. *Neuroscience*, **11**, 443-462.

Eyigor, O. & Jennes, L. (1998) Identification of kainate-preferring glutamate receptor subunit GluR7 mRNA and protein in the rat median eminence. *Brain Res*, **814**, 231-235.

Eyigor, O. & Jennes, L. (2000) Kainate receptor subunit-positive gonadotropin-releasing hormone neurons express c-Fos during the steroid-induced luteinizing hormone surge in the female rat. *Endocrinology*, **141**, 779-786.

Franceschini, I., Lomet, D., Cateau, M., Delsol, G., Tillet, Y. & Caraty, A. (2006) Kisspeptin immunoreactive cells of the ovine preoptic area and arcuate nucleus co-express estrogen receptor alpha. *Neurosci Lett*, **401**, 225-230.

Fukudome, Y., Ohno-Shosaku, T., Matsui, M., Omori, Y., Fukaya, M., Tsubokawa, H., Taketo, M.M., Watanabe, M., Manabe, T. & Kano, M. (2004) Two distinct classes of muscarinic action on hippocampal inhibitory synapses: M2-mediated direct suppression and M1/M3-mediated indirect suppression through endocannabinoid signalling. *The European Journal of Neuroscience*, **19**, 2682-2692.

Genazzani, A.R., Bernardi, F., Pluchino, N., Begliuomini, S., Lenzi, E., Casarosa, E. & Luisi, M. (2005) Endocrinology of menopausal transition and its brain implications. *CNS Spectr*, **10**, 449-457.

Gerdeman, G. & Lovinger, D.M. (2001) CB1 cannabinoid receptor inhibits synaptic release of glutamate in rat dorsolateral striatum. *J Neurophysiol*, **85**, 468-471.

Gillard, S.E., Tzaferis, J., Tsui, H.C. & Kingston, A.E. (2003) Expression of metabotropic glutamate receptors in rat meningeal and brain microvasculature and choroid plexus. *J Comp Neurol*, **461**, 317-332.

Goodman, R.L., Lehman, M.N., Smith, J.T., Coolen, L.M., de Oliveira, C.V., Jafarzadehshirazi, M.R., Pereira, A., Iqbal, J., Caraty, A., Ciofi, P. & Clarke, I.J. (2007) Kisspeptin neurons in the arcuate nucleus of the ewe express both dynorphin A and neurokinin B. *Endocrinology*, **148**, 5752-5760.

Gottsch, M.L., Cunningham, M.J., Smith, J.T., Popa, S.M., Acohido, B.V., Crowley, W.F., Seminara, S., Clifton, D.K. & Steiner, R.A. (2004) A role for kisspeptins in the regulation of gonadotropin secretion in the mouse. *Endocrinology*, **145**, 4073-4077.

Guran, T., Tolhurst, G., Bereket, A., Rocha, N., Porter, K., Turan, S., Gribble, F.M., Kotan, L.D., Akcay, T., Atay, Z., Canan, H., Serin, A., O'Rahilly, S., Reimann, F., Semple, R.K. & Topaloglu, A.K. (2009) Hypogonadotropic hypogonadism due to a novel missense mutation in the first extracellular loop of the neurokinin B receptor. *J Clin Endocrinol Metab*, **94**, 3633-3639.

Han, S.K., Gottsch, M.L., Lee, K.J., Popa, S.M., Smith, J.T., Jakawich, S.K., Clifton, D.K., Steiner, R.A. & Herbison, A.E. (2005) Activation of gonadotropin-releasing hormone neurons by kisspeptin as a neuroendocrine switch for the onset of puberty. *J Neurosci*, **25**, 11349-11356.

Hayashi, M., Yamada, H., Uehara, S., Morimoto, R., Muroyama, A., Yatsushiro, S., Takeda, J., Yamamoto, A. & Moriyama, Y. (2003) Secretory granule-mediated co-secretion of L-glutamate and glucagon triggers glutamatergic signal transmission in islets of Langerhans. *J Biol Chem*, **278**, 1966-1974.

Herbison, A.E. (1998) Multimodal influence of estrogen upon gonadotropin-releasing hormone neurons. *Endocr Rev*, **19**, 302-330.

Herbison, A.E. (2008) Estrogen positive feedback to gonadotropin-releasing hormone (GnRH) neurons in the rodent: the case for the rostral periventricular area of the third ventricle (RP3V). *Brain Res Rev*, **57**, 277-287.

Herbison, A.E. & Theodosis, D.T. (1992) Localization of oestrogen receptors in preoptic neurons containing neurotensin but not tyrosine hydroxylase, cholecystokinin or luteinizing hormone-releasing hormone in the male and female rat. *Neuroscience*, **50**, 283-298.

Herkenham, M., Lynn, A.B., de Costa, B.R. & Richfield, E.K. (1991) Neuronal localization of cannabinoid receptors in the basal ganglia of the rat. *Brain Res*, **547**, 267-274.

Herzog, E., Bellenchi, G.C., Gras, C., Bernard, V., Ravassard, P., Bedet, C., Gasnier, B., Giros, B. & El Mestikawy, S. (2001) The existence of a second vesicular glutamate transporter specifies subpopulations of glutamatergic neurons. *J Neurosci*, **21**, RC181.

Hoffman, A.F. & Lupica, C.R. (2000) Mechanisms of cannabinoid inhibition of GABA(A) synaptic transmission in the hippocampus. *J Neurosci*, **20**, 2470-2479.

Hokfelt, T., Broberger, C., Xu, Z.Q., Sergeyev, V., Ubink, R. & Diez, M. (2000) Neuropeptides--an overview. *Neuropharmacology*, **39**, 1337-1356.

Hokfelt, T., Elfvin, L.G., Elde, R., Schultzberg, M., Goldstein, M. & Luft, R. (1977) Occurrence of somatostatin-like immunoreactivity in some peripheral sympathetic noradrenergic neurons. *Proc Natl Acad Sci U S A*, **74**, 3587-3591.

Hrabovszky, E., Kallo, I., Hajszan, T., Shughrue, P.J., Merchenthaler, I. & Liposits, Z. (1998) Expression of estrogen receptor-beta messenger ribonucleic acid in oxytocin and vasopressin neurons of the rat supraoptic and paraventricular nuclei. *Endocrinology*, **139**, 2600-2604.

Irwig, M.S., Fraley, G.S., Smith, J.T., Acohido, B.V., Popa, S.M., Cunningham, M.J., Gottsch, M.L., Clifton, D.K. & Steiner, R.A. (2004) Kisspeptin activation of gonadotropin releasing hormone neurons and regulation of KiSS-1 mRNA in the male rat. *Neuroendocrinology*, **80**, 264-272.

Jarry, H., Leonhardt, S., Schwarze, T. & Wuttke, W. (1995) Preoptic rather than mediobasal hypothalamic amino acid neurotransmitter release regulates GnRH secretion during the estrogen-induced LH surge in the ovariectomized rat. *Neuroendocrinology*, **62**, 479-486.

Jennes, L., Jennes, M.E., Purvis, C. & Nees, M. (1992) c-fos expression in noradrenergic A2 neurons of the rat during the estrous cycle and after steroid hormone treatments. *Brain Res*, **586**, 171-175.

Jirikowski, G.F., Caldwell, J.D., Pedersen, C.A. & Stumpf, W.E. (1988) Estradiol influences oxytocin-immunoreactive brain systems. *Neuroscience*, **25**, 237-248.

Kalra, S.P. & Crowley, W.R. (1992) Neuropeptide Y: a novel neuroendocrine peptide in the control of pituitary hormone secretion, and its relation to luteinizing hormone. *Front Neuroendocrinol*, **13**, 1-46.

Karsch, F.J. & Foster, D.L. (1975) Sexual differentiation of the mechanism controlling the preovulatory discharge of luteinizing hormone in sheep. *Endocrinology*, **97**, 373-379.

Katona, I., Rancz, E.A., Acsady, L., Ledent, C., Mackie, K., Hajos, N. & Freund, T.F. (2001) Distribution of CB1 cannabinoid receptors in the amygdala and their role in the control of GABAergic transmission. *J Neurosci*, **21**, 9506-9518.

Katona, I., Sperlagh, B., Sik, A., Kafalvi, A., Vizi, E.S., Mackie, K. & Freund, T.F. (1999) Presynaptically located CB1 cannabinoid receptors regulate GABA release from axon terminals of specific hippocampal interneurons. *J Neurosci*, **19**, 4544-4558.

Kauffman, A.S., Gottsch, M.L., Roa, J., Byquist, A.C., Crown, A., Clifton, D.K., Hoffman, G.E., Steiner, R.A. & Tena-Sempere, M. (2007) Sexual differentiation of Kiss1 gene expression in the brain of the rat. *Endocrinology*, **148**, 1774-1783.

Kawakami, S. (2000) Glial and neuronal localization of ionotropic glutamate receptor subunit-immunoreactivities in the median eminence of female rats: GluR2/3 and GluR6/7 colocalize with vimentin, not with glial fibrillary acidic protein (GFAP). *Brain Res*, **858**, 198-204.

Kawakami, S., Ichikawa, M., Murahashi, K., Hirunagi, K., Tsukamura, H. & Maeda, K. (1998a) Excitatory amino acids act on the median eminence nerve terminals to induce gonadotropin-releasing hormone release in female rats. *Gen Comp Endocrinol*, **112**, 372-382.

Kawakami, S.I., Hirunagi, K., Ichikawa, M., Tsukamura, H. & Maeda, K.I. (1998b) Evidence for terminal regulation of GnRH release by excitatory amino acids in the median eminence in female rats: a dual immunoelectron microscopic study. *Endocrinology*, **139**, 1458-1461.

Keenan, P.A., Ezzat, W.H., Ginsburg, K. & Moore, G.J. (2001) Prefrontal cortex as the site of estrogen's effect on cognition. *Psychoneuroendocrinology*, **26**, 577-590.

Kinoshita, M., Tsukamura, H., Adachi, S., Matsui, H., Uenoyama, Y., Iwata, K., Yamada, S., Inoue, K., Ohtaki, T., Matsumoto, H. & Maeda, K. (2005) Involvement of central metastin in the regulation of preovulatory luteinizing hormone surge and estrous cyclicity in female rats. *Endocrinology*, **146**, 4431-4436.

Kiss, J., Kocsis, K., Csaki, A. & Halasz, B. (2003) Evidence for vesicular glutamate transporter synapses onto gonadotropin-releasing hormone and other neurons in the rat medial preoptic area. *Eur J Neurosci*, **18**, 3267-3278.

Kiyama, H., Sato, K. & Tohyama, M. (1993) Characteristic localization of non-NMDA type glutamate receptor subunits in the rat pituitary gland. *Brain Res Mol Brain Res*, **19**, 262-268.

Knobil, E. (1980) The neuroendocrine control of the menstrual cycle. *Recent progress in hormone research*, **36**, 53-88.

Knobil, E. (1990) The GnRH pulse generator. *Am J Obstet Gynecol*, **163**, 1721-1727.

Korach, K.S., Couse, J.F., Curtis, S.W., Washburn, T.F., Lindzey, J., Kimbro, K.S., Eddy, E.M., Migliaccio, S., Snedeker, S.M., Lubahn, D.B., Schomberg, D.W. & Smith, E.P. (1996) Estrogen receptor gene disruption: molecular characterization and experimental and clinical phenotypes. *Recent progress in hormone research*, **51**, 159-186; discussion 186-158.

Koutras, D.A. (1997) Disturbances of menstruation in thyroid disease. *Ann N Y Acad Sci*, **816**, 280-284.

Krajewski, S.J., Anderson, M.J., Iles-Shih, L., Chen, K.J., Urbanski, H.F. & Rance, N.E. (2005) Morphologic evidence that neurokinin B modulates gonadotropin-releasing hormone secretion via neurokinin 3 receptors in the rat median eminence. *J Comp Neurol*, **489**, 372-386.

Krizbai, I.A., Deli, M.A., Pestenacz, A., Siklos, L., Szabo, C.A., Andras, I. & Joo, F. (1998) Expression of glutamate receptors on cultured cerebral endothelial cells. *J Neurosci Res*, **54**, 814-819.

Krsmanovic, L.Z., Hu, L., Leung, P.K., Feng, H. & Catt, K.J. Pulsatile GnRH secretion: roles of G protein-coupled receptors, second messengers and ion channels. *Mol Cell Endocrinol*, **314**, 158-163.

Krsmanovic, L.Z., Stojilkovic, S.S. & Catt, K.J. (1996) Pulsatile gonadotropin-releasing hormone release and its regulation. *Trends Endocrinol Metab*, **7**, 56-59.

Kuiper, G.G., Enmark, E., Pelto-Huikko, M., Nilsson, S. & Gustafsson, J.A. (1996) Cloning of a novel receptor expressed in rat prostate and ovary. *Proc Natl Acad Sci U S A*, **93**, 5925-5930.

Laflamme, N., Nappi, R.E., Drolet, G., Labrie, C. & Rivest, S. (1998) Expression and neuropeptidergic characterization of estrogen receptors (ERalpha and ERbeta) throughout the rat brain: anatomical evidence of distinct roles of each subtype. *J Neurobiol*, **36**, 357-378.

Lehman, M.N. & Karsch, F.J. (1993) Do gonadotropin-releasing hormone, tyrosine hydroxylase-, and beta-endorphin-immunoreactive neurons contain estrogen receptors? A double-label immunocytochemical study in the Suffolk ewe. *Endocrinology*, **133**, 887-895.

Lehman, M.N. & Silverman, A.J. (1988) Ultrastructure of luteinizing hormone-releasing hormone (LHRH) neurons and their projections in the golden hamster. *Brain Res Bull*, **20**, 211-221.

Leranth, C., MacLusky, N.J., Sakamoto, H., Shanabrough, M. & Naftolin, F. (1985) Glutamic acid decarboxylase-containing axons synapse on LHRH neurons in the rat medial preoptic area. *Neuroendocrinology*, **40**, 536-539.

Li, C., Chen, P. & Smith, M.S. (1999) Morphological evidence for direct interaction between arcuate nucleus neuropeptide Y (NPY) neurons and gonadotropin-releasing hormone neurons and the possible involvement of NPY Y1 receptors. *Endocrinology*, **140**, 5382-5390.

Limonta, P., Montagnani Marelli, M. & Moretti, R.M. (2001) LHRH analogues as anticancer agents: pituitary and extrapituitary sites of action. *Expert Opin Investig Drugs*, **10**, 709-720.

Lin, W., McKinney, K., Liu, L., Lakhlani, S. & Jennes, L. (2003) Distribution of vesicular glutamate transporter-2 messenger ribonucleic Acid and protein in the septum-hypothalamus of the rat. *Endocrinology*, **144**, 662-670.

Liposits, Z., Merchenthaler, I., Wetsel, W.C., Reid, J.J., Mellon, P.L., Weiner, R.I. & Negro-Vilar, A. (1991) Morphological characterization of immortalized hypothalamic neurons synthesizing luteinizing hormone-releasing hormone. *Endocrinology*, **129**, 1575-1583.

Liposits, Z. & Setalo, G. (1980) Descending luteinizing hormone-releasing hormone (LH-RH) nerve fibers to the midbrain of the rat. *Neurosci Lett*, **20**, 1-4.

Liposits, Z., Setalo, G. & Flerko, B. (1984) Application of the silver-gold intensified 3,3'-diaminobenzidine chromogen to the light and electron microscopic detection of the luteinizing hormone-releasing hormone system of the rat brain. Neuroscience, 13, 513-525.

Livshits, A. & Seidman, D.S. (2009) Fertility issues in women with diabetes. *Womens Health (Lond Engl)*, **5**, 701-707.

Marshall, J.C. & Griffin, M.L. (1993) The role of changing pulse frequency in the regulation of ovulation. *Hum Reprod*, **8 Suppl 2**, 57-61.

Matagne, V., Lebrethon, M.C., Gerard, A. & Bourguignon, J.P. (2005) Kainate/estrogen receptor involvement in rapid estradiol effects in vitro and intracellular signaling pathways. *Endocrinology*, **146**, 2313-2323.

Matesic, D.F., Germak, J.A., Dupont, E. & Madhukar, B.V. (1993) Immortalized hypothalamic luteinizing hormone-releasing hormone neurons express a connexin 26-like protein and display functional gap junction coupling assayed by fluorescence recovery after photobleaching. *Neuroendocrinology*, **58**, 485-492.

Mechoulam, R., Ben-Shabat, S., Hanus, L., Ligumsky, M., Kaminski, N.E., Schatz, A.R., Gopher, A., Almog, S., Martin, B.R., Compton, D.R. & et al. (1995) Identification of an endogenous 2-monoglyceride, present in canine gut, that binds to cannabinoid receptors. *Biochem Pharmacol*, **50**, 83-90.

Meister, B. & Hokfelt, T. (1988) Peptide- and transmitter-containing neurons in the mediobasal hypothalamus and their relation to GABAergic systems: possible roles in control of prolactin and growth hormone secretion. *Synapse*, **2**, 585-605.

Meister, B., Hokfelt, T., Geffard, M. & Oertel, W. (1988) Glutamic acid decarboxylase- and gamma-aminobutyric acid-like immunoreactivities in corticotropin-releasing factor-containing parvocellular neurons of the hypothalamic paraventricular nucleus. *Neuroendocrinology*, **48**, 516-526.

Mellon, P.L., Windle, J.J., Goldsmith, P.C., Padula, C.A., Roberts, J.L. & Weiner, R.I. (1990) Immortalization of hypothalamic GnRH neurons by genetically targeted tumorigenesis. *Neuron*, **5**, 1-10.

Merchenthaler, I. (2005) Estrogen stimulates galanin expression within luteinizing hormone-releasing hormone-immunoreactive (LHRH-i) neurons via estrogen receptor-beta (ERbeta) in the female rat brain. *Neuropeptides*, **39**, 341-343.

Merchenthaler, I., Culler, M.D., Petrusz, P., Flerko, B. & Negro-Vilar, A. (1989) Immunocytochemical localization of the gonadotropin-releasing hormone-associated peptide portion of the LHRH precursor in the hypothalamus and extrahypothalamic regions of the rat central nervous system. *Cell Tissue Res*, **255**, 5-14.

Merchenthaler, I., Kovacs, G., Lavasz, G. & Setalo, G. (1980) The preoptico-infundibular LH-RH tract of the rat. *Brain Res*, **198**, 63-74.

Miller, C.A. & Golden, N.H. An introduction to eating disorders: clinical presentation, epidemiology, and prognosis. *Nutr Clin Pract*, **25**, 110-115.

Mitchner, N.A., Garlick, C. & Ben-Jonathan, N. (1998) Cellular distribution and gene regulation of estrogen receptors alpha and beta in the rat pituitary gland. *Endocrinology*, **139**, 3976-3983.

Moenter, S.M., Caraty, A. & Karsch, F.J. (1990) The estradiol-induced surge of gonadotropin-releasing hormone in the ewe. *Endocrinology*, **127**, 1375-1384.

Moenter, S.M., Chu, Z. & Christian, C.A. (2009) Neurobiological mechanisms underlying oestradiol negative and positive feedback regulation of gonadotrophin-releasing hormone neurones. *J Neuroendocrinol*, **21**, 327-333.

Moenter, S.M., DeFazio, A.R., Pitts, G.R. & Nunemaker, C.S. (2003) Mechanisms underlying episodic gonadotropin-releasing hormone secretion. *Front Neuroendocrinol*, **24**, 79-93.

Morrison, J.H., Brinton, R.D., Schmidt, P.J. & Gore, A.C. (2006) Estrogen, menopause, and the aging brain: how basic neuroscience can inform hormone therapy in women. *J Neurosci*, **26**, 10332-10348.

Mounzih, K., Lu, R. & Chehab, F.F. (1997) Leptin treatment rescues the sterility of genetically obese ob/ob males. *Endocrinology*, **138**, 1190-1193.

Navarro, V.M., Gottsch, M.L., Chavkin, C., Okamura, H., Clifton, D.K. & Steiner, R.A. (2009) Regulation of gonadotropin-releasing hormone secretion by kisspeptin/dynorphin/neurokinin B neurons in the arcuate nucleus of the mouse. *J Neurosci*, **29**, 11859-11866.

Negoro, H., Visessuwan, S. & Holland, R.C. (1973) Unit activity in the paraventricular nucleus of female rats at different stages of the reproductive cycle and after ovariectomy, with or without oestrogen or progesterone treatment. *J Endocrinol*, **59**, 545-558.

Nelson, H.D., Humphrey, L.L., Nygren, P., Teutsch, S.M. & Allan, J.D. (2002) Postmenopausal hormone replacement therapy: scientific review. *JAMA*, **288**, 872-881.

Noris, G., Hol, D., Clapp, C. & Martinez de la Escalera, G. (1995) Histamine directly stimulates gonadotropin-releasing hormone secretion from GT1-1 cells via H1 receptors coupled to phosphoinositide hydrolysis. *Endocrinology*, **136**, 2967-2974.

Oakley, A.E., Clifton, D.K. & Steiner, R.A. (2009) Kisspeptin signaling in the brain. *Endocr Rev*, **30**, 713-743.

Ohtsuka, S., Nishizaki, T., Tasaka, K., Miyake, A., Tanizawa, O., Yamatodani, A. & Wada, H. (1989) Estrogen stimulates gonadotropin-releasing hormone release from rat hypothalamus independently through catecholamine and histamine in vitro. *Acta Endocrinol (Copenh)*, **120**, 644-648.

Pagotto, U., Marsicano, G., Cota, D., Lutz, B. & Pasquali, R. (2006) The emerging role of the endocannabinoid system in endocrine regulation and energy balance. *Endocrine reviews*, **27**, 73-100.

Panula, P., Pirvola, U., Auvinen, S. & Airaksinen, M.S. (1989) Histamine-immunoreactive nerve fibers in the rat brain. *Neuroscience*, **28**, 585-610.

Panula, P., Yang, H.Y. & Costa, E. (1984) Histamine-containing neurons in the rat hypothalamus. *Proc Natl Acad Sci U S A*, **81**, 2572-2576.

Pau, K.Y., Berria, M., Hess, D.L. & Spies, H.G. (1993) Preovulatory gonadotropin-releasing hormone surge in ovarian-intact rhesus macaques. *Endocrinology*, **133**, 1650-1656.

Petersen, S. & McCrone, S. (1994) Characterization of the receptor complement of individual neurons using dual-label in situ hybridization histochemistry. In JH Eberwine, Valentino, K., Barchas, J. (eds) *In situ hybridization in neurobiology. Advances in methodology*. Oxford University Press, New York, pp. 78-94.

Petersen, S.L., Ottem, E.N. & Carpenter, C.D. (2003) Direct and indirect regulation of gonadotropin-releasing hormone neurons by estradiol. *Biol Reprod*, **69**, 1771-1778.

Pielecka-Fortuna, J., Chu, Z. & Moenter, S.M. (2008) Kisspeptin acts directly and indirectly to increase gonadotropin-releasing hormone neuron activity and its effects are modulated by estradiol. *Endocrinology*, **149**, 1979-1986.

Ping, L., Mahesh, V.B., Bhat, G.K. & Brann, D.W. (1997) Regulation of gonadotropin-releasing hormone and luteinizing hormone secretion by AMPA receptors. Evidence for a physiological role of AMPA receptors in the steroid-induced luteinizing hormone surge. *Neuroendocrinology*, **66**, 246-253.

Ping, L., Mahesh, V.B., Wiedmeier, V.T. & Brann, D.W. (1994) Release of glutamate and aspartate from the preoptic area during the progesterone-induced LH surge: in vivo microdialysis studies. *Neuroendocrinology*, **59**, 318-324.

Prevot, V., Bouret, S., Stefano, G.B. & Beauvillain, J. (2000) Median eminence nitric oxide signaling. *Brain Res Brain Res Rev*, **34**, 27-41.

Ramaswamy, S., Guerriero, K.A., Gibbs, R.B. & Plant, T.M. (2008) Structural interactions between kisspeptin and GnRH neurons in the mediobasal hypothalamus of the male rhesus monkey (Macaca mulatta) as revealed by double immunofluorescence and confocal microscopy. *Endocrinology*, **149**, 4387-4395.

Rance, N.E., McMullen, N.T., Smialek, J.E., Price, D.L. & Young, W.S., 3rd (1990) Postmenopausal hypertrophy of neurons expressing the estrogen receptor gene in the human hypothalamus. *J Clin Endocrinol Metab*, **71**, 79-85.

Rance, N.E., Young, W.S., 3rd & McMullen, N.T. (1994) Topography of neurons expressing luteinizing hormone-releasing hormone gene transcripts in the human hypothalamus and basal forebrain. *J Comp Neurol*, **339**, 573-586.

Revel, F.G., Masson-Pevet, M., Pevet, P., Mikkelsen, J.D. & Simonneaux, V. (2009) Melatonin controls seasonal breeding by a network of hypothalamic targets. *Neuroendocrinology*, **90**, 1-14.

Richardson, S.B., Prasad, J.A. & Hollander, C.S. (1982) Acetylcholine, melatonin, and potassium depolarization stimulate release of luteinizing hormone-releasing hormone from rat hypothalamus in vitro. *Proc Natl Acad Sci U S A*, **79**, 2686-2689.

Rometo, A.M., Krajewski, S.J., Voytko, M.L. & Rance, N.E. (2007) Hypertrophy and increased kisspeptin gene expression in the hypothalamic infundibular nucleus of postmenopausal women and ovariectomized monkeys. *J Clin Endocrinol Metab*, **92**, 2744-2750.

Sarkar, D.K., Chiappa, S.A., Fink, G. & Sherwood, N.M. (1976) Gonadotropin-releasing hormone surge in pro-oestrous rats. *Nature*, **264**, 461-463.

Saunders, P.T., Millar, M.R., Williams, K., Macpherson, S., Harkiss, D., Anderson, R.A., Orr, B., Groome, N.P., Scobie, G. & Fraser, H.M. (2000) Differential expression of estrogen receptor-alpha and -beta and androgen receptor in the ovaries of marmosets and humans. *Biol Reprod*, **63**, 1098-1105.

Sawchenko, P.E., Swanson, L.W., Grzanna, R., Howe, P.R., Bloom, S.R. & Polak, J.M. (1985) Colocalization of neuropeptide Y immunoreactivity in brainstem catecholaminergic neurons that project to the paraventricular nucleus of the hypothalamus. *J Comp Neurol*, **241**, 138-153.

Sawyer, C.H. (1955) Rhinencephalic involvement in pituitary activation by intraventricular histamine in the rabbit under nembutal anesthesia. *Am J Physiol*, **180**, 37-46.

Schwanzel-Fukuda, M. & Pfaff, D.W. (1990) The migration of luteinizing hormone-releasing hormone (LHRH) neurons from the medial olfactory placode into the medial basal forebrain. *Experientia*, **46**, 956-962.

Seminara, S.B., Messager, S., Chatzidaki, E.E., Thresher, R.R., Acierno, J.S., Jr., Shagoury, J.K., Bo-Abbas, Y., Kuohung, W., Schwinof, K.M., Hendrick, A.G., Zahn, D., Dixon, J., Kaiser, U.B., Slaugenhaupt, S.A., Gusella, J.F., O'Rahilly, S., Carlton, M.B., Crowley, W.F., Jr., Aparicio, S.A. & Colledge, W.H. (2003) The GPR54 gene as a regulator of puberty. *N Engl J Med*, **349**, 1614-1627.

Seminara, S.B., Oliveira, L.M., Beranova, M., Hayes, F.J. & Crowley, W.F., Jr. (2000) Genetics of hypogonadotropic hypogonadism. *J Endocrinol Invest*, **23**, 560-565.

Semple, R.K., Achermann, J.C., Ellery, J., Farooqi, I.S., Karet, F.E., Stanhope, R.G., O'Rahilly, S. & Aparicio, S.A. (2005) Two novel missense mutations in g protein-coupled receptor 54 in a patient with hypogonadotropic hypogonadism. *J Clin Endocrinol Metab*, **90**, 1849-1855.

Shahab, M., Mastronardi, C., Seminara, S.B., Crowley, W.F., Ojeda, S.R. & Plant, T.M. (2005) Increased hypothalamic GPR54 signaling: a potential mechanism for initiation of puberty in primates. *Proc Natl Acad Sci U S A*, **102**, 2129-2134.

Sherwin, B.B. (2003) Estrogen and cognitive functioning in women. *Endocr Rev*, **24**, 133-151.

Shivers, B.D., Harlan, R.E., Morrell, J.I. & Pfaff, D.W. (1983) Absence of oestradiol concentration in cell nuclei of LHRH-immunoreactive neurones. *Nature*, **304**, 345-347.

Shughrue, P.J., Komm, B. & Merchenthaler, I. (1996) The distribution of estrogen receptor-beta mRNA in the rat hypothalamus. *Steroids*, **61**, 678-681.

Shughrue, P.J., Lane, M.V. & Merchenthaler, I. (1997) Comparative distribution of estrogen receptor-alpha and -beta mRNA in the rat central nervous system. *J Comp Neurol*, **388**, 507-525.

Shughrue, P.J. & Merchenthaler, I. (2001) Distribution of estrogen receptor beta immunoreactivity in the rat central nervous system. *J Comp Neurol*, **436**, 64-81.

Simerly, R.B., Chang, C., Muramatsu, M. & Swanson, L.W. (1990) Distribution of androgen and estrogen receptor mRNA-containing cells in the rat brain: an in situ hybridization study. *J Comp Neurol*, **294**, 76-95.

Simonovic, I., Motta, M. & Martini, L. (1974) Acetylcholine and the release of the follicle-stimulating hormone-releasing factor. *Endocrinology*, **95**, 1373-1379.

Skowsky, W.R., Swan, L. & Smith, P. (1979) Effects of sex steroid hormones on arginine vasopressin in intact and castrated male and female rats. *Endocrinology*, **104**, 105-108.

Smith, C.G., Smith, M.T., Besch, N.F., Smith, R.G. & Asch, R.H. (1978) Effect of delta 9-tetrahydrocannabinol (THC) on female reproductive function. *Adv Biosci*, **22-23**, 449-467.

Smith, J.T., Clifton, D.K. & Steiner, R.A. (2006) Regulation of the neuroendocrine reproductive axis by kisspeptin-GPR54 signaling. *Reproduction (Cambridge, England)*, **131**, 623-630.

Sullivan, S.D., DeFazio, R.A. & Moenter, S.M. (2003) Metabolic regulation of fertility through presynaptic and postsynaptic signaling to gonadotropin-releasing hormone neurons. *J Neurosci*, **23**, 8578-8585.

Teles, M.G., Bianco, S.D., Brito, V.N., Trarbach, E.B., Kuohung, W., Xu, S., Seminara, S.B., Mendonca, B.B., Kaiser, U.B. & Latronico, A.C. (2008) A GPR54-activating mutation in a patient with central precocious puberty. *N Engl J Med*, **358**, 709-715.

Temple, J.L., Laing, E., Sunder, A. & Wray, S. (2004) Direct action of estradiol on gonadotropin-releasing hormone-1 neuronal activity via a transcription-dependent mechanism. *J Neurosci*, **24**, 6326-6333.

Terasawa, E. (1998) Cellular mechanism of pulsatile LHRH release. *Gen Comp Endocrinol*, **112**, 283-295.

Tobet, S.A., Chickering, T.W., King, J.C., Stopa, E.G., Kim, K., Kuo-Leblank, V. & Schwarting, G.A. (1996) Expression of gamma-aminobutyric acid and gonadotropin-releasing hormone during neuronal migration through the olfactory system. *Endocrinology*, **137**, 5415-5420.

Topaloglu, A.K., Reimann, F., Guclu, M., Yalin, A.S., Kotan, L.D., Porter, K.M., Serin, A., Mungan, N.O., Cook, J.R., Ozbek, M.N., Imamoglu, S., Akalin, N.S., Yuksel, B., O'Rahilly, S. & Semple, R.K. (2009) TAC3 and TACR3 mutations in familial hypogonadotropic hypogonadism reveal a key role for Neurokinin B in the central control of reproduction. *Nat Genet*, **41**, 354-358.

Tsuruo, Y., Kawano, H., Kagotani, Y., Hisano, S., Daikoku, S., Chihara, K., Zhang, T. & Yanaihara, N. (1990) Morphological evidence for neuronal regulation of luteinizing hormone-releasing hormone-containing neurons by neuropeptide Y in the rat septo-preoptic area. *Neurosci Lett*, **110**, 261-266.

Urbanski, H.F. & Ojeda, S.R. (1987) Activation of luteinizing hormone-releasing hormone release advances the onset of female puberty. *Neuroendocrinology*, **46**, 273-276.

van den Pol, A.N., Wuarin, J.P. & Dudek, F.E. (1990) Glutamate, the dominant excitatory transmitter in neuroendocrine regulation. *Science*, **250**, 1276-1278.

Van Tol, H.H., Bolwerk, E.L., Liu, B. & Burbach, J.P. (1988) Oxytocin and vasopressin gene expression in the hypothalamo-neurohypophyseal system of the rat during the estrous cycle, pregnancy, and lactation. *Endocrinology*, **122**, 945-951.

Vida, B., Deli, L., Hrabovszky, E., Kalamatianos, T., Caraty, A., Coen, C.W., Liposits, Z. & Kalló, I. (2010) Evidence for suprachiasmatic vasopressin neurons innervating kisspeptin neurons in the rostral periventricular area of the mouse brain: regulation by oestrogen. *(2010) J. Neuroendocrinol. (In press)*.

Vizi, E.S., Katona, I. & Freund, T.F. (2001) Evidence for presynaptic cannabinoid CB(1) receptor-mediated inhibition of noradrenaline release in the guinea pig lung. *Eur J Pharmacol*, **431**, 237-244.

Vizi, E.S. & Kiss, J.P. (1998) Neurochemistry and pharmacology of the major hippocampal transmitter systems: synaptic and nonsynaptic interactions. *Hippocampus*, **8**, 566-607.

Wang, H., Ward, A.R. & Morris, J.F. (1995) Oestradiol acutely stimulates exocytosis of oxytocin and vasopressin from dendrites and somata of hypothalamic magnocellular neurons. *Neuroscience*, **68**, 1179-1188.

Wenger, T., Rettori, V., Snyder, G.D., Dalterio, S. & McCann, S.M. (1987) Effects of delta-9-tetrahydrocannabinol on the hypothalamic-pituitary control of luteinizing hormone and follicle-stimulating hormone secretion in adult male rats. *Neuroendocrinology*, **46**, 488-493.

Wetsel, W.C., Valenca, M.M., Merchenthaler, I., Liposits, Z., Lopez, F.J., Weiner, R.I., Mellon, P.L. & Negro-Vilar, A. (1992) Intrinsic pulsatile secretory activity of immortalized luteinizing hormone-releasing hormone-secreting neurons. *Proc Natl Acad Sci U S A*, **89**, 4149-4153.

Wildt, L., Hausler, A., Marshall, G., Hutchison, J.S., Plant, T.M., Belchetz, P.E. & Knobil, E. (1981) Frequency and amplitude of gonadotropin-releasing hormone stimulation and gonadotropin secretion in the rhesus monkey. *Endocrinology*, **109**, 376-385.

Witkin, J.W. (1999) Synchronized neuronal networks: the GnRH system. *Microsc Res Tech*, **44**, 11-18.

Witkin, J.W. & Silverman, A.J. (1985) Synaptology of luteinizing hormone-releasing hormone neurons in rat preoptic area. *Peptides*, **6**, 263-271.

Wojcik, S.M., Rhee, J.S., Herzog, E., Sigler, A., Jahn, R., Takamori, S., Brose, N. & Rosenmund, C. (2004) An essential role for vesicular glutamate transporter 1 (VGLUT1) in postnatal development and control of quantal size. *Proc Natl Acad Sci U S A*, **101**, 7158-7163.

Wray, S., Grant, P. & Gainer, H. (1989) Evidence that cells expressing luteinizing hormone-releasing hormone mRNA in the mouse are derived from progenitor cells in the olfactory placode. *Proc Natl Acad Sci U S A*, **86**, 8132-8136.

Yin, W., Mendenhall, J.M., Bratton, S.B., Oung, T., Janssen, W.G., Morrison, J.H. & Gore, A.C. (2007) Novel localization of NMDA receptors within neuroendocrine gonadotropin-releasing hormone terminals. *Exp Biol Med (Maywood)*, **232**, 662-673.

Zhang, C., Bosch, M.A., Ronnekleiv, O.K. & Kelly, M.J. (2009) Gamma-aminobutyric acid B receptor mediated inhibition of gonadotropin-releasing hormone neurons is suppressed by kisspeptin-G protein-coupled receptor 54 signaling. *Endocrinology*, **150**, 2388-2394.

VI/2 AZ ÉRTEKEZÉS ALAPJÁUL SZOLGÁLÓ SAJÁT KÖZLEMÉNYEK JEGYZÉKE

(1) Fekete Cs., Strutton P.H., Cagampang F.R.A., **Hrabovszky E.,** Kalló I., Shughrue PJ., Dobó E., Mihály E., Baranyi L., Okada H., Panula P., Merchenthaler I., Coen C.W. and Liposits Zs. (1999): Estrogen receptor-immunoreactivity is present in the majority of central histaminergic neurons: evidence for a new neuroendocrine pathway associated with luteinizing hormone-releasing hormone-synthesising neurons in rats and humans. ***Endocrinology:*** 140:4335-4341

(2) **Hrabovszky E.**, Shughrue P.J, Merchenthaler I, Hajszán T, Liposits Zs, Carpenter C.D. and Petersen S.L. (2000): Detection of estrogen receptor-β messenger ribonucleic acid and ^{125}I [estrogen] binding sites in luteinizing hormone-releasing hormone neurons of the rat brain. ***Endocrinology:*** 141:3506-3509

(3) **Hrabovszky E.,** Steinhauser A., Barabás K., Shughrue P.J, Petersen S.L., Merchenthaler I. and Liposits Zs. (2001): Estrogen receptor-β immunoreactivity in luteinizing hormone-releasing hormone neurons of the rat brain. ***Endocrinology:*** 142:3261-3264

(4) **Hrabovszky E.** and Petersen S.L. (2002): Increased concentrations of radioisotopically-labeled complementary ribonucleic acid probe, dextran sulfate and dithiothreitol in the hybridization buffer can improve results of *in situ* hybridization histochemistry. ***J. Histochem. Cytochem.:*** 50:1389-1400

(5) Turi F.G., Liposits Zs., Moenter S.M., Fekete Cs. and **Hrabovszky E**. (2003): Origin of neuropeptide Y-containing afferents to gonadotropin-releasing hormone neurons in male mice. ***Endocrinology:*** 144:4967-4974

(6) **Hrabovszky E**., Kalló I., Steinhauser A., Merchenthaler I., Coen C.W.,. Petersen S.L. and Liposits Zs (2004): Estrogen receptor-β in oxytocin and vasopressin neurons of the rat and human hypothalamus. Immunocytochemical and *in situ* hybridization studies. ***J. Comp. Neurol.:*** 473: 315-333

(7) **Hrabovszky E**., Turi G.F., Kalló I. and Liposits Z. (2004): Expression of vesicular glutamate transporter-2 in gonadotropin-releasing hormone neurons of the adult male rat. ***Endocrinology:*** 145: 4018-4021

(8) **Hrabovszky E.,** Wittmann G., Turi G.F. Liposits Z. and Fekete C. (2005): Hypophysiotropic thyrotropin-releasing hormone and corticotropin-releasing hormone neurons of the rat contain vesicular glutamate transporter-2. ***Endocrinology:*** 146: 341-347

(9) **Hrabovszky E**., Turi G.F. Liposits Z. (2005): Presence of vesicular glutamate transporter-2 in hypophysiotropic somatostatin but not growth hormone-releasing hormone neurons of the male rat. ***Eur. J. Neurosci.:*** 21(8): 2120-2126

(10) **Hrabovszky E**., Csapó Á.K., Kalló I., Wilheim T., Túri G.F. and Liposits Zs. (2006): Localization and osmotic regulation of vesicular glutamate transporter-2 in magnocellular neurons of the rat hypothalamus. ***Neurochem. Int.:*** 48:753-761

(11) **Hrabovszky E**., Kalló I., Turi G.F., May K., Wittmann G., Fekete C. and Liposits Zs. (2006): Expression of vesicular glutamate transporter-2 in gonadotrope and thyrotrope cells of the rat pituitary. Regulation by estrogen and thyroid hormone status. ***Endocrinology:*** 147(8):3818-3825

(12) **Hrabovszky E**., Deli L., Turi G.F., Kalló I. and Liposits Zs. (2007): Glutamatergic innervation of the hypothalamic median eminence and posterior pituitary of the rat. ***Neuroscience:*** 144: 1383-1392

(13) Wittmann G., Deli L., Kalló I., **Hrabovszky E.**, Watanabe M., Liposits Zs. and Fekete C. (2007): Distribution of type 1 cannabinoid receptor (CB1) immunoreactive axons in the mouse hypothalamus. ***J. Comp. Neurol.:*** 503: 270-279

(14) **Hrabovszky E**. and Liposits Z. (2007) Glutamatergic phenotype of hypothalamic neurosecretory systems: a novel aspect of central neuroendocrine regulation. ***Clinical Neuroscience/Ideggyógyászati Szemle:*** 60: 177-181

(15) **Hrabovszky E**., kalló I., Szlávik N., Keller É., Merchenthaler I. and Liposits Zs. (2007) Gonadotropin-releasing hormone neurons express estrogen receptor-β. ***J. Clin. Endocr. Metab.:*** 92(7): 2827-2830

(16) Turi G.F., Liposits Z. and **Hrabovszky E.** (2008) Cholinergic afferents to gonadotropin-releasing hormone neurons of the rat. ***Neurochem. Int.:*** 52 (4-5):723-728

(17) **Hrabovszky E**. and Liposits Z. (2008) Novel aspects of glutamatergic signalling in the neuroendocrine system ***J. Neuroendocrinol.:*** 20 (6): 743-751

(18) Varju P., 1, Ken Chang, C.N. **Hrabovszky E**., Merchenthaler I. and Liposits Z. (2009) Temporal profile of estrogen-dependent gene expression in LHRH-producing GT1-7 cells. ***Neurochem. Int.:*** 54:(2) 119-134

(19) Sarvari M., **Hrabovszky E.,** Kallo I., Galamb O., Solymosi N., Liko I., Molnar B., Tihanyi K., Szombathelyi Z., Liposits Z. (2010) Gene expression profiling identifies key estradiol targets in the frontal cortex of the rat. ***Endocrinology:*** 151(3):1161-1176

(20) Kocsis Z.S., Molnár C.S., Watanabe, M., Daneels G., Moechars D., Liposits Z. and **Hrabovszky E**. (2010) Demonstration of vesicular glutamate transporter-1 in corticotroph cells in the anterior pituitary of the rat. ***Neurochem. Int.:*** 56(3):479-486

(21) **Hrabovszky E**., Ciofi P., Vida B., Horvath M.C., Keller É., Caraty A., Bloom S.R., Ghatei M.A., Dhillo W.S., Liposits Z. and Kallo I. (2010) The kisspeptin system of the human hypothalamus. Sexual dimorphism and relationship with gonadotropin-releasing hormone and neurokinin B neurons. ***Eur. J. Neurosci.:*** 31:1984-1998

(22) Sarvari M., Kallo I., **Hrabovszky E**., Solymosi N., Toth K., Likó I., Molnar B., Tihanyi K. and Liposits Z. (2010) Estradiol replacement alters expression of genes related to neurotransmission and immune surveillance in the frontal cortex of middle-aged ovariectomized rats. ***Endocrinology:*** 151: 3847-3862

(23) Farkas I., Kallo I., Deli L., Vida B., **Hrabovszky E.,** Fekete C., Moenter S.M., Watanabe M. and Liposits Z. (2010) Retrograde Endocannabinoid Signaling Reduces GABA-ergic Synaptic Transmission to Gonadotropin-Releasing Hormone Neurons. ***Endocrinology:*** (In press)

VI/3 A PHD FOKOZAT MEGSZERZÉSE ÓTA MEGJELENT EGYÉB SAJÁT KÖZLEMÉNYEK

(1) Wittman G., Sarkar S., **Hrabovszky E**., Liposits Z., Lechan R.M. and Fekete C. (2004): Galanin but not galanin-like peptide (GALP)-containing axon terminals innervate hypophysiotropic thyrotropin-releasing hormone (TRH)-synthesizing neurons in the hypothalamic paraventricular nucleus. ***Brain Res.:*** 1002: 43-50

(2) Kalamatianos T., van der Walt L., **Hrabovszky E.,** Kalló I., Marsh P., Bennett N.C. and Coen C.W. (2005): Characterization of gonadotrophin releasing hormone precursor cDNA in the old world mole-rat cryptomys hottentotus pretoriae: high homology with the new world guinea pig sequence. ***J. Neuroendocrinol.:*** 17(5): 265-268

(3) **Hrabovszky E**., Halász J., Meelis W., Kruk M.R., Liposits Z., Halász J. (2005): Neurochemical characterization of hypothalamic neurons involved in attack behavior: glutamatergic dominance and co-expression of thyrotropin-releasing hormone in a subset of glutamatergic neurons. ***Neuroscience:*** 133(3): 657-666

(4) Menyhért J., Wittmann G., **Hrabovszky E.,** Keller É., Liposits Zs. and Fekete Cs. (2006): Interconnection between orexigenic neuropeptide Y- and anorexigenic α-

melanocyte stimulating hormone-synthesizing neuronal systems of the human hypothalamus. ***Brain Res.:*** 1076(1):101-105

(5) Menyhért J., Wittmann G., **Hrabovszky E.,** Szlávik N., Keller É., Horváth T.L., Tschöp M.H., Liposits Zs. and Fekete Cs. (2006): Distribution of ghrelin-immunoreactive neuronal networks in the human hypothalamus. ***Brain Res.:*** 1125(1):31-36

(6) Halasz J., Toth M., Mikics E., **Hrabovszky E.,** Barsy B., Barsvari B. and Haller J. (2008): The effect of NK1 receptor blockade on territorial aggression and in a model of violent aggression. ***Biol. Psychiatry:*** 63(3): 271-278

(7) Kiss J., Halász, B., Csáki Á., Liposits Z. and **Hrabovszky E.** (2007) Vesicular glutamate transporter 2 protein and mRNA containing neurons in the hypothalamic suprachiasmatic nucleus of the rat. ***Brain Res. Bull.:*** 74: 397-405

(8) Kalló I., Jekkel C., **Hrabovszky E**., Jurányi Z., Vida B., Járási A., Wilheim T., Harsing L.G., Jr. and Liposits Z. (2007) Immunohistochemical and *in situ* hybridization studies on glycine transporter 1 after transient ischemia in the rat forebrain. ***Neurochem. Int.:*** 52 (4-5): 799-808

(9) Farkas I., Varju P., Szabo E., **Hrabovszky E**., Okada N., Okada H. and Liposits Z. (2008) Estrogen enhances expression of the complement C5a receptor and the C5a-agonist evoked calcium influx in hormone secreting neurons of the hypothalamus. ***Neurochem. Int.:*** 52 (4-5): 846-856

(10) Csercsik D., Farkas I., Szederkenyi G., **Hrabovszky E**., Liposits Z. and Hangos K. (2010) The Hodgkin-Huxley type modelling and parameter estimation of GnRH neurons. ***Biosystems:*** 100(3):198-207

(11) Vida B., **Hrabovszky E.,** Kalamatianos T., Coen C.W., Liposits Z. and Kalló I. (2008) Oestrogen receptor α and β in the suprachiasmatic nucleus of the male and female mice ***J. Neuroendocrinol.:*** 20(11): 1270-1277

(12) Vida B., Deli L., **Hrabovszky E.,** Kalamatianos T., Caraty A., Coen C.W., Liposits Z. and Kalló I. (2010) Evidence for suprachiasmatic vasopressin neurons innervating kisspeptin neurons in the rostral periventricular area of the mouse brain: regulation by oestrogen ***J. Neuroendocrinol.:*** 22(9):1032-1039

VII. KÖSZÖNETNYILVÁNÍTÁS

Kutatói pályám elindításáért és további támogatásáért Liposits Zsoltnak professzor úrnak szeretnék köszönetet mondani.

Az *in situ* hibridizációs módszer elsajátítására Sandra L. Petersen laboratóriumában töltött posztdoktori éveim során kaptam lehetőséget.

Hálás vagyok az Endokrin Neurobiológia Laboratórium valamennyi volt és jelenlegi tagjának az alkotó és pozitív szakmai légkör megteremtéséért, köztük Kalló Imre, Fekete Csaba, Gereben Balázs, Hajszán Tibor, Farkas Imre, Sárvári Miklós, Túri Gergely, Wittmann Gábor és Molnár Csilla kollégáimnak, továbbá a munkámat támogató, magas színvonalú asszisztensi segítségért Bekó Norbertnének. Munkakapcsolatom a Semmelweis Egyetem Igazságügyi Orvostani Intézetében Dr. Keller Éva professzor asszonnyal a humán szövettani vizsgálatok elvégzését tette lehetővé.

Szüleimnek köszönöm kitartó támogatásukat és szeretetüket.

1. számú melléklet

0013-7227/99/$03.00/0
Endocrinology

Vol. 140, No. 9
Printed in U.S.A.

Estrogen Receptor Immunoreactivity Is Present in the Majority of Central Histaminergic Neurons: Evidence for a New Neuroendocrine Pathway Associated with Luteinizing Hormone-Releasing Hormone-Synthesizing Neurons in Rats and Humans*

CS. FEKETE, P. H. STRUTTON, F. R. A. CAGAMPANG, E. HRABOVSZKY, I. KALLÓ, P. J. SHUGHRUE, E. DOBÓ, E. MIHÁLY, L. BARANYI, H. OKADA, P. PANULA, I. MERCHENTHALER, C. W. COEN, AND ZS. LIPOSITS

Institute of Experimental Medicine (Cs.F., E.H., Zs.L.), Hungarian Academy of Sciences, Budapest, Hungary; Biomedical Sciences Division (P.H.S., F.R.A.C., C.W.C.), King's College, London, United Kingdom; Department of Anatomy (I.K., E.D., E.M.), Albert Szent-Györgyi Medical University, Szeged, Hungary, The Women's Health Research Institute (P.J.S., I.M.), Wyeth-Ayerst Research, Radnor, Pennsylvania; Department of Molecular Biology (H.O.), Nagoya City University School of Medicine, Nagoya, Japan; Department of Biology (P.P.), Abo Akademi University, Turku, Finland; Department of Membrane Biochemistry (L.B.), Walter Reed Army Institute for Research, Washington D.C.

ABSTRACT

The central regulation of the preovulatory LH surge requires a complex sequence of interactions between neuronal systems that impinge on LH-releasing hormone (LHRH)-synthesizing neurons. The reported absence of estrogen receptors (ERs) in LHRH neurons indicates that estrogen-receptive neurons that are afferent to LHRH neurons are involved in mediating the effects of this steroid. We now present evidence indicating that central histaminergic neurons, exclusively located in the tuberomammillary complex of the caudal diencephalon, serve as an important relay in this system. Evaluation of this system revealed that 76% of histamine-synthesising neurons display ERα-immunoreactivity in their nucleus; furthermore histaminergic axons exhibit axo-dendritic and axo-somatic appositions onto LHRH neurons in both the rodent and the human brain. Our *in vivo* studies show that the intracerebroventricular administration of the histamine-1 (H1) receptor antagonist, mepyramine, but not the H2 receptor antagonist, ranitidine, can block the LH surge in ovariectomized estrogen-treated rats. These data are consistent with the hypothesis that the positive feedback effect of estrogen in the induction of the LH surge involves estrogen-receptive histamine-containing neurons in the tuberomammillary nucleus that relay the steroid signal to LHRH neurons via H1 receptors. (*Endocrinology* **140:** 4335–4341, 1999)

THE POSITIVE feedback effect of elevated plasma estradiol levels in proestrous animals initiates a surge of LH from the anterior pituitary gland, which is triggered by an increased discharge of LH-releasing hormone (LHRH) from nerve terminals in the median eminence into the hypophysial portal circulation (1). Although the LHRH secretion unequivocally depends on available estrogen levels, efforts to detect a significant uptake of estradiol (2) or estrogen receptor (ER) immunoreactivity (3–5) in LHRH neurons have been unsuccessful until very recently (see *Note Added in Proof*). Consequently, it has been assumed that the positive feedback effect of estrogen upon LHRH neurons is mediated by estrogen-sensitive interneurons. The neuronal circuits that relay information to LHRH neurons about the circulating levels of gonadal steroid hormones have been the subject of intensive investigation (1). Any candidate neurotransmitter system for mediating the feedback effects of estrogen on LHRH neurons must satisfy the criteria of (a) expressing ERs, (b) innervating LHRH neurons, and (c) exerting a regulatory influence upon LHRH neurons via specific neurotransmitter receptors.

In this report, we present data consistent with the hypothesis that the histaminergic neuronal system of the brain, the perikarya of which are confined to the tuberomammillary nuclear (TM) complex, provides an interneuron system capable of mediating the feedback effects of estrogen on LHRH neurons. This study was prompted by reports indicating (a) that administration of estrogen into the medium of perifused hypothalamic blocks stimulates the release of histamine (6), (b) that numerous histaminergic fibers project to the preoptico-septal area of the rat brain (7), the site at which most of the LHRH neurons are located in rats, (c) that histamine administered intracerebroventricularly stimulates ovulation in the rabbit (8), and (d) that an immortalized LHRH cell-line (GT1) expresses H1 receptors (9). The present studies demonstrate ERα-immunoreactivity in histamine-containing neurons, reveal the histaminergic pathway to LHRH neurons and provide *in vivo* pharmacological evidence concerning the

Received January 27, 1999.

Address all correspondence and requests for reprints to: Dr. Zsolt Liposits, Institute of Experimental Medicine, Hungarian Academy of Sciences, 1083 Budapest, Szigony u. 43, Hungary. E-mail: liposits@koki.hu.

* This study was supported by grants from National Science Foundation of Hungary (OTKA T0–16354 and F-22711), the BBSRC, the Wellcome Trust, the Royal Society, and NATO.

histamine receptor subtype involved in regulating the LHRH surge.

Materials and Methods

Tissue samples

Human brains. Diencephalic tissue samples were obtained from routine autopsies of five individuals (2 males and 3 females) whose clinical and pathological histories included neither neurological nor endocrine disturbances. The autopsy and tissue processing were carried out in accordance with the regulation and permission (No. 372) of the Ethics Board of the Albert Szent-Györgyi Medical University.

Rat brains. The animal experiments were performed on adult female Wistar rats that were ovariectomised bilaterally (day 0), treated with colchicine intracerebroventricularly (50 μg/100 g body wt.; day 14), and killed by transcardiac fixation (day 15) under Nembutal anesthesia (35 mg/kg). Each histological study detailed below comprised sections from 5 animals.

Immunocytochemical studies

Fixation

Human tissue. The diencephalic blocks were fixed by immersion, first in buffered 4% 1-ethyl-3(3-dimethylaminopropyl)-carbodiimide (EDCDI; Sigma Chemical Co.) (8 days), then in 4% formaldehyde (4 days).

Rat tissue. Following an initial flushing with 0.1 M PBS, the animals were perfused with 50 ml phosphate buffered 4% EDCDI. The brains were postfixed either in EDCDI (4 days) and then in 2% formaldehyde (1 day), or, for the purposes of estrogen receptor colocalization, in 4% formaldehyde (1 day).

Section preparation. Serial frozen sections were cut from the human and rat hypothalami at 30 μm and 20 μm thickness, respectively.

Immunocytochemical single-labeling. The detailed immunocytochemical protocol using the PAP technique has been published elsewhere (10).

Detection of histamine-containing neuronal elements. Sections including the rat TM complex were incubated with a polyclonal antiserum raised against histamine (1:25,000) (11). Preabsorption of the primary antiserum with the histamine-ovalbumin conjugate that was used for immunization abolished all the immunoreactivity.

Localization of estrogen receptor-immunoreactivity. ER-immunoreactive (IR) neurons of the TM were detected by three different polyclonal anti-ERα sera: AS409 rabbit antirat ERα (1:25,000) (12), 715 rabbit antirat ERα (1:1,000) (13) and ZS08–174 rabbit antihuman ERα (Zymed Laboratories, Inc., San Francisco, CA) (0.5 μg/ml). Nickel-3,3′-diaminobenzidine (Ni-DAB) was used as the chromogen in the peroxidase reaction; this was then silver-intensified (14). Preabsorption of ERα antibodies 715 and ZS08–174 with the corresponding synthetic ER peptides (1 μg/ml, overnight) resulted in loss of all immunoreactivity.

Immunocytochemical double-labeling. For the simultaneous detection of two antigens, a previously reported double-labeling technique was used (15). This utilizes the color difference between the DAB (*brown*) and silver-intensified Ni-DAB (*black*) reaction products.

Simultaneous detection of histamine-containing axons and LHRH neurons in human and rat hypothalami. At first, histamine immunoreactivity was detected by means of the PAP method with the silver-intensified Ni-DAB chromogen. Following incubation in monoclonal antibodies generated against LHRH (1:1,000) (16), the LHRH-IR neurons were visualized with the DAB reaction product. Some of the double-labeled sections from rats were embedded in Epon-resin for preparation of semithin sections.

Colocalization of ER and histamine in the tuberomammillary nucleus of the rat. The immunostained ERα-IR nuclei were identified by the *black* silver-intensified Ni-DAB chromogen, whereas the histamine-IR perikarya were detected with the *brown* DAB alone. In addition to mapping the distribution of ER- and histamine-immunoreactive neurons in the subnuclei (E_1–E_5) of the TM complex (17), the ratio of signal coexpression was also assessed by counting single- and double-labeled histamine-IR neurons. This analysis included every sixth section from serial samples taken through the posterior hypothalamus of three rats (16 sections from each animal). The data are presented as the mean ± SE (SEM).

Effects of H1 and H2 receptor antagonists on the LH surge: in vivo studies

Animals. Adult female Wistar rats (250–320 g) were maintained under controlled conditions (lights on from 0600 to 1800 h, dim red light from 1800 to 0600 h; temperature 21 ± 1 C). Food and water were available *ad libitum*. All animals were bilaterally ovariectomized; 7 days later an icv cannula (C313G; Plastics One, Roanoke, VA) was implanted into the lateral cerebral ventricle. After a further 3–4 days an iv cannula was implanted into the right atrium of the heart via the external jugular vein. This cannula was directed sc and passed into a cranial attachment, which allowed for the Luer lock fitting of a protective flexible metal coil (Instech Laboratories, Plymouth Meeting, PA). On the following day, each animal was given a sc injection of oestradiol benzoate (50 μg/0.2 ml arachis oil) at 1200 h (day 1 of the experiment). These experiments were undertaken in accordance with the UK Animals (Scientific Procedures) Act, 1986, and associated guidelines.

Experimental protocol. At 1000 h on the day of sampling (day 4 of the experiment), an icv injection cannula (C313I; Plastics One) was attached to the central channel of a dual channel swivel (Instech Laboratories); this cannula was filled with the drug or the vehicle and inserted into the icv guide cannula. The iv cannula was attached to the second channel of the swivel. Blood sampling commenced 3 h later at 1300 h; an automated sampling system was used to withdraw two 25-μl blood samples within a period of 5 min every 30 min for 12 h (from 1300 to 0100 h). The samples were stored at −20 C before RIA for LH. Pyrilamine maleate (mepyramine; Research Biochemicals International, Natick, MA) or ranitidine (RBI) was dissolved in 0.9% sterile saline at 100 nmol/30 μl. After an initial sampling period of 1 h, mepyramine or ranitidine or vehicle was infused icv at a rate of 0.5 μl/min for 6 h using a 250 μl gas tight microsyringe driven by a syringe pump.

RIA and statistical analysis. The whole blood LH concentrations were measured in a single RIA as described previously (18). Within group comparisons were made using one-way repeated measures ANOVA followed by the Tukey multiple comparison test; between group comparisons were made using the unpaired Student's *t* test.

Results

Colocalization of estrogen receptor- and histamine-immunoreactivity in the tuberomammillary nucleus

Histamine-immunoreactive (IR) neurons appeared in all of the five subgroups (E1–E5) of the tuberomammillary complex (Figs. 1b and 2, a–d), corroborating the results of previous immunocytochemical studies (11, 19). The largest population of these neurons was found in the E_2 subnucleus. Most histamine-IR neurons were multipolar; however, scattered, fusiform neurons were also observed. Neurons exhibiting ERα-IR nuclei were identified in all subgroups of the tuberomammillary complex, and they also occurred in other regions of the caudal hypothalamus, including the ventromedial, dorsomedial, arcuate, ventral premammillary, and lateral mammillary nuclei (Figs. 1a and 2, a–d). Immunostaining with three different ERα antibodies revealed a comparable distribution of ERα-IR nuclei. Using an immunocytochemical double-labeling method, we found that nuclear ERα immunoreactivity was present within the majority of histamine-IR perikarya (Figs. 1, c–d, and 2, a–d). In the double-labeled neurons, the cytoplasmic expression of his-

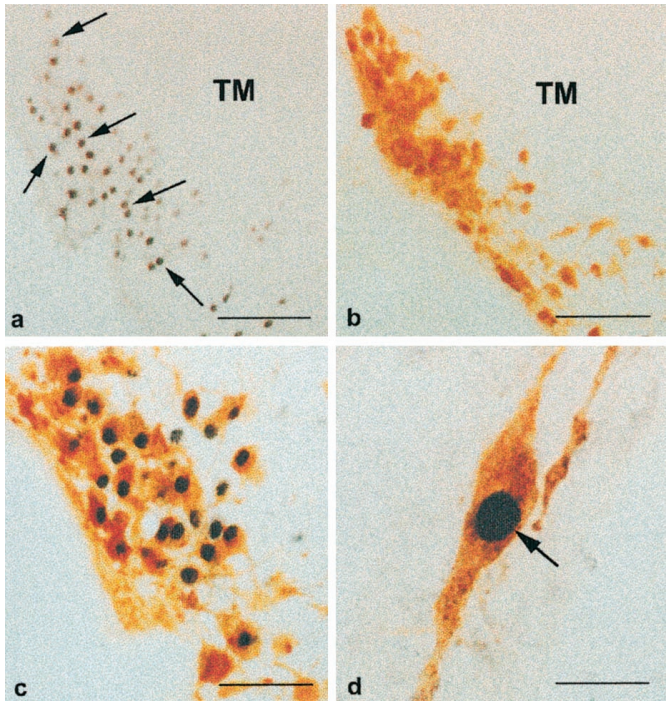

FIG. 1. Localization of ERα-IR and histamine-IR neurons in the TM of the rat. a, Neurons of the E_2-subnucleus possessing strong nuclear labeling (*arrows*) for ERs. b, Histamine-IR neurons clustered in the E_2-subnucleus of the TM. c, *Black* ERα-IR nuclei located within *brown* histamine-IR neurons. d, High power picture of a histamine-IR neuron displaying an ERα-IR nucleus (*arrow*). *Scale bar*: a–b, 150 μm; c, 75 μm; d, 25 μm.

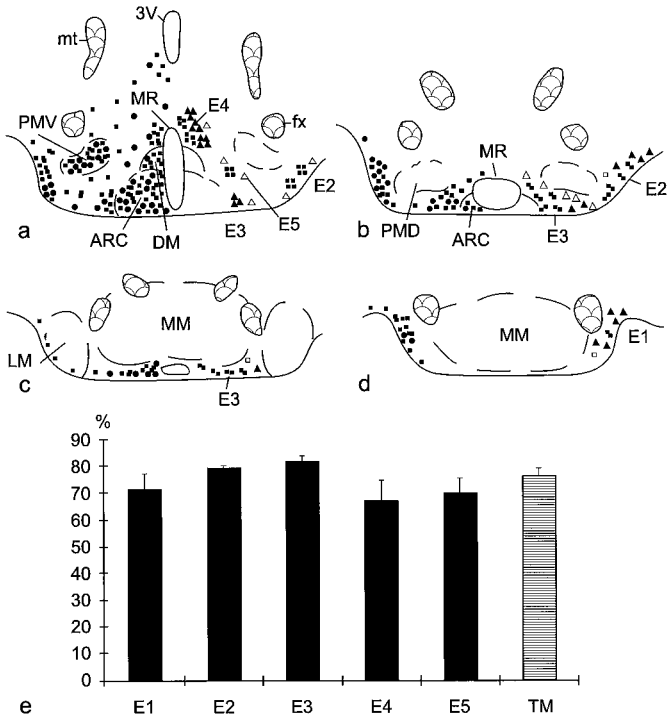

FIG. 2. Distribution of ERα-IR and histamine-IR neurons in the TM of the rat diencephalon. a–d, Schematic representation of coronal sections from the TM complex indicating the location of the five major histaminergic subnuclei (E_1–E_5). The *left half* of each figure depicts the distribution of ERα-IR neurons; the *right half* shows the pattern of colocalization for ERα and histamine. e, *Bar diagram* indicating the percentage of histamine-IR cells that coexpress ERα within the different subdivisions (E_1–E_5) of the TM. ●, ERα-positive cells; ▲, 1 ERα- + histamine-IR neuron; ■, 10 ERα- + histamine-IR neurons; △; 1 ERα-negative, histamine-positive neuron; □; 5 ERα-negative, histamine-positive neurons. Arc, Arcuate nucleus; DM, dorsomedial nucleus; E_1–E_5, subnuclei of the tuberomammillary nucleus; MM, medial mammillary nucleus; MR, mammillary recess; PMD, dorsal premammillary nucleus; PMV, ventral premammillary nucleus; 3V: 3rd ventricle.

tamine was clearly segregated from the ERα-immunoreactivity of the cell nuclei (Fig. 1, c and d). Analysis of the double-immunostained sections indicated ERα-immunoreactivity in 66–81% of the histamine-synthesizing neurons in the different subgroups of the tuberomammillary complex (Fig. 2e); the mean percentage of histaminergic neurons that were immunoreactive for ERα was 76 ± 3.2 (SEM).

Histaminergic innervation of LHRH neurons in the rat

In accordance with previous reports (7), a dense plexus of histamine-IR fibers was detected in the bed nucleus of stria terminalis, in the vicinity of the organum vasculosum of the lamina terminalis (OVLT), and along the vertical and horizontal limbs of the diagonal band of Broca. Our immunocytochemical double-labeling studies of the preoptic region revealed an intimate relationship between histamine-IR axons and LHRH-IR neurons (Fig. 3, a–b). Histaminergic axons approached LHRH neurons and exhibited axo-somatic (Fig. 3a) and axo-dendritic (Fig. 3b) appositions; 40 ± 2.3% of the LHRH neurons were apposed by histamine-IR axons.

Histaminergic innervation of LHRH neurons in the human

Immunocytochemical double-labeling techniques applied to human hypothalamic sections revealed LHRH-IR neurons embedded in a rich network of varicose histamine-IR axons in both the preoptic and the infundibular regions. Histamine-IR fibers were found to approach LHRH neurons and, in many instances, to be juxtaposed to their perikarya and dendrites (Fig. 3, c–d). Histaminergic axons winding around LHRH cells and exhibiting serial appositions (Fig. 3d) were also apparent. At least one juxtaposition with histamine-IR fibers was observed in association with 51 ± 3.0% of the LHRH neurons.

In vivo effects of H1- and H2-histaminergic receptor antagonists on the LH surge in rats

To elucidate the involvement of H1- and H2-histaminergic receptors in the regulation of the estrogen-induced LH surge *in vivo*, whole blood LH concentrations were monitored in ovariectomised estrogen-treated rats during intracerebroventricular (icv) infusion of an H1 or H2 receptor antagonist or the vehicle between 1400 and 2000 h. A significant rise in LH concentrations was observed in the animals ($P < 0.05$; Fig. 4, a–b) that received the vehicle. Infusion of the H1 antagonist, mepyramine, (100 nmol/h) prevented the occurrence of the estrogen-induced surge (Fig. 4a). In contrast, the surge remained unaffected (Fig. 4b) in the presence of the H2 antagonist, ranitidine (100 nmol/h). The treatments with

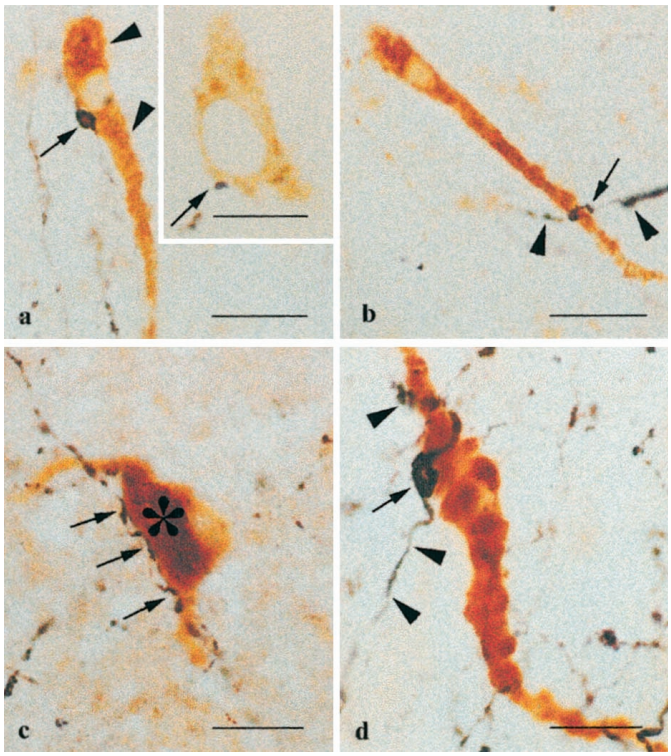

FIG. 3. Juxtapositions between the central histamine- and LHRH-immunoreactive (IR) systems of the rat (a, b) and human (c, d). a, *Black* histaminergic bouton (*arrow*) juxtaposed to a *brown*, LHRH-IR perikaryon (*arrowheads*) in the preoptic area; the *inset* shows a similar axo-somatic apposition (*arrow*) at higher power in a 1 μm thick specimen. b, Histamine-IR fiber (*arrowheads*) apposed (*arrow*) to the dendritic process of a fusiform LHRH neuron in the preoptic region. c, Histamine-IR axon forming multiple *en passant*-type appositions (*arrows*) with a multipolar LHRH cell (*asterisk*) located in the preoptic area of the human brain. d, A histamine-IR axon (*arrowheads*) making an axo-somatic apposition (*arrow*) with a fusiform LHRH neuron located in the human infundibular nucleus. *Scale bar*: a–d, 20 μm; *inset*, 10 μm.

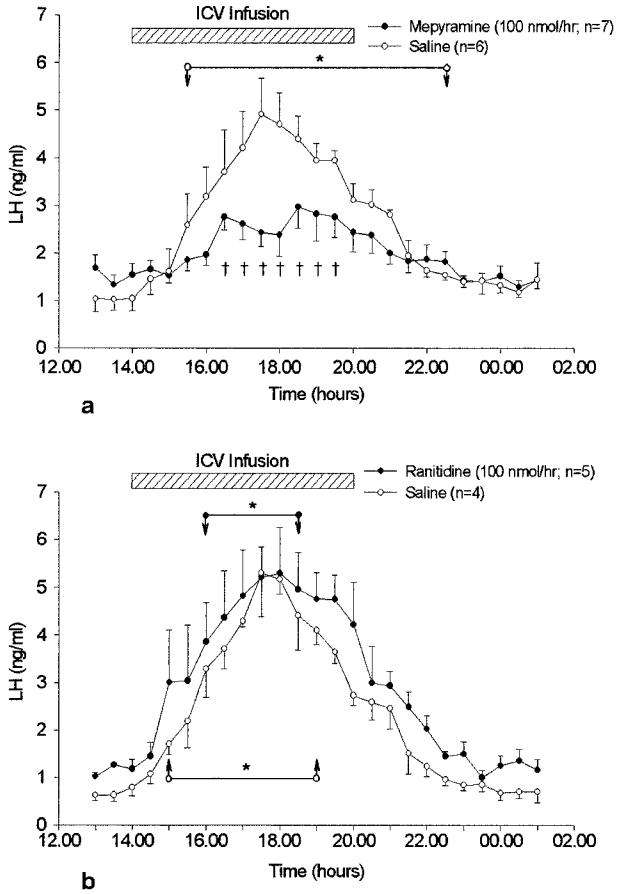

FIG. 4. Mean (±SEM) whole blood LH concentrations in ovariectomized rats at times indicated on day 4 following sc treatment with 50 μg estradiol benzoate at 1200 h on day 1. Animals were given an intracerebroventricular infusion between 14.00 and 20.00h of (a) the H1 receptor antagonist mepyramine (100 nmol/30 μl/h) or (b) the H2 receptor antagonist ranitidine (100 nmol/30 μl/h) or the vehicle (30 μl/h) in concurrently treated control groups. *, $P < 0.05$ with respect to the level at 1300 h within the same group. †, $P < 0.05$ with respect to the concurrent level in the vehicle-treated group.

mepyramine or ranitidine were not associated with any apparent changes in the behavior of the animals.

Discussion

The results of the present studies are consistent with the hypothesis that one of the routes by which estrogen influences LHRH neurons involves the central histaminergic system and that this action, in the context of the LH surge, is restricted to H1 receptors. It has been previously demonstrated that the release of histamine *in vitro* from the perifused mediobasal hypothalamus can be stimulated by estradiol (6). The possibility that this steroid has direct actions on histamine-containing neurons is indicated by the present discovery of ERα-immunoreactivity in 76% of these cells. The pioneering work of Pfaff and Keiner (20) demonstrated estradiol uptake in the lateral mammillary region with a distribution that is comparable to the immunocytochemical map of ERα-IR cells in the E_2 and E_3 subgroups of the TM presented here. The estrogen receptor antisera used in our work have been widely used for the visualization of the classical estrogen receptor ERα. Recently, a novel type of estrogen receptor, ERβ has been cloned (21); the messenger RNA (mRNA) for this receptor has been detected in various regions of the rat brain including the TM (22, 23). Consequently, the role of ERβ in mediating estrogenic effects within the TM merits attention in further studies. Whether ERβ is present in the histaminergic neurons remains to be determined.

Histamine was first implicated in the regulation of gonadotropin secretion with the discovery that it was capable of inducing ovulation when injected intracerebroventricularly into pentobarbital anaesthetised rabbits (8). It was subsequently shown that this amine stimulates LHRH and LH secretion from an *in vitro* preparation containing the medial basal hypothalamus and pituitary of female rats (24); this stimulatory effect can also be achieved using an H1 but not an H2 agonist and can be blocked by an H1 antagonist (24). In contrast, *in vitro* studies on tissues taken from male rats have reported that histamine is without effect not only on LH release when the pituitary is perifused alone (24) but also on LHRH release from the mediobasal hypothalamus (25). A permissive role for estrogen in the stimulatory action of

histamine on LH is suggested by the discovery that the central administration of this amine stimulates LH release in rats on the day of proestrus; no such effect was observed on other days of the estrous cycle or in male rats (26). Other studies have shown that intracerebroventricular histamine stimulates LH release in ovariectomized rats treated with a relatively high dose of estrogen and progesterone (27, 28) but not in orchidectomized rats following the same steroid treatment (28); only a weak stimulatory effect has been observed in the presence of a lower dose of estrogen (29). Our present observation of histaminergic fibers apposed to the perikarya and dendrites of LHRH neurons in both the rat and the human suggests that the effects of histamine on LH secretion may include direct actions on the LHRH neurons. This does not, however, exclude additional sites of interaction; an axo-axonic-type regulation might also occur at the level of the median eminence where scattered histaminergic fibers are found (30).

It should be noted that the method of postfixation used in this study was developed in our laboratory to optimize the detection of histamine-IR axons while retaining immunoreactivity for the other products examined. By using this procedure, we were able to demonstrate for the first time the relationship between histaminergic axons and an immunocytochemically characterized population of neurons (*i.e.* LHRH neurons in the rat and human brain). The requirements of our double-label immunohistochemistry were satisfied by postfixing the tissues in EDCDI over 4 or 8 days (for rat and human tissue, respectively) before the paraformaldehyde treatment; because this procedure provided poor membrane preservation, it was not appropriate to investigate the material at the electron microscopic level. Alternative methods will be required to establish whether the appositions identified in this study involve synaptic specializations or, alternatively, whether locally released histamine can affect the LHRH neurons via extrasynaptically located receptors.

The *in vivo* pharmacological data presented here demonstrate that central treatment with an antagonist against H1 but not H2 receptors blocks the estrogen-induced LH surge in rats. This study was designed to assess the involvement of these receptors in the spontaneous surge while minimizing the nonspecific disturbances that can affect its timing, amplitude, and occurrence. The drug- and vehicle-treated groups were sampled concurrently and received the intracerebroventricular infusion via a syringe pump located outside the cage; furthermore, the use of an automated blood sampling system permitted the frequent withdrawal of small blood samples (25 μl) with minimal stress to the animals. The discovery that the LH surge can be suppressed by mepyramine suggests that the histaminergic fibers that exhibit multiple appositions onto LHRH neurons may exert their effects via H1 receptors. This notion is supported by recent evidence (9) showing that H1 receptors are expressed in GT-1 cells, a cell line derived from LHRH-producing neurons (31). Furthermore, it has been found that the stimulation by estrogen of LHRH release from the hypothalamus *in vitro* can be blocked by an H1 but not an H2 antagonist (24).

The positive feedback actions of estrogen upon LHRH neurons are likely to operate via more than a single estrogen-sensitive neuronal system. Considerable evidence indicates that estrogen has potent regulatory effects on GABA transmission in the medial preoptic area and that changes in GABA-ergic tone in this region contribute to the induction of the LH surge (32–34). Within the context of the present study the evidence that all histaminergic neurons also contain GABA (35) may be highly significant; nevertheless, the region of the preoptic area in which the LHRH cells are located is also densely populated with GABA-ergic neurons (34). Additional neurotransmitter systems that have been implicated in the positive feedback action of estrogen include the central noradrenergic and adrenergic systems (36–39). Other systems that might mediate the effects of estrogen on LHRH neurons include those employing neuropeptide-Y and substance P; both have been shown to innervate LHRH neurons and to express estrogen receptors (40–43). In contrast to the various neuronal systems that are already recognized as potential sites for the action of estrogen in the context of LHRH regulation, the histaminergic neurons are not only concentrated in a particularly circumscribed part of the brain but also show a very high incidence (76%) of ERα-immunoreactivity.

Our understanding of the mechanisms underlying the positive feedback actions of estrogen in the human brain is limited. As in the case of several other species, morphological data indicate that human LHRH neurons do not express estrogen receptors (44). Among the neurotransmitters/modulators that might regulate human LHRH neurons via afferent connections neuropeptide Y (45), catecholamines (46), and substance P (47) have been implicated by double-label immunocytochemistry. The present study has revealed that histamine-IR fibres form close appositions with human LHRH neurons. Our current understanding of the role of histamine in the regulation of LH release in humans is restricted to a series of studies that predominantly involved H2 antagonists administered peripherally (48–55); no H2 receptor-specific effects on circulating levels of LH have been demonstrated. In contrast, the reported effects of H1 antagonists include the suppression of LH in women and its elevation in men (50); paradoxically, comparable sex-dependent effects were achieved with peripherally administered histamine (50). Nevertheless, the H1 antagonist employed in another study (49) was without effect on LH levels in either sex. It should be noted that research designed to assess histamine involvement in the regulation of either the LH surge or LH pulses in humans remains to be undertaken.

In summary, the morphological and functional data presented here demonstrate that (a) the majority of histamine-IR neurons within the tuberomammillary nuclear complex exhibit ERα immunoreactivity in their cell nucleus, (b) histamine-IR neurons of the TM exhibit axo-dendritic and axo-somatic appositions onto LHRH neurons in both rats and humans; and (c) intracerebroventricular administration of the H1 receptor antagonist, mepyramine, but not the H2 receptor antagonist, ranitidine, can block the LH surge induced by estrogen in ovariectomized rats. These data indicate that the positive feedback effect of estradiol on the preovulatory LH surge may involve estrogen-receptive histamine-containing neurons within the TM that relay their steroid-influenced signal to LHRH neurons via H1 receptors.

Acknowledgments

The authors would like to express their appreciation to Dr. S. Hayashi for the generous gift of the ER antibody (AS409), and to Dr. H. F. Urbanski for the kind donation of the monoclonal LHRH antibodies. We also thank A. Kobolák for her valuable technical assistance.

Note Added in Proof

During the editorial processing of this paper, a report was published showing that 17% of the LHRH neurons are immunoreactive for ER-α in the rat. (Butler J, Sjöberg M, Coen CW 1999 Evidence for estrogen receptor α immunoreactivity in gonadotropin-releasing hormone expressing neurons. J Neuroendocrinol 11:331–335).

References

1. **Freeman ME** 1994 The neuroendocrine control of the ovarian cycle of the rat. In: Knobil E, Neill JD (eds) The Physiology of Reproduction. Raven Press, New York, vol 2:613–658
2. **Shivers BD, Harlan RE, Morrell JI, Pfaff DW** 1983 Absence of oestradiol concentration in cell nuclei of LHRH-immunoreactive neurones. Nature 304:345–347
3. **Herbison AE, Theodosis DT** 1992 Localization of oestrogen receptors in preoptic neurons containing neurotensin but not tyrosine hydroxylase, cholecystokinin or luteinizing hormone-releasing hormone in the male and female rat. Neuroscience 50:283–298
4. **Lehman MN, Karsch FJ** 1993 Do gonadotropin-releasing hormone, tyrosine hydroxylase-, and β-endorphin-immunoreactive neurons contain estrogen receptors? A double-label immunocytochemical study in the Suffolk ewe. Endocrinology 133:887–895
5. **Sullivan KA, Witkin JW, Ferin M, Silverman AJ** 1995 Gonadotropin-releasing hormone neurons in the rhesus macaque are not immunoreactive for the estrogen receptor. Brain Res 685:198–200
6. **Ohtsuka S, Nishizaki T, Tasaka K, Miyake A, Tanizawa O, Yamatodani A, Wada H** 1989 Estrogen stimulates gonadotropin-releasing hormone release from rat hypothalamus independently through catecholamine and histamine *in vitro*. Acta Endocrinol (Copenh) 120:644–648
7. **Panula P, Pirvola U, Auvinen S, Airaksinen MS** 1989 Histamine-immunoreactive nerve fibers in the rat brain. Neuroscience 28:585–610
8. **Sawyer CH** 1955 Rhinencephalic involvement in pituitary activation by intraventricular histamine in the rabbit under nembutal anesthesia. Am J Physiol 205:37–46
9. **Noris G, Hol D, Clapp C, Martinez de la Escalera G** 1995 Histamine directly stimulates gonadotropin-releasing hormone secretion from GT1–1 cells via H1 receptors coupled to phosphoinositide hydrolysis. Endocrinology 136:2967–2974
10. **Liposits Z, Sétáló G, Flerkó B** 1984 Application of the silver-gold intensified 3,3′-diaminobenzidine chromogen to the light and electron microscopic detection of the luteinizing hormone-releasing hormone system of the rat brain. Neuroscience 13:513–525
11. **Panula P, Yang HY, Costa E** 1984 Histamine-containing neurons in the rat hypothalamus. Proc Natl Acad Sci USA 81:2572–2576
12. **Okamura H, Yamamoto K, Hayashi S, Kuroiwa A, Muramatsu M** 1992 A polyclonal antibody to the rat oestrogen receptor expressed in *Escherichia coli*: characterization and application to immunohistochemistry. J Endocrinol 135:333–341
13. **Furlow JD, Ahrens H, Mueller GC, Gorski J** 1990 Antisera to a synthetic peptide recognize native and denatured rat estrogen receptors. Endocrinology 127:1028–1032
14. **Liposits Z, Kalló I, Coen CW, Paull WK, Flerkó B** 1990 Ultrastructural analysis of estrogen receptor immunoreactive neurons in the medial preoptic area of the female rat brain. Histochemistry 93:233–239
15. **Liposits Z, Sherman D, Phelix C, Paull WK** 1986 A combined light and electron microscopic immunocytochemical method for the simultaneous localization of multiple tissue antigens. Tyrosine hydroxylase immunoreactive innervation of corticotropin releasing factor synthesizing neurons in the paraventricular nucleus of the rat. Histochemistry 85:95–106
16. **Urbanski HF** 1991 Monoclonal antibodies to luteinizing hormone-releasing hormone: production, characterization, and immunocytochemical application. Biol Reprod 44:681–686
17. **Inagaki N, Toda K, Taniuchi I, Panula P, Yamatodani A, Tohyama M, Watanabe T, Wada H** 1990 An analysis of histaminergic efferents of the tuberomammillary nucleus to the medial preoptic area and inferior colliculus of the rat. Exp Brain Res 80:374–380
18. **Strutton PH, Coen CW** 1996 Sodium pentobarbitone and the suppression of luteinizing hormone pulses in the female rat: the role of hypothermia. J Neuroendocrinol 8:941–946
19. **Watanabe T, Taguchi Y, Shiosaka S, Tanaka J, Kubota H, Terano Y, Tohyama M, Wada H** 1984 Distribution of the histaminergic neuron system in the central nervous system of rats; a fluorescent immunohistochemical analysis with histidine decarboxylase as a marker. Brain Res 295:13–25
20. **Pfaff D, Keiner M** 1973 Atlas of estradiol-concentrating cells in the central nervous system of the female rat. J Comp Neurol 151:121–158
21. **Kuiper G, Enmark E, Pelto-Huiko M, Nilsson S, Gustafsson J-A** 1996 Cloning of a novel estrogen receptor expressed in rat prostate and ovary. Proc Natl Acad Sci USA 93:5925–5930
22. **Shughrue PJ, Komm B, Merchenthaler I** 1996 The distribution of estrogen receptor-β mRNA in the rat hypothalamus. Steroids 61:678–681
23. **Shughrue PJ, Lane MV, Merchenthaler I** 1997 Comparative distribution of estrogen receptor-α and β mRNA in the rat central nervous system. J Comp Neurol 388:507–525
24. **Miyake A, Ohtsuka S, Nishizaki T, Tasaka K, Aono T, Tanizawa O, Yamatodani A, Watanabe T, Wada H** 1987 Involvement of H1 histamine receptor in basal and estrogen-stimulated luteinizing hormone-releasing hormone secretion in rats in vitro. Neuroendocrinology. 45:191–196
25. **Charli JL, Rotszejn WH, Pattou E, Kordon C** 1978 Effect of neurotransmitters on in *vitro* release of luteinizing-hormone-releasing hormone from the mediobasal hypothalamus of male rats. Neurosci Lett 10:159–163
26. **Donoso AO** 1978 Induction of prolactin and luteinizing hormone release by histamine in male and female rats and the influence of brain transmitter antagonists. J Endocrinol 76:193–202
27. **Donoso AO, Banzan AM, Borzino MI** 1976 Prolactin and luteinizing hormone release after intraventricular injection of histamine in rats. J Endocrinol 68:171–172
28. **Donoso AO, Banzan AM** 1978 Failure of histamine to induce the release of luteinizing hormone in castrated rats primed with sex steroids. J Endocrinol 78:447–448
29. **Libertun C, McCann SM** 1976 The possible role of histamine in the control of prolactin and gonadotropin release. Neuroendocrinology 20:110–120
30. **Inagaki N, Yamatodani A, Shinoda K, Panula P, Watanabe T, Shiotani Y, Wada H** 1988 Histaminergic nerve fibers in the median eminence and hypophysis of rats demonstrated immunocytochemically with antibodies against histidine decarboxylase and histamine. Brain Res 439:402–405
31. **Mellon PL, Windle JJ, Goldsmith PC, Padula CA, Roberts JL, Weiner RI** 1990 Immortalization of hypothalamic GnRH neurons by genetically targeted tumorigenesis. Neuron 5:1–10
32. **Jarry H, Perschl A, Wuttke W** 1988 Further evidence that preoptic anterior hypothalamic GABAergic neurons are part of the GnRH pulse and surge generator. Acta Endocrinol (Copenh) 118:573–579
33. **Herbison AE, Dyer RG** 1991 Effect on luteinizing hormone secretion of GABA receptor modulation in the medial preoptic area at the time of proestrous luteinizing hormone surge. Neuroendocrinology 53:317–320
34. **Herbison AE** 1997 Estrogen regulation of GABA transmission in rat preoptic area. Brain Res Bull 44:321–326
35. **Airaksinen MS, Alanen S, Szabat E, Visser TJ, Panula P** 1992 Multiple neurotransmitters in the tuberomammillary nucleus: comparison of rat, mouse, and guinea pig. J Comp Neurol 323:103–116
36. **Barraclough CA, Wise PM** 1982 The role of catecholamines in the regulation of pituitary luteinizing hormone and follicle-stimulating hormone secretion. Endocr Rev 3:91–119
37. **Sar M, Stumpf WE** 1981 Central noradrenergic neurones concentrate 3H-oestradiol. Nature 289:500–502
38. **Simonian SX, Herbison AE** 1997 Differential expression of estrogen receptor and neuropeptide Y by brainstem A1 and A2 noradrenaline neurons. Neuroscience 76:517–529
39. **Coen CW** 1993 The central control of luteinizing hormone release: a provisional model. In: Lehrnert H, Murison H, Weiner D, Hellhammer, Beyer J (eds) Endocrine and Nutritional Control of Basic Biological Functions. Hogrefe & Huber Publishers, vol 1:441–454
40. **Tsuruo Y, Kawano H, Kagotani Y, Hisano S, Daikoku S, Chihara K, Zhang T, Yanaihara N** 1990 Morphological evidence for neuronal regulation of luteinizing hormone-releasing hormone-containing neurons by neuropeptide Y in the rat septo-preoptic area. Neurosci Lett 110:261–266
41. **Sar M, Sahu A, Crowley WR, Kalra SP** 1990 Localization of neuropeptide-Y immunoreactivity in estradiol-concentrating cells in the hypothalamus. Endocrinology 127:2752–2756
42. **Tsuruo Y, Kawano H, Hisano S, Kagotani Y, Daikoku S, Zhang T, Yanaihara N** 1991 Substance P-containing neurons innervating LHRH-containing neurons in the septo-preoptic area of rats. Neuroendocrinology 53:236–245
43. **Okamura H, Yokosuka M, Hayashi S** 1994 Induction of substance P-immunoreactivity by estrogen in neurons containing estrogen receptors in the anteroventral periventricular nucleus of female but not male rats. J Neuroendocrinol 6:609–615
44. **Rance NE, McMullen NT, Smialek JE, Price DL, Young WSD** 1990 Postmenopausal hypertrophy of neurons expressing the estrogen receptor gene in the human hypothalamus. J Clin Endocrinol Metab 71:79–85
45. **Dudás B, Dobó E, Merchenthaler I, Liposits Zs,** Human luteinizing hormone-releasing hormone-synthesizing neurons receive neuropeptide-Y-immunoreactive innervation. Program of the Annual Meeting of the Society for Neuroscience, Washington DC, 1996, p 1588 (Abstract)
46. **Dudás B, Dobó E, Merchenthaler I, Liposits Zs,** Catecholaminergic axons

innervate luteinizing hormone-releasing hormone immunocreative neurons of the human diencephalon. Program of the Annual Meeting of the Society for Neuroscience, New Orleans, LA, 1997, p 1506 (Abstract)
47. **Dudás B, Dobó E, Merchenthaler I, Liposits Zs,** Luteinizing hormone-releasing hormone (LHRH)-synthesizing neurons are innervated by substance-P immunoreactive axons in the human diencephalon. Program of the Annual Meeting of the Society for Neuroscience, Los Angeles, CA, 1998, p 2073 (Abstract)
48. **Knigge U, Dejgaard A, Wollesen F, Ingerslev O, Bennett P, Christiansen PM** 1983 The acute and long term effect of the H2-receptor antagonists cimetidine and ranitidine on the pituitary-gonadal axis in men. Clin Endocrinol (Oxf) 18:307–313
49. **Segrestaa JM, Gueris J, Lefaucheur C, Orriere P** 1982 Role of histaminergic H1 and H2 receptors in prolactin release in humans. Pathol Biol (Paris) 30:715–718
50. **Pontiroli AE, De Castro S, Mazzoleni F, Alberetto M, Baio G, De Pasqua A, Stella L, Girardi AM, Pozza G** 1981 The effect of histamine and H1 and H2 receptors on prolactin and luteinizing hormone release in humans: sex differences and the role of stress. J Clin Endocrinol Metab 52:924–928
51. **Delitala G, Stubbs WA, Wass JA, Jones A, Williams S, Besser GM** 1979 Effects of the H2 receptor antagonist cimetidine on pituitary hormones in man. Clin Endocrinol (Oxf) 11:161–167
52. **Peden NR, Boyd EJ, Browning MC, Saunders JH, Wormsley KG** 1981 Effects of two histamine H2-receptor blocking drugs on basal levels of gonadotrophins, prolactin, testosterone and oestradiol-17 beta during treatment of duodenal ulcer in male patients. Acta Endocrinol (Copenh) 96:564–568
53. **Masaoka K, Niibe T, Kumasaka T, Saito M** 1983 Effect of a histamine H2-receptor antagonist, cimetidine, on prolactin secretion in women. Nippon Sanka Fujinka Gakkai Zasshi 35:1627–1633
54. **Biagi P, Galli M, Brettoni A, Rizzo AA, Massafra C** 1983 H2 histamine antagonists and the hypothalamo-hypophyseal-gonadal axis: effect of short-term treatment on serum levels of prolactin, FSH, LH and testosterone in male ulcer patients. Quad Sclavo Diagn 19:313–321
55. **Knigge U, Thuesen B, Dejgaard A, Bennett P, Christiansen PM** 1989 Plasma concentrations of pituitary and peripheral hormones during ranitidine treatment for two years in men with duodenal ulcer. Eur J Clin Pharmacol 37: 305–307

dc_27_10

2. számú melléklet

0013-7227/00/$03.00/0
Endocrinology

dc_27_10

Vol. 141, No. 9
Printed in U.S.A.

Detection of Estrogen Receptor-β Messenger Ribonucleic Acid and ^{125}I-Estrogen Binding Sites in Luteinizing Hormone-Releasing Hormone Neurons of the Rat Brain

ERIK HRABOVSZKY, PAUL J. SHUGHRUE, ISTVÁN MERCHENTHALER, TIBOR HAJSZÁN, CLIFFORD D. CARPENTER, ZSOLT LIPOSITS AND SANDRA L. PETERSEN*

Department of Biology (EH, CDC, SLP), University of Massachusetts, Amherst, MA 01003, USA; The Women's Health Research Institute (PJS, IM), Wyeth-Ayerst Research, Radnor, PA 19087, USA; Department of Neurobiology (TH and ZSL), Institute of Experimental Medicine, Hungarian Academy of Sciences, Budapest, 1083 Hungary

ABSTRACT

Luteinizing hormone-releasing hormone (LHRH) neurons of the forebrain play a pivotal role in the neuroendocrine control of reproduction. Although serum estrogen levels influence many aspects of LHRH neuronal activity in the female, earlier studies were unable to detect estrogen receptors (ERs) within LHRH neurons, thus shaping a consensus view that the effects of estradiol on the LHRH neuronal system are mediated by interneurons and/or the glial matrix. The present studies used dual-label *in situ* hybridization histochemistry (ISHH) and combined LHRH-immunocytochemistry/^{125}I-estrogen binding to readdress the estrogen-receptivity of LHRH neurons in the female rat. In ISHH experiments we found that the majority of LHRH neurons exhibited hybridization signal for the "β" form of ER (ER-β). The degree of colocalization was similar in topographically distinct populations of LHRH neurons and was not significantly altered by estradiol (67.2±1.8 % in ovariectomized and 73.8±4.2 % in ovariectomized and estradiol-treated rats). In contrast, the mRNA encoding the classical ER-α could not be detected within LHRH neurons. In addition, *in vivo* binding studies using ^{125}I-estrogen revealed a subset of LHRH-immunoreactive neurons (8.8%) which accumulated the radioligand, thus providing evidence for the translation of ER protein(s) within these cells. The findings that most LHRH neurons in the female rat express ER-β mRNA and at least some are capable of binding ^{125}I-estrogen challenge the current opinion that estrogen does not exert direct effects upon the LHRH neuronal system.

KEY WORDS

estradiol, estrogen binding, estrogen receptor, gonadotropin-releasing hormone, *in situ* hybridization, luteinizing hormone-releasing hormone

Introduction

Luteinizing hormone-releasing hormone (LHRH) neurons of the forebrain play a pivotal role in the central regulation of female reproduction. Many aspects of LHRH neuronal activity are modulated by circulating estrogens. Estradiol regulates the biosynthesis and secretion of LHRH, and it determines the sexually dimorphic pattern and estrous cycle variations of galanin expression by LHRH neurons (ref. 1 for a review). Previous studies, however, could not detect specific concentration of tritiated estradiol (2), estrogen receptor-α (ER-α) immunoreactivity (3) or ER-β messenger ribonucleic acid (mRNA; 4) in LHRH neurons of the rat. The lack of evidence for ER expression in these cells shaped a consensus view that LHRH neurons are not receptive to estrogen, but rather, the estrogen signal is communicated to them by interneurons and/or the glial matrix. However, somewhat conflicting data suggest that estrogen might have direct actions upon the LHRH neuronal system. For example, estrogen response elements are present within the promoter region of the primate LHRH gene (5) and immortalized LHRH-producing cells take up estradiol (6) and express ER-α mRNA (7). Recent immunocytochemical studies (8) demonstrate ER-α-like immunoreactivity in 17±1% of LHRH neurons of rats. These findings reopened the debate on the presence and putative functions of ERs within LHRH neurons.

In the present studies, we used dual-label *in situ* hybridization histochemistry (ISHH; 9) and combined *in vivo* ^{125}I-estrogen binding/LHRH-immunocytochemistry to revisit the issue of whether the LHRH neuronal system of the rat is directly regulated by estrogen.

*Correspondence is requested to
Dr. Sandra L. Petersen
Dept. of Biology, 221 Morrill Sci. Ctr., Univ. of Massachusetts, Amherst, MA 01003 USA
Phone: 1-413-545-1808
Fax: 1-413-545-3243
E-mail: Sandyp@bio.umass.edu
Received 04/25/00.

Materials and Methods

All animals were treated in accordance with the NIH Guide for the Care and Use of Laboratory Animals and the University of Massachusetts IAUCC.

Dual-label ISHH studies

Sprague-Dawley rats (n=10; 225-250 g bw) were ovariectomized (OVX), and on postovariectomy day 12 (1000 h) implanted with two subcutaneous Silastic capsules (Dow Corning; l=30 mm, ID=1.58mm, OD=3.18mm) containing either sesame oil (n=5; OVX group) or 17β-estradiol (Sigma; 200μg/ml in sesame oil; n=5; OVX+E_2 group). On day 14 (1000h), all rats were sacrificed and their brains removed and snap-frozen on pulverized dry ice. Then, 12-μm coronal sections through the region containing the organum vasculosum of the lamina terminalis (OVLT) and the medial preoptic area (MPOA) were collected on gelatin-coated slides and processed for dual-label ISHH (9).

The synthesis and application of the digoxigenin-labeled complementary RNA (cRNA) probe to LHRH mRNA, as well as the detection of the non-isotopic ISHH signal with anti-digoxigenin antibodies conjugated to horseradish peroxidase (Boehringer Mannheim; anti-digoxigenin-POD, Fab fragment, 1:200), were described elsewhere (9). For improved detection of LHRH neurons, the peroxidase-catalyzed deposition of biotinylated tyramine (Renaissance kit; NEN), followed by the incubation of sections with the ABC-Elite reagent (Vector) was added to the procedure. Neurons expressing ER-α or ER-β mRNA were targeted with ^{35}S-labeled cRNA probes which were added at 40,000-120,000 cpm/μl/probe concentration to the hybridization buffer (50% formamide, 20% dextran sulfate, 1X Denhardt's solution, 300 mM sodium chloride, 30 mM sodium citrate, 0.5 mg/ml yeast tRNA, 0.5 mg/ml heparin sodium salt, 1 mg/ml sodium pyrophosphate, 80 mg/ml dithiothreitol; pH 7.0). The ER-α-specific cRNA probe was complementary to nucleotides 1224-2090 of the rat ER-α mRNA (10). To detect the expression of ER-β transcripts in LHRH neurons, two strategies were used. In the first set of experiments, dual-label ISHH was performed on proteinase K-pretreated (Sigma; 0.1μg/ml, 15 min) sections using a cRNA probe corresponding to nucleotides 6-1458 of the rat ER-β mRNA (11). A second series of sections was hybridized with a mixture of two shorter ER-β cRNA transcripts targeting nucleotides 52-610 and 1809-2094. The selection of these probe sequences (12) prevented a potential cross-hybridization with the ER-α mRNA. Following the immunocytochemical detection of the digoxigenin-labeled cRNA probe to LHRH mRNA, the slides were dipped in NTB-3 photographic emulsion (Kodak; diluted 1:1 with distilled water), exposed for 6 weeks, then the autoradiograms were developed. Some sections were counterstained with toluidine blue before coverslipping. Effects of E_2 on colocalization were evaluated using Students' t-tests.

In vivo binding/ ICC studies

On postnatal day 21, female rats (n=7) were ovariectomized. On postovariectomy day 11, five animals were injected subcutaneously with 2 μg/kg bw of 17α-iodovinyl-11β-methoxyestradiol (^{125}I-estrogen, specific activity 2200 Ci/mMol; 13) in 200μl of vehicle (50% DMSO, 50% PBS). Control animals (n=2) were injected with 250 μg/kg bw of 17β-estradiol 1 hour prior to the administration of ^{125}I-estrogen to compete off the radiolabeled compound and verify the specificity of ^{125}I-estrogen uptake in this animal paradigm. Four to six hours after injection of ^{125}I-estrogen, the rats were anesthetized and transcardially perfused with 4% paraformaldehyde. The brains were removed and postfixed in 4% paraformaldehyde for 20 hours at 4°C. Vibratome sections (35 μm) were collected in ice cold PBS and following pretreatment (13), they were incubated at 4°C with a rabbit polyclonal LHRH antiserum (#H-16) for 18 hours. The detection of LHRH immunoreactivity was completed with the Vector Elite kit. The sections were mounted on gelatin-coated slides, air-dried, then washed (13), dipped in distilled water and allowed to dry at room temperature. Finally, the slides were coated with liquid nuclear emulsion (Kodak; NTB-2, diluted 1:1 with distilled water), air-dried and stored at 4°C in a light-tight desiccator until development (10-20 days).

Results

The results of ISHH studies showed that the mRNA encoding the classical ER-α (Figs a-c) occurred at much higher cellular abundance than ER-β mRNA (Figs d-i) in regions of the preoptic area that contained LHRH neurons. In addition, we found that the autoradiographic signal increased, with slight compromise in background levels, when higher probe concentrations (120,000 cpm/μl, in Figs b and c, vs 40,000 cpm/μl, in Fig a) were used. Most LHRH neurons were entirely devoid of the autoradiographic ISHH signal for ER-α (Figs a-c). In a few instances (4 out of 502 LHRH neurons; <1%) the two signals overlapped partially. Such cases were not interpreted as colocalization (Fig c). In contrast to the lack of evidence for ER-α mRNA in LHRH neurons, a relatively weak autoradiographic signal for ER-β mRNA was frequently detected over the cell bodies of LHRH neurons. The incidence of this colocalization was high in neurons of the diagonal band of Broca (DBB; Fig d), medial septum (MS; Fig e), OVLT (Fig f), median preoptic nucleus (MPN; Fig g) and MPOA (Fig h). We found that 319 of 465 LHRH neurons in OVX, and 539 of 725 neurons in OVX+E_2 rats expressed ER-β mRNA. There was no statistically significant difference between OVX (67.2±1.8%, mean±SEM); and OVX+E_2 (73.8±4.2%) animals in the percentage of colocalization. The finding of ER-β mRNA in LHRH neurons using the 1453-base cRNA probe (Figs d-h) was successfully replicated with the combined application of the two short ER-β probe constructs (Fig i). In further control experiments, the ER-β hybridization signal was absent if the hybridization was performed on sections pretreated with RNAse A (not shown) or if ER-β probes were substituted with ^{35}S-labeled "sense" strand RNA transcripts (Fig j). The absence of grain cluster formation over LHRH profiles using either the antisense probe for ER-α (Figs a-c) or the sense probes for ER-β (Fig j) confirmed our previous observation that DAB does not cause positive chemography on the NTB-3 emulsion (9).

The results of dual *in vivo* binding/ICC experiments showed that a small population of LHRH-immunoreactive neurons (8.8%; 145 out of 1635) in the OVLT/MPOA concentrated the radioactive label in their nuclei (Figs k, l). Only scattered (0-2%) double-labeled cells were observed in the MS. All ^{125}I-estrogen binding to LHRH neurons was eliminated by estradiol pretreatment of the animals, indicating the specificity of radioligand uptake.

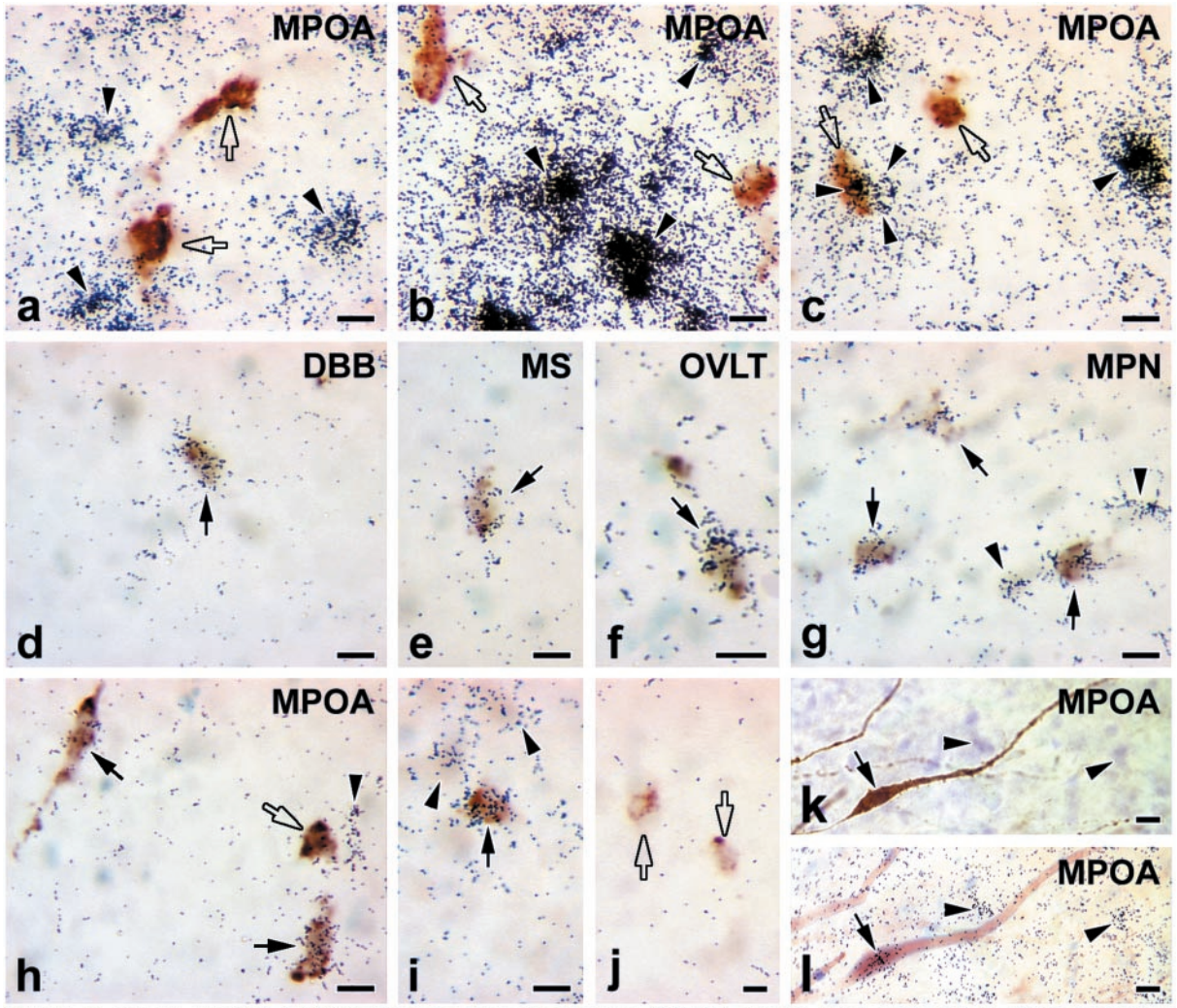

Studies of estrogen-receptive luteinizing hormone-releasing hormone (LHRH) neurons using dual-label *in situ* hybridization histochemistry (ISHH; Figs a-j) and combined *in vivo* ^{125}I-estrogen binding/LHRH-immunocytochemistry (Figs k, l). a-c: The autoradiographic ISHH signal for ER-α (clustered silver grains; arrowheads) is heavily expressed in cells of the medial preoptic area (MPOA), but is absent from LHRH neurons (brown histochemical staining; empty arrows). Note the strong ER-α signal and the somewhat compromised autoradiographic background in "**b**" and "**c**", due to the use of higher probe concentrations (120,000 cpm/μl) than in "**a**" (40,000 cpm/μl). The grain cluster in figure "**c**" identified by three arrowheads overlaps only partially with an LHRH profile. **d-h**: Large numbers of LHRH neurons in the diagonal band of Broca (DBB; **d**), medial septum (MS; **e**), organum vasculosum of the lamina terminalis (OVLT; **f**), median preoptic nucleus (MPN; **g**) and MPOA (**h**) express the autoradiographic ISHH signal to ER-β. Dual- (solid arrows) and single-labeled (empty arrow in "**h**") LHRH neurons, in addition to non-LHRH cells expressing ER-β mRNA (arrowheads) are present in ovariectomized (**f**) as well as ovariectomized+estradiol-treated (**d, e, g, h**) animals. The detection of ER-β mRNA was performed with the 1453-base probe. Control studies using the combination of two short ER-β probe constructs in "**i**" confirm the finding of ER-β mRNA expression in LHRH neurons. **j:** Results of dual-label ISHH with the 1453-base sense strand probe for ER-β mRNA show no signal, further confirming the specific binding of the antisense probe and also showing that positive chemographic artifacts do not occur over DAB-stained LHRH neurons (empty arrows). **k, l**: An LHRH-immunoreactive neuron (diaminobenzidine chromogen; brown cytoplasm), photographed at two different focus planes, exhibits *in vivo* accumulation of ^{125}I-estrogen (autoradiographic signal). Note the concentration of silver grains over the cell nucleus of the LHRH neuron (arrows), in addition to the nuclei of non-LHRH cells (arrowheads). Scale bars=10 μm.

Discussion

The results of our dual-label ISHH studies demonstrated that the majority of LHRH neurons in the female rat contain ER-β mRNA. However, a similar methodology failed to detect any expression of ER-α mRNA in these cells. In addition, the observation of *in vivo* ^{125}I-estrogen binding to a subset of LHRH neurons in the OVLT/MPOA provided strong evidence for the translation of functional ER protein(s) at least within some LHRH neurons.

Although much methodological effort, including the application of increased probe concentrations, has been invested successfully to improve the detection of ER mRNAs, our ISHH experiments could not confirm the recent ICC finding of ER-α expression in LHRH neurons of the rat (8). However, we recognize the possibility that very low cellular levels of ER-α mRNA might not be detected in our ISHH studies.

Recently, Laflamme et al. reported the absence of ER-β mRNA in LHRH neurons of the rat (4). In contrast, we detected ER-β mRNA expression in high percentages of LHRH neurons. The different results of our experiments are most likely due to the technical modifications that enhanced the detection sensitivity of the colocalization method. It is noteworthy that we used 4- to 12-fold higher concentration of ER-β hybridization probe and a 4-fold longer autoradiographic exposure than did the cited study.

The *in vivo* uptake of ^{125}I-estrogen indicates the presence of ER protein(s) in a population of LHRH neurons, although LHRH neurons showing accumulation of the radioligand were less numerous then those co-expressing ER-β and LHRH transcripts. This discrepancy might be attributable to differences in sensitivities of the methodologies, together with a functional heterogenity of LHRH neurons in the cellular abundance of translated ER protein(s).

While this manuscript was in preparation, Skynner and co-workers demonstrated ER-α and ER-β mRNA transcripts in individual LHRH neurons of mice using a single-cell multiplex RT-PCR method (14). Because both the RT-PCR and our ISHH approaches are based on the detection of cellular mRNAs, the discrepancies between the results of these two studies are somewhat surprising. The RT-PCR method showed the predominance of ER-α over ER-β mRNA in LHRH neurons in mice, whereas our ISHH experiments could not provide evidence for the presence of ER-α mRNA in rat LHRH neurons. Furthermore, the RT-PCR study detected ER-β expression in a much lower percentage of LHRH neurons in mice (0-19%, the highest in estrous animals), than did our ISHH study in rats (67.2 % in OVX, 73.8 % in OVX+E_2 animals). Finally, the RT-PCR method showed the disappearance of ER-β mRNA from non-LHRH as well as LHRH neurons of the preoptic area in mice at proestrous, when estrogen levels are high. In contrast, we did not observe this dramatic down-regulation of ER-β mRNA by estradiol in the preoptic area; moreover, the incidence of ER-β mRNA expression in LHRH neurons was similar in the presence or absence of E_2. These discrepancies may be attributable to methodological or species differences.

The mechanism whereby estrogen signaling via ER-β within LHRH neurons can modulate reproductive functions will be the subject of further investigation. It is currently impossible to separate direct effects of estrogen from those mediated by interneurons and glial cells. Also, future studies are needed to determine the contributions of the two types of ER to the modulation of LHRH neuronal functions.

In summary, our studies demonstrated the expression of ER-β, but not ER-α, mRNA in large numbers of LHRH neurons and the presence of ^{125}I-estrogen binding sites within a smaller population of these neurons in adult female rats. These data together provide a strong argument against the widely-held view that the LHRH neuronal system is not estrogen-receptive.

Supported by grant HD27305 from the the National Institute of Health of the USA and in part by grants from the National Science Foundation of Hungary (OTKA F22711, TO16354) and the Hungarian Medical Research Council (ETT 638/96 and 139/98).

References

1. **Herbison, AE 1998** Multimodal influence of estrogen upon gonadotropin-releasing hormone neurons. Endocr Rev 19: 302-30
2. **Shivers BD, Harlan RE, Morrell JI, Pfaff DW** 1983 Absence of oestradiol concentration in cell nuclei of LHRH-immunoreactive neurones. Nature 304:345-347
3. **Herbison AE, Theodosis DT** 1992 Localization of oestrogen receptors in preoptic neurons containing neurotensin but not tyrosine hydroxylase, cholecystokinin or luteinizing hormone-releasing hormone in the male and female rat. Neuroscience 50:283-298
4. **Laflamme N, Nappi RE, Drolet G, Labrie C, Rivest S** 1998 Expression and neuropeptidergic characterization of estrogen receptors (ERalpha and ERbeta) throughout the rat brain: anatomical evidence of distinct roles of each subtype. J Neurobiol 36:357-378
5. **Radovick S, Wray S, Muglia L, Westphal H, Olsen B, Smith E, Patriquin E, Wondisford FE** 1994 Steroid hormone regulation and tissue-specific expression of the human GnRH gene in cell culture and transgenic animals. Horm Behav 28:520-529
6. **Poletti A, Melcangi RC, Negri-Cesi P, Maggi R, Martini L** 1994 Steroid binding and metabolism in the luteinizing hormone-releasing hormone-producing neuronal cell line GT1-1. Endocrinology 135:2623-2628
7. **Shen ES, Meade EH, Perez MC, Deecher DC, Negro-Vilar A, Lopez FJ** 1998 Expression of functional estrogen receptors and galanin messenger ribonucleic acid in immortalized luteinizing hormone-releasing hormone neurons: estrogenic control of galanin gene expression. Endocrinology 139:939-948
8. **Butler JA, Sjoberg M, Coen CW** 1999 Evidence for oestrogen receptor alpha-immunoreactivity in gonadotrophin-releasing hormone-expressing neurones. J Neuroendocrinol 11:331-335
9. **Petersen SL, McCrone S** 1994 Characterization of the receptor complement of individual neurons using dual-label in situ hybridization histochemistry. In JH Eberwine, KL Valentino and JD Barchas (Eds.), In situ hybridization in neurobiology. Advances in methodology, Oxford University Press, New York, pp. 78-94
10. **Koike S, Sakai M, Muramatsu M** 1987 Molecular cloning and characterization of rat estrogen receptor cDNA. Nucleic Acids Res 15:2499-2513
11. **Kuiper GG, Enmark E, Pelto Huikko M, Nilsson S, Gustafsson JA** 1996 Cloning of a novel receptor expressed in rat prostate and ovary. Proc Natl Acad Sci USA 93:5925-5930
12. **Shughrue PJ, Komm B, Merchenthaler I** 1996 The distribution of estrogen receptor-beta mRNA in the rat hypothalamus. Steroids 61:678-681
13. **Shughrue PJ, Scrimo PJ, Merchenthaler I** 2000 Estrogen binding and estrogen receptor characterization (ERalpha and ERbeta) in the cholinergic neurons of the rat basal forebrain, Neuroscience 96:41-49
14. **Skynner MJ, Sim JA, Herbison AE** 1999 Detection of estrogen receptor alpha and beta messenger ribonucleic acids in adult gonadotropin-releasing hormone neurons Endocrinology 140:5195-5201

3. számú melléklet

0013-7227/00/$03.00/0
Endocrinology

dc_27_10

Vol. 142, No. 7
Printed in U.S.A.

Estrogen Receptor-β Immunoreactivity in Luteinizing Hormone-Releasing Hormone Neurons of the Rat Brain

ERIK HRABOVSZKY, ANNAMÁRIA STEINHAUSER, KLAUDIA BARABÁS, PAUL J. SHUGHRUE*, SANDRA L. PETERSEN, ISTVÁN MERCHENTHALER AND ZSOLT LIPOSITS**

Department of Neurobiology (EH, AS, KB,ZSL), Institute of Experimental Medicine, Hungarian Academy of Sciences, Budapest, 1083 Hungary; The Women's Health Research Institute (PJS, IM), Wyeth-Ayerst Research, Radnor, PA 19087, USA; Department of Biology (SLP), University of Massachusetts, Amherst, MA 01003, USA

ABSTRACT
Feedback regulation of luteinizing hormone-releasing hormone (LHRH) neurons by estradiol plays important roles in the neuroendocrine control of reproduction. Recently, we found that the majority of LHRH neurons in the rat contain estrogen receptor-β (ER-β) mRNA, whereas, they seemed to lack ER-α mRNA expression. In addition, we observed nuclear uptake of ^{125}I-estrogen by a subset of these cells. These data suggest that ER-β is the chief receptor isoform mediating direct estrogen effects upon LHRH neurons. To verify the translation of ER-β protein within LHRH cells, the present studies applied dual-label immunocytochemistry (ICC) to free-floating sections obtained from the preoptic area of rats. The improved ICC method using the silver-gold intensification of nickel-diaminobenzidine chromogen, enabled the observation of nuclear ER-β-immunoreactivity in the majority of LHRH cells. The incidence of ER-β expression was similarly high in LHRH neurons of ovariectomized female (87.8±2.3%, mean±SEM), estradiol-primed female (74.9±3.2%) and intact male (85.0±4.7%) rats. The presence of ER-β mRNA, ER-β immunoreactivity and ^{125}I-estrogen binding sites in LHRH neurons of the rat provide strong support for the notion that these cells are directly regulated by estradiol, through ER-β. The gene targets and molecular mechanisms of this regulation remain unknown.

KEY WORDS
estradiol, estrogen, estrogen receptor, gonadotropin-releasing hormone, immunocytochemistry, steroid receptor

Introduction

The luteinizing hormone-releasing hormone (LHRH) neurosecretory system represents the final common pathway in the neuroendocrine control of reproduction. The ovarian steroid hormone 17β-estradiol (E_2) regulates LHRH neurons through feedback actions, which have been reviewed recently (1). The lack of evidence for estrogen receptor (ER) expression in LHRH neurons (2-4) shaped a consensus view that estrogen-receptive interneurons are necessary to communicate estrogen signals to the LHRH neuronal system. Very recently, this notion was challenged by the identification of ER-α immunoreactivity (5), ER mRNA transcripts (6, 7), and ^{125}I-estrogen binding sites (7) in LHRH neurons of rodents. Using dual-label *in situ* hybridization histochemistry (ISHH), our group found ER-β, but not ER-α mRNA expression, within the majority of LHRH neurons in rats (7). Furthermore, we successfully combined radio-labeled estrogen binding with LHRH immunocytochemistry (ICC) to demonstrate ^{125}I-estrogen uptake within a subset of LHRH neurons (7). To establish the functional link between ER-β mRNA expression and ^{125}I-estrogen binding, evidence for the translation of ER-β protein in LHRH neurons is still missing.

*Present address: Department of Pharmacology, Merck Research Laboratories, West Point, PA 19486 USA
**Correspondence is requested to
Dr. Zsolt Liposits
Dept. of Neurobiology, Institute of Experimental Medicine, Hungarian Academy of Sciences, Szigony u. 43., 1083 Budapest, Hungary
Phone and **Fax:** 36-1-210-6147; **E-mail: liposits@koki.hu**
Received 04/09/01.

The present studies used dual-label ICC to localize ER-β immunoreactivity in LHRH neurons of ovariectomized female, E_2-primed female, and intact male rats.

Materials and Methods

Rats were treated in accordance with Guides by the Animal Care and Use Committee of IEM, the NIH guidelines for the Care and Use of Laboratory animals and the IACUC of the University of Massachusetts.

Dual-label ICC studies

Female (n=12; 225-250 g bw) and male (n=6; 225-250 g bw) Wistar rats were purchased from Charles-River. Females were bilaterally ovariectomized under Nembutal anesthesia (35mg/kg bw, ip) and on post-ovariectomy day 5 (1000 h), 6 of them were reanesthetized and implanted subcutaneously with a pair of Silastic capsules (Dow Corning; L=30mm, ID=1.58mm, OD=3.18mm) containing 200μg/ml of E_2 (Sigma; OVX+E_2 group) in sesame oil. The remainder of female rats (n=6; OVX group) did not receive steroid replacement. On post-ovariectomy day 7 (1000 h), all animals, were anesthetized with Nembutal and perfused transcardially with 150 ml fixative solution containing 2% paraformaldehyde (Sigma) and 4% acrolein (Aldrich) in 0.1M phosphate buffered saline (pH 7.4). Tissue blocks containing the preoptic area were dissected out and infiltrated with 30% sucrose overnight. Then coronal sections (20μm) comprising the diagonal band of Broca (DBB), organum vasculosum of the lamina terminalis (OVLT), medial septum (MS), medial preoptic area (mPOA) and median preoptic nucleus (MPN) were prepared using a

freezing microtome. The sections were rinsed in Tris buffered saline (TBS; 0.1M Tris-HCl/0.9% sodium chloride; pH 7.8), then pretreated with 1% sodium borohydride (Sigma) in TBS (30 min), 10% thioglycolic acid (Sigma; 30 min), 0.5% H_2O_2 in TBS (10 min), and finally, with 2% normal horse serum (NHS) in TBS (30 min). Subsequently, they were incubated (five days; 4 °C) in the ER-β primary antiserum (Z8P; Zymed Laboratories; dissolved at 33 ng/ml in TBS/2% NHS/0.1% merthiolate/0.4% Triton X-100). These antibodies were generated in rabbit against a synthetic peptide corresponding to the carboxy-terminal 18 amino acids of murine ER-β (15/18 amino acid identity with the rat ER-β sequence). Control sections were incubated in Z8P antiserum preabsorbed with 0.1 μg/ml of the immunization antigen. Cross-reaction of the Z8P antibody with the rat ER-β as well as the specificity of immunostaining in the rat, were demonstrated recently by co-authors of this paper (8). The peroxidase reaction was visualized with nickel-diaminobenzidine (Ni-DAB) chromogen following tissue incubations in biotinylated antirabbit IgG (Jackson, 1:1000; 2 hours), then in horseradish peroxidase-conjugated streptavidin (Jackson, 1:1000; 1 hour). The signal was amplified using silver-gold post-intensification (9). Subsequently, the sections were incubated in rabbit primary antibodies to LHRH (LR1; 1:100.000), biotinylated antirabbit IgG, and then, horseradish peroxidase-conjugated streptavidin. Finally, the peroxidase reaction was developed using brown DAB as chromogen substrate.

Dual-label ISHH studies

Three female and four male rats (Sprague-Dawley; 225-250 g bw) were purchased from Zivic-Miller. Females were ovariectomized and allowed to recover from the surgery for 7 days. Male animals were kept intact. Rats of both genders were sacrificed by decapitation and their brains snap-frozen on powdered dry ice. Twelve-μm coronal sections through the OVLT/mPOA region were collected on double gelatin-coated microscopic slides. Dual-label ISHH detection of LHRH and ER-β mRNAs was carried out as described previously (7). First, brown DAB chromogen was used to detect immunocytochemically the digoxigenin-labeled cRNA probe to LHRH mRNA, and then, the ^{35}S-labeled cRNA probes to ER-β mRNA (7, 10) were visualized on emulsion autoradiographs.

Results

Dual-label ICC studies

Consistent with recent light microscopic observations (8), the ICC application of the Z8P ER-β antibodies produced exclusively nuclear immunolabeling in the preoptic region of the rat. The silver-gold intensification procedure (9) greatly enhanced the intensity of this immunocytochemical staining. Heavily labeled cell nuclei were observed in the vicinity of the third ventricle (Figs 2A and B; anteroventral periventricular nucleus /AVPV/). In addition, a substantial number of cell nuclei showed light immunolabeling in regions populated by LHRH neurons, including the mPOA (Figs 2A and B) and the OVLT. This pattern of ER-β immunostaining was highly reminiscent of ER-β mRNA distribution (7, 10), thus serving as a positive control for specificity. Furthermore, both heavy and light immunostaining for ER-β could be fully eliminated by preabsorption of the primary antiserum with the ER-β antigen (negative control; Fig 2F). A high percentage of LHRH neurons contained ER-β immunoreactivity in their cell nuclei, usually at moderate or low levels (Figs 2B and E). Dark nuclear immunostaining of LHRH neurons was also observed occasionally (Figs 2C and D). The incidence of ER-β expression was similarly high in LHRH neurons of the OVX (87.8±2.3%, mean±SEM), the OVX+E_2 (74.9±3.2%) and the male (85.0±4.7%) groups (Fig 1). Corroborating previous ISHH data (7), no regional heterogeneity was noticed in the distribution of dual-labeled LHRH neurons.

Dual-label ISHH studies

Similar to the results of our previous ISHH study (7), we found autoradiographic ISHH signal for ER-β mRNA in the majority of LHRH neurons (61.0±5.7%) in OVX female rats (Figs 1 and 2G). In addition, most LHRH neurons in the intact male rat (72.9±4.18%; Figs 1 and 2H) also expressed hybridization signal for ER-β mRNA. As we previously demonstrated no effect of estrogen on the incidence of LHRH/ER-β mRNA co-expression (7), the present study did not readdress this issue.

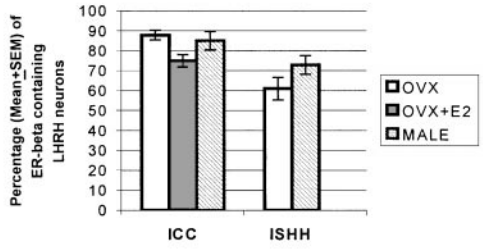

Figure 1 The percent ratio of estrogen receptor-β (ER-β) containing LHRH neurons. Results of immunocytochemical (ICC) and ***in situ*** hybridization (ISHH) studies demonstrate ER-β expression in the majority of LHRH neurons in ovariectomized female (OVX), ovariectomized and estradiol-primed female (OVX+E_2) and intact male (MALE) rats.

Discussion

Results of these dual-label ICC studies demonstrate the presence of ER-β immunoreactivity in the majority of LHRH neurons in the rat. The observations complement our previous data that LHRH neurons in the rat express ER-β mRNA and accumulate ^{125}I-estrogen (7).

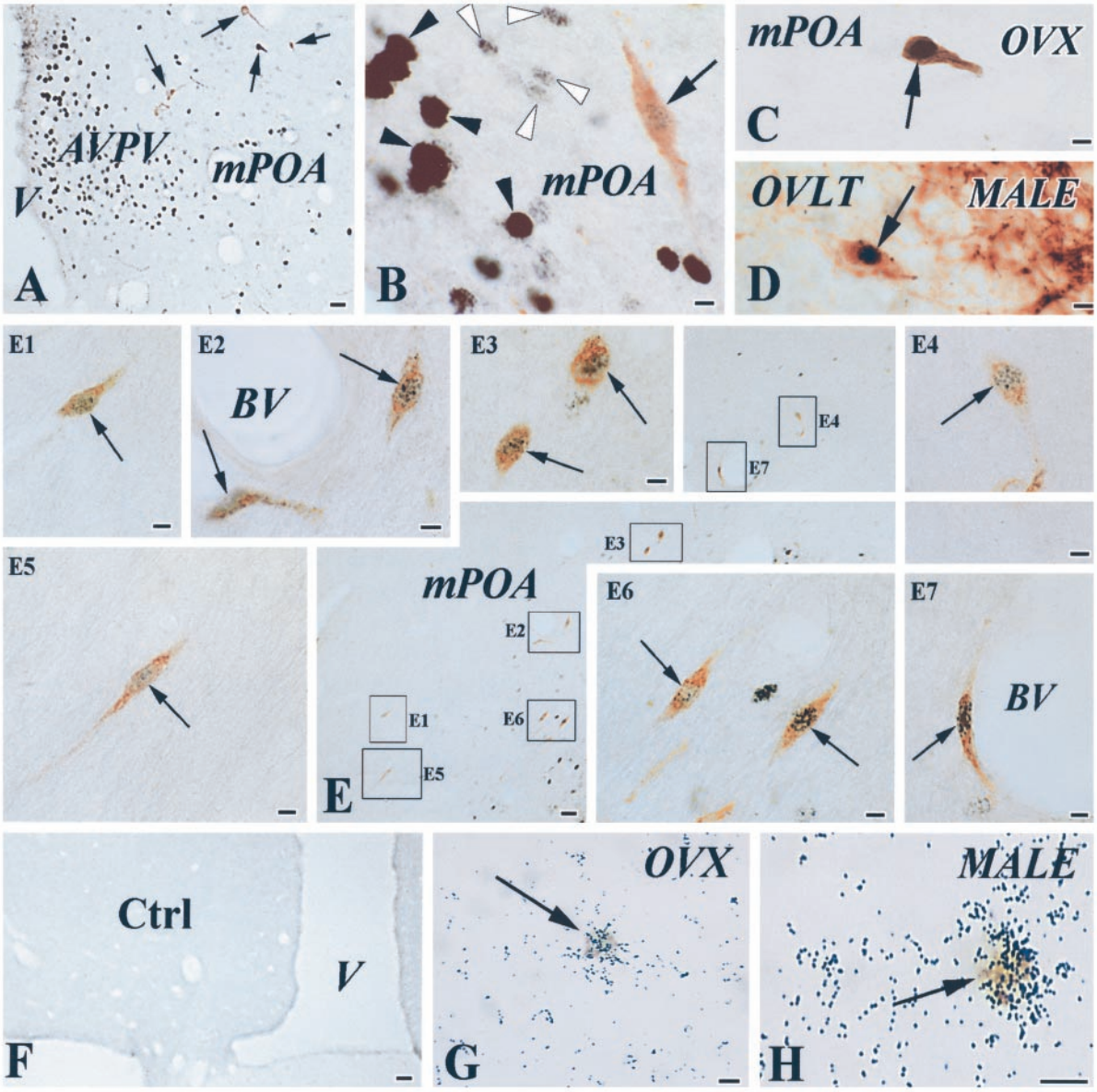

Figure 2 Evidence for estrogen receptor-β (ER-β) immunoreactivity (A-F) and mRNA expression (G, H) within luteinizing hormone-releasing hormone (LHRH) neurons of the rat. A: Detection of immunoreactive ER-β using the silver-gold-intensified Ni-DAB chromogen (gray-to-black color) reveals heavy nuclear labeling in neurons of the anteroventral periventricular nucleus (AVPV) neighboring the third ventricle (*V*). In contrast, mainly light immunostaining (pale cell nuclei) can be obtained in the medial preoptic area (mPOA), where high numbers of LHRH neurons (brown cytoplasmic staining; arrows) reside. **B:** Characteristically, LHRH neurons (arrow) and surrounding non-LHRH cells in the mPOA exhibit light nuclear immunostaining for ER-β. Note the contrast between cell nuclei accumulating high (black arrowheads in the AVPV) or low (white arrowheads in the mPOA) amounts of the chromogen. **C-D:** Occasionally, dark nuclear labeling can be observed in LHRH neurons of the (mPOA; **C**) and the organum vasculosum of the lamina terminalis (OVLT; **D**). Dual-labeled LHRH neurons are detectable in both female (**C**) and male (**D**) animals. *OVX*, ovariectomized female. **E:** Insets ($\mathbf{E}_{1\text{-}7}$) corresponding to framed areas in low-power central figure (**E**) demonstrate that the majority of LHRH neurons in the mPOA exhibit ER-β-positive cell nucleus (arrows). *BV*, blood vessels. **F:** Preabsorption of the primary antiserum with the ER-β antigen prevents immunostaining of the control section (Ctrl). **G-H:** Dual-label *in situ* hybridization experiments reveal ER-β mRNA expression (autoradiographic grain clusters) in LHRH neurons (arrows; brown histochemical staining) of OVX female (**G**) as well as intact male (**H**) rats. Scale bars=100 μm in A, E and F, and 10 μm in other figures.

We established that similarly high percentages of LHRH neurons express ER-β mRNA or protein in the two genders. These findings indicate that if sex differences exist, they are likely subtle.

In agreement with our previous observations (7), dual-label ICC experiments did not reveal major differences in the percentage of ER-β expressing LHRH neurons in OVX female and OVX+E_2 female rats. Somewhat conflicting these ISHH and ICC findings in the rat, a single-cell RT-PCR study of mouse LHRH neurons demonstrated steroid-dependent variations in the incidence of ER-β mRNA expression by LHRH neurons (19 % in estrous and 0 % in proestrous) (6).

It is reasonable to hypothesize that ER-β immunoreactivity in LHRH neurons corresponds to the ^{125}I-estrogen binding sites that we reported previously (7). In the light of the present ICC data indicating that most LHRH neurons in the rat contain ER-β protein, it is likely that the lower percentage (8.8%) of LHRH neurons that accumulated the radio-labeled estrogen was due to limitations of the combined estrogen binding/ICC method. This notion is supported by the relative paucity of ER-β mRNA and protein in LHRH cells that required the use of improved ISHH (7) and ICC methods for detection.

It remains to be determined whether or not LHRH neurons possess ER-α (5, 6) or other currently unknown isoforms of ER, in addition to ER-β (6, 7). As previous evidence for ER-α mRNA in LHRH neurons (6) was not confirmed (7, 11), further research will need to determine the molecular source of ER-α immunoreactivity in LHRH neurons (5).

Due to the inadequacy of *in vivo* approaches to distinguish direct from trans-synaptic, or ER-α- from ER-β-mediated estrogen effects, only speculations can be made about the identity of genes directly regulated by ER-β in LHRH cells. One of these gene candidates encodes galanin, the expression pattern of which exhibits estrogen-dependent variations within LHRH neurons (12, 13). A second important matter of consideration is the involvement of ER-β in the negative feedback regulation of the LHRH gene. Consistent with this idea is the repression of the LHRH promoter by E_2 in LHRH-producing GT1 cells (14). Unfortunately, the reported presence of both ER isoforms in this cell line (14) makes it difficult to determine the contribution of ER-β to this effect. It is worth noting that a recent *in vitro* study demonstrated high constitutive transactivation of the vasopressin gene promoter by the unliganded ER-β. This effect was exerted at non-ERE sites of the promoter and it could be reversed by E_2 (15). Hypothetically, a similar interaction of ER-β with the LHRH gene could inhibit the transcription of LHRH mRNA, as observed during episodes of negative estrogen feedback.

In summary, the identification of ER-β immunoreactivity in LHRH neurons corroborates our previous ISHH data. The combined information indicates that the majority of LHRH neurons in female and male rats can be directly regulated by E_2, through ER-β. The gene targets and molecular mechanisms of this regulation are presently unknown.

This work was supported by grants from the National Science Foundation of Hungary (OTKA F22711, T031770), the Hungarian Medical Research Council (ETT 280/2000), the Fifth EC Framework Program (QLG3 2000-00844) and HD27305 from the National Institute of Health of the USA. The authors wish to thank Dr. R. Benoit for the kind donation of the LR1 LHRH antibody.

References

1. **Herbison AE** 1998 Multimodal influence of estrogen upon gonadotropin-releasing hormone neurons. Endocr Rev 19:302-330
2. **Shivers BD, Harlan RE, Morrell JI, Pfaff** DW 1983 Absence of oestradiol concentration in cell nuclei of LHRH-immunoreactive neurones. Nature 304:345-347
3. **Herbison AE, Theodosis DT** 1992 Localization of oestrogen receptors in preoptic neurons containing neurotensin but not tyrosine hydroxylase, cholecystokinin or luteinizing hormone-releasing hormone in the male and female rat. Neuroscience 50:283-298
4. **Watson R, Langub M, Landis J** 1992 Further evidence that most luteinizing hormone-releasing hormone neurons are not directly estrogen-responsive: simultaneous localization of luteinizing hormone-releasing hormone and estrogen receptor immunoreactivity in the guinea pig brain. J Neuroendocrinol 4:311-318
5. **Butler JA, Sjoberg M, Coen CW** 1999 Evidence for oestrogen receptor alpha-immunoreactivity in gonadotrophin- releasing hormone-expressing neurones. J Neuroendocrinol 11:331-335
6. **Skynner MJ, Sim JA, Herbison AE** 1999 Detection of estrogen receptor alpha and beta messenger ribonucleic acids in adult gonadotropin-releasing hormone neurons. Endocrinology 140:5195-5201
7. **Hrabovszky E, Shughrue PJ, Merchenthaler I, Hajszán T, Carpenter CD, Liposits Z, Petersen SL** 2000 Detection of estrogen receptor-beta messenger ribonucleic acid and ^{125}I-estrogen binding sites in luteinizing hormone-releasing hormone neurons of the rat brain. Endocrinology 141:3506-3509
8. **Shughrue J, Merchenthaler I** 2001 The distribution of estrogen receptor beta immunoreactivity in the rat central nervous system. J Comp Neurol (In press)
9. **Liposits Z, Sétáló G, Flerkó B** 1984 Application of the silver-gold intensified 3,3'-diaminobenzidine chromogen to the light and electron microscopic detection of the luteinizing hormone-releasing hormone system of the rat brain. Neuroscience 13:513-525
10. **Shughrue PJ, Lane MV, Merchenthaler I** 1997 Comparative distribution of estrogen receptor-alpha and -beta mRNA in the rat central nervous system. J Comp Neurol 388:507-525
11. **Herbison A, Skynner M, Sim J** 2001 Lack of detection of estrogen receptor-alpha transcripts in mouse gonadotropin-releasing hormone neurons. Endocrinology 142 (Erratum)
12. **Liposits Z, Reid JJ, Negro-Vilar A, Merchenthaler I** 1995 Sexual dimorphism in copackaging of luteinizing hormone-releasing hormone and galanin into neurosecretory vesicles of hypophysiotrophic neurons: estrogen dependency. Endocrinology 136:1987-1992
13. **Merchenthaler I** 1998 LHRH and sexual dimorphism. Ann N Y Acad Sci 863:175-187
14. **Roy D, Angelini NL, Belsham** DD 1999 Estrogen directly respresses gonadotropin-releasing hormone (GnRH) gene expression in estrogen receptor-alpha (ERalpha)- and ERbeta-expressing GT1-7 GnRH neurons. Endocrinology 140:5045-5053
15. **Shapiro RA, Xu C, Dorsa DM** 2000 Differential transcriptional regulation of rat vasopressin gene expression by estrogen receptor alpha and beta. Endocrinology 141:4056-4064

4. számú melléklet

Volume 50(10): 1389–1400, 2002
The Journal of Histochemistry & Cytochemistry
http://www.jhc.org

ARTICLE

Increased Concentrations of Radioisotopically-labeled Complementary Ribonucleic Acid Probe, Dextran Sulfate, and Dithiothreitol in the Hybridization Buffer Can Improve Results of In Situ Hybridization Histochemistry

Erik Hrabovszky and Sandra L. Petersen

Department of Biology, University of Massachusetts, Amherst, Massachusetts (EH,SLP), and Department of Neurobiology, Institute of Experimental Medicine, Hungarian Academy of Sciences, Budapest, Hungary (EH)

SUMMARY The goal of the present studies was to optimize mRNA detection with radioisotopic in situ hybridization histochemistry (ISHH). Test experiments performed on sections of rat brain tissue used computer-assisted image analysis to compare autoradiographic signals resulting when varying concentrations of ^{35}S-labeled cRNA probes, dextran sulfate (DS), and dithiothreitol (DTT) were used for ISHH. We found that greatly enhanced corrected signal density (total density of signal area minus background density) was obtained using concentrations of probe and/or DS that were several-fold higher than those widely recommended in published ISHH procedures (probe concentration $>4 \times 10^4$ cpm/μl; DS concentration >10%). Extended hybridization reaction (>16 hr) also significantly augmented the corrected signal density. Finally, nonspecific probe binding was greatly reduced and corrected signal density enhanced by including 750–1000 mM, rather than the widely used 10–200 mM DTT, in the hybridization buffer. These observations indicate that the low efficiency of hybridization and the formation of high background may largely compromise the sensitivity of routine ISHH procedures. We suggest that the new method using increased concentrations of ^{35}S-labeled cRNA probe, DS, and DTT will be especially important for the cellular localization of rare mRNA species.

(J Histochem Cytochem 50:1389–1400, 2002)

KEY WORDS
autoradiography
background
brain
complementary ribonucleic acid probes
dextran sulfate
dithiothreitol
image analysis
in situ hybridization
quantitation
radioisotope

DETECTION of mRNA expression with in situ hybridization histochemistry (ISHH; Gall and Pardue 1969) uses radioisotopically- or non-radioisotopically-labeled nucleic acid probes with antisense nucleotide sequences (Höfler et al. 1998). Variables that influence the sensitivity of the ISHH technique include (a) the type, quality, and method of detection of the hybridization probe, (b) the effects of tissue fixation on target mRNA preservation and accessibility to probe, (c) the efficiency of hybrid formation, (d) the stability of in situ formed hybrids during posthybridization treatments and, finally, (e) background noise masking the hybridization signal (Höfler et al. 1998). Strategies designed to optimize these variables can improve the sensitivity of ISHH (e.g., Nunez et al. 1989; Petersen and McCrone 1994; Guiot and Rahier 1995; Zoeller et al. 1997).

The detection of rare mRNA species in individual neurons of the brain requires ISHH techniques that provide high sensitivity and also allow single-cell resolution. Recently, we observed that increasing concentrations of ^{35}S-labeled cRNA hybridization probes, dextran sulfate (DS), and dithiothreitol (DTT) in the hybridization solution could noticeably enhance the autoradiographic hybridization signal for mRNAs encoding estrogen receptor isoforms. Application of this reformulated, but not the standard, hybridization solution enabled us to detect low expression levels of es-

Correspondence to: Dr. Erik Hrabovszky, Dept. of Neurobiology, Inst. of Experimental Medicine, Hungarian Academy of Sciences, Budapest 1083, Hungary. E-mail: hrabovszky@koki.hu

Received for publication February 5, 2002; accepted May 1, 2002 (2A5741).

0022-1554/02/$3.30

trogen receptor-β (ERβ) mRNA in the majority of luteinizing hormone-releasing hormone neurons (Hrabovszky et al. 2000). It is critical to note that several control approaches, including recent immunocytochemical studies (Hrabovszky et al. 2001), confirmed the specificity of ERβ hybridization signal generated by the modified ISHH method. The unexpected dependence of hybridization signal on probe concentration conflicted with the common assumption that the conditions of the ISH reaction should satisfy the criterion to "saturate" target mRNA molecules in the tissue specimen (Nunez et al. 1989; Davenport 1998). Our findings raised the possibility that suboptimal hybridization conditions represent a general, albeit commonly overlooked, source of sensitivity loss in hybridization experiments.

The present studies were conducted to formally establish whether routine hybridization procedures provide submaximal hybridization signals. In addition, strategies were developed to improve the detection sensitivity of the ISHH method. To accomplish these aims, we assessed the impact of increased radioisotopic probe (>40,000 cpm/μl), DS (>10%), and DTT (>200 mM) concentrations in the hybridization solution, and also evaluated the influence of an extended hybridization time (>16 hr) on levels of autoradiographic hybridization signal and background.

Materials and Methods

Tissue Preparation

Adult female Sprague–Dawley rats (n=3; 225 g bw) were maintained and treated in accordance with the NIH Guide for the Care and Use of Laboratory Animals and the University of Massachusetts IAUCC. After sacrifice of animals with CO_2, brains were removed and snap-frozen on pulverized dry ice. Twelve-μm coronal sections through the cerebral cortex were prepared on a cryostat, thaw-mounted onto double gelatin-coated microscopic slides, dried, and stored in slide boxes at −80C as described previously (Petersen and McCrone 1994).

Preparation of cDNA Templates for In Vitro RNA Transcription

Both sense and antisense RNA probe sequences were used for hybridization assays. To ensure that results obtained were not probe-specific, we used several cRNA probes, each of which produced hybridization signal in the cerebral cortex. The cDNA template for androgen receptor (AR; Lubahn et al. 1988) was a 1016-bp fragment corresponding to bases 2821–3838 (generously provided by Dr. R. Handa). To prepare probes to the γ2 subunit of GABA-A receptor mRNA, a 304-bp cDNA template (gift from Dr. C.D. Carpenter), corresponding to nucleotides 1530–1833 (Shivers et al. 1989), was used. The 678-bp galanin cDNA was kindly provided by Dr. M.E. Vrontakis (Vrontakis et al. 1987). Finally, the 548-bp BamH1-Sal1 fragment of the rat progesterone receptor (PR) cDNA [rPR-1; generously provided by Dr. O.K. Park–Sarge (Park–Sarge and Mayo 1994)], was used as template for in vitro RNA transcription.

In Vitro Transcription of Antisense and Sense RNA Probes

The 10-μl transcription reactions were composed of the following ingredients: [^{35}S]-UTP (NEN Life Science Products; Boston, MA), 120 pmol; linearized cDNA template, 1 μg; 5 × transcription buffer, 2 μl; 100 mM DTT (Sigma Chemical; St Louis, MO), 1 μl; 10 mM ATP, CTP, and GTP, 0.5 μl of each; 20 U/μl RNasin (Promega; Madison, WI), 0.5 μl; appropriate RNA polymerase (T3, T7, or SP6; Promega), 10 U. The reaction was allowed to proceed for 30 min at 37C. Then a second aliquot of RNA polymerase (10 U) was added and the mixture incubated for a second period of 30 min. After incubation, the volume was brought up to 90 μl with nuclease-free water, and we added 5 μl 1 M Tris-HCl buffer (pH 8.0), 1 μl tRNA, (25 mg/ml; Sigma), 1 μl 1 M $MgCl_2$, 0.5 μl 20 U/μl RNasin (Promega), and 0.5 μl 10 U/μl DNase I (Roche Diagnostics; Indianapolis, IN). The template DNA was digested for 30 min at 37C, and finally the probe was purified by extraction with phenol/chloroform/isoamyl alcohol, then with chloroform/isoamyl alcohol. Unincorporated nucleotides were removed by two sequential NaCl/ethanol precipitations. The probe pellets were finally dissolved in 0.1% sodium dodecyl sulfate (SDS; Sigma) and radioactivity concentrations (in terms of cpm/μl) determined using a Beckman LS 6000 SC β-counter.

Preparation of Hybridization Buffer

The standard hybridization buffer was modified from a previously described formulation (Petersen and McCrone 1994) and contained the following: 50% ultra-pure formamide (Sigma), 2 × standard saline citrate (SSC) solution (1 × SSC = 0.15 M NaCl/0.015 M sodium citrate, pH 7.0), 10–30% DS (500,000 MW; Sigma), 1 × Denhardt's solution (0.02% each of bovine serum albumin, Ficoll, and polyvinylpyrrolidone; Sigma), 500 μg/ml yeast tRNA (Sigma), 500 μg/ml heparin sodium salt (Sigma), and 0.1% sodium pyrophosphate (Sigma). Immediately before use, the hybridization buffer was warmed to 56C and 200–1000 mM DTT (Sigma) was added and dissolved by vortexing. Changes in various components of this buffer are described for single test experiments.

Prehybridization Tissue Treatment Steps

Before ISHH, the slides were removed from the −80C freezer, warmed to RT (10 min), and loaded into RNase-free metal racks. The racks were placed in RNase-free plastic containers and sections were processed through the following prehybridization steps: 30-min fixation in phosphate-buffered (pH 7.4) 4% formaldehyde solution; 2-min rinse in 2 × SSC solution; 10 min acetylation in 0.25% acetic anhydride (Sigma)/0.9% NaCl/0.1 M triethanolamine (pH 8.0; Sigma) (Tecott et al. 1987); a brief rinse in 2 × SSC solution; dehydration in 70, 80, 95, and 100% ethanol (2 min each); delipidation in chloroform (5 min), then partial rehydration in 100% followed by 95% ethanol (2 min each). The slides were finally air-dried on trays.

In Situ Hybridization

The slides were placed in Nalgene boxes in which the air was humidified using caps of 50-ml centrifuge tubes containing distilled water. Twenty-five μl of hybridization solution was pipetted onto each section and covered with a glass coverslip. The standard hybridization reaction was carried out at 56C for 16 hr (overnight).

Posthybridization Tissue Treatment Steps

The coverslips were floated off the slides in 1 × SSC solution and the excess of hybridization solution was rinsed off in three changes of 1 × SSC solution. Then the slides were loaded into metal racks and the following incubation steps were carried out under agitation: 1 × SSC (RT), twice for 20 min; 50% formamide/2 × SSC mixture (52C), twice for 30 min; 2 × SSC (RT), 10 min; 50 μg/ml RNase A (Roche Diagnostics) dissolved in 500 mM NaCl/10 mM Tris-HCl/1 mM EDTA, pH 7.8, 37C), 30 min; rinse in 2 × SSC (RT), 10 min; 50% formamide/2 × SSC (52C), 30 min. Finally, the slides were rinsed in 2 × SSC buffer at RT (10 min), dipped briefly in distilled water (2 sec), rinsed in 70% ethanol (10 min), and air-dried on slide trays.

X-ray Autoradiography

For X-ray autoradiography, the slides were aligned in exposure cassettes and apposed to Kodak β-Max autoradiographic films for 2–14 days. The autoradiographs were developed with a Konica SRX-101A automated film processor.

Emulsion Autoradiography

After the development of film autoradiographs, the slides were dipped in Kodak NTB-3 nuclear emulsion (diluted at 1:1 with distilled water) and exposed for 1–4 weeks. The images were developed using Dektol developer (Kodak; Rochester, NY) for 2 min, rinsed with distilled water for 30 sec, and fixed with Kodak fixer for 5 min. Then the sections were rinsed in distilled water for 5 min and dried on slide trays.

Coverslipping of Sections

The sections were immersed in xylenes for 2 min, then coverslipped using DPX mounting medium (Fluka Chemie; Buchs, Switzerland) and used for light microscopic evaluation.

Computerized Semi-quantitative Image Analysis of X-ray Film Autoradiographs

X-ray films were placed on a light box and images were captured and digitized using a BioQuant Windows image analysis system (R and M Biometrics; Nashville, TN) interfaced with a CCD video camera (Hitachi Denshi; Tokyo, Japan) and an AF MicroNikkor 60-mm objective. The average gray level of highlighted pixels (on a 0–255 scale) was measured over a similar region of the cingulate cortex or the retrosplenial cortex in each section to determine the total density of the signal area ("total signal density"). In addition, "background density" measurement was taken over the white matter of the corpus callosum in each section. The background density measurement was subtracted from the total signal density to obtain the "corrected signal density" value. The mean of replicate measurements was determined for each test group, and means were compared by ANOVA. Newman–Keuls tests were performed post hoc when indicated.

Processing of Photographic Images

Representative film autoradiographs from each group were used for photographic illustrations. In addition, emulsion autoradiographs were examined using a Nikon light microscope and photographed with the CCD video camera. Digital images were processed using Adobe Photoshop 4.0 software (Tucson, AZ). In each experiment, representative photographs were merged into a single table before editing to maintain a reliable visual comparison of individual panels.

Preparation of RNase A-pretreated Sections for Control Studies

The slides were removed from the −80C freezer, placed in Coplin jars, and fixed for 10 min in acetone. The sections were air-dried briefly, then incubated in RNase A solution (50 μg/ml; Roche Diagnostics) for 30 min, as described above. To remove residual RNase A from the sections, the slides were rinsed abundantly with 2 × SSC solution (five times for 5 min). Formaldehyde fixation and further prehybridization treatment steps of the RNase-treated sections were performed in the same way as for untreated sections.

Results

Application of 1000 mM Instead of 200 mM DTT to Reduce Background Density of X-ray Film Autoradiographs

In practice, the use of high amounts of radioisotopic probe is limited by the formation of unacceptably high nonspecific background. In an attempt to overcome this problem, we addressed the advantage of increasing the concentration of DTT from 200 mM to 1000 mM in the hybridization solution. A sense-strand RNA transcript to the GABA A γ2 receptor subunit was used for the first hybridization experiment in the presence of either 200 mM or 1000 mM DTT. Because the pattern of background generated by this probe was not similar to the distribution of neuronal cells (Figures 1A–1D), it was unlikely that cross-hybridization of the probe to tissue nucleic acids contributed to the background we observed. Test experiments were performed using our standard hybridization solution containing 40,000 cpm/μl probe and 10% DS, as well as a modified hybridization solution that included a largely elevated probe concentration (200,000 cpm/μl) and 20% instead of 10% DTT, which further increased the effective concentration of the probe (Wahl et al. 1979). For research design, see overlays in Figures 1A–1D and table in Figure 2. Background levels over both the white matter (corpus callosum) and the gray matter (cingulate cortex) were analyzed and com-

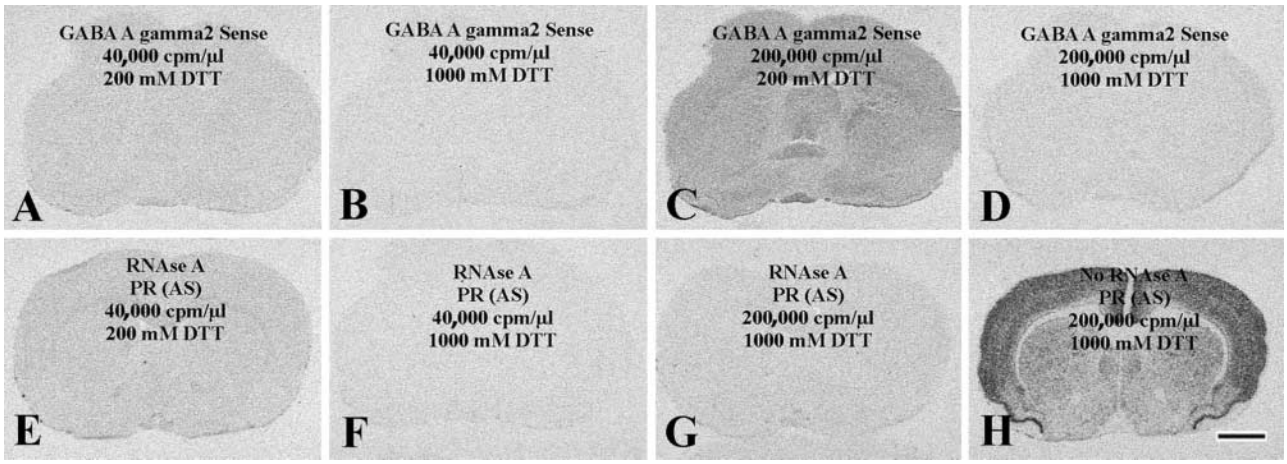

Figure 1 Reduced nonspecific probe binding after application of 1000 mM instead of 200 mM DTT in the hybridization solution. (**A–D**) Comparative use of 200 mM (**A,C**) vs 1000 mM (**B,D**) DTT in a standard (40,000 cpm/µl probe–10% DS; **A,B**) and a reformulated (200,000 cpm/µl probe–20% DS; **C,D**) hybridization solution. Lower background resulted if sections were hybridized with the ^{35}S-labeled sense-strand GABA-A γ2 RNA transcript in the presence of elevated DTT (compare **B** to **A** and **D** to **C**). (**E–G**) Differential effects of 200 mM (**E**) and 1000 mM (**F,G**) DTT on nonspecific binding of the antisense PR probe to RNase A-pretreated sections. Elevated DTT (1000 mM) decreased nonspecific probe binding using common probe (40,000 cpm/µl) and DS (10%) concentrations (compare **F** to **E**) and efficiently prevented background formation if greatly enhanced probe (200,000 cpm/µl) and DS (20%) concentrations were applied (**G**). (**H**) High probe (200,000 cpm/µl) and DS (20%), in the presence of high DTT (1000 mM), was a successful approach to generate low background (white matter regions) and high signal density (e.g., in the cerebral cortex) in the RNase A-untreated control section. Bar = 2.5 mm.

pared using three-way ANOVA, with main effects of DTT concentration (200 mM vs 1000 mM), probe DS contents (40,000 cpm/µl-10% vs. 200,000 cpm/µl-20% DS) of the hybridization solution, and tissue characteristics (white matter vs gray matter).

We found that the use of DTT at 1000 mM instead of 200 mM significantly reduced background density ($F=1463.18$; $p<0.05$). Compare Figures 1B to 1A and Figures 1D to 1C and blocks 2B to 2A and 2D to 2C in Figure 2. The extent of reduction was high when increased amounts of probe (200,000 cpm/µl) and DS (20%) were used (32% in the white matter; compare blocks 2D to 2C in Figure 2), as opposed to the slight (but significant; $p<0.05$) reduction observed using the standard probe (40,000 cpm/µl) and DS (10%) concentrations of our procedure (18% in the white matter; compare blocks 2B to 2A in Figure 2).

The inclusion of enhanced probe/DS concentrations in the hybridization solution significantly augmented background density ($F=549.64$; $p<0.05$), as shown by the comparison of Figure 1C to Figures 1A and 1D to Figure 1B and blocks in Figure 2C to 2A and Figure 2D to 2B. Background density enhancements were robust if the hybridization buffer contained 200 mM DTT (30%; compare blocks 2C to 2A in Figure 2) and slight if the hybridization solution contained 1000 mM DTT (7%; compare blocks 2D to 2B in Figure 2).

Tissue characteristics (white or gray matter) also exerted a statistically significant effect on background ($F=9.94$; $p<0.05$). Newman–Keuls test showed that film density over the white matter was significantly higher ($p<0.01$) than over the gray matter (Figure 1C; compare the two columns in block C of Figure 2) if high probe/DS were combined with low DTT. In contrast, background was evenly distributed between the white matter and the gray matter when we used the low probe/DS combination with low DTT ($p=0.18$; Figure 1A; compare the two columns in block A of Figure 2), low probe/DS with high DTT ($p=0.59$; Figure 1B; two columns in block B of Figure 2) or high probe/DS in the presence of high DTT ($p=0.79$; Figure 1D; two columns in block D of Figure 2).

A second experiment used RNase A-pretreated sections for hybridization with an antisense PR probe. This approach was designed to prevent any hybridization to occur between the probe and tissue RNA molecules (Tecott et al. 1987; Höfler et al. 1998; Sunday 1998). The effects of DTT concentration (200 mM vs 1000 mM), probe–DS concentrations (40,000 cpm/µl probe–10% DS vs 200,000 cpm/µl probe–20% DS) and tissue characteristics (white vs gray matter) on background density were significant ($p<0.05$; analysis not detailed) and entirely reminiscent to the observations made using the sense-strand GABA A γ2 receptor subunit probe (compare Figures 1E to 1A, 1F to 1B, and 1G to 1D in representative photomicrographs obtained using identical probe, DS, and DTT concentrations). In addition, the modified hybridization procedure simultaneously using high DTT (1000 mM), high probe (200,000 cpm/µl), and high DS (20%) concentrations in RNase A-untreated control sections generated autoradiographic images characterized by high

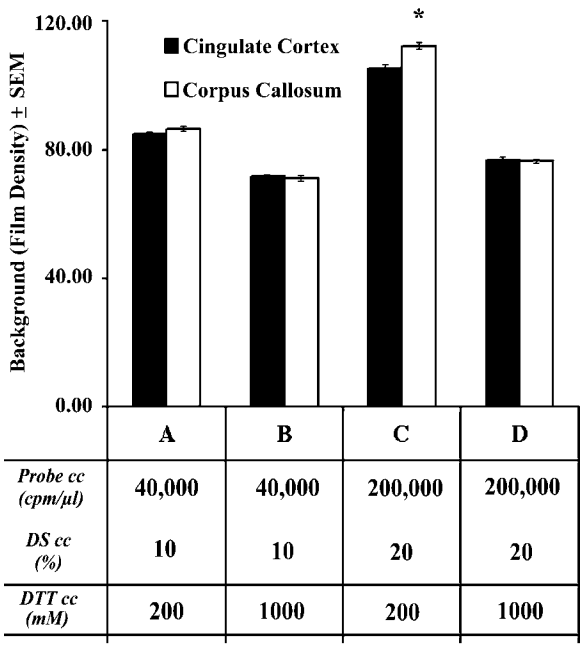

Figure 2 Quantitative analysis of autoradiographic background as an effect of elevated DTT concentration, increased (sense) probe–DS concentrations, and tissue characteristics. The application of 1000 mM (**B,D**) vs 200 mM (**A,C**) DTT significantly ($p<0.05$) reduced background density, whether 40,000 cpm/µl GABA-A γ2 sense probe in combination with 10% DS (**B** vs **A**) or 200,000 cpm/µl probe together with 20% DS (**D** vs **C**) was used. Enhanced probe–DS concentrations significantly ($p<0.05$) elevated background in **C** vs **A** and **D** vs **B**. Tissue characteristics (white vs gray matter) only exerted significant effect on background when the combination of high probe–DS and low DTT concentrations (**C**) was used. *Background was significantly higher in white vs gray matter ($p<0.05$). Representative sections of each group are illustrated in Figures 1A–1D. Statistical analysis is discussed in the text.

signal and low background labeling (compare signal density in gray matter vs background density in white matter structures in Figure 1H).

Effects of Increased Probe, Increased DS, or Both, on Hybridization Signals

To address the potential advantage of using increased probe and increased DS concentrations in the hybridization solution, consecutive sections were divided into nine groups (six to eight sections/group) and hybridized for 16 hr with the antisense probe to the γ2 subunit of the GABA-A receptor, using three different concentrations of probe (40,000, 80,000, or 120,000 cpm/µl) and DS (10, 20, or 30%) in the hybridization solution. High amounts of DTT (750 mM) were added to the hybridization buffer to suppress nonspecific probe binding. After posthybridization treatments, the slides were exposed to X-ray films for 50 hr, then the autoradiographs were developed (Figure 3). Corrected signal density was determined in each treatment group (Figure 5) and two-way ANOVA, with DS concentration and probe concentration as main effects, was performed. Autoradiographs derived from ^{14}C standards (using empty film density for background correction) were also analyzed to determine the ^{14}C radioisotope concentrations causing identical corrected density to individual groups of hybridized sections. Finally, the full set of sections used in this experiment was coated with nuclear track emulsion. The emulsion autoradiographs were developed after 7 days of exposure and were used for light microscopic evaluation of hybridization signals in the cingulate cortex (Figure 4).

The distribution pattern of hybridization signal for the GABA A γ2 mRNA was identical using any combination of DS and probe concentrations, but film density differed largely in each group (Figure 3). Corrected signal density of the cingulate cortex showed robust enhancements as probe and/or DS contents of the hybridization solution increased (Figure 5). The influences of probe ($F=63.59$; $p<0.01$) and DS ($F=864.80$; $p<0.01$) concentrations were statistically significant. Furthermore, they showed significant interaction ($F_{1,2}=3.67$; $p<0.01$) (Figure 5). The corrected signal density produced by our routine hybridization procedure was increased approximately fourfold in this experiment by raising probe and DS concentrations (compare the last column to the first column in Figure 5 and Figures 3I to 3A). A similar enhancement of corrected density could be generated by a tenfold increase in ^{14}C radioisotope concentration (radioactivity/area), as we established by the analysis of co-exposed ^{14}C standards. In addition, emulsion autoradiographs of the cingulate cortex (Figures 4A–4I) demonstrated that individual neurons gained improved definition by the clustering of silver grains when probe and/or DS was used at increased concentrations. Diffuse background, represented by homogeneously scattered grains in the molecular layer of the cingulate cortex (middle portion of individual panels in Figure 4), was negligible in all groups.

Use of a Series of Different Test Probes to Extend the Validity of the Concept that Routine Hybridization Conditions Produce Submaximal Hybridization Signals

We used a series of test probes to various targets (galanin, PR, and AR mRNAs) and of different lengths to address the issue of whether increased concentrations of probe and/or DS can further increase hybridization signals (corrected signal density). Results of ISHH studies using the galanin (Figures 6A–6D), the PR (Figures 6E and 6F), and the AR (Figures 6G and 6H) probes under various test conditions uniformly indicated that increased signal intensities could be achieved as probe and/or DS concentrations were in-

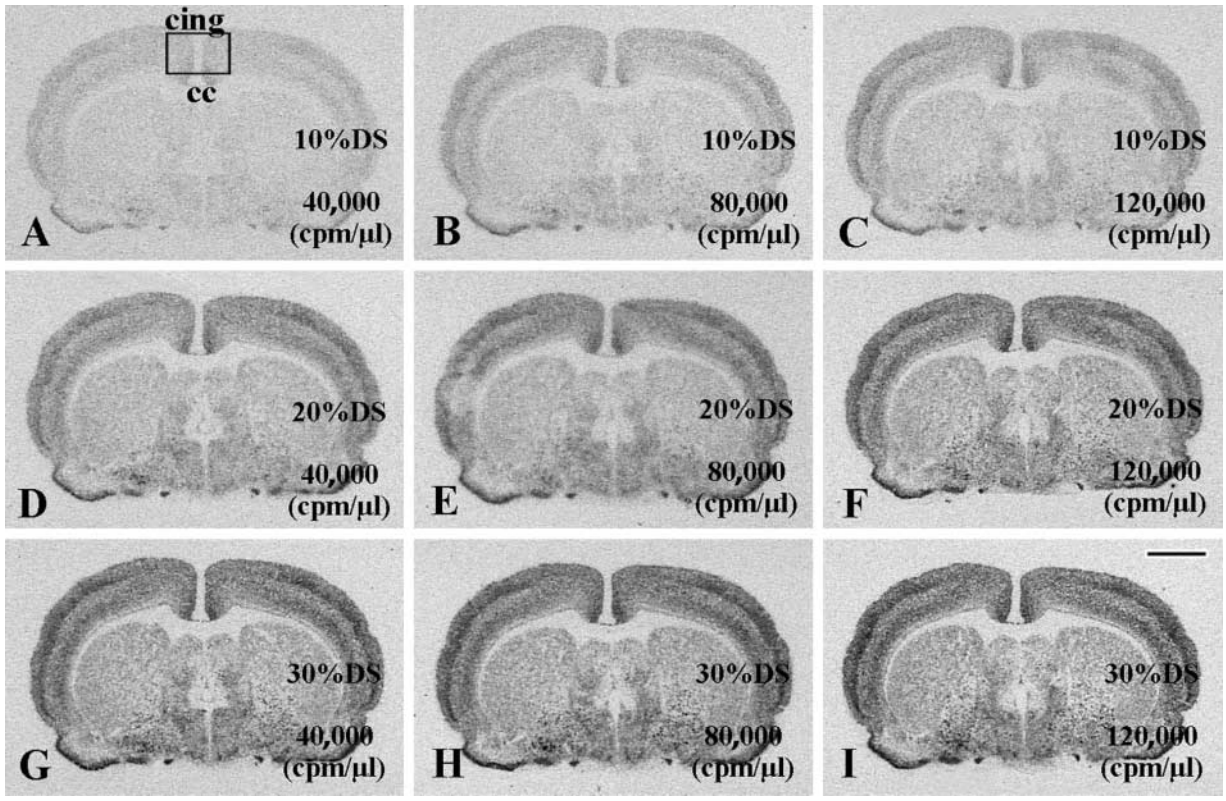

Figure 3 X-ray film autoradiographs illustrating enhanced hybridization signals after application of increased GABA-A γ2 probe and DS concentrations. The lowest signal produced by the standard formulation of hybridization solution (40,000 cpm/µl probe and 10% DS) in **A** could be greatly enhanced by using increased concentrations of probe (from left to right), DS (downward), or both. Emulsion autoradiographs of **A–I** (corresponding to the framed area of the cingulate cortex in **A**) are shown in Figure 4. For corrected signal density of single groups, see Figure 5. cing, cingulate cortex. Bar = 2.5 mm.

creased in the presence of 800 mM DTT. For each test probe, the effects of increased probe (in Figures 6B vs 6A, Figures 6F vs 6E) and increased DS (in Figures 6D vs 6B and Figures 6H vs 6G) concentration on corrected signal densities were statistically significant by one-way ANOVA ($p<0.05$). These findings corroborated the idea that the lower probe and DS concentrations did not allow target mRNA saturation to occur.

Use of Extended Hybridization Time as an Alternative to Increased Probe to Further Verify the Concept that Regular Hybridization Reactions are Incomplete

On the basis of the concept that incomplete hybridization reactions should provide higher signals if allowed to proceed longer, the hybridization time was extended from the commonly used 16 hr (overnight hybridization; Angerer and Angerer 1981) to 40 hr. High DTT (800 mM) in the hybridization solution was used to suppress nonspecific probe binding. The first group of slides was removed from the incubator after 16 hr of hybridization with the antisense PR probe, then processed through posthybridization treatments. The second set of slides was hybridized for 40 hr and then processed through identical posthybridization steps. Using any probe–DS combinations, the extended hybridization reaction (40 hr vs 16 hr) augmented significantly (one-way ANOVA; $p<0.05$) the corrected signal density of the retrosplenial cortex (compare Figures 7E to 7A, 7F to 7B, 7G to 7C, and 7H to 7D). This observation was in harmony with the concept that hybridization reactions did not come to completion after 16 hr.

Titration of The Probe Concentration that Generates Maximal Corrected Signal Density

A broad range of probe concentrations were tested to establish hybridization conditions that provide maximal corrected signal density in a 16-hr hybridization reaction. To minimize background associated with high amounts of radioisotope in the hybridization solutions, the test experiment used a PR probe that was labeled to low specific activity in the presence of 108 µM UTP and 12 µM [^{35}S]-UTP. Using this approach,

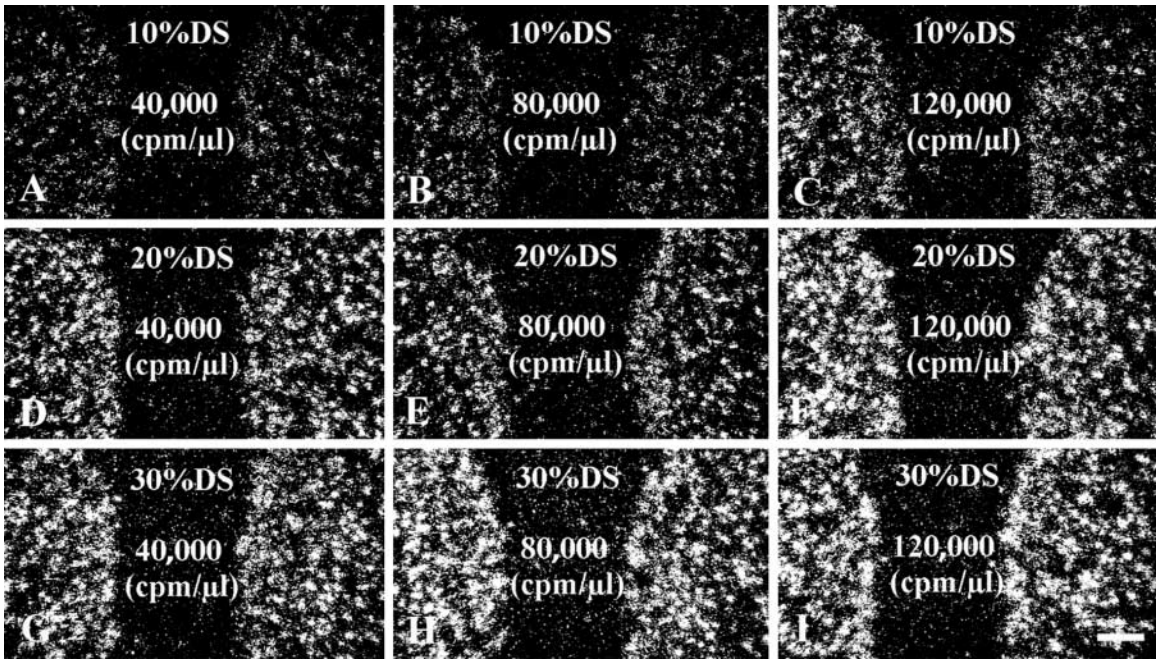

Figure 4 Emulsion autoradiographs showing enhanced hybridization signals after application of increased GABA-A γ2 probe and DS concentrations. **(A–I)** Increasing GABA A γ2 probe (left to right) and dextran sulfate (DS; downwards) concentrations, alone or in combination, enhanced the hybridization signal (amounts of silver grains) in individual cortical neurons. The standard ISHH procedure (40,000 cpm/μl probe and 10% DS) produced only low levels of autoradiographic signal in **A** (note the poor clustering tendency of silver grains over individual neurons of the cingulate cortex), whereas well-defined grain clusters were obtained by the application of increased probe and/or DS. Scattered silver grains in layer 1 of the cerebral cortex (middle portion of each panel) represent low levels of background, which was a clear benefit of high DTT content (750 mM) in the hybridization buffers. Bar = 350 μm.

the "plateau" phase of the hybridization reaction was expected at tenfold lower radioisotope concentration than using a probe labeled to maximal specific activity (in the absence of unlabeled UTP). Probe concentrations ranging from 4,000 cpm/μl to 176,000 cpm/μl were tested in a hybridization buffer that contained 20% DS and 1000 mM DTT. For each section group hybridized, mean total density, background density, and corrected signal density values were determined from film autoradiographs. For experimental design, see columns in Figure 8. Results of this study established that the highest value of corrected signal density (asterisk in Figure 8) was obtained using 20% DS and 40,000–64,000 cpm/μl probe. When compared with results of the standard procedure (10% DS and 4,000 cpm/μl of the low specific-activity test probe), this represented a threefold total increase of corrected signal density, of which 80% was already achieved by simultaneously raising DS from 10% to 20% and probe from 4000 to 16,000 cpm/μl. We also found that increasing the concentration of probe from 64,000 cpm/μl to 88,000 cpm/μl or further tended to slightly decrease the computable value of corrected signal density. This phenomenon was a consequence of a sudden rise in background density (Figure 8).

Discussion

The results of these studies demonstrate that the sensitivity of conventional ISHH procedures can be improved significantly by increasing the concentrations of ^{35}S-labeled cRNA probe (>40,000 cpm/μl), DS (>10%), and DTT (>200 mM) in the hybridization solution, or by using an extended hybridization reaction time (>16 hr). These modifications will facilitate the cellular localization of low-abundance mRNAs in brain and other tissues.

The Concept of Target mRNA Occupation (Saturation)

A plateau phase in hybrid formation was demonstrated in vitro using immobilized nucleic acid targets (Galau et al. 1977a,b). Although the kinetics of the ISH reaction are far more complex, various hybridization protocols used in the literature are based on the assumption that most targeted mRNA molecules in the tissues would be bound to probe by the end of the hybridization period (saturation phenomenon) (Nunez et al. 1989; Davenport 1998). In contrast to this concept, the results of the present studies demonstrate that the corrected signal density is still submaximal when ^{35}S-labeled cRNA probe and DS are used at the

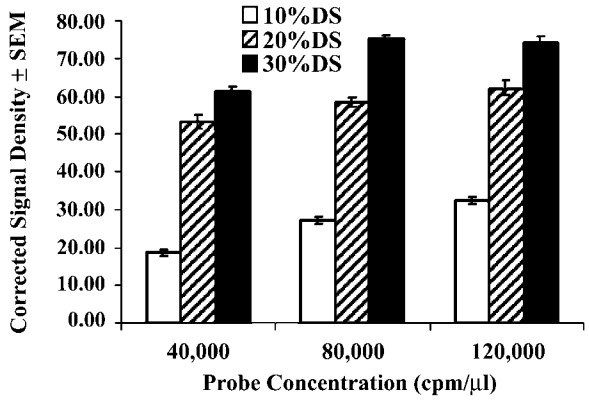

Figure 5 Effects of varying GABA-A γ2 probe (40,000, 80,000, or 120,000 cpm/μl) and DS (10, 20, or 30%) concentrations on corrected signal density of the cerebral cortex. Increased probe and increased DS concentrations significantly ($p<0.01$) enhanced the computable values of corrected signal density, and their effects were synergistic ($p<0.01$). Representative sections of each group were used for photographic illustrations in Figures 3 and 4. For detailed statistics, see text.

highest concentrations we encountered in the literature. It is important to point out that the enhancement of corrected signal density by increased probe and/or increased DS required an improved protection against background formation, which we were able to achieve by the inclusion of 750–1000 mM instead of 10–200 mM DTT in the hybridization mixture. Without this modification we found that the use of increased probe and/or DS generated extremely high background over both signal and background regions, often reducing the corrected signal density value. Although specific probe binding (hybridization) to the signal area was probably increased in the presence of low DTT concentrations, the enhancement of background density appeared to exceed the enhancement of total cortical density (resulting from enhanced specific and nonspecific probe binding), with a net result of a reduced corrected signal density. Studies showing the non-linear optical density response of X-ray films to radiation (film grayness increases to a lesser extent than does radioactivity in the corresponding tissue area; Kuhar et al. 1985; Davenport 1998) provide a partial explanation of this phenomenon. It also follows that the "maximal corrected signal density" and the "highest signal-to-background ratio" in a saturation experiment using gradually increasing concentrations of probe for hybridization indicate mRNA target saturation only if background noise can be kept at a constant level. Because the simultaneous use of 1000 mM DTT and a low specific activity PR probe in our saturation experiment generated background levels that were unaffected by a broad range of probe concentrations, it is probable that the probe concentrations approaching the corrected signal density plateau, were close to "saturation" of most of the hybridizable mRNA targets. The formation of a corrected signal density plateau at stable background levels was a fundamental observation in this study, supporting the basic concept that a finite number of target molecules were present in the tissue for hybridization with the PR probe.

DTT Concentration

Although the mechanism by which DTT reduces nonspecific background is only partially understood (Zoeller et al. 1997), DTT at 10–200 mM represents a basic component of the hybridization solution. Our hybridization experiments using either sense-strand RNA transcripts or antisense probes on RNase A-pre-

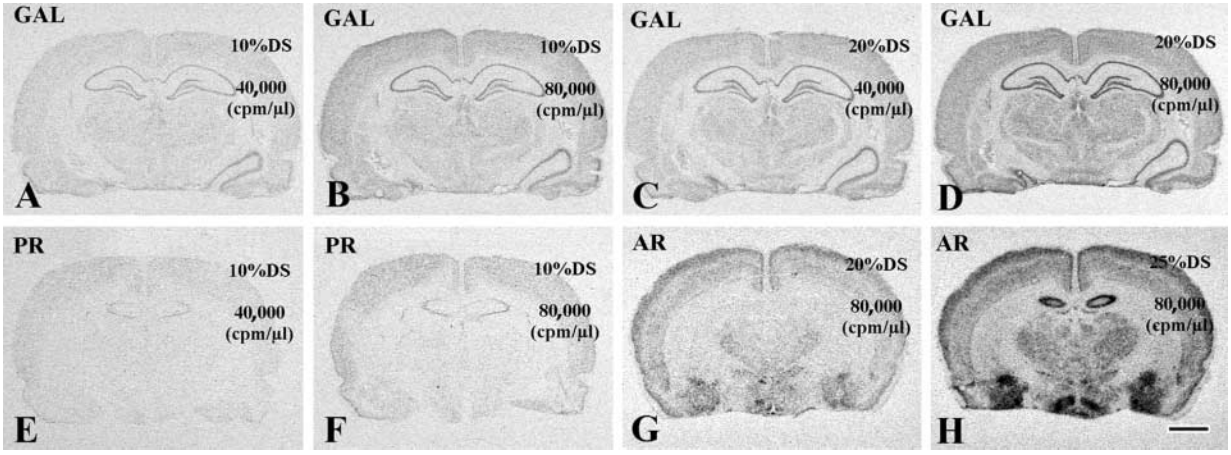

Figure 6 Enhanced ISHH signals after use of increased probe or DS concentrations. Use of test probes to galanin (**A–D**), PR (**E,F**), and AR (**G,H**) mRNAs established that either increased probe (compare **B** to **A**, **D** to **C**, and **F** to **E**) or increased DS (compare **C** to **A**, **D** to **B**, and **H** to **G**) concentrations were able to enhance the ISHH signals. Corrected signal densities by ANOVA differed significantly ($p<0.05$) among these treatment pairs. Bar = 2.5 mm.

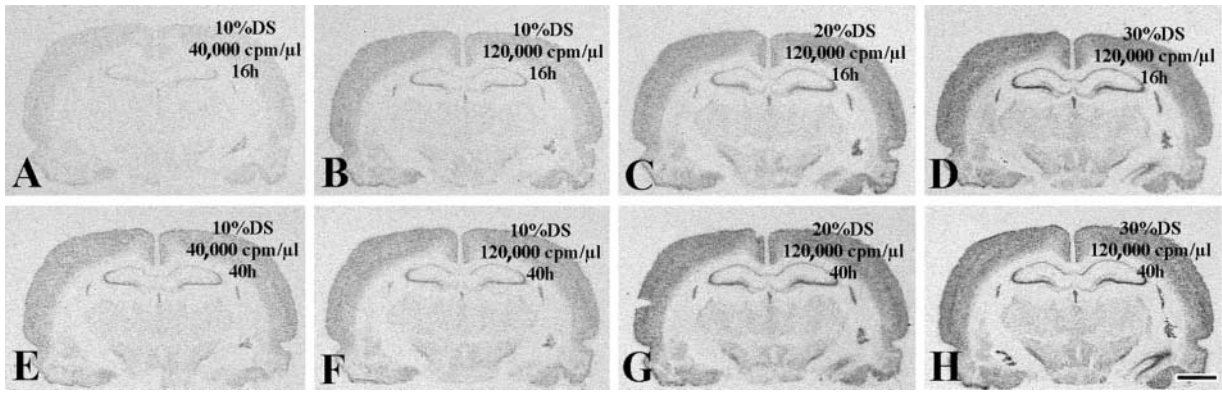

Figure 7 Use of extended hybridization reactions to enhance the ISHH signals. **(A–H)** The application of 40-hr (lower panels) instead of 16-hr (overnight; upper panels) hybridization reactions provided enhanced hybridization signals using various amounts of probe and DS in the hybridization solution. Corrected signal densities were significantly higher ($p<0.05$) in lower than in corresponding upper panels, indicating that saturation of target mRNA was not accomplished in 16 hr. Bar = 2.5 mm.

treated sections established that the ability of DTT to reduce background can be largely enhanced by raising its concentration from 200 mM up to 1000 mM in the hybridization solution. Increased DTT was able to reduce background at any probe and DS concentrations we tested, but its use became critically important when elevated probe and/or DS concentrations were present in the hybridization solution. These data encourage the routine application of 750–1000 mM DTT in the hybridization solution as an efficient tool to prevent high background.

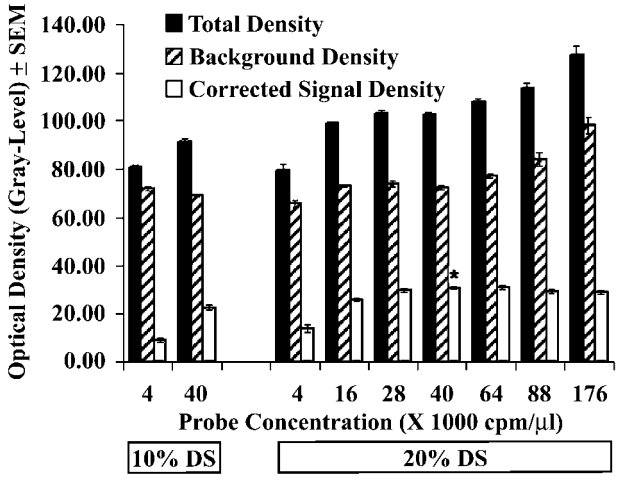

Figure 8 Total cortical density, background density and corrected signal density of ISH autoradiographs using increasing amounts of a low specific-activity PR probe for a saturation experiment. Compared to the standard procedure (here: 4,000 cpm/µl probe and 10% DS; first column), the maximal corrected signal density (asterisk) required the use of a tenfold probe excess (40,000 cpm/µl) and 20% instead of 10% DS in the hybridization solution. Note that background remained relatively stable below 64,000 cpm/µl probe, but then it suddenly increased, thus producing a slight reduction of corrected signal density at the highest probe concentrations.

The Rate of Hybrid Formation

Nucleic acid hybridization to immobilized targets follows pseudo-first-order kinetics if probe is in large access (Galau et al. 1977a,b). Despite its higher complexity, the ISHH reaction has been postulated to follow similar reaction kinetics (Tecott et al. 1987). It is interesting to note that the strong impact of probe concentration on hybridization signal, which we report here, is incompatible with pseudo-first-order reaction kinetics.

Probe Concentration

The enhancements of corrected signal density after application of increased probe concentrations were robust and reproducible using a variety of cRNA probes to different mRNA targets and of various lengths. Application of the low specific-activity PR probe in the presence of 1000 mM DTT revealed that a corrected density plateau was approached only with probe concentrations an order of magnitude higher than those recommended in published ISHH procedures and with 20%, instead of 10% DS, in the hybridization buffer, which further enhanced the effective probe concentration (Wahl et al. 1979). The use of increased probe and DTT concentrations represents a promising and novel approach to enhancing the sensitivity of in situ mRNA detection. Nevertheless, the high cost of the radioisotope and the increased problem of radioactive waste management are important issues that must be considered.

DS Concentration

Consistent with the concept that DS increases the effective probe concentration by excluding probe molecules from the volume occupied by the polymer (Wahl et al. 1979), when the same probe concentration was used the application of 20% or 30% DS in the hybrid-

ization buffer yielded consistently higher autoradiographic signals (corrected signal densities) than did 10% DS. Therefore, high amounts of DS or substitute macromolecules in the hybridization mixture offer efficient and inexpensive alternatives to the use of high-radioisotopic probe concentrations.

Detection Sensitivity

The practical value of using probe, DS, and DTT at increased concentrations will be the enhanced detection sensitivity of the isotopic ISHH procedure. This expectation is supported by our recent observation of ER-β mRNA expression in the majority of LHRH neurons, which required the simultaneous application of high probe, high DS, and high DTT in the hybridization solution (Hrabovszky et al. 2000). In our present studies using the GABA A γ2 cRNA probe, the advantage of these modifications was confirmed by the markedly improved clustering of silver grains over individual cortical neurons. In the same experiment, the difference we found between the lowest and the highest corrected signal density of film autoradiographs was comparable to a 10-fold difference in ^{14}C radioisotope concentration on co-exposed radioisotope standards. Although without the use of appropriate tissue paste calibration standards (Davenport et al. 1988; Davenport 1998; Palfi et al. 1998; Vizi and Gulya 2000) and precise background correction methods, these data did not enable us to precisely determine the extent to which target mRNA molecules remained unoccupied using the standard hybridization procedure. Similarities between ^{14}C plastic standards and ^{35}S-labeled brain tissue paste standards (Miller 1991) indicate that the lowest probe and DS concentrations left most target mRNA molecules unhybridized in this study.

Autoradiographic Background

One must be aware that increased probe and DS may amplify hybridization artifacts, in addition to the advantage of enhancing detection sensitivity. Two distinct categories of nonspecific probe–tissue interactions we have to consider (Höfler et al. 1998) include the binding of probe to non-nucleic acid tissue constituents and the cross-hybridization of probes with nucleic acids exhibiting partial sequence homology with the target (Crabbe 1985). It has been proposed that the first type of background is largely contributed by the oxidation of tissue sulfhydryls, followed by the interaction of the resulting disulfides with the phosphorothioate moiety ($O_3P = {}^{35}S$) of the probe (Zoeller et al. 1997). Whereas most hybridization procedures in the literature use DTT at 10–100 mM to minimize this type of background, results of our present studies indicate that DTT above 200 mM can further reduce nonspecific probe binding without any obvious disadvantage. The most dramatic effects of elevated DTT (750–1000 mM) could be observed when elevated concentrations of probe and/or DS were used.

The second important source of nonspecific probe binding is cross-hybridization of probes with rRNA and mRNA sequences that are partially homologous with the targeted mRNA (Crabbe 1985; Höfler et al. 1998; Sunday 1998). If hybridization stringency allows such cross-hybridization to occur, we reason that improved hybridization conditions will amplify nonspecific as well as specific hybridization events because these reactions are driven by identical chemical forces. In the light of this reasoning, it was important that high probe and DS concentrations did not generate cross-hybridization artifacts, as evidenced by the lack of neuronal-type density distribution on X-ray films when we used high concentrations of the sense-strand GABA-A γ2 RNA transcript. However, whenever high probe and DS concentrations are used one should consider the increased importance of specificity controls (Tecott et al. 1987; Davenport 1998; Höfler et al. 1998; Sunday 1998).

Use of Corrected Signal Density to Indicate the Completeness of Hybridization Reaction

Digital subtraction of background (e.g., background produced by a sense control probe; Davenport et al. 1988; Molenaar et al. 1993) from the total signal density is a commonly applied correction method to approximate the specific hybridization signal and, at the same time, to compensate for variations in autoradiographic background. Although this procedure has the great practical value of simplicity, it is important to recognize that variable background can introduce a new error to the quantification procedure. If nonspecific probe binding increases similarly within the signal area and within the background area, the enhancement of background density will exceed the increase of total density in the signal area, thus reducing the corrected signal density value as a net effect. This phenomenon results from the non-linear optical density response of the X-ray film to radiation (Kuhar et al. 1985; Davenport 1998). A second factor that causes corrected signal density to decrease in the presence of high background is the preferential accumulation of background in white matter structures (e.g., the corpus callosum) that we used here for background correction. In the light of the above two phenomena, we reason that as long as increasing amounts of probe cause a growing corrected signal density in spite of the opposite effects of rising background, the hybridization reaction is incomplete. Although we can use this argument to justify the application of "growing corrected signal density " to indicate that free probe bind-

ing sites are available for hybridization in the tissues, it is also important to recognize that this index is not very sensitive, despite the practical value of its simplicity. Unless background levels are stabilized using a wide range of increasing probe concentrations, the corrected signal density usually peaks much before the plateau phase of hybridization reaction (Nunez et al. 1989; Davenport 1998) is reached. This phenomenon may become a pitfall in studies attempting to correlate the maximal corrected signal density (or the maximal signal-to-background ratio) with the saturation of mRNA targets. In our saturation experiment, the simultaneous application of a low specific-activity PR probe and 1000 mM DTT in the hybridization solution ensured stable background levels that were unaffected by a broad range of probe concentrations. Therefore, probe concentrations generating a corrected signal density plateau were probably close to occupying most mRNA targets. It is interesting to note that saturation of hybridization signal in this experiment required 20% instead of 10% DS and probe concentrations one order of magnitude higher than those used in standard hybridization procedures.

To summarize our data, we demonstrated that the low efficiency of hybrid formation and the generation of high oxidative background may largely compromise the sensitivity of in situ mRNA detection using ^{35}S-labeled cRNA probes. We suggest that the use of increased concentrations of ^{35}S-labeled cRNA probe, DS, and DTT will greatly facilitate the cellular localization of rare mRNA species in brain and other tissues.

Acknowledgments

Supported by grant HD27305 from the National Institutes of Health (Bethesda, MD).

We wish to thank Drs C.D. Carpenter, R. Handa, O.K. Park–Sarge, and M.E. Vrontakis for their kind donation of cDNAs.

Literature Cited

Angerer LM, Angerer RC (1981) Detection of poly A+ RNA in sea urchin eggs and embryos by quantitative in situ hybridization. Nucleic Acids Res 9:2819–2840

Crabbe MJ (1985) Partial sequence homologies between cytoskeletal proteins, c-myc, Rous sarcoma virus and adenovirus proteins, transducin, and beta- and gamma-crystallins. Biosci Rep 5:167–174

Davenport A (1998) Quantification of in situ hybridization macroautoradiograms. In Polak JM, McGee JO'D, eds. In Situ Hybridization. Principles and Practice. 2nd ed. Oxford, Oxford Medical Publications, 21–33

Davenport AP, Beresford IJM, Hall MD, Hill RG, Hughes J (1988) Quantitative autoradiography in neuroscience. In Van Leeuwen FW, Buijs RM, Pool CW, Pach O, eds. Molecular Neuroanatomy. Amsterdam, Elsevier Science, 121–145

Galau GA, Britten RJ, Davidson EH (1977a) Studies on nucleic acid reassociation kinetics: rate of hybridization of excess RNA with DNA, compared to the rate of DNA renaturation. Proc Natl Acad Sci USA 74:1020–1023

Galau GA, Smith MJ, Britten RJ, Davidson EH (1977b) Studies on nucleic acid reassociation kinetics: retarded rate of hybridization of RNA with excess DNA. Proc Natl Acad Sci USA 74:2306–2310

Gall JG, Pardue ML (1969) Formation and detection of RNA-DNA hybrid molecules in cytological preparations. Proc Natl Acad Sci USA 63:378–383

Guiot Y, Rahier J (1995) The effects of varying key steps in the nonradioactive in situ hybridization protocol: a quantitative study. Histochem J 27:60–68

Höfler H, Mueller J, Werner M (1998) Principles of in situ hybridization. In Polak JM, McGee JO'D, eds. In Situ Hybridization. Principles and Practice, 2nd ed. Oxford, Oxford Medical Publications, 1–19

Hrabovszky E, Shughrue PJ, Merchenthaler I, Hajszan T, Carpenter CD, Liposits Z, Petersen SL (2000) Detection of estrogen receptor-beta messenger ribonucleic acid and 125I-estrogen binding sites in luteinizing hormone-releasing hormone neurons of the rat brain. Endocrinology 141:3506–3509

Hrabovszky E, Steinhauser A, Barabas K, Shughrue PJ, Petersen SL, Merchenthaler I, Liposits Z (2001) Estrogen receptor-beta immunoreactivity in luteinizing hormone-releasing hormone neurons of the rat brain. Endocrinology 142:3261–3264

Kuhar MJ, Unnerstall JR, De Souza EB (1985) Receptor mapping in neuropharmacology by autoradiography: some technical problems. NIDA Res Monogr 62:1–12

Lubahn DB, Joseph DR, Sar M, Tan J, Higgs HN, Larson RE, French FS, et al. (1988) The human androgen receptor: complementary deoxyribonucleic acid cloning, sequence analysis and gene expression in prostate. Mol Endocrinol 2:1265–1275

Miller JA (1991) The calibration of 35S or 32P with 14C-labeled brain paste 14C-plastic standards for quantitative autoradiography using LKB Ultrofilm or Amersham Hyperfilm. Neurosci Lett 121:211–214

Molenaar P, O'Reilly G, Sharkey A, Kuc RE, Harding DP, Plumpton C, Gresham GA, et al. (1993) Characterization and localization of endothelin receptor subtypes in the human atrioventricular conducting system and myocardium. Circ Res 72:526–538

Nunez DJ, Davenport AP, Emson PC, Brown MJ (1989) A quantitative 'in-situ' hybridization method using computer-assisted image analysis. Validation and measurement of atrial-natriuretic-factor mRNA in the rat heart. Biochem J 263:121–127

Palfi A, Hatvani L, Gulya K (1998) A new quantitative film autoradiographic method of quantifying mRNA transcripts for in situ hybridization. J Histochem Cytochem 46:1141–1149

Park–Sarge OK, Mayo KE (1994) Regulation of the progesterone receptor gene by gonadotropins and cyclic adenosine 3′,5′-monophosphate in rat granulosa cells. Endocrinology 134:709–718

Petersen SL, McCrone S (1994) Characterization of the receptor complement of individual neurons using dual-label in situ hybridization histochemistry. In Eberwine JH, Valentino K, Barchas J, eds. In Situ Hybridization in Neurobiology. Advances in Methodology. New York, Oxford University Press, 78–94

Shivers BD, Killisch I, Sprengel R, Sontheimer H, Kohler M, Schofield PR, Seeburg PH (1989) Two novel GABA A receptor subunits exist in distinct neuronal subpopulations. Neuron 3:327–337

Sunday M (1998) The design and generation of probes for in situ hybridization. In Polak JM, McGee JO'D, eds. In Situ Hybridization. Principles and Practice. 2nd ed. Oxford, Oxford Medical Publications, 21–33

Tecott L, Eberwine J, Barchas J, Valentino K (1987) Methodological considerations in the utilization of in situ hybridiztion. In Valentino K, Eberwine J, Barchas J, eds. In Situ Hybridization: Applications to Neurobiology, 2nd ed. New York, Oxford University Press, 1–23

Vizi S, Gulya K (2000) Calculation of maximal hybridization capacity (Hmax) for quantitative in situ hybridization: a case study for multiple calmodulin mRNAs. J Histochem Cytochem 48:893–904

Vrontakis ME, Peden LM, Duckworth ML, Friesen HG (1987) Isolation and characterization of a complementary DNA (galanin) clone from estrogen-induced pituitary tumor messenger RNA. J Biol Chem 262:16755–16758

Wahl GM, Stern M, Stark GR (1979) Efficient transfer of large DNA fragments from agarose gels to diazobenzyloxymethyl-paper and rapid hybridization by using dextran sulfate. Proc Natl Acad Sci USA 76:3683–3687

Zoeller RT, Fletcher DL, Butnariu O, Lowry CA, Moore FL (1997) N-ethylmaleimide (NEM) can significantly improve in situ hybridization results using 35S-labeled oligodeoxynucleotide or complementary RNA probes. J Histochem Cytochem 45:1035–1041

5. számú melléklet

0013-7227/03/$15.00/0
Printed in U.S.A.

dc_27_10

Endocrinology 144(11):4967–4974

doi: 10.1210/en.2003-0470

Origin of Neuropeptide Y-Containing Afferents to Gonadotropin-Releasing Hormone Neurons in Male Mice

GERGELY F. TURI, ZSOLT LIPOSITS, SUZANNE M. MOENTER, CSABA FEKETE, AND ERIK HRABOVSZKY

Department of Endocrine and Behavioral Neurobiology (G.F.T., Z.L., C.F., E.H.), Institute of Experimental Medicine, Hungarian Academy of Sciences, H-1083 Budapest, Hungary; and Departments of Medicine and Cell Biology (S.M.M.), University of Virginia, Charlottesville, Virginia 22908

The origin of neuropeptide Y (NPY) afferents to GnRH neurons was investigated in male mice. Neonatal lesioning of the hypothalamic arcuate nuclei (ARC) with monosodium glutamate markedly reduced the number of NPY fibers in the preoptic area as well as the frequency of their contacts with perikarya and proximal dendrites of GnRH neurons. Dual-label immunofluorescence studies to determine the precise contribution of the ARC to the innervation of GnRH neurons by NPY axons were carried out on transgenic mice in which enhanced green fluorescent protein was expressed under the control of the GnRH promoter (GnRH-enhanced green fluorescent protein mice). The combined application of red Cy3 and blue AMCA fluorochromogenes established that 49.1 ± 7.3% of NPY axons apposed to green GnRH neurons also contained agouti-related protein (AGRP), a selective marker for NPY axons arising from the ARC. Immunoelectronmicroscopic analysis detected symmetric synapses between AGRP fibers and GnRH-immunoreactive perikarya. Additional triple-fluorescence experiments revealed the presence of dopamine-β-hydroxylase immunoreactivity within 25.4 ± 3.3% of NPY afferents to GnRH neurons. This enzyme marker enabled the selective labeling of NPY pathways ascending from noradrenergic/adrenergic cell populations of the brain stem, thus defining a second important source for NPY-containing fibers regulating GnRH cells. The absence of both topographic markers (AGRP and dopamine-β-hydroxylase) within 26% of NPY contacts suggests that additional sources of NPY fibers to GnRH neurons exist. Future studies will address distinct functions of the two identified NPY systems in the afferent neuronal regulation of the GnRH system. (*Endocrinology* 144: 4967–4974, 2003)

NEUROPEPTIDE Y (NPY), A 36-AMINO-ACID peptide of the pancreatic polypeptide family plays important roles in the regulation of reproduction via acting at both the hypothalamic and pituitary levels (1). Centrally, a chronic increase in NPY tone has been implicated in hypogonadism that accompanies malnutrition (2), obesity (3), or diabetes (4). Inhibition of the gonadotropic axis can also be induced experimentally in male rats and mice by the central infusion of either NPY or Y5 receptor agonist (5). Furthermore, high central NPY levels coincide with the lack of fertility in the leptin-deficient *ob/ob* mice (6). The inhibition of reproduction is likely caused by the hyperfunction of leptin receptor-expressing NPY neurons in the hypothalamic arcuate nucleus (ARC) (7) because leptin replacement to these animals suppresses hypothalamic NPY gene expression with a concomitant occurrence of normal LH secretion and fertility (6). Moreover, cross-breeding of *ob/ob* mice with NPY-knockout animals also results in significant improvement of the reproductive phenotype (8).

Although chronic increase in NPY tone inhibits gonadotropin release (5), delays sexual maturation (9), and suppresses estrous cyclicity (10), the direction of acute NPY effects is markedly influenced by the sexual steroid status of the experimental animals. Likewise, in castrated rats, rabbits, and monkeys, central administration of NPY decreases gonadotropin secretion (11–16), whereas, in intact or gonadectomized and steroid-primed rodents, NPY increases serum gonadotropin levels (5, 12, 15–18).

NPY influences gonadotropin secretion via acting at multiple levels of the reproductive axis. It potentiates gonadotropin release in response to a GnRH challenge (19) by increasing the number of GnRH binding sites on pituitary gonadotrophs (20). In addition, it also stimulates GnRH secretion via acting centrally on GnRH axon terminals in the mediobasal hypothalamus (21–23). The major site of central NPY actions appears to be the preoptic area (POA). The majority of GnRH neurons are located in this region, gain abundant innervation from NPY-containing axon terminals (24–26), and express the Y5 receptor isoform (27).

One putative source of NPY-containing afferents to GnRH neurons is the ARC because neonatal lesioning of this region by monosodium glutamate (MSG) treatment markedly reduced the density of NPY fibers in the POA (28). Indeed, injection of retrograde tracer around GnRH neurons labeled a population of NPY cells in the ARC (26), and anterograde tracing of NPY axons from the ARC revealed their direct appositions to GnRH neurons of the POA (25). Nearly all NPY neurons in the ARC express another orexigenic peptide, agouti-related protein (AGRP). Given that these cells represent a unique source for AGRP in the central nervous system (28), the presence of this neuropeptide can serve as a distinctive marker for NPY axons arising from the ARC. An additional likely source for the origin of NPY afferents to

Abbreviations: AGRP, Agouti-related protein; ARC, arcuate nucleus; bw, body weight; DAB, diaminobenzidine; DBH, dopamine-β-hydroxylase; GABA, γ-aminobutyric acid; GFP, green fluorescent protein; MSG, monosodium glutamate; NPY, neuropeptide Y; PB, phosphate buffer; POA, preoptic area; TBS, Tris-buffered saline.

GnRH neurons is the brain stem in which NPY colocalizes with epinephrine and norepinephrine (26, 29, 30). Retrograde tracing studies found that norepinephrine neurons projecting to the vicinity of GnRH cells coexpress NPY in the ventrolateral medulla (A1 catecholamine cell group) but not in the nucleus tractus solitarii (A2 cells) (26). The putative functional heterogeneity of central NPY pathways motivated the present studies to determine the relative contribution of neurochemically distinct NPY systems to the innervation of GnRH neurons.

We performed a series of immunocytochemical experiments to quantitatively address the involvement of the ARC as well as noradrenergic/adrenergic cell groups of the brain stem in the afferent regulation of GnRH neurons by NPY. To estimate the contribution of NPY cells in the ARC to this innervation, first we compared the frequency of AGRP-containing *vs.* NPY-containing axonal contacts on GnRH neurons, using dual-label immunocytochemistry for bright-field light microscopy. As a second approach, we determined the lost fraction of NPY-immunoreactive juxtapositions to GnRH neurons in neonatally MSG-treated mice with lesioned ARC. The ultrastructural relationship between AGRP-immunoreactive NPY afferents form the ARC and GnRH neurons was also addressed by immunoelectronmicroscopy. Finally, studies using three-color fluorescent microscopy were conducted in preoptic sections of GnRH-enhanced green fluorescent protein (GFP) transgenic mice (31). The immunofluorescent identification of AGRP in NPY afferents to GnRH-GFP neurons was used to label innervation from the ARC, whereas a second set of experiments used the detection of dopamine-β-hydroxylase (DBH) in NPY-containing contacts to identify afferents ascending from noradrenergic/adrenergic cells.

Materials and Methods

Experimental animals

Adult (8 wk old) male GnRH-GFP transgenic mice (n = 16) in which the GnRH promoter drives selective GFP expression in the majority of GnRH neurons (31) were bred and housed at the Institute of Experimental Medicine under conditions of 12 h of light (lights on at 0700 h) with constant access to food and water. The animals were treated in accordance with NIH Guidelines for the Care and Use of Laboratory Animals. All experimental protocols were reviewed and approved by the Animal Welfare Committee at the Institute of Experimental Medicine.

Neonatal MSG treatment

To eliminate NPY fibers arising from the ARC, the chemical lesion of this region was performed by MSG treatment of four neonatal mice. Briefly, the neonatal animals were injected sc with increasing volumes of an 8% MSG solution (dissolved in water), using a treatment paradigm adapted from Légrádi and Lechan (32): postnatal d 1 and 3, 4 mg/g body weight (bw); postnatal d 5, 7, and 9, 8 mg/g bw. The treated animals and four age-matched untreated mice were allowed to reach postnatal wk 8 and then killed by transcardiac perfusion. Brain tissues from the two groups were processed in parallel for comparative histological studies of the ARC and POA.

Transcardiac perfusion

All animals used in these studies were deeply anesthetized with sodium pentobarbital (45 mg/kg bw, ip) and perfused via the ascending aorta first, with 20 ml of 0.01 M PBS (pH 7.4) and then with 100 ml fixative solution. Tissues were fixed with 4% paraformaldehyde (Sigma Chemical Co., St. Louis, MO) in 0.01 M phosphate buffer (PB) for light and fluorescent microscopy and with a mixture of 2% paraformaldehyde and 4% acrolein (Aldrich Chemical Co., Milwaukee, WI) in PB for electron microscopy.

Section preparation

Brains used for light and fluorescent microscopy were immersed into 30% sucrose in PBS overnight, snap frozen on powdered dry ice, and sectioned at 25 μm with a Leica CM 3050 S cryostat (Meyer Instruments, Houston, TX). For preembedding immunoelectronmicroscopy, preoptic sections (35 μm) were prepared on a Vibratome (Technical Products International, St. Louis, MO).

Immunocytochemical studies

A series of immunocytochemical studies were performed using different chromogen combinations for bright-field light microscopy, electron microscopy, and fluorescent microscopy. Specificity of labeling was tested by the omission of primary or secondary antibodies, which resulted in the absence of any staining with the AGRP-, DBH-, NPY-, and GnRH antisera. The distribution of immunoreactive neuronal structures was in agreement with data of previous mapping studies for these antigens.

Experiment 1: light microscopic analysis of NPY- and AGRP-containing fibers in contact with GnRH neurons of neonatally MSG-treated mice vs. untreated controls

Single-label immunocytochemistry. Coronal sections through the ARC were obtained from neonatally MSG-treated mice as well as untreated controls and stained with cresyl violet to verify the chemical lesion in the former group. Sections containing the POA were used for comparative immunocytochemical studies of NPY and AGRP immunoreactivities in these two groups, as outlined below. Sections were rinsed in PBS and pretreated with 10% thioglycolic acid (Sigma) for 30 min to suppress tissue argyrophilia (33) and with 0.5% H_2O_2 in Tris-buffered saline (TBS) (0.1 M Tris-HCl with 0.9% NaCl; pH 7.8) for 15 min to eliminate endogenous peroxidase activity. Nonspecific antibody binding sites were blocked and tissues permeabilized with 2% normal horse serum in TBS/0.4% Triton X-100 (Sigma) for 20 min. Every other preoptic section was transferred into a 1:100,000 dilution of a polyclonal sheep antiserum to NPY (FJL no. 14/3A; diluted with Triton X-100-free blocking reagent) (34), which was generously provided by Dr. István Merchenthaler (Wyeth Research, Collegeville, PA), and applied to the sections for 48 h at 4 C. The remaining sections were incubated in a 1:8000 dilution of a polyclonal rabbit antiserum to human AGRP (H-003-053; Phoenix Pharmaceuticals, Inc., Mountain View, CA) (35). Immunoreactivities were detected after tissue incubations in species-specific biotinylated secondary antibodies (Jackson ImmunoResearch Laboratories, West Grove, PA; 1:1000), then in ABC-Elite reagent (Vector Laboratories, Burlingame, CA; 1:1000 dilutions of solutions A and B in TBS), for 1 h each. The peroxidase developer contained 10 mg diaminobenzidine (DAB), 30 mg nickel-ammonium-sulfate, and 0.002% H_2O_2 in 24 ml TBS. Then silver intensification of the peroxidase reaction product was carried out as described by Liposits *et al.* (33).

Dual-label immunocytochemistry. The majority of sections immunostained for AGRP and NPY were processed further for the immunocytochemical identification of GnRH neurons, using sequential incubations in rabbit polyclonal antibodies to GnRH (LR-1; 1:25,000; gift from Dr. R. Benoit, Montréal, Canada) for 48 h, biotinylated secondary antibodies (Jackson ImmunoResearch Laboratories; 1:1000) for 1 h, and then ABC Elite working solution for 1 h. The developer solution contained 10 mg DAB and 0.001% H_2O_2 in 50 ml TBS. The single- and dual-immunostained sections were mounted on microscope slides, dehydrated with ethanol, coverslipped with DPX mounting medium (Fluka Chemie, Buchs, Switzerland), and studied with an Axiophot microscope (Zeiss, Göttingen, Germany) equipped with an RT Spot digital camera (Diagnostic Instrument, Sterling Heights, MI).

Quantitative analysis of dual-labeled sections

Sections dual immunostained for NPY and GnRH from MSG-treated and untreated control animals as well as sections dual-labeled for AGRP and GnRH from control animals were mounted on microscope slides according to a pattern that allowed later identification of section sources. The slides were coverslipped, sections individually labeled with a code, and in each the number of axonal contacts along the outlines of GnRH neurons analyzed using a ×100 objective lens with immersion oil by an investigator who was blind to the experimental procedures and the pattern of section mounting. Studies of sections in random sequence ensured the homogenous analysis of groups to compare. A case was considered contact based only on highly stringent criteria that were applied consistently. The axon and GnRH neuron had to occur in the same focus plane without the presence of an intervening gap, and instances of partial overlap were excluded from the counting.

Two different approaches were used in parallel to estimate the ratio of NPY afferents of ARC origin to GnRH neurons. First, the average number of AGRP immunoreactive neuronal appositions to GnRH cells was calculated in intact animals (after the analysis of 561 GnRH neurons at high power) and compared with the mean of NPY immunoreactive contacts on individual GnRH cells (with 546 GnRH neurons analyzed). Second, the average number of NPY-containing juxtapositions to single GnRH cells was calculated for neonatally MSG-treated mice (analysis included 408 GnRH neurons) and related to the number determined for the untreated controls. The final results of the analysis were expressed as mean ± SEM.

Experiment 2: electron microscopic analysis of AGRP afferents to GnRH neurons

Preembedding dual-label immunoelectronmicroscopy was used for the ultrastructural analysis of neuronal contacts between AGRP-immunoreactive axons and GnRH cells of the POA. The methodology for dual labeling was adapted from a procedure published recently (36). Briefly, sections were treated with 0.5% sodium borohydride in PBS for 30 min to eliminate residual aldehydes, infiltrated with sucrose for cryoprotection (15% for 1 h and then, 30% overnight), and permeabilized by three repeated freeze-thaw cycles on liquid nitrogen. The immunocytochemical detection of AGRP used sequential incubations in primary antibodies to AGRP (Phoenix; 1:2000) for 4 d, biotinylated antirabbit antibodies (Jackson ImmunoResearch Laboratories; 1: 1000) for 2 h, and ABC working solution (Vector Laboratories; 1: 1000) for 1 h. Triton X-100 was omitted from all solutions and immunoreactivity to AGRP was visualized with a DAB in the peroxidase developer. The detection of AGRP axons was followed by a 4-d incubation (4 C) of sections in rabbit polyclonal antibodies to GnRH (LR-1; 1:25,000), a 30-min blocking step using 0.1% cold-water fish gelatin (Electron Microscopy Sciences, Fort Washington, PA) and 1% BSA (fraction V; Sigma) in PBS, and then, a 1-h incubation in goat antirabbit IgG conjugated with 0.8 nm colloidal gold (Electron Microscopy Sciences; diluted at 1:100 with the blocking reagent). The sections were rinsed briefly with the same blocking reagent and then with PBS, treated for 10 min with 1.25% glutaraldehyde in PBS, and rinsed in 0.2 M sodium citrate (pH 7.5). The silver intensification of gold particles was carried out according to instructions provided with the IntenSE kit (Amersham, Arlington Heights, IL). The dual-labeled sections were osmicated (1% osmium tetroxide in 0.1 M PB; 30 min) and dehydrated in serial dilutions of ethanol. A 30-min contrasting step using 2% uranyl acetate in 70% ethanol was inserted in this procedure and the fully dehydrated sections were finally infiltrated with propylene oxide and flat embedded in Durcupan ACM epoxy resin (Fluka, Ronkonkoma, NY) on liquid release agent (Electron Microscopy Sciences)-coated microscope slides at 56 C. Ultrathin section (50–60 nm) were cut from the resin blocks with an ultracut UCT ultramicrotome (Leica Microsystems AG, Wetzlar, Germany), collected onto Formvar-coated single-slot grids, and examined with a Jeol-100C transmission electron microscope (JEOL, Tokyo, Japan).

Experiment 3: triple-fluorescent analysis of AGRP/NPY and DBH/NPY contacts with GnRH-GFP neurons

To determine the relative contributions of the ARC and brain stem to the innervation of GnRH neurons, a triple-fluorescence strategy was developed, enabling the detection of NPY in axonal contacts to GnRH neurons simultaneously with the immunofluorescent visualization of a site-of-origin-specific topographic marker. The presence of AGRP in NPY axons showed their origin in the ARC, whereas the identification of the adrenergic/noradrenergic biosynthetic enzyme DBH in NPY fibers served as a selective marker for NPY axons arising from catecholamine cell groups of the brain stem. Although DBH is present exclusively in adrenergic/noradrenergic cells of the brain stem, the fine distinction among various catecholamine cell groups that express NPY differentially (26, 29, 30) was not possible via the use of this marker.

First, a cocktail of two primary antibodies (sheep anti-NPY, 1:12,000 and rabbit anti-AGRP, 1:4000; sheep anti-NPY, 1:12,000, and rabbit anti-DBH, 1:8000) (37) was applied to the sections for 48 h at 4 C. This was followed by sequential incubations in a mixture of secondary antibodies, donkey biotin-conjugated antirabbit IgG (1:1,000; Jackson ImmunoResearch Laboratories), and antisheep-Cy3 (1:250; Jackson ImmunoResearch Laboratories), and then in the ABC-Elite working solution (Vector Laboratories) for 1 h each. The detection of AGRP and DBH fibers was completed by treating sections with biotin tyramid working solution (described below) for 30 min and finally with avidin-conjugated AMCA fluorochrom (1:200; Vector Laboratories). To prepare the biotin tyramid solution, a stock solution was first synthesized according to instruction by Adams (38). This stock was stored in frozen aliquots and diluted at 1:1000 in TBS/0.005% H_2O_2 immediately before use. Following steps of this dual-immunofluorescent labeling procedure, sections were mounted on microscope slides and coverslipped with Vectashield mounting medium (Vector Laboratories). Fibers immunoreactive for NPY appeared in red, AGRP-, or DBH-containing axons appeared in blue, and GnRH-GFP neurons appeared in green using the following epifluorescent filter sets: for Cy3, excitation of 540–590 nM, bandpass of 595 nm, and emission of 600–660 nm; for AMCA, excitation of 320–400 nm, bandpass of 400 nm, and emission of 430–490 nm; for GFP, excitation of 460–500 nm, bandpass of 505 nm, and emission of 510–560 nm.

To determine the percent ratios of dual-labeled NPY fibers in each set of experiment, individual NPY juxtapositions were analyzed at high magnification and categorized as being either positive or negative for the topographic markers, AGRP, or DBH. Each study included the analysis of more than 200 NPY-containing neuronal contacts with GnRH neuronal cell bodies and proximal dendrites and percent data were expressed as mean from four animals ± SEM. The fluorescent specimen was analyzed using a ×100 objective lens with immersion oil. First, NPY contacts apposed to GnRH profiles were identified using the same stringent criteria as for bright-field microscopy. Then in each contact identified, we determined whether the NPY axon contained AGRP (or DBH) by switching between the fluorescent filter sets.

Results

Experiment 1: light microscopic analysis of NPY- and AGRP-containing fibers in contact with GnRH neurons of neonatally MSG-treated mice vs. untreated controls

Comparison of cresyl-violet-stained sections from MSG-treated mice (Fig. 1B) *vs.* untreated controls (Fig. 1A) showed a marked reduction in the size of the ARC, whereas neurons of the ventromedial nuclei remained intact.

Results of immunocytochemical experiments showed that the density of NPY-immunoreactive fibers was largely reduced in the POA of ARC-lesioned animals (Fig. 1D), in comparison with untreated controls (Fig. 1C). This observation indicated that a major, albeit not the sole, source of NPY fibers to the POA is the ARC. Axons containing AGRP immunoreactivity (Fig. 1E) formed a somewhat less dense plexus in the POA than NPY fibers (Fig. 1C) in control animals. As opposed to NPY immunostaining (Fig. 1D), AGRP immunoreactivity was almost completely absent from the POA (Fig. 1D) in MSG-treated animals, corroborating previous data that the ARC is the only brain region in which this neuropeptide is synthesized (28).

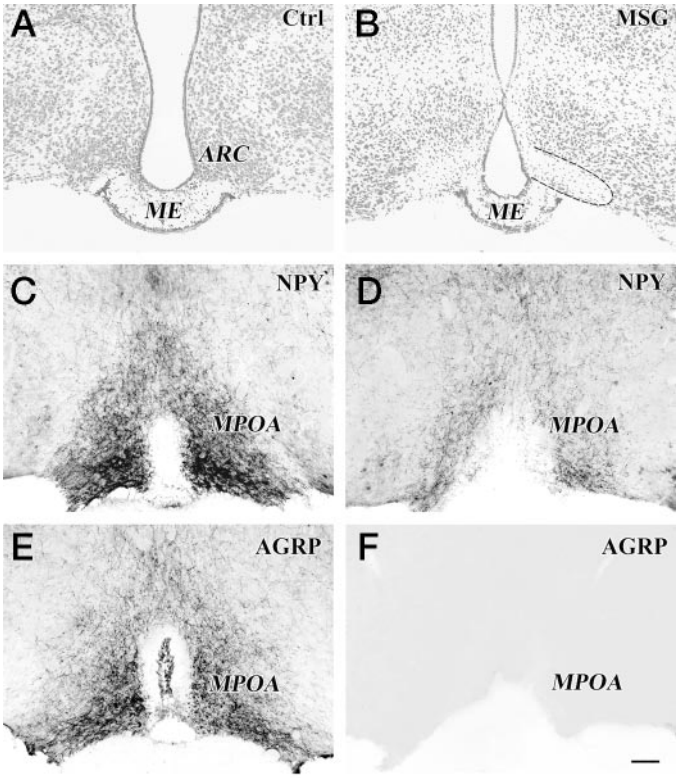

FIG. 1. Effects of neonatal MSG treatment on the morphology of the ARC and innervation pattern of the medial POA (MPOA) by NPY and AGRP fibers. A, Cresyl violet-stained section shows the normal structure of the ARC. B, Neonatal MSG treatment of mice results in a marked shrinkage and cell paucity of this region (*dashed line*) due to a major neuronal cell loss. Note that the lesion is region specific, and neurons outside the ARC escape the effects of treatment. C and D, Innervation of the MPOA by NPY-immunoreactive axons is largely reduced in the ARC-lesioned animal (D) *vs.* the control (C). The source of the NPY network that survives the treatment is likely outside the ARC. E and F, Neuronal fibers immunoreactive to AGRP densely innervate the MPOA in untreated animals (E). Because the ARC is the only brain region synthesizing AGRP, immunoreactive axons almost completely disappear after neonatal lesioning of the ARC by MSG treatment (F). Note that the loss of NPY fibers in D and AGRP fibers in F reflect death of neurons that synthesize both AGRP and NPY in the ARC. *Scale bar*, 100 μm (A–F).

The analysis of dual-labeled sections from intact mice demonstrated numerous contacts between NPY-immunoreactive axons and the perikarya and proximal dendrites of GnRH neurons (Fig. 2A). The frequency of NPY-containing axonal appositions to individual GnRH cells was significantly higher by ANOVA ($P < 0.05$) than the frequency at which AGRP immunoreactive neuronal contacts occurred on GnRH neurons (Fig. 2B). The number of AGRP immunopositive contacts was 56.5 ± 9.8% of that of NPY immunoreactive contacts. Furthermore, significantly less ($P < 0.05$) NPY-containing neuronal contacts were visible in neonatally MSG-treated animals (Fig. 2C) *vs.* controls. The lesion of the ARC caused a 63.7 ± 5.0% loss of NPY-immunopositive juxtapositions. Altogether, the two different methodological approaches suggested that about 56.5–63.7% of NPY axons to GnRH cells arise from NPY neurons of the ARC.

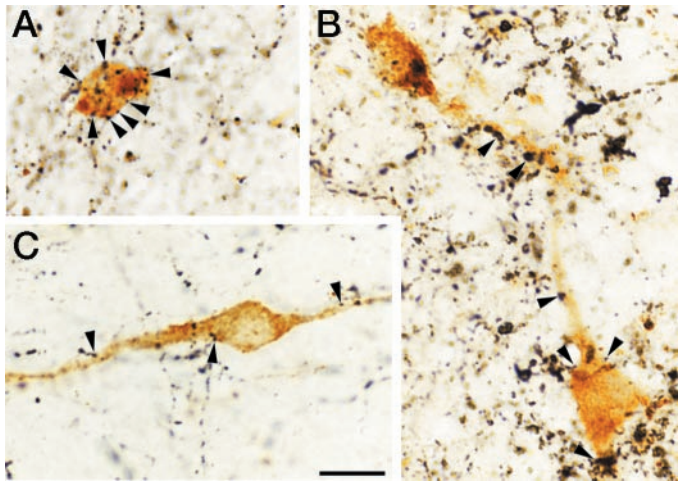

FIG. 2. Innervation of GnRH neurons by NPY and AGRP fibers. Effects of neonatal MSG treatment. A, Axons immunoreactive to NPY form juxtapositions (*arrowheads*) with the cell bodies and proximal dendrites of GnRH neurons. B, Neuronal contacts (*arrowheads*) between AGRP-immunoreactive axons and GnRH cells are less frequent. C, GnRH neurons of neonatally MSG-treated mice are contacted (*arrowheads*) by significantly less NPY axons than GnRH cells of untreated controls (A). *Scale bar*, 10 μm (A–C).

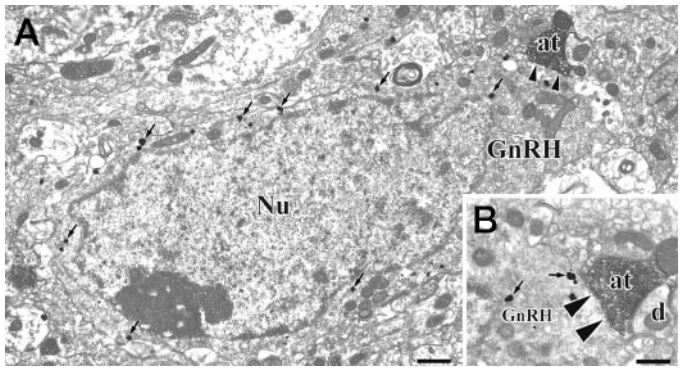

FIG. 3. Electron microscopic evidence for synaptic communication between AGRP-containing axons and GnRH neurons. A and B, An AGRP-immunoreactive axon terminal (at) labeled by electron-dense DAB deposits is closely apposed to the perikaryon of a GnRH-immunoreactive neuron (GnRH), which contains highly electron-dense silver-intensified gold particles (*arrows*). High-power image in B reveals axosomatic synaptic communication between the labeled structures. *Arrowheads* point to the postsynaptic density of a symmetrical synapse. Also note the presence of a symmetric synapse between the same AGRP-immunoreactive terminal and an unlabeled dendrite (d). *Scale bars*, 0.8 μm in A and 0.5 μm in B.

Experiment 2: electron microscopic analysis of AGRP afferents to GnRH neurons

At the ultrastructural level, AGRP-immunoreactive fibers contained electron-dense DAB deposits, and they were frequently apposed to GnRH neurons accumulating highly electron-dense silver-gold particles (Fig. 3, A and B). Synapses of symmetric morphology were observed between AGRP axons and GnRH neurons as well as non-GnRH structures (Fig. 3B). The absence of metal particles over AGRP fibers indicated that antibody cross-reaction did not arise from the species identity of the two primary antibodies.

Experiment 3: triple-fluorescent analysis of AGRP/NPY and DBH/NPY contacts with GnRH-GFP neurons

The distributions of NPY- (Fig. 4A) and AGRP-containing (Fig. 4B) fibers largely overlapped (Fig. 4C) in the POA, and the heaviest immunolabeling for both was observed in the ventral aspect of this region. Axons double labeled for NPY and AGRP often formed serial contacts with the cell bodies and proximal dendrites (Fig. 4, D–F) of GnRH-GFP neurons, which exhibited bright green fluorescence. High-power analysis of the fluorescent specimen established that 49.1 ± 7.3% of NPY-containing neuronal contacts also contained AGRP (Figs. 4, D–F). In addition, nearly all AGRP fibers were immunoreactive to NPY.

Similar to AGRP immunoreactive axons, fibers containing DBH (Fig. 4G) showed overlapping distribution with that of NPY axons in the POA (Fig. 4H). High-power analysis of immunostained axons established the presence of DBH in 25.4 ± 3.3% of NPY-containing fibers in contact with GnRH neurons (Fig. 4, J–L). Other types of fibers observed in the POA contained NPY without DBH or DBH without NPY (Figs. 4, J–L), and they were apposed to GnRH neurons.

Discussion

NPY plays a rather complex role in the regulation of reproduction. Although evidence exists for direct stimulation of pituitary gonadotrophs by NPY (19–21, 39), the majority of work indicates that NPY mainly acts centrally to modulate gonadotropin secretion (3, 5, 9–14, 16–18, 21, 22, 40, 41) and that GnRH neurons of the POA are direct target cells to central NPY actions (23–27). In the present study, the origins of NPY-containing neurons afferents to GnRH cells were investigated. Our results indicate that NPY neurons of the ARC give rise to 49–64% of the NPY-immunoreactive axonal contacts on the somata and proximal dendrites of GnRH neurons (depending on the calculation approach we used), and an additional 25% of juxtapositions originate in adrenergic/noradrenergic cell groups of the brain stem. These quantitative data supplement results of a previous report by Simonian *et al.* (26), who described retrograde labeling of NPY neurons in both the ARC and ventrolateral medulla of the rat after tracer injection around GnRH neurons.

Receptors mediating NPY effects belong to the family of the seven-transmembrane domain, G protein-coupled receptors, which act primarily via inhibiting adenylate cyclase (42). Pharmacological studies using selective ligands to Y receptor subtypes for intracerebroventricular acute injections to castrated rats (13) and chronic infusions to intact male rats and mice (5) provided evidence that the Y5 receptor isoform plays a crucial role in the inhibitory control of gonadotropin release by NPY. Given that 55% of GnRH neuronal perikarya bear this receptor isoform (27), the Y5 receptor-mediated reproductive actions of NPY may be exerted, at least partly, on GnRH cells. In pentobarbital-blocked, proestrous rats, iv pulses of Y1 receptor antagonist blocked the endogenous LH surges and prevented the amplification of the LHRH-induced LH surges by NPY, implicating Y1 receptor activation in the stimulatory control of LH secretion (43). Morphological evidence supports the presence of the Y1 receptor isoform in axon terminals of GnRH neurons in the median eminence as well as in NPY fibers that innervate GnRH neurons from the ARC (25). It is reasonable to speculate that Y1 receptors presynaptic to GnRH neurons may modulate the synaptic release of NPY, AGRP, or a putative major neurotransmitter of these neurons, γ-aminobutyric acid (GABA) (44). Accordingly, NPY agonism

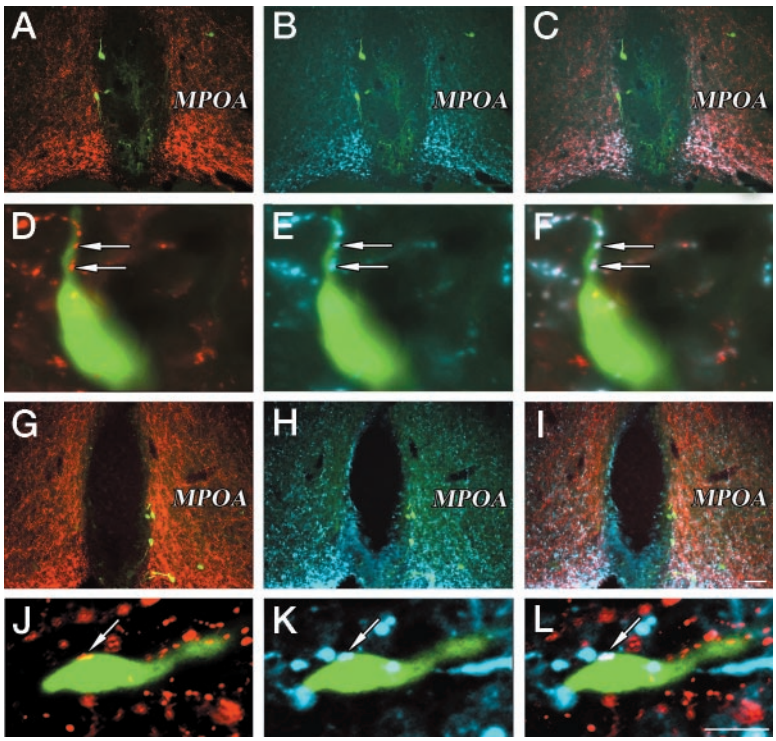

FIG. 4. Immunofluorescent identification of AGRP and DBH in NPY afferents to GnRH neurons. A–C, Both NPY (A; *red* Cy-3 fluorochrom) and AGRP (B; *blue* AMCA fluorochrom) immunoreactive fibers form dense plexus in the medial POA (MPOA). The *purple-to-white* color that dominates over *red* in the merged figure (C) indicates that many NPY axons cocontain AGRP. Note the *bright green* fluorescence in GnRH neurons (A–C) due to the presence of the GnRH-GFP transgene product. D–F, High-power photomicrographs reveal an NPY axon (D) that also contains AGRP (E). *Arrows* indicate the same points of contact between a dual-labeled NPY/AGRP axon and a GnRH neuron in unmerged (D, E) and merged (F) digital images. G–I, The distribution of NPY axons (G; *red* Cy-3 fluorochrom) also overlaps with that of DBH containing fibers (H; *blue* AMCA fluorochrom) in the MPOA. Note that this match (*purple-to-white color* in the merged panel; I) is of lower degree than in case of NPY and AGRP immunoreactive fibers (C). J–L, A noradrenergic/adrenergic axon that contains NPY (J) as well as DBH (K) establishes contact (*arrows*) with the soma of a GnRH neurons. The merged image in L clearly shows that many NPY axons (*red color*) are devoid of DBH, and vice versa, DBH-immunoreactive axons (*blue color*) often remain immunonegative for NPY. *Scale bars*, 100 μm in A–C and G–I and 10 μm in D–F and J–L.

on presynaptic Y1 and Y2 receptors has been shown to inhibit glutamate (45) GABA (46) and norepinephrine (47) release.

The use of AGRP immunoreactivity as a marker for NPY axons of ARC origin was based on previous evidence that AGRP and NPY neurons of the ARC are essentially identical (28). Results of our triple-fluorescence studies indicate that NPY/AGRP neurons of the ARC give rise to 49% of NPY axons that form contacts with the somata and proximal dendrites of GnRH neurons. A similar ratio for NPY axons of ARC origin (56%) was calculated in experiment 1 from the comparison of AGRP-immunoreactive *vs.* NPY-immunoreactive contacts on GnRH neurons. A somewhat heavier innervation appear to originate from the ARC (64%) if the lost fraction of NPY contacts in MSG-treated animals is considered. To analyze the nature of the putative neuronal communication between AGRP axons and GnRH neurons, we carried out electron microscopic studies and demonstrated that AGRP axons establish synapses with GnRH neurons. From a functional viewpoint, it is important to note that AGRP axons formed only symmetric-type synapses with GnRH as well as non-GnRH neurons of the POA. This observation is in concert with the previous findings of symmetric synapses between NPY axons and GnRH neurons of the POA (24). Furthermore, this synaptic morphology also characterizes GABAergic synapses (48). Therefore, the identification of the biosynthetic enzyme of GABA, GAD-65, in 30% of NPY neurons in the ARC (49) along with the light and electron microscopic demonstration of GABA immunoreactivity in subsets of NPY axons in the POA (44) highly indicate that at least some AGRP/NPY terminals that innervate GnRH neurons may cocontain GABA. Although this hypothesis awaits confirmation, recent evidence supports the physiological importance of a GABA/NPY interplay in the regulation of gonadotropin secretion (44).

Little is currently known about the role of AGRP, an endogenous antagonist of melanocortin 3 and 4 receptors (MC3-R and MC4-R), in the regulation of the reproductive axis. It is likely that AGRP primarily stimulates gonadotropin secretion via acting at hypothalamic sites. Increased gonadotropin secretion was observed 40 min after intracerebroventricular injection of AGRP to male rats, whereas AGRP was unable to alter either basal- or GnRH-stimulated gonadotropin secretion from dispersed pituitary cells (50). Furthermore, AGRP also stimulated GnRH release from mediobasal hypothalamic explants *in vitro*, and this effect was prevented by the presence of α-MSH in the medium (50), indicating that AGRP partially acts via antagonizing melanocortin receptors in the ARC-median eminence region. The synaptic communication revealed by our studies between AGRP axons and GnRH neurons of the POA represents an additional anatomical route for AGRP to influence the reproductive axis. The type and location of receptors involved in this synaptic interaction requires clarification. Future research will also need to address any difference of chronic *vs.* acute AGRP effects on gonadotropin secretion as well as the potential sexual steroid dependence of AGRP actions, features well characterized for the regulation of the reproductive axis by NPY.

In addition to AGRP/NPY contacts of arcuate origin, our analysis found DBH immunofluorescence within 25% of NPY immunoreactive axonal contacts on GnRH neurons. This observation indicates that noradrenergic/adrenergic pathways directly regulate GnRH neurons and corroborates previous data by others (26, 51, 52) that noradrenergic cell groups project to the immediate vicinity of GnRH neurons in the rat. The adrenergic/noradrenergic input to GnRH cells is consistent with a large body of evidence in the literature indicating the important role of adrenergic stimuli in the regulation of the ovarian cycle and the steroid-induced gonadotropin surge (53). The present work did not address the ultrastructural characteristics of DBH-immunoreactive juxtapositions to GnRH neurons. One previous study (54) suggested that noradrenergic neurons can communicate with GnRH cells through classical synaptic mechanisms, whereas other investigators (55) debated the abundance of such synapses.

Potential difficulties to reveal synaptic specializations between adrenergic/noradrenergic terminals and GnRH neurons may indicate the involvement of nonsynaptic routes in the catecholamine-GnRH communication. Although this concept will require formal support by the immunoelectronmicroscopic analysis of DBH contacts on GnRH cells, there is little doubt that the proposed nonsynaptic mechanisms often play a role in noradrenergic neurotransmission. For example, only a small fraction of DBH-immunoreactive juxtapositions establish classical synapses with neurons of the cerebral cortex and the subcellular distribution of $\alpha 2_A$ adrenoceptors is not restricted to the postsynaptic membranes (56). It is also worth noting that a large subset of DBH-immunopositive axons in contact with GnRH cells was devoid of NPY immunoreactivity, in concert with the finding that NPY is expressed differentially among distinct noradrenergic/adrenergic cell groups (26, 29, 30). Likewise, high percentages of C1–3 adrenergic neurons and A1 noradrenergic neurons were found to contain NPY, whereas A2 and A6 noradrenergic neurons often lacked any NPY immunostaining (26, 29). Finally, while it is likely that at least some of the AGRP/NPY input that reaches GnRH neurons from the ARC is GABAergic (44, 49), the recent demonstration of vesicular glutamate transporter-2 in C1 adrenergic and other catecholamine neurons of the brain stem (57), which also synthesize NPY (29), raises the possibility that the excitatory neurotransmitter glutamate is coreleased with NPY and epinephrine/norepinephrine from afferents to GnRH neurons.

Although the ARC and brain stem are generally viewed as the most important sources of central NPY, neuronal perikarya-synthesizing NPY occur in many further brain regions, including the dorsomedial hypothalamic nucleus, bed nucleus of the stria terminalis, anterior horn of the anterior commissure, lateral preoptic area, dorsal hypothalamic area, mesencephalic central gray, and ventrolateral geniculate nucleus (58). It is likely that some of the above or other NPY cell groups contribute to the innervation of GnRH neurons. The calculated percentage of these alternative afferents can be up to 20–26% of NPY fibers form the ARC are identified by their AGRP content but somewhat lower (11%) if the percent loss of NPY afferents in MSG-treated animals is considered. Several explanations for this discrepancy may exist. It is possible that MSG treatment altered other NPY systems, in addition to induce the lesion of ARC neurons.

Alternatively, the ratio of NPY afferents reaching GnRH neurons from the ARC may be somewhat higher than we estimated on the basis of their AGRP content. A subset of NPY neurons in the ARC (5%) seem to be devoid of AGRP (28), and these cells may contribute to the innervation of GnRH neurons. Finally, we cannot rule out the possibility that the immunocytochemical assay conditions were suboptimal to reveal low levels of DBH or AGRP in subsets of NPY axons, despite the high detection sensitivity provided by the tyramid signal amplification technique (38).

The AGRP and DBH contents of NPY afferents to GnRH neurons were analyzed in GnRH-GFP transgenic mice (31) in which green fluorescence is detectable in the vast majority of GnRH neurons, without a significant ectopic expression of the transgene (31). This approach alleviated the need of using three primary antibodies, all of which should be generated in different species to avoid cross-reactions. A second technical consideration is that the innervation pattern we observed reflects only the situation on the somata and proximal dendrites of GnRH neurons. Because distal dendrites of GnRH neurons may not contain GFP fluorescence, our studies do not allow us to conclude about their putative regulation by NPY afferents.

In summary, the quantitative data we present here reveal the relative contributions of two major NPY systems to the afferent regulation of GnRH neurons. Using different detection approaches, 49–64% of NPY contacts on GnRH neurons were found to originate from the ARC, cocontain AGRP, and establish symmetric synapses with GnRH neurons. An additional 25% of NPY afferents contain DBH, indicating their origin in noradrenergic/adrenergic cell groups of the brain stem. This information will stimulate future research for the functional characterization of NPY afferents to GnRH neurons and the input-specific use of pre-, post-, and/or extrasynaptic receptors by distinct afferent systems.

Acknowledgments

The authors thank Dr. R. Benoit for the kind donation of the LR1 antibody to GnRH and Dr. I. Merchenthaler for the FJL no. 14/3A antiserum to NPY.

Received April 15, 2003. Accepted July 18, 2003.

Address all correspondence and requests for reprints to: Erik Hrabovszky, Department of Endocrine- and Behavioral Neurobiology, Institute of Experimental Medicine, Hungarian Academy of Sciences, Szigony u. 43., 1083 Budapest, Hungary. E-mail: hrabovszky@koki.hu.

This work was supported by grants from the National Science Foundation of Hungary (OTKA T031770 and T043407), the Hungarian Medical Research Council (ETT 280/2000), and the Fifth EC Framework Program (QLG3 2000-00844).

References

1. **Kalra SP, Crowley WR** 1992 Neuropeptide Y: a novel neuroendocrine peptide in the control of pituitary hormone secretion, and its relation to luteinizing hormone. Front Neuroendocrinol 13:1–46
2. **Kalra SP, Dube MG, Sahu A, Phelps CP, Kalra PS** 1991 Neuropeptide Y secretion increases in the paraventricular nucleus in association with increased appetite for food. Proc Natl Acad Sci USA 88:10931–10935
3. **Zarjevski N, Cusin I, Vettor R, Rohner-Jeanrenaud F, Jeanrenaud B** 1993 Chronic intracerebroventricular neuropeptide-Y administration to normal rats mimics hormonal and metabolic changes of obesity. Endocrinology 133:1753–1758
4. **Williams G, Steel JH, Cardoso H, Ghatei MA, Lee YC, Gill JS, Burrin JM, Polak JM, Bloom SR** 1988 Increased hypothalamic neuropeptide Y concentrations in diabetic rat. Diabetes 37:763–772
5. **Raposinho PD, Pierroz DD, Broqua P, White RB, Pedrazzini T, Aubert ML** 2001 Chronic administration of neuropeptide Y into the lateral ventricle of C57BL/6J male mice produces an obesity syndrome including hyperphagia, hyperleptinemia, insulin resistance, and hypogonadism. Mol Cell Endocrinol 185:195–204
6. **Mounzih K, Lu R, Chehab FF** 1997 Leptin treatment rescues the sterility of genetically obese ob/ob males. Endocrinology 138:1190–1193
7. **Baskin DG, Breininger JF, Schwartz MW** 1999 Leptin receptor mRNA identifies a subpopulation of neuropeptide Y neurons activated by fasting in rat hypothalamus. Diabetes 48:828–833
8. **Erickson JC, Hollopeter G, Palmiter RD** 1996 Attenuation of the obesity syndrome of ob/ob mice by the loss of neuropeptide Y. Science 274:1704–1707
9. **Pierroz DD, Gruaz NM, d'Alieves V, Aubert ML** 1995 Chronic administration of neuropeptide Y into the lateral ventricle starting at 30 days of life delays sexual maturation in the female rat. Neuroendocrinology 61:293–300
10. **Catzeflis C, Pierroz DD, Rohner-Jeanrenaud F, Rivier JE, Sizonenko PC, Aubert ML** 1993 Neuropeptide Y administered chronically into the lateral ventricle profoundly inhibits both the gonadotropic and the somatotropic axis in intact adult female rats. Endocrinology 132:224–234
11. **Kerkerian L, Guy J, Lefevre G, Pelletier G** 1985 Effects of neuropeptide Y (NPY) on the release of anterior pituitary hormones in the rat. Peptides 6:1201–1204
12. **Kalra SP, Crowley WR** 1984 Norepinephrine-like effects of neuropeptide Y on LH release in the rat. Life Sci 35:1173–1176
13. **Raposinho PD, Broqua P, Pierroz DD, Hayward A, Dumont Y, Quirion R, Junien JL, Aubert ML** 1999 Evidence that the inhibition of luteinizing hormone secretion exerted by central administration of neuropeptide Y (NPY) in the rat is predominantly mediated by the NPY-Y5 receptor subtype. Endocrinology 140:4046–4055
14. **Kaynard AH, Pau KY, Hess DL, Spies HG** 1990 Third-ventricular infusion of neuropeptide Y suppresses luteinizing hormone secretion in ovariectomized rhesus macaques. Endocrinology 127:2437–2444
15. **Khorram O, Pau KY, Spies HG** 1987 Bimodal effects of neuropeptide Y on hypothalamic release of gonadotropin-releasing hormone in conscious rabbits. Neuroendocrinology 45:290–297
16. **Sahu A, Crowley WR, Tatemoto K, Balasubramaniam A, Kalra SP** 1987 Effects of neuropeptide Y, NPY analog (norleucine4-NPY), galanin and neuropeptide K on LH release in ovariectomized (ovx) and ovx estrogen, progesterone-treated rats. Peptides 8:921–926
17. **Allen LG, Kalra PS, Crowley WR, Kalra SP** 1985 Comparison of the effects of neuropeptide Y and adrenergic transmitters on LH release and food intake in male rats. Life Sci 37:617–623
18. **Berria M, Pau KY, Spies HG** 1991 Evidence for α1-adrenergic involvement in neuropeptide Y-stimulated GnRH release in female rabbits. Neuroendocrinology 53:480–486
19. **Bauer-Dantoin AC, McDonald JK, Levine JE** 1992 Neuropeptide Y potentiates luteinizing hormone (LH)-releasing hormone-induced LH secretion only under conditions leading to preovulatory LH surges. Endocrinology 131:2946–2952
20. **Parker SL, Kalra SP, Crowley WR** 1991 Neuropeptide Y modulates the binding of a gonadotropin-releasing hormone (GnRH) analog to anterior pituitary GnRH receptor sites. Endocrinology 128:2309–2316
21. **Crowley WR, Kalra SP** 1987 Neuropeptide Y stimulates the release of luteinizing hormone-releasing hormone from medial basal hypothalamus *in vitro*: modulation by ovarian hormones. Neuroendocrinology 46:97–103
22. **Woller MJ, Terasawa E** 1991 Infusion of neuropeptide Y into the stalk-median eminence stimulates *in vivo* release of luteinizing hormone-release hormone in gonadectomized rhesus monkeys. Endocrinology 128:1144–1150
23. **Urban JH, Das I, Levine JE** 1996 Steroid modulation of neuropeptide Y-induced luteinizing hormone releasing hormone release from median eminence fragments from male rats. Neuroendocrinology 63:112–119
24. **Tsuruo Y, Kawano H, Kagotani Y, Hisano S, Daikoku S, Chihara K, Zhang T, Yanaihara N** 1990 Morphological evidence for neuronal regulation of luteinizing hormone-releasing hormone-containing neurons by neuropeptide Y in the rat septo-preoptic area. Neurosci Lett 110:261–266
25. **Li C, Chen P, Smith MS** 1999 Morphological evidence for direct interaction between arcuate nucleus neuropeptide Y (NPY) neurons and gonadotropin-releasing hormone neurons and the possible involvement of NPY Y1 receptors. Endocrinology 140:5382–5390
26. **Simonian SX, Spratt DP, Herbison AE** 1999 Identification and characterization of estrogen receptor á-containing neurons projecting to the vicinity of the gonadotropin-releasing hormone perikarya in the rostral preoptic area of the rat. J Comp Neurol 411:346–358
27. **Campbell RE, Ffrench-Mullen JM, Cowley MA, Smith MS, Grove KL** 2001 Hypothalamic circuitry of neuropeptide Y regulation of neuroendocrine function and food intake via the Y5 receptor subtype. Neuroendocrinology 74: 106–119
28. **Broberger C, Johansen J, Johansson C, Schalling M, Hokfelt T** 1998 The neuropeptide Y/agouti gene-related protein (AGRP) brain circuitry in normal, anorectic, and monosodium glutamate-treated mice. Proc Natl Acad Sci USA 95:15043–15048
29. **Sawchenko PE, Swanson LW, Grzanna R, Howe PR, Bloom SR, Polak JM**

1985 Colocalization of neuropeptide Y immunoreactivity in brainstem catecholaminergic neurons that project to the paraventricular nucleus of the hypothalamus. J Comp Neurol 241:138–153
30. **Everitt BJ, Hokfelt T, Terenius L, Tatemoto K, Mutt V, Goldstein M** 1984 Differential co-existence of neuropeptide Y (NPY)-like immunoreactivity with catecholamines in the central nervous system of the rat. Neuroscience 11: 443–462
31. **Suter KJ, Song WJ, Sampson TL, Wuarin JP, Saunders JT, Dudek FE, Moenter SM** 2000 Genetic targeting of green fluorescent protein to gonadotropin-releasing hormone neurons: characterization of whole-cell electrophysiological properties and morphology. Endocrinology 141:412–419
32. **Legradi G, Lechan RM** 1998 The arcuate nucleus is the major source for neuropeptide Y-innervation of thyrotropin-releasing hormone neurons in the hypothalamic paraventricular nucleus. Endocrinology 139:3262–3270
33. **Liposits Z, Setalo G, Flerko B** 1984 Application of the silver-gold intensified 3, 3′-diaminobenzidine chromogen to the light and electron microscopic detection of the luteinizing hormone-releasing hormone system of the rat brain. Neuroscience 13:513–525
34. **Wittmann G, Liposits Z, Lechan RM, Fekete C** 2002 Medullary adrenergic neurons contribute to the neuropeptide Y-ergic innervation of hypophysiotropic thyrotropin-releasing hormone-synthesizing neurons in the rat. Neurosci Lett 324:69–73
35. **Mihaly E, Fekete C, Tatro JB, Liposits Z, Stopa EG, Lechan RM** 2000 Hypophysiotropic thyrotropin-releasing hormone-synthesizing neurons in the human hypothalamus are innervated by neuropeptide Y, agouti-related protein, and á-melanocyte-stimulating hormone. J Clin Endocrinol Metab 85: 2596–2603
36. **Fekete C, Legradi G, Mihaly E, Huang QH, Tatro JB, Rand WM, Emerson CH, Lechan RM** 2000 á-Melanocyte-stimulating hormone is contained in nerve terminals innervating thyrotropin-releasing hormone-synthesizing neurons in the hypothalamic paraventricular nucleus and prevents fasting-induced suppression of prothyrotropin-releasing hormone gene expression. J Neurosci 20:1550–1558
37. **Chen IL, Hansen JT, Yates RD** 1985 Dopamine β-hydroxylase-like immunoreactivity in the rat and cat carotid body: a light and electron microscopic study. J Neurocytol 14:131–144
38. **Adams JC** 1992 Biotin amplification of biotin and horseradish peroxidase signals in histochemical stains. J Histochem Cytochem 40:1457–1463
39. **Crowley WR, Hassid A, Kalra SP** 1987 Neuropeptide Y enhances the release of luteinizing hormone (LH) induced by LH-releasing hormone. Endocrinology 120:941–945
40. **Gore AC, Mitsushima D, Terasawa E** 1993 A possible role of neuropeptide Y in the control of the onset of puberty in female rhesus monkeys. Neuroendocrinology 58:23–34
41. **Kalra PS, Bonavera JJ, Kalra SP** 1995 Central administration of antisense oligodeoxynucleotides to neuropeptide Y (NPY) mRNA reveals the critical role of newly synthesized NPY in regulation of LHRH release. Regul Pept 59:215–220
42. **Blomqvist AG, Herzog H** 1997 Y-receptor subtypes—how many more? Trends Neurosci 20:294–298
43. **Leupen SM, Besecke LM, Levine JE** 1997 Neuropeptide Y Y1-receptor stimulation is required for physiological amplification of preovulatory luteinizing hormone surges. Endocrinology 138:2735–2739
44. **Horvath TL, Pu S, Dube MG, Diano S, Kalra SP** 2001 A GABA-neuropeptide Y (NPY) interplay in LH release. Peptides 22:473–481
45. **van den Pol AN, Obrietan K, Chen G, Belousov AB** 1996 Neuropeptide Y-mediated long-term depression of excitatory activity in suprachiasmatic nucleus neurons. J Neurosci 16:5883–5895
46. **Chen G, van den Pol AN** 1996 Multiple NPY receptors coexist in pre- and postsynaptic sites: inhibition of GABA release in isolated self-innervating SCN neurons. J Neurosci 16:7711–7724
47. **Simonneaux V, Ouichou A, Craft C, Pevet P** 1994 Presynaptic and postsynaptic effects of neuropeptide Y in the rat pineal gland. J Neurochem 62:2464–2471
48. **Peters A, Palay SL, Webster H deF** 1991 The fine structure of the nervous system. Neurons and their supporting cells. New York: University Press
49. **Horvath TL, Bechmann I, Naftolin F, Kalra SP, Leranth C** 1997 Heterogeneity in the neuropeptide Y-containing neurons of the rat arcuate nucleus: GABAergic and non-GABAergic subpopulations. Brain Res 756:283–286
50. **Stanley SA, Small CJ, Kim MS, Heath MM, Seal LJ, Russell SH, Ghatei MA, Bloom SR** 1999 Agouti related peptide (Agrp) stimulates the hypothalamo pituitary gonadal axis *in vivo*, *in vitro* in male rats. Endocrinology 140:5459–5462
51. **Wright DE, Jennes L** 1993 Origin of noradrenergic projections to GnRH perikarya-containing areas in the medial septum-diagonal band and preoptic area. Brain Res 621:272–278
52. **Simonian SX, Herbison AE** 1997 Differential expression of estrogen receptor and neuropeptide Y by brainstem A1 and A2 noradrenaline neurons. Neuroscience 76:517–529
53. **Herbison AE** 1997 Noradrenergic regulation of cyclic GnRH secretion. Rev Reprod 2:1–6
54. **Miller MM, Zhu L** 1995 Ovariectomy and age alter gonadotropin hormone releasing hormone-noradrenergic interactions. Neurobiol Aging 16:613–625
55. **Leranth C, MacLusky NJ, Shanabrough M, Naftolin F** 1988 Catecholaminergic innervation of luteinizing hormone-releasing hormone and glutamic acid decarboxylase immunopositive neurons in the rat medial preoptic area. An electron-microscopic double immunostaining and degeneration study. Neuroendocrinology 48:591–602
56. **Aoki C, Venkatesan C, Go CG, Forman R, Kurose H** 1998 Cellular and subcellular sites for noradrenergic action in the monkey dorsolateral prefrontal cortex as revealed by the immunocytochemical localization of noradrenergic receptors and axons. Cereb Cortex 8:269–277
57. **Stornetta RL, Sevigny CP, Guyenet PG** 2002 Vesicular glutamate transporter DNPI/VGLUT2 mRNA is present in C1 and several other groups of brainstem catecholaminergic neurons. J Comp Neurol 444:191–206
58. **Chronwall BM, DiMaggio DA, Massari VJ, Pickel VM, Ruggiero DA, O'Donohue TL** 1985 The anatomy of neuropeptide-Y-containing neurons in rat brain. Neuroscience 15:1159–1181

dc_27_10

6. számú melléklet

THE JOURNAL OF COMPARATIVE NEUROLOGY 473:315–333 (2004)

Estrogen Receptor-β in Oxytocin and Vasopressin Neurons of the Rat and Human Hypothalamus: Immunocytochemical and In Situ Hybridization Studies

ERIK HRABOVSZKY,[1,2] IMRE KALLÓ,[1,3] ANNAMÁRIA STEINHAUSER,[1] ISTVÁN MERCHENTHALER,[4] CLIVE W. COEN,[3] SANDRA L. PETERSEN,[2] AND ZSOLT LIPOSITS[1]*

[1]Laboratory of Endocrine Neurobiology, Institute of Experimental Medicine, Hungarian Academy of Sciences, Budapest 1083, Hungary
[2]Department of Biology, University of Massachusetts Amherst, Amherst, Massachusetts 01003
[3]Centre for Neuroscience Research, King's College London, London SE1 1UL, United Kingdom
[4]Women's Health and Bone, Wyeth Research, Collegeville, Pennsylvania 19426

ABSTRACT

Topographical distribution of estrogen receptor-β (ER-β)-synthesizing oxytocin (OT) and vasopressin (VP) neurons was studied in the hypothalamic paraventricular and supraoptic nuclei (PVH; SO) of ovariectomized rats. In distinct subregions, 45–98% of OT neurons and 88–99% of VP neurons exhibited ER-β immunoreactivity that was confined to cell nuclei. Neuronal populations differed markedly with respect to the intensity of the ER-β signal. Magnocellular OT neurons in the PVH, SO, and accessory cell groups typically contained low levels of the ER-β signal; in contrast, robust receptor labeling was displayed by OT cells in the ventral subdivision of medial parvicellular subnucleus and in the caudal PVH (dorsal subdivision of medial parvicellular subnucleus and lateral parvicellular subnucleus). Estrogen receptor-β signal was generally more intense and present in higher proportions of magnocellular and parvicellular VP vs. OT neurons of similar topography. Immunocytochemical observations were confirmed via triple-label in situ hybridization, an approach combining use of digoxigenin-, fluorescein-, and ^{35}S-labeled cRNA hybridization probes. Further, ER-β mRNA was also detectable in corticotropin-releasing hormone neurons in the parvicellular PVH. Finally, double-label immunocytochemical analysis of human autopsy samples showed that subsets of OT and VP neurons also express ER-β in the human. These neuroanatomical studies provide detailed information about the topographical distribution and cellular abundance of ER-β within subsets of hypothalamic OT and VP neurons in the rat. The variable receptor content may indicate the differential responsiveness to estrogen in distinct OT and VP neuronal populations. In addition, a relevance of these findings to the human hypothalamus is suggested. J. Comp. Neurol. 473:315–333, 2004.

Indexing terms: corticotropin releasing hormone; estradiol; magnocellular neurons; paraventricular nucleus, parvicellular neuron; supraoptic nucleus

Grant sponsor: National Science Foundation of Hungary; Grant number: OTKA T031770; Grant number: T043407; Grant sponsor: Hungarian Medical Research Council; Grant number: ETT 280/2000; Grant sponsor: Fifth EC Framework Program; Grant number: QLG3 2000-00844; Grant sponsor: National Institutes of Health; Grant number: HD27305; Grant sponsor: the Wellcome Trust; Grant number: 060202/Z/00/Z (C.W.C.).

*Correspondence to: Zsolt Liposits, Laboratory of Endocrine Neurobiology, Institute of Experimental Medicine, Hungarian Academy of Sciences, Szigony u. 43., Budapest 1083, Hungary. E-mail: liposits@koki.hu

Received 12 August 2003; Revised 2 January 2004; Accepted 7 January 2004

DOI 10.1002/cne.20127

Published online in Wiley InterScience (www.interscience.wiley.com).

Oxytocin (OT) and vasopressin (VP)-synthesizing neurons (OT neurons; VP neurons) of the hypothalamic paraventricular and supraoptic nuclei (PVH; SO) regulate a wide array of neuroendocrine and autonomic functions. Magnocellular OT and VP neurons project to the neurohypophysis (Scharrer and Scharrer, 1954; Burbach et al., 2001), thus forming the hypothalamo-neurohypophysial neurosecretory system that is involved in the control of reproductive functions (Fuchs and Saito, 1971; Wakerley et al., 1973; Pederson et al., 1985) and water-electrolyte balance (Robertson, 1976). Additional large subsets of OT and VP neurons are located in distinct parvicellular subdivisions of the PVH; they send axon projections to the hypophysial portal circulation in the external zone of the median eminence (Vandesande et al., 1977), brain stem, and spinal cord (Swanson and Kuypers, 1980; Tucker and Saper, 1985; Cechetto and Saper, 1988; Hallbeck and Blomqvist, 1999; Veronneau-Longueville et al., 1999; Hallbeck et al., 2001; Stern and Zhang, 2003) as well as limbic and olfactory areas (Buijs and Swaab, 1979; Sofroniew and Schrell, 1980; Hermes et al., 1988) to modulate a variety of endocrine and autonomic functions.

Circulating estrogens regulate many aspects of OT and VP neuronal functions in the rat. These include neuronal OT and VP mRNA expression (Van Tol et al., 1988; Caldwell et al., 1989; Nomura et al., 2002; Shughrue et al., 2002) and peptide (Jirikowski et al., 1988; Levin and Sawchenko, 1993) levels, serum (Skowsky et al., 1979; Yamaguchi et al., 1979), and pituitary (Van Tol et al., 1988; Levin and Sawchenko, 1993) levels of OT and VP, axonal (Crowley et al., 1978; Skowsky et al., 1979; Yamaguchi et al., 1979; Amico et al., 1981), and dendritic (Wang et al., 1995) release of OT, as well as the regulation of electrical activity of OT neurons (Negoro et al., 1973; Akaishi and Sakuma, 1985). The reported absence or only low level of expression of the classical estrogen receptor (ER-α) in the PVH and the SO (Simerly et al., 1990; Shughrue et al., 1997) of the rat, together with recent identification of the second isoform of estrogen receptor (ER-β) (Kuiper et al., 1996) within subsets of OT and VP neurons (Simonian and Herbison, 1997; Alves et al., 1998; Hrabovszky et al., 1998; Laflamme et al., 1998; Shughrue et al., 2002; Somponpun and Sladek, 2003; Stern and Zhang, 2003), indicate that direct estrogen effects on OT and VP neurons may be primarily exerted via the newly discovered ER-β. However, published reports of the topographical location of ER-β-containing OT and VP neurons have not been consistent thus far. Two studies have indicated greater expression of ER-β mRNA (Hrabovszky et al., 1998) and ER-β immunoreactivity (Alves et al., 1998) within VP as opposed to OT-containing cells of the SO. In contrast, other reports have described no ER-β immunoreactivity in the SO at all (Simonian and Herbison, 1997) or localized ER-β mRNA within OT neurons of the SO only (Laflamme et al., 1998). There has also been discrepancy with respect to the ER-β content of magnocellular neurons in the PVH; while one group reported ER-β mRNA expression in some magnocellular OT but not VP neurons (Laflamme et al., 1998), others (Hrabovszky et al., 1998; Somponpun and Sladek, 2003) found ER-β mRNA in magnocellular OT as well as VP neurons in the PVH. In contrast, some reports have indicated no ER-β immunoreactivity in magnocellular OT or VP neurons of the PVH (Simonian and Herbison, 1997; Alves et al., 1998). These discrepancies prompted the present investigations of ER-β protein and mRNA expression by OT and VP neurons in distinct anatomical compartments of the PVH (Swanson and Sawchenko, 1983; Swanson, 1998) and in the SO. First, we mapped ER-β-immunoreactive (IR) OT and VP neurons using double-label immunocytochemistry and highly specific polyclonal antibodies to mouse ER-β (Z8P; Zymed, San Francisco, CA) that also react with the rat ER-β sequence in tissue sections (Hrabovszky et al., 2001; Kallo et al., 2001; Shughrue et al., 2001). The subcellular distribution of ER-β was addressed using immunoelectron microscopy. Second, to supplement the ICC experiments, we examined the expression of ER-β mRNA in OT and VP mRNA-expressing neurons by means of a novel triple-labeling technique. This approach combined a sensitive methodology for radioisotopic in situ hybridization histo-

Abbreviations

ACC	accessory magnocellular cell groups
AHN	anterior hypothalamic nucleus
am	anterior magnocellular subnucleus of the hypothalamic paraventricular nucleus
AP	alkaline phosphatase
ap	anterior parvicellular subnucleus of the hypothalamic paraventricular nucleus
BST	bed nucleus of the stria terminalis
cDNA	complementary deoxyribonucleic acid
CRH	corticotropin releasing hormone
cRNA	complementary ribonucleic acid
DAB	3,3′-diaminobenzidine tetrahydrochloride
dm	dorsomedial nucleus
dp	dorsal parvicellular subnucleus of the hypothalamic paraventricular nucleus
DS	dextran sulfate
DTT	dithiothreitol
ER-α	estrogen receptor-α
ER-β	estrogen receptor-β
f	fornical subnucleus of the hypothalamic paraventricular nucleus
fx	fornix
ICC	immunocytochemical
IR	immunoreactive
ISHH	in situ hybridization histochemistry
lp	lateral parvicellular subnucleus of the hypothalamic paraventricular nucleus
mpd	hypothalamic paraventricular nucleus, dorsal subdivision of the medial parvicellular subnucleus
mpv	hypothalamic paraventricular nucleus, ventral subdivision of the medial parvicellular subnucleus
Ni-DAB	nickel-diaminobenzidine
OCH	optic chiasma
opt	optic tract
OT	oxytocin
pml	hypothalamic paraventricular nucleus, lateral subdivision of the posterior magnocellular subnucleus
pmm	hypothalamic paraventricular nucleus, medial subdivision of the posterior magnocellular subnucleus
pv	periventricular subnucleus of the hypothalamic paraventricular nucleus
PVH	hypothalamic paraventricular nucleus
RCH	retrochiasmatic area
SCH	suprachiasmatic nucleus
SO	hypothalamic supraoptic nucleus
SOr	retrochiasmatic portion of the hypothalamic supraoptic nucleus
VP	vasopressin
V3	third cerebral ventricle
ZI	zona incerta

chemistry (ISHH) (Hrabovszky and Petersen, 2002) to detect ER-β mRNA with the simultaneous nonisotopic ISHH identification of OT as well as VP neurons. The occurrence of ER-β mRNA was also investigated in parvicellular neurons containing corticotropin releasing hormone (CRF) mRNA. Finally, to study the presence of ER-β in OT and VP cells of the human hypothalamus, tissue samples from human autopsies were used in double-label immunocytochemical (ICC) experiments.

MATERIALS AND METHODS

Experimental animals

Adult female Sprague-Dawley rats (n = 16; 200–225 g) were purchased from Charles-River Hungary (Isaszeg, Hungary). The animals were housed in light- and temperature-controlled environment with free access to food and water and treated in accordance with the legal requirements of the Animal Care and Use Committee of the Institute of Experimental Medicine and the European Community (Decree 86/609/EEC). All experimental protocols were reviewed and approved by the Animal Welfare Committee at the Institute of Experimental Medicine. Following 1 week of acclimation, the rats were ovariectomized bilaterally under pentobarbital anesthesia (35 mg/kg, ip) and allowed to survive for 14 days before sacrifice.

Immunocytochemical detection of oxytocin and vasopressin neurons with estrogen receptor-β in the rat hypothalamus

Tissue preparation. Ovariectomized rats (n = 4) were anesthetized and sacrificed by transcardiac perfusion with 150 ml fixative solution containing 2% paraformaldehyde (Sigma Chemical, St. Louis, MO) and 4% acrolein (Aldrich Chemical, Milwaukee, WI) in 0.1M phosphate buffered saline (PBS; pH 7.4). The perfused hypothalami were dissected out, immersed in 25% sucrose overnight, and labeled by micropunches to allow for the subsequent identification of section sources. Then the tissue blocks were snap-frozen on dry ice and 20 μm free-floating sections according to plates 22–27 of Swanson's (1998) brain atlas were prepared in the coronal plane using a Leica CM 3050 S cryostat (Leica Microsystems, Nussloch, Germany). The sections were collected serially in four groups, each combining every fourth section from four animals. The processing of combined section pools throughout the ICC labeling procedures precluded the signal variability that must be expected when batches are processed separately. Following the ICC procedures detailed below, the sections were transferred into 0.3% polyvinyl alcohol (Mol. Wt. 70,000–100,000; Sigma) and mounted in a rostral-caudal sequence onto glass microscope slides. Then sections were air-dried, dehydrated in graded ethanol (95%, followed by 100%; 5 minutes in each), cleared in xylene (2 × 5 minutes) and coverslipped with DPX mounting medium (Fluka, Buchs, Switzerland).

Immunocytochemical detection of estrogen receptor-β. The ICC detection of ER-β was carried out as reported recently (Hrabovszky et al., 2001; Kallo et al., 2001; Shughrue and Merchenthaler, 2001). Sections of all four groups were first treated with 0.5% sodium borohydride (Sigma; 30 minutes) in PBS to remove residual aldehydes, then with 10% thioglycolic acid (Sigma) to suppress tissue argyrophylia (30 minutes) (Gallyas, 1982) and finally, with 0.5% H_2O_2 (15 minutes) to eliminate endogenous peroxidase activity. Nonspecific antibody binding sites were blocked using a 30-minute preincubation with a blocking solution which consisted of 2% normal horse serum (NHS), 0.4% Triton X-100, and 0.1% merthiolate in TBS (0.1M Tris-HCl with 0.9% NaCl; pH 7.8). The sections were incubated for 5 days at 4°C in Z8P rabbit primary antibodies to mouse ER-β (Zymed; 1:5,000 dilution with TBS; pH 7.8, containing 2% NHS, 0.4% Triton X-100, and 0.1% merthiolate). Estrogen-receptor-β immunoreactivity was detected using sequential incubations in biotinylated secondary antibodies (donkey, biotin-SP-antirabbit IgG; Jackson ImmunoResearch Laboratories, West Grove, PA; 1:1,000), then in ABC-Elite reagent (Vector, Burlingame, CA; 1:1,000 dilution of solutions "A" and "B" in TBS). The developer contained 10 mg diaminobenzidine (DAB), 30 mg nickel-ammonium-sulfate (Ni), and 0.003% H_2O_2 in 24 ml Tris-HCl buffer solution (0.05M; pH 8.0). Then the silver intensification of the peroxidase reaction product (in this case Ni-DAB) was carried out as detailed elsewhere by Liposits et al. (1984). One section group was used to analyze the regional distribution of ER-β. The second group was mounted on gelatin-coated slides in a rostral-caudal sequence, air-dried, and stained with Cresyl violet to facilitate the anatomical localization of ER-β cells in distinct paraventricular subnuclei. The remaining two sets of sections were processed further for the ICC detection of OT and VP neurons.

Immunocytochemical detection of oxytocin and vasopressin. The ICC detection of either OT or VP was carried out using monoclonal antibodies against OT-neurophysin (PS-38; 1:500) (Zhang et al., 2002) (the monoclonal antibodies PS-38 and PS-41 to OT and VP, respectively, were generous gifts from Dr. H. Gainer, NIH, Bethesda, MD) and a commercially available polyclonal rabbit antiserum to VP (647171; ICN Immunobiologicals, Lisle, IL; 1:4,000). Following a 48-hour incubation in primary antibodies, the sections were transferred into appropriate species-specific biotinylated secondary antibodies (Jackson; 1:1,000) and then into ABC-Elite solution (Vector) for 1 hour each. The peroxidase reaction was developed using the DAB chromogen (10 mg DAB and 0.005% H_2O_2 in 50 ml TBS) in the absence of nickel ions, resulting in brown cytoplasmic color in OT and VP neurons, readily distinguishable from the gray-to-black chromogen deposition within ER-β-IR cell nuclei. To prevent the masking of faint nuclear ER-β signals by DAB deposition, care was taken to avoid the development of excessive cytoplasmic staining (Axelson and van Leeuwen, 1990).

Immunocytochemical control experiments. Specificity of the ER-β labeling was tested by omission of the primary or secondary antibodies and by immunoneutralization of the ER-β antiserum (5 μg neutralizing peptide/ml working dilution of the antiserum) with a synthetic peptide corresponding to the final 19 amino acids at the carboxy terminus of rat ER-β (Kallo et al., 2001). All of these changes in the ICC procedure resulted in complete absence of labeling. Specificity of OT and VP labeling was tested by the double-immunofluorescent detection of OT and VP in the same control sections. Consistent with the expression of the two peptides by different cell populations, the different fluorochromes were found to label distinct cells in the PVH and the SO, with a minimal degree of overlap as reported previously for nonlactating rats (Mezey and Kiss, 1991).

Analysis of estrogen receptor-β-immunoreactive neurons in the paraventricular and supraoptic nuclei. Single- and double-labeled sections were first categorized into one of six rostrocaudal planes according to Swanson's brain atlas (levels 22–27) (Swanson, 1998) based on the morphological appearance of the PVH. The distribution of ER-β-containing cells was examined in distinct subnuclei of the PVH, in the SO and in accessory magnocellular cell groups (ACC) at each level using the single-immunolabeled sections. The ER-β signals typical of each region were characterized on a scale of five intensities of labeling, with "+" meaning "very low," "++" meaning "low," "+++" meaning "medium," "++++" meaning "high," and "+++++" meaning "very high."

Then, using the double-labeled specimens, OT and VP neurons were analyzed individually at high magnification to determine the percentages of ER-β-containing OT and VP cells in each subdivision of the PVH, in the SO, and in the ACC. In addition, the characteristic intensity of ER-β labeling was determined for each OT and VP cell population and presented on the same scale of five as described for single-labeling studies. Digital photomicrographs were prepared with an RT Spot digital camera (Diagnostic Instrument, Sterling Heights, MI) mounted on a Zeiss Axiophot microscope (Zeiss, Göttingen, Germany). The digital images were processed with the Adobe PhotoShop 5.5 computer software at 300 dpi resolution and printed on Hewlett Packard photo-quality printer paper. Examples of ER-β signals considered characteristic of the most important subsets of OT and VP neurons are illustrated in high-power photomicrographs.

Electron microscopic detection of estrogen receptor-β in the paraventricular nucleus of the rat

Four male rats were used to study the subcellular distribution of ER-β in parvicellular and magnocellular neurons of the PVH. The anesthetized animals were perfused via the ascending aorta, first with 30 ml of PBS (pH 7.4; 420 mOsM) followed by 300 ml of 1% paraformaldehyde and 1% glutaraldehyde in PBS. The brains were removed and serial coronal sections (25 μm) were cut on a Vibratome (Technical Products International, St. Louis, MO). The sections were infiltrated with sucrose (15% for 1 hour, then 30% overnight) and permeabilized by three repeated freeze–thaw cycles over liquid nitrogen. The ICC detection of ER-β was performed as described above for light microscopy, except for the omission of Triton-X 100 from the antibody solutions. The antigenic sites were detected by silver-gold intensified DAB chromogen (Liposits et al., 1984). Small tissue blocks containing the PVH were dissected, osmicated (1% osmium tetroxide in distilled water for 30 minutes), and dehydrated in a graded series of ethanol (30%, 50, 70, 90, 96, and 100%, 10 minutes each). A 30-minute contrasting step using 2% uranyl acetate in 70% ethanol was inserted in the dehydration process and finally the fully dehydrated sections were infiltrated with propylene oxide and flat-embedded in Durcupan ACM epoxy resin (Fluka, Ronkonkoma, NY). Semithin (1 μm) and ultrathin (50–60 nm) sections were cut from the hardened resin blocks with a Leica Ultracut UCT ultramicrotome (Leica Microsystems, Wetzlar, Germany). The ultrathin sections were collected on Formvar-coated single-slot grids, contrasted with Reynold's lead citrate and examined with Jeol-100C transmission electron microscope.

Triple-label in situ hybridization studies in rats

Tissue preparation. Ovariectomized rats (n = 4) were euthanized by CO_2 asphyxiation and decapitated. The brains were removed rapidly and frozen on powdered dry ice. Twelve-μm coronal sections corresponding to plates 22–27 of Swanson's (1998) brain atlas were cut serially from the PVH and the SO on a cryostat and thaw-mounted on gelatin-coated microscope slides. The sections were dried, transferred into slide boxes, and stored at −80°C until used.

Preparation of cDNA templates for in vitro RNA transcription.

Estrogen receptor-β cDNA templates. Total hypothalamic RNA was prepared with the STAT-60 total RNA isolation reagent (Tel-Test, Friendswood, TX) and reverse-transcribed with MMLV reverse transcriptase (Stratagene, La Jolla, CA) using rat ER-β-specific reverse primers. Then, two cDNA fragments complementary to bases 918–1667 and 2043–2535, respectively, of the rat ER-β cDNA (Kuiper et al., 1996) were amplified using a Mastercycler Gradient thermal cycler (Eppendorf Scientific, Westbury, NY). The amplicons were cloned using the TOPO TA Cloning kit from Invitrogen (Carlsbad, CA). Plasmids containing the cDNAs were grown in TOPO cells (Invitrogen), isolated with the QIAfilter Plasmid Midi kit (Qiagen, Valencia, CA) and linearized at the EcoRV restriction site. Finally, the transcription templates were purified with phenol/chloroform/isoamyl alcohol (PCI), followed by chloroform/isoamyl alcohol (CI) extractions, then precipitation with NaCl and ethanol.

Rat oxytocin cDNA template. Total hypothalamic RNA was isolated and OT cDNA reverse-transcribed using the OT-specific reverse PCR primer. Then, a 175-bp cDNA fragment corresponding to bases 1–175 of the rat OT mRNA (Rehbein et al., 1986) was amplified with polymerase chain reaction and cloned with the TOPO TA Cloning kit. A plasmid preparation (QIAfilter Plasmid Midi kit; Qiagen) was digested at the BamHI restriction site of the TOPO vector and the transcription template was purified with PCI and CI extractions and then precipitation with NaCl and ethanol.

Rat vasopressin cDNA template. A 241-bp PstI fragment of the VP cDNA was inserted into the pGEM3 vector (the VP cDNA was kindly provided by Dr. Thomas Sherman, University Medical Center, Washington, DC). To generate a transcription template, the vector was linearized at the EcoRI restriction site and purified.

Probe preparation by in vitro RNA transcription. Two antisense RNA probes targeting different segments of the ER-β mRNA were transcribed from the cDNA templates with SP6 RNA polymerase in the presence of ^{35}S-UTP (NEN Life Science Products, Boston, MA) as detailed (Hrabovszky and Petersen, 2002). The 10-μl transcription reactions were composed of the following ingredients: linearized cDNA template, 1 μg; 5× transcription buffer, 2 μl; 100 mM dithiothreitol (DTT), 1 μl; 10 mM ATP, CTP, and GTP, 0.5 μl each; ^{35}S-UTP (NEN), 120 pmol; 20 U/μl RNAsin (Promega, Madison, WI), 0.5 μl; 20 U/μl T7 RNA polymerase (Promega), 0.5 μl. The reaction was allowed to proceed for 30 minutes at 37°C. A second aliquot of RNA polymerase was then added and the cocktail incubated

further for an additional 30 minutes. The volume was brought up to 90 μl with nuclease-free water, and the cDNA template was degraded for 30 minutes at 37°C after the addition of 1 μl 10 U/μl DNase I (Roche Diagnostics, Indianapolis, IN), 5 μl 1 M Tris/HCl buffer (pH 8.0), 1 μl transfer RNA (tRNA; 25 mg/ml), 1 μl 1 M $MgCl_2$ and 0.5 μl RNasin (40 U/μl) to the reaction mixture. Finally, the probes were purified by extractions with PCI and CI. Unincorporated nucleotides were eliminated by performing two sequential NaCl/ethanol precipitations. The probe pellets were dissolved in 0.1% sodium dodecyl sulfate and combined in the hybridization cocktail at 80,000 cpm/μl hybridization buffer concentrations of each probe.

To generate a digoxigenin-labeled cRNA probe to VP, the cDNA template was transcribed in vitro with SP6 RNA polymerase in the presence of digoxigenin-11-UTP (Roche Diagnostics, Indianapolis, IN) as described previously (Petersen and McCrone, 1994). Briefly, the reaction mixture consisted of the following ingredients: linearized template DNA, 1 μg; 5× transcription buffer, 2 μl; 100 mM DTT, 1 μl; 10 mM of ATP, CTP, and GTP, 0.5 μl each; 10 mM digoxigenin-11-UTP, 0.5 μl; 1 mM UTP, 1 μl; 40 U/μl RNAsin (Promega), 0.5 μl; 20 U/μl SP6 RNA polymerase (Promega), 1 μl. Following a 1-hour incubation of the cocktail at 37°C, a second 20 U aliquot of SP6 RNA polymerase was added and the reaction incubated for an additional 1 hour. The cDNA template was digested as described for the preparation of radioisotopic ER-β probes. The probe was purified by sodium chloride/ethanol precipitation and the pellet dissolved in 100 μl of 0.1% sodium dodecyl sulfate. Test hybridization experiments were used to determine the optimal concentration of VP probe in the hybridization solution (typically 1/50–1/300).

A fluorescein-labeled complementary RNA probe to OT was transcribed from the linearized cDNA template with T7 RNA polymerase as described for the digoxigenin-labeled VP probe, except for the substitution of fluorescein-12-UTP (NEN) for digoxigenin-11-UTP.

Probe hybridization and signal visualization. Prior to hybridization, the slides were removed from the freezer, warmed to room temperature for 10 minutes, and processed through the following prehybridization steps: 30-minute fixation in phosphate-buffered 4% paraformaldehyde solution, 2-minute rinse in standard saline citrate solution (2× SSC; 1× SSC = 0.15 M NaCl/0.015 M sodium citrate, pH 7.0), 10-minute acetylation in 0.25% acetic anhydride/0.9% NaCl/0.1 M triethanolamine (pH 8.0; Sigma), 2-minute rinse in 2× SSC, dehydration in 70, 80, 95, and 100% ethanol (2 minutes each), delipidation in chloroform (5 minutes), and finally, partial rehydration in 100%, followed by 95% ethanol (2 minutes each). The slides were then air-dried on slide trays.

The sections were hybridized with a mixture of nonisotopic and radioisotopic cRNA probes in hybridization buffer (50% formamide, 2× SSC, 20% dextran sulfate (DS), 1× Denhardt's solution, 500 μg/ml yeast tRNA, 500 μg/ml heparin sodium salt, 0.1% sodium pyrophosphate, 750 mM DTT). The detection sensitivity for ER-β mRNA was enhanced by the use of increased probe (80,000 cpm/μl hybridization solution of each probe), increased DS (20%, instead of the widely used 10%) and increased DTT (750 mM, instead of the commonly used 50–200 mM) concentrations (Hrabovszky and Petersen, 2002). The slides were transferred into plastic Nalgene boxes and a 25-μl volume of hybridization mixture was pipetted onto each section. The hybridization solution was covered with glass coverslips and the hybridization was allowed to proceed at 50°C for 16 h. To moisturize air, several centrifuge tube (50 ml) caps containing water were placed in the hybridization chambers.

The glass coverslips were floated off from the hybridized sections in a beaker containing 1× SSC solution (room temperature, RT), and then most of the excess hybridization solution was removed by agitating the slides manually in three changes of 1× SSC solution (RT). The subsequent posthybridization steps were performed on an orbital shaker in stainless steel racks: 1× SSC, 2 × 20 minutes (RT); 50 μg/ml RNAse A (dissolved in 0.5 M NaCl/10 mM Tris-HCl/1 mM EDTA; pH 7.8), 30 minutes (37°C); 2× SSC, 10 minutes (RT); 0.1× SSC, 2× 30 minutes (52°C); 2× SSC, 10 minutes (RT). Finally, the slides were rinsed with TBS for 30 minutes.

Prior to the immunocytochemical detection of nonisotopic hybridization signals, the sections were treated with 0.2% Triton X-100 (Sigma) in TBS for 20 minutes, then to minimize the nonspecific binding of antibodies, preincubated for 30 minutes with a blocking solution containing 2% blocking reagent for nucleic acid hybridization and detection (Roche) and 0.9% NaCl in 100 mM maleate buffer (pH 7.5). The cocktail of antibodies used next contained the same blocking solution, anti-digoxigenin antibodies conjugated to alkaline phosphatase (anti-digoxigenin-AP; Fab fragment; 1:1,000; Roche) and antifluorescein antibodies conjugated to horseradish peroxidase (antifluorescein-HRP conjugate; NEN; 1:500). This mixture was applied to the sections for 48 hours at 4°C with the aid of press-seal probe clips (Sigma). To visualize the enzyme reactions, the slides were first rinsed in TBS, then incubated for 30 minutes in biotin tyramide solution (diluted at 1:1,000 with TBS/0.002% H_2O_2 from a stock prepared according to Adams, 1992). Following the deposition of biotin tyramide reporter in OT neurons (IR to fluorescein), the AP signal in VP neurons (IR to digoxigenin) was visualized using the 5-bromo-4-chloro-3-indolyl-phosphate/4-nitro blue tetrazolium BCIP/NBT chromogen system (Roche) according to the manufacturer's instructions. The development of purple color reaction was monitored at intervals and stopped after 30–60 minutes. The sections were rinsed briefly in TBS and transferred into the ABC-Elite reagent (Vector) for 1 hour in order to introduce HRP to the sites of biotin tyramide deposition in OT neurons. The peroxidase reaction was finally detected with DAB (prepared and used as described for ICC experiments), which resulted in brown chromogen deposition in OT perikarya. Double-stained sections were rinsed copiously in TBS (30 minutes), dipped quickly into MQ water, dehydrated in a graded series of ethanol (70, 80, 95, 100%; 2 minutes each), then dried on slide trays.

Detection of nonisotopic probes to OT and VP was followed by the autoradiographic visualization of the ER-β probes. To prevent chemographic artifacts by the BCIP/NBT chromogen in the NTB-3 (Kodak, Rochester, NY) photographic emulsion (Young and Hsu, 1991; Petersen and McCrone, 1994), the slides were dipped sequentially twice into 1% solution of Parlodion (Mallinckrodt, St. Louis, MO) dissolved in amyl acetate and air-dried (Hrabovszky et al., 1995). Then, they were coated with thawed (42°C) NTB-3 emulsion (diluted 1:1 with distilled water), dried, and exposed for 6 weeks in light-tight exposure boxes at 4°C. The slide autoradiographs were developed with prechilled (15°C) Dektol developer (Kodak; di-

luted 1:1 with MQ water; 2 minutes), rinsed with MQ water (30 seconds), and fixed with Kodak fixer (5 minutes). Then, the sections were rinsed in several changes of chilled MQ water, air-dried on slide trays overnight, dehydrated in ethanol (95%, 5 minutes; 100%, 2 × 5 minutes), transferred briefly into xylenes (30 seconds) and coverslipped. Digital photomicrographs were prepared and processed as described for ICC studies.

In situ hybridization control experiments. To check for specificity of radioisotopic as well as nonisotopic hybridization signals, RNase A-pretreated sections were used as a negative control approach. These control sections were processed in parallel with the experimental specimens and found to lack any labeling for OT, VP, and ER-β. The OT and VP probe sequences were designed to prevent cross-hybridization artifacts due to the very high homology at the neurophysin segments in OT-neurophysin and VP-neurophysin mRNAs. In addition, the distribution of hybridization signals for OT and VP mRNAs matched the ICC signal patterns, serving as further evidence for hybridization specificity. In the case of ER-β probes, a positive control approach was the separate and combined use of the "ER-β 750" and "ER-β 498" probes on neighboring test sections. The discovery that the two different probes generated identical patterns of signal distribution when applied to the sections individually, and an increased signal intensity when combined in the hybridization solution, provided additional evidence for hybridization specificity.

In situ hybridization detection of estrogen receptor-β mRNA in corticotropin-releasing hormone neurons

To partially reveal the neurochemistry of parvicellular neurons containing ER-β mRNA, dual-label ISHH studies were carried out on paraventricular sections of ovariectomized rats (n = 4) with the combined use of a digoxigenin-labeled cRNA probe to corticotropin-releasing hormone (CRH) mRNA and the two ^{35}S-labeled cRNA probes to ER-β mRNA. The 1100-bp segment of rat CRH cDNA (the CRH cDNA was a gift from Dr. K. Mayo, Northwestern University, Evanston, IL) used as transcription template was inserted into the pGEM 4Z vector. The vector was linearized at the Hind III restriction site and antisense CRH probe was transcribed with SP6 RNA polymerase in the presence of digoxigenin-11-UTP, according to the procedure described for the preparation of the VP probe. The ISHH studies were performed as detailed for triple-labeling experiments and the two signal components detected as published recently (Hrabovszky et al., 2000, 2001). To visualize the nonisotopic signal for CRH, the sections were incubated for 2 days with antidigoxigenin antibodies conjugated to horseradish peroxidase (anti-digoxigenin-POD; Fab fragment; 1/200; Roche). This was followed by the POD-catalyzed deposition of biotin tyramide, incubation with the ABC working solution, and finally, detection of the POD signal using DAB in the developer, as detailed for the visualization of OT cells in the present triple-labeling experiments.

Immunocytochemical studies of human hypothalami

Human hypothalamic samples were obtained from autopsy at the Forensic Medicine Department of Semmelweis University (Budapest, Hungary). Protocols were reviewed and approved by the Regional Committee of Science and Research Ethics (TUKEB 49/1999). To examine the expression of ER-β in OT and VP neurons of the human PVH and SO, hypothalamic tissue blocks from three human individuals (a 33-year-old male and two females age 34 and 72 years) with no history of neurological disorders were used. Small tissue blocks containing the SO and the PVH were dissected and immersed into 4% paraformaldehyde for 72 hours, infiltrated with 25% sucrose for 72 hours, and then sectioned at 25 μm with a cryostat. Double-label immunocytochemistry was performed as follows: sections were pretreated with 0.4% Triton X-100 for 30 minutes and 0.5% H_2O_2 for 15 minutes, then incubated in 1:20,000 dilution of primary antibodies raised in a sheep against human ER-β (P3) (the human ER-β antiserum was generously provided by Dr. Philippa T.K. Saunders, MRC Human Reproductive Sciences Unit, Centre for Reproductive Biology, Edinburgh, UK) (Saunders et al., 2000). The primary serum incubation was followed by treatment with the secondary antibodies (biotin-SP-antisheep IgG; Jackson; 1:1,000) and the ABC reagent for 1 hour each. Then ER-β signal was visualized with the Ni-DAB chromogen. Subsequently, OT or VP neurons were also immunostained with the biotinylated secondary antibody-ABC technique using PS-38 and PS-41 (Zhang et al., 2002) as primary antibodies, respectively, and DAB as the chromogen.

RESULTS

Immunocytochemical detection of oxytocin and vasopressin neurons with estrogen receptor-β in the rat hypothalamus

Light microscopic analysis of single-labeled sections revealed the presence of ER-β-IR cells in all subdivisions of the PVH and in the SO (Fig. 1). Immunolabeling appeared to be confined to cell nuclei and the intensity of the ER-β signal was highly variable among, and even within, anatomical subdivisions of the PVH (Swanson and Kuypers, 1980; Swanson, 1998) (for illustration of results, see Fig. 1). The periventricular subnucleus of the PVH (pv; levels 22–27) contained a few ER-β-IR cells, which were usually labeled weakly (+; ++; +++). The anterior magnocellular (am; level 22) and anterior parvicellular (ap; levels 22–24) subnuclei of the PVH exhibited labeled cells somewhat more frequently than the pv of the PVH, with signal intensities ranging from very low to medium (+; ++; +++). The number of labeled cells was relatively low in the dorsal parvicellular subnucleus of the PVH (dp; levels 25 and 26); the typical intensity of labeling was very low or low (+; ++), but a few heavily labeled cells (++++) were also present. The relatively frequent ER-β-IR cells in the dorsal subdivision of the medial parvicellular subnucleus of the PVH (mpd; levels 25, 26) exhibited a wide range of labeling intensities from very low to medium (+; ++; +++). The medial subdivision of the posterior magnocellular subnucleus of the PVH (pmm; level 25) was rich in labeled cell nuclei that showed low or medium intensity of labeling (++; +++). Heavy labeling (++++) characterized a high proportion of cells in the lateral subdivision of the posterior magnocellular subnucleus of the PVH (pml; level 26), but cells exhibiting very low or low signal (+; ++) were also observed. The ventral subdivision of the medial parvicellular subnucleus (mpv; level 26) as well as

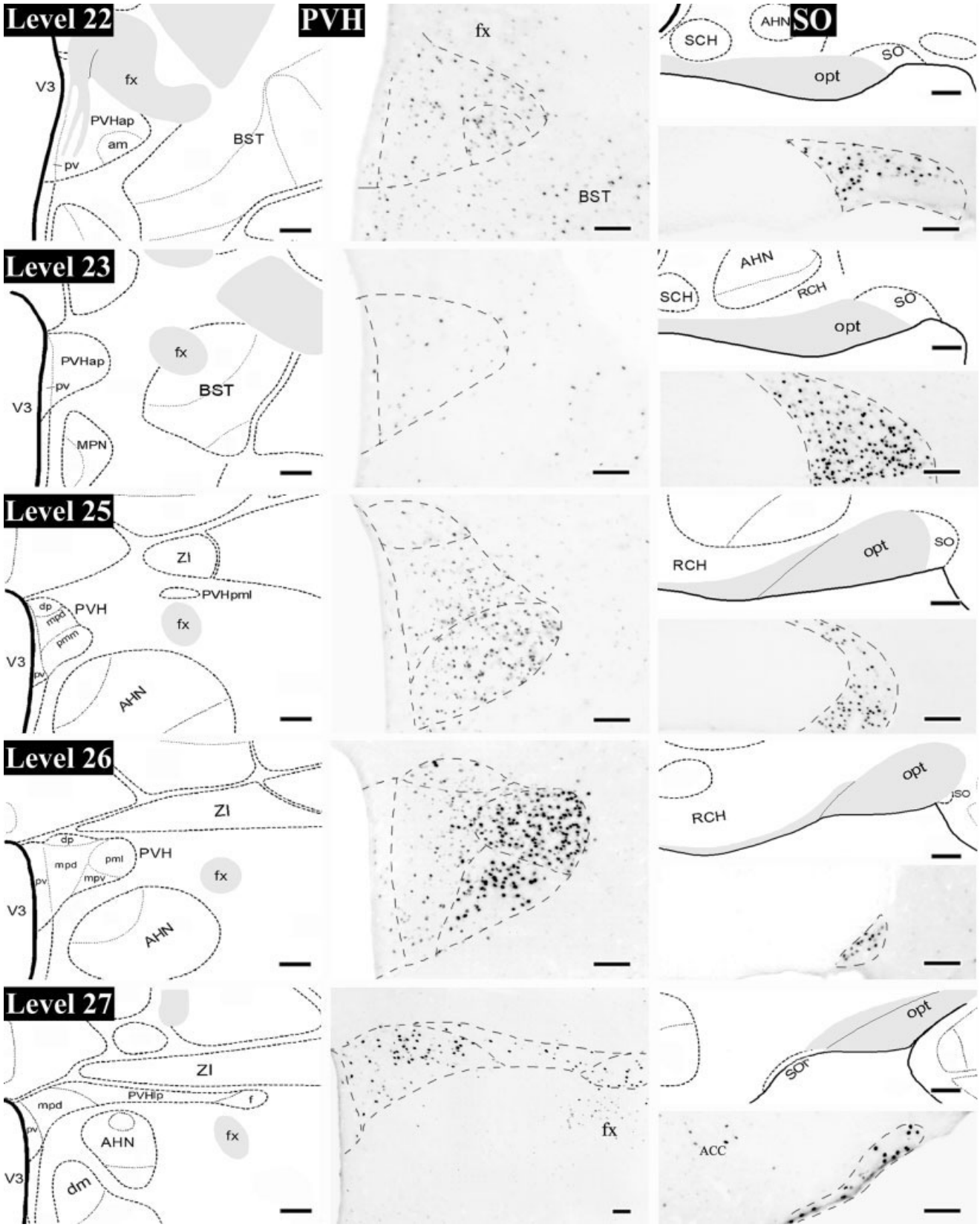

Fig. 1. Distribution of estrogen receptor-β (ER-β) immunoreactivity in the hypothalamic paraventricular and supraoptic nuclei (PVH; SO). Most subdivisions of the hypothalamic PVH, except for the pv, contain a large number of cells labeled for ER-β at variable intensities. The most intense nuclear labeling for ER-β can be observed within the mpd-lp and the mpv subdivisions of the PVH at levels 27 and 26, respectively, of Swanson's brain atlas (Swanson, 1998). Heavy signals are also present in the pml, f, and dp subdivisions of the PVH, throughout the SO, and in accessory magnocellular cell groups (ACC; right lower panel). Scale bars = 200 μm in atlas schemas; 100 μm in photomicrographs.

the mpd and the lateral parvicellular subnuclei (lp; level 27) of the PVH showed a very high signal level for ER-β (+++++). The fornical subnucleus of the PVH (f), the rostrocaudal extent of the SO, and accessory magnocellular cell groups contained cells labeled at either high (++++) or very low-to-medium intensity (+; ++; +++).

In double-labeled sections, the regional distribution of OT-IR and VP-IR neurons agreed with previous findings (Hou Yu et al., 1986). High percentages of OT (45.0–97.7%) and VP (88.1–99.1%) neurons contained nuclear ER-β labeling in all regions. Nevertheless, the labeling intensity for ER-β varied markedly among distinct cell groups and even among neurons that belonged to the same anatomical subdivision. The general description below concerns the most characteristic appearance(s) of OT and VP cells in the different anatomical subdivisions; representative images are shown in Figure 2. The numbers of OT-IR and VP-IR neurons analyzed, the percentages of OT-IR and VP-IR neurons expressing ER-β, and the most frequently observed labeling intensity patterns are summarized in Table 1.

The rostrocaudal extent of the pv subnucleus of the PVH typically contained OT neurons unlabeled or weakly labeled (+; ++) for ER-β (Fig. 2B). The double-labeled cells constituted 45.0 ± 2.0% of all OT-IR neurons; this represented the lowest incidence of coexpression observed in this study. Most of the VP-IR cells (90.4 ± 3.8%) were stained for ER-β, but typically only weakly (+; ++). Oxytocin-IR neurons predominated over VP-IR cells in the am (level 22; Fig. 2A) and ap (levels 22–24) subnuclei of the PVH; approximately half of these OT-IR neurons (52.2 ± 4.8%, SEM) and most of the VP-IR neurons (91.1 ± 1.9%) were labeled for ER-β, typically at very low (+), low (++), or medium (+++) intensity (Fig. 2C). Level 25 contained high numbers of magnocellular OT and VP neurons intermingled within the pmm subnucleus of the PVH (Fig. 2G,I); although the labeling intensity for ER-β ranged only from very low (+) to medium (+++) in these neurons, the majority of OT-IR (71.1 ± 3.9%) and VP-IR (97.6 ± 1.1%; Fig. 2H) neurons displayed ER-β immunoreactivity, the heaviest signal (+++) being observed in the latter cell population (Fig. 2H). Estrogen receptor-β signal strength for the scattered OT-IR and VP-IR neurons located in the mpd subnucleus of the PVH at levels 25–26 was variable. Here, 64.4 ± 5.1% of OT-IR cells and 88.4 ± 5.8% of VP-IR cells were labeled for ER-β at very low to medium intensity (+; ++; +++). In the dp subnucleus of the PVH at levels 25 (Fig. 2G,H) and 26 (Fig. 2J), OT/ER-β neurons constituted 52.6 ± 7.9% of all OT-IR cells. The less numerous VP-IR neurons in this region were usually labeled for ER-β (88.1 ± 2.5%). Some of the OT-IR (Fig. 2H) and VP-IR cells in the dp subnucleus of the PVH were labeled heavily for ER-β (+++; ++++); however, weakly labeled (+; ++) or unlabeled cells were also observed. The pml subnucleus of the PVH at level 26 (Fig. 2J) contained a major population of magnocellular VP neurons (Fig. 2L), 94.2 ± 0.6% of which were labeled for ER-β. A frequently encountered labeling intensity in these cells was heavy (++++), but a large subset (about 50%) of the VP-IR neurons contained only a weak ER-β signal (+; ++). The central core of VP neurons in the pml of the PVH was surrounded by magnocellular OT neurons (Fig. 2J); of these OT neurons, 65.6 ± 7.6% were labeled for ER-β, but, in contrast to the local VP cells, their labeling intensity was only very low or low (+; ++). Oxytocin-IR neurons exhibiting the most intense labeling for ER-β in the whole hypothalamus were located in the mpv subnucleus of the PVH at level 26 (Fig. 2J,K) and in the mpd-lp subnuclei of the PVH at level 27 (Fig. 2M). These OT-IR cells exhibited a homogeneously very heavy signal for ER-β (+++++) and nearly all of the cells (97.7 ± 1.3% in the mpv and 97.2 ± 1.1% in the mpd-lp subnuclei of the PVH) were double-labeled. Similarly, most of the VP-IR neurons in these sites (99.1 ± 0.9% in the mpv and 97.8 ± 1.3% in the mpd-lp subnuclei) were also labeled for ER-β, but typically somewhat less heavily (++++) than in the case of the OT neurons. While OT-IR neurons predominated within the mpd subunit of the PVH at level 27, the incidence of VP neurons increased laterally, outnumbering OT-IR neurons in the lateral part of the lp and in the f subdivisions of the PVH. Most of the VP-IR cells (94.4 ± 2.8%; Fig. 2N) and a lower percentage of the OT-IR cells (60.2 ± 2.4%) in the f subnucleus of the PVH were double-labeled for ER-β. From this subnucleus, VP-IR and OT-IR neurons followed the arched course of blood vessels towards the retrochiasmatic portion of the SO at the ventral surface of the brain, coalescing into accessory magnocellular cell groups. Oxytocin-IR and VP-IR neurons in the f subnucleus of the PVH, in accessory nuclei, and across the rostrocaudal extent of the SO (Fig. 2D–F,O) had common labeling characteristics in that a heavy ER-β signal (++++) was typical for a large subset of VP-IR cells neurons (Fig. 2F,O), but OT neurons were labeled to much lower intensities (+; ++; +++). It is noteworthy that a significant subset of magnocellular VP neurons (e.g., approximately half of the ER-β-IR VP neurons in the SO) contained only weak ER-β labeling (+; ++). Estrogen receptor-β immunoreactivity was present in 88.4 ± 0.9% of VP neurons in the SO, 92.5 ± 1.1% of VP neurons in accessory magnocellular cell groups, 59.5 ± 4.3% of OT neurons in the SO, and 54.9 ± 3.3% of OT neurons in accessory magnocellular cell groups.

Electron microscopic detection of ER-β in the paraventricular nucleus of the rat

Semithin sections of the PVH displayed cell nuclei that were labeled for ER-β at variable intensities (Fig. 3A). The nucleoli remained typically unstained. The electron micro-

Fig. 2. Intensity of estrogen receptor-β (ER-β) signal in distinct subsets of oxytocin (OT) and vasopressin (VP) neurons at different rostrocaudal levels of the hypothalamus. Oxytocin and VP neurons double-labeled for ER-β are indicated by white and black arrows, respectively. **A,B:** Most OT neurons in the pv exhibit only weak, if any, labeling. A,**C:** Weak signal is also typical for OT cells of the am subnucleus. **D,E:** The SO contains heavily labeled cells in its ventral aspect, with a pattern distinct from the distribution of OT neurons. Double-labeled OT cells in the SO exhibit lightly ER-β immunoreactive cell nuclei. **F:** Approximately half of the magnocellular VP neurons in the SO display heavy ER-β signals. **G,H:** Although ER-β-positive OT neurons in the dp are usually labeled weakly, a subset (arrows) of OT neurons exhibits intense immunostaining for the receptor. **I:** Magnocellular VP neurons in the pmm exhibit low to medium signal intensity. **J,K:** The highest intensity for the ER-β signal is found in OT neurons of the mpv. **L:** A large subset of VP cells in the central core of the pml are labeled heavily. **M:** OT cells of the mpd and lp subdivisions at level 27 exhibit similarly intense ER-β immunoreactivity to those in the mpv. **N,O:** Many VP cells in the f subnucleus of the PVH and in the SOr are labeled heavily. Scale bars = 75 μm in A,D,G,J,M; 25 μm in B,C,E,F,H,I,K,L,N,O.

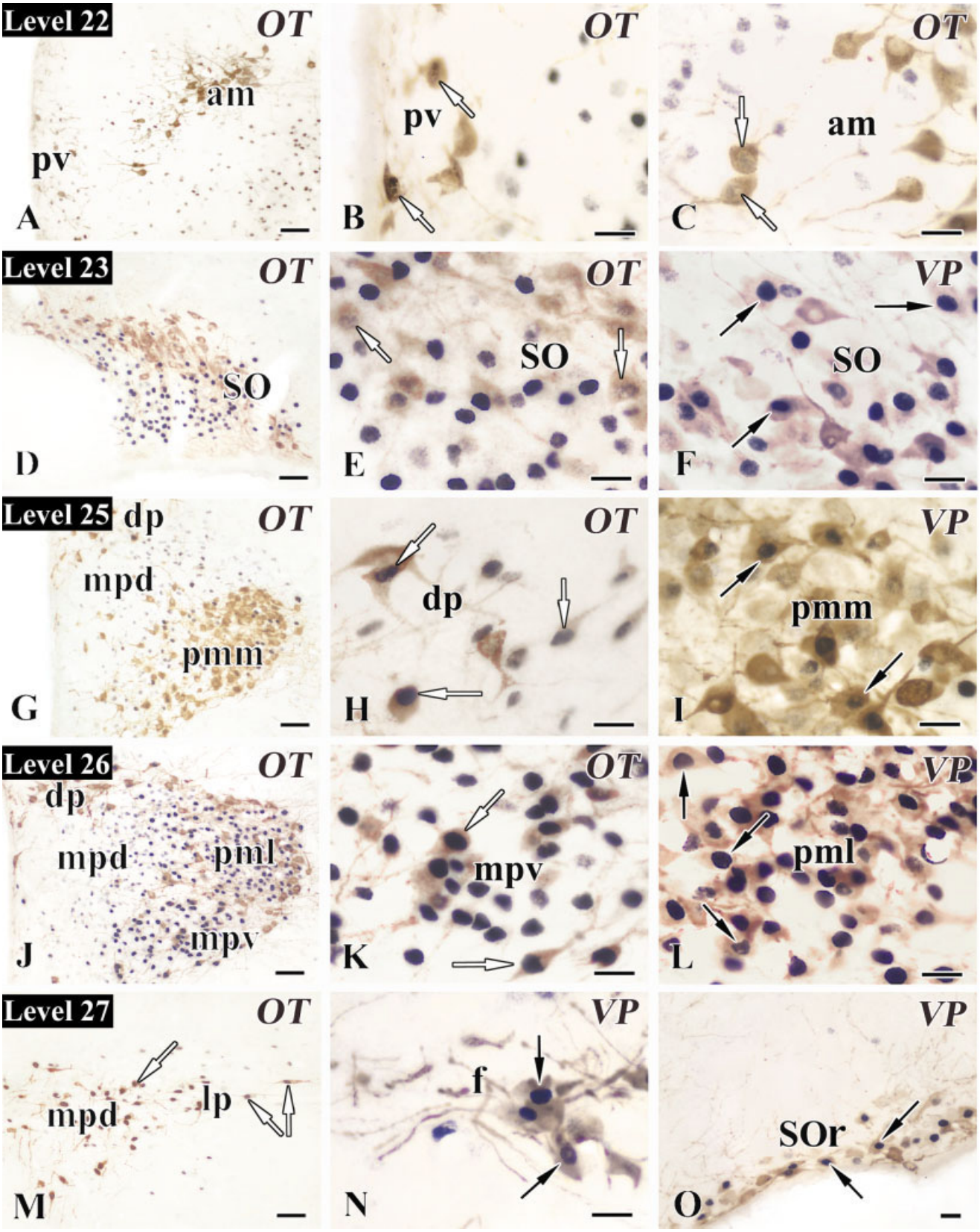
Level 22
OT
am
pv
A
OT
pv
B
OT
am
C
Level 23
OT
SO
D
OT
SO
E
VP
SO
F
Level 25
dp
OT
mpd
pmm
G
OT
dp
H
VP
pmm
I
Level 26
OT
dp
mpd
pml
mpv
J
OT
mpv
K
VP
pml
L
Level 27
OT
mpd
lp
M
VP
f
N
VP
SOr
O

Figure 2

TABLE 1. Percentage of Oxytocin and Vasopressin Neurons Immunoreactive for Estrogen Receptor-β in Distinct Subdivisions of the Paraventricular and Supraoptic Nuclei (PVH; SO) and in Accessory Magnocellular Neurons (ACC) at Rostrocaudal Levels Specified by Swanson (1998)

Region			VP neurons			OT neurons		
Nucleus	Subnucleus	Rostrocaudal level	Number of neurons analyzed	Percentage with ER-β (% ± SEM)	Observed labeling intensities for ER-β	Number of neurons analyzed	Percentage with ER-β (% ± SEM)	Observed labeling intensities for ER-β
PVH	ap/am	22–24	332	91.1 ± 1.9	+, ++, +++	835	52.2 ± 4.8	+, ++, +++
	pv	22–27	147	90.4 ± 3.8	+, ++	534	45.0 ± 2.0	+, ++
	pmm	25	818	97.6 ± 1.1	+, ++ | +++	1544	71.1 ± 3.9	+, ++
	mpd	25–26	146	88.4 ± 5.8	+ | ++ | +++	88	64.4 ± 5.1	+ | ++ | +++
	dp	25–26	87	88.1 ± 2.5	+, ++ | ++++	326	52.6 ± 7.9	+, ++ | ++++
	mpv	26	95	99.1 ± 0.9	++++	251	97.7 ± 1.3	+++++
	pml	26	897	94.2 ± 0.6	+, ++ | ++++	380	65.6 ± 7.6	+, ++, ++
	mpd-lp	27	236	97.8 ± 1.3	++++	871	97.2 ± 1.1	+++++
	f	27	185	94.4 ± 2.8	+, ++ | ++++	151	60.2 ± 2.4	+, ++, ++
SO		22–27	4775	88.4 ± 0.9	+, ++ | ++++	3579	59.5 ± 4.3	+, ++, ++
ACC		22–27	995	92.5 ± 1.1	+, ++ | ++++	1589	54.9 ± 3.3	+, ++, ++

The most frequently encountered labeling intensities are indicated using a five point scale: "+", "very low;" "++", "low;" "+++", "medium;" "++++", "high;" "+++++", "very high."

scopic analysis revealed that ER-β immunoreactivity was exclusively coupled to neurons, leaving glial cells and constituents of blood vessels unlabeled. Both magnocellular (Fig. 3B) and parvicellular (Fig. 3C) neurosecretory cells of the PVH displayed the ICC signal for ER-β. The majority of silver-gold particles were located within the cell nuclei (Fig. 3B,C) coupled to the chromatin matrix (Fig. 3D). A few scattered grains were also noted in the cytoplasm of the labeled neurons.

Triple-label in situ hybridization studies in rats

The nonisotopic ISHH detection of OT and VP mRNA-containing neurons produced distinct signal patterns in the hypothalamic SO and PVH. The contrasting colors of the brown DAB and the purple BCIP/NBT chromogens distinguished OT from VP-expressing neurons in the SO (Fig. 4A) and the PVH (Fig. 4D). In triple-label ISHH studies employing optimal color development for OT and VP mRNA-containing cell populations (Fig. 4B,C,E), silver grain clusters representing ER-β mRNA could be observed above OT and VP cells (Fig. 4B,C,E). The proportions of double-labeled VP and OT neurons were calculated for the SO, the pml of the PVH, and the ACC. Histochemical staining intensities in these neurons were optimized to allow the observation of weak autoradiographic signals. The expression of ER-β mRNA was apparent in 72.1 ± 3.6% of OT-positive and 84.0 ± 3.0% of VP-positive neurons in the SO, in 81.6 ± 4.1% of OT neurons and 98.5 ± 0.6% of VP neurons in the pml of the PVH (Fig. 4E), and in 67.9 ± 55% of OT-positive neurons and 88.4 ± 2.5% of VP-positive neurons in the ACC. The stronger ER-β mRNA expression in VP neurons in comparison to OT neurons and the higher proportion of double-labeled magnocellular VP as opposed to OT neurons were consistent with the ICC observations.

In situ hybridization detection of ER-β mRNA in corticotropin-releasing hormone neurons

The autoradiographic hybridization signal for ER-β mRNA was detectable in a large subset of parvicellular neurons in the PVH, including cells in the mpd subnucleus at levels 25–26. Here, a large population of hypophysiotropic CRH neurons was found to exhibit a weak labeling for the receptor mRNA (Fig. 4F).

Immunocytochemical studies of human hypothalami

ER-β was identified in the human PVH, SO, and other hypothalamic regions. The signal was predominantly nuclear but, in some cases, also present in the cytoplasm; this extranuclear labeling has been previously noted by others (Ishunina et al., 2000). Nuclear ER-β immunoreactivity (illustrated in the specimen from the 33-year-old male; Fig. 5) was observed in varying numbers of OT and VP neurons in all three brains. Given the low number and heterogeneity of the human hypothalami investigated here, quantitative analysis of the percentages of ER-β-expressing OT and VP neurons was not attempted.

DISCUSSION

Double-label ICC and triple-label ISHH studies presented here describe the regional distribution and cellular abundance of ER-β in distinct subpopulations of OT-expressing and VP-expressing neurons in the rat hypothalamus. The demonstration of ER-β signal in OT-IR and VP-IR neurons of human hypothalami indicates comparability with the observations made in the rat.

Estrogen receptor expression in oxytocin-synthesizing and vasopressin-synthesizing neurons

The first morphological evidence for the estrogen responsiveness of a subset of paraventricular OT neurons was provided using studies of tritiated estradiol uptake by Pfaff and Keiner (1973) and Rhodes et al. (1981, 1982). In the autoradiographic studies by Rhodes et al., estrogen receptive OT neurons were found in the caudal PVH as well as in the ventromedial aspect of the middle PVH. These sites also exhibited the highest level of ER-β mRNA and protein expression in our present and previous studies (Hrabovszky et al., 1998). According to the nomenclature used in Swanson's (1998) brain maps, we identified these sites as the mpd-lp (level 27) and the mpv (level 26) subnuclei of the PVH. The very high levels of ER-β mRNA and protein in these regions suggest that the previously reported binding of ^{3}H-estrogen (Rhodes et al., 1981, 1982) was due to ER-β. It should be noted that the cytoarchitectonic similarities of these two PVH sites have been identified by Kiss et al. (1991). Those authors defined these

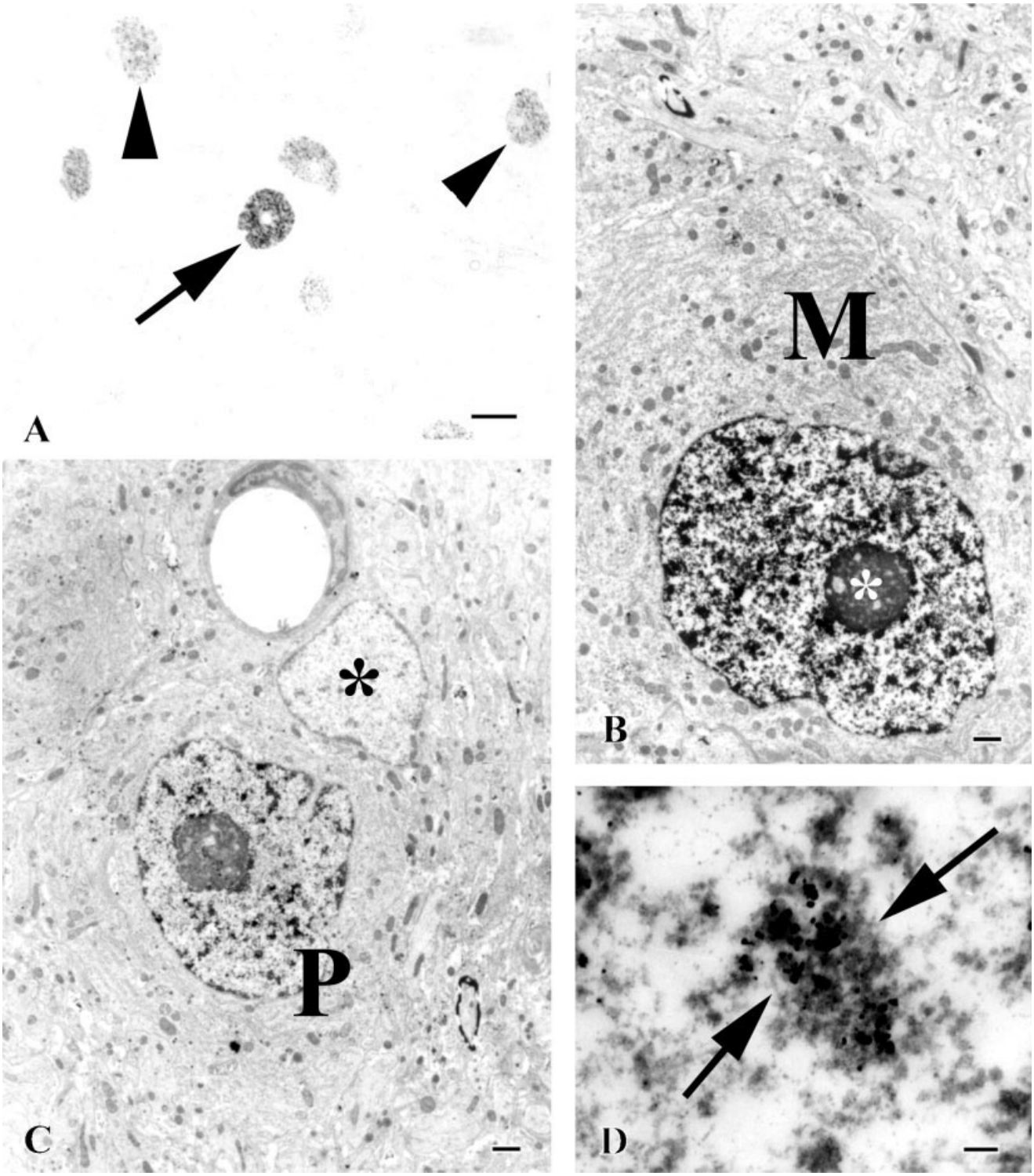

Fig. 3. Ultrastructural detection of estrogen receptor-β (ER-β) immunoreactivity in the hypothalamic paraventricular nucleus of the rat **A:** Semithin section (1 μm) demonstrates immunolabeled cell nuclei with intense (arrow) or moderate (arrowheads) receptor signal. **B:** A magnocellular neurosecretory cell (M) exhibits a heavily labeled cell nucleus. The silver-gold particles, indicating receptor immunoreactivity, are scattered throughout the nucleus. **C:** A parvicellular neuron (P) displays moderate nuclear labeling for ER-β. The asterisk marks an immunonegative cell nucleus. **D:** High-power electron micrograph demonstrates the association (arrows) of the immunolabel with the chromatin substance. Scale bars = 10 μm in A; 1 μm in B,C; 0.2 μm in D.

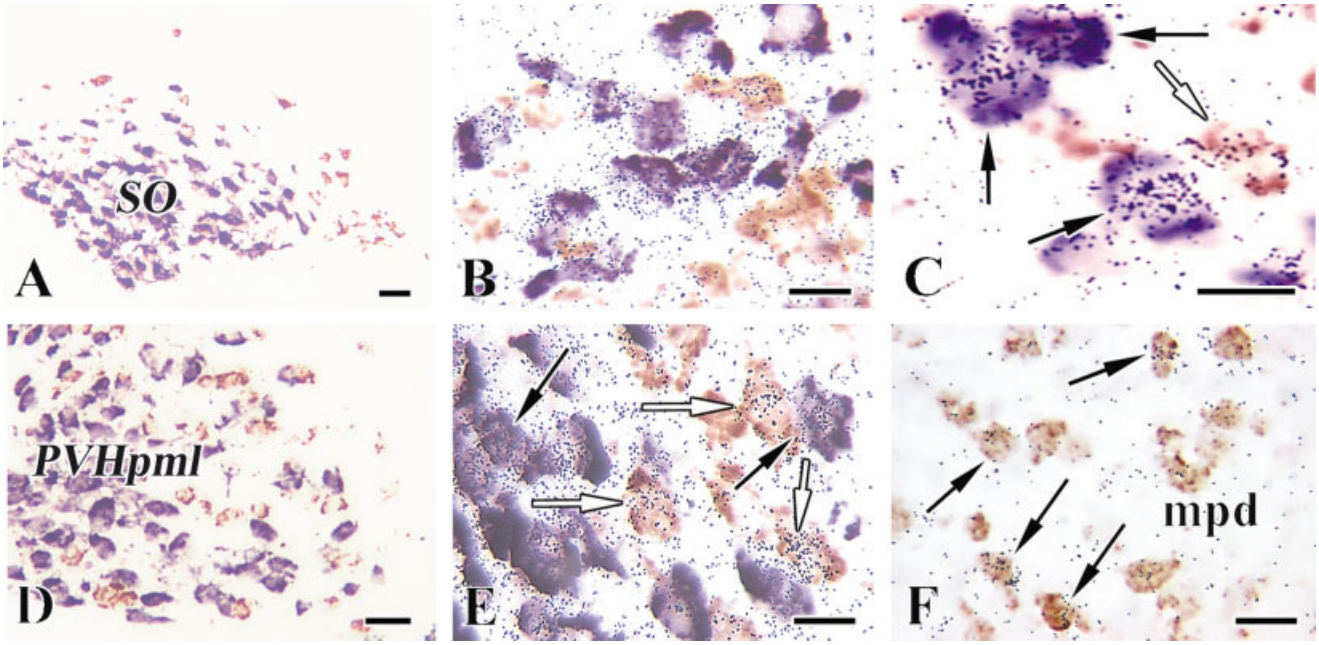

Fig. 4. In situ hybridization detection of estrogen receptor-β mRNA expression in magnocellular oxytocin and vasopressin neurons (A–E) and parvicellular corticotropin releasing hormone neurons (F). **A,D:** The combined use of the purple BCIP/NBT and the brown DAB histochemical stains yields contrasting colors, enabling the distinction of vasopressin (VP) from oxytocin (OT) neurons, respectively, in the SO (A) and in the pml of the PVH (D). **B,C,E:** Triple-label ISHH detection of OT (brown cytoplasmic stain), VP (purple color) and ER-β (autoradiographic signal) mRNAs in the SO (B,C) and the pml (E) provides for the identification of ER-β mRNA expressing OT (white arrows) and VP (black arrows) neurons in both regions. **F:** A population of parvicellular neurons (arrows) in the mpd expresses ER-β mRNA (autoradiographic signal) as well as corticotropin releasing hormone mRNA (brown DAB chromogen). Scale bars = 50 μm in A,D; 25 μm in B,C,E,F.

two regions as the posterior subdivision of the mediocellular subnucleus, based on morphometric and cell packing density analyses. In addition to the very heavy ER-β signal in the mpv subnucleus at level 26 and the mpd-lp subnuclei at level 27 of the PVH, our present studies detected cells with lower levels of ER-β expression in all additional populations of OT-containing and VP-containing neurons in the PVH and in the SO; this suggests that previous ligand binding studies (Pfaff and Keiner, 1973; Sar and Stumpf, 1980; Rhodes et al., 1981, 1982) revealed the estrogen receptivity of neurons that express the highest levels of ER-β immunoreactivity. In this context, it should be noted that the absence of ^{3}H-estradiol uptake by luteinizing hormone-releasing hormone (LHRH) neurons has long served as a major argument against the direct estrogen responsiveness of these cells (Shivers et al., 1983). Nevertheless, recent methodological improvements have provided evidence for ER-β mRNA expression (Skynner et al., 1999; Hrabovszky et al., 2000, 2001), ER-β immunoreactivity (Hrabovszky et al., 2001; Kallo et al., 2001) and ^{125}I-estrogen uptake (Hrabovszky et al., 2000) in LHRH neurons of rodents.

The autoradiographic observations of estrogen uptake by a subset of neurons in the PVH and the SO (Pfaff and Keiner, 1973; Sar and Stumpf, 1980; Rhodes et al., 1981, 1982) were followed by a series of apparently incompatible ICC and ISHH studies which reported the absence of the classical estrogen receptor isoform (ER-α) (Herbison, 1994) and its encoding mRNA (Simerly et al., 1990; Shughrue et al., 1997) within the SO and either no (Shughrue et al., 1997) or only weak (Simerly et al., 1990) ER-α mRNA expression in the PVH of the rat. These findings raised the possibility that mechanisms whereby estrogen regulates OT and VP neurons are primarily transsynaptic. Indeed, various forebrain regions expressing high levels of ER-α were reported to communicate with the SO and the PVH, providing putative anatomical pathways for indirect estrogen actions (Voisin et al., 1997). The discovery of the second isoform of ER (ER-β) (Kuiper et al., 1996) and high levels of its expression in both the SO and the PVH (Shughrue et al., 1996, 1997) readdressed the possibility that estradiol may directly influence gene expression of OT-containing and VP-containing neuronal systems. In strong support of this idea, recent colocalization studies using double-label immunocytochemistry (Simonian and Herbison, 1997; Alves et al., 1998) and combined immunocytochemistry and ISHH (Hrabovszky et al., 1998; Laflamme et al., 1998) provided morphological evidence for the presence of ER-β immunoreactivity (Simonian and Herbison, 1997; Alves et al., 1998) and ER-β mRNA expression (Hrabovszky et al., 1998; Laflamme et al., 1998) within distinct subpopulations of OT-containing and VP-containing neurons. Nevertheless, the observations concerning the topographical distribution of ER-β-containing OT and VP neurons in those reports (Simonian and Herbison, 1997; Alves et al., 1998; Hrabovszky et al., 1998; Laflamme et al., 1998) were not consistent; this provided the rationale for the present studies. One important issue of debate (Alves et al., 1998; Simonian and Herbison, 1997) has been the presence (Hrabovszky et al.,

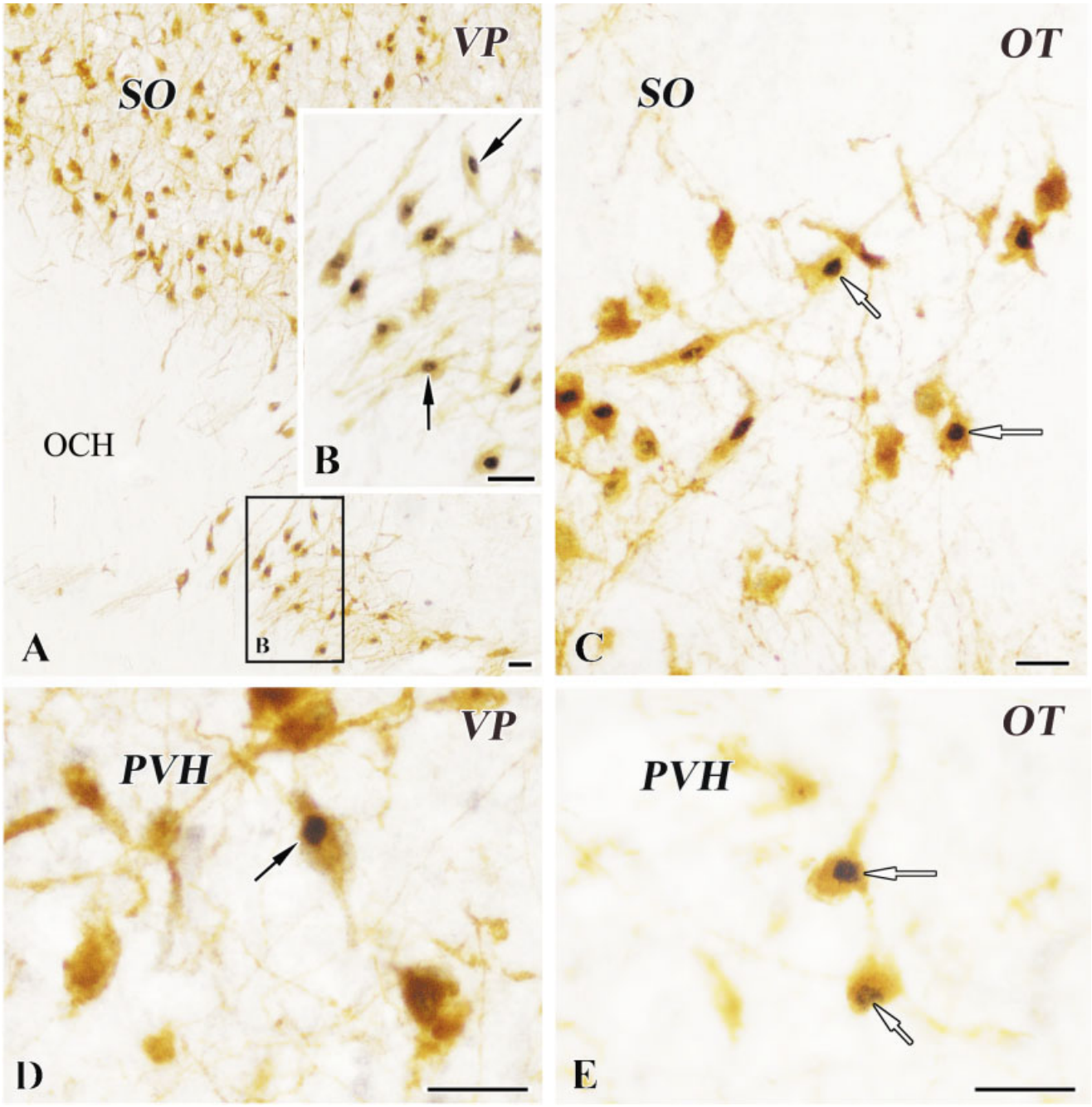

Fig. 5. **A–D:** Identification of estrogen receptor-β (ER-β)-immunoreactive oxytocin (OT) and vasopressin (VP) neurons in the human supraoptic and paraventricular nuclei (SO; PVH). Black arrows in B and D indicate ER-β-positive cell nuclei of VP neurons in the SO and PVH, respectively (OCH in A = optic chiasma). White arrows in C and E indicate ER-β-containing OT neurons in the SO and PVH, respectively. Scale bars = 50 μm.

1998) of ER-β in magnocellular VP neurons of the PVH (Hrabovszky et al., 1998), a finding confirmed recently by others (Somponpun and Sladek, 2003) as well as by the present ICC and ISHH studies. The neurochemical identity of ER-β-containing cells in the SO provided an additional major discrepancy in the published data. While results of two studies indicated preferential expression of ER-β mRNA (Hrabovszky et al., 1998) and ER-β immunoreactivity (Alves et al., 1998) in VP as opposed to OT neurons, other investigators found either no ER-β immunoreactivity in the SO at all (Simonian and Herbison, 1997), or detected ER-β in OT-IR, but not VP-IR, neurons in this nucleus (Laflamme et al., 1998). Nevertheless, a recent report (Somponpun and Sladek, 2003) and our present ICC and ISHH studies have confirmed that ER-β mRNA and protein are expressed by VP-containing as well

as OT-containing neurons in the SO, albeit in higher percentages of cells and at much higher levels in VP-containing than in OT-containing cell populations (typically high as opposed to very low or low levels, respectively). A similar tendency for differential signal expression was observed in accessory magnocellular OT and VP cells and in magnocellular neurons of the pml subnucleus of the PVH. Further, we found that magnocellular VP neurons in the pmm subnucleus of the PVH tended to be labeled somewhat more heavily than OT neurons located in the same anatomical subunit. Novel observations in the present double-label ICC and triple-label ISHH studies included the differential expression of ER-β protein and its encoding mRNA among and even within distinct subsets of OT and VP neurons, and very low levels of these products in large subsets of OT and VP neurons. These observations suggest that the inconsistent results of previous colocalization studies were partly due to variable sensitivity of the ICC and ISHH techniques employed to detect ER-β neurons; in agreement with this, our preliminary experiments showed that the percentages of ER-β-positive cells depended on the sensitivity of the detection method. In view that the physiological significance of low vs. very high ER-β content may be considerable, we deemed it critical to characterize individual subsets of OT and VP neurons in terms of the typical appearance of the ER-β signal, in addition to providing data on the percentages of their ER-β coexpression.

Location of oxytocin and vasopressin neurons with the highest cellular levels of ER-β expression

Magnocellular VP neurons in the SO, in the pml, and in accessory magnocellular cell groups generally had high ER-β signals, whereas magnocellular OT cells in the same regions displayed only very low or low signal intensity. This tendency was also apparent for the pmm of the PVH, where signal levels were relatively low in both cell populations (low or medium in VP-IR neurons vs. very low or low in OT-IR neurons). In comparison with the magnocellular cell groups, the distinct subpopulations of parvicellular OT-IR and VP-IR neurons exhibited more complex patterns of ER-β staining and considerable signal variability. It is noteworthy that the OT cell population of the mpd-lp subdivisions at level 27 and the mpv subdivision at level 26 offers an excellent model system for investigating ER-β-mediated genomic actions, since nearly all of these OT-synthesizing cells exhibit a very high intensity of labeling for ER-β mRNA and protein. Oxytocin neurons at these locations concentrate tritiated estradiol and give rise to descending projections to the dorsal vagal complex (Corodimas and Morrell, 1990) and to the sexually dimorphic spinal nucleus of the bulbocavernosus muscle (Wagner et al., 1993). Recent studies by Stern and Zhang (2003) have demonstrated that a high percentage of ER-β-containing autonomic neurons in these regions project to the rostroventrolateral medulla. In addition to their very high ER-β content, more than half of the OT neurons in the mpv of the PVH contain androgen receptors (Zhou et al., 1994) and may play a critically important role in autonomic mechanisms and sexual behavior in both genders. A large population of ER-β-containing neurons with a similar topographical distribution in the PVH has recently been shown to express the mRNA for the novel opioid neuropeptide, orphanin FQ and its receptor, ORL1 (Isgor et al., 2003). The physiological significance of this colocalization remains to be investigated.

Oxytocin and vasopressin gene regulation by estrogen

Although estrogen response elements are present in the promoter regions of the OT-neurophysin (Mohr and Schmitz, 1991) and the VP-neurophysin (Shapiro et al., 2000) genes, the issue of whether estrogen can directly regulate OT and VP gene transcription in the PVH and in the SO is highly controversial (Caldwell et al., 1989; Miller et al., 1989; Burbach et al., 1990; Chung et al., 1991; Amico et al., 1995; Crowley et al., 1995; Nomura et al., 2002; Shughrue et al., 2002). Elevated levels of the mRNAs for OT and, to a lesser extent, for VP were observed during pregnancy and lactation (Lightman and Young, 1987; Van Tol et al., 1988; Zingg and Lefebvre, 1988; Crowley and Amico, 1993), but ovariectomy and estrogen replacement in earlier reports did not appear to significantly alter OT (Miller et al., 1989; Burbach et al., 1990; Amico et al., 1995) or VP (Roy et al., 1999) mRNA levels. It should be noted that the ERE motifs do not necessarily contribute to the transactivation of OT and VP genes by ERs. In transient transfection experiments, out of two EREs observed in the rat VP-neurophysin gene promoter, only the distal element was functional during transactivation by the liganded ER-α, and, notably, neither was involved in the constitutive transactivation of the VP gene by the unliganded ER-β (Shapiro et al., 2000).

In contrast to the controversy regarding the estrogenic regulation of the OT and VP genes in magnocellular neurons of the SO and the PVH, there is a consensus that VP-neurophysin gene expression is highly stimulated by estrogen and aromatizable androgen in the bed nucleus of the stria terminalis (BST) and the medial amygdaloid nucleus (van Leeuwen et al., 1985; de Vries et al., 1986, 1992; Brot et al., 1993). This difference in regulation from VP neurons of the SO and PVH may be attributable to ER-α involvement in ligand-dependent transactivation of VP neurons in the BST and the medial amygdala (Axelson and van Leeuwen, 1990), in contrast to VP neurons of the PVH and the SO (Simerly et al., 1990; Herbison, 1994; Shughrue et al., 1997; Laflamme et al., 1998). Consistent with this idea, ER-α has, indeed, been shown to induce transactivation of the VP gene in vitro in a ligand-dependent manner, by acting on the distal ERE of the VP gene promoter (Shapiro et al., 2000). In vitro observations on the effects of ER-β on the VP-neurophysin gene promoter may be relevant to VP-IR neurons of the PVH and the SO. The results of cotransfection studies with the VP promoter and the ER-β expression vector showed a constitutive transactivation of VP-neurophysin gene in the absence of receptor ligands; estradiol could block this effect through ER-β (Shapiro et al., 2000). It has been proposed that the ligand-dependent transcriptional repression is exerted at CRE or AP1 motifs of the VP promoter (Shapiro et al., 2000).

It is currently difficult to understand the mechanisms underlying the observed upregulation of the OT-neurophysin gene by sequential exposure to estrogen and progesterone, followed by progesterone withdrawal (Crowley et al., 1995). Although this hormonal context may be physiologically relevant to the activation of OT neurons before parturition (Weisz and Ward, 1980), the paucity of

progesterone receptors in the PVH and the SO (Auger and de Vries, 2002) suggests an indirect mechanism for these actions. The controversy regarding estrogenic regulation of the OT and VP genes may be partially due to differences in animal models and hormone treatment paradigms used previously. A recent time-course study found significantly reduced OT mRNA expression in the PVH of ovariectomized female rats 6 hours after the injection of a single dose of estradiol; the mRNA levels returned to baseline value 48 hours postinjection (Shughrue et al., 2002). In contrast, in gonadectomized male mice the continuous presence of estradiol benzoate pellets for 21 days produced significantly increased OT mRNA levels in the PVH (Nomura et al., 2002). The mRNA for VP was regulated inversely in the PVH and reduced significantly by this treatment (Nomura et al., 2002). This study also established a clear role for ER-β in mediating these estrogenic effects because both regulatory actions were absent in βERKO mice (Nomura et al., 2002).

Other putative gene targets for regulation by ER-β within oxytocin-synthesizing and vasopressin-synthesizing neurons

Several studies show that various neuropeptides in the PVH respond to changes in estrogen levels. For example, estrogen interferes with the induction of preproenkephalin gene in the PVH by hypertonic saline injections (Yukhananov and Handa, 1997). In addition, estrogen interacts with stress to regulate the expression of a human preproenkephalin promoter-beta galactosidase fusion gene-construct in transgenic mice (Priest et al., 1997). Further, estradiol increases the incidence of colocalization of angiotensin II and dynorphin with VP (Levin and Sawchenko, 1993). An additional candidate for regulation by ER-β is the ER-β gene itself, since estradiol has been found to decrease ER-β mRNA in the PVH; in contrast, the phytoestrogens coumestrol and genistein exerted the opposite effect (Patisaul et al., 1999, 2002). Although the mechanism of these differential actions is not understood, the preferential binding of phytoestrogens to the ER-β receptor isoform (Kuiper et al., 1997) suggests that at least the effects of coumestrol and genistein are exerted directly on the PVH via ER-β. A recent report by Somponpun and Sladek (2003) showed robust downregulation of ER-β mRNA and immunoreactivity in the SO and PVH of osmotically stimulated rats. This interesting finding raises the possibility that dynamic change in the cellular abundance of this receptor, in addition to variation in the level of circulating estrogen, may be an important factor in transcriptional regulation through ER-β.

Detection of ER-β mRNA in parvicellular corticotropin-releasing hormone neurons

In addition to detect ER-β mRNA expression and immunoreactivity in parvicellular OT and VP neurons, we observed hybridization signal for ER-β in further subsets of parvicellular neurons in the PVH, including hypophysiotopic CRH neurons in the mpd subnucleus at levels 25–26. This observation is novel and likely contributed by the high sensitivity of the radioisotopic ISHH technique, as previous studies have not found significant overlap between parvicellular CRH and ER-β neurons (Alves et al., 1998) or reported ER-β mRNA expression in magnocellular but not parvicellular CRH neurons of the PVH (Laflamme et al., 1998).

Ultrastructural studies of ER-β in the paraventricular nucleus

Our studies examined the ultrastructural location of ER-β immunoreactivity in the PVH. In agreement with the concept that ER-β mainly acts as a ligand-dependent and/or ligand-independent transcription factor (Hall et al., 2001; Nilsson et al., 2001), ER-β immunoreactivity was found predominantly at nuclear sites in association with the chromatin. Despite recent evidence for the involvement of ER-β in estrogenic inhibition of NMDA-stimulated OT and VP release (Somponpun and Sladek, 2002), we only observed a few silver grains outside the cell nucleus; it was not clear from these results whether the scattered extranuclear silver grains represent sites for new receptor synthesis or, alternatively, sites for extranuclear receptor function. It is noteworthy that the only ER-β isoforms identified to date which tend to be sequestered in the cytoplasmic compartment are the exon 4-deleted variants, ER-β1δ4 and ER-β2δ4. These receptor forms lack the nuclear localization signal as well as estrogen-binding capacity (Price et al., 2000). Although their relative abundance is high in the hippocampus and the lateral septum, they are only expressed at low levels in most brain regions, including the PVH and the SO (Price et al., 2000). Future studies will be required to elucidate the receptor-related mechanisms for nongenomic estrogen effects on magnocellular neurons, including the rapid degranulation of OT neurons by estradiol in vitro (Wang et al., 1995).

ER-β in human oxytocin and vasopressin neurons

Double-label ICC studies established the presence of nuclear ER-β immunoreactivity in some OT-IR and VP-IR neurons in the human SO and PVH. Marked anatomical and neurochemical differences exist between the human (Koutcherov et al., 2000) and rat PVN and SO. Of particular interest to our work is the reported abundance of ER-α in neurons of the human (Ishunina et al., 2000; Osterlund et al., 2000), but not the rat (Simerly et al., 1990; Shughrue et al., 1997), PVH and SO. However, as in the case of the rat, the human PVH and SO also express ER-β immunoreactivity and mRNA (Ishunina et al., 2000; Osterlund et al., 2000). Ishunina et al. (2000) reported cytoplasmic as well as nuclear ER-α and ER-β immunoreactivities in magnocellular VP neurons of the human SO; the relative abundance of receptor signals in these cellular compartments exhibited sexual dimorphism and age-related changes. Confirming these previous observations, the human tissue used in our studies also displayed some cytoplasmic in addition to nuclear ER-β staining; both nuclear and extranuclear immunostaining could be entirely prevented by preabsorption of ER-β antibodies with the immunization antigen.

Methodological considerations

Immunocytochemistry. The parameters employed for the present double-label ICC (type of fixative, antibody concentrations, length of serum incubations, etc.) were determined in preliminary tests to achieve an optimal sensitivity for ER-β detection together with that of OT and

VP cells. In order to evaluate the presence/absence of ER in the cell nucleus, we and others (Axelson and van Leeuwen, 1990) have found it necessary to allow development of only a light cytoplasmic color in OT and VP neurons. This precaution may have somewhat compromised the number of OT and VP neurons detected and analyzed for ER-β immunoreactivity. We found that the use of the silver-gold intensified Ni-DAB chromogen had clear advantages over nonintensified Ni-DAB in that it rendered even the weakest ER-β signal granular in appearance, which facilitated the identification of ER-β-positive neurons at high magnification.

Primary antisera to ER-β applied previously to colocalization studies with OT and VP were from two different sources. Both the PA1-310 antibodies from Affinity BioReagents (Golden, CO) (Simonian and Herbison, 1997; Alves et al., 1998) and the more recently used Z8P antibodies from Zymed (Shughrue et al., 2002; Stern and Zhang, 2003; Somponpun and Sladek, 2003; present studies) were directed to the C-terminal sequence of ER-β. Therefore, it is likely that different results are mostly due to the different quality of antibodies and differences in the immunocytochemical assay conditions. While all of the above studies agreed that the heaviest immunocytochemical signal levels for ER-β are found in OT neurons of the caudal PVH (described in our present study as the mpv subnucleus at level 26 and the mpd-lp subnuclei at level 27), the use of the Z8P antibodies generally revealed a wider distribution of ER-β immunoreactivity. For example, specific labeling for ER-β in magnocellular neurons of the PVH has only been reported using the Z8P antibodies (Shughrue et al., 2002; Somponpun and Sladek, 2003; present studies). Assay conditions may further influence the success of colocalization studies using Z8P antibodies. While some of the recent studies used paraformaldehyde-fixed tissues for colocalization studies with the Z8P antibodies (Stern and Zhang, 2003), we have formally established that better results can be obtained on tissues fixed with the mixture of 2% paraformaldehyde and 4% acrolein (Kallo et al., 2001; Shughrue and Merchenthaler, 2001). The use of acrolein/paraformaldehyde-fixed tissues and the silver-intensification of signal could contribute to the success of the present studies to reveal often very low levels of ER-β in subpopulations of OT and VP neurons.

In situ hybridization. The triple-label ISHH method represents a modification of a double-labeling technique developed previously (Petersen and McCrone, 1994), which combined radioisotopic and digoxigenin-labeled nonisotopic cRNA probes. Introducing a third hybridization signal to this method allowed the simultaneous visualization of OT-synthesizing and VP-synthesizing neurons in the same tissue sections; this greatly facilitated the topographical analysis of ER-β mRNA expression by these cells. The additional nonisotopic cRNA probe was labeled with fluorescein; the use of the fluorescein-labeled cRNA probe without further amplification resulted in a relatively low detection sensitivity when compared with digoxigenin-labeled probes. However, the fluorescein label could be markedly enhanced by incubating the sections sequentially in antifluorescein-HRP conjugate, then in biotin tyramide (Adams, 1992) and ABC Elite working solutions (Vector), as described previously (Ottem et al., 2002).

A further important methodological consideration was to protect the Kodak autoradiographic emulsion from direct contact with the BCIP/NBT histochemical stain, in order to eliminate positive chemography observed previously (Young, 1989; Petersen and McCrone, 1994). This phenomenon could be prevented by dipping the slides sequentially twice into a 1% solution of Parlodion (Mallinckrodt) prior to emulsion autoradiography (Young, 1989; Hrabovszky et al., 1995). When Parlodion-coated slides were used, we found it important to keep the developing and fixing reagents at a low temperature (<15°C) to avoid detachment of the photographic emulsion. Alternatively, the emulsion could also be stabilized by covering the Parlodion with a layer of gelatin prior to emulsion-coating of slides.

To minimize the proportion of OT-synthesizing and VP-synthesizing neurons that might be falsely negative for ER-β mRNA, several technical modifications were introduced to the isotopic ISHH procedure. Important methodological changes included the combined application of two different cRNA hybridization probes to ER-β (Shughrue et al., 1996, 1997; Hrabovszky et al., 1998, 2000, 2001). Furthermore, we used our recently developed method which greatly enhances the sensitivity of radioisotopic ISHH procedures by the simultaneous application of unusually high concentrations of radioisotopic cRNA probes (80,000 cpm/μl hybridization buffer of each probe), DS (20%, instead of 10%), and DTT (750 mM, instead of the widely used 10–200 mM) in the hybridization solution (Hrabovszky and Petersen, 2002). Our previous success in visualizing ER-β mRNA expression in the majority of LHRH neurons has been enabled by these changes in the composition of the hybridization solution (Hrabovszky et al., 2000, 2001). The use of improved hybridization methodology was also critical for detecting low cellular levels of ER-β mRNA in the present triple-label ISHH study. For example, while other investigators found ER-β mRNA in less then 5% of VP neurons in the hypothalamus (Laflamme et al., 1998), or recently, in 5% of VP neurons in the SO and 20% of VP neurons in the PVH (Isgor et al., 2003), we observed that the vast majority of magnocellular VP neurons in the SO (84.0 ± 3.0%), pml (98.5 ± 0.6%) and ACC (88.4 ± 2.5%) displayed hybridization signal for ER-β mRNA. Further, very low levels of ER-β mRNA expression became detectable in all subsets of OT and VP neurons, of which several were previously reported not to express any ER-β mRNA (Laflamme et al., 1998; Isgor et al., 2003) or ER-β-IR (Simonian and Herbison, 1997; Alves et al., 1998). Finally, the similarly high percentages of double-labeled magnocellular OT and VP neurons identified by the mRNA and protein detection methods indicated that the sensitivity of the triple-label ISHH technique was comparable to that of double-label ICC.

In summary, the present double-label ICC and triple-label ISHH studies have provided a detailed topographical description of OT and VP neurons that express ER-β mRNA and ER-β immunoreactivity in the PVH and the SO of the rat. Relevance of these data to the human was indicated by the finding of ER-β immunoreactivity in OT and VP neurons of human hypothalami in autopsy specimens. Future studies will examine gene targets regulated by ER-β in separate subsets of OT and VP neurons.

ACKNOWLEDGMENTS

The authors thank Dr. H. Gainer (Bethesda, MD) for the kind donation of PS-38 and PS-41 antibodies, Dr. Philippa

T.K. Saunders (Edinburgh, UK) for the human ER-β antiserum, Dr. Thomas Sherman (Washington, DC) for the VP cDNA, and Dr. K. Mayo (Evanston, IL) for the CRH cDNA.

LITERATURE CITED

Adams JC. 1992. Biotin amplification of biotin and horseradish peroxidase signals in histochemical stains. J Histochem Cytochem 40:1457–1463.

Akaishi T, Sakuma Y. 1985. Estrogen excites oxytocinergic, but not vasopressinergic cells in the paraventricular nucleus of female rat hypothalamus. Brain Res 335:302–305.

Alves SE, Lopez V, McEwen BS, Weiland NG. 1998. Differential colocalization of estrogen receptor beta (ERbeta) with oxytocin and vasopressin in the paraventricular and supraoptic nuclei of the female rat brain: an immunocytochemical study. Proc Natl Acad Sci U S A 95:3281–3286.

Amico JA, Seif SM, Robinson AG. 1981. Oxytocin in human plasma: correlation with neurophysin and stimulation with estrogen. J Clin Endocrinol Metab 52:988–993.

Amico JA, Crowley RS, Insel TR, Thomas A, O'Keefe JA. 1995. Effect of gonadal steroids upon hypothalamic oxytocin expression. Adv Exp Med Biol 395:23–35.

Auger CJ, De Vries GJ. 2002. Progestin receptor immunoreactivity within steroid-responsive vasopressin-immunoreactive cells in the male and female rat brain. J Neuroendocrinol 14:561–567.

Axelson JF, van Leeuwen FW. 1990. Differential localization of estrogen receptors in various vasopressin synthesizing nuclei of the rat brain. J Neuroendocrinol 2:209–216.

Brot MD, De Vries GJ, Dorsa DM. 1993. Local implants of testosterone metabolites regulate vasopressin mRNA in sexually dimorphic nuclei of the rat brain. Peptides 14:933–940.

Buijs RM, Swaab DF. 1979. Immuno-electron microscopical demonstration of vasopressin and oxytocin synapses in the limbic system of the rat. Cell Tissue Res 204:355–365.

Burbach JPH, Adan RAH, Van Tol HHM, Verbeeck MAE, Axelson JF, Leeuwen FW, Beekman JM, Ab G. 1990. Regulation of the rat oxytocin gene by estradiol. J Neuroendocrinol 2:633–639.

Burbach JP, Luckman SM, Murphy D, Gainer H. 2001. Gene regulation in the magnocellular hypothalamo-neurohypophysial system. Physiol Rev 81:1197–1267.

Caldwell JD, Brooks PJ, Jirikowski GF, Barakat AS, Lund PK, Pedersen CA. 1989. Estrogen alters oxytocin mRNA in the preoptic area. J Neuroendocrinol 1:1–7.

Cechetto DF, Saper CB. 1988. Neurochemical organization of the hypothalamic projection to the spinal cord in the rat. J Comp Neurol 272:579–604.

Chung SK, McCabe JT, Pfaff DW. 1991. Estrogen influences on oxytocin mRNA expression in preoptic and anterior hypothalamic regions studied by in situ hybridization. J Comp Neurol 307:281–295.

Corodimas KP, Morrell JI. 1990. Estradiol-concentrating forebrain and midbrain neurons project directly to the medulla. J Comp Neurol 291:609–620.

Crowley RS, Amico JA. 1993. Gonadal steroid modulation of oxytocin and vasopressin gene expression in the hypothalamus of the osmotically stimulated rat. Endocrinology 133:2711–2718.

Crowley WR, O'Donohue TL, George JM, Jacobowitz DM. 1978. Changes in pituitary oxytocin and vasopressin during the estrous cycle and after ovarian hormones: evidence for mediation by norepinephrine. Life Sci 23:2579–2585.

Crowley RS, Insel TR, O'Keefe JA, Kim NB, Amico JA. 1995. Increased accumulation of oxytocin messenger ribonucleic acid in the hypothalamus of the female rat: induction by long term estradiol and progesterone administration and subsequent progesterone withdrawal. Endocrinology 136:224–231.

de Vries GJ, Duetz W, Buijs RM, van Heerikhuize J, Vreeburg JT. 1986. Effects of androgens and estrogens on the vasopressin and oxytocin innervation of the adult rat brain. Brain Res 399:296–302.

de Vries GJ, Crenshaw BJ, al-Shamma HA. 1992. Gonadal steroid modulation of vasopressin pathways. Ann N Y Acad Sci 652:387–396.

Fuchs AR, Saito S. 1971. Pituitary oxytocin and vasopressin content of pregnant rats before, during and after parturition. Endocrinology 88: 574–578.

Gallyas F. 1982. Suppression of argyrophil III reaction by mercapto-compounds. A prerequisite for intensification of histochemical reactions by physical developers. Acta Histochem 70:99–105.

Hall JM, Couse JF, Korach KS. 2001. The multifaceted mechanisms of estradiol and estrogen receptor signaling. J Biol Chem 276:36869–36872.

Hallbeck M, Blomqvist A. 1999. Spinal cord-projecting vasopressinergic neurons in the rat paraventricular hypothalamus. J Comp Neurol 411:201–211.

Hallbeck M, Larhammar D, Blomqvist A. 2001. Neuropeptide expression in rat paraventricular hypothalamic neurons that project to the spinal cord. J Comp Neurol 433:222–238.

Herbison AE. 1994. Immunocytochemical evidence for oestrogen receptors within GABA neurones located in the perinuclear zone of the supraoptic nucleus and GABAA receptor beta 2/beta 3 subunits on supraoptic oxytocin neurones. J Neuroendocrinol 6:5–11.

Hermes ML, Buijs RM, Masson-Pevet M, Pevet P. 1988. Oxytocinergic innervation of the brain of the garden dormouse (Eliomys quercinus L.). J Comp Neurol 273:252–262.

Hou Yu A, Lamme AT, Zimmerman EA, Silverman AJ. 1986. Comparative distribution of vasopressin and oxytocin neurons in the rat brain using a double-label procedure. Neuroendocrinology 44:235–246.

Hrabovszky E, Petersen SL. 2002. Increased concentrations of radioisotopically-labeled complementary ribonucleic acid probe, dextran sulfate, and dithiothreitol in the hybridization buffer can improve results of in situ hybridization histochemistry. J Histochem Cytochem 50:1389–1400.

Hrabovszky E, Vrontakis ME, Petersen SL. 1995. Triple-labeling method combining immunocytochemistry and in situ hybridization histochemistry: demonstration of overlap between Fos-immunoreactive and galanin mRNA-expressing subpopulations of luteinizing hormone-releasing hormone neurons in female rats. J Histochem Cytochem 43:363–370.

Hrabovszky E, Kalló I, Hajszán T, Shughrue PJ, Merchenthaler I, Liposits Z. 1998. Expression of estrogen receptor-beta mRNA in oxytocin and vasopressin neurons of the rat supraoptic and paraventricular nuclei. Endocrinology 139:2600–2604.

Hrabovszky E, Shughrue PJ, Merchenthaler I, Hajszan T, Carpenter CD, Liposits Z, Petersen SL. 2000. Detection of estrogen receptor-beta messenger ribonucleic acid and ^{125}I-estrogen binding sites in luteinizing hormone-releasing hormone neurons of the rat brain. Endocrinology 141:3506–3509.

Hrabovszky E, Steinhauser A, Barabas K, Shughrue PJ, Petersen SL, Merchenthaler I, Liposits Z. 2001. Estrogen receptor-beta immunoreactivity in luteinizing hormone-releasing hormone neurons of the rat brain. Endocrinology 142:3261–3264.

Isgor C, Shieh KR, Akil H, Watson SJ. 2003. Colocalization of estrogen beta-receptor messenger RNA with orphanin FQ, vasopressin and oxytocin in the rat hypothalamic paraventricular and supraoptic nuclei. Anat Embryol (Berl) 206:461–469.

Ishunina TA, Kruijver FP, Balesar R, Swaab DF. 2000. Differential expression of estrogen receptor alpha and beta immunoreactivity in the human supraoptic nucleus in relation to sex and aging. J Clin Endocrinol Metab 85:3283–3291.

Jirikowski GF, Caldwell JD, Pedersen CA, Stumpf WE. 1988. Estradiol influences oxytocin-immunoreactive brain systems. Neuroscience 25: 237–248.

Kallo I, Butler JA, Barkovics-Kallo M, Goubillon ML, Coen CW. 2001. Oestrogen receptor beta-immunoreactivity in gonadotropin releasing hormone-expressing neurones: regulation by oestrogen. J Neuroendocrinol 13:741–748.

Kiss JZ, Martos J, Palkovits M. 1991. Hypothalamic paraventricular nucleus: a quantitative analysis of cytoarchitectonic subdivisions in the rat. J Comp Neurol 313:563–573.

Koutcherov Y, Mai JK, Ashwell KW, Paxinos G. 2000. Organization of the human paraventricular hypothalamic nucleus. J Comp Neurol 423: 299–318.

Kuiper GG, Enmark E, Pelto Huikko M, Nilsson S, Gustafsson JA. 1996. Cloning of a novel receptor expressed in rat prostate and ovary. Proc Natl Acad Sci U S A 93:5925–5930.

Kuiper GG, Carlsson B, Grandien K, Enmark E, Haggblad J, Nilsson S, Gustafsson JA. 1997. Comparison of the ligand binding specificity and transcript tissue distribution of estrogen receptors alpha and beta. Endocrinology 138:863–870.

Laflamme N, Nappi RE, Drolet G, Labrie C, Rivest S. 1998. Expression and neuropeptidergic characterization of estrogen receptors (ERalpha and

ERbeta) throughout the rat brain: anatomical evidence of distinct roles of each subtype. J Neurobiol 36:357–378.

Levin MC, Sawchenko PE. 1993. Neuropeptide co-expression in the magnocellular neurosecretory system of the female rat: evidence for differential modulation by estrogen. Neuroscience 54:1001–1018.

Lightman SL, Young WS 3rd. 1987. Vasopressin, oxytocin, dynorphin, enkephalin and corticotrophin-releasing factor mRNA stimulation in the rat. J Physiol 394:23–39.

Liposits Z, Setalo G, Flerko B. 1984. Application of the silver-gold intensified 3,3′-diaminobenzidine chromogen to the light and electron microscopic detection of the luteinizing hormone-releasing hormone system of the rat brain. Neuroscience 13:513–525.

Mezey E, Kiss JZ. 1991. Coexpression of vasopressin and oxytocin in hypothalamic supraoptic neurons of lactating rats. Endocrinology 129: 1814–1820.

Miller FD, Ozimek G, Milner RJ, Bloom FE. 1989. Regulation of neuronal oxytocin mRNA by ovarian steroids in the mature and developing hypothalamus. Proc Natl Acad Sci U S A 86:2468–2472.

Mohr E, Schmitz E. 1991. Functional characterization of estrogen and glucocorticoid responsive elements in the rat oxytocin gene. Brain Res Mol Brain Res 9:293–298.

Negoro H, Visessuwan S, Holland RC. 1973. Unit activity in the paraventricular nucleus of female rats at different stages of the reproductive cycle and after ovariectomy, with or without oestrogen or progesterone treatment. J Endocrinol 59:545–558.

Nilsson S, Makela S, Treuter E, Tujague M, Thomsen J, Andersson G, Enmark E, Pettersson K, Warner M, Gustafsson JA. 2001. Mechanisms of estrogen action. Physiol Rev 81:1535–1565.

Nomura M, McKenna E, Korach KS, Pfaff DW, Ogawa S. 2002. Estrogen receptor-beta regulates transcript levels for oxytocin and arginine vasopressin in the hypothalamic paraventricular nucleus of male mice. Brain Res Mol Brain Res 109:84–94.

Osterlund MK, Gustafsson JA, Keller E, Hurd YL. 2000. Estrogen receptor beta (ERbeta) messenger ribonucleic acid (mRNA) expression within the human forebrain: distinct distribution pattern to ERalpha mRNA. J Clin Endocrinol Metab 85:3840–3866.

Ottem EN, Godwin JG, Petersen SL. 2002. Glutamatergic signaling through the N-methyl-D-aspartate receptor directly activates medial subpopulations of luteinizing hormone-releasing hormone (LHRH) neurons, but does not appear to mediate the effects of estradiol on LHRH gene expression. Endocrinology 143:4837–4845.

Patisaul HB, Whitten PL, Young LJ. 1999. Regulation of estrogen receptor beta mRNA in the brain: opposite effects of 17beta-estradiol and the phytoestrogen, coumestrol. Brain Res Mol Brain Res 67:165–171.

Patisaul HB, Melby M, Whitten PL, Young LJ. 2002. Genistein affects ER beta- but not ER alpha-dependent gene expression in the hypothalamus. Endocrinology 143:2189–2197.

Pederson CA, Asher JA, Monroe YL, Prange AJ. 1985. Oxytocin induces maternal behavior in virgin female rats. Science 216:648–649.

Petersen SL, McCrone S. 1994. Characterization of the receptor complement of individual neurons using dual-label in situ hybridization histochemistry. In: Eberwine JH, Valentino KL, Barchas JD, editors. In situ hybridization in neurobiology. Advances in methodology. New York: Oxford University Press. p 78–94.

Pfaff D, Keiner M. 1973. Atlas of estradiol-concentrating cells in the central nervous system of the female rat. J Comp Neurol 151:121–158.

Price RH Jr, Lorenzon N, Handa RJ. 2000. Differential expression of estrogen receptor beta splice variants in rat brain: identification and characterization of a novel variant missing exon 4. Brain Res Mol Brain Res 80:260–268.

Priest CA, Borsook D, Pfaff DW. 1997. Estrogen and stress interact to regulate the hypothalamic expression of a human proenkephalin promoter-beta-galactosidase fusion gene in a site-specific and sex-specific manner. J Neuroendocrinol 9:317–326.

Rehbein M, Hillers M, Mohr E, Ivell R, Morley S, Schmale H, Richter D. 1986. The neurohypophyseal hormones vasopressin and oxytocin. Precursor structure, synthesis and regulation. Biol Chem Hoppe Seyler 367:695–704.

Rhodes CH, Morrell JI, Pfaff DW. 1981. Distribution of estrogen-concentrating, neurophysin-containing magnocellular neurons in the rat hypothalamus as demonstrated by a technique combining steroid autoradiography and immunohistology in the same tissue. Neuroendocrinology 33:18–23.

Rhodes CH, Morrell JI, Pfaff DW. 1982. Estrogen-concentrating neurophysin-containing hypothalamic magnocellular neurons in the vasopressin-deficient (Brattleboro) rat: a study combining steroid autoradiography and immunocytochemistry. J Neurosci 2:1718–1724.

Robertson GL. 1976. The regulation of vasopressin function in health and disease. Recent Prog Horm Res 33:333–385.

Roy BN, Reid RL, Van Vugt DA. 1999. The effects of estrogen and progesterone on corticotropin-releasing hormone and arginine vasopressin messenger ribonucleic acid levels in the paraventricular nucleus and supraoptic nucleus of the rhesus monkey. Endocrinology 140:2191–2198.

Sar M, Stumpf WE. 1980. Simultaneous localization of [^{3}H]estradiol and neurophysin I or arginine vasopressin in hypothalamic neurons demonstrated by a combined technique of dry-mount autoradiography and immunohistochemistry. Neurosci Lett 17:179–184.

Saunders PT, Millar MR, Williams K, Macpherson S, Harkiss D, Anderson RA, Orr B, Groome NP, Scobie G, Fraser HM. 2000. Differential expression of estrogen receptor-alpha and -beta and androgen receptor in the ovaries of marmosets and humans. Biol Reprod 63:1098–1105.

Scharrer E, Scharrer B. 1954. Hormones produced by neurosecretory cells. Rec Prog Horm Res 10:183–240.

Shapiro RA, Xu C, Dorsa DM. 2000. Differential transcriptional regulation of rat vasopressin gene expression by estrogen receptor alpha and beta. Endocrinology 141:4056–4064.

Shivers BD, Harlan RE, Morrell JI, Pfaff DW. 1983. Absence of oestradiol concentration in cell nuclei of LHRH-immunoreactive neurones. Nature 304:345–347.

Shughrue PJ, Merchenthaler I. 2001. Distribution of estrogen receptor beta immunoreactivity in the rat central nervous system. J Comp Neurol 436:64–81.

Shughrue PJ, Komm B, Merchenthaler I. 1996. The distribution of estrogen receptor-beta mRNA in the rat hypothalamus. Steroids 61:678–681.

Shughrue PJ, Lane MV, Merchenthaler I. 1997. The comparative distribution of estrogen receptor alpha and beta mRNAs in the rat central nervous system. J Comp Neurol 388:507–525.

Shughrue PJ, Dellovade TL, Merchenthaler I. 2002. Estrogen modulates oxytocin gene expression in regions of the rat supraoptic and paraventricular nuclei that contain estrogen receptor-beta. Prog Brain Res 139:15–29.

Simerly RB, Chang C, Muramatsu M, Swanson LW. 1990. Distribution of androgen and estrogen receptor mRNA-containing cells in the rat brain: an in situ hybridization study. J Comp Neurol 294:76–95.

Simonian SX, Herbison AE. 1997. Differential expression of estrogen receptor alpha and beta immunoreactivity by oxytocin neurons of rat paraventricular nucleus. J Neuroendocrinol 9:803–806.

Skowsky WR, Swan L, Smith P. 1979. Effects of sex steroid hormones on arginine vasopressin in intact and castrated male and female rats. Endocrinology 104:105–108.

Skynner MJ, Sim JA, Herbison AE. 1999. Detection of estrogen receptor alpha and beta messenger ribonucleic acids in adult gonadotropin-releasing hormone neurons. Endocrinology 140:5195–5201.

Sofroniew MV, Schrell U. 1980. Hypothalamic neurons projecting to the rat caudal medulla oblongata, examined by immunoperoxidase staining of retrogradely transported horseradish peroxidase. Neurosci Lett 19: 257–263.

Somponpun S, Sladek CD. 2002. Role of estrogen receptor-beta in regulation of vasopressin and oxytocin release in vitro. Endocrinology 143: 2899–2904.

Somponpun SJ, Sladek CD. 2003. Osmotic regulation of estrogen receptor-beta in rat vasopressin and oxytocin neurons. J Neurosci 23:4261–4269.

Stern JE, Zhang W. 2003. Preautonomic neurons in the paraventricular nucleus of the hypothalamus contain estrogen receptor beta. Brain Res 975:99–109.

Swanson L. 1998. Brain maps: structure of the rat brain. Amsterdam: Elsevier.

Swanson LW, Kuypers HG. 1980. The paraventricular nucleus of the hypothalamus: cytoarchitectonic subdivisions and organization of projections to the pituitary, dorsal vagal complex, and spinal cord as demonstrated by retrograde fluorescence double-labeling methods. J Comp Neurol 194:555–570.

Swanson LW, Sawchenko PE. 1983. Hypothalamic integration: organization of the paraventricular and supraoptic nuclei. Annu Rev Neurosci 6:269–324.

Tucker DC, Saper CB. 1985. Specificity of spinal projections from hypotha-

lamic and brainstem areas which innervate sympathetic preganglionic neurons. Brain Res 360:159–164.

van Leeuwen FW, Caffe AR, De Vries GJ. 1985. Vasopressin cells in the bed nucleus of the stria terminalis of the rat: sex differences and the influence of androgens. Brain Res 325:391–394.

Van Tol HH, Bolwerk EL, Liu B, Burbach JP. 1988. Oxytocin and vasopressin gene expression in the hypothalamo-neurohypophyseal system of the rat during the estrous cycle, pregnancy, and lactation. Endocrinology 122:945–951.

Vandesande F, Dierickx K, De Mey J. 1977. The origin of the vasopressinergic and oxytocinergic fibres of the external region of the median eminence of the rat hypophysis. Cell Tissue Res 180:443–452.

Veronneau-Longueville F, Rampin O, Freund-Mercier MJ, Tang Y, Calas A, Marson L, McKenna KE, Stoeckel ME, Benoit G, Giuliano F. 1999. Oxytocinergic innervation of autonomic nuclei controlling penile erection in the rat. Neuroscience 93:1437–1447.

Voisin DL, Simonian SX, Herbison AE. 1997. Identification of estrogen receptor-containing neurons projecting to the rat supraoptic nucleus. Neuroscience 78:215–228.

Wagner CK, Sisk CL, Clemens LG. 1993. Neurons in the paraventricular nucleus of the hypothalamus that project to the sexually dimorphic lower lumbar spinal cord concentrate ^{3}H-estradiol in the male rat. J Neuroendocrinol 5:545–551.

Wakerley J, Dyball R, Lincoln D. 1973. Milk-ejection in the rat: the result of a selective release of oxytocin. J Endocrinol 57:557–558.

Wang H, Ward AR, Morris JF. 1995. Oestradiol acutely stimulates exocytosis of oxytocin and vasopressin from dendrites and somata of hypothalamic magnocellular neurons. Neuroscience 68:1179–1188.

Weisz J, Ward IL. 1980. Plasma testosterone and progesterone titers of pregnant rats, their male and female fetuses, and neonatal offspring. Endocrinology 106:306–316.

Yamaguchi K, Akaishi T, Negoro H. 1979. Effect of estrogen treatment on plasma oxytocin and vasopressin in ovariectomized rats. Endocrinol Jpn 26:197–205.

Young WS. 1989. Simultaneous use of digoxigenin- and radiolabeled oligodeoxyribonucleotide probes for hybridization histochemistry. Neuropeptides 13:271–275.

Young WS 3rd, Hsu AC. 1991. Observations on the simultaneous use of digoxigenin- and radiolabeled oligodeoxyribonucleotide probes for hybridization histochemistry. Neuropeptides 18:75.

Yukhananov RY, Handa RJ. 1997. Estrogen alters proenkephalin RNAs in the paraventricular nucleus of the hypothalamus following stress. Brain Res 764:109–116.

Zhang BJ, Kusano K, Zerfas P, Iacangelo A, Young WS 3rd, Gainer H. 2002. Targeting of green fluorescent protein to secretory granules in oxytocin magnocellular neurons and its secretion from neurohypophysial nerve terminals in transgenic mice. Endocrinology 143:1036–1046.

Zhou L, Blaustein JD, De Vries GJ. 1994. Distribution of androgen receptor immunoreactivity in vasopressin- and oxytocin-immunoreactive neurons in the male rat brain. Endocrinology 134:2622–2627.

Zingg HH, Lefebvre DL. 1988. Oxytocin and vasopressin gene expression during gestation and lactation. Brain Res 464:1–6.

dc_27_10

7. számú melléklet

0013-7227/04/$15.00/0
Printed in U.S.A.

dc_27_10

Endocrinology 145(9):4018–4021

doi: 10.1210/en.2004-0589

Expression of Vesicular Glutamate Transporter-2 in Gonadotropin-Releasing Hormone Neurons of the Adult Male Rat

ERIK HRABOVSZKY, GERGELY F. TURI, IMRE KALLÓ, AND ZSOLT LIPOSITS

Laboratory of Endocrine Neurobiology, Institute of Experimental Medicine, Hungarian Academy of Sciences, Budapest 1083, Hungary

Isoforms of the recently cloned vesicular glutamate transporters (VGLUT1–3) selectively accumulate glutamic acid into synaptic vesicles in excitatory axon terminals and are viewed as reliable markers for glutamatergic neurons. Our present studies provided dual-label *in situ* hybridization evidence that virtually all (99.5%) GnRH neurons express VGLUT2 mRNA in the preoptic region of the adult male rat. Dual-label immunofluorescent experiments were carried out to examine the presence of VGLUT2 protein in GnRH axon terminals. Confocal laser microscopic analysis of the organum vasculosum of the lamina terminalis and the external zone of the median eminence, the major termination fields for GnRH-secreting axons, demonstrated the frequent occurrence of VGLUT2 immunoreactivity in GnRH axon terminals. Together these mRNA hybridization and immunocytochemical data indicate that GnRH neurons of the adult male rat possess marked glutamatergic characteristics. The physiological significance of endogenous glutamate in the regulation of gonadotropin secretion requires clarification. (*Endocrinology* 145: 4018–4021, 2004)

RECENT DISCOVERY OF the three distinct vesicular glutamate transporter isoforms (VGLUT1–3) that selectively accumulate glutamic acid into synaptic vesicles has enabled the histochemical identification of excitatory neurons that use glutamate for neuronal transmission. The abundance of glutamatergic neurons expressing VGLUT2 mRNA in the hypothalamic paraventricular nucleus (1, 2) and the high density of VGLUT2-immunoreactive (VGLUT2-IR) axon terminals (1) and ionotropic glutamate receptors (3, 4) in the external zone of the median eminence (ME) raised the possibility that peptidergic neuroendocrine cells regulating anterior pituitary functions secrete glutamate as an autocrine/paracrine modulator of their neurohormone output.

Hypophysiotropic GnRH neurons regulating reproduction differentiate from the olfactory placode and migrate to the forebrain during fetal development (5, 6); migrating GnRH cells in rodents and humans exhibit immunoreactivity to γ-aminobutyric acid (GABA) (7). In postnatal rodents, the majority of GnRH-containing neuronal perikarya occupy their final position in the organum vasculosum of the lamina terminalis (OVLT), medial preoptic area (MPO), and medial septum, regions also populated by high numbers of glutamatergic neurons containing VGLUT2 (1, 2). In the present studies we examined the possibility that mature GnRH neurons in these regions possess glutamatergic characteristics. Dual-labeling experiments using *in situ* hybridization histochemistry (ISHH) investigated the expression of VGLUT2 mRNA in GnRH neurons of the adult male rat. In addition, dual-label immunofluorescent studies using confocal laser scanning microscopy addressed the putative VGLUT2 content of GnRH-IR axon terminals in the OVLT and ME, the major projection fields of GnRH-secreting neurons.

Abbreviations: FITC, Fluorescein isothiocyanate; GABA, γ-aminobutyric acid; IR, immunoreactive; ISHH, *in situ* hybridization histochemistry; ME, median eminence; MPO, medial preoptic area; OVLT, organum vasculosum of the lamina terminalis; VGLUT, vesicular glutamate transporter.

***Endocrinology* is published monthly by The Endocrine Society (http://www.endo-society.org), the foremost professional society serving the endocrine community.**

Materials and Methods

Adult male Wistar rats (n = 8; 220–240 g body weight) were purchased from Charles River Hungary Ltd. (Isaszeg, Hungary) and housed in a light- and temperature-controlled environment with food and water *ad libitum*. Experimental procedures were approved by the animal welfare committee at the Institute of Experimental Medicine.

Dual-label ISHH studies

Four adult rats were decapitated, and their brains were snap-frozen on powdered dry ice. Twelve-micrometer thick coronal sections through the OVLT and the MPO were cut with a CM 3050 S cryostat (Leica, Deerfield, IL) and collected serially on gelatin-coated microscope slides. Every sixth section was processed for dual-label ISHH detection of the GnRH and VGLUT2 mRNAs. The ^{35}S-labeled VGLUT2–879 probe corresponded to bases 522-1400 of VGLUT2 mRNA (GenBank accession no. NM_053427). As a positive control for hybridization specificity, a second series of dual-label ISHH experiment was carried out with a distinct VGLUT2 probe (VGLUT2–734, gift from Dr. J. P. Herman, University of Cincinnati Medical Center, Cincinnati, OH) that was complementary to bases 1704–2437. Negative control experiments were performed with the combined use of the GnRH probe and the sense strand VGLUT2 RNA transcripts. According to a recently introduced novel approach to enhance hybridization sensitivity (8), we applied unusually high radioisotopic probe (80,000 cpm/μl), dextran sulfate (25%), and dithiothreitol (1000 mM) concentrations in the hybridization solution and extended the time of hybridization from 16 to 40 h. After hybridization (52 C) and posthybridization treatments (9), the digoxigenin-labeled cRNA probe to GnRH mRNA (transcribed from a 330-bp cDNA template; a gift from Dr. J. P. Adelman, Vollume Institute, Oregon Health Science University, Portland, OR) was detected immunocytochemically as detailed previously (9), using sequential incubations with antidigoxigenin antibodies conjugated to horseradish peroxidase (1:200; antidig-POD, Roche, St.

Louis, MO) for 48 h, biotin tyramide amplification solution for 1 h, and ABC Elite working solution (Vector Laboratories, Inc., Burlingame, CA) for 1 h. The signal was visualized with diaminobenzidine chromogen in the peroxidase developer. Subsequently, the ^{35}S-labeled cRNA probe to VGLUT2 mRNA was detected on autoradiographic emulsion (NTB-3; Eastman Kodak Co., Rochester, NY) (8, 9) after a 2-wk exposure.

Dual-label immunofluorescent studies

Four rats were anesthetized with pentobarbital (35 mg/kg body weight, ip) and perfused transcardially with 150 ml fixative solution containing 2% paraformaldehyde (Sigma-Aldrich Corp., St. Louis, MO) and 4% acrolein (Sigma-Aldrich Corp.) in 0.1 M PBS (pH 7.4) (9, 10). Tissue blocks were dissected out and infiltrated with 25% sucrose overnight. Then 20-μm thick, free floating coronal sections were prepared from the OVLT/MPO region and the mediobasal hypothalamus with a cryostat. The sections were rinsed in Tris-buffered saline (0.1 M Tris-HCl/0.9% sodium chloride, pH 7.8), treated with 0.5% sodium borohydride (Sigma-Aldrich Corp.; 30 min) and 0.5% H_2O_2 (15 min), and finally treated with a mixture of 0.2% Triton X-100 (Sigma-Aldrich Corp.) and 2% normal horse serum in Tris-buffered saline (30 min). After these pretreatments, the sections were incubated (72 h; 4 C) in anti-VGLUT2 primary antibodies raised in a guinea pig (AB 5907; Chemicon International, Temecula, CA; 1:1000). Steps to enhance the fluorescent signal included sequential incubations with biotinylated antiguinea pig IgG (Jackson ImmunoResearch Laboratories, West Grove, PA; 1:1000; 2 h), ABC Elite solution (Vector Laboratories, Inc.; 1 h), biotin tyramide working solution prepared and used as described previously (9) (1:1000; 1 h), and streptavidin-conjugated fluorescein isothiocyanate (FITC) fluorochrome (Jackson ImmunoResearch Laboratories; 1:200; 12 h). Immunoreactivity for GnRH was detected with rabbit LR-1 primary antibodies (1:30,000; gift from Dr. R. Benoit, Montréal, Canada). This antiserum was applied to the sections for 48 h (4 C) and then reacted with Cy3-conjugated antirabbit IgG (Jackson ImmunoResearch Laboratories; 1:200; 12 h). The colocalization of VGLUT2 and GnRH immunoreactivities was examined with a Radiance 2100 confocal microscope (Bio-Rad Laboratories, Hemel Hempstead, UK) using laser excitation lines 488 nm for FITC and 543 nm for Cy3 and dichroic/emission filters 560 nm/500–530 nm for FITC and 560–610 nm for Cy3. To distinguish axonal colocalizations from cases of overlap, individual optical slices of minimal thickness (<0.7 μm) were obtained using a ×60 objective lens (with immersion oil) and an optimized pinhole. Parallel control experiments used VGLUT2 antibodies preabsorbed with 10 μM immunization antigen (AG209, Chemicon International). As a positive control for the specificity of VGLUT2 immunostaining, dual-immunofluorescent experiments were carried out with the combined use of guinea pig anti-VGLUT2 primary antibodies (AB 5907, Chemicon) and rabbit anti-VGLUT2 primary antibodies (1:5000; AB 135103; SYnaptic SYstems, Gottingen, Germany). The primary antibodies were detected with antiguinea pig-FITC (Jackson ImmunoResearch Laboratories; 1:200) and antirabbit-Cy3 (Jackson ImmunoResearch Laboratories; 1:200) conjugates, respectively, and were analyzed by confocal microscopy.

Results

Dual-label ISHH results

Development of emulsion autoradiographs exposed for 2 wk resulted in strong hybridization signal for VGLUT2 mRNA in the horizontal and vertical limbs of the diagonal band of Broca, the OVLT, the MPO, and the median preoptic nucleus (Fig. 1A). Heavy accumulation of silver grains was observed frequently above glutamatergic cells in the vicinity of GnRH neurons (Fig. 1, A_1, A_2, and B). Virtually all (mean ± SEM, 99.5 ± 0.2%) of the total 438 GnRH neurons analyzed (Fig. 1, A_1–A_3) also contained VGLUT2 hybridization signal, usually at moderate levels. Confirmative results obtained with a distinct VGLUT2 probe (Fig. 1B) and the lack of VGLUT2 signal using the sense strand VGLUT2–879 RNA transcript (Fig. 1C) provided support for hybridization specificity.

Dual-label immunofluorescent results

Both glutamatergic and GnRH-containing fibers formed dense plexus in the OVLT (Fig. 1D) and the external zone of the ME (Fig. 1F). High power confocal images demonstrated extensive terminal coexpression of VGLUT2 with GnRH immunoreactivities in both circumventricular organs (Fig. 1, E and G). Although most dual-labeled axons occurred laterally in the ME, a dense VGLUT2 plexus was also observed medially (Fig. 1F). VGLUT2-IR axons (Fig. 1H) were eliminated (Figs. 1I) from the ME when using primary antibodies preabsorbed with 10 μM immunization antigen. In addition, simultaneous use of the two different primary antisera against VGLUT2 labeled identical axons throughout the hypothalamus, in further support of labeling specificity (Fig. 1, J–L).

Discussion

Demonstration of VGLUT2 mRNA expression and VGLUT2 immunoreactivity in GnRH neurons provides conclusive evidence that these cells possess a marked glutamatergic phenotype in the adult male rat.

Glutamate is a critically important neurotransmitter in the regulation of the GnRH neuronal system. Intravenous *N*-methyl-D,L-aspartate infusion can induce precocious puberty in immature rats (11) and activation of ionotropic glutamate receptors plays a crucial role in both pulse (12) and surge (13) modes of GnRH secretion. Although glutamate can regulate GnRH neurons at the level of GnRH cell bodies and dendrites that receive VGLUT2-IR synapses (1, 14) and exhibit immunoreactivity for ionotropic glutamate receptors (15, 16), compelling evidence indicates that an additional major site of action for glutamate is the ME. GnRH terminals in the ME are apposed to glutamatergic axons (1, 4) and express immunoreactivity for the KA2 and NR1 ionotropic glutamate receptor subunits (4). Further, glutamate and agonists of ionotropic glutamate receptors can induce Ca^{2+}-dependent release of GnRH from superfused ME fragments (3). Our ISHH finding that virtually all GnRH neurons expressed VGLUT2 mRNA in the adult male rat strongly suggests that the glutamatergic chemotype is a critically important feature of the GnRH neuronal system. The molecular mechanisms by which glutamate endogenous to GnRH neurons regulates reproduction require future clarification.

The reason why previous confocal and electron microscopic studies (1, 3, 4, 14) failed to reveal the glutamatergic phenotype of the GnRH neuronal system is not clear. In view of the only moderate VGLUT2 mRNA and protein levels we found in GnRH cells, the use of amplification methods could be essential for our colocalization studies to succeed. Furthermore, although VGLUT2 mRNA was present in virtually all GnRH neurons, VGLUT2 immunoreactivity often remained undetectable in GnRH terminals. This discrepancy may be attributable to a general limitation of the immunocytochemical detection method. Another possibility is the heterogeneity of GnRH axon varicosities, in that some may mostly contain dense core vesicles with GnRH and only few small clear vesicles with VGLUT2.

It is important to note that the ME also contained a large number of VGLUT2-IR terminals that were devoid of im-

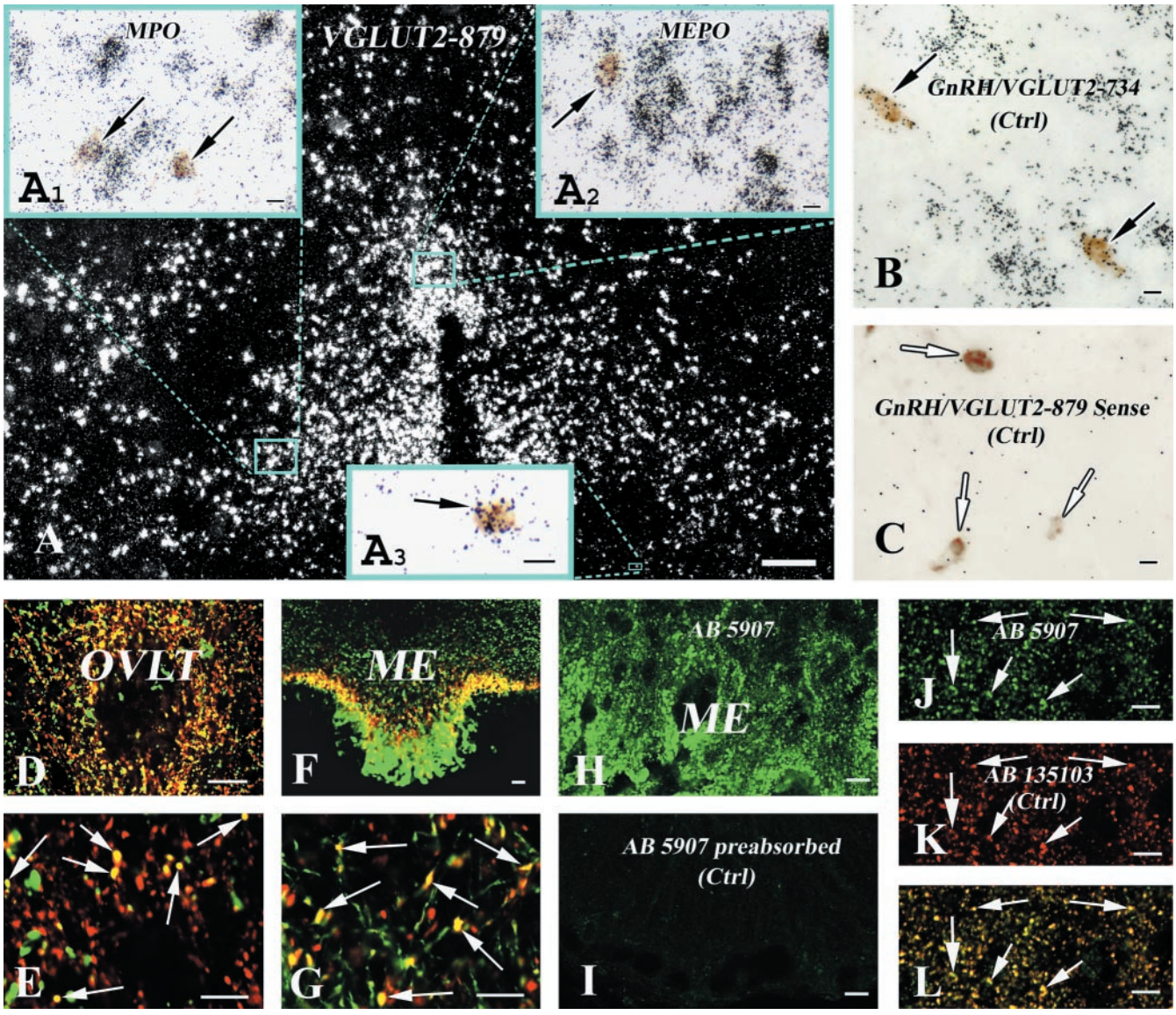

FIG. 1. GnRH neurons of the adult male rat contain VGLUT2. Dual-label ISHH experiments reveal high expression levels of VGLUT2 mRNA (autoradiographic grain clusters in A) in regions also populated by GnRH neurons (*brown* histochemical staining in A_1–A_3), including the medial preoptic area (MPO) and the median preoptic nucleus (MEPO). High power insets (A_1–A_3) illustrate moderate levels of VGLUT2 mRNA in GnRH neurons (*arrows*) from frames in A after use of the VGLUT2–879 probe. Demonstration of VGLUT2 mRNA-containing GnRH neurons with a distinct antisense probe (VGLUT2–734; B) and lack of such dual-labeled GnRH neurons after use of the sense strand VGLUT2–879 RNA transcript (C) serve as controls for hybridization specificity. Dual-immunofluorescent images (D and F) illustrate the overlapping distribution of fibers immunoreactive for VGLUT2 (*green* fluorochrome) and GnRH (*red*) in the OVLT (D) and the ME (F). Although sites of overlap (*yellow*) occur mostly in the lateral part of the ME, the dense VGLUT2-IR plexus is also present medially (F). *Arrows* in high power confocal images (E and G) point to dual-labeled axon varicosities (*yellow*) immunoreactive for both GnRH and VGLUT2. The specificity of VGLUT2 immunostaining in the ME (H) is indicated by the lack of labeled axons after adding the immunization antigen (10 μM) to the working dilution of AB 5907 (I). In addition, dual-immunofluorescent labeling of hypothalamic axons (*arrows* in confocal images J, K, and merged panel L) using two distinct primary antibodies for VGLUT2 further supports the authenticity of VGLUT2 immunoreactivity. *Scale bars*, 200 μm in A, 30 μm in D and F, and 10 μm in the other panels.

munostaining for GnRH. A likely source of some of these fibers is the parvicellular part of the hypothalamic paraventricular nucleus, where VGLUT2-expressing neurons occur in high numbers (1, 2).

A large subset of GnRH neurons in rats, mice, and humans exhibit GABA immunoreactivity (7) during fetal migration from the olfactory placode to the forebrain (5, 6). Tobet and co-workers (7) found no GABA immunoreactivity in GnRH neurons that migrated further caudal to the olfactory bulbs, suggesting that GnRH neurons may switch from the GABAergic to the glutamatergic phenotype perinatally. If the concept of this developmental conversion is valid, then its biological significance and exact time of onset need to be investigated. The possibilities also remain that VGLUT2 is already expressed prenatally in the GnRH system when these neurons still display GABA-ergic features and/or that

GABA synthetic enzymes and the vesicular GABA transporter continue to be expressed together with VGLUT2 in adult GnRH neurons.

In summary, in the present studies we provide conclusive evidence for a marked glutamatergic phenotype of GnRH neurons in the adult male rat by demonstrating VGLUT2 mRNA expression in the perikaryon and VGLUT2 immunoreactivity in the main axon projections of these cells. The physiological significance of endogenous glutamate in the regulation of GnRH secretion requires clarification.

Acknowledgments

We are grateful to Drs. J. P. Herman and J. P. Adelman for providing their VGLUT2 and GnRH cDNAs, respectively, to Dr. R. A. Benoit for the LR-1 antibodies to GnRH, and to Gyöngyi Kékesi for technical assistance.

Received May 10, 2004. Accepted June 7, 2004.

Address all correspondence and requests for reprints to: Dr. Erik Hrabovszky, Laboratory of Endocrine Neurobiology, Institute of Experimental Medicine, Hungarian Academy of Sciences, Budapest 1083, Hungary. E-mail: hrabovszky@koki.hu.

This work was supported by grants from the National Science Foundation of Hungary (OTKA T43407 and T46574), OMFB-01806/2002 from the Ministry of Education, the Sixth European Community Framework Program (LSHM-CT-2003-503041), and Project Grant 060202/Z/00/Z from the Wellcome Trust.

This publication reflects the authors' views and not necessarily those of the European Union. The information in this document is provided as is, and no guarantee or warranty is given that the information is fit for any particular purpose. The user thereof uses the information at its sole risk and liability.

References

1. **Lin W, McKinney K, Liu L, Lakhlani S, Jennes L** 2003 Distribution of vesicular glutamate transporter-2 messenger ribonucleic acid and protein in the septum-hypothalamus of the rat. Endocrinology 144:662–670
2. **Ziegler DR, Cullinan WE, Herman JP** 2002 Distribution of vesicular glutamate transporter mRNA in rat hypothalamus. J Comp Neurol 448:217–229
3. **Kawakami S, Ichikawa M, Murahashi K, Hirunagi K, Tsukamura H, Maeda K** 1998 Excitatory amino acids act on the median eminence nerve terminals to induce gonadotropin-releasing hormone release in female rats. Gen Comp Endocrinol 112:372–382
4. **Kawakami SI, Hirunagi K, Ichikawa M, Tsukamura H, Maeda KI** 1998 Evidence for terminal regulation of GnRH release by excitatory amino acids in the median eminence in female rats: a dual immunoelectron microscopic study. Endocrinology 139:1458–1461
5. **Schwanzel-Fukuda M** 1999 Origin and migration of luteinizing hormone-releasing hormone neurons in mammals. Microsc Res Tech 44:2–10
6. **Wray S, Grant P, Gainer H** 1989 Evidence that cells expressing luteinizing hormone-releasing hormone mRNA in the mouse are derived from progenitor cells in the olfactory placode. Proc Natl Acad Sci USA 86:8132–8136
7. **Tobet SA, Chickering TW, King JC, Stopa EG, Kim K, Kuo-Leblank V, Schwarting GA** 1996 Expression of γ-aminobutyric acid and gonadotropin-releasing hormone during neuronal migration through the olfactory system. Endocrinology 137:5415–5420
8. **Hrabovszky E, Petersen SL** 2002 Increased concentrations of radioisotopically-labeled complementary ribonucleic acid probe, dextran sulfate, and dithiothreitol in the hybridization buffer can improve results of in situ hybridization histochemistry. J Histochem Cytochem 50:1389–1400
9. **Hrabovszky E, Kallo I, Steinhauser A, Merchenthaler I, Coen CW, Liposits Z** 2004 Estrogen receptor-β in oxytocin and vasopressin neurons of the rat and human hypothalamus. Immunocytochemical and in situ hybridization studies. J Comp Neurol 473:315–333
10. **Hrabovszky E, Steinhauser A, Barabás K, Shughrue JP, Petersen SL, Merchenthaler I, Liposits Z** 2001 Estrogen receptor-β immunoreactivity in luteinizing hormone-releasing hormone neurons of the rat brain. Endocrinology 142:3261–3264
11. **Urbanski HF, Ojeda SR** 1987 Activation of luteinizing hormone-releasing hormone release advances the onset of female puberty. Neuroendocrinology 46:273–276
12. **Bourguignon JP, Gerard A, Mathieu J, Simons J, Franchimont P** 1989 Pulsatile release of gonadotropin-releasing hormone from hypothalamic explants is restrained by blockade of *N*-methyl-D,L-aspartate receptors. Endocrinology 125:1090–1096
13. **Ping L, Mahesh VB, Bhat GK, Brann DW** 1997 Regulation of gonadotropin-releasing hormone and luteinizing hormone secretion by AMPA receptors. Evidence for a physiological role of AMPA receptors in the steroid-induced luteinizing hormone surge. Neuroendocrinology 66:246–253
14. **Kiss J, Kocsis K, Csaki A, Halasz B** 2003 Evidence for vesicular glutamate transporter synapses onto gonadotropin-releasing hormone and other neurons in the rat medial preoptic area. Eur J Neurosci 18:3267–3278
15. **Gore AC, Wu TJ, Rosenberg JJ, Roberts JL** 1996 Gonadotropin-releasing hormone and NMDA receptor gene expression and colocalization change during puberty in female rats. J Neurosci 16:5281–5289
16. **Eyigor O, Jennes L** 2000 Kainate receptor subunit-positive gonadotropin-releasing hormone neurons express c-Fos during the steroid-induced luteinizing hormone surge in the female rat. Endocrinology 141:779–786

***Endocrinology* is published monthly by The Endocrine Society (http://www.endo-society.org), the foremost professional society serving the endocrine community.**

8. számú melléklet

0013-7227/05/$15.00/0
Printed in U.S.A.

dc_27_10

Endocrinology 146(1):341–347

doi: 10.1210/en.2004-0856

Hypophysiotropic Thyrotropin-Releasing Hormone and Corticotropin-Releasing Hormone Neurons of the Rat Contain Vesicular Glutamate Transporter-2

Erik Hrabovszky, Gábor Wittmann, Gergely F. Turi, Zsolt Liposits, and Csaba Fekete

Laboratory of Endocrine Neurobiology, Institute of Experimental Medicine, Hungarian Academy of Sciences, Budapest 1083, Hungary

TRH and CRH are secreted into the hypophysial portal circulation by hypophysiotropic neurons located in parvicellular subdivisions of the hypothalamic paraventricular nucleus (PVH). Recently these anatomical compartments of the PVH have been shown to contain large numbers of glutamatergic neurons expressing type 2 vesicular glutamate transporter (VGLUT2). In this report we presented dual-label *in situ* hybridization evidence that the majority (>90%) of TRH and CRH neurons in the PVH of the adult male rat express the mRNA encoding VGLUT2. Dual-label immunofluorescent studies followed by confocal laser microscopic analysis of the median eminence also demonstrated the occurrence of VGLUT2 immunoreactivity within TRH and CRH axon varicosities, suggesting terminal glutamate release from these neuroendocrine systems. These data together indicate that the hypophysiotropic TRH and CRH neurons possess glutamatergic characteristics. Future studies will need to address the physiological significance of the endogenous glutamate content in these neurosecretory systems in the neuroendocrine regulation of thyroid and adrenal functions. (*Endocrinology* 146: 341–347, 2005)

GLUTAMATE IS A major excitatory synaptic transmitter in neuroendocrine regulation (1, 2). The recent discovery of vesicular glutamate transporters (VGLUTs) 1–3, which selectively accumulate glutamic acid into synaptic vesicles, has provided histochemical markers for the identification of glutamatergic neurons. The three molecular forms of VGLUT appear to be expressed by distinct populations of glutamatergic neurons; VGLUT2 represents the dominant isoform synthesized in hypothalamic excitatory neurons (3–12). The occurrence of VGLUT2 mRNA and immunoreactivity has been observed in hypothalamic regions that play crucial roles in neuroendocrine regulation (10, 11), including the parvicellular compartments of the hypothalamic paraventricular nucleus (PVH), which comprise hypophysiotropic TRH and CRH neurons, among other peptidergic neuronal phenotypes. The observations of glutamate- (13) and VGLUT2-immunoreactive (IR) (11, 14) axons in the external zone of the median eminence (ME) have raised the possibility that some of the parvicellular neurosecretory systems may accumulate glutamic acid into synaptic vesicles for terminal corelease with hypophysiotropic neuropeptides. Also in support of this idea, we have recently shown that GnRH neurons forming the final common pathway in the neuroendocrine control of reproduction express VGLUT2 mRNA in their perikaryon and exhibit VGLUT2 immunoreactivity in their axons terminating in the organum vasculosum of the lamina terminalis and the ME (14).

In these studies we addressed the putative glutamatergic phenotype of hypophysiotropic TRH and CRH neurons in the adult male rat. First, we performed dual-label *in situ* hybridization histochemistry (ISHH) to analyze VGLUT2 mRNA expression in TRH and CRH neurons of the PVH. In addition, we carried out dual-label immunofluorescent studies followed by confocal laser microscopic analysis of the ME to localize VGLUT2 immunoreactivity within neurosecretory TRH and CRH axon terminals.

Materials and Methods

Animals

Adult male Wistar rats (n = 8; 200–225 g body weight) were purchased from Charles River Hungary Ltd. (Isaszeg, Hungary) and maintained in a light- and temperature-controlled environment (lights on 0500–1900 h; 22 C) with free access to food and water. Experimental protocols were reviewed and approved by the Animal Welfare Committee of the Institute of Experimental Medicine.

Dual-label in situ hybridization experiments

Four rats were decapitated and their brains were rapidly removed and frozen on powdered dry ice. Coronal, 12-μm-thick sections were cut with a CM 3050 S cryostat (Leica Microsystems Nussloch Gmbh, Nussloch, Germany) and collected serially on gelatin-coated microscope slides. Mounted sections were processed either for the simultaneous detection of VGLUT2 with TRH mRNAs or VGLUT2 with CRH mRNAs. Dual-label ISHH was carried out as described recently for the demonstration of VGLUT2 mRNA expression in GnRH neurons (14). Briefly, sections were hybridized at 52 C with a mixture of a ^{35}S-labeled cRNA hybridization probe to VGLUT2 mRNA and a digoxigenin-labeled

First Published Online October 14, 2004

Abbreviations: ap, Anterior parvicellular subnucleus; DAB, diaminobenzidine; FITC, fluorescein isothiocyanate; GABA, γ-aminobutyric acid; IR, immunoreactive; ISHH, *in situ* hybridization histochemistry; ME, median eminence; mpd, dorsal subdivision of the medial parvicellular subnucleus; NMDA, *N*-methyl-D-aspartate; POD, peroxidase; pv, periventricular subnucleus; PVH, hypothalamic paraventricular nucleus; RT, reticular nucleus of the thalamus; VGLUT, vesicular glutamate transporter.

***Endocrinology* is published monthly by The Endocrine Society (http://www.endo-society.org), the foremost professional society serving the endocrine community.**

cRNA probe to either proTRH or proCRH mRNA. After hybridization and posthybridization treatments, the nonisotopic probes were reacted with horseradish peroxidase (POD)-conjugated antidigoxigenin antibodies (1:200; Roche Diagnostics Co., Indianapolis, IN). The POD signals were enhanced with biotin tyramide amplification using a procedure (15) adapted from Adams (16) and finally visualized with diaminobenzidine (DAB) chromogen (14, 15). To reduce autoradiographic background, we added 1000 mM dithiothreitol to the hybridization solution (17). To enhance autoradiographic hybridization signal for VGLUT2 mRNA, we also applied high concentrations of radioisotopic probe (80,000 cpm/μl) and dextran sulfate (25%) to the sections and extended the time of hybridization from 16 to 40 h. The advantages of these changes have been formally established in a methodological report (17) and confirmed in recent dual- and triple-label ISHH studies from our laboratory (14, 15, 18, 19). The autoradiographs were detected on NTB-3 nuclear track emulsion (Kodak, Rochester, NY) after 2 wk of exposure (14).

Procedures to label radioisotopic and nonisotopic cRNA probes and details of the dual-label ISHH method have been described elsewhere (15). The cDNA templates to generate proTRH (1.2 kb) and proCRH (1.1 kb) probes were kindly provided by Drs. R. M. Lechan (New England Medical Center, Boston, MA) and K. Mayo (Northwestern University, Evanston, IL), respectively, and used in previous nonisotopic ISHH experiments (15, 20). The mRNA encoding VGLUT2 was detected with a ^{35}S-labeled probe to bases 522-1400 of VGLUT2 mRNA (GenBank accession no. NM 053427) (14). TRH and CRH neurons exhibiting DAB labeling were analyzed individually for the autoradiographic VGLUT2 signal at high power. The percent ratios of TRH and CRH neurons with VGLUT2 mRNA were determined using two sections per animal for each region of interest. Results of dual-labeling were expressed as mean ± SEM of four animals.

In situ hybridization control experiments

Test sections from the PVH were hybridized using a distinct antisense probe to VGLUT2 mRNA (VGLUT2–734; complementary to bases 1704–2437). The plasmid template for *in vitro* transcription of this probe (10) was a kind gift from Dr. J. P. Herman (University of Cincinnati Medical Center, Cincinnati, OH), and results served as positive control for hybridization specificity. Furthermore, control sections were hybridized with the combined application of the digoxigenin-labeled antisense TRH probe and the isotopically labeled sense-strand VGLUT2–879 or VGLUT2–734 transcripts.

Tissue preparation for immunocytochemistry

Four rats were anesthetized with pentobarbital (35 mg/kg body weight, ip) and perfused transcardially with 150 ml fixative solution containing 2% paraformaldehyde (Sigma Chemical Co., St. Louis, MO) and 4% acrolein (Aldrich Chemical Co., Milwaukee, WI) in 0.1 M PBS (pH 7.4). The hypothalami were dissected and soaked in 25% sucrose overnight for cryoprotection. Then 20-μm-thick free-floating coronal sections were cut from the hypothalami using a cryostat. The sections were rinsed in Tris-buffered saline [0.1 M Tris-HCl/0.9% sodium chloride (pH 7.8)] and treated with 0.5% sodium borohydride (Sigma, 30 min), then 0.5% H_2O_2 + 0.5% Triton X-100 (15 min), and finally 2% normal horse serum in Tris-buffered saline (30 min) (15).

Immunocytochemical procedures

After pretreatments, the sections were incubated in a polyclonal VGLUT2 antiserum raised in a guinea pig (AB5907; 1:1000; Chemicon, Temecula, CA) for 72 h at 4 C. The primary antibodies were reacted with donkey, biotin-SP-antiguinea pig IgG (1:1000; Jackson ImmunoResearch Laboratories, West Grove, PA) for 2 h and then with streptavidine-conjugated Cy3 fluorochrome (1:200; Vector Laboratories, Burlingame, CA) for 2 h. Subsequently immunoreactivities for either TRH or CRH were detected with a rabbit antiserum against TRH (no. 31) at 1:2500 dilution (a gift from Dr. R. M. Lechan) and a rabbit CRH antiserum (1:300; Peninsula Laboratories Inc., San Carlos, CA), respectively, which were applied to the sections for 48 h (4 C) and then reacted with fluorescein isothiocyanate (FITC)-conjugated antirabbit IgG (1:200; 12 h; Jackson ImmunoResearch). Dual-immunofluorescent specimens were analyzed at high power (×60 objective lens) with a Radiance 2100 confocal microscope (Bio-Rad Laboratories, Hemel Hempstead, UK) using laser excitation lines 488 nm for FITC and 543 nm for Cy3 and dichroic/emission filters 560/500–530 nm for FITC and 560–610 nm for Cy3. The analysis of individual optical layers (<0.7 μm) was used for the demonstration of the axonal colocalization phenomenon and its photographic illustration (14).

Immunocytochemical control experiments

Negative and positive control studies to assess specificity of VGLUT2 immunolabeling were carried out as described recently (14). Primary antibodies (AB5907) preabsorbed with 10 μM of the immunization antigen (AG209; Chemicon) were applied to test sections in parallel with the experimental specimens (14). In addition, the AB5907 guinea pig VGLUT2 antibodies (Chemicon) were used in combination with rabbit VGLUT2 antibodies (AB 135103; 1:5000; Synaptic Systems, Göttingen, Germany) for dual-immunofluorescent experiments. The different primary antibodies were reacted with appropriate secondary antibody-fluorochrome conjugates (antiguinea pig-FITC and antirabbit-Cy3, respectively; Jackson ImmunoResearch) for 12 h, and colocalization of the two signals was assessed in the hypothalamus with confocal microscopy (14).

Results

Dual-label in situ hybridization results

Silver grain clusters were abundant in the diencephalon after 2 wk of autoradiographic exposure (Fig 1A). Virtually all anatomical compartments of the PVH through its rostrocaudal extent (Fig. 1, B–D), including the anterior parvicellular (ap) and periventricular (pv) subnuclei as well as the dorsal subdivision of the medial parvicellular subnucleus (mpd), exhibited numerous cells expressing VGLUT2 mRNA. Very heavy grain clusters accumulated in the lateral hypothalamic area (LHA; Fig. 1A), which is known to contain nonhypophysiotropic TRH neurons in large numbers. In contrast, the reticular nucleus of the thalamus (RT), which exhibits cells containing proTRH mRNA but not TRH tripeptide (21), was devoid of VGLUT2 hybridization signal (Fig. 1A).

Using bright-field illumination of dual-labeled sections, the majority of DAB-labeled TRH neurons in the PVH, including nonhypophysiotropic TRH neurons in the ap subnucleus (Fig. 2A) and hypophysiotropic TRH neurons in the pv (Fig. 2B) and mpd (Fig. 2C) subnuclei, exhibited moderate levels of isotopic hybridization signal for VGLUT2 mRNA. In sections hybridized for CRH and VGLUT2 mRNAs, most CRH neurons in the PVH also expressed the signal for VGLUT2 mRNA (Fig. 2D). The counted ratio of dual-labeled TRH neurons was 97.4 ± 1.1% in the ap, 93.8 ± 1.4% in the pv, and 94.3 ± 1.4% in the mpd subnuclei of the PVH. Furthermore, 90.5 ± 1.3% of CRH neurons in the mpd subnucleus, which includes most hypophysiotropic CRH neurons, exhibited autoradiographic signal for the glutamatergic marker, VGLUT2. In addition to occurring within TRH and CRH neurons in the PVH, it is worth noting that TRH neurons with the heaviest cellular levels of VGLUT2 signal were identified in the LHA (Fig. 2E). Of these cells, 98.6 ± 0.7% exhibited VGLUT2 labeling. In contrast, only 18.9 ± 4.5% of the TRH neurons in the perifornical region (Fig. 2F) contained the VGLUT2 signal, and proTRH mRNA-expressing

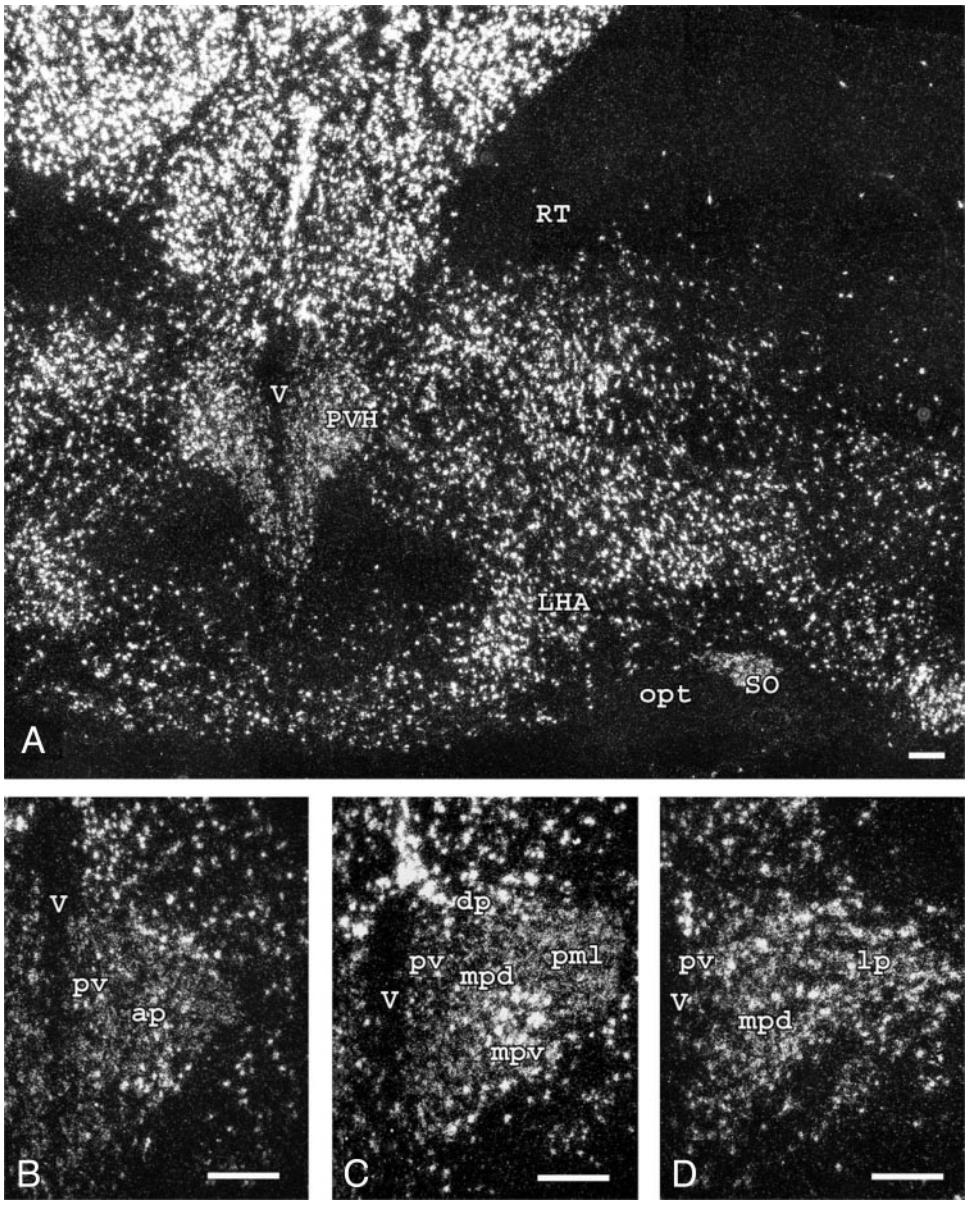

FIG. 1. *In situ* hybridization detection of VGLUT2 mRNA at the level of the PVH. A, Heavy and moderate expression levels of VGLUT2 mRNA (autoradiographic grain clusters) can be observed in the LHA and PVH, respectively. In contrast, the hybridization signal is absent from the RT. B–D, Large numbers of glutamatergic neurons are present in virtually all subnuclei of the PVH in its rostral (B), middle (C), and caudal (D) portions. In addition to occurring in various parvicellular compartments, the hybridization signal is also expressed in magnocellular neurons of the PVH (lateral subdivision of the posterior magnocellular subnucleus; pml) and the supraoptic nucleus (SO). dp, Dorsal parvicellular subnucleus (PVH); lp, lateral parvicellular subnucleus (PVH); mpv, ventral subdivision of the medial parvicellular subnucleus (PVH); opt, optic tract; V, third cerebral ventricle. *Scale bars*, 200 μm.

neurons in the RT (Fig. 2G) did not accumulate silver grains. Sections dual labeled for CRH and VGLUT2 mRNAs also included CRH neurons in the central amygdaloid nucleus. In contrast to CRH neurons of the PVH, these cells remained unlabeled for VGLUT2 (Fig. 2H). In control experiments, application of the sense VGLUT2 probes (Fig. 2, J and L) did not generate any patterned labeling of sections exceeding background labeling. TRH and CRH neurons in these sections were devoid of silver grain clusters, also indicating lack of potential positive chemography on the DAB chromogen. Furthermore, the distribution of cells labeled for VGLUT2 mRNA was identical using either the VGLUT2–879 probe (Fig. 2I; also used in Fig. 1 and Fig. 2, A–H) or the control probe (VGLUT2–734; Fig. 2K) that recognized nonoverlapping segments of VGLUT2 mRNA; dual-labeled neurons were also clearly identifiable with the latter (Fig. 2K), in strong support of hybridization specificity.

Dual-label immunofluorescent results

Immunofluorescent studies revealed a dense plexus of VGLUT2-immunoreactive axons in the external zone of the ME (Fig. 2O), which overlapped with the distribution of hypophysiotropic peptidergic axons. Confocal laser microscopic analysis established an extensive terminal coexpression of VGLUT2 with TRH (Fig. 2M) and VGLUT2 with CRH (Fig. 2N) immunoreactivities. The two types of signal showed a clear segregation within individual terminal varicosities (Fig. 2N), supporting the assumption that VGLUT2 (and the glutamate transmitter pool) and the neuropeptides are contained in distinct vesicular components. Specificity control experiments showed that preabsorption of VGLUT2 antibodies (AB5907) with 10 μM of the immunization antigen (AG209) eliminated the axonal labeling from the ME (Fig. 2O). Furthermore, VGLUT2 antibodies from Chemicon and

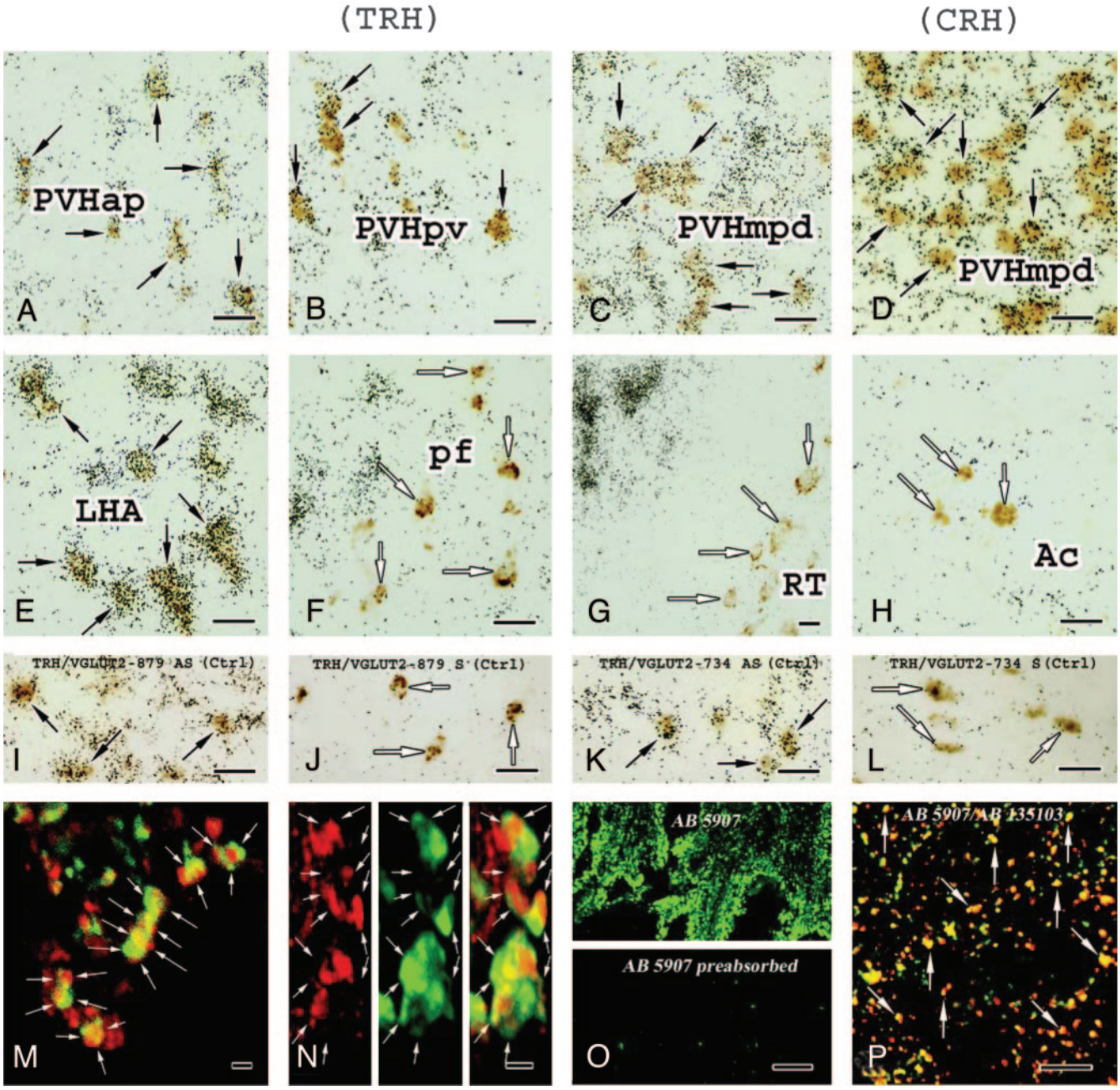

FIG. 2. Histochemical detection of VGLUT2 mRNA expression and immunoreactivity in TRH and CRH neurons of the diencephalon. *Black arrows* in dual-label *in situ* hybridization images (A–L) point to TRH or CRH neurons (*brown* DAB chromogen) that also express VGLUT2 mRNA (*silver* grain clusters), whereas *white arrows* indicate TRH or CRH neurons that lack the autoradiographic signal. A–C, The VGLUT2 hybridization signal is expressed at moderate levels by the majority of nonhypophysiotropic TRH neurons (*brown* DAB chromogen) in the anterior parvicellular subnucleus of the paraventricular nucleus (PVHap; A). Similarly, most hypophysiotropic TRH neurons in the periventricular subnucleus (PVHpv; B) and the dorsal subdivision of the medial parvicellular subnucleus (PVHmpd; C) contain VGLUT2 mRNA. D, The mpd compartment also includes a large number of CRH neurons with VGLUT2 mRNA. E–G, TRH neurons in the LHA (E) are labeled heavily for VGLUT2, whereas more than 80% of TRH neurons in the perifornical region (pf; F) and all proTRH mRNA-expressing neurons in the RT (G) are devoid of the VGLUT2 hybridization signal. H, Similarly, VGLUT2 mRNA is not detectable in CRH neurons of the central amygdala (Ac). I–L, Serial sections from the PVH used for control (Ctrl) purposes were hybridized in parallel using two distinct antisense (AS; I, K) and sense (S; J, L) VGLUT2 transcripts (VGLUT2–879 and VGLUT2–734) together with the digoxigenin-labeled antisense probe to TRH mRNA. The autoradiographic VGLUT2 signal and dual-labeled TRH neurons (clustered *silver* grains over *brown* DAB deposits) are present using either one of the two antisense (I, K) but none of the two sense (J, L) VGLUT2 probe sequences, providing strong support for hybridization specificity. M and N, Dual-label immunofluorescent studies using confocal laser microscopy reveal a dense plexus of VGLUT2-IR axons (*red* fluorochrome) in the external layer of the ME, which overlaps with the distribution of hypophysiotropic TRH (M) and CRH (N) axons (*green* fluorochrome). The high-power confocal images of single optical layers (<0.7 μm) demonstrate an extensive axonal colocalization of VGLUT2 with TRH (M; merged figure) and VGLUT2 with CRH (N) immunoreactivities. *Arrows* delineate dual-labeled terminal varicosities. The three panels in N also illustrate the intraaxonal segregation of organelles containing VGLUT2 (*red*; *left panel*) and CRH (*green*; *middle panel*) immunoreactivities.

those from Synaptic Systems consequently labeled identical axon varicosities in the hypothalamus (Fig. 2P), serving as positive control for the specificity of axonal VGLUT2 immunolabeling (14).

Discussion

In this report we present evidence that the majority of TRH and CRH neurons in the PVH express the mRNA for VGLUT2. Furthermore, their neurosecretory axon terminals in the ME contain VGLUT2 immunoreactivity.

Classical nonpeptide neurotransmitters including L-glutamate are transported into synaptic vesicles by vesicular neurotransmitter transporters before their quantal release by exocytosis (22). Recently it has been established that the brain-specific Na^+-dependent inorganic phosphate cotransporter (23) fulfills the criteria required for the vesicular glutamate transporter, and hence, the molecule was renamed VGLUT1 (3, 24). Subsequently several laboratories have shown that differentiation-associated Na^+-dependent inorganic phosphate cotransporter represents a second member of the VGLUT family, VGLUT2 (4, 6, 25–28). Although VGLUT1 and VGLUT2 occur in distinct classes of glutamatergic neurons establishing asymmetric synapses typical of excitatory neurons (4–6, 29), the roles of the third member of the VGLUT family, VGLUT3 (7–9), are less well understood given its unexpected occurrence in serotonergic (7–9), cholinergic (7–9), and even γ-aminobutyric acid (GABAergic) (7) neurons, presence in neuronal cell bodies and dendrites, in addition to axon terminals (7–9), and involvement in symmetric, in addition to asymmetric synapses (7, 8). The VGLUT2 isoform we identified in various groups of diencephalic TRH and CRH neurons is considered an authentic marker for the glutamatergic neuronal phenotype.

Together the expression of the mRNA for the glutamatergic marker VGLUT2 in the majority of TRH- and CRH-synthesizing neuronal perikarya in hypophysiotropic subdivisions of the PVH and the occurrence of VGLUT2 immunoreactivity in TRH and CRH IR terminals in the ME indicate that the hypophysiotropic TRH and CRH neurosecretory systems release glutamate, in addition to neuropeptides, into the pericapillary space of hypophysial portal vessels. The physiological role of this glutamate cosecretion with TRH and CRH remains to be investigated.

One possibility is that glutamate released from hypophysiotropic terminals reaches the anterior pituitary at high enough concentrations to exert physiological effects. This putative hypophysial site of glutamatergic actions would be compatible with the reported presence of glutamate receptors on thyrotrophs (30). However, it is even more likely that glutamate acts centrally at the level of the ME. Central glutamatergic mechanisms are clearly crucial in thyroid regulation, which is indicated by decreased serum TSH and thyroid hormone levels in response to intracerebroventricular administration of antagonists to 2-amino-3-hydroxy-5-methyl-4-isoxazol propionic acid and *N*-methyl-D-aspartate (NMDA) receptors (31). In contrast, exclusively central glutamatergic mechanisms appear to be involved in adrenal regulation. Plasma ACTH levels rise after systemic (32–34) or central (35) administration of NMDA and kainate, whereas NMDA, kainate, or glutamate does not directly elicit ACTH release from incubated pituitaries (34). Moreover, the observation that ACTH release induced by systemic NMDA or kainate injections can be blocked by antisera to CRH also suggests that the central actions of glutamate may involve CRH terminals in the ME (34). It is reasonable to speculate that glutamate actions in the ME can be partly exerted directly on neurosecretory terminals. Indeed, some of these axon terminals have been shown to express immunoreactivity for the KA2 and NR1 ionotropic glutamate receptor subunits (13, 36). Such receptors, assuming they are also present on TRH and CRH terminals, may be involved in autocrine/paracrine regulatory mechanisms on binding glutamate secreted from endogenous sources in TRH and CRH axon terminals. In addition, a further possibility is that the secreted glutamate regulates important glial functions at the sites of release. Tanycytes and astrocytes in the ME were found to contain mRNAs and immunoreactivity for kainate receptors (37–39) and to express c-Fos immunoreactivity on kainate stimulation (37). Because tanycytic processes regulate the neurohemal junction in the ME, it is an intriguing possibility that glutamate induces plastic changes in this cell type to regulate the access of secretion products to the hypophysial portal vessels. Finally, intrinsic glutamate released by hypophysiotropic TRH and CRH terminals may also act on vascular elements. Although somewhat controversial (40), the presence of functional metabotropic (41, 42) and ionotropic (42, 43) glutamate receptors has been described on cerebral microvascular endothelial cells. It is interesting to note that the stimulation of NMDA receptors increases nitric oxide production within the ME (44), which is considered to be of endothelial origin (45). Nitric oxide, in turn, is an important regulator of CRH release from the ME (45), proposed to act via increasing cGMP and/or prostaglandin E2 production in hypophysiotropic axon terminals (45). Actions mediated by the soluble nitric oxide may also propagate the glutamatergic signal to a larger group of neurosecretory terminals and to a higher distance from the site of glutamate release.

The observation of VGLUT2 in functionally and neurochemically diverse neurosecretory endings also suggests that intrinsic glutamate fulfills similar regulatory functions in several neuroendocrine systems. A putative general mechanism would be its contribution to regulate episodic secretion, which equally characterizes the TRH and CRH systems (46, 47). Whereas the concept requires experimental support, it is tempting to speculate that the endogenous glutamate

The *yellow color* in merged figure (*right panel*) likely occurs at sites containing both small clear and dense core vesicles. O, Specificity of VGLUT2 immunostaining in the ME (*upper panel*) is indicated by the lack of labeled axons (*lower panel*) after adding 10 μM of the immunization antigen to the working dilution of AB 5907. P, Furthermore, glutamatergic axons in the external layer of the ME can be dual immunolabeled with two distinct VGLUT2 antisera (AB 5907 and AB 135103) and using *green* and *red* fluorochromes, respectively. Presence of mostly dual-labeled axon varicosities (*yellow color*; *arrows*) serves as a strong evidence for the authenticity of VGLUT2 immunolabeling. *Scale bars*,1 μm in M, N; 10 μm in P; and 20 μm in other panels.

content of these systems contributes to common signaling mechanisms that generate the pulsatile patterns in neurohormone output.

It is worth noting that, whereas VGLUT2 mRNA was identifiable in the vast majority of the hypophysiotropic TRH and CRH neurons in the PVH, the ME contained both TRH and CRH axon terminals that were not immunoreactive for VGLUT2. A methodological explanation for this discrepancy may be the superior detection sensitivity of the ISHH *vs.* the immunocytochemical technique. Alternatively, the nonhomogeneous intraaxonal distribution of VGLUT2 *vs.* TRH/CRH immunoreactivities in our confocal microscopic studies raises the possibility that the segregation of vesicular pools containing VGLUT2 and the hypophysiotropic neuropeptides could partly account for the observation of VGLUT2-immunonegative TRH and CRH terminals. Finally, of particular interest to our observation that VGLUT2 mRNA is expressed in the vast majority of CRH neurons in the PVH is a previous report on glutamic acid decarboxylase and GABA immunoreactivities in a small subset of parvicellular CRH neurons in this nucleus (48). Whether these apparently GABA-synthesizing CRH neurons constitute a subpopulation of the CRH/VGLUT2 neurons or they correspond to the small subset (<10%) of CRH neurons that showed no VGLUT2 mRNA expression in our present study remains to be established.

In addition to being expressed in hypophysiotropic TRH and CRH neurons, VGLUT2 mRNA also occurred in several nonhypophysiotropic TRH neuronal populations. Hybridization results have shown that nonhypophysiotropic TRH neurons in the anterior PVH and the LHA (49, 50) exhibit common glutamatergic characteristics. In contrast, proTRH mRNA synthesizing neurons in the RT region were devoid of VGLUT2 mRNA, in accordance with the predominant GABAergic phenotype of this brain region (51). We were similarly unable to find VGLUT2 mRNA expression in the majority (>80%) of TRH neurons in the perifornical region. It remains unclear whether perifornical TRH cells consist of glutamatergic and nonglutamatergic (putative GABAergic) subpopulations or else their majority contains VGLUT2 mRNA at levels below the detection threshold of our isotopic ISHH approach. Evidence exists that the perifornical TRH neurons are neurochemically and functionally distinct from the TRH neurons of the PVH in that they contain enkephalin and project to the lateral septum (52). A neurochemical diversity also exists for distinct CRH-containing neuronal cell groups with regard to their amino acid transmitter cocontent. CRH has been localized to GABAergic neurons in the bed nucleus of the stria terminalis and central amygdaloid nucleus (53), which appears to be in agreement with our present data on the absence of VGLUT2 hybridization signal in CRF neurons of the central amygdala.

In summary, in the present ISHH and immunocytochemistry studies, we provide evidence that hypophysiotropic TRH and CRH neurons of the PVH synthesize VGLUT2 mRNA and protein in the male rat. The functional significance of this marked glutamatergic phenotype, which is shared by several neurosecretory systems, requires clarification.

Acknowledgments

This publication reflects the authors' views and not necessarily those of the European Union. The information in this document is provided as is, and no guarantee or warranty is given that the information is fit for any particular purpose. The user thereof uses the information at its sole risk and liability. The authors are grateful to Drs. J. P. Herman and K. Mayo for providing their VGLUT2 and proCRH cDNAs, respectively, to Dr. R. M. Lechan for the proTRH cDNA and TRH antibodies and to Gyöngyi Kékesi for the excellent technical assistance.

Received July 6, 2004. Accepted October 5, 2004.

Address all correspondence and requests for reprints to: Dr. Erik Hrabovszky, Laboratory of Endocrine Neurobiology, Institute of Experimental Medicine, Hungarian Academy of Sciences, Szigony u. 43, Budapest 1083, Hungary. E-mail: hrabovszky@koki.hu.

This work was supported by grants from the National Science Foundation of Hungary (OTKA T43407, T46574, T46492), the Ministry of Education (OMFB-01806/2002), and the European Union FP6 funding (contract LSHM-CT-2003-503041).

References

1. **van den Pol AN, Wuarin JP, Dudek FE** 1990 Glutamate, the dominant excitatory transmitter in neuroendocrine regulation. Science 250:1276–1278
2. **Brann DW** 1995 Glutamate: a major excitatory transmitter in neuroendocrine regulation. Neuroendocrinology 61:213–225
3. **Bellocchio EE, Reimer RJ, Fremeau Jr RT, Edwards RH** 2000 Uptake of glutamate into synaptic vesicles by an inorganic phosphate transporter. Science 289:957–960
4. **Fremeau Jr RT, Troyer MD, Pahner I, Nygaard GO, Tran CH, Reimer RJ, Bellocchio EE, Fortin D, Storm-Mathisen J, Edwards RH** 2001 The expression of vesicular glutamate transporters defines two classes of excitatory synapse. Neuron 31:247–260
5. **Fujiyama F, Furuta T, Kaneko T** 2001 Immunocytochemical localization of candidates for vesicular glutamate transporters in the rat cerebral cortex. J Comp Neurol 435:379–387
6. **Herzog E, Bellenchi GC, Gras C, Bernard V, Ravassard P, Bedet C, Gasnier B, Giros B, El Mestikawy S** 2001 The existence of a second vesicular glutamate transporter specifies subpopulations of glutamatergic neurons. J Neurosci 21:RC181
7. **Fremeau Jr RT, Burman J, Qureshi T, Tran CH, Proctor J, Johnson J, Zhang H, Sulzer D, Copenhagen DR, Storm-Mathisen J, Reimer RJ, Chaudhry FA, Edwards RH** 2002 The identification of vesicular glutamate transporter 3 suggests novel modes of signaling by glutamate. Proc Natl Acad Sci USA 99:14488–14493
8. **Gras C, Herzog E, Bellenchi GC, Bernard V, Ravassard P, Pohl M, Gasnier B, Giros B, El Mestikawy S** 2002 A third vesicular glutamate transporter expressed by cholinergic and serotoninergic neurons. J Neurosci 22:5442–5451
9. **Schafer MK, Varoqui H, Defamie N, Weihe E, Erickson JD** 2002 Molecular cloning and functional identification of mouse vesicular glutamate transporter 3 and its expression in subsets of novel excitatory neurons. J Biol Chem 277:50734–50748
10. **Ziegler DR, Cullinan WE, Herman JP** 2002 Distribution of vesicular glutamate transporter mRNA in rat hypothalamus. J Comp Neurol 448:217–229
11. **Lin W, McKinney K, Liu L, Lakhlani S, Jennes L** 2003 Distribution of vesicular glutamate transporter-2 messenger ribonucleic acid and protein in the septum-hypothalamus of the rat. Endocrinology 144:662–670
12. **Sakata-Haga H, Kanemoto M, Maruyama D, Hoshi K, Mogi K, Narita M, Okado N, Ikeda Y, Nogami H, Fukui Y, Kojima I, Takeda J, Hisano S** 2001 Differential localization and colocalization of two neuron-types of sodium-dependent inorganic phosphate cotransporters in rat forebrain. Brain Res 902:143–155
13. **Kawakami SI, Hirunagi K, Ichikawa M, Tsukamura H, Maeda KI** 1998 Evidence for terminal regulation of GnRH release by excitatory amino acids in the median eminence in female rats: a dual immunoelectron microscopic study. Endocrinology 139:1458–1461
14. **Hrabovszky E, Turi GF, Kallo I, Liposits Z** 2004 Expression of vesicular glutamate transporter-2 in gonadotropin-releasing hormone neurons of the adult male rat. Endocrinology 145:4018–4021
15. **Hrabovszky E, Kallo I, Steinhauser A, Merchenthaler I, Coen CW, Liposits Z** 2004 Estrogen receptor-β in oxytocin and vasopressin neurons of the rat and human hypothalamus. Immunocytochemical and *in situ* hybridization studies. J Comp Neurol 473:315–333
16. **Adams JC** 1992 Biotin amplification of biotin and horseradish peroxidase signals in histochemical stains. J Histochem Cytochem 40:1457–1463
17. **Hrabovszky E, Petersen SL** 2002 Increased concentrations of radioisotopically labeled complementary ribonucleic acid probe, dextran sulfate, and dithiothreitol in the hybridization buffer can improve results of *in situ* hybridization histochemistry. J Histochem Cytochem 50:1389–1400

18. **Hrabovszky E, Shughrue PJ, Merchenthaler I, Hajszan T, Carpenter CD, Liposits Z, Petersen SL** 2000 Detection of estrogen receptor-β messenger ribonucleic acid and ^{125}I-estrogen binding sites in luteinizing hormone-releasing hormone neurons of the rat brain. Endocrinology 141:3506–3509
19. **Hrabovszky E, Steinhauser A, Barabas K, Shughrue PJ, Petersen SL, Merchenthaler I, Liposits Z** 2001 Estrogen receptor-β immunoreactivity in luteinizing hormone-releasing hormone neurons of the rat brain. Endocrinology 142:3261–3264
20. **Fekete C, Legradi G, Mihaly E, Huang QH, Tatro JB, Rand WM, Emerson CH, Lechan RM** 2000 α-Melanocyte-stimulating hormone is contained in nerve terminals innervating thyrotropin-releasing hormone-synthesizing neurons in the hypothalamic paraventricular nucleus and prevents fasting-induced suppression of prothyrotropin-releasing hormone gene expression. J Neurosci 20:1550–1558
21. **Segerson TP, Hoefler H, Childers H, Wolfe HJ, Wu P, Jackson IM, Lechan RM** 1987 Localization of thyrotropin-releasing hormone prohormone messenger ribonucleic acid in rat brain *in situ* hybridization. Endocrinology 121: 98–107
22. **Masson J, Sagne C, Hamon M, El Mestikawy S** 1999 Neurotransmitter transporters in the central nervous system. Pharmacol Rev 51:439–464
23. **Ni B, Rosteck Jr PR, Nadi NS, Paul SM** 1994 Cloning and expression of a cDNA encoding a brain-specific Na(+)-dependent inorganic phosphate cotransporter. Proc Natl Acad Sci USA 91:5607–5611
24. **Takamori S, Rhee JS, Rosenmund C, Jahn R** 2000 Identification of a vesicular glutamate transporter that defines a glutamatergic phenotype in neurons. Nature 407:189–194
25. **Bai L, Xu H, Collins JF, Ghishan FK** 2001 Molecular and functional analysis of a novel neuronal vesicular glutamate transporter. J Biol Chem 276:36764–36769
26. **Hayashi M, Otsuka M, Morimoto R, Hirota S, Yatsushiro S, Takeda J, Yamamoto A, Moriyama Y** 2001 Differentiation-associated Na+-dependent inorganic phosphate cotransporter (DNPI) is a vesicular glutamate transporter in endocrine glutamatergic systems. J Biol Chem 276:43400–43406
27. **Takamori S, Rhee JS, Rosenmund C, Jahn R** 2001 Identification of differentiation-associated brain-specific phosphate transporter as a second vesicular glutamate transporter (VGLUT2). J Neurosci 21:RC182
28. **Varoqui H, Schafer MK, Zhu H, Weihe E, Erickson JD** 2002 Identification of the differentiation-associated Na+/PI transporter as a novel vesicular glutamate transporter expressed in a distinct set of glutamatergic synapses. J Neurosci 22:142–155
29. **Bellocchio EE, Hu H, Pohorille A, Chan J, Pickel VM, Edwards RH** 1998 The localization of the brain-specific inorganic phosphate transporter suggests a specific presynaptic role in glutamatergic transmission. J Neurosci 18:8648–8659
30. **Bhat GK, Mahesh VB, Chu ZW, Chorich LP, Zamorano PL, Brann DW** 1995 Localization of the *N*-methyl-D-aspartate R1 receptor subunit in specific anterior pituitary hormone cell types of the female rat. Neuroendocrinology 62:178–186
31. **Arufe MC, Duran R, Perez-Vences D, Alfonso M** 2002 Endogenous excitatory amino acid neurotransmission regulates thyroid-stimulating hormone and thyroid hormone secretion in conscious freely moving male rats. Endocrine 17:193–197
32. **Farah Jr JM, Rao TS, Mick SJ, Coyne KE, Iyengar S** 1991 *N*-methyl-D-aspartate treatment increases circulating adrenocorticotropin and luteinizing hormone in the rat. Endocrinology 128:1875–1880
33. **Jezova D, Oliver C, Jurcovicova J** 1991 Stimulation of adrenocorticotropin but not prolactin and catecholamine release by *N*-methyl-aspartic acid. Neuroendocrinology 54:488–492
34. **Chautard T, Boudouresque F, Guillaume V, Oliver C** 1993 Effect of excitatory amino acid on the hypothalamo-pituitary-adrenal axis in the rat during the stress-hyporesponsive period. Neuroendocrinology 57:70–78
35. **Makara GB, Stark E** 1975 Effect of intraventricular glutamate on ACTH release. Neuroendocrinology 18:213–216
36. **Kawakami S, Ichikawa M, Murahashi K, Hirunagi K, Tsukamura H, Maeda K** 1998 Excitatory amino acids act on the median eminence nerve terminals to induce gonadotropin-releasing hormone release in female rats. Gen Comp Endocrinol 112:372–382
37. **Eyigor O, Jennes L** 1998 Identification of kainate-preferring glutamate receptor subunit GluR7 mRNA and protein in the rat median eminence. Brain Res 814:231–235
38. **Kawakami S** 2000 Glial and neuronal localization of ionotropic glutamate receptor subunit-immunoreactivities in the median eminence of female rats: GluR2/3 and GluR6/7 colocalize with vimentin, not with glial fibrillary acidic protein (GFAP). Brain Res 858:198–204
39. **Diano S, Naftolin F, Horvath TL** 1998 Kainate glutamate receptors (GluR5–7) in the rat arcuate nucleus: relationship to tanycytes, astrocytes, neurons and gonadal steroid receptors. J Neuroendocrinol 10:239–247
40. **Morley P, Small DL, Murray CL, Mealing GA, Poulter MO, Durkin JP, Stanimirovic DB** 1998 Evidence that functional glutamate receptors are not expressed on rat or human cerebromicrovascular endothelial cells. J Cereb Blood Flow Metab 18:396–406
41. **Gillard SE, Tzaferis J, Tsui HC, Kingston AE** 2003 Expression of metabotropic glutamate receptors in rat meningeal and brain microvasculature and choroid plexus. J Comp Neurol 461:317–332
42. **Krizbai IA, Deli MA, Pestenacz A, Siklos L, Szabo CA, Andras I, Joo F** 1998 Expression of glutamate receptors on cultured cerebral endothelial cells. J Neurosci Res 54:814–819
43. **Parfenova H, Fedinec A, Leffler CW** 2003 Ionotropic glutamate receptors in cerebral microvascular endothelium are functionally linked to heme oxygenase. J Cereb Blood Flow Metab 23:190–197
44. **Bhat GK, Mahesh VB, Ping L, Chorich L, Wiedmeier VT, Brann DW** 1998 Opioid-glutamate-nitric oxide connection in the regulation of luteinizing hormone secretion in the rat. Endocrinology 139:955–960
45. **Prevot V, Bouret S, Stefano GB, Beauvillain J** 2000 Median eminence nitric oxide signaling. Brain Res Brain Res Rev 34:27–41
46. **Mershon JL, Sehlhorst CS, Rebar RW, Liu JH** 1992 Evidence of a corticotropin-releasing hormone pulse generator in the macaque hypothalamus. Endocrinology 130:2991–2996
47. **Okauchi Y, Takahashi H, Mizobuchi M, Bando H, Saito S** 1996 Thyrotropin-releasing hormone release in normal and hyperthyroid rats as measured by microdialysis. Tokushima J Exp Med 43:93–100
48. **Meister B, Hokfelt T, Geffard M, Oertel W** 1988 Glutamic acid decarboxylase- and γ-aminobutyric acid-like immunoreactivities in corticotropin-releasing factor-containing parvocellular neurons of the hypothalamic paraventricular nucleus. Neuroendocrinology 48:516–526
49. **Merchenthaler I, Liposits Z** 1994 Mapping of thyrotropin-releasing hormone (TRH) neuronal systems of rat forebrain projecting to the median eminence and the OVLT. Immunocytochemistry combined with retrograde labeling at the light and electron microscopic levels. Acta Biol Hung 45:361–374
50. **Kawano H, Tsuruo Y, Bando H, Daikoku S** 1991 Hypophysiotrophic TRH-producing neurons identified by combining immunohistochemistry for pro-TRH and retrograde tracing. J Comp Neurol 307:531–538
51. **Houser CR, Vaughn JE, Barber RP, Roberts E** 1980 GABA neurons are the major cell type of the nucleus reticularis thalami. Brain Res 200:341–354
52. **Merchenthaler I** 1991 Colocalization of enkephalin and TRH in perifornical neurons of the rat hypothalamus that project to the lateral septum. Brain Res 544:177–180
53. **Veinante P, Stoeckel ME, Freund-Mercier MJ** 1997 GABA- and peptide-immunoreactivities colocalize in the rat central extended amygdala. Neuroreport 8:2985–2989

***Endocrinology* is published monthly by The Endocrine Society (http://www.endo-society.org), the foremost professional society serving the endocrine community.**

dc_27_10

9. számú melléklet

European Journal of Neuroscience, Vol. 21, pp. 2120–2126, 2005

Presence of vesicular glutamate transporter-2 in hypophysiotropic somatostatin but not growth hormone-releasing hormone neurons of the male rat

Erik Hrabovszky, Gergely F. Turi and Zsolt Liposits
Laboratory of Endocrine Neurobiology, Institute of Experimental Medicine, Hungarian Academy of Sciences, Szigony u. 43., Budapest, 1083 Hungary

Keywords: arcuate nucleus, confocal microscopy, *in situ* hybridization, median eminence, periventricular nucleus

Abstract

Recent evidence indicates that hypophysiotropic gonadotropin-releasing hormone (GnRH), corticotropin-releasing hormone (CRH) and thyrotropin-releasing hormone (TRH) neurons of the adult male rat express mRNA and immunoreactivity for type-2 vesicular glutamate transporter (VGLUT2), a marker for glutamatergic neuronal phenotype. In the present study, we investigated the issue of whether these glutamatergic features are shared by growth hormone-releasing hormone (GHRH) neurons of the hypothalamic arcuate nucleus (ARH) and somatostatin (SS) neurons of the anterior periventricular nucleus (PVa), the two parvicellular neurosecretory systems that regulate anterior pituitary somatotrophs. Dual-label *in situ* hybridization studies revealed relatively few cells that expressed VGLUT2 mRNA in the ARH; the GHRH neurons were devoid of VGLUT2 hybridization signal. In contrast, VGLUT2 mRNA was expressed abundantly in the PVa; virtually all (97.5 ± 0.4%) SS neurons showed labelling for VGLUT2 mRNA. In accordance with these hybridization results, dual-label immunofluorescent studies followed by confocal laser microscopic analysis of the median eminence established the absence of VGLUT2 immunoreactivity in GHRH terminals and its presence in many neurosecretory SS terminals. The GHRH terminals, in turn, were immunoreactive for the vesicular γ-aminobutyric acid (GABA) transporter, used in these studies as a marker for GABA-ergic neuronal phenotype. Together, these results suggest the paradoxic cosecretion of the excitatory amino acid neurotransmitter glutamate with the inhibitory peptide SS and the cosecretion of the inhibitory amino acid neurotransmitter GABA with the stimulatory peptide GHRH. The mechanisms of action of intrinsic amino acids in hypophysiotropic neurosecretory systems require clarification.

Introduction

L-Glutamate is the major excitatory neurotransmitter in the central nervous system (Monaghan *et al*., 1989; Collingridge & Singer, 1990; Headley & Grillner, 1990), whereas γ-aminobutyric acid (GABA) functions as the primary mediator of inhibitory synaptic transmission (Decavel & Van den Pol, 1990). The palisade zone of the hypothalamic median eminence (ME) represents the termination field for hypophysiotropic axons which secrete releasing and release-inhibiting hormones into the pericapillary space of the hypophysial portal system. This region receives a dense GABA-ergic innervation (Meister & Hokfelt, 1988); moreover, the marker enzyme for GABA, glutamic acid decarboxylase, has been localized specifically to growth hormone-releasing hormone (GHRH)-, tyrosine hydroxylase (dopaminergic marker)-, neurotensin- and galanin-immunoreactive (IR), but not to somatostatin (SS)-IR hypophysiotropic axon terminals (Meister & Hokfelt, 1988). The hypothalamus also hosts a large number of glutamatergic cell bodies that express the mRNA for type-2 vesicular glutamate transporter (VGLUT2) selectively (Herzog *et al*., 2001; Takamori *et al*., 2001; Lin *et al*., 2003). A subset of these VGLUT2-IR neurons are located in hypophysiotropic regions and innervate the ME (Lin *et al*., 2003; Varoqui *et al*., 2002); recent studies have shown that glutamatergic fibres of the ME are partly identical with hypophysiotropic gonadotropin-releasing hormone (GnRH; Hrabovszky *et al*., 2004b)-, thyrotropin-releasing hormone (TRH; Hrabovszky *et al*., 2005)- and corticotropin-releasing hormone (CRH; Hrabovszky *et al*., 2005)-IR terminals.

The putative cosecretion of glutamate from additional hypophysiotropic neurosecretory systems, including GHRH and SS neurons, has not been addressed. The synthesis of growth hormone (GH) and its release from the somatotrophs is under the dual control of the stimulatory GHRH and the inhibitory SS; these two peptide neurohormones are synthesized in neuronal perikarya located in the arcuate and the anterior periventricular nuclei (ARH; PVa), respectively (Tannenbaum *et al*., 1990). In the present studies, we used dual-label *in situ* hybridization histochemistry (ISHH) to address the expression of VGLUT2 mRNA in the perikaryon of hypophysiotropic GHRH and/or SS neurons. In addition, we conducted dual-label immunofluorescent studies to investigate VGLUT2 immunoreactivity in GHRH and/or SS axon terminals of the ME. Based on a previous report indicating that hypophysiotropic GHRH neurons might be GABAergic (Meister & Hokfelt, 1988), instead of glutamatergic, we also examined the putative occurrence of the vesicular GABA transporter (VGAT) in GHRH terminals. Although VGAT is used in common for vesicular neurotransmitter uptake by glycinergic and GABAergic inhibitory neurons, it represents an authentic GABA marker within hypophysiotropic GHRH terminals which originate in the ARH, a

Correspondence: Dr Erik Hrabovszky, as above.
E-mail: hrabovszky@koki.hu

Received 21 October 2004, revised 26 January 2005, accepted 2 February 2005

doi:10.1111/j.1460-9568.2005.04076.x

region devoid of glycinergic (Zeilhofer *et al*., 2005) and rich in GABAergic (Meister & Hokfelt, 1988) cell bodies.

Recently, we have used similar *in situ* hybridization and immunocytochemical approaches to demonstrate the occurrence of VGLUT2 mRNA and protein, respectively, in the hypophysiotropic GnRH, TRH and CRH neurosecretory systems (Hrabovszky *et al*., 2004b, 2005).

Materials and methods

Animals

Adult male Wistar rats ($n = 8$; 220–240 g body weight) were purchased from Charles River Hungary Ltd. (Isaszeg, Hungary) and housed in a light- and temperature-controlled environment, with food and water available *ad libitum*. Experimental procedures were approved by the Animal Welfare Committee at the Institute of Experimental Medicine.

In situ *hybridization studies*

Tissue preparation

Four rats were decapitated and their brains snap-frozen on powdered dry ice. Then 12-μm thick coronal sections through the PVa and the ARH regions were cut with a Leica CM 3050 S cryostat, collected serially on gelatin-coated microscope slides and processed for dual-label ISHH studies using procedures adapted from recent work (Hrabovszky *et al*., 2004a). Sections from the PVa were processed for dual-label ISHH detection of SS and VGLUT2 mRNAs, whereas sections from the ARH were used for the simultaneous visualization of GHRH and VGLUT2 mRNAs.

Probe preparation

The preparation of ^{35}S-labelled antisense and sense 'VGLUT2-879' cRNA probes (targeted to bases 522–1400 of rat VGLUT2 mRNA; GenBank Acc. # NM053427) has been detailed elsewhere (Hrabovszky *et al*., 2004b). The 514-bp cDNA template for *in vitro* transcription of a digoxigenin-labelled SS probe to bases 3–516 of the rat somatostatin mRNA (GenBank Acc. # M2589) was cloned with polymerase chain reaction from rat hypothalamic cDNA using the TOPO TA Cloning® kit from Invitrogen (Carlsbad, CA, USA). The plasmid containing the SS amplicon was grown in TOPO cells (Invitrogen), isolated with the QIAfilter Plasmid Maxi kit (Qiagen; Valencia, CA, USA) and digested at the BamHI restriction site. The linearized transcription template was purified with phenol/chloroform/isoamyl alcohol and chloroform/isoamyl alcohol extractions, precipitated with NaCl and ethanol and reconstituted. The digoxigenin-labelled cRNA probe was transcribed with T7 RNA polymerase in the presence of digoxigenin-11-UTP (Roche Diagnostics Co., Indianapolis, IN, USA), as described previously (Petersen & McCrone, 1994; Hrabovszky *et al*., 2004a). A pGEM 4 plasmid containing bases 285–489 of the rat GHRH cDNA (GenBank Acc. # M73486) was kindly provided by Dr R.A. Steiner (University of Washington, Seattle, WA, USA) for the generation of the digoxigenin-labelled antisense GHRH probe. The vector was linearized at the *Eco*RI site and transcribed with T7 RNA polymerase.

Dual-label ISHH

Prehybridization, hybridization and posthybridization procedures have been adapted from similar studies that investigated VGLUT2 mRNA expression by hypophysiotropic GnRH, TRH and CRH neurons (Hrabovszky *et al*., 2004b, 2005). Based on a recently introduced methodological approach (Hrabovszky & Petersen, 2002), hybridization sensitivity for VGLUT2 has been enhanced by applying high radioisotopic probe (80 000 c.p.m./mL), dextran sulphate (25%) and dithiothreitol (1000 mM) concentrations in the hybridization solution and extending the hybridization time from 16 to 40 h. Following posthybridization treatments (Hrabovszky *et al*., 2004a), the digoxigenin-labelled cRNA probe to GHRH or SS mRNA was detected immunocytochemically using sequential incubations with anti-digoxigenin antibodies conjugated to horseradish peroxidase (1 : 200; Roche) for 48 h, biotin tyramide amplification solution for 1 h, and ABC Elite working solution (Vector; Burlingame, CA, USA; 1 : 1000 dilution of solutions 'A' and 'B' in TBS) for 1 h. The signal was visualized with diaminobenzidine chromogen in the peroxidase developer. Subsequently, the ^{35}S-labelled cRNA probe to VGLUT2 mRNA was visualized on Kodak NTB-3 autoradiographic emulsion following 2 weeks of exposure. To confirm VGLUT2 hybridization specificity in positive control experiments, the 'VGLUT2-879' probe was replaced with the 'VGLUT2-734' probe kindly provided by Dr J. P. Herman (Ziegler *et al*., 2002; Hrabovszky *et al*., 2004b, 2005), targeting a nonoverlapping segment (bases 1704–2437) of VGLUT2 mRNA. Negative control experiments for VGLUT2 hybridization specificity (Hrabovszky *et al*., 2004b, 2005) were conducted with the combined use of the nonisotopic antisense SS probe and the radioisotopically labelled sense-strand VGLUT2-879 transcript.

Dual-label immunofluorescent studies of VGLUT2 in GHRH and SS axons

To analyse the putative occurrence of VGLUT2 immunoreactivity in hypophysiotropic GHRH and SS axons, four rats were anaesthetized with pentobarbital (35 mg/kg body weight, i.p.) and perfused transcardially with 150 mL fixative solution containing 2% paraformaldehyde (Sigma Chemical Co., St. Louis, MO, USA) and 4% acrolein (Aldrich Chemical Co., Milwaukee, WI, USA) in 0.1 M phosphate-buffered saline (PBS; pH 7.4). Tissue blocks were dissected out and infiltrated with 25% sucrose overnight. Then 20-μm-thick free-floating coronal sections were prepared through the mediobasal hypothalami with a cryostat. The sections were rinsed in Tris-buffered saline (TBS; 0.1 M Tris-HCl/0.9% NaCl; pH 7.8). Free aldehydes were inactivated with 0.5% sodium borohydride (Sigma; 30 min) and the tissues permeabilized and blocked against nonspecific antibody binding with a mixture of 0.2% Triton X-100 (Sigma) and 2% normal horse serum in TBS (30 min). Following pretreatments, two-thirds of the sections were incubated in anti-VGLUT2 primary antibodies raised in guinea pig (AB 5907; Chemicon; Temecula, CA, USA; 1 : 1000) for 72 h at 4 °C, then in biotinylated anti-guinea pig IgG (Jackson ImmunoResearch Laboratories, West Grove, PA, USA; 1 : 1000) for 2 h, and in streptavidine-conjugated Cy3 fluorochrome (Jackson ImmunoResearch; 1 : 200) for 12 h. Half of these sections were used to detect GHRH using sheep primary antibodies (FMS/FJL #19–4; 1 : 30 000; kind gift from Dr I. Merchenthaler; University of Maryland, School of Medicine, Baltimore, MD, USA). This antiserum was applied to the sections for 48 h at 4 °C and then, reacted with FITC-conjugated antisheep IgG (Jackson ImmunoResearch; 1 : 200) for 12 h at room temperature. The second pool of ME sections already immunostained for VGLUT2 was used for the detection of SS-IR neuronal elements. The SS antiserum (a kind gift from Dr A. J. Harmar, School of Biomedical and Clinical Laboratory Sciences, Edinburgh, UK) was generated in rabbit (R12, 1 : 4000) and recognized both the SS14 and SS28 molecular forms of SS (Pierotti

& Harmar, 1985). The primary antibodies were applied to the sections for 48 h at 4 °C and then reacted with FITC-conjugated anti-rabbit IgG (Jackson ImmunoResearch, 1 : 200) for 12 h at 4 °C. The remaining third of the mediobasal hypothalamic sections was used in control experiments and in dual-labelling studies to localize VGAT in the axon terminals of GHRH neurons. The dual-immunofluorescent procedure, used to demonstrate the GABAergic marker in GHRH terminals, was performed as described above for the VGLUT2/GHRH double-labelling, except by substituting the VGLUT2 antibodies with VGAT antibodies that were also raised in a guinea pig (AB5855; Chemicon; 1 : 2000). The fluorescently labelled specimen was examined with a Radiance 2100 confocal microscope (Bio-Rad Laboratories, Hemel Hempstead, UK) using laser excitation lines 488 nm for FITC and 543 nm for Cy3 and dichroic/emission filters 560 nm/500–530 nm for FITC and 560–610 nm for Cy3. Individual optical slices were collected for the analysis in 'lambda strobing' mode. This way, only one excitation laser and the corresponding emission detector were active during a line scan, to eliminate emission crosstalk.

Colocalization was assessed using a 60 × objective lens with immersion oil and an optimized pinhole, allowing optical slices below 0.7 μm (Hrabovszky *et al*., 2004b, 2005). Control experiments to prove the specificity of VGLUT2 immunolabelling included preabsorption of primary antibodies with 10 μM of the immunization antigen (AG209; Chemicon). In addition, the AB5907 guinea pig anti-VGLUT2 antibodies from Chemicon were used in combination with the rabbit anti-VGLUT2 antibodies from SYnaptic SYstems (AB 135103; 1 : 5000; Göttingen, Germany) in dual-immunofluorescent experiments. The primary antibodies raised in different species were reacted with secondary antibody-fluorochrome conjugates, which resulted in dual-immunofluorescent labelling of identical axonal profiles (Hrabovszky *et al*., 2004b, 2005).

Results

In situ *hybridization results*

The nonisotopic ISHH procedure visualized numerous GHRH mRNA-expressing neurons in the ARH (Fig. 1A) and SS mRNA-expressing neurons in the PVa (Fig. 1B). The development of emulsion autoradiographs exposed for 2 weeks resulted in the heavy accumulation of grain clusters in several diencephalic nuclei, including the ventromedial hypothalamic nucleus (VMH; Fig. 1A) and the PVa (Fig. 1B). The ARH contained only few VGLUT2 neurons, most of which were localized laterally within the nucleus. These glutamatergic cells were labelled lightly or moderately and their distribution overlapped with the area also containing GHRH neurons. Nevertheless, microscopic analysis of every third section through the rostrocaudal extent of the ARH of each of four rats found no evidence for the coexpression of GHRH and VGLUT2 mRNAs at this level of detection sensitivity (Fig. 1A). In contrast, silver grain clusters clearly distinct from the homogeneous background grains were associated with most SS neurons in the PVa (Fig. 1B). The analysis of 787 SS neurons (from two representative PVa sections of each of four rats) showed hybridization signal (accumulation of silver grains) for VGLUT2 mRNA in 97.5 ± 0.4% of SS neurons. The periventricular and medial parvicellular (high-power inset in Fig. 1B) subdivisions of the paraventricular nucleus (PVH) contained a further large population of SS neurons. Of 688 neurons analysed in these subnuclei (from two PVH sections of each of four rats), 96.0 ± 1.4% were clearly dual-labelled. The series of sections hybridized for SS and VGLUT2 mRNAs also included additional populations of SS neurons in the suprachiasmatic nucleus and the rostral-most part of the ARH. No VGLUT2 hybridization signal was associated with these nonhypophysiotropic SS neurons. Detection of dual-labelled SS neurons using a distinct VGLUT2 probe ('VGLUT2-734') and lack of autoradiographic signal (grain clustering) using the sense VGLUT2 transcipt provided evidence for hybridization specificity, corroborating the results of previously used control experiments (Hrabovszky *et al*., 2004b, 2005).

Immunocytochemical results

The immunocytochemical studies detected a high density of glutamatergic axons in the external zone of the ME (Fig. 1C and E); here the glutamatergic axons intermingled with peptidergic terminals containing GHRH (Fig. 1C) and SS (Fig. 1E). High-power confocal microscopic analysis found no evidence for a colocalization of VGLUT2 and GHRH immunoreactivities (Fig. 1C), whereas the GHRH terminals often contained immunoreactivity for the GABAergic marker, VGAT (Fig. 1D). In contrast with the absence of VGLUT2 from GHRH-IR axons, many of the SS-IR terminals contained VGLUT2 immunoreactivity (Fig. 1E), in accordance with the ISHH observation of VGLUT2 mRNA synthesis in SS perikarya of the PVa and the PVH. Omission of primary antibodies eliminated all labelling from the ME. Additional controls studies detailed elsewhere (Hrabovszky *et al*., 2004b, 2005) confirmed specificity of the immunocytochemical labelling for the VGLUT2 protein.

Discussion

In this report we present ISHH and immunocytochemical evidence that GHRH neurons, unlike neurons of the hypophysiotropic GnRH, TRH and CRH systems, do not appear to synthesize VGLUT2 mRNA and protein; instead, we found that their neurosecretory terminals contain immunoreactivity for the GABAergic marker, VGAT. In contrast with GHRH neurons, nearly all of the cell bodies of hypophysiotropic SS neurons in the PVa and in the medial parvicellular subdivision of the PVH express VGLUT2 mRNA and their projections to the ME contain immunoreactivity for VGLUT2. These observations indicate the capability of the inhibitory SS neurosecretory system to cosecrete the excitatory amino acid neurotransmitter, L-glutamate.

Glutamate is an important regulator of anterior pituitary functions, including regulation of GH synthesis and secretion (Brann, 1995). Subcutaneous *N*-methyl-DL-aspartic acid or kainate injections to adult male rats increases serum GH levels (Mason *et al*., 1983) and similar stimulatory effects have also been observed in other species (Estienne *et al*., 1989; Shahab *et al*., 1993). Some of the actions of glutamate on the somatotropic axis may also be exerted at the hypophysial level. Ionotropic and metabotropic glutamate receptors are expressed by anterior pituitary cells (Bhat *et al*., 1995; Caruso *et al*., 2004) and *N*-methyl-D-aspartic acid (NMDA), kainate and glutamate can stimulate dose-dependently GH secretion from perifused somatotrophs (Lindstrom & Ohlsson, 1992; Niimi *et al*., 1994). Several lines of evidence also indicate that glutamate exerts central actions on GH secretion in which GHRH neurons play a crucial role. In accordance with this idea, the *N*-methyl-D,L-aspartic acid-induced GH release can be blocked by antibodies to GHRH or prevented by the ablation of the ARH where the hypophysiotropic GHRH neurons reside (Acs *et al*., 1990). In further support of the concept that endogenous glutamate stimulates the GHRH neurosecretory system, systemic treatment of rats with an NMDA receptor antagonist can reduce hypothalamic

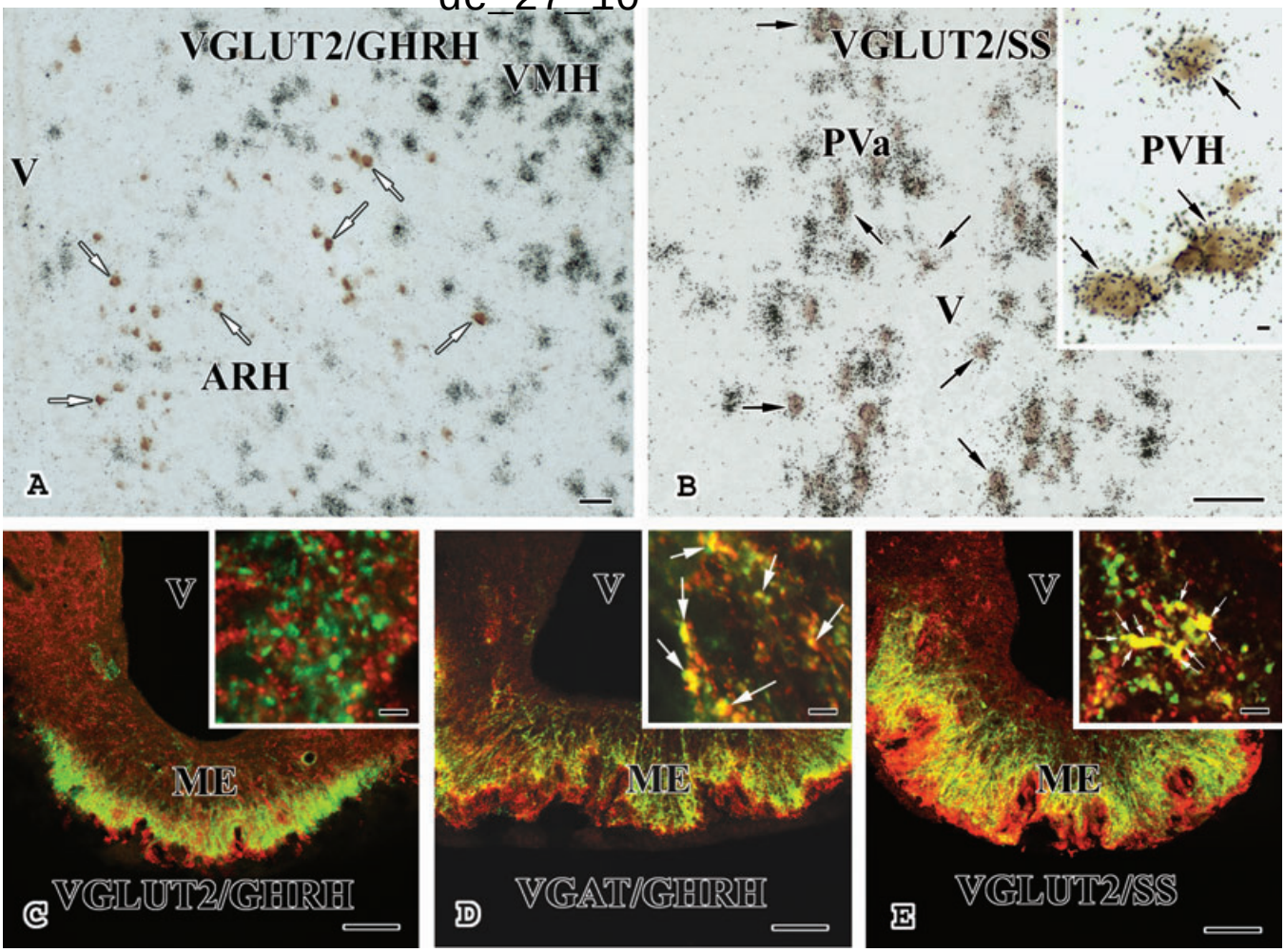

FIG. 1. Morphological evidence for the the glutamatergic phenotype of somatostatine (SS) secreting and the GABA-ergic phenotype of growth hormone-releasing hormone (GHRH) secreting hypophysiotropic neurons. (A) Results of dual-label *in situ* hybridization studies show heavy expression levels of VGLUT2 mRNA (autoradiographic grain clusters) in the ventromedial hypothalamic nucleus (VMH), whereas the arcuate nucleus (ARH) comprising hypophysiotropic GHRH neurons (brown DAB chromogen) contains relatively few and lightly labelled glutamatergic neurons. The GHRH cells (white arrows) are devoid of the autoradiographic hybridization signal for VGLUT2 mRNA. (B) The anterior periventricular nucleus (PVa) shows high levels of VGLUT2 mRNA expression on the two sides of the third cerebral ventricle (V). Virtually all hypophysiotropic somatostatin (SS) neurons (brown DAB chromogen) in this nucleus as well as in the medial parvicellular subdivision of the hypothalamic paraventricular nucleus (PVH; high-power inset) express VGLUT2 mRNA, as indicated by the presence of silver grain clusters. Black arrows point to dual-labelled SS neurons. (C) Confocal laser microscopic analysis of the median eminence (ME) shows the overlapping distribution of GHRH-immunoreactive (IR; green colour) and VGLUT2-IR (red colour) terminals in the external layer of the ME. High-power image (inset in right upper corner) of a 0.45-μm single optical slice demonstrates that VGLUT2 fibres are distinct from GHRH fibres. (D) In contrast, the vesicular GABA transporter (VGAT; red colour), used as a GABAergic marker, is often detectable in GHRH-IR axons (green colour). Arrows in high-power inset point to dual-labelled VGAT/GHRH axon varicosities (yellow colour). (E) Somatostatin-IR terminals (green colour) in the external layer of the ME exhibit an overlapping distribution with that of VGLUT2-IR (red colour) terminals. Arrows in high-power inset reveal that SS terminals cocontain immunoreactivity for VGLUT2 (yellow colour). Scale bars, 5 μm (B–E insets); 50 μm (other panels).

GHRH mRNA expression in the ARH and GHRH immunoreactivity in the ME (Cocilovo *et al*., 1992).

The central glutamatergic regulation of different neurosecretory systems, including GHRH and SS neurons, likely involves synaptic mechanisms. In addition, the dense VGLUT2-IR axon plexus observed recently in the external zone of the ME (Lin *et al*., 2003; Hrabovszky *et al*., 2004b, 2005) also raises the possibility that central glutamatergic pathways may directly act on the axon terminals of hypophysiotropic neurons. Confocal microscopic studies of the ME have revealed that many of these glutamatergic fibres are identical with the neurosecretory terminals of GnRH, TRH and CRH neurons (Hrabovszky *et al*., 2004b, 2005). To pursue the neurochemical characterization of glutamatergic axons in the ME, in the present study we investigated the putative occurrence of VGLUT2 in hypophysiotropic GHRH and SS neurons. The results of ISHH and immunocytochemical experiments established that, of these two systems, SS but not GHRH neurons are glutamatergic.

The functional importance of endogenous glutamate release from distinct types of hypophysiotropic neurosecretory systems will be difficult to determine. We found that at least four neuropeptidergic phenotypes (GnRH, TRH, CRH and SS) contribute to glutamate release in the ME and experimental tools are currently unavailable to separately manipulate the excitatory amino acid output from each of these systems. From a functional point of view, it seems more likely that glutamate acts locally in the ME, rather than influencing adenohypophysial cells as a hypophysiotropic factor. The findings that glutamatergic agents increase plasma ACTH levels *in vivo* (Makara & Stark, 1975; Farah *et al*., 1991; Jezova *et al*., 1991;

dc_27_10

Chautard *et al*., 1993) but do not elicit ACTH release from incubated pituitaries (Chautard *et al*., 1993), indicate that hypophysial actions do not play a major role in the glutamatergic regulation of the adrenal axis. There is evidence that central effects also dominate in the glutamatergic regulation of the gonadotropic axis; glutamate can elevate serum luteinizing hormone levels when injected into the third cerebral ventricle (Ondo *et al*., 1976), whereas neither its hypophysial injection (Ondo *et al*., 1976) nor its *in vitro* application to pituitary culture (Tal *et al*., 1983) can stimulate luteinizing hormone secretion. Despite the existing evidence that glutamate can act directly on somatotrophs (Lindstrom & Ohlsson, 1992; Niimi *et al*., 1994), its central actions through GHRH neurons appear to be dominant (Acs *et al*., 1990).

The target cells to the actions of glutamate in the ME and the receptorial mechanisms involved, are unclear. It is reasonable to speculate that the release of endogenous glutamate exerts autocrine actions or paracrine effects on hypophysiotropic neurosecretory axon terminals. The existence of autocrine/paracrine glutamatergic mechanisms in the central regulation of GnRH secretion received substantial support from: (i) the capability of ionotropic glutamate receptor agonists to elicit GnRH release from the mediobasal hypothalami (Donoso *et al*., 1990; Lopez *et al*., 1992; Arias *et al*., 1993; Zuo *et al*., 1996; Kawakami *et al*., 1998a); (ii) the identification of immunoreactivity for the KA2 and the NR1 ionotropic glutamate receptor subunits on GnRH terminals (Kawakami *et al*., 1998a, b); and (iii), our recent observation that GnRH neurons contain VGLUT2, an indication for glutamate release from endogenous stores (Hrabovszky *et al*., 2004b). However, the putative presence and actions of glutamate receptors on SS containing and other types of neuroendocrine terminals remain to be established. Glutamate might also affect the glial and endothelial cell functions in the microenvironment of release. In strong support of this idea, tanycytes lining the ventral wall of the third ventricle and astrocytes in the ME were found to contain mRNAs and immunoreactivity for kainate receptors (Diano *et al*., 1998; Eyigor & Jennes, 1998; Kawakami, 2000) and to express c-Fos immunoreactivity in response to stimulation by kainate (Eyigor & Jennes, 1998). Although somewhat controversial (Morley *et al*., 1998), evidence also exists for the presence of functional metabotropic (Krizbai *et al*., 1998; Gillard *et al*., 2003) and ionotropic (Krizbai *et al*., 1998; Parfenova *et al*., 2003) glutamate receptors on cerebral microvascular endothelial cells. Endothelial cells in the ME have been implicated in the generation of nitric oxide (Aguan *et al*., 1996; Prevot *et al*., 2000) which is an important regulator of GnRH and CRH release from the ME (Prevot *et al*., 2000). The stimulation of NMDA receptors within the ME, indeed, increases nitric oxide production (Bhat *et al*., 1998). It is interesting to note that the glutamate-induced release of GnRH from mediobasal hypothalami can be blocked by a nitric oxid synthase inhibitor or a nitric oxide scavenger (Rettori *et al*., 1994). The proposed mechanism whereby nitric oxide elicits CRH and GnRH release is by increasing the cGMP and/or prostaglandin E2 production within hypophysiotropic axon terminals (Prevot *et al*., 2000). Nevertheless, the putative involvement of endothelial cells and nitric oxide specifically in the regulation of GHRH and SS release need to be investigated.

In accordance with the earlier observation of glutamic acid decarboxylase immunoreactivity in GHRH terminals (Meister & Hokfelt, 1988), the present confocal microscopic studies identified another GABA marker, VGAT, in GHRH axons. The putative sites of action of tuberoinfundibular GABA, secreted primarily by GHRH and dopaminergic terminals (Meister & Hokfelt, 1988), can be the anterior pituitary as well as the ME. Corroborating the hypophysial actions of GABA, GABA A receptors have been identified on anterior pituitary cells (Berman *et al*., 1994). In addition, somatotrophs and lactotrophs, but no other types of adenohypophysial cells, are capable of internalizing [^{3}H]GABA through mechanisms that are currently unknown (Duvilanski *et al*., 2000). Somewhat contradicting the idea that the secreted GABA regulates the anterior pituitary is the finding that GABA levels are not higher in the hypophysial portal vs. the peripheral blood (Mulchahey & Neill, 1982). Therefore, GABA released from hypophysiotropic GHRH terminals may also act primarily at the level of the ME, as we propose for glutamate. In case of both glutamate and GABA, morphological studies will need to clear whether or not, they have autoreceptors on glutamatergic and GABAergic axon terminals, respectively. Alternatively, if GABA receptors occur on glutamatergic terminals and reversely, glutamate receptors occur on GABAergic terminals in the ME, the amino acid cotransmitters could also be involved in a crosstalk among neurosecretory terminals of different amino acid phenotypes.

It is tempting to speculate that the endogenous glutamate content of GnRH, TRH, CRH and SS axon terminals contributes to the synchronized neurohormone output from individual axon terminals, a prerequisite for pulsatile neurohormone secretion. In support of this concept, the blockade of NMDA receptors is capable of abolishing the endogenous pulsatility of GnRH secretion from incubated mediobasal hypothalami (Bourguignon *et al*., 1989). The lack of glutamate from GHRH neurons that also secrete episodically (Nakamura *et al*., 2003) somewhat complicates this hypothesis, although it is possible that glutamatergic signals originating from other types of terminals are involved in generating GHRH secretory pulses. Although this concept requires experimental support, the synchronization in the patterned release of SS and GHRH clearly appears to exist. Recent *in vivo* studies of female monkeys using push–pull perfusion of the stalk–ME complex identified that the majority of GHRH secretory pulses either coincide with SS peaks or occur simultaneously with the SS troughs (Nakamura *et al*., 2003). Finally, although these ISHH and immunocytochemical data reveal a clear difference between hypophysiotropic SS and GHRH neurons in their VGLUT2 content, the possibility should be recognized that GHRH neurons may contain low levels of VGLUT2 which remained undetected in the present studies.

In summary, in the present ISHH and immunocytochemical studies we provide evidence that the neurons of the hypophysiotropic SS system, similarly to GnRH, TRH and CRH neurons, express the mRNA and immunoreactivity for the glutamatergic marker, VGLUT2. Whereas GHRH-secreting neurons appeared to lack VGLUT2, their axon terminals contained the GABAergic marker VGAT. Together, these results suggest the paradoxic cosecretion of the inhibitory amino acid neurotransmitter GABA with the stimulatory peptide releasing hormone GHRH, and the cosecretion of the excitatory amino acid neurotransmitter glutamate with the inhibitory peptide SS. The physiological significance of endogenous amino acid neurotransmitter cosecretion from these hypophysiotropic neuronal systems, as well as from others, requires clarification.

Acknowledgements

This research was supported by grants from the National Science Foundation of Hungary (OTKA T43407, T46574), the Ministry of Education (OMFB-01806/2002) and the EU FP6 funding (contract no. LSHM-CT-2003–503041). This publication reflects the author's views and not necessarily those of the EU. The information in this document is provided as is and no guarantee of warranty is given that the information is fit for any particular purpose. The user thereof uses the information at its sole risk and liability. The authors are grateful

to Drs J. P. Herman and R. A. Steiner for providing their VGLUT2 and GHRH cDNAs, respectively, to Dr I. Merchenthaler for the GHRH antibodies, to Dr A. J. Harmar for the SS antiserum and to Gyöngyi Kékesi for the excellent technical assistance.

Abbreviations

ARH, arcuate nucleus of the hypothalamus; CRH, corticotropin-releasing hormone; GABA, γ-aminobutyric acid; GH, growth hormone; GHRH, growth hormone-releasing hormone; GnRH, gonadotropin-releasing hormone; mRNA, messenger ribonucleic acid; ME, median eminence; IR, immunoreactive; ISHH, *in situ* hybridization histochemistry; NMDA, *N*-methyl-D-aspartic acid; SS, somatostatin; PVa, anterior periventricular nucleus of the hypothalamus; PVH, paraventricular nucleus of the hypothalamus; TBS, Tris-buffered saline; TRH, thyrotropin-releasing hormone; VGAT, vesicular GABA transporter; VGLUT2, type 2 vesicular glutamate transporter; VMH, ventromedial nucleus of the hypothalamus.

References

Acs, Z., Lonart, G. & Makara, G.B. (1990) Role of hypothalamic factors (growth-hormone-releasing hormone and gamma-aminobutyric acid) in the regulation of growth hormone secretion in the neonatal and adult rat. *Neuroendocrinology*, **52**, 156–160.

Aguan, K., Mahesh, V.B., Ping, L., Bhat, G. & Brann, D.W. (1996) Evidence for a physiological role for nitric oxide in the regulation of the LH surge: effect of central administration of antisense oligonucleotides to nitric oxide synthase. *Neuroendocrinology*, **64**, 449–455.

Arias, P., Jarry, H., Leonhardt, S., Moguilevsky, J.A. & Wuttke, W. (1993) Estradiol modulates the LH release response to N-methyl-D-aspartate in adult female rats: studies on hypothalamic luteinizing hormone-releasing hormone and neurotransmitter release. *Neuroendocrinology*, **57**, 710–715.

Berman, J.A., Roberts, J.L. & Pritchett, D.B. (1994) Molecular and pharmacological characterization of GABAA receptors in the rat pituitary. *J. Neurochem.*, **63**, 1948–1954.

Bhat, G.K., Mahesh, V.B., Chu, Z.W., Chorich, L.P., Zamorano, P.L. & Brann, D.W. (1995) Localization of the N-methyl-D-aspartate R1 receptor subunit in specific anterior pituitary hormone cell types of the female rat. *Neuroendocrinology*, **62**, 178–186.

Bhat, G.K., Mahesh, V.B., Ping, L., Chorich, L., Wiedmeier, V.T. & Brann, D.W. (1998) Opioid-glutamate-nitric oxide connection in the regulation of luteinizing hormone secretion in the rat. *Endocrinology*, **139**, 955–960.

Bourguignon, J.P., Gerard, A., Mathieu, J., Simons, J. & Franchimont, P. (1989) Pulsatile release of gonadotropin-releasing hormone from hypothalamic explants is restrained by blockade of N-methyl-D,1-aspartate receptors. *Endocrinology*, **125**, 1090–1096.

Brann, D.W. (1995) Glutamate: a major excitatory transmitter in neuroendocrine regulation. *Neuroendocrinology*, **61**, 213–225.

Caruso, C., Bottino, M.C., Pampillo, M., Pisera, D., Jaita, G., Duvilanski, B., Seilicovich, A. & Lasaga, M. (2004) Glutamate Induces Apoptosis in Anterior Pituitary Cells through Group II Metabotropic Glutamate Receptor Activation. *Endocrinology*, **145**, 4677–4684.

Chautard, T., Boudouresque, F., Guillaume, V. & Oliver, C. (1993) Effect of excitatory amino acid on the hypothalamo-pituitary-adrenal axis in the rat during the stress-hyporesponsive period. *Neuroendocrinology*, **57**, 70–78.

Cocilovo, L., de Gennaro Colonna, V., Zoli, M., Biagini, G., Settembrini, B.P., Muller, E.E. & Cocchi, D. (1992) Central mechanisms subserving the impaired growth hormone secretion induced by persistent blockade of NMDA receptors in immature male rats. *Neuroendocrinology*, **55**, 416–421.

Collingridge, G.L. & Singer, W. (1990) Excitatory amino acid receptors and synaptic plasticity. *Trends Pharmacol. Sci.*, **11**, 290–296.

Decavel, C. & Van den Pol, A.N. (1990) GABA: a dominant neurotransmitter in the hypothalamus. *J. Comp. Neurol.*, **302**, 1019–1037.

Diano, S., Naftolin, F. & Horvath, T.L. (1998) Kainate glutamate receptors (GluR5–7) in the rat arcuate nucleus: relationship to tanycytes, astrocytes, neurons and gonadal steroid receptors. *J. Neuroendocrinol.*, **10**, 239–247.

Donoso, A.O., Lopez, F.J. & Negro-Vilar, A. (1990) Glutamate receptors of the non-N-methyl-D-aspartic acid type mediate the increase in luteinizing hormone-releasing hormone release by excitatory amino acids in vitro. *Endocrinology*, **126**, 414–420.

Duvilanski, B.H., Perez, R., Seilicovich, A., Lasaga, M., Diaz, M.C. & Debeljuk, L. (2000) Intracellular distribution of GABA in the rat anterior pituitary. An electron microscopic autoradiographic study. *Tissue Cell*, **32**, 284–292.

Estienne, M.J., Schillo, K.K., Green, M.A., Hileman, S.M. & Boling, J.A. (1989) N-methyl-d, l-aspartate stimulates growth hormone but not luteinizing hormone secretion in the sheep. *Life Sci.*, **44**, 1527–1533.

Eyigor, O. & Jennes, L. (1998) Identification of kainate-preferring glutamate receptor subunit GluR7 mRNA and protein in the rat median eminence. *Brain Res.*, **814**, 231–235.

Farah, J.M. Jr, Rao, T.S., Mick, S.J., Coyne, K.E. & Iyengar, S. (1991) N-methyl-D-aspartate treatment increases circulating adrenocorticotropin and luteinizing hormone in the rat. *Endocrinology*, **128**, 1875–1880.

Gillard, S.E., Tzaferis, J., Tsui, H.C. & Kingston, A.E. (2003) Expression of metabotropic glutamate receptors in rat meningeal and brain microvasculature and choroid plexus. *J. Comp. Neurol.*, **461**, 317–332.

Headley, P.M. & Grillner, S. (1990) Excitatory amino acids and synaptic transmission: the evidence for a physiological function. *Trends Pharmacol. Sci.*, **11**, 205–211.

Herzog, E., Bellenchi, G.C., Gras, C., Bernard, V., Ravassard, P., Bedet, C., Gasnier, B., Giros, B. & El Mestikawy, S. (2001) The existence of a second vesicular glutamate transporter specifies subpopulations of glutamatergic neurons. *J. Neurosci.*, **21**, RC181.

Hrabovszky, E., Kallo, I., Steinhauser, A., Merchenthaler, I., Coen, C.W. & Liposits, Z. (2004a) Estrogen receptor-beta in oxytocin and vasopressin neurons of the rat and human hypothalamus. Immunocytochemical and in situ hybridization studies. *J. Comp. Neurol.*, **473**, 315–333.

Hrabovszky, E. & Petersen, S.L. (2002) Increased concentrations of radioisotopically-labeled complementary ribonucleic acid probe, dextran sulfate, and dithiothreitol in the hybridization buffer can improve results of in situ hybridization histochemistry. *J. Histochem. Cytochem.*, **50**, 1389–1400.

Hrabovszky, E., Turi, G.F., Kallo, I. & Liposits, Z. (2004b) Expression of vesicular glutamate transporter-2 in gonadotropin-releasing hormone neurons of the adult male rat. *Endocrinology*, **145**, 4018–4021.

Hrabovszky, E., Wittmann, G., Túri, F.G., Liposits, Z. & Fekete, C. (2005) Hypophysiotropic thyrotropin-releasing hormone and corticotropin-releasing hormone neurons of the rat contain vesicular glutamate transporter-2. *Endocrinology*, **146**, 346–347.

Jezova, D., Oliver, C. & Jurcovicova, J. (1991) Stimulation of adrenocorticotropin but not prolactin and catecholamine release by N-methyl-aspartic acid. *Neuroendocrinology*, **54**, 488–492.

Kawakami, S. (2000) Glial and neuronal localization of ionotropic glutamate receptor subunit-immunoreactivities in the median eminence of female rats: GluR2/3 and GluR6/7 colocalize with vimentin, not with glial fibrillary acidic protein (GFAP). *Brain Res.*, **858**, 198–204.

Kawakami, S.I., Hirunagi, K., Ichikawa, M., Tsukamura, H. & Maeda, K.I. (1998b) Evidence for terminal regulation of GnRH release by excitatory amino acids in the median eminence in female rats: a dual immunoelectron microscopic study. *Endocrinology*, **139**, 1458–1461.

Kawakami, S., Ichikawa, M., Murahashi, K., Hirunagi, K., Tsukamura, H. & Maeda, K. (1998a) Excitatory amino acids act on the median eminence nerve terminals to induce gonadotropin-releasing hormone release in female rats. *Gen. Comp. Endocrinol.*, **112**, 372–382.

Krizbai, I.A., Deli, M.A., Pestenacz, A., Siklos, L., Szabo, C.A., Andras, I. & Joo, F. (1998) Expression of glutamate receptors on cultured cerebral endothelial cells. *J. Neurosci. Res.*, **54**, 814–819.

Lin, W., McKinney, K., Liu, L., Lakhlani, S. & Jennes, L. (2003) Distribution of vesicular glutamate transporter-2 messenger ribonucleic Acid and protein in the septum-hypothalamus of the rat. *Endocrinology*, **144**, 662–670.

Lindstrom, P. & Ohlsson, L. (1992) Effect of N-methyl-D,1-aspartate on isolated rat somatotrophs. *Endocrinology*, **131**, 1903–1907.

Lopez, F.J., Donoso, A.O. & Negro-Vilar, A. (1992) Endogenous excitatory amino acids and glutamate receptor subtypes involved in the control of hypothalamic luteinizing hormone-releasing hormone secretion. *Endocrinology*, **130**, 1986–1992.

Makara, G.B. & Stark, E. (1975) Effect of intraventricular glutamate on ACTH release. *Neuroendocrinology*, **18**, 213–216.

Mason, G.A., Bissette, G. & Nemeroff, C.B. (1983) Effects of excitotoxic amino acids on pituitary hormone secretion in the rat. *Brain Res.*, **289**, 366–369.

Meister, B. & Hokfelt, T. (1988) Peptide- and transmitter-containing neurons in the mediobasal hypothalamus and their relation to GABAergic systems: possible roles in control of prolactin and growth hormone secretion. *Synapse*, **2**, 585–605.

Monaghan, D.T., Bridges, R.J. & Cotman, C.W. (1989) The excitatory amino acid receptors: their classes, pharmacology, and distinct properties in the

function of the central nervous system. *Annu. Rev. Pharmacol. Toxicol.*, **29**, 365–402.

Morley, P., Small, D.L., Murray, C.L., Mealing, G.A., Poulter, M.O., Durkin, J.P. & Stanimirovic, D.B. (1998) Evidence that functional glutamate receptors are not expressed on rat or human cerebromicrovascular endothelial cells. *J. Cereb. Blood Flow Metab.*, **18**, 396–406.

Mulchahey, J.J. & Neill, J.D. (1982) Gamma amino butyric acid (GABA) levels in hypophyseal stalk plasma of rats. *Life Sci.*, **31**, 453–456.

Nakamura, S., Mizuno, M., Katakami, H., Gore, A.C. & Terasawa, E. (2003) Aging-related changes in in vivo release of growth hormone-releasing hormone and somatostatin from the stalk-median eminence in female rhesus monkeys (Macaca mulatta). *J. Clin. Endocrinol. Metab.*, **88**, 827–833.

Niimi, M., Sato, M., Murao, K., Takahara, J. & Kawanishi, K. (1994) Effect of excitatory amino acid receptor agonists on secretion of growth hormone as assessed by the reverse hemolytic plaque assay. *Neuroendocrinology*, **60**, 173–178.

Ondo, J.G., Pass, K.A. & Baldwin, R. (1976) The effects of neurally active amino acids on pituitary gonadotropin secretion. *Neuroendocrinology*, **21**, 79–87.

Parfenova, H., Fedinec, A. & Leffler, C.W. (2003) Ionotropic glutamate receptors in cerebral microvascular endothelium are functionally linked to heme oxygenase. *J. Cereb. Blood Flow Metab.*, **23**, 190–197.

Petersen, S. & McCrone, S. (1994) Characterization of the receptor complement of individual neurons using dual-label in situ hybridization histochemistry. In: Eberwine, J.H., Valentino, K. & Barchas, J. (eds) *In Situ Hybridization in Neurobiology. Advances in Methodology.* Oxford University Press, New York, pp. 78–94.

Pierotti, A.R. & Harmar, A.J. (1985) Multiple forms of somatostatin-like immunoreactivity in the hypothalamus and amygdala of the rat: selective localization of somatostatin-28 in the median eminence. *J. Endocrinol.*, **105**, 383–389.

Prevot, V., Bouret, S., Stefano, G.B. & Beauvillain, J. (2000) Median eminence nitric oxide signaling. *Brain Res. Brain Res. Rev.*, **34**, 27–41.

Rettori, V., Kamat, A. & McCann, S.M. (1994) Nitric oxide mediates the stimulation of luteinizing-hormone releasing hormone release induced by glutamic acid in vitro. *Brain Res. Bull.*, **33**, 501–503.

Shahab, M., Nusser, K.D., Griel, L.C. & Deaver, D.R. (1993) Effect of a single intravenous injection of N-methyl-D,1-aspartic acid on secretion of luteinizing hormone and growth hormone in Holstein bull calves. *J. Neuroendocrinol.*, **5**, 469–473.

Takamori, S., Rhee, J.S., Rosenmund, C. & Jahn, R. (2001) Identification of differentiation-associated brain-specific phosphate transporter as a second vesicular glutamate transporter (VGLUT2). *J. Neurosci.*, **21**, RC182.

Tal, J., Price, M.T. & Olney, J.W. (1983) Neuroactive amino acids influence gonadotrophin output by a suprapituitary mechanism in either rodents or primates. *Brain Res.*, **273**, 179–182.

Tannenbaum, G.S., Painson, J.C., Lapointe, M., Gurd, W. & McCarthy, G.F. (1990) Interplay of somatostatin and growth hormone-releasing hormone in genesis of episodic growth hormone secretion. *Metabolism*, **39**, 35–39.

Varoqui, H., Schafer, M.K., Zhu, H., Weihe, E. & Erickson, J.D. (2002) Identification of the differentiation-associated Na+/PI transporter as a novel vesicular glutamate transporter expressed in a distinct set of glutamatergic synapses. *J. Neurosci.*, **22**, 142–155.

Zeilhofer, H.U., Studler, B., Arabadzisz, D., Schweizer, C., Ahmadi, S., Layh, B., Bosl, M.R. & Fritschy, J.M. (2005) Glycinergic neurons expressing enhanced green fluorescent protein in bacterial artificial chromosome transgenic mice. *J. Comp. Neurol.*, **482**, 123–141.

Ziegler, D.R., Cullinan, W.E. & Herman, J.P. (2002) Distribution of vesicular glutamate transporter mRNA in rat hypothalamus. *J. Comp. Neurol.*, **448**, 217–229.

Zuo, Z., Mahesh, V.B., Zamorano, P.L. & Brann, D.W. (1996) Decreased gonadotropin-releasing hormone neurosecretory response to glutamate agonists in middle-aged female rats on proestrus afternoon: a possible role in reproductive aging? *Endocrinology*, **137**, 2334–2338.

dc_27_10

10. számú melléklet

Available online at www.sciencedirect.com
SCIENCE DIRECT®
Neurochemistry International 48 (2006) 753–761
NEUROCHEMISTRY International
www.elsevier.com/locate/neuint

Localization and osmotic regulation of vesicular glutamate transporter-2 in magnocellular neurons of the rat hypothalamus

E. Hrabovszky [a,*], Á.K. Csapó [a], I. Kalló [a,b], T. Wilheim [a], G.F. Túri [a], Zs. Liposits [a,b]

[a] *Laboratory of Endocrine Neurobiology, Institute of Experimental Medicine, Hungarian Academy of Sciences, Szigony u. 43, Budapest 1083, Hungary*
[b] *Department of Neuroscience, Faculty of Information Technology, Péter Pázmány Catholic University, Budapest, Hungary*

Received 8 November 2005; accepted 21 December 2005
Available online 14 February 2006

Abstract

In this report we present immunocytochemical and in situ hybridization evidence that magnocellular vasopressin and oxytocin neurons in the hypothalamic supraoptic and paraventricular nuclei express type-2 vesicular glutamate transporter, a marker for their glutamatergic neuronal phenotype. To address the issue of whether an increase in magnocellular neuron activity coincides with the altered synthesis of the endogenous glutamate marker, we have introduced a new dual-label in situ hybridization method which combines fluorescent and autoradiographic signal detection components for vasopressin and vesicular glutamate transporter-2 mRNAs, respectively. Application of this technique provided evidence that 2% sodium chloride in the drinking water for 7 days produced a robust and significant increase of vesicular glutamate transporter-2 mRNA in vasopressin neurons of the supraoptic nucleus. The immunocytochemical labeling of pituitary sections, followed by the densitometric analysis of vesicular glutamate transporter-2 immunoreactivity in the posterior pituitary, revealed a concomitant increase in vesicular glutamate transporter-2 protein levels at the major termination site of the magnocellular axons. These data demonstrate that magnocellular oxytocin as well as vasopressin cells contain the glutamatergic marker vesicular glutamate transporter-2, similarly to most of the parvicellular neurosecretory neurons examined so far. The robust increase in vesicular glutamate transporter-2 mRNA and immunoreactivity after salt loading suggests that the cellular levels of vesicular glutamate transporter-2 in vasopressin neurons are regulated by alterations in water–electrolyte balance. In addition to the known synaptic actions of excitatory amino acids in magnocellular nuclei, the new observations suggest novel mechanisms whereby glutamate of endogenous sources can regulate magnocellular neuronal functions.

Keywords: Glutamatergic; Neurosecretion; Oxytocin; Vasopressin; VGLUT; VGLUT2

1. An introductory statement

Prior to exocytotic neurotransmitter release, classical non-peptide transmitters are accumulated into synaptic vesicles by vesicular neurotransmitter transporters (Masson et al., 1999). Previous studies (Bellocchio et al., 2000; Takamori et al., 2000) established that the vesicular transporter for L-glutamate (VGLUT1) is identical to a molecule previously known as the brain-specific Na^+-dependent inorganic phosphate cotransporter (BNPI) (Ni et al., 1994). Subsequently, two additional members of the VGLUT family (VGLUT2, VGLUT3) were identified (Bai et al., 2001; Fremeau et al., 2001; Hayashi et al., 2001; Herzog et al., 2001; Takamori et al., 2001; Fremeau et al., 2002; Gras et al., 2002; Schafer et al., 2002; Varoqui et al., 2002). Results of initial mapping studies for these peptides formed a consensus opinion that the different VGLUT isoforms tend to occur in distinct classes of glutamatergic neurons (Bellocchio et al., 1998; Fremeau et al., 2001; Fujiyama et al., 2001; Herzog et al., 2001). The diencephalon mainly seems to contain glutamatergic neurons of the VGLUT2 phenotype (Lin et al., 2003). Furthermore, the excitatory glutamatergic neurons in several hypothalamic nuclei now appear to be partly identical with neurosecretory

Abbreviations: AP, alkaline phosphatase; BCIP, 5-bromo-4-chloro-3-indolyl-phosphate; CRH, corticotropin-releasing hormone; DAB, diaminobenzidine tetrahydrochloride; GnRH, gonadotropin-releasing hormone; HRP, horseradish peroxidase; ISH-ICC, immunocytochemical-in situ hybridization; mRNA, messenger ribonucleic acid; NBT, 4-nitro blue tetrazolium; OT, oxytocin; PVH, hypothalamic paraventricular nucleus; SO, hypothalamic supraoptic nucleus; TBS, Tris-buffered saline; TRH, thyrotropin-releasing hormone; VP, vasopressin; VGLUT2, type-2 vesicular glutamate transporter

* Corresponding author. Tel.: +36 1 210 9400x366; fax: +36 1 210 9944.
E-mail address: hrabovszky@koki.hu (E. Hrabovszky).

0197-0186/$ – see front matter © 2006 Elsevier Ltd. All rights reserved.
doi:10.1016/j.neuint.2005.12.013

peptidergic neurons that regulate adenohypophysial functions. Accordingly, recent studies from our laboratory using dual-label in situ hybridization (ISH) and dual-label immunocytochemistry have demonstrated the presence of VGLUT2 mRNA and protein, respectively, in the vast majority of hypophysiotropic gonadotropin-releasing hormone (GnRH) (Hrabovszky et al., 2004b), thyrotropin-releasing hormone (TRH) (Hrabovszky et al., 2005b), corticotropin-releasing hormone (CRH) (Hrabovszky et al., 2005b) and somatostatin (Hrabovszky et al., 2005a), but not growth hormone-releasing hormone (Hrabovszky et al., 2005a), neurons in the rat. Based on the (i) previous detection of VGLUT2 mRNA and immunoreactivity in magnocellular neurons of the hypothalamic paraventricular and supraoptic nuclei (PVH, SO) (Hisano and Nogami, 2002; Ziegler et al., 2002; Lin et al., 2003) and (ii) earlier reports on glutamate immunoreactivity within magnocellular neurosecretory terminals in the posterior pituitary (Meeker et al., 1991), in the present studies we investigated the occurrence of VGLUT2 mRNA in oxytocin (OT) and/or vasopressin (VP) neurons. To also address the issue of whether the cellular amounts of VGLUT2 are regulated at times of increased magnocellular neuronal activity, we studied the effect of hypertonic saline in the drinking water on the VGLUT2 mRNA content of VP neurons and on the VGLUT2 immunoreactivity of the posterior pituitary.

2. Experimental procedures

2.1. Animals

Adult male Wistar rats ($N = 14$; 220–240 g bw) were purchased from the local breeding colony of the Medical Gene Technology Unit of the Institute of Experimental Medicine. The animals were kept under a 12 h day–12 h night schedule (lights off at 07:00 h, lights on at 19:00 h), in a temperature (22 ± 2 °C) and humidity ($60 \pm 10\%$) controlled environment with free access to laboratory rat food (Sniff Spezialdiaeten GmbH, Soest, Germany) and tap water. Experiments were carried out in accordance with the European Communities Council Directive of 24 November 1986 (86/609/EEC) and were reviewed and approved by the Animal Welfare Committee at the Institute of Experimental Medicine.

For studies to assess the effect of chronic osmotic stimulation on the VGLUT2 content of VP neurons, one group of rats (Salt+ group; $N = 8$) were provided 2% (w/v) sodium chloride in the drinking water for 7 days (Sheikh et al., 1998; Joanny et al., 2000; Burbach et al., 2001; Theodosis et al., 2004), whereas control rats (Ctrl group; $N = 6$) continued to receive tap water. The animals were decapitated, their brains removed and snap-frozen on powdered dry ice. Twelve-μm thick coronal sections were cut serially from the SO and the PVH with a Leica CM 3050 S cryostat (Leica Microsystems Nussloch Gmbh, Nussloch, Germany) and mounted serially on gelatin-coated microscope slides (Hrabovszky et al., 2004a). The sections were stored at −80 °C until processed for ISH studies. The pituitaries of the same animals were immersed in 4% paraformaldehyde fixative for 5 days. Following fixation, five pituitaries from Ctrl rats and six pituitaries from Salt+ rats were aligned in embedding molds for subsequent immersion into egg yolk in a way that two separate blocks contained the pituitaries of the two distinct groups. The supporting medium of the blocks (Martin et al., 1983) was hardened in formalin fume (48 h). The tissues were infiltrated with 20% sucrose (5 days), snap-frozen on dry ice and cut serially at 30 μm with a Leica SM 2000R freezing microtome (Leica Microsystems). The sections were stored in anti-freeze medium at −20 °C until processing for immunocytochemistry.

2.2. Single-label ISH detection of VGLUT2 mRNA in the SO and the PVH

Every tenth section was processed for single-label ISH detection of VGLUT2 mRNA using a ^{35}S-UTP (NEN Life Science Products, Boston, MA, USA)-labeled cRNA probe (“VGLUT2-879”; complementary to bases 522-1400 of GenBank Acc. # NM 053427) and hybridization procedures detailed elsewhere (Hrabovszky et al., 2004a, 2004b). The autoradiographic signal for VGLUT2 mRNA was enhanced by the application of unusually high concentrations of dithiothreitol (750 mM), hybridization probe (80,000 cpm/μl) and dextran sulfate (20%) in the hybridization solution and the use of an extended hybridization time (40 h) (Hrabovszky and Petersen, 2002). Following posthybridization procedures, the slides were coated with thawed (42 °C) NTB-3 emulsion (Kodak; Rochester, NY, USA; diluted 1:1 with distilled water), dried, and exposed for 2 weeks in light-tight exposure boxes at 4 °C. The slide autoradiographs were developed with pre-chilled (15 °C) D19 developer (Kodak; diluted 1:1 with MQ water; 2 min), rinsed with MQ water (30 s), and fixed with Kodak fixer (5 min). Then, the sections were rinsed in several changes of MQ water, air-dried on slide trays, dehydrated in ethanol (95%, 5 min; 100%, 2 × 5 min), transferred briefly into xylene (30 s) and coverslipped with DPX mounting medium (Fluka Chemie; Buchs, Switzerland).

As described recently, the specificity of VGLUT2 hybridization signal was confirmed in a series of control studies. The sense-strand VGLUT2 RNA transcript (negative control) provided no labeling, whereas a different antisense VGLUT2 probe complementary to bases 1704-2437 (gift from Dr. J.P. Herman, University of Cincinnati Medical Center, Cincinnati, OH; used as positive control) generated signal patterns identical to those obtained with the VGLUT2-879 probe (Hrabovszky et al., 2004b).

2.3. Triple-label ISH detection of VGLUT2 mRNA in OT and VP neurons

To investigate whether VGLUT2 is expressed in OT neurons, VP neurons or both, a procedure for triple-label ISH detection of OT, VP and VGLUT2 mRNAs was adapted from a recent study that localized estrogen receptor-β mRNA expression to magnocellular OT and VP neurons. The generation and use of the fluorescein-labeled, 175-base OT probe and the digoxigenin-labeled 241-base VP probe (the VP cDNA was kindly made available by Dr. Thomas Sherman, University Medical Center, Washington, DC, USA), as well as the detailed stepwise triple-labeling protocol has been provided in this report (Hrabovszky et al., 2004a) and used in the present studies with the difference that the ^{35}S-labeled estrogen receptor-β probe was substituted with the VGLUT2-879 probe. Following hybridization of every tenth hypothalamic section with the probe cocktail and posthybridization treatments, the sections were permeabilized with 0.2% Triton X-100 (Sigma Chemical Company, St. Louis, MO, USA) in Tris-buffered saline (TBS; 0.1 M Tris–HCl with 0.9% NaCl; pH 7.8) for 20 min, prior to the ICC detection of the non-isotopic hybridization signals. To reduce non-specific binding of antibodies, the sections were preincubated for 30 min with a solution containing 2% blocking reagent for nucleic acid hybridization and detection (Roche Diagnostics Co., Indianapolis, IN, USA) in 100 mM maleate buffer (pH 7.5). The antibody cocktail, used next, contained the blocking solution, anti-digoxigenin antibodies conjugated to alkaline phosphatase (anti-digoxigenin-AP; Fab fragment; 1:1000; Roche) and antifluorescein antibodies conjugated to horseradish peroxidase (antifluorescein-HRP; NEN; 1:500). This mixture was applied to the sections for 48 h at 4 °C with the aid of press-seal probe clips (Sigma). To visualize the non-isotopic probes, the slides were first rinsed in TBS, then incubated for 30 min in biotin tyramide solution (diluted at 1:1000 with TBS/0.002% H_2O_2 from a stock prepared according to Adams) (Adams, 1992). Following the deposition of biotin tyramide reporter in OT neurons, the AP signal in VP neurons was visualized using the 5-bromo-4-chloro-3-indolyl-phosphate/4-nitro blue tetrazolium BCIP/NBT chromogen system, according to the manufacturer’s instructions (Roche). The development of purple color reaction was allowed to proceed for 30 min. The sections were rinsed briefly in TBS and transferred into the ABC-Elite reagent (Vector; Burlingame, CA, USA; 1:1000 dilution of solutions “A” and “B” in TBS) for 1 h in order to introduce horseradish peroxidase (HRP) to the sites of biotin tyramide deposition (in OT neurons). The HRP reaction was finally detected with 10 mg 3,3′-diaminobenzidine tetrahydrochloride (DAB), and 0.001% H_2O_2 in 50 ml TBS solution,

resulting in brown chromogen deposition in OT perikarya which was clearly distinguishable form the purple color in VP neurons. Double-stained sections were rinsed copiously in TBS (30 min), dipped quickly into MQ water, transferred into 70% ethanol with 300 mM ammonium acetate, dehydrated in a graded series of ethanol (70, 80, 95, 100%; 2 min each), then dried on slide trays. The visualization of non-isotopic probes to OT and VP this way was followed by the autoradiographic detection of the VGLUT2 probe. To prevent chemographic artifacts by the BCIP/NBT chromogen in the NTB-3 (Kodak; Rochester, NY) photographic emulsion (Young and Hsu, 1991), the slides were coated twice with a 1% solution of Parlodion (Mallinckrodt; dissolved in amyl acetate) and air-dried (Hrabovszky et al., 2004a). Then, the autoradiographic detection was carried out as described above for single-labeling ISH studies.

2.4. Immunocytochemical detection of VGLUT2 in the posterior pituitary

Before detecting VGLUT2 immunoreactivity in the posterior pituitary using peroxidase immunocytochemistry, the pituitary sections were treated for 30 min with 1% H_2O_2 and 0.2% Triton X-100 (Sigma) in PBS to eliminate endogenous peroxidase activity and facilitate antibody penetration. The pretreated sections were rinsed in PBS and incubated sequentially in mouse primary VGLUT2 antibodies (MAB 5504; 1:500; Chemicon) or rabbit primary VGLUT2 antibodies (#135103, 1:2000; SYnaptic SYstems, Göttingen, Germany) for 5 days on a shaking platform at 4 °C, followed by biotinylated secondary antibodies (Jackson ImmunoResearch; 1:1000) for 2 h (RT) and ABC Elite working solution (1:1000) for 1 h (RT). The HRP signals were visualized with DAB, in the presence or absence of nickel ions. The immunostained sections were mounted on microscope slides from Elvanol, air-dried, dehydrated with 95% (5 min), followed by 100% (2 × 5 min) ethanol, cleared with xylene (2 × 5 min) and coverslipped with DPX mounting medium (Fluka).

The specificity of VGLUT2 immuno-labeling was also confirmed using simultaneously the two different VGLUT2 antibodies for dual-immunofluorescent labeling. In this case, the rabbit and mouse primary antibodies as well as the fluorochrom-conjugated secondary antibodies (FITC-conjugated donkey anti-mouse IgG, 1:250 and Cy3-conjugated donkey anti-rabbit IgG, 1:250, Jackson ImmunoResearch) were applied to the sections in the form of cocktails, for 72 and 16 h, respectively. The dual-fluorescent specimens were mounted on glass slides, air-dried, coverslipped with Vectashield (Vector), and analyzed with a Radiance 2100 confocal microscope (Bio-Rad Laboratories, Hemel Hempstead, UK) using laser excitation lines 488 nm for FITC and 543 nm for Cy3 and dichroic/emission filters 560 nm/500–530 nm for FITC and 560–610 nm for Cy3. Individual optical slices were collected for the analysis in ''lambda strobing'' mode so that only one excitation laser and the corresponding emission detector were active during a line scan, to eliminate emission cross-talk (Hrabovszky et al., 2005a). Colocalization was demonstrated in single optical slices (<0.7 μm).

2.5. Studies of the effect of salt loading on the VGLUT2 mRNA content of VP neurons

A new quantification approach combining fluorescent and radioisotopic ISH detections was developed and used to address the effect of salt loading on the VGLUT2 mRNA content of VP neurons. First, the digoxigenin-labeled VP probe and the ^{35}S-labeled VGLUT2 probe were used in combination for ISH. Then, instead of using a stable histochemical staining (DAB or BCIP/NBT) for the detection of the non-isotopic signal component, VP neurons were visualized with the red fluorochrome rhodamin as follows. After incubations in anti-digoxigenin antibodies conjugated with HRP (1/200; Roche), rhodamin-tyramide (1/500 dilution with TBS/0.002% H_2O_2 of a stock prepared as described by Hopman et al., 1998) was deposited to the HRP sites. The sections were dehydrated with ethanol, coated with Kodak NTB-3 photographic emulsion and exposed for 2 weeks. Following the development of emulsion autoradiographs, the sections were coverslipped with Vectashield and examined with an Axiophot microscope (Zeiss; Göttingen, Germany) equipped with an RT Spot digital camera (Diagnostic Instrument, Sterling Heights, MI). The rhodamine signal in VP neurons was viewed with an epifluorescent filter set (excitation of 540–590 nM, bandpass of 595 nm, and emission of 600–660 nm), whereas the autoradiographic signal in the same field was visualized with dark-field illumination. The optimal photographic settings were determined for both the fluorescent and the dark-field images and then the manual exposure settings were locked. Digital photographs were prepared from the SO with a 20× objective lens and archived. The entire specimen to be analyzed quantitatively was photographed in a single session, using a random sequence of sections from salt-loaded and control animals. To collect VGLUT2 hybridization signals characteristic for VP neurons, the digital files were processed further with the Adobe Photoshop 5.5 software, as follows. The fluorescent image of VP neurons (labeled with the red fluorochrom) was transferred into a new layer of the file which contained the autoradiographic signal for VGLUT2. By selecting the ''screen'' mode for this new layer, the two types of signal became simultaneously visible. Autoradiographic grain clusters above individual VP neurons (red color) were then selected with the lasso tool from the background layer and transferred into a new Photoshop file with dark background. While this sample collection approach and subsequent analysis was ideal to characterize the VGLUT2 signals that were obviously derived from individual VP neurons, the VP and VGLUT2 signals were often confluent due to the compactness of the SO. Therefore, an alternative sample collection approach was also used to characterize the VGLUT2 mRNA content of VP neurons. A fixed size (50 μm × 50 μm) frame was placed on regions of each SO that were rich in VP neurons, without considering the number of VP neurons giving rise to signals. Then the autoradiographic images under the selection frame were copied into new Photoshop files for the analysis. On average, 40 VP neurons and 45 frames were used to characterize individual animals. Using both sample collection methods, the photographs to be analyzed were saved in grayscale mode as TIF files (one single file for each animal) and opened with the Image J image analysis software (public domain at http://rsb.info.nih.gov/ij/download/src/). The threshold was determined in a way to highlight all silver grains but not the background. Individual VP neurons (first sample collection approach) as well as VP-rich areas of fixed size (second sample collection method) in each animal were characterized with the area covered by highlighted pixels. Group differences were assessed with one-way ANOVA.

2.6. Effect of salt loading on VGLUT2 immunoreactivity of the posterior pituitary

To eliminate any technical variation from the immunocytochemical (ICC) staining procedure, the egg yolk-embedded pituitary sections from the two animal groups were processed in parallel for the ICC detection of VGLUT2. Four sections of each block were chosen for comparative studies of VGLUT2 immunoreactivity in the two groups of animal. Each of the selected sections contained large surfaces of all posterior lobes.

First, the sections were treated for 30 min with 1% H_2O_2 and 0.2% Triton X-100 (Sigma) in PBS to eliminate endogenous peroxidase activity and facilitate antibody penetration. The pretreated sections were rinsed in PBS and incubated in mouse primary VGLUT2 antibodies (MAB 5504; 1:500; Chemicon) for 5 days (4 °C), then in biotinylated anti-mouse IgG (Jackson ImmunoResearch; 1:1000) for 2 h (RT) and in ABC Elite working solution for 1 h (RT). The HRP signals were visualized with a DAB-containing developer. The immunostained sections were mounted on microscope slides from Elvanol, air-dried, dehydrated with 95% (5 min), followed by 100% (2 × 5 min) ethanol, cleared with xylene (2 × 5 min) and coverslipped with DPX mounting medium (Fluka). Digital photomicrographs were taken from the neural lobes (four photographs from each posterior pituitary). Attention was paid to ensure homogeneous specimen illumination and to use identical exposure settings (manual, instead of automatic) throughout the photography of the whole series of sections. The photographs were initially processed with the Adobe Photoshop 5.5 software. The posterior lobe was selected with the lasso tool from each hypophysis and copied and aligned in separate layers of a new photoshop (PSD) file on white background. Each file containing four images of one animal was flattened, converted to grayscale mode and saved in TIF format. The files were opened with the Image J image analysis software. The threshold was set to highlight the entire surface of the lightest hypophysis but to exclude background. The mean gray value of the highlighted pixels was measured in each photograph and the mean of four photographs was used to characterize each animal. The values of Ctrl and Salt+ animals were compared using one-way ANOVA.

3. Results

3.1. VGLUT2 is expressed in magnocellular OT and VP neurons

Single-label ISH studies of VGLUT2 mRNA revealed its abundant expression in the diencephalon, including both the PVH and the SO which contain magnocellular neurosecretory neurons (Fig. 1A). Similarly to our recent observations (Hrabovszky et al., 2004b, 2005a, 2005b), hybridization specificity was indicated by the absence of any labeling using the sense RNA transcript and the identical patterns of hybridization signals using the two distinct antisense VGLUT2 probes. As expected from these ISH data, the ICC studies of pituitary sections revealed the presence of VGLUT2 immunoreactivity in the posterior pituitary which contains the terminating magnocellular axons. Labeling specificity was indicated by the similarity of labeling patterns provided by VGLUT2 antibodies from two different sources (Fig. 1B and C) and by the immunostaining of identical fibers in dual-immunofluorescent experiments (insets in Fig. 1B and C). The successful triple-ISH labeling of hypothalamic sections yielded distinct brown and purple labeling of OT and VP neurons, respectively, as well as autoradiographic grain clusters throughout the diencephalon (Fig. 2A). The high-power analysis revealed that although magnocellular neurons typically contained only moderate levels of the VGLUT2 hybridization signal, this glutamatergic marker was expressed in most OT as well as VP neurons of the SO, the PVH and accessory magnocellular nuclei (Fig. 2B–D).

3.2. Salt loading enhances VGLUT2 mRNA in magnocellular VP neurons and VGLUT2 immunoreactivity in the neural lobe

The combined fluorescent/radioisotopic ISH method allowed the simultaneous visualization of VP and VGLUT2 mRNA expressing neurons in the SO (Fig. 2E) and the collection of the two different hybridization images in separate layers of Adobe Photoshop files, without signal interference. This approach was found compatible with the quantitative analysis of autoradiographic hybridization signals that were derived from individual VP neurons (Fig. 3A and B) as well as from groups of VP neurons situated within the arbitrarily set 50 μm × 50 μm frames

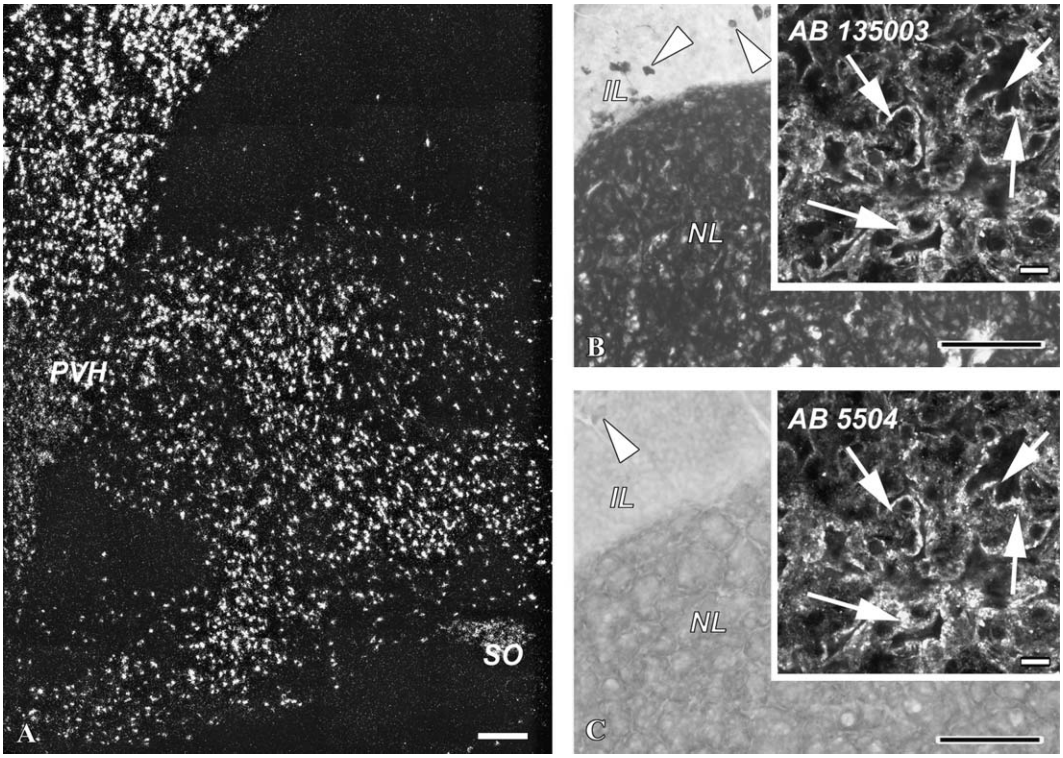

Fig. 1. In situ hybridization (ISH) and immunocytochemical (ICC) evidence for type-2 vesicular glutamate transporter (VGLUT2) expression in magnocellular neurons. (A) Results of ISH studies indicate a wide distribution of glutamatergic cells (autoradiographic grain clusters) in the diencephalon and moderate levels of VGLUT2 mRNA expression in the hypothalamic supraoptic and paraventricular nuclei (SO; PVH). (B and C) Results of ICC studies with two different VGLUT2 antibodies demonstrate the presence of authentic VGLUT2 protein in the neural lobe of the pituitary (NL) which represents the termination field of the magnocellular axons. Compare the staining intensity of the NL to that in the intermediate lobe (IL), which only contains a few scattered cells (arrowheads) labeled for VGLUT2. Panel B illustrates immunoreactivity following the use of the rabbit polyclonal antibodies AB 135003, with Ni-DAB chromogen in the peroxidase developer, whereas panel C shows the results of immunostaining with the mouse monoclonal antibodies AB 5504 and DAB chromogen. Confocal images (insets in B and C) demonstrate the result of a dual-immunofluorescent labeling with the combined use of the above primary antibodies as well as species-specific secondary antibodies conjugated to different fluorochroms. Arrows point to identical neuronal fibers that are dual-labeled with Cy3 and FITC fluorochromogens. Dual-labeling serves as proof for the specificity of immunocytochemistry. Scale bars = 200 μm in A–C and 20 μm in insets in panels B and C.

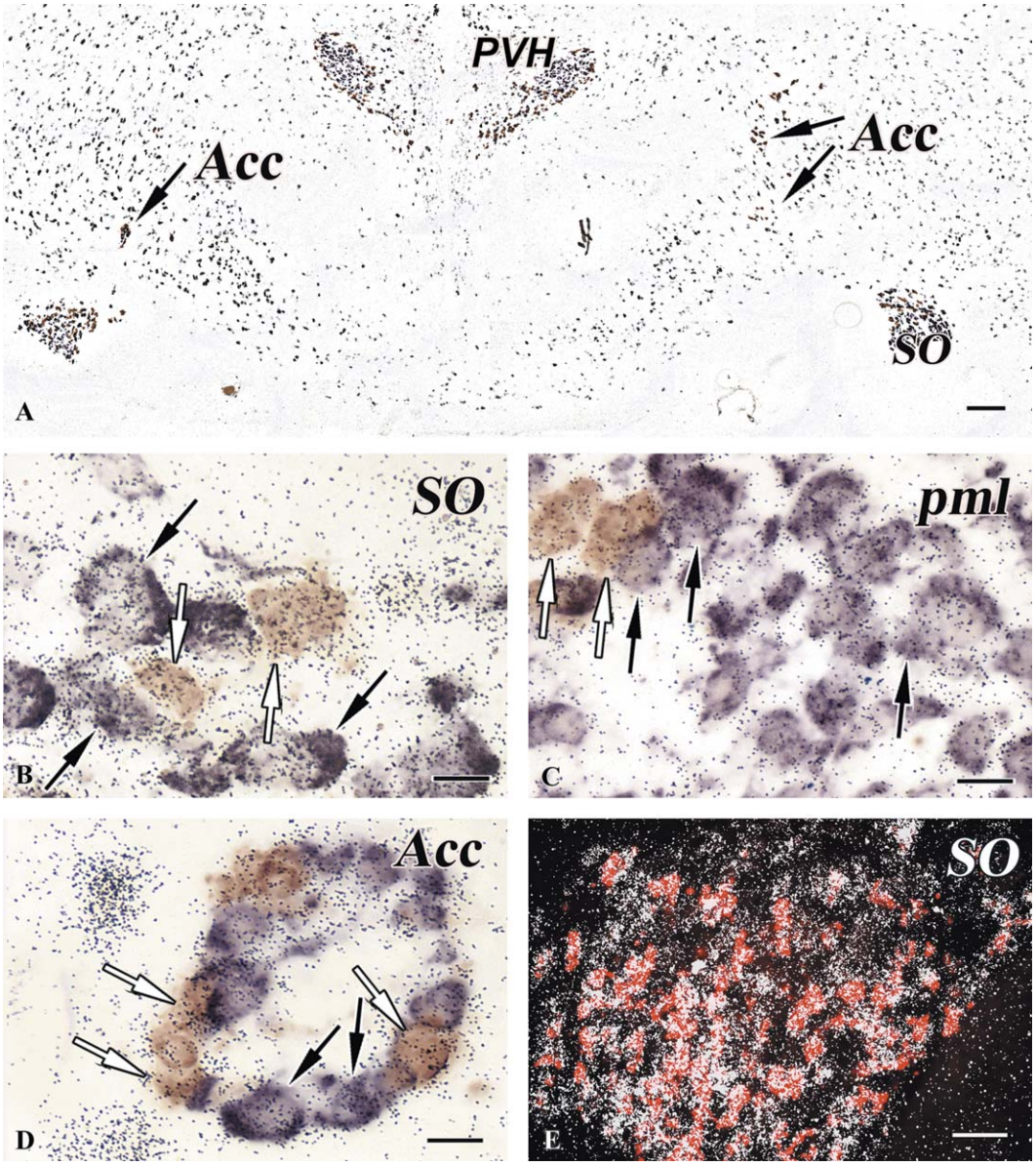

Fig. 2. Dual- and triple-label in situ hybridization (ISH) detection of VGLUT2 mRNA in distinct subsets of magnocellular oxytocin (OT) and vasopressin (VP) neurons. (A) Low-power photomicrograph illustrates the simultaneous triple-label ISH detection of VP (BCIP/NBT chromogen; purple color), OT (DAB chromogen; brown color) and VGLUT2 mRNAs (black grain clusters in the emulsion autoradiograph) in the hypothalamus. *Note*: the presence of OT and VP mRNA signals in the supraoptic (SO) and paraventricular (PVH) nuclei and in neurons of accessory magnocellular cell groups (Acc; arrows), whereas glutamatergic neurons are more widely distributed in the hypothalamus. (B–D) High-power photomicrographs show that moderate levels of VGLUT2 mRNA expression are detectable in the vast majority of magnocellular OT and VP neurons. The combined use of the purple BCIP/NBT and the brown DAB histochemical stains yields contrasting colors, enabling the distinction of VP from OT neurons, respectively, in the SO (B), in the VP cell-dominated lateral subdivision of the posterior magnocellular subnucleus of the PVH (pml; C), and in the Acc (D). Black arrows indicate dual-labeled VP neurons, whereas white arrows point to VGLUT2 mRNA expressing OT neurons. (E) Combined use of rhodamine fluorochrom to detect VP mRNA and autoradiography (dark-field illumination; white grain clusters) to detect VGLUT2 mRNA in the same cells of the SO. After placing the images in separate layers of Adobe Photoshop files, individual grain clusters corresponding to VP neurons or as an alternative approach, autoradiographic signals above groups of VP neurons can be selected for the quantitative image analysis of VGLUT2 hybridization signals, as detailed in the text and illustrated in Fig. 3. Scale bars = 200 in A, 25 μm in B–D and 50 μm in E.

(Fig. 3D and E). Seven days of salt loading resulted in a robust and highly significant increase in the VGLUT2 mRNA signal which was associated with single VP neurons (area covered by VGLUT2 signal/VP neuron) by one-way ANOVA [$F(1,12) = 26.703$; $p = 0.00023$] (Fig. 3A–C) and VGLUT2 mRNA signal which was detectable under the 50 μm × 50 μm frames over groups of VP neurons [$F(1,12) = 23.562$, $p = 0.00040$] (Fig. 3D–F). The increase in VGLUT2 mRNA expression was also accompanied by a significant enhancement [$F(1,9) = 9.747$; $p = 0.0123$ by one-way ANOVA] of VGLUT2 immunoreactivity (mean gray value) in the neural lobe of the hypophysis (Fig. 3G–I).

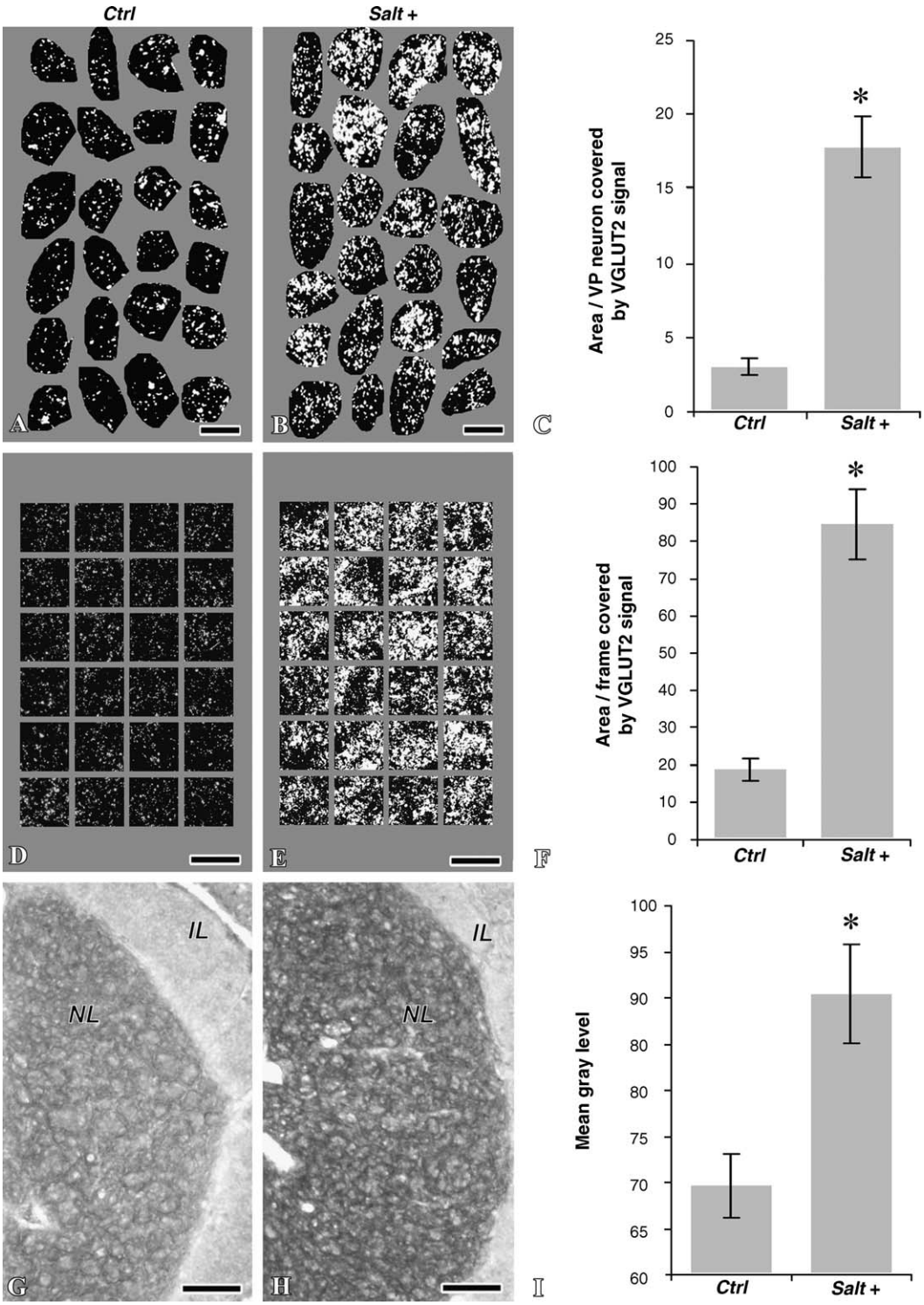

Fig. 3. Effects of a 7-day salt loading on VGLUT2 mRNA content of magnocellular VP neurons and on VGLUT2 immunoreactivity of the posterior pituitary. (A and B) Examples for autoradiographic VGLUT2 hybridization signals derived from individual VP/VGLUT2 neurons of the supraoptic nucleus (SO) from control (Ctrl) and salt-loaded (Salt+) animals. Neurons were selected from similar dual-labeled images as shown in Fig. 2E. Representative autoradiographs in A and B and results of image analysis in C demonstrate a robust enhancement of VGLUT2 hybridization signal (signal area/VP neurons; arbitrary units) in single VP neurons of the SO. (D–F) An alternative approach to characterize the amounts of VGLUT2 mRNA signal in VP neurons was to analyze and compare autoradiographic images within arbitrary 50 μm × 50 μm frames selected above VP cell groups. This second strategy could establish a similar increase in the VGLUT2 mRNA content of VP neurons in response to salt loading (F; see text for details of the analysis and for statistics). (G–I) Immunocytochemical analysis of mean gray values in the neurohypophyses that were immunostained with DAB for VGLUT2, established a significant increase in the VGLUT2-immunoreactive protein content of the posterior pituitary, concomitant to the increased VGLUT2 mRNA expression in SO neurons. Scale bars = 25 μm in A and B, 50 μm in D and E and 100 μm in G and H.

4. Discussion

In these studies we present ISH and ICC evidence that magnocellular OT as well as VP neurons of the SO and PVH express the glutamatergic phenotype marker VGLUT2. In addition, robust increases in VGLUT2 mRNA expression of VP neurons and neurohypophysial VGLUT2 immunoreactivity were observed following a seven-day osmotic stimulation by 2% sodium chloride in the drinking water.

L-Glutamate is the major excitatory neurotransmitter in the hypothalamus (van den Pol et al., 1990) and also a key regulator of the magnocellular neurosecretory systems (Meeker, 2002). Magnocellular neurons respond to osmotic stimulation by increased expression (Lightman and Young, 1987) and secretion (Onaka and Yagi, 2001) of both OT and VP. A series of other genes co-expressed with VP and OT has been found upregulated by osmotic challenges, including secretogranin II, chromogranin B, VGF, dynorphin, enkephalin, neuropeptide Y, corticotropin-releasing hormone, etc. (for a review, see Burbach et al., 2001). The mechanisms underlying the stimulatory effects of high plasma osmolality on magnocellular neurons are thought to be dual. First, magnocellular neurons are intrinsically osmosensitive; they possess stretch-inactivated mechanoreceptors in their plasma membranes which can open a non-selective cation channel (Oliet and Bourque, 1993). On the other hand, magnocellular neurons in the SO (Csaki et al., 2002) and the PVH (Csaki et al., 2000) receive abundant glutamatergic innervation from hypothalamic nuclei as well as from extrahypothalamic regions. Osmosensitive glutamatergic neurons in the subfornical organ, the organum vasculosum of the lamina terminalis and the median preoptic nucleus appear to be particularly important in communicating osmotic signals to the magnocellular neurosecretory system (Bourque et al., 1994; Leng et al., 1999). Antagonists to NMDA and non-NMDA type glutamate receptors impair vasopressin release after osmotic stimuli in in vitro preparations (Sladek et al., 1998; Swenson et al., 1998) as well as in vivo (Xu and Herbert, 1998) and about 25% of the synapses in the SO are glutamatergic (Meeker et al., 1993). Both metabotropic and all three classes of ionotropic glutamate receptors have been detected on magnocellular neurons (Meeker et al., 1994; Al-Ghoul et al., 1997; Herman et al., 2000). Recent studies have also established that salt loading increases the density of glutamatergic innervation to supraoptic magnocellular neurons (Mueller et al., 2005). A concomittant upregulation of NMDA-R1 expression by dehydration (Decavel and Curras, 1997) may serve as a mechanism to amplify the glutamatergic afferent stimulation of magnocellular neurons. The direct mechanosensitivity is thought to further facilitate the activation of magnocellular neurons by the extrinsic glutamatergic synaptic inputs (Bourque et al., 1994).

Beyond a large body of evidence that glutamate is the most important excitatory neurotransmitter in the synaptic regulation of magnocellular neurons, recent studies showing that magnocellular neurons express the mRNAs for VGLUT2 (Ziegler et al., 2002; Lin et al., 2003), and in one report also for VGLUT1 (Ziegler et al., 2002), together with our present observations and the previous detection of glutamate immunoreactivity in magnocellular neurons (Meeker et al., 1989, 1991), raise the possibility that glutamate can be packaged into synaptic vesicles for terminal and/or somatic/dendritic release from the magnocellular OT and VP neurons. It appears that several parvicellular neurosecretory systems share a similar glutamatergic feature with VP and OT neurons, which was established via the previous identification of VGLUT2 mRNA and immunoreactivity in GnRH, TRH, CRH and SS neurons of the rat (Hrabovszky et al., 2004b, 2005a, 2005b). Currently only speculations can be made about the role of endogenous glutamate in these neuroendocrine systems. Whereas in the case of the parvicellular systems, the possibility exists that glutamate may reach sufficient concentrations in the hypophysial portal circulation to influence anterior pituitary functions, in the case of the magnocellular OT and VP neurons it is very unlikely that glutamate exerts any other than local effects at its most likely release site, i.e. the posterior pituitary. As we have previously proposed for parvicellular terminals in the median eminence (Hrabovszky et al., 2004b, 2005a, 2005b), the actions of endogenous glutamate may include autocrine/paracrine effects via glutamate receptors that are located on the neuroendocrine terminals. In this context, it is important to note that the posterior pituitary of the rat exhibits an especially high density of kainic acid binding sites which may, at least partly, account for such putative preterminal actions (Unnerstall and Wamsley, 1983). Other cell types than neurons may also be targets for the glutamatergic actions, including astrocytes, pituicytes and the endothelial cells of blood vessels. While the exact roles of VGLUT2 in magnocellular neurons require clarification, the robust enhancement in the VGLUT2 content of VP neurons following salt loading suggests important regulatory functions.

The new approach we used for the quantitative image analysis of VGLUT2 hybridization signal in VP neurons might have wide applications in studies that require the quantitative image analysis of autradiographic hybridization signal in an identified neuronal phenotype. Although stable histochemical chromogenes including DAB or BCIP/NBT are more widely used than fluorochromes to demonstrate the coexpression of two mRNAs of interest, technical difficulties may occur while quantifying the autoradiographic signal component. When such quantification is required, the gray value of the autoradiographic signal (or the measured area covered by grains) is increased by the gray value of the underlying enzyme reaction products. One solution to this problem is epiilumination which uses reflected, instead of transmitted, light which does not pass through the chromogens in the specimens. Our new quantification approach offers an alternative by combining a fluorescent detection method with emulsion autradiography. In the present studies we presented two examples of how this combination can be exploited in quantitative studies of VGLUT2 mRNA expression selectively within the VP population of magnocellular neurons. One approach analyzed the VGLUT2 mRNA signal of individual VP neurons and detected a highly significant difference in the average VGLUT2 mRNA content of VP neurons sampled from salt-treated versus control rats.

One limitation of this approach in data collection was due to the packed nature of magnocellular neurons. This has often prevented us from attributing the autoradiographic grain clusters to individual VP neurons. This problem was overcome by the second sampling strategy which analyzed VGLUT2 mRNA levels in areas of fixed size which were occupied by VP neurons. The choice from these approaches or other alternatives will depend on the specific application. Future studies will use similar dual-labeling strategies to address whether and how chronic osmotic stimulation regulates VGLUT2 mRNA in OT neurons of the SO.

While this work was prepared for publication, an independent single-label ISH study was published by Kawasaki et al. (2005) which found increased VGLUT2 mRNA expression in the SO and the magnocellular PVH regions of osmotically stimulated rats. In addition to the similarity of the observed regional changes in VGLUT2 mRNA expression and the results of our single-cell quantification of VGLUT2 mRNA in VP neurons, several important differences exist between these two studies. Notably, while Kawasaki and colleagues found a decrease of VGLUT2 immunoreactivity in the neural lobe of the hypophysis, in our study we observed an increase of VGLUT2 immunoreactivity in the region containing the magnocellular axon terminals. In addition, while Kawasaki and co-workers reported the preferential expression of VGLUT2 mRNA in VP cells, our triple-label ISH data rather indicate that both types of magnocellular neurons share the glutamatergic phenotype. The reasons for the partly different conclusions will require clarification.

In summary, these studies have demonstrated that magnocellular OT as well as VP neurons contain VGLUT2 mRNA. Salt loading was found to produce a robust and significant increase in the VGLUT2 mRNA of VP neurons and in the VGLUT2 immunoreactivity of the posterior pituitary. The functional significance of the presence and pretranslational regulation of VGLUT2 in magnocellular neurons requires clarification.

Acknowledgements

This research was supported by grants from the National Science Foundation of Hungary (OTKA T43407, T46574), NKFP 1A/002/2004 and the European Union FP6 funding (contract no. LSHM-CT-2003-503041). This publication reflects the authors' views and not necessarily those of the European Union. The information in this document is provided as is, and no guarantee or warranty is given that the information is fit for any particular purpose. The user thereof uses the information at its sole risk and liability. The authors are grateful to Drs. J.P. Herman and T. Sherman for providing the VGLUT2-734 and VP cDNAs, respectively, for these studies and to Gyöngyi Kékesi for the excellent technical assistance.

References

Adams, J.C., 1992. Biotin amplification of biotin and horseradish peroxidase signals in histochemical stains. J. Histochem. Cytochem. 40, 1457–1463.

Al-Ghoul, W.M., Meeker, R.B., Greenwood, R.S., 1997. Differential expression of five *N*-methyl-D-aspartate receptor subunit mRNAs in vasopressin and oxytocin neuroendocrine cells. Brain Res. Mol. Brain Res. 44, 262–272.

Bai, L., Xu, H., Collins, J.F., Ghishan, F.K., 2001. Molecular and functional analysis of a novel neuronal vesicular glutamate transporter. J. Biol. Chem. 276, 36764–36769.

Bellocchio, E.E., Hu, H., Pohorille, A., Chan, J., Pickel, V.M., Edwards, R.H., 1998. The localization of the brain-specific inorganic phosphate transporter suggests a specific presynaptic role in glutamatergic transmission. J. Neurosci. 18, 8648–8659.

Bellocchio, E.E., Reimer, R.J., Fremeau Jr., R.T., Edwards, R.H., 2000. Uptake of glutamate into synaptic vesicles by an inorganic phosphate transporter. Science 289, 957–960.

Bourque, C.W., Oliet, S.H., Richard, D., 1994. Osmoreceptors, osmoreception, and osmoregulation. Front. Neuroendocrinol. 15, 231–274.

Burbach, J.P., Luckman, S.M., Murphy, D., Gainer, H., 2001. Gene regulation in the magnocellular hypothalamo-neurohypophysial system. Physiol. Rev. 81, 1197–1267.

Csaki, A., Kocsis, K., Halasz, B., Kiss, J., 2000. Localization of glutamatergic/aspartatergic neurons projecting to the hypothalamic paraventricular nucleus studied by retrograde transport of [3H]D-aspartate autoradiography. Neuroscience 101, 637–655.

Csaki, A., Kocsis, K., Kiss, J., Halasz, B., 2002. Localization of putative glutamatergic/aspartatergic neurons projecting to the supraoptic nucleus area of the rat hypothalamus. Eur. J. Neurosci. 16, 55–68.

Decavel, C., Curras, M.C., 1997. Increased expression of the *N*-methyl-D-aspartate receptor subunit, NR1, in immunohistochemically identified magnocellular hypothalamic neurons during dehydration. Neuroscience 78, 191–202.

Fremeau Jr., R.T., Burman, J., Qureshi, T., Tran, C.H., Proctor, J., Johnson, J., Zhang, H., Sulzer, D., Copenhagen, D.R., Storm-Mathisen, J., Reimer, R.J., Chaudhry, F.A., Edwards, R.H., 2002. The identification of vesicular glutamate transporter 3 suggests novel modes of signaling by glutamate. Proc. Natl. Acad. Sci. U.S.A. 99, 14488–14493.

Fremeau Jr., R.T., Troyer, M.D., Pahner, I., Nygaard, G.O., Tran, C.H., Reimer, R.J., Bellocchio, E.E., Fortin, D., Storm-Mathisen, J., Edwards, R.H., 2001. The expression of vesicular glutamate transporters defines two classes of excitatory synapse. Neuron 31, 247–260.

Fujiyama, F., Furuta, T., Kaneko, T., 2001. Immunocytochemical localization of candidates for vesicular glutamate transporters in the rat cerebral cortex. J. Comp. Neurol. 435, 379–387.

Gras, C., Herzog, E., Bellenchi, G.C., Bernard, V., Ravassard, P., Pohl, M., Gasnier, B., Giros, B., El Mestikawy, S., 2002. A third vesicular glutamate transporter expressed by cholinergic and serotoninergic neurons. J. Neurosci. 22, 5442–5451.

Hayashi, M., Otsuka, M., Morimoto, R., Hirota, S., Yatsushiro, S., Takeda, J., Yamamoto, A., Moriyama, Y., 2001. Differentiation-associated Na+-dependent inorganic phosphate cotransporter (DNPI) is a vesicular glutamate transporter in endocrine glutamatergic systems. J. Biol. Chem. 276, 43400–43406.

Herman, J.P., Eyigor, O., Ziegler, D.R., Jennes, L., 2000. Expression of ionotropic glutamate receptor subunit mRNAs in the hypothalamic paraventricular nucleus of the rat. J. Comp. Neurol. 422, 352–362.

Herzog, E., Bellenchi, G.C., Gras, C., Bernard, V., Ravassard, P., Bedet, C., Gasnier, B., Giros, B., El Mestikawy, S., 2001. The existence of a second vesicular glutamate transporter specifies subpopulations of glutamatergic neurons. J. Neurosci. 21, RC181.

Hisano, S., Nogami, H., 2002. Transporters in the neurohypophysial neuroendocrine system, with special reference to vesicular glutamate transporters (BNPI and DNPI): a review. Microsc. Res. Tech. 56, 122–131.

Hopman, A.H., Ramaekers, F.C., Speel, E.J., 1998. Rapid synthesis of biotin-, digoxigenin-, trinitrophenyl-, and fluorochrome-labeled tyramides and their application for in situ hybridization using CARD amplification. J. Histochem. Cytochem. 46, 771–777.

Hrabovszky, E., Kallo, I., Steinhauser, A., Merchenthaler, I., Coen, C.W., Petersen, S.L., Liposits, Z., 2004a. Estrogen receptor-beta in oxytocin and vasopressin neurons of the rat and human hypothalamus: Immunocy-

tochemical and in situ hybridization studies. J. Comp. Neurol. 473, 315–333.

Hrabovszky, E., Petersen, S.L., 2002. Increased concentrations of radioisotopically-labeled complementary ribonucleic acid probe, dextran sulfate, and dithiothreitol in the hybridization buffer can improve results of in situ hybridization histochemistry. J. Histochem. Cytochem. 50, 1389–1400.

Hrabovszky, E., Turi, G.F., Kallo, I., Liposits, Z., 2004b. Expression of vesicular glutamate transporter-2 in gonadotropin-releasing hormone neurons of the adult male rat. Endocrinology 145, 4018–4021.

Hrabovszky, E., Turi, G.F., Liposits, Z., 2005a. Presence of vesicular glutamate transporter-2 in hypophysiotropic somatostatin but not growth hormone-releasing hormone neurons of the male rat. Eur. J. Neurosci. 21, 2120–2126.

Hrabovszky, E., Wittmann, G., Turi, G.F., Liposits, Z., Fekete, C., 2005b. Hypophysiotropic thyrotropin-releasing hormone and corticotropin-releasing hormone neurons of the rat contain vesicular glutamate transporter-2. Endocrinology 146, 341–347.

Joanny, P., Steinberg, J., Guerrero, F., Sauze, N., Oliver, C., Grino, M., 2000. The effects of ionotropic agonists of excitatory amino acids on the release of arginine vasopressin in rat hypothalamic slices. J. Neuroendocrinol. 12, 970–976.

Kawasaki, A., Hoshi, K., Kawano, M., Nogami, H., Yoshikawa, H., Hisano, S., 2005. Up-regulation of VGLUT2 expression in hypothalamic-neurohypophysial neurons of the rat following osmotic challenge. Eur. J. Neurosci. 22, 672–680.

Leng, G., Brown, C.H., Russell, J.A., 1999. Physiological pathways regulating the activity of magnocellular neurosecretory cells. Prog. Neurobiol. 57, 625–655.

Lightman, S.L., Young 3rd, W.S., 1987. Vasopressin, oxytocin, dynorphin, enkephalin and corticotrophin-releasing factor mRNA stimulation in the rat. J. Physiol. 394, 23–39.

Lin, W., McKinney, K., Liu, L., Lakhlani, S., Jennes, L., 2003. Distribution of vesicular glutamate transporter-2 messenger ribonucleic acid and protein in the septum-hypothalamus of the rat. Endocrinology 144, 662–670.

Martin, G.K., Wise, R.P., Lonsbury-Martin, B.L., 1983. Frozen-section autoradiography of the cochlea: evidence for differential distribution of amino acids. Ann. Otol. Rhinol. Laryngol. 92, 254–258.

Masson, J., Sagne, C., Hamon, M., El Mestikawy, S., 1999. Neurotransmitter transporters in the central nervous system. Pharmacol. Rev. 51, 439–464.

Meeker, R.B., 2002. Metabotropic and NMDA glutamate receptor interactions with osmotic stimuli in supraoptic neurons. Pharmacol. Biochem. Behav. 73, 475–484.

Meeker, R.B., Greenwood, R.S., Hayward, J.N., 1994. Glutamate receptors in the rat hypothalamus and pituitary. Endocrinology 134, 621–629.

Meeker, R.B., Swanson, D.J., Greenwood, R.S., Hayward, J.N., 1991. Ultrastructural distribution of glutamate immunoreactivity within neurosecretory endings and pituicytes of the rat neurohypophysis. Brain Res. 564, 181–193.

Meeker, R.B., Swanson, D.J., Greenwood, R.S., Hayward, J.N., 1993. Quantitative mapping of glutamate presynaptic terminals in the supraoptic nucleus and surrounding hypothalamus. Brain Res. 600, 112–122.

Meeker, R.B., Swanson, D.J., Hayward, J.N., 1989. Light and electron microscopic localization of glutamate immunoreactivity in the supraoptic nucleus of the rat hypothalamus. Neuroscience 33, 157–167.

Mueller, N.K., Di, S., Paden, C.M., Herman, J.P., 2005. Activity-dependent modulation of neurotransmitter innervation to vasopressin neurons of the supraoptic nucleus. Endocrinology 146, 348–354.

Ni, B., Rosteck Jr., P.R., Nadi, N.S., Paul, S.M., 1994. Cloning and expression of a cDNA encoding a brain-specific Na(+)-dependent inorganic phosphate cotransporter. Proc. Natl. Acad. Sci. U.S.A. 91, 5607–5611.

Oliet, S.H., Bourque, C.W., 1993. Mechanosensitive channels transduce osmosensitivity in supraoptic neurons. Nature 364, 341–343.

Onaka, T., Yagi, K., 2001. Involvement of *N*-methyl-D-aspartic acid receptor activation in oxytocin and vasopressin release after osmotic stimuli in rats. J. Neuroendocrinol. 13, 166–174.

Schafer, M.K., Varoqui, H., Defamie, N., Weihe, E., Erickson, J.D., 2002. Molecular cloning and functional identification of mouse vesicular glutamate transporter 3 and its expression in subsets of novel excitatory neurons. J. Biol. Chem. 277, 50734–50748.

Sheikh, S.P., Feldthus, N., Orkild, H., Goke, R., McGregor, G.P., Turner, D., Moller, M., Stuenkel, E.L., 1998. Neuropeptide Y2 receptors on nerve endings from the rat neurohypophysis regulate vasopressin and oxytocin release. Neuroscience 82, 107–115.

Sladek, C.D., Badre, S.E., Morsette, D.J., Sidorowicz, H.E., 1998. Role of non-NMDA receptors in osmotic and glutamate stimulation of vasopressin release: effect of rapid receptor desensitization. J. Neuroendocrinol. 10, 897–903.

Swenson, K.L., Badre, S.E., Morsette, D.J., Sladek, C.D., 1998. *N*-methyl-D-aspartic acid stimulation of vasopressin release: role in osmotic regulation and modulation by gonadal steroids. J. Neuroendocrinol. 10, 679–685.

Takamori, S., Rhee, J.S., Rosenmund, C., Jahn, R., 2000. Identification of a vesicular glutamate transporter that defines a glutamatergic phenotype in neurons. Nature 407, 189–194.

Takamori, S., Rhee, J.S., Rosenmund, C., Jahn, R., 2001. Identification of differentiation-associated brain-specific phosphate transporter as a second vesicular glutamate transporter (VGLUT2). J. Neurosci. 21, RC182.

Theodosis, D.T., Schachner, M., Neumann, I.D., 2004. Oxytocin neuron activation in NCAM-deficient mice: anatomical and functional consequences. Eur. J. Neurosci. 20, 3270–3280.

Unnerstall, J.R., Wamsley, J.K., 1983. Autoradiographic localization of high-affinity [3H]kainic acid binding sites in the rat forebrain. Eur. J. Pharmacol. 86, 361–371.

van den Pol, A.N., Wuarin, J.P., Dudek, F.E., 1990. Glutamate, the dominant excitatory transmitter in neuroendocrine regulation. Science 250, 1276–1278.

Varoqui, H., Schafer, M.K., Zhu, H., Weihe, E., Erickson, J.D., 2002. Identification of the differentiation-associated Na+/PI transporter as a novel vesicular glutamate transporter expressed in a distinct set of glutamatergic synapses. J. Neurosci. 22, 142–155.

Xu, Z., Herbert, J., 1998. Effects of intracerebroventricular dizocilpine (MK801) on dehydration-induced dipsogenic responses, plasma vasopressin and c-fos expression in the rat forebrain. Brain Res. 784, 91–99.

Young 3rd, W.S., Hsu, A.C., 1991. Observations on the simultaneous use of digoxigenin- and radiolabeled-oligodeoxyribonucleotide probes for hybridization histochemistry. Neuropeptides 18, 75.

Ziegler, D.R., Cullinan, W.E., Herman, J.P., 2002. Distribution of vesicular glutamate transporter mRNA in rat hypothalamus. J. Comp. Neurol. 448, 217–229.

11. számú melléklet

0013-7227/06/$15.00/0
Printed in U.S.A.

dc_27_10

Endocrinology 147(8):3818–3825

doi: 10.1210/en.2005-1229

Expression of Vesicular Glutamate Transporter-2 in Gonadotrope and Thyrotrope Cells of the Rat Pituitary. Regulation by Estrogen and Thyroid Hormone Status

Erik Hrabovszky, Imre Kalló, Gergely F. Turi, Katalin May, Gábor Wittmann, Csaba Fekete, and Zsolt Liposits

Laboratory of Endocrine Neurobiology (E.H., I.K., G.F.T., K.M., G.W., C.F., Z.S.L.), Institute of Experimental Medicine, Hungarian Academy of Sciences, Budapest, 1083 Hungary; Department of Neuroscience (I.K., Z.S.L.), Faculty of Information Technology, Péter Pázmány Catholic University, Budapest, 1083 Hungary; and Tupper Research Institute and Department of Medicine (C.F.), Division of Endocrinology, Diabetes, and Metabolism, Tufts-New England Medical Center, Boston, Massachusetts 02111

Immunocytochemical studies of the rat adenohypophysis identified a cell population that exhibits immunoreactivity for type-2 vesicular glutamate transporter (VGLUT2), a marker for glutamatergic neuronal phenotype. The *in situ* hybridization detection of VGLUT2 mRNA expression in adenohypophysial cells verified that VGLUT2 immunoreactivity is due to local synthesis of authentic VGLUT2. Dual-immunofluorescent studies of the hypophyses from male rats showed the presence of VGLUT2 in high percentages of LH (93.3 ± 1.3%)-, FSH (44.7 ± 3.9%)-, and TSH (70.0 ± 5.6%)-immunoreactive cells and its much lower incidence in cells of the prolactin, GH, and ACTH phenotypes. Quantitative *in situ* hybridization studies have established that the administration of a single dose of 17-β-estradiol (20 μg/kg; sc) to ovariectomized rats significantly elevated VGLUT2 mRNA in the adenohypophysis 16 h postinjection. Thyroid hormone dependence of VGLUT2 expression was addressed by the comparison of hybridization signals in animal models of hypo- and hyperthyroidism to those in euthyroid controls. Although hyperthyroidism had no effect on VGLUT2 mRNA, hypothyroidism increased adenohypophysial VGLUT2 mRNA levels. This coincided with a decreased ratio of VGLUT2-immunoreactive TSH cells, regarded as a sign of enhanced secretion. The presence of the glutamate marker VGLUT2 in gonadotrope and thyrotrope cells, and its up-regulation by estrogen or hypothyroidism, address the possibility that endocrine cells of the adenohypophysis may cosecrete glutamate with peptide hormones in an estrogen- and thyroid status-regulated manner. The exact roles of endogenous glutamate observed primarily in gonadotropes and thyrotropes, including its putative involvement in autocrine/paracrine regulatory mechanisms, will require clarification. (*Endocrinology* 147: 3818–3825, 2006)

VESICULAR GLUTAMATE transporters (VGLUT1–3) selectively accumulate L-glutamate into synaptic vesicles; these proteins are thus also viewed as histochemical markers for excitatory neurons that use L-glutamate for synaptic communication. The three molecular forms of VGLUT are expressed by distinct classes of glutamatergic neurons in the central nervous system (1–10). Recent studies have established that several hypothalamic regions involved in neuroendocrine regulation synthesize the mRNA and protein for the VGLUT2 isoform (8, 9). Hypophysiotropic neurosecretory systems shown to possess VGLUT2 mRNA and protein include GnRH neurons of the preoptic area (11), TRH (12), and CRH (12) neurons of the paraventricular nucleus and somatostatin (13) neurons of the paraventricular and anterior periventricular nuclei. The identification of VGLUT2 immunoreactivity in neurosecretory terminals in the external zone of the median eminence indicates that these systems may corelease L-glutamate with the peptide neurohormones (11). It is currently unclear whether the putative secretory glutamate acts locally on cellular elements of the median eminence, or else is carried away by the portal circulation to regulate ultimately adenohypophysial cells bearing glutamate receptors (14, 15). In addition to the glutamatergic characteristics of various parvicellular neuroendocrine systems, recent studies have also provided evidence for the VGLUT2 phenotype of magnocellular neurosecretory oxytocin and vasopressin neurons (16, 17).

Beyond the putative cosecretion of glutamate from neuroendocrine axon terminals, there is emerging evidence that the VGLUT isoforms can also occur in nonneural endocrine tissues (18). The pineal gland contains both the VGLUT1 and the VGLUT2 isoforms (19, 20) and various endocrine cells of the gastrointestinal tract, including α and F cells of the pancreatic Langerhans islets and intestinal L cells (20, 21), also synthesize VGLUT2. In the present studies, we used immunocytochemistry and *in situ* hybridization (ISH) to investigate the putative synthesis of VGLUT2 in peptide hormone-secreting cells of the adenohypophysis. The functional phenotype of VGLUT2-immunoreactive adenohypophysial cells was addressed by dual-immunofluorescent histochemistry followed by confocal laser microscopic analysis. Based on preliminary results of these experiments which identified

First Published Online May 4, 2006

Abbreviations: bw, Body weight; DAB, 3,3′-diaminobenzidine tetrahydrochloride; ISH, *in situ* hybridization; OVX, ovariectomized; OVX + E2, ovariectomized and estradiol-treated; PRL, prolactin; VGUT, vesicular glutamate transporter.

***Endocrinology* is published monthly by The Endocrine Society (http://www.endo-society.org), the foremost professional society serving the endocrine community.**

VGLUT2 immunoreactivity in gonadotrope and thyrotrope cells, the issues of whether and how the estrogen status and the thyroid hormone status regulate adenohypophysial VGLUT2 mRNA expression, have been addressed. Quantitative ISH studies were carried out to compare VGLUT2 hybridization signals in adenohypophysial sections from ovariectomized *vs.* ovariectomized and estrogen-treated female rats and from hypothyroid *vs.* euthyroid *vs.* hyperthyroid male rats. Subsequent dual-immunofluorescent studies also analyzed putative alterations of VGLUT2 immunoreactivity within adenohypophysial cells of these endocrine models.

Materials and Methods

Tissue preparations

Adult male [n = 33; 200–225 g body weight (bw)] and female (n = 17; 200–225 g bw) Wistar rats were purchased from the local breeding colony of the Medical Gene Technology Unit of the Institute of Experimental Medicine. The animals were maintained under a 12-h d/12-h night schedule (lights on 0700–1900 h), in a temperature (22 ± 2 C) and humidity (60 ± 10%) controlled environment with free access to laboratory rat food (Sniff Spezialdiaeten GmbH, Soest, Germany) and tap water. All experiments were carried out in accordance with the Council Directive of 24 November 1986 of the European Communities (86/609/EEC) and were reviewed and approved by the Animal Welfare Committee of the Institute of Experimental Medicine (47/003/2005).

Tissue preparation for light and confocal microscopic studies

To collect pituitaries for immunocytochemical experiments, rats were deeply anesthetized with pentobarbital (35 mg/kg bw, ip) and perfused transcardially, first with 20 ml of 0.1 M PBS (pH 7.4), and then with 150 ml fixative solution containing 4% paraformaldehyde (Sigma Chemical Co., St. Louis, MO) in PBS. To provide a firm support for floating hypophysial sections, the glands were immersed in fresh egg-yolk and exposed to formalin fumes for 48 h, as recommended for the processing of soft histological specimens by others (22). The hardened blocks were trimmed, soaked in 20% sucrose for 72 h, and snap-frozen on powdered dry ice. Then, 20-μm-thick free-floating sections were prepared with a Leica SM 2000R freezing microtome (Leica Microsystems, Nussloch Gmbh, Nussloch, Germany). Endogenous peroxidase activity was eliminated, and sections were permeabilized by a 30-min incubation in 1% H_2O_2 and 0.4% Triton X-100 in PBS. Then the tissues were treated with 2% normal horse serum in TBS (0.1 M Tris-HCl with 0.9% NaCl; pH 7.8) to prevent nonspecific binding of the antibodies.

Tissue preparation for ISH studies

Four rats used for the ISH detection of adenohypophysial VGLUT2 mRNA were briefly anesthetized in a CO_2 atmosphere and decapitated. The hypophysis of each animal was removed, placed in a metal mold containing Jung tissue freezing medium (Leica Microsystems, Nussloch Gmbh; diluted 1:1 with 0.9% sodium chloride solution) and aligned. The blocks were snap-frozen on powdered dry ice. Sixteen-micrometer-thick coronal sections were cut from the frozen pituitary blocks with a Leica CM 3050 S cryostat (Leica Microsystems), thaw-mounted on gelatin-coated microscope slides, and air-dried.

Experiment 1: demonstration of VGLUT2 immunoreactive adenohypophysial cells using peroxidase immunocytochemistry

Paraformaldehyde-fixed pituitary sections of five male rats were incubated in either mouse primary VGLUT2 antibodies (MAB 5504, 1:500; Chemicon, Temecula, CA) or rabbit primary VGLUT2 antibodies (135103, 1:2000; SYnaptic SYstems, Göttingen, Germany) for 5 d on a shaking platform at 4 C. This was followed by sequential treatments with species-specific biotinylated secondary antibodies (Jackson ImmunoResearch Laboratories, West Grove, PA; 1:1000) for 2 h (room temperature) and ABC Elite working solution (1:1000; Vector Laboratories, Burlingame, CA) for 1 h (room temperature). The peroxidase signals were visualized with 3,3′-diaminobenzidine tetrahydrochloride (DAB) in the peroxidase developer, in either the presence or the absence of nickel ions. After chromogen deposition, the immunostained pituitary sections were mounted on microscope slides from Elvanol, air-dried, dehydrated with 95% (5 min) followed by 100% (2 × 5 min) ethanol, cleared with xylene (2 × 5 min), coverslipped with DPX mounting medium (Fluka Chemie, Buchs, Switzerland), and studied with an Axiophot microscope (Zeiss, Göttingen, Germany) equipped with an RT Spot digital camera (Diagnostic Instrument, Sterling Heights, MI).

Experiment 2: dual-immunofluorescent detection of VGLUT2 immunoreactive adenohypophysial cells in positive control studies

Positive control experiments to confirm the authenticity of VGLUT2 immunoreactivity applied the mixture of the two different VGLUT2 antibodies to the same tissue sections for dual-immunofluorescent labeling, similarly to strategies used recently (11, 12). The mouse and rabbit primary antibodies (used at 1:300 and 1:1000 dilutions, respectively) were reacted for 12 h with a cocktail of Cy3-conjugated antimouse IgG and FITC-conjugated antirabbit IgG (Jackson ImmunoResearch Laboratories; 1:100 each). The immunofluorescent specimens were mounted on glass slides from 0.05 M Tris/HCl solution (pH 7.8), dried, and coverslipped with Vectashield mounting medium (Vector Laboratories). Confocal microscopic analysis of the specimens was carried out as detailed under experiment 4.

Experiment 3: demonstration of VGLUT2 mRNA expression in adenohypophysial cells using ISH

To provide further confirmation to the concept that VGLUT2 immunoreactivity in adenohypophysial cells is due to local synthesis of the authentic VGLUT2 molecules, slide-mounted hypophysial sections from four male rats were processed for the ISH detection of VGLUT2 mRNA with a sensitized radioisotopic ISH procedure (23). The preparation and use of a 879-base ^{35}S-labeled cRNA hybridization probe to bases 522-1400 of VGLUT2 mRNA (GenBank accession no. NM 053427) have been detailed in recent publications from our laboratory (11–13). After post-hybridization treatments which included the RNase A digestion (50 μg/ml, 30 min at 37 C) of probe excess (24), the sections were dehydrated, air-dried, and coated with NTB-3 autoradiographic emulsion (Kodak, Rochester, NY), diluted 1:1 with MQ water. After 2 wk of exposure, the slide autoradiographs were developed with D19 developer (Kodak; diluted 1:1 with MQ water; 2 min), rinsed with MQ water (30 sec), and fixed with Kodak fixer (5 min). Then, the slides were rinsed in several changes of chilled MQ water, counter-stained lightly with toluidine blue, air-dried, transferred briefly into xylene (30 sec) and coverslipped with DPX mounting medium (Fluka Chemie). Negative control experiments included the use of ^{35}S-labeled sense probes for ISH studies and the omission of primary antibodies for immunocytochemistry. A positive control for ISH labeling specificity (11–13) was to substitute the VGLUT2–879 probe with a distinct probe ("VGLUT2–734", a kind gift from Dr. J. P. Herman, University of Cincinnati Medical Center, Cincinnati, OH) against a nonoverlapping segment of VGLUT2 mRNA (8).

Experiment 4: immunofluorescent experiments to determine the functional phenotype of VGLUT2 expressing adenohypophysial cells

To determine the functional phenotype of adenohypophysial cells that exhibit VGLUT2 immunoreactivity, a series of dual-immunofluorescent studies was carried out for the simultaneous detection of VGLUT2 and different adenohypophysial hormones. Sections from five male animals were first incubated in the mouse monoclonal VGLUT2 antibodies (1:300, Chemicon) for 72 h and then, in Cy3-conjugated secondary antibodies (Jackson ImmunoResearch Laboratories; 1:100) for 12 h. Subsequently, the sections were incubated in rabbit polyclonal

antisera from Accurate (Westbury, NY) against rat GH (1:1000), ACTH (1:1000), LH (1:1000), FSH (1:1000), TSH (1:1000), or rat prolactin [S13 anti-prolactin (PRL); 1:1000; kind gift from Dr. György Nagy, Semmelweis University, Budapest Hungary] (25, 26). The incubation in the primary antibodies was followed by FITC-conjugated antirabbit secondary antibodies (Jackson ImmunoResearch Laboratories; 1:100) for 12 h. The dual-immunofluorescent specimens were mounted on glass slides from 0.05 M Tris/HCl (pH 7.8) solution, dried, and coverslipped with Vectashield medium (Vector Laboratories). Cells that were immunoreactive for VGLUT2 thus appeared in red, whereas peptide-immunoreactive cells appeared in green using the following epifluorescent filter sets of the Zeiss Axiophot epifluorescent microscope: for Cy3, excitation of 540–590 nm, bandpass of 595 nm, and emission of 600–660 nm; for FITC, excitation of 460–500 nm, bandpass of 505 nm, and emission of 510–560 nm. Dual-immunofluorescent specimens were analyzed further with a Radiance 2100 confocal microscope (Bio-Rad Laboratories, Hemel Hempstead, UK) using laser excitation lines 488 nm for FITC and 543 nm for Cy3 and dichroic/emission filters 560 nm/500–530 nm for FITC and 560–610 nm for Cy3. To eliminate emission cross-talk, single optical slices (<0.7 μm) were collected in "λ strobing" mode so that only one excitation laser and the corresponding emission detector were active during a line scan (13). The digital images were processed with the Adobe PhotoShop 7.0 software at 300 dpi resolution.

To determine the percent ratios of double-labeled LH, FSH, and TSH cells in each set of dual-labeling experiment, individual hormone-immunoreactive cells were analyzed at high magnification for the presence/absence of the VGLUT2 immunofluorescent signal, by switching between the epifluorescent filter sets for Cy3 and FITC. The percent ratios of VGLUT2 containing PRL, GH, and ACTH cells were analyzed on confocal images. Each quantitative analysis included at least 100 randomly selected adenohypophysial cells from each of five male animals and results were expressed as mean from the five animals ± SEM.

Experiment 5: studies on the estrogenic regulation of adenohypophysial VGLUT2 mRNA

Nine female rats were bilaterally ovariectomized under pentobarbital anesthesia (35 mg/kg bw, ip). On postovariectomy d 11, five of these gonadectomized rats [ovariectomized and estradiol-treated (OVX + E2) group] received a single sc injection of 17-β-estradiol (20 μg/kg, bw) in sunflower oil, whereas control rats [n = 4; ovariectomized (OVX) group] were injected with the vehicle. This dose of 17-β-estradiol was chosen to safely saturate tissue estrogen receptors (27). Sixteen hours after the injections, the rats were decapitated and the hypophyses were embedded into freezing medium (diluted 1:1 with 0.9% NaCl solution) and frozen on dry ice. Sixteen-micrometer-thick sections were prepared from each pituitary, thaw-mounted, and dried on glass slides and hybridized with the antisense "VGLUT2–879" probe as described under experiment 3. After posthybridization treatments, the sections were exposed to Fujifilm imaging plates for 48 h. The images were scanned with a Fujifilm FLA-3000 phosphorimager system and archived in TIF mode. The files were opened for the analysis with the Image J image analysis software (public domain at http://rsb.info.nih.gov/ij/download/src/). The threshold was set to highlight the entire tissue surface. The adenohypophysis was selected and its mean gray level was determined. Each animal was characterized with the mean of four measurements (from four hypophysial sections). The mean gray levels in the OVX and the OVX + E2 groups were compared with one-way ANOVA.

Experiment 6: studies on the effects of thyroid hormone status on adenohypophysial VGLUT2 mRNA

The issues of whether and how the thyroid hormone status regulates VGLUT2 mRNA expression in the adenohypophysis have been addressed using a similar quantitative ISH strategy to the one described for experiment 5. Methods to generate hypothyroid and hyperthyroid rat models have been detailed elsewhere (28–30). In brief, adult male Wistar rats were made hypothyroid by a treatment with 0.02% methimazole in the drinking water for 3 wk. Control euthyroid rats (n = 8) received regular tap water. Hyperthyroid rats (n = 8) received tap water and were injected daily for 10 d with 10 μg T_4 (i.p). The animals were decapitated, and their hypophysis was processed for quantitative ISH studies of VGLUT2 mRNA expression as described under experiment 5. The effect of treatments was analyzed with one-way ANOVA, followed by Newman-Keuls test.

Experiment 7: effects of endocrine status on adenohypophysial VGLUT2 immunoreactivity

Dual-immunofluorescent studies to localize VGLUT2 immunoreactivity within LH, TSH, and other adenohypophysial cell types have been replicated in methimazole-treated hypothyroid (n = 4) *vs.* euthyroid control (n = 4) male rats and in OVX (n = 4) *vs.* OVX + E2 (n = 4) female rats. The percent ratios of VGLUT2 immunoreactive LH, TSH, and PRL cells in different animal models were compared by one-way ANOVA to see whether endocrine alterations affect the incidence of these colocalizations.

Results

Experiment 1: demonstration of VGLUT2 immunoreactive adenohypophysial cells using peroxidase immunocytochemistry

The results of immunocytochemical experiments revealed VGLUT2 immunoreactivity in magnocellular axon terminals of the neural lobe (Fig 1A), corroborating recent findings by our group (16) and others (17). In addition to this fiber staining in the neurohypophysis, many adenohypophysial cells in the anterior lobe and a few in the intermediate lobe exhibited VGLUT2 immunoreactivity in their cytoplasm (Fig. 1A). High-power microscopic analysis of the anterior lobe using either the mouse or the rat VGLUT2 antibodies (Fig. 1, B and C) revealed that the labeled elements corresponded to relatively large endocrine cells dispersed throughout the gland (Fig. 1, B and C).

Experiment 2: dual-immunofluorescent detection of VGLUT2 immunoreactive adenohypophysial cells in positive control studies

The combined use of the two different VGLUT2 primary antibodies, followed by appropriate species-specific secondary antibodies which were conjugated with different fluorochroms, resulted in dual-immunofluorescent labeling of immunoreactive adenohypophysial cells, in strong support of labeling specificity for VGLUT2 (Fig. 2, A–C).

Experiment 3: demonstration of VGLUT2 mRNA expression in adenohypophysial cells using ISH histochemistry

ISH experiments identified well-defined clusters of silver grains in the emulsion autoradiographs after 2 wk of exposure (Fig. 1, D and E). These ISH results served as further proof of authentic VGLUT2 synthesis by a subset of adenohypophysial cells. Hybridization specificity was confirmed by the similar results obtained with the two distinct antisense VGLUT2 probes and the absence of grain clusters when using sense RNA transcripts for negative control (data not shown).

Experiment 4: immunofluorescent experiments to determine the functional phenotype of VGLUT2 expressing adenohypophysial cells

The analysis of a series of sections dual-labeled for VGLUT2 and one of the hypophysial peptide hormones, established that VGLUT2 immunoreactivity was absent from

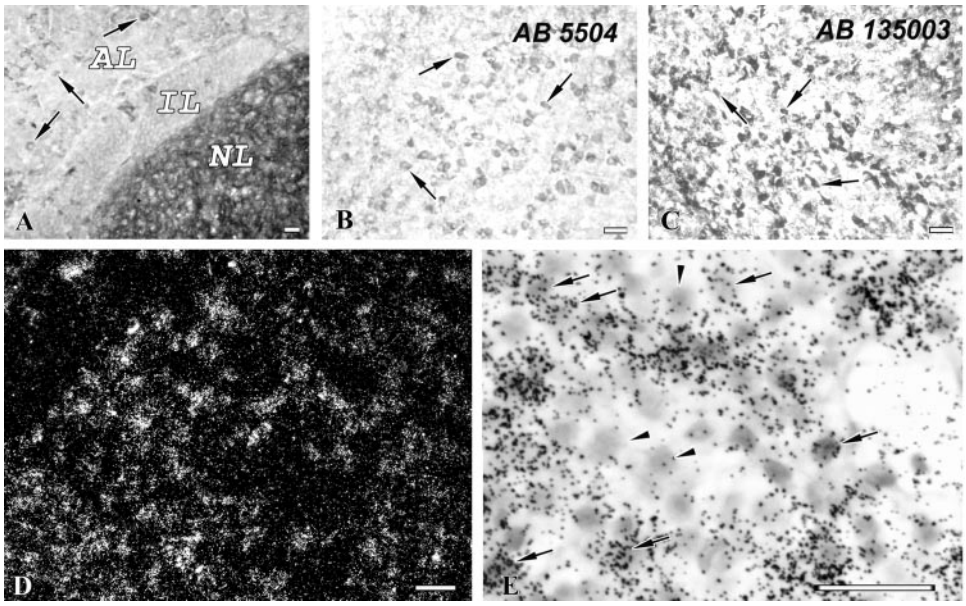

FIG. 1. Immunocytochemical and ISH detection of VGLUT2 and its encoding mRNA in the adenohypophysis. A, Low-power digital photomicrograph of a hypophysial section immunostained for VGLUT2 with mouse monoclonal VGLUT2 antibodies (AB 5504) and peroxidase immunocytochemistry (DAB chromogen) illustrates VGLUT2-immunoreactive fibers in the neural lobe (NL) as well as immunopositive cells in the intermediate lobe (IL) and in the anterior lobe (AL; *arrows*). B and C, Similar staining patterns in the anterior lobe using the mouse monoclonal (AB 5504; B) and the rabbit polyclonal (AB 135003; C; Ni-DAB chromogen) antibodies suggest the specificity of immunoreactions. D, Dark-field image of an emulsion autoradiograph showing VGLUT2 mRNA hybridization signal (clusters of autoradiographic silver grains) in the anterior lobe indicates that VGLUT2 immunoreactivity is due to local VGLUT2 synthesis by the pituitary cells. The hybridization was carried out with the ^{35}S-labeled antisense VGLUT2–879 probe. E, *Arrows* in a high-power bright-field image point to toluidine blue-stained nuclei of endocrine cells that exhibit autoradiographic hybridization signal (grain clusters) for VGLUT2 mRNA. Note also the presence of many unlabeled cells (*arrowheads*) in the adenohypophysis. *Scale bars*, 50 μm.

the vast majority of the corticotrope (Fig. 2D), somatotrope (Fig. 2E), and lactotrope (Fig. 2F) cells, although a few cells of each phenotype (<8%; see *inset* in Fig. 2F) cocontained the VGLUT2 signal. In contrast, the immunocytochemical signal for VGLUT2 tended to be specifically associated with three different phenotypes of glycoprotein-secreting endocrine cells that were immunoreactive to LH, FSH, and TSH (Fig. 2, G, H, and I). The quantitative analysis to estimate the ratios of double-labeled cells in male rats identified VGLUT2 immunoreactivity in 93.3 ± 1.3% of LH-, 44.7 ± 3.9% of FSH-, 70.0 ± 5.6% of TSH-, 7.7 ± 4.2% of PRL-, 6.6 ± 1.6% of GH-, and 3.3 ± 0.6% of ACTH-immunoreactive cells (Fig. 3).

Experiment 5: studies on the estrogenic regulation of adenohypophysial VGLUT2 mRNA

The quantitative densitometric analysis of autoradiographic images captured on a phosphorimager screen established that the adenohypophyses of OVX + E2 female rats contained significantly higher levels of VGLUT2 mRNA (higher mean gray value) than did the anterior lobes of the OVX group [$F(1;7) = 9.40$; $P = 0.0182$] (Fig. 4).

Experiment 6: studies on the effects of thyroid hormone status on adenohypophysial VGLUT2 mRNA

The quantitative analysis of ISH autoradiographs from hypothyroid, euthyroid, and hyperthyroid rats identified a significant effect [$F(2;21) = 42.25$; $P = 0.0001$] of thyroid status on adenohypophysial VGLUT2 mRNA levels (mean gray value). There was no difference between VGLUT2 signals in the hyperthyroid and euthyroid groups ($P = 0.8089$), whereas hypothyroid animals exhibited significantly higher VGLUT2 mRNA expression than did euthyroid ($P = 0.0001$) and hyperthyroid ($P = 0.0001$) rats (Fig. 5).

Experiment 7: effects of endocrine status on adenohypophysial VGLUT2 immunoreactivity

Nearly all of the LH cells in both the OVX (94.6 ± 2.0%) and the OVX + E2 (96.9 ± 0.7%) groups contained VGLUT2 immunoreactivity (Fig. 5, A–D). Robust alterations were observed in the morphology of TSH cells in the hypothyroid male rats, corroborating previous findings by others (31). The activated thyrotropes increased in number as well as in size, and they displayed a decreased immunolabeling for TSH (Fig. 6G). A significantly lower ratio [$(F(1;6) = 44.4$; $P = 0.0005$) by ANOVA] of TSH cells contained the immunofluorescent signal for VGLUT2 in hypothyroid (29.7 ± 5.0%) than in euthyroid control (64.8 ± 0.8%) rats (Fig. 6, E–H). The analysis of VGLUT2 immunoreactivity in hypothyroid and euthyroid male rats and in OVX and OVX + E2 female rats showed that VGLUT2 was mainly detectable in the same cell types, gonadotropes and thyrotropes, as in intact male rats. The incidence of VGLUT2 colocalization was low in PRL cells of OVX female (6.2 ± 0.5%) and euthyroid male (7.9 ± 2.0%) rats, and it was not altered as a result of estrogen treatment or hypothyroidism, respectively (by ANOVA).

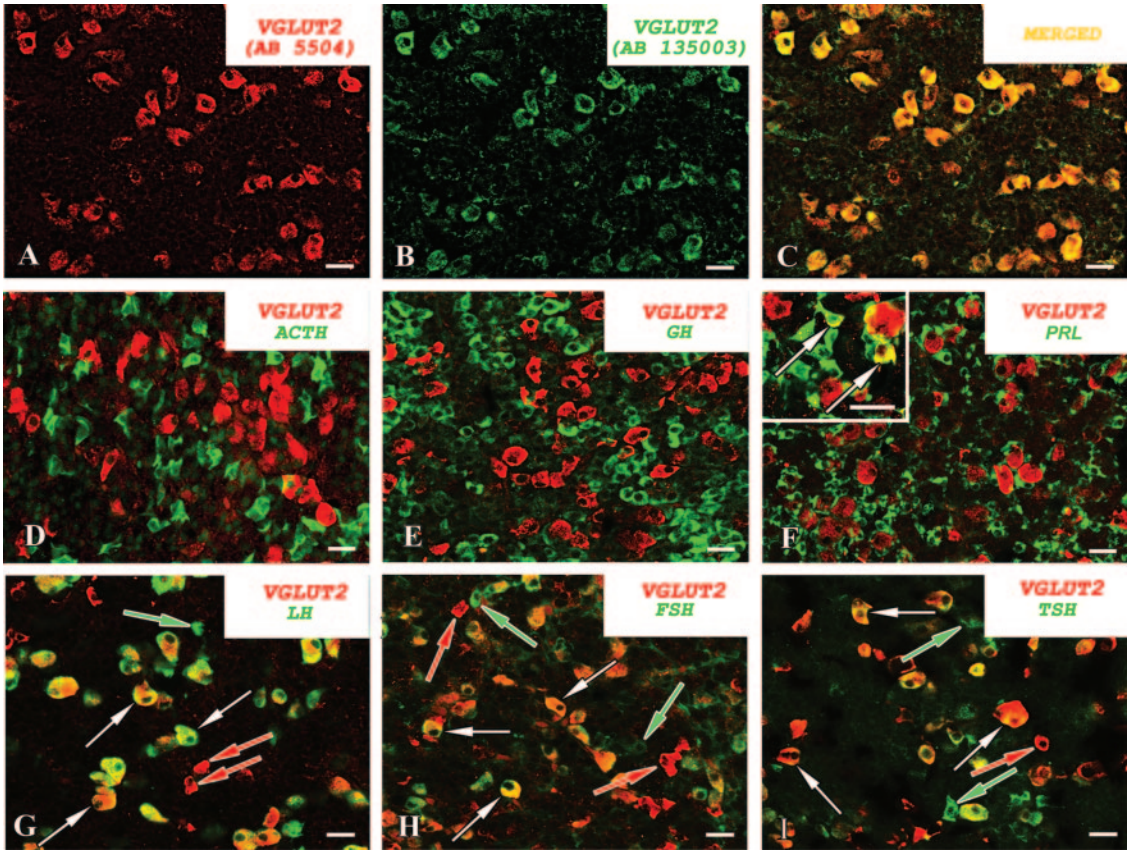

FIG. 2. Dual-immunofluorescent labeling and confocal microscopy for the chemical identification of the phenotype of VGLUT2-immunoreactive adenohypophysial cells. A–C, Dual-labeling of adenohypophysial cells (*yellow color* in merged panel; C) after the combined use of the mouse (AB 5504; A) and rabbit (AB 135003; B) VGLUT2 antibodies and species-specific secondary antibodies conjugated to Cy3 and FITC fluorochroms, respectively, verifies that the authentic VGLUT2 protein is detected. D–F, The sequential detection of VGLUT2 and ACTH (ACTH; D), VGLUT2 and GH (E), or VGLUT2 and PRL (F) results in the absence of double-labeling (lack of *yellow color* in merged figures). However, a few cells with a relatively weak VGLUT2 labeling are always present (high-power *inset* in F; *white arrows*). G–I, In contrast, results of dual-immunofluorescent labeling for VGLUT2 and LH (G), VGLUT2 and FSH (H), or VGLUT2 and TSH (I) reveal frequent cases of signal coexpression (*yellow cells* indicated by *white arrows*), with intense VGLUT2 signal. *Green* and *red arrows* indicate anterior lobe cells that only contain one type of immunoreactivity. *Scale bars*, 25 μm.

Discussion

The results of this study provided immunocytochemical and ISH evidence that the authentic VGLUT2 molecule, a marker for the glutamatergic neuronal phenotype, is present in high percentages of gonadotrope and thyrotrope cells and also occurs in small subsets of corticotrope, somatotrope, and lactotrope cells of the rat adenohypophysis. The quantitative comparison of adenohypophysial VGLUT2 mRNA levels in

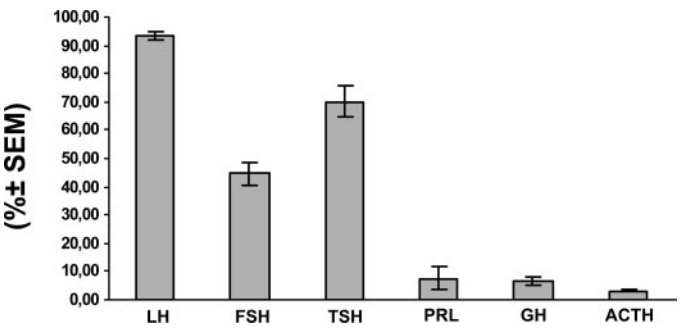

FIG. 3. The percent ratio of different adenohypophysial cell types that exhibit VGLUT2 immunoreactivity in intact male rats. Varying subsets of the different adenohypophysial cell phenotypes exhibit the immunofluorescent signal for VGLUT2 in the male rat. Whereas gonadotrope and thyrotrope cells clearly tend to cocontain VGLUT2, the glutamatergic marker is present in less than 10% of lactotrope, somatotrope, or corticotrope cells.

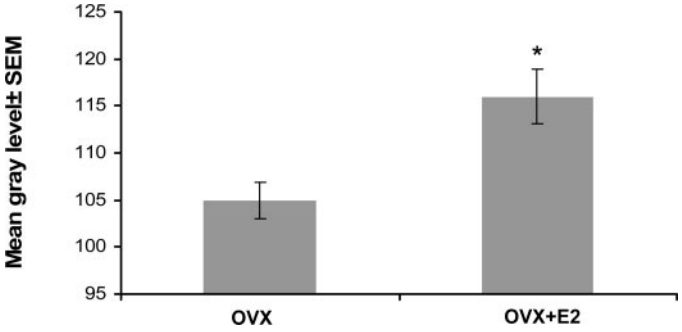

FIG. 4. The effect of estrogen administration to ovariectomized rats on the levels of adenohypophysial VGLUT2 mRNA. A single sc injection of 17-β-estradiol (20 μg/kg) to female rats on postovariectomy d 11 results in a significant increase of VGLUT2 mRNA expression (mean gray value) in the anterior lobe 16 h after the treatment. See text for the details of the analysis and statistics. *, $P = 0.0182$ *vs.* OVX by ANOVA.

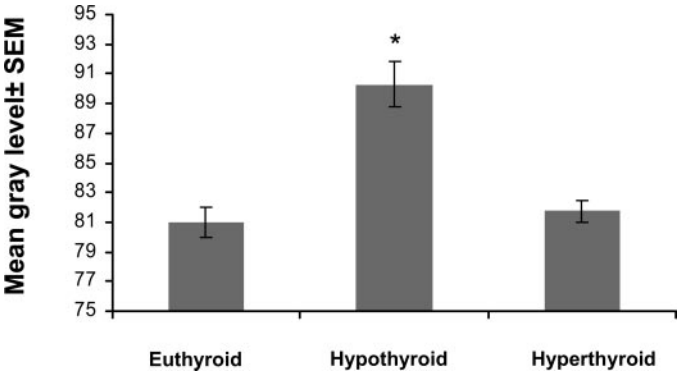

FIG. 5. The effect of thyroid hormone status on adenohypophysial VGLUT2 mRNA expression. Hypothyroidism (induced by a 3-wk treatment of male rats with 0.02% methimazole in the drinking water) caused a significant increase in adenohypophysial VGLUT2 mRNA expression (mean gray value), compared with signal levels found in the untreated euthyroid controls. In contrast, hyperthyroidism induced by daily T_4 injections (10 mg ip., for 10 d) did not affect the VGLUT2 hybridization signals. *, $P = 0.0001$ *vs.* hyperthyroid and euthyroid groups by ANOVA followed by Newman-Keuls.

ovariectomized *vs.* ovariectomized and estrogen-injected female rats revealed the up-regulation of VGLUT2 mRNA expression 16 h after *sc.* administration of a single dose of 17-β-estradiol. VGLUT2 levels were also significantly increased in hypothyroid rats after a 3-wk treatment with methimazole in the drinking water, whereas the hyperthyroid state (induced by daily T_4 injections for 10 d) did not influence VGLUT2 mRNA levels.

Before quantal exocytotic release, classical neurotransmitters including L-glutamate are packaged into synaptic vesicles by vesicular neurotransmitter transporters (32). The brain-specific Na^+-dependent inorganic phosphate cotransporter (33) was shown to fulfill the criteria required for the VGLUT, and hence, was renamed VGLUT1 (1, 34). Intense investigations have subsequently identified the second and third isoforms of VGLUT (VGLUT2 and VGLUT3) (2, 4–7, 20, 35–37). In addition to the presynaptic occurrence of the different VGLUT isoforms in excitatory synapses (2–4, 38), several phenotypes of neurosecretory axons in the median eminence were also found to contain the glutamatergic marker VGLUT2 (11–13). As synaptic specializations at this neurosecretion site are rare (39), glutamatergic mechanisms acting in the median eminence apparently differ from the classical glutamatergic synaptic neurotransmission. The secretory glutamate may exert autocrine/paracrine effects on the putative neuronal glutamate receptors of axon terminals. Furthermore, it may also influence neighboring glial elements containing glutamate receptors (40, 41) or endothelial cells.

The present study, to analyze the putative expression of VGLUT2 in peptide hormone secreting cells of the anterior pituitary, was strongly motivated by recent data showing VGLUT2 in peripherial endocrine organs including cells of the pancreatic Langerhans islets (20), as well as our preliminary observation of VGLUT2-like immunoreactivity in the anterior lobe of the rat pituitary during studies of VGLUT2 immunoreactivity in magnocellular axon terminals in the neurohypophysis (16). The authenticity of adenohypophysial VGLUT2 immunoreactivity was confirmed using simultaneously two distinct VGLUT2 antibodies for dual-immunofluorescent labeling and the ISH demonstration of VGLUT2 mRNA expression in these cells. In the absence of ultrastructural data, it is presently unclear whether VGLUT2 and the various peptide hormones are localized to the same or to separate vesicular compartments. Anterior pituitary cells are known to possess both secretory granules and synaptic-like microvesicles (42, 43). In the central nervous system, VGLUT1 and VGLUT2 are contained in small clear vesicles of synaptic terminals (2–4, 38). Furthermore, although the analogous organelles, synaptic-like microvesicles contain the VGLUT1 and VGLUT2 isoforms in the pineal gland (19), Hayashi *et al.* (21) reported that the α-cells of the pancreatic Langerhans islets contain VGLUT2 in glucagone-containing secretory granules, and cosecrete stoichiometric amounts of glutamate and glucagone under low glucose conditions. The putative localization of VGLUT2 in adenohypophysial microvesicles appears to gain support from our unpublished observation that gonadotrope and thyrotrope cells are strongly immunoreactive to "SV2", an immunocytochemical marker of synaptic-like microvesicles. However, the presence of VGLUT2 in microvesicles awaits direct ultrastructural confirmation.

The functional significance of VGLUT2 we found in gonadotrope and thyrotrope cells is unclear. In view of recent data showing low-glucose-induced corelease of glutamate with glucagone from endocrine cells of the Langerhans islet (21), glutamate secretion from stimulated adenohypophysial cells is highly possible. Of particular note in the context of the proposed glutamate cosecretion is our observation that the activated thyrotropes of hypothyroid male rats showed not only a decreased TSH immunoreactivity, but their immunostaining for VGLUT2 was also attenuated. The increased secretion rate offers an explanation for the apparent paradox between the increased synthesis and the decreased visibility of both secretory compounds. If glutamate is, indeed, secreted, it likely exerts autocrine and paracrine effects upon the endocrine cells. Corroborating this concept, ionotropic as well as metabotropic glutamate receptors have been identified in adenohypophysial cells (14, 15). However, it is worth noting that a previous study demonstrated N-methyl-D-aspartate R1 subunit expression in only relatively low percentages of adenohypophysial cells (<12% for each cell type) and, unlike we found for VGLUT2, there was no preferential association of N-methyl-D-aspartate R1 with any particular cell type (14). Furthermore, it seems somewhat paradoxical that group II metabotropic glutamate receptors (mGLUR2/3) have been identified in the somatotrope and lactotrope cells (15) most of which were found in the present study not to contain VGLUT2. One explanation for such a discrepancy may be a putative cross-talk between adenohypophysial cell types (gonadotropes and thyrotropes) secreting glutamate and those having receptors for it. The intimate relationship of lactotrope cells with VGLUT2 expressing gonadotropes, that we observed in the present studies, may support this idea. An example for such a paracrine glutamatergic regulation has been described in the Langerhans islets. Although insulin-secreting β-cells are devoid of VGLUTs (21), the stimulation of α-amino-3-hydroxy-5-methyl-4-isoxazole propionic acid-type ionotropic glutamate receptors on these cells,

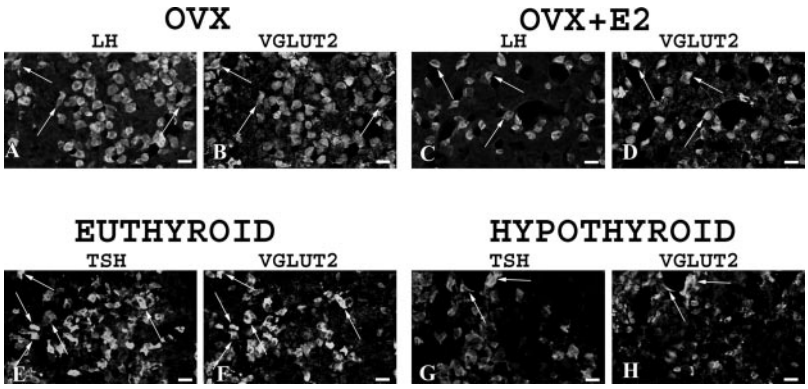

FIG. 6. The effects of estrogen treatment and hypothyroidism on the morphology and VGLUT2 immunoreactivity of gonadotrope and thyrotrope cells. A–D, Black-and-white confocal images of adenohypophysial LH (A, C) and VGLUT2 (B, D) cells indicate that nearly all LH cells contain VGLUT2 in OVX as well as in OVX + E2 rats. *Arrows* point to examples of dual-labeled cells (identical cells in the corresponding panels). E–H, A large subset of thyrotrope cells (E) also contain VGLUT2 (F) in euthyroid rat, whereas hypothyroidism, induced with methimazole in the drinking water, significantly decreased the ratio of VGLUT2-containing thyrotrope cells. *Arrows* point to dual-labeled cells in corresponding panels (E and F; G and H). Note the increased size and the attenuated TSH immunostaining of the activated cells (G), in addition to the disappearance of VGLUT2 from many of them. *Scale bars*, 25 μm.

which is likely exerted by the paracrine action of α-cell-derived glutamate, can enhance the secretion of GABA from synaptic-like microvesicles (21). We also have to recognize that adenohypophysial cell types not showing VGLUT2 immunoreactivity in the present study may contain low levels of VGLUT2 that are below the detection threshold of our method. In particular, the low percentage (<8%) of lactotrope, somatotrope, and corticotrope cells that we found to contain VGLUT2 appears to support the hypothesis that these cells may also store glutamate under certain functional conditions. Alternatively, other than the VGLUT2 isoform of VGLUTs may occur in these cells and confer a glutamatergic phenotype. Further studies thus will be needed to address the amino acid content of these cell types.

The up-regulation of adenohypophysial VGLUT2 mRNA levels by estradiol or hypothyroidism may be indicative of increased VGLUT2 protein synthesis when estrogen levels rise or thyroid hormone levels decrease. As gonadotrope cells possess estrogen receptors (44, 45), and several phenotypes of anterior lobe cells, including thyrotropes and gonadotropes, also possess thyroid hormone receptors (46), it is possible that nuclear hormone receptors directly regulate VGLUT2 gene expression in these cells. Alternatively, the rise of VGLUT2 mRNA may be secondary to synthetic and secretory changes induced by the altered estrogen and thyroid hormone feedback to the pituitary and/or to the endocrine hypothalamus. The exact mechanisms of these changes and the issue of whether the increased VGLUT2 expression in estrogen-treated and hypothyroid rats is due to an increase in the number of VGLUT2 synthesizing cells, an increase in VGLUT2 mRNA copy number in individual gonadotropes and thyrotropes, or both, will require clarification.

In summary, the present immunocytochemical and ISH studies established the presence of the authentic VGLUT2 molecule in large subsets of gonadotrope and thyrotrope cells and smaller subsets of other cell types in the adenohypophysis. Furthermore, either an estrogen regimen administered to ovariectomized rats, or hypothyroidism induced by methimazole in the drinking water of male rats, could up-regulate adenohypophysial VGLUT2 mRNA levels. Finally, despite the increased VGLUT2 mRNA synthesis in hypothyroid rats, the activated TSH cells of hypothyroid rats exhibited less VGLUT2 immunoreactivity, which may be indicative of an increased rate of glutamate secretion. The physiological significance of endogeneous glutamate stores in adenohypohysial cells will require clarification.

Acknowledgments

The authors are grateful to Drs. J. P. Herman and G. Nagy for providing the VGLUT2–734 cDNA and PRL antibodies, respectively, and to Gyöngyi Kékesi and Hajni Bekó for the excellent technical assistance.

Received September 26, 2005. Accepted April 27, 2006.

Address all correspondence and requests for reprints to: Dr. Erik Hrabovszky, Laboratory of Endocrine Neurobiology, Institute of Experimental Medicine, Hungarian Academy of Sciences, Szigony u. 43, Budapest, 1083 Hungary. E-mail: hrabovszky@koki.hu.

This research was supported by grants from the National Science Foundation of Hungary (OTKA T43407, T46574, T46492), NKFP 1A/002/2004, and the European Union FP6 funding (contract no. LSHM-CT-2003-50304). This publication reflects the authors' views and not necessarily those of the European Union. The information in this document is provided as is, and no guarantee or warranty is given that the information is fit for any particular purpose. The user thereof uses the information at its sole risk and liability.

Disclosure: All of the authors have nothing to declare.

References

1. **Bellocchio EE, Reimer RJ, Fremeau Jr RT, Edwards RH** 2000 Uptake of glutamate into synaptic vesicles by an inorganic phosphate transporter. Science 289:957–960
2. **Fremeau Jr RT, Troyer MD, Pahner I, Nygaard GO, Tran CH, Reimer RJ, Bellocchio EE, Fortin D, Storm-Mathisen J, Edwards RH** 2001 The expression of vesicular glutamate transporters defines two classes of excitatory synapse. Neuron 31:247–260
3. **Fujiyama F, Furuta T, Kaneko T** 2001 Immunocytochemical localization of candidates for vesicular glutamate transporters in the rat cerebral cortex. J Comp Neurol 435:379–387
4. **Herzog E, Bellenchi GC, Gras C, Bernard V, Ravassard P, Bedet C, Gasnier B, Giros B, El Mestikawy S** 2001 The existence of a second vesicular glutamate transporter specifies subpopulations of glutamatergic neurons. J Neurosci 21:RC181
5. **Fremeau Jr RT, Burman J, Qureshi T, Tran CH, Proctor J, Johnson J, Zhang H, Sulzer D, Copenhagen DR, Storm-Mathisen J, Reimer RJ, Chaudhry FA, Edwards RH** 2002 The identification of vesicular glutamate transporter 3 suggests novel modes of signaling by glutamate. Proc Natl Acad Sci USA 99:14488–14493
6. **Gras C, Herzog E, Bellenchi GC, Bernard V, Ravassard P, Pohl M, Gasnier B, Giros B, El Mestikawy S** 2002 A third vesicular glutamate transporter expressed by cholinergic and serotoninergic neurons. J Neurosci 22:5442–5451
7. **Schafer MK, Varoqui H, Defamie N, Weihe E, Erickson JD** 2002 Molecular cloning and functional identification of mouse vesicular glutamate transporter 3 and its expression in subsets of novel excitatory neurons. J Biol Chem 277:50734–50748
8. **Ziegler DR, Cullinan WE, Herman JP** 2002 Distribution of vesicular glutamate transporter mRNA in rat hypothalamus. J Comp Neurol 448:217–229
9. **Lin W, McKinney K, Liu L, Lakhlani S, Jennes L** 2003 Distribution of vesicular glutamate transporter-2 messenger ribonucleic acid and protein in the septum-hypothalamus of the rat. Endocrinology 144:662–670
10. **Sakata-Haga H, Kanemoto M, Maruyama D, Hoshi K, Mogi K, Narita M, Okado N, Ikeda Y, Nogami H, Fukui Y, Kojima I, Takeda J, Hisano S** 2001 Differential localization and colocalization of two neuron-types of sodium-dependent inorganic phosphate cotransporters in rat forebrain. Brain Res 902:143–155
11. **Hrabovszky E, Turi GF, Kallo I, Liposits Z** 2004 Expression of vesicular

glutamate transporter-2 in gonadotropin-releasing hormone neurons of the adult male rat. Endocrinology 145:4018–4021
12. **Hrabovszky E, Wittmann G, Turi GF, Liposits Z, Fekete C** 2005 Hypophysiotropic thyrotropin-releasing hormone and corticotropin-releasing hormone neurons of the rat contain vesicular glutamate transporter-2. Endocrinology 146:341–347
13. **Hrabovszky E, Turi GF, Liposits Z** 2005 Presence of vesicular glutamate transporter-2 in hypophysiotropic somatostatin but not growth hormone-releasing hormone neurons of the male rat. Eur J Neurosci 21:2120–2126
14. **Bhat GK, Mahesh VB, Chu ZW, Chorich LP, Zamorano PL, Brann DW** 1995 Localization of the *N*-methyl-D-aspartate R1 receptor subunit in specific anterior pituitary hormone cell types of the female rat. Neuroendocrinology 62:178–186
15. **Caruso C, Bottino MC, Pampillo M, Pisera D, Jaita G, Duvilanski B, Seilicovich A, Lasaga M** 2004 Glutamate induces apoptosis in anterior pituitary cells through group II metabotropic glutamate receptor activation. Endocrinology 145:4677–4684
16. **Hrabovszky E, Csapo AK, Kallo I, Wilheim T, Turi GF, Liposits Z** 2006 Localization and osmotic regulation of vesicular glutamate transporter-2 in magnocellular neurons of the rat hypothalamus. Neurochem Intl 48:753–761
17. **Kawasaki A, Hoshi K, Kawano M, Nogami H, Yoshikawa H, Hisano S** 2005 Up-regulation of VGLUT2 expression in hypothalamic-neurohypophysial neurons of the rat following osmotic challenge. Eur J Neurosci 22:672–680
18. **Moriyama Y, Yamamoto A** 2004 Glutamatergic chemical transmission: look! Here, there, and anywhere. J Biochem (Tokyo) 135:155–163
19. **Morimoto R, Hayashi M, Yatsushiro S, Otsuka M, Yamamoto A, Moriyama Y** 2003 Co-expression of vesicular glutamate transporters (VGLUT1 and VGLUT2) and their association with synaptic-like microvesicles in rat pinealocytes. J Neurochem 84:382–391
20. **Hayashi M, Otsuka M, Morimoto R, Hirota S, Yatsushiro S, Takeda J, Yamamoto A, Moriyama Y** 2001 Differentiation-associated Na^+-dependent inorganic phosphate cotransporter (DNPI) is a vesicular glutamate transporter in endocrine glutamatergic systems. J Biol Chem 276:43400–43406
21. **Hayashi M, Yamada H, Uehara S, Morimoto R, Muroyama A, Yatsushiro S, Takeda J, Yamamoto A, Moriyama Y** 2003 Secretory granule-mediated cosecretion of L-glutamate and glucagon triggers glutamatergic signal transmission in islets of Langerhans. J Biol Chem 278:1966–1974
22. **Martin GK, Wise RP, Lonsbury-Martin BL** 1983 Frozen-section autoradiography of the cochlea: evidence for differential distribution of amino acids. Ann Otol Rhinol Laryngol 92:254–258
23. **Hrabovszky E, Petersen SL** 2002 Increased concentrations of radioisotopically-labeled complementary ribonucleic acid probe, dextran sulfate, and dithiothreitol in the hybridization buffer can improve results of in situ hybridization histochemistry. J Histochem Cytochem 50:1389–1400
24. **Hrabovszky E, Kallo I, Steinhauser A, Merchenthaler I, Coen CW, Liposits Z** 2004 Estrogen receptor-β in oxytocin and vasopressin neurons of the rat and human hypothalamus. Immunocytochemical and in situ hybridization studies. J Comp Neurol 473:315–333
25. **Demaria JE, Nagy GM, Freeman ME** 2000 Immunoneutralization of prolactin prevents stimulatory feedback of prolactin on hypothalamic neuroendocrine dopaminergic neurons. Endocrine 12:333–337
26. **Léránt AA, Nagy GM** 1994 Analysis of autocrine and paracrine interactions in the pituitary gland by the reverse hemolytic plaque assay. Neuroprotocols 5:198–208
27. **Brown TJ, Naftolin F, Maclusky NJ** 1992 Sex differences in estrogen receptor binding in the rat hypothalamus: effects of subsaturating pulses of estradiol. Brain Res 578:129–134
28. **Segerson TP, Hoefler H, Childers H, Wolfe HJ, Wu P, Jackson IM, Lechan RM** 1987 Localization of thyrotropin-releasing hormone prohormone messenger ribonucleic acid in rat brain in situ hybridization. Endocrinology 121: 98–107
29. **Kakucska I, Rand W, Lechan RM** 1992 Thyrotropin-releasing hormone gene expression in the hypothalamic paraventricular nucleus is dependent upon feedback regulation by both triiodothyronine and thyroxine. Endocrinology 130:2845–2850
30. **Raptis S, Fekete C, Sarkar S, Rand WM, Emerson CH, Nagy GM, Lechan RM** 2004 Cocaine- and amphetamine-regulated transcript co-contained in thyrotropin-releasing hormone (TRH) neurons of the hypothalamic paraventricular nucleus modulates TRH-induced prolactin secretion. Endocrinology 145:1695–1699
31. **DeFesi CR, Astier HS, Surks MI** 1979 Kinetics of thyrotrophs and somatotrophs during development of hypothyroidism and L-triiodothyronine treatment of hypothyroid rats. Endocrinology 104:1172–1180
32. **Masson J, Sagne C, Hamon M, El Mestikawy S** 1999 Neurotransmitter transporters in the central nervous system. Pharmacol Rev 51:439–464
33. **Ni B, Rosteck Jr PR, Nadi NS, Paul SM** 1994 Cloning and expression of a cDNA encoding a brain-specific Na^+-dependent inorganic phosphate cotransporter. Proc Natl Acad Sci USA 91:5607–5611
34. **Takamori S, Rhee JS, Rosenmund C, Jahn R** 2000 Identification of a vesicular glutamate transporter that defines a glutamatergic phenotype in neurons. Nature 407:189–194
35. **Bai L, Xu H, Collins JF, Ghishan FK** 2001 Molecular and functional analysis of a novel neuronal vesicular glutamate transporter. J Biol Chem 276:36764–36769
36. **Takamori S, Rhee JS, Rosenmund C, Jahn R** 2001 Identification of differentiation-associated brain-specific phosphate transporter as a second vesicular glutamate transporter (VGLUT2). J Neurosci 21:RC182
37. **Varoqui H, Schafer MK, Zhu H, Weihe E, Erickson JD** 2002 Identification of the differentiation-associated Na^+/PI transporter as a novel vesicular glutamate transporter expressed in a distinct set of glutamatergic synapses. J Neurosci 22:142–155
38. **Bellocchio EE, Hu H, Pohorille A, Chan J, Pickel VM, Edwards RH** 1998 The localization of the brain-specific inorganic phosphate transporter suggests a specific presynaptic role in glutamatergic transmission. J Neurosci 18:8648–8659
39. **Kobayashi H, Matsui T, Ishii S** 1970 Functional electron microscopy of the hypothalamic median eminence. Int Rev Cytol 29:281–381
40. **Diano S, Naftolin F, Horvath TL** 1998 Kainate glutamate receptors (GluR5–7) in the rat arcuate nucleus: relationship to tanycytes, astrocytes, neurons and gonadal steroid receptors. J Neuroendocrinol 10:239–247
41. **Eyigor O, Jennes L** 1998 Identification of kainate-preferring glutamate receptor subunit GluR7 mRNA and protein in the rat median eminence. Brain Res 814:231–235
42. **Cussac D, Leblanc P, L'Heritier A, Bertoglio J, Lang P, Kordon C, Enjalbert A, Saltarelli D** 1996 Rho proteins are localized with different membrane compartments involved in vesicular trafficking in anterior pituitary cells. Mol Cell Endocrinol 119:195–206
43. **Majo G, Aguado F, Blasi J, Marsal J** 1998 Synaptobrevin isoforms in secretory granules and synaptic-like microvesicles in anterior pituitary cells. Life Sci 62:607–616
44. **Mitchner NA, Garlick C, Ben-Jonathan N** 1998 Cellular distribution and gene regulation of estrogen receptors α and β in the rat pituitary gland. Endocrinology 139:3976–3983
45. **Vaillant C, Chesnel F, Schausi D, Tiffoche C, Thieulant ML** 2002 Expression of estrogen receptor subtypes in rat pituitary gland during pregnancy and lactation. Endocrinology 143:4249–4258
46. **Sasaki S, Nakamura H, Tagami T, Osamura Y, Imura H** 1991 Demonstration of nuclear 3,5,3′-triiodothyronine receptor proteins in gonadotrophs and corticotrophs in rat anterior pituitary by double immunohistochemical staining. Endocrinology 129:511–516

***Endocrinology* is published monthly by The Endocrine Society (http://www.endo-society.org), the foremost professional society serving the endocrine community.**

12. számú melléklet

Neuroscience 144 (2007) 1383–1392

GLUTAMATERGIC INNERVATION OF THE HYPOTHALAMIC MEDIAN EMINENCE AND POSTERIOR PITUITARY OF THE RAT

E. HRABOVSZKY,[a]* L. DELI,[a] G. F. TURI,[a] I. KALLÓ[a,b] AND Z. LIPOSITS[a,b]

[a]*Laboratory of Endocrine Neurobiology, Institute of Experimental Medicine, Hungarian Academy of Sciences, P.O. Box 67, 1450 Budapest, Hungary*

[b]*Department of Neuroscience, Faculty of Information Technology, Péter Pázmány Catholic University, 1083 Budapest, Hungary*

Abstract—Recent studies have localized the glutamatergic cell marker type-2 vesicular glutamate transporter (VGLUT2) to distinct peptidergic neurosecretory systems that regulate hypophysial functions in rats. The present studies were aimed to map the neuronal sources of VGLUT2 in the median eminence and the posterior pituitary, the main terminal fields of hypothalamic neurosecretory neurons. Neurons innervating these regions were identified by the uptake of the retrograde tract-tracer Fluoro-Gold (FG) from the systemic circulation, whereas glutamatergic perikarya of the hypothalamus were visualized via the radioisotopic *in situ* hybridization detection of VGLUT2 mRNA. The results of dual-labeling studies established that the majority of neurons accumulating FG and also expressing VGLUT2 mRNA were located within the paraventricular, periventricular and supraoptic nuclei and around the organum vasculosum of the lamina terminalis and the preoptic area. In contrast, only few FG-accumulating cells exhibited VGLUT2 mRNA signal in the arcuate nucleus. Dual-label immunofluorescent studies of the median eminence and posterior pituitary to determine the subcellular location of VGLUT2, revealed the association of VGLUT2 immunoreactivity with SV2 protein, a marker for small clear vesicles in neurosecretory endings. Electron microscopic studies using pre-embedding colloidal gold labeling confirmed the localization of VGLUT2 in small clear synaptic vesicles.

These data suggest that neurosecretory neurons located mainly within the paraventricular, anterior periventricular and supraoptic nuclei and around the organum vasculosum of the lamina terminalis and the preoptic area secrete glutamate into the fenestrated vessels of the median eminence and posterior pituitary. The functional aspects of the putative neuropeptide/glutamate co-release from neuroendocrine terminals remain to be elucidated.

Key words: glutamate, hypophysiotropic, neurosecretion, portal circulation, synaptic vesicle, VGLUT2.

*Corresponding author. Tel: +36-1-210-9400x366; fax: +36-1-210-9944.
E-mail address: hrabovszky@koki.hu (E. Hrabovszky).

Abbreviations: ARH, arcuate nucleus of the hypothalamus; BSA, bovine serum albumin; FG, Fluoro-Gold; ME, median eminence; OVLT, organum vasculosum of the lamina terminalis; PBS, phosphate-buffered saline; Pe, periventricular nucleus of the hypothalamus; POA, preoptic area; PP, posterior pituitary; PVH, paraventricular nucleus of the hypothalamus; SO, supraoptic nucleus of the hypothalamus; SSC, standard saline citrate; TBS, Tris-buffered saline; VGLUT, vesicular glutamate transporter.

The major excitatory synaptic transmitter L-glutamate (van den Pol et al., 1990; Brann, 1995) is accumulated into synaptic vesicles by three molecular forms of vesicular glutamate transporters (VGLUT1-3) which are expressed by distinct subsets of glutamatergic excitatory neurons (Bellocchio et al., 2000; Fremeau et al., 2001, 2002; Fujiyama et al., 2001; Herzog et al., 2001; Sakata-Haga et al., 2001; Gras et al., 2002; Schafer et al., 2002; Ziegler et al., 2002; Lin et al., 2003). The *in situ* hybridization detection of VGLUT2 mRNA has established high expression levels of the VGLUT2 transporter isoform in several anatomical regions that are critically important in neuroendocrine regulation; these include the preoptic area (POA), the organum vasculosum of the lamina terminalis (OVLT) and the paraventricular (PVH), supraoptic (SO) and anterior periventricular (Pe) hypothalamic nuclei (Ziegler et al., 2002; Collin et al., 2003; Lin et al., 2003; Eyigor et al., 2004; Hrabovszky et al., 2004, 2005a,b,c, 2006). As opposed to these hypophysiotropic regions populated densely by excitatory glutamatergic neurons, the hypothalamic arcuate nucleus (ARH), which plays a crucially important role in the regulation of growth hormone and prolactin secretion, is dominated by inhibitory GABA containing neurons over glutamatergic cells (Hrabovszky et al., 2005a). Results of recent colocalization experiment by dual-label *in situ* hybridization and dual-label immunocytochemistry have also demonstrated that some glutamatergic cells in hypophysiotropic regions are identical with the known hypophysiotropic neurons secreting classical peptide releasing and release-inhibiting hormones into the hypophysial portal circulation. Parvicellular neurosecretory systems synthesizing VGLUT2 mRNA and protein, include gonadotropin-releasing hormone neurons in the POA and the OVLT (Hrabovszky et al., 2004), thyrotropin-releasing hormone (Hrabovszky et al., 2005c) and corticotropin-releasing hormone (Hrabovszky et al., 2005c) neurons in the PVH and somatostatin (Hrabovszky et al., 2005b) neurons in the PVH and the anterior Pe. In addition, magnocellular oxytocin and vasopressin neurons in both the PVH and the SO share the VGLUT2 phenotype with these parvicellular systems (Kawasaki et al., 2005; Hrabovszky et al., 2006). In contrast, tubero-infundibular dopaminergic (Meister and Hokfelt, 1988) and growth hormone-releasing hormone synthesizing (Meister and Hokfelt, 1988; Hrabovszky et al., 2005b) neurons of the ARH appear to exhibit a GABA amino acid neurotransmitter phenotype.

The goal of the present studies was to map the distribution of VGLUT2-synthesizing glutamatergic neurons that regulate hypophysial functions via innervating the median eminence (ME) and the posterior pituitary (PP). To this

0306-4522/07$30.00+0.00
doi:10.1016/j.neuroscience.2006.10.053

aim, we have used the neuronal uptake of the retrograde tracer, Fluoro-Gold (FG) from the systemic circulation, as a marker of neurosecretory systems which project their axon outside of the blood–brain barrier (Schmued and Fallon, 1986; Merchenthaler, 1991b). The immunofluorescent visualization of FG was combined with the *in situ* hybridization detection of VGLUT2 mRNA in histological sections, in order to identify the hypophysiotropic glutamatergic neuronal systems. The subcellular distribution of VGLUT2 protein in neurosecretory terminals was also addressed with a series of immunofluorescent and pre-embedding immunoelectron microscopic studies of neuroendocrine axon terminals in the ME and PP.

EXPERIMENTAL PROCEDURES

Animals

Prepubertal male Wistar rats (N=10; 150 g bw) were purchased from Charles-River Hungary Ltd. (Isaszeg, Hungary) and maintained in a light- and temperature-controlled environment (lights on 05:00–19:00 h; 22 °C) with free access to standard laboratory food (Sniff Spezialdiaeten GmbH, Soest, Germany) and tap water. All experiments were carried out in accordance with the Council Directive of 24 November 1986 of the European Communities (86/609/EEC) and were reviewed and approved by the Animal Welfare Committee of the Institute of Experimental Medicine (47/003/2005). All protocols were designed to minimize both the total number of animals used and their suffering.

Localization of glutamatergic cell bodies projecting outside the blood–brain barrier

Retrograde labeling of hypophysiotropic neurons with FG. To label hypophysiotropic neurons via the uptake and retrograde transport of FG from the systemic circulation (Merchenthaler, 1991b), four rats at the age of 6 weeks were injected i.p. with 16 mg/kg, bw of FG (hydroxystilbamidine methanesulfonate; Molecular Probes, Eugene, OR, USA; dissolved in distilled water) and allowed to survive for 2 weeks.

Tissue collection for combined immunocytochemical/in situ *hybridization studies.* The FG-injected rats were anesthetized with pentobarbital (35 mg/kg bw, i.p.) and perfused transcardially with 150 ml fixative solution containing 4% paraformaldehyde (Sigma Chemical Company, St. Louis, MO, USA) in 0.1 M phosphate-buffered saline (PBS; pH 7.4). The hypothalami were dissected and soaked in 20% sucrose overnight for cryoprotection. Then, they were snap-frozen on powdered dry ice and 20-μm-thick free-floating coronal sections were prepared from the preoptic-hypothalamic region using a Leica CM 3050 S cryostat (Leica Microsystems Nussloch Gmbh, Nussloch, Germany).

Immunofluorescent detection of FG. The tissue mRNAs were protected against enzymatic degradation by adding 1000 U/ml of heparin sodium salt (Hofler et al., 1987) to the immunocytochemical reagents and by using diethyl pyrocarbonate-pretreated and autoclaved 0.1 M PBS (pH 7.4) as a rinsing solution between the incubation steps. The sections were blocked against non-specific antibody binding with 1% bovine serum albumin (BSA; fraction V; Sigma) in PBS for 30 min and transferred into anti-FG antiserum (AB153; Chemicon, Temecula, CA, USA; 1:5000) for 24 h. The primary antibodies were reacted with biotin-SP-anti-rabbit IgG (Jackson ImmunoResearch Laboratories, West Grove, PA, USA; 1:1000) and streptavidin conjugated to the red fluorochrome Cy3 (Jackson; 1:250) for 4 h. The sections were mounted from sterile buffer solution onto microscope slides coated with (3-aminopropyl) triethoxy-silane (Sigma), air-dried and processed for the radioisotopic *in situ* hybridization detection of VGLUT2 mRNA, as described elsewhere for fresh-frozen tissue sections (Hrabovszky et al., 2004, 2005c).

Detection of VGLUT2 mRNA with radioisotopic in situ *hybridization.* Prior to hybridization, the section were re-fixed in 4% paraformaldehyde for 5 min, acetylated with 0.25% acetic anhydride in 0.9% NaCl/0.1 M triethanolamine (Sigma Chemical Company; pH 8.0) for 10 min, rinsed in standard saline citrate solution (2× SSC; 1× SSC=0.15 M NaCl/0.015 M sodium citrate, pH 7.0) for 2 min, dehydrated in 70, 80, 95 and 100% ethanol (2 min each), delipidated in chloroform for 5 min, and finally, rehydrated partially in 100%, followed by 95% ethanol, for 2 min each. The slides were then air-dried on slide trays and hybridized with a ^{35}S-labeled complementary RNA hybridization probe targeting bases 522–1400 of VGLUT2 mRNA (GenBank acc. # NM 053427); the "VGLUT2-879" complementary DNA template to transcribe this probe has been prepared in our laboratory and validated in previous *in situ* hybridization experiments (Hrabovszky et al., 2004, 2005c). To prevent the formation of high autoradiographic background, 1000 mM dithiothreitol has been added to the hybridization solution (Hrabovszky and Petersen, 2002). Further, an enhanced hybridization signal has been achieved via using high concentrations of radioisotopic probe (80,000 cpm/μl) and dextran sulfate (20%) in the hybridization solution, as formally established in previous experiments (Hrabovszky and Petersen, 2002). After the overnight hybridization at 52 °C, the non-specifically bound probe was digested with 50 μg/ml ribonuclease A (Sigma; dissolved in 0.5 M NaCl/10 mMTris–HCl/1 mM EDTA; pH 7.8) for 60 min at 37 °C, followed by a stringent treatment step to further clear the signal (55 °C in 0.1× SSC solution for 60 min). The slides were dipped into MQ water for 2 s, rinsed in 70% ethanol for 5 min and air-dried. The autoradiographs were visualized on Kodak NTB-3 nuclear track emulsion (Kodak; Rochester, NY, USA) with Kodak processing chemicals after 2 weeks of exposure at 4 °C in the dark. The sections were finally dehydrated with graded ethanol (95%, followed by 100%; 5 min each), cleared in xylene (2×5 min), coverslipped with DPX mounting medium (Fluka Chemie; Buchs, Switzerland) and examined with a Zeiss Axiophot epifluorescent microscope (Zeiss; Göttingen, Germany) using an epifluorescent filter set with the following parameters: excitation of 540–590 nM, bandpass of 595 nm, and emission of 600–660 nm. The autoradiographic signal was examined under dark-field illumination. The fluorescent and autoradiographic images of the same section area were captured with an RT Spot digital camera (Diagnostic Instruments, Sterling Heights, MI, USA), processed as separate layers using the Adobe Photoshop 7.0.1 software (Adobe Systems Inc., Berkeley, CA, USA). The colocalization of the signals for FG and VGLUT2 mRNA was demonstrated on merged digital images.

In situ *hybridization control experiments.* For positive control, test sections from the hypothalami were hybridized using a distinct antisense probe to VGLUT2 mRNA ("VGLUT2-734"; complementary to bases 1704–2437), as described earlier (Hrabovszky et al., 2004, 2005c). The complementary DNA template to prepare this probe was kindly donated by Dr. J. P. Herman (University of Cincinnati Medical Center, Cincinnati, OH, USA). As a negative control approach, sense RNA transcripts were applied to the sections.

Immunofluorescent analysis of glutamatergic axon terminals in the ME and PP

Tissue preparation for immunocytochemistry. Three adult male rats were anesthetized with pentobarbital (35 mg/kg bw, i.p.) and perfused transcardially with 150 ml fixative solution containing 4% paraformaldehyde. The hypothalami were dissected and soaked in 25% sucrose overnight for cryoprotection. The pituitaries were first

embedded into egg yolk which was hardened in formalin fume (Hrabovszky et al., 2006) and then soaked in 25% sucrose. Then, 20-μm-thick free-floating coronal sections were cut through the ME and the PP using a cryostat. The sections were rinsed in Tris-buffered saline (TBS; 0.1 M Tris–HCl/0.9% sodium chloride; pH 7.8), treated with a mixture of 0.5% H_2O_2 and 0.2% Triton X-100 (Sigma) for 20 min, and finally incubated in blocking solution (2% normal horse serum/NHS/in TBS) for 30 min.

Immunocytochemical procedures. Following pretreatments, the sections were incubated in a polyclonal anti-VGLUT2 antiserum raised in a guinea pig (AB5907; Chemicon; 1:1000) for 72 h at 4 °C. The primary antibodies were reacted with donkey, biotin-SP-anti-guinea-pig IgG (Jackson ImmunoResearch; 1:1000) for 2 h and then with streptavidin-conjugated to the red Cy3 fluorochrome (Jackson ImmunoResearch; 1:250) for 2 h. The detection of VGLUT2 was followed by the immunofluorescent visualization of SV2 protein which was found selectively associated with small clear vesicles within neurosecretory terminals (Walch-Solimena et al., 1993; Zhang et al., 2000). The anti-SV2 monoclonal antibodies (Developmental Studies Hybridoma Bank; The University of Iowa, Iowa City, IA, USA) (Buckley and Kelly, 1985), which recognized both the SV2A and SV2B isoforms (Bajjalieh et al., 1993), were applied to the sections for 48 h at 4 °C and then, reacted with FITC-conjugated anti-mouse antibodies (Jackson, 1:200; 12 h). The dual-labeled sections were mounted on microscope slides from 0.05 M Tris–HCl solution (pH 7.8), dried and coverslipped with Vectashield mounting medium (Vector). Dual-immunofluorescent specimens were analyzed with a Radiance 2100 confocal microscope (Bio-Rad Laboratories, Hemel Hempstead, UK) using laser excitation lines 488 nm for FITC and 543 nm for Cy3 and dichroic/emission filters 560 nm/500–530 nm for FITC and 560–610 nm for Cy3. Individual optical slices were collected for the analysis in "lambda strobing" mode so that only one excitation laser and the corresponding emission detector were active during a line scan. This has eliminated emission-type cross-talk. Individual optical slices were used to study and illustrate the phenomenon of axonal colocalization (Hrabovszky et al., 2005b).

Immunocytochemical control experiments. Negative and positive control strategies to assess the specificity of VGLUT2 immunolabeling were used as described recently (Hrabovszky et al., 2004). The previous approach included use of primary antibodies (AB5907) preabsorbed with 10 μM of the immunization antigen (AG209; Chemicon) (Hrabovszky et al., 2004). In positive control studies, the AB5907 guinea-pig anti-VGLUT2 antibodies from Chemicon were used in combination with rabbit anti-VGLUT2 antibodies from SYnaptic SYstems (AB 135103; 1:5,000; Göttingen, Germany) for dual-immunofluorescent experiments. The different primary antibodies were reacted with appropriate secondary antibody-fluorochrome conjugates (anti-guinea-pig-FITC and anti-rabbit-Cy3, respectively; Jackson ImmunoResearch) for 12 h. The colocalization of the two signals was confirmed in the hypothalamus with confocal microscopy.

Electron microscopic localization of VGLUT2 in hypophysiotropic axon terminals in the ME and PP

Tissue preparation for immunocytochemistry. Three adult male rats were anesthetized with pentobarbital (35 mg/kg bw, i.p.) and killed by decapitation. The hypothalami and pituitaries were removed rapidly and fixed for 24 h by immersion into a freshly-made fixative solution containing 4% paraformaldehyde, 0.3% glutaraldehyde and 15% (V/V) saturated picric acid in 0.1 M PBS (pH 7.4). The tissues were fixed further for 3 days in the same fixative, with the omission of glutaraldehyde. The basal hypothalamus and the pituitaries were sliced at 50 μm with a Vibratome (Technical Products International, St. Louis, MO, USA).

Preembedding colloidal gold labeling. Pre-embedding immuno-electron microscopy was used for the ultrastructural analysis of VGLUT2 immunoreactivity in the ME and PP. The sections were first treated with 0.5% sodium borohydride in 0.1 M PBS (pH 7.4) for 20 min to eliminate residual aldehydes and then infiltrated with increasing concentrations of sucrose in 0.1 M PBS (pH 7.4) for cryoprotection (7.5%, 15% and 30%; 20 min for each). Subsequently the tissues were permeabilized by three repeated freeze-thaw cycles on liquid nitrogen. For the immunocytochemical detection of VGLUT2, the sections were incubated for four days in a 1:1000 dilution of the rabbit primary antibodies against VGLUT2 (AB 135103; SYnaptic SYstems). These antibodies performed better than the guinea-pig anti-VGLUT2 antibodies following the use of glutaraldehyde in the tissue fixative. The primary antibody incubation was followed by a 30-min blocking step using 0.1% cold-water fish gelatin (Electron Microscopy Sciences, Fort Washington, PA, USA) and 1% BSA (fraction V; Sigma) in 0.1 M PBS (pH 7.4), and then, an overnight incubation in goat anti-rabbit IgG conjugated with 1.4 nM ultra small gold particles (Electron Microscopy Sciences; diluted at 1:100 with the blocking reagent). The sections were rinsed briefly with the same blocking reagent, followed by PBS. Then they were treated with 2% glutaraldehyde in PBS for 10 min and rinsed in distilled water (3×5 min). The silver-intensification of gold particles was carried out according to the instructions provided with the Aurion R-Gent SE-LM silver enhancing kit (AURION ImmunoGold Reagents & Accessories, Wageningen, The Netherlands). Hypothalamic and hypophysial sections were osmicated (0.5% osmium tetroxide in 0.1 M PBS, 20 min) and dehydrated in serial dilutions of ethanol. A 30-min contrasting step using 1% uranyl acetate in 70% ethanol was inserted in this procedure and the fully dehydrated sections were finally infiltrated with propylene oxide and flat-embedded at 60 °C in TAAB 812 Embedding resin (TAAB Laboratory Equipments Ltd., Aldermaston, Berks, UK) on microscope slides that were pre-coated with liquid release agent (Electron Microscopy Sciences). Ultrathin (50–60 nm) sections were cut from the resin blocks with a Leica ultracut UCT ultramicrotome (Leica Microsystems AG, Wetzlar, Germany), collected onto Formvar-coated single-slot grids and examined with a Hitachi 7100 (Yokohama, Japan) transmission electron microscope.

RESULTS

Localization of glutamatergic cell bodies projecting outside the blood–brain barrier

The immunofluorescent visualization of FG was combined successfully with the subsequent *in situ* hybridization detection of VGLUT2 mRNA in hypothalamic tissue sections. The distribution of FG-accumulating neuronal cell bodies projecting outside the blood–brain barrier was in agreement with previous reports (Merchenthaler et al., 1986; Lopez et al., 1991; Merchenthaler, 1991a, 1992; Merchenthaler and Lennard, 1991; Lennard et al., 1993; Liposits et al., 1993; Merchenthaler and Liposits, 1994). Such neurons were visualized in high numbers within regions known to regulate hypophysial functions, including both the parvicellular and magnocellular subdivisions of the PVH (Fig. 1B), the dorso-medial and ventro-lateral subdivisions of the ARH (Fig. 1F), the anterior Pe, the SO (Fig. 1I), the OVLT and the POA regions (Merchenthaler, 1991b). Diencephalic neurons expressing VGLUT2 mRNA occurred as clusters of silver grains on the autoradiographs (Fig. 1A, E, H) and hypothalamic neurons exhibited a wide range of VGLUT2 hybridization signal. Corroborating previous re-

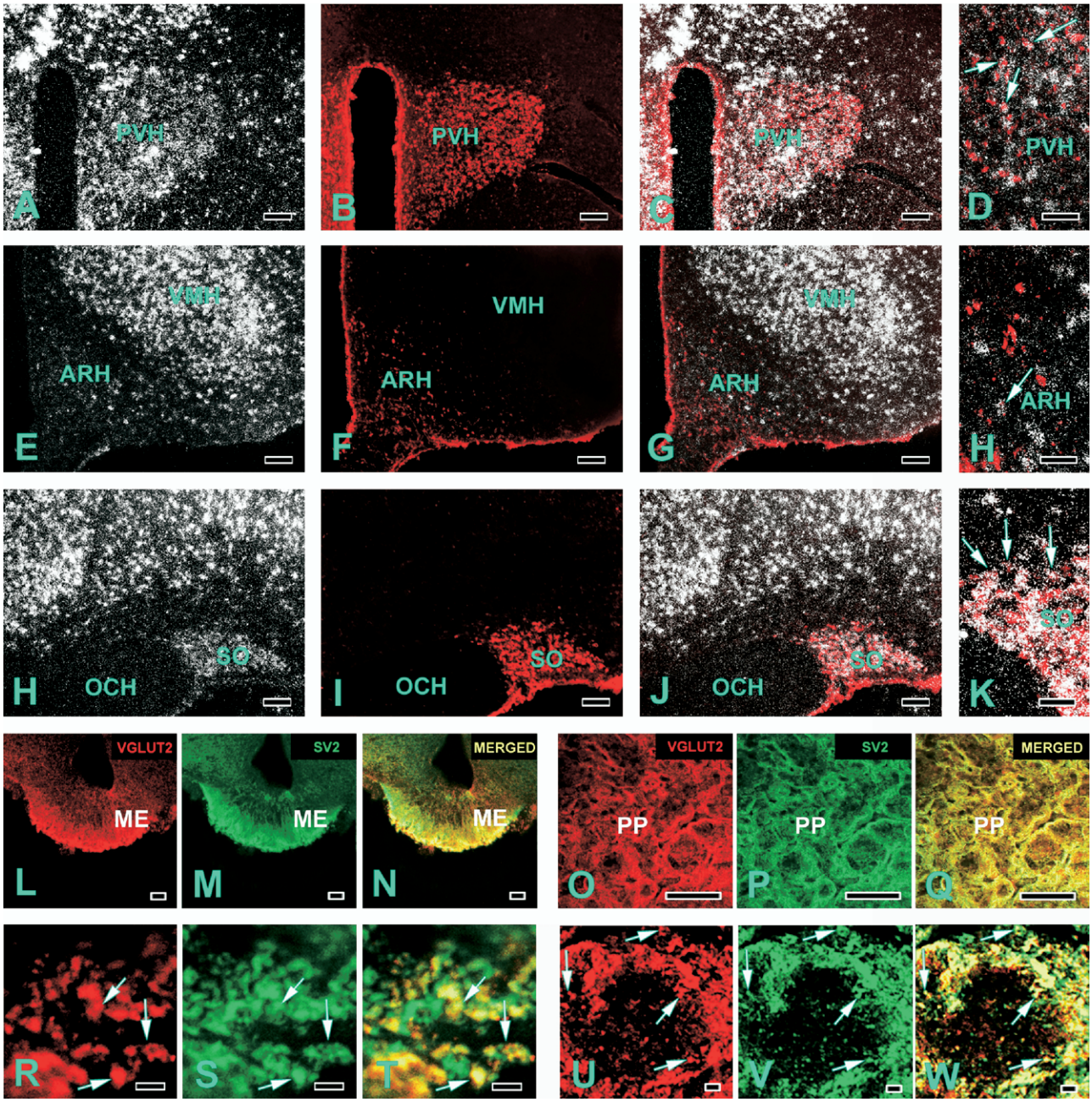

Fig. 1. Localization of glutamatergic neuronal elements innervating the hypothalamic ME and the PP. Combined detection of the glutamatergic neuronal cell marker type-2 vesicular glutamate transporter (VGLUT2) mRNA (*in situ* hybridization autoradiographs; A, E, H) and FG accumulation (red immuno-fluorescent signal; B, F, I) reveals hypothalamic glutamatergic systems that have an access to the peripheral circulation. Merged panels (C and J) reveal that the parvicellular (medially) and magnocellular (laterally) subdivisions of the PVH as well as the SO, comprise numerous glutamatergic cells that terminate outside the blood–brain barrier. Arrows in high-power images point to parvicellular neurons of the PVH (D) and magnocellular neurons of the SO (K) that also exhibit the immuno-fluorescent signal for FG. In contrast with the abundance of VGLUT2-expressing cells in these nuclei, the ARH contains only a few and weakly labeled glutamatergic cells (E) which mostly occur laterally. Although FG-positive cells are abundant in the ARH (F), with very few exceptions (e.g. arrow in H) they are distinct from the glutamatergic neurons of the ARH (H). Simultaneous immuno-fluorescent visualization of VGLUT2 (L, O, R, U) and SV2 (a synaptic vesicle marker in neurosecretory endings; M, P, S, V) reveals similarities in the two distribution patterns in both the external zone of the ME and the PP. The prominent yellow color in merged panels (N and Q) indicates the association of VGLUT2 with small clear vesicles in the ME and the PP. White arrows in high-power images of the ME (R–T) point to axon varicosities dual-labeled for VGLUT2 and SV2. Single-labeled profiles also seen in the ME (green color in T) likely represent terminals containing some classical neurotransmitter different from glutamate. High magnification panels from the PP (U–V) demonstrate that most immunoreactive profiles are dual-labeled (arrows), suggesting the major neurotransmitter of synaptic vesicles is glutamate in the PP. Scale bars=2 μm in R–T; 5 μm in U–W; 50 μm in D, H, K, O–Q; and 100 μm in the other panels.

ports (Ziegler et al., 2002; Collin et al., 2003; Lin et al., 2003; Eyigor et al., 2004), glutamatergic neurons formed prominent cell populations in several hypothalamic nuclei that play important roles in neuroendocrine regulation, in-

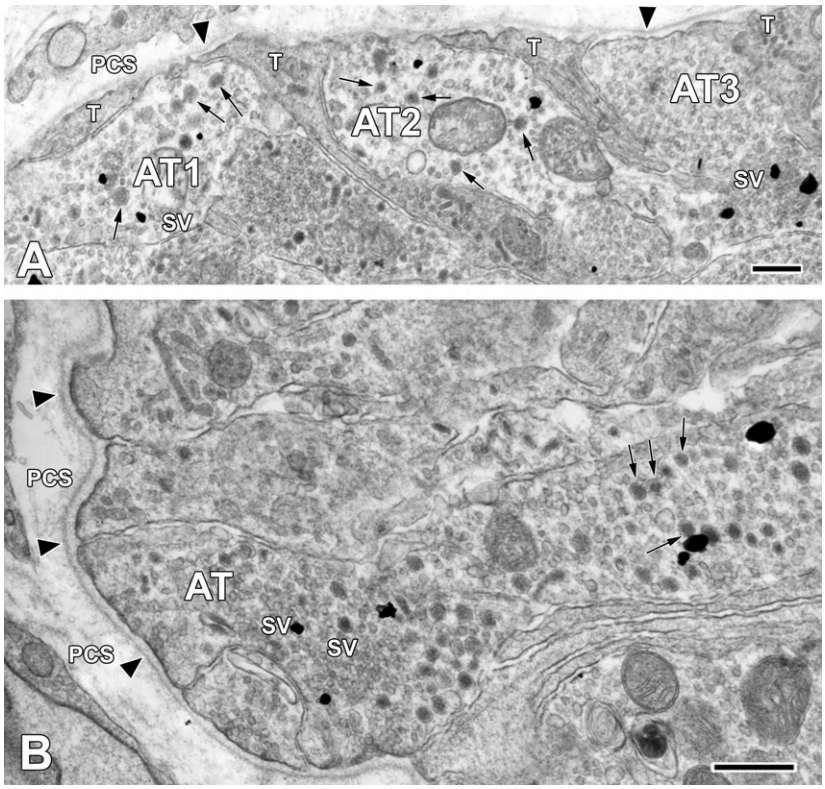

Fig. 2. Electron microscopic localization of VGLUT2 immunoreactivity in the external zone of the ME. (A) Three neuroendocrine axon terminals (AT1-3) freely communicate with the pericapillary space (PCS) of portal blood vessels. Arrowheads delineate the basal lamina. AT1 and AT2 contain both dense-core vesicles (DV; arrows) and small clear vesicles (SV), whereas AT3 comprises SVs only. The silver-intensified gold particles identify the VGLUT2 content of the terminals. Note that the immunocytochemical label is preferentially associated with subcellular sites densely populated by SVs, indicating that VGLUT2 is contained in SVs. (B) A glutamatergic axon terminal (AT) terminates on the external limiting membrane (arrowheads) of a portal capillary. Arrowheads delineate the basal lamina. Note the presence of DVs (arrows) as well as SVs in the same terminal profile and the association of the VGLUT2 immune signal with SVs. Scale bars=0.5 μm.

cluding various parvicellular and magnocellular subdivisions of the PVH (Fig. 1A), the anterior Pe, the SO (Fig. 1H), the OVLT and the POA. The non-hypophysiotropic ventromedial nucleus consisted of a particularly prominent glutamatergic cell mass. The heavy labeling of this nucleus contrasted the paucity of VGLUT2 expressing neurons in the ARH (Fig. 1E). Neurons accumulating FG and also expressing VGLUT2 mRNA occurred in high numbers in the OVLT, in the POA, in the Pe, in parvicellular as well as magnocellular subdivisions of the PVH (Fig. 1C, D) and in the SO (Fig. 1J, K). Accessory magnocellular neurons between the PVH and the SO were also dual-labeled for FG and VGLUT2 mRNA. In contrast, FG-labeled hypophysiotropic neurons in the dorso-medial and ventro-lateral subdivisions of the ARH were devoid of VGLUT2 mRNA (Fig. 1G, H). Except for a few cases, the relatively weakly-labeled glutamatergic neurons in the lateral ARH were devoid of FG signal, indicating that they do not project to the ME (Fig. 1G, H).

Immunofluorescent characterization of glutamatergic terminals in the ME and PP

Dual-immunofluorescent studies revealed a dense plexus of VGLUT2-immunoreactive axons in the external zone of the ME. The heaviest VGLUT2 immunostaining occurred superficially in the external layer where the hypophysiotropic axons terminate (Fig. 1L, R). No significant VGLUT2 signal was detected according to the cross-sectioned magnocellular tract traversing in the internal layer toward the posterior lobe. This distribution pattern exhibited an excellent match with that of the small clear vesicle marker protein, SV2 (Fig. 1L–N; 1R–T). The presence of SV2-immunoreactive structures without VGLUT2 signal was also obvious, suggesting that not all synaptic vesicles contain the glutamatergic marker in the ME (Fig. 1T). In the PP, the VGLUT2 immunoreactive elements were organized into lobular structures surrounding capillaries (Fig. 1O). Most VGLUT2 immunoreactive profiles were apparently identical with the SV2 immunoreactive elements (Fig. 1O–Q; 1U–W).

Ultrastructural localization of VGLUT2 in neurosecretory axons terminating in the ME and PP

Pre-embedding colloidal gold labeling for VGLUT2 identified numerous glutamatergic axon terminals in the external layer of the ME. Many of these axons established direct contact with the external limiting membrane of portal vessels (Fig. 2A, B), indicating they represent neurosecretory terminals. The labeled structures contained small clear as well as dense-core vesicles at a highly variable ratio. The

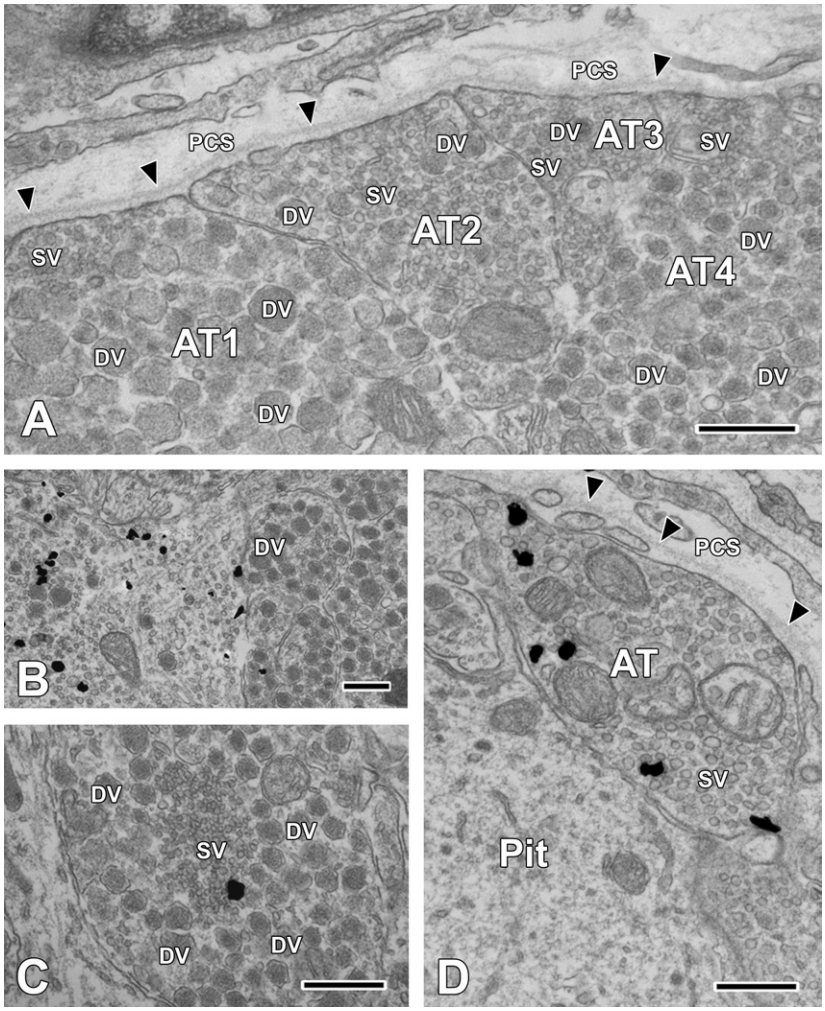

Fig. 3. Ultrastructural localization of VGLUT2 immunoreactivity in the PP. (A) Neuroendocrine axon terminals (AT1–4) in contact with the basal lamina (arrowheads) contain dense-core vesicles (DV) as well as varying amounts of small clear vesicles (SV). Note a typical accumulation of SVs in the immediate proximity of the pericapillary space (PCS) in AT1 and AT4. The profiles of AT2 and AT3 are dominated by SVs, and contain a few DVs only. (B) Pre-embedding colloidal-gold labeling for VGLUT2, followed by silver intensification, reveals the preferential distribution of immunocytochemical signal in axonal profiles dominated by SVs. Note the absence of metal particles in non-terminal neuroendocrine axons (right half of panel) which mostly contain DVs. (C) High-power image of a non-terminal immuno-labeled neuroendocrine axon demonstrates DVs peripherally and a group of SVs centrally. (D) A neuroendocrine axon terminal immunolabeled for VGLUT2, contains SVs exclusively, indicating further the association of VGLUT2 with SVs and not DVs. While on the left the terminal is neighbored by a pituicyte (Pit), on the right it is in open communication toward the PCS. Arrowheads delineate the basal lamina. Scale bars=0.5 μm.

immunocytochemical labeling clearly tended to occur at subcellular domains occupied primarily by small clear vesicles (Fig. 2A, B). Neuroendocrine fibers of the PP contained small clear as well as dense-core vesicles (Fig. 3A). As a tendency, non-terminal axons in the PP were dominated by large dense-core vesicles (Fig. 3B), whereas the terminal segments of magnocellular axons contacting the basal lamina typically contained numerous small clear vesicles (Fig. 3A). The immunocytochemical labeling for VGLUT2 tended to occur in neuronal profiles that were dominated by small clear vesicles (Fig. 3B). Axons with mixed vesicular content typically contained the labeling around groups of small clear vesicles (Fig. 3C). Finally, the concept that VGLUT2 is found in small clear vesicles was further strengthened by numerous examples of heavily immunolabeled axon terminals which contained small clear vesicles only (Fig. 3D).

DISCUSSION

In this study, we mapped the distribution of preoptic/hypothalamic neurons that project to areas devoid of blood–brain barrier, including the ME and the PP, and also express a marker for glutamatergic neuronal phenotype, VGLUT2. In addition, ultrastructural observations indicate that VGLUT2, unlike the secretory peptide neurohormones, is localized to small clear vesicles within the neuroendocrine axon terminals.

When administered into the systemic circulation, FG is only taken up by nerve terminals in regions devoid of

blood–brain barrier. These include circumventricular organs, such as the ME, the OVLT, the subfornical organ, the area postrema, the pineal gland and the PP (Ambalavanar and Morris, 1989; Merchenthaler, 1991b). This property of FG has been successfully exploited in a large number of studies which identified the hypophysiotropic subsets of various peptidergic neuronal systems (Merchenthaler et al., 1986, 1989; Witkin, 1990; Lopez et al., 1991; Merchenthaler, 1991a, 1992; Merchenthaler and Lennard, 1991; Lennard et al., 1993; Liposits et al., 1993; Merchenthaler and Liposits, 1994). Beyond the convenience of this approach compared with the use of previous surgical techniques to directly inject retrograde tracers into the ME (Setalo and Merchenthaler, 1990), some uncertainty always exists as to the actual site of tracer uptake when using systemic FG injections, as discussed by Merchenthaler (1991b). While this also adds some complexity to the interpretation of our findings, the ME and the PP undoubtedly represent the most significant projection fields of hypothalamic neurons outside the blood–brain barrier (Merchenthaler, 1991b).

The findings of the present studies that FG-accumulating glutamatergic neurons are widely distributed around the OVLT/POA region, in different parvicellular and magnocellular subdivisions of the PVH, in the SO and in the Pe, are in accordance with our previous reports which established VGLUT2 mRNA expression within classical parvicellular and magnocellular neurosecretory neurons at the same locations (Hrabovszky et al., 2004, 2005b,c, 2006). In addition to visualize these cells as double-labeled neurons, in the present studies we may have observed FG-accumulating glutamatergic neurons potentially distinct from the hypophysiotropic gonadotropin-releasing hormone, thyrotropin releasing hormone, corticotropin-releasing hormone and somatostatin neurons. Merchenthaler and co-workers have described large populations of FG-accumulating cells in the PVH which contained galanin (Merchenthaler, 1991a) enkephalin (Merchenthaler, 1992) or neurotensin (Merchenthaler and Lennard, 1991). In view that i) as a rule, peptidergic neurons also contain some classical neurotransmitter (Hokfelt, 1991), ii) VGLUT2 mRNA is widely distributed in all subdivisions of the PVH, and iii) GABA containing neurons are rare within this nucleus (Hrabovszky et al., 2005c), it is very likely that the amino acid phenotype of galanin, enkephalin and neurotensin containing paraventricular neurons is also glutamatergic. It still remains to be determined to what extent these peptidergic cell populations overlap with hypophysiotropic neurons that secrete the classical releasing and release inhibiting hormones into the portal circulation. The absence of VGLUT2 from neuroendocrine neurons of the ARH corroborates the previous observations that tuberoinfundibular dopaminergic and GHRH neurons exhibit a GABA-ergic neuronal phenotype (Meister and Hokfelt, 1988; Schimchowitsch et al., 1991; Hrabovszky et al., 2005b). In addition, as dopaminergic neurons innervating the intermediate lobe of the hypophysis also exhibit a GABA/dopamine dual-phenotype (Schimchowitsch et al., 1991), they also likely occurred as single-labeled neurons for FG in the present study. Finally, the neurochemical identity of the weakly VGLUT2-positive non-neuroendocrine neurons in the lateral ARH remains to be determined. The results of previous studies make it likely that these neurons are, at least partly, identical with proopiomelanocortin cells (Collin et al., 2003; Kiss et al., 2005).

The ultrastructural distribution of VGLUT2 in small clear, and not dense-core, vesicles agrees with the presumed site of location of classical neurotransmitters, including L-glutamate. This location is also in agreement with the association of VGLUT1 and VGLUT2 immunoreactivities with small clear vesicles in excitatory synapses (Fremeau et al., 2001; Fujiyama et al., 2001; Herzog et al., 2001) but differs from the reported subcellular distribution of VGLUT2 in the alpha cells of the pancreatic Langerhans islets which secrete stoichiometric amounts of glucagon and glutamate under low glucose conditions and contain VGLUT2 in glucagon-containing secretory granules, instead of synaptic-like microvesicles (Hayashi et al., 2003). It is worth noting that neuroendocrine axons were particularly rich in small clear vesicles close to their termination around the pericapillary space both in the ME and the PP. Inversely, dense-core granules were often decreased in number as the neuroendocrine axons approached the basal lamina. Previous studies have revealed a similar change in the vesicular composition of corticotropin-releasing hormone containing axons in the ME in that dense-core vesicles dominated the preterminals, whereas small clear vesicles became more characteristic to terminals reaching the pericapillary space (Liposits and Paull, 1985). Glutamate immunoreactive small clear vesicles also had a tendency to accumulate at the terminal segment of magnocellular axons in the PP (Meeker et al., 1991), which is in line with our present finding of VGLUT2 immunoreactive small clear vesicles in magnocellular terminals. To some extent the differential distribution of the two types of vesicles is also reminiscent to their relationship at chemical synapses of various species. The presynaptic specialization contains primarily small clear vesicles, whereas dense-core granules do not tend to occur close to the synaptic specializations (Buma and Roubos, 1986; Zhu et al., 1986).

Regulated exocytosis of synaptic vesicles and dense-core vesicles is partially based on conserved mechanisms and in both cases involves the elevation of intracellular calcium levels in response to stimulation. However, the exocytosis of synaptic vesicles is induced by lower-frequency stimuli which may elevate calcium levels primarily near calcium channels, and cargo release is short (milliseconds) (Morgan and Burgoyne, 1997). In contrast, the exocytosis of dense-core granules is induced by stimuli (e.g. high frequency electrical stimuli) that may elevate calcium levels at greater distances from calcium channels in the bulk cytoplasm, resulting in a long-lasting (minutes) cargo release (Dutton and Dyball, 1979; Morgan and Burgoyne, 1997). In theory, this difference implies that glutamate may already be elicited from neuroendocrine terminals by stimuli that do not evoke phasic neuropeptide release if local Ca^{2+} levels rise sufficiently around small

clear vesicles. Using the tannic acid method, Morris and Pow (1991) have provided evidence that in the hypothalamus only a fraction of the peptidergic vesicles is exocytosed into the synaptic cleft. Similar studies of the magnocellular neurosecretory system also revealed that all parts of their extensive terminal arborization in the PP are capable of exocytosing peptide neurosecretory granules. In contrast, the obvious accumulation of small clear vesicles within neurosecretory endings both in the ME and the PP and the identification of VGLUT2 immunoreactivity in these terminals suggest that glutamate release is spatially more restricted than that of neuroendocrine peptides.

To elucidate the role of glutamate co-secretion in neuroendocrine regulation, it is of prime importance to first find and characterize glutamate receptors in the ME and PP. Theoretically, such receptors may be located on the neuroendocrine terminals to inhibit or facilitate peptide neurosecretion. The putative existence of autocrine/paracrine glutamatergic mechanisms in the terminal regulation of gonadotropin-releasing hormone neurosecretion receives substantial support from i) the recent observation that gonadotropin-releasing hormone terminals contain VGLUT2 (Hrabovszky et al., 2004), ii) the identification of immunoreactivities for the kainate-2 and the *N*-methyl-D-aspartate-1 ionotropic glutamate receptor subunits on gonadotropin releasing hormone-immunoreactive terminals (Kawakami et al., 1998a,b) and iii) the ability of ionotropic glutamate receptor agonists to elicit gonadotropin-releasing hormone release from the mediobasal hypothalamus (Donoso et al., 1990; Lopez et al., 1992; Arias et al., 1993; Zuo et al., 1996; Kawakami et al., 1998b). Glutamate receptors may also be present on glial and vascular elements of the ME and PP to influence their functions, possibly including morphological plasticity. Tanycytes lining the ventral wall of the third ventricle and astrocytes of the ME were, indeed, found to contain mRNAs and immunoreactivity for kainate receptors (Diano et al., 1998; Eyigor and Jennes, 1998; Kawakami, 2000) and to also express the activity marker c-Fos immunoreactivity in response to stimulation by kainate (Eyigor and Jennes, 1998). From the occurrence of VGLUT2 in functionally and neurochemically diverse neurosecretory endings, it is tempting to speculate that intrinsic L-glutamate fulfills similar regulatory functions in several neuroendocrine systems and may contribute to the generation of the pulsatile patterns of neurohormone output. Nevertheless, this hypothesis would require experimental support.

CONCLUSION

In summary, in this study we show that the glutamatergic innervation of the ME and PP is primarily derived from neurons around the OVLT/POA, in the anterior Pe, PVH and SO. We also provide ultrastructural evidence for the association of VGLUT2 with small clear vesicles which tend to occupy the terminal segments of neurosecretory systems in the ME and the PP. The functional significance of endogenous glutamate in neuroendocrine cells requires clarification.

Acknowledgments—This research was supported by grants from the National Science Foundation of Hungary (OTKA T43407, T46574), NKFP 1A/002/2004 and the European Union FP6 funding (contract no. LSHM-CT-2003-50304). This publication reflects the authors' views and not necessarily those of the European Union. The information in this document is provided as is, and no guarantee or warranty is given that the information is fit for any particular purpose. The user thereof uses the information at its sole risk and liability. The study was supported in part by Gedeon Richter Ltd. (Hungary). The authors are grateful to Dr. J. P. Herman for providing the VGLUT2-734 plasmid and to Hajni Bekó for the excellent technical assistance.

REFERENCES

Ambalavanar R, Morris R (1989) Fluoro-Gold injected either subcutaneously or intravascularly results in extensive retrograde labelling of CNS neurones having axons terminating outside the blood-brain barrier. Brain Res 505:171–175.

Arias P, Jarry H, Leonhardt S, Moguilevsky JA, Wuttke W (1993) Estradiol modulates the LH release response to N-methyl-D-aspartate in adult female rats: studies on hypothalamic luteinizing hormone-releasing hormone and neurotransmitter release. Neuroendocrinology 57:710–715.

Bajjalieh SM, Peterson K, Linial M, Scheller RH (1993) Brain contains two forms of synaptic vesicle protein 2. Proc Natl Acad Sci U S A 90:2150–2154.

Bellocchio EE, Reimer RJ, Fremeau RT Jr, Edwards RH (2000) Uptake of glutamate into synaptic vesicles by an inorganic phosphate transporter. Science 289:957–960.

Brann DW (1995) Glutamate: a major excitatory transmitter in neuroendocrine regulation. Neuroendocrinology 61:213–225.

Buckley K, Kelly RB (1985) Identification of a transmembrane glycoprotein specific for secretory vesicles of neural and endocrine cells. J Cell Biol 100:1284–1294.

Buma P, Roubos EW (1986) Ultrastructural demonstration of nonsynaptic release sites in the central nervous system of the snail Lymnaea stagnalis, the insect Periplaneta americana, and the rat. Neuroscience 17:867–879.

Collin M, Backberg M, Ovesjo ML, Fisone G, Edwards RH, Fujiyama F, Meister B (2003) Plasma membrane and vesicular glutamate transporter mRNAs/proteins in hypothalamic neurons that regulate body weight. Eur J Neurosci 18:1265–1278.

Diano S, Naftolin F, Horvath TL (1998) Kainate glutamate receptors (GluR5-7) in the rat arcuate nucleus: relationship to tanycytes, astrocytes, neurons and gonadal steroid receptors. J Neuroendocrinol 10:239–247.

Donoso AO, Lopez FJ, Negro-Vilar A (1990) Glutamate receptors of the non-N-methyl-D-aspartic acid type mediate the increase in luteinizing hormone-releasing hormone release by excitatory amino acids in vitro. Endocrinology 126:414–420.

Dutton A, Dyball RE (1979) Phasic firing enhances vasopressin release from the rat neurohypophysis. J Physiol 290:433–440.

Eyigor O, Jennes L (1998) Identification of kainate-preferring glutamate receptor subunit GluR7 mRNA and protein in the rat median eminence. Brain Res 814:231–235.

Eyigor O, Lin W, Jennes L (2004) Identification of neurones in the female rat hypothalamus that express oestrogen receptor-alpha and vesicular glutamate transporter-2. J Neuroendocrinol 16: 26–31.

Fremeau RT Jr, Burman J, Qureshi T, Tran CH, Proctor J, Johnson J, Zhang H, Sulzer D, Copenhagen DR, Storm-Mathisen J, Reimer RJ, Chaudhry FA, Edwards RH (2002) The identification of vesicular glutamate transporter 3 suggests novel modes of signaling by glutamate. Proc Natl Acad Sci U S A 99:14488–14493.

Fremeau RT Jr, Troyer MD, Pahner I, Nygaard GO, Tran CH, Reimer RJ, Bellocchio EE, Fortin D, Storm-Mathisen J, Edwards RH

(2001) The expression of vesicular glutamate transporters defines two classes of excitatory synapse. Neuron 31:247–260.

Fujiyama F, Furuta T, Kaneko T (2001) Immunocytochemical localization of candidates for vesicular glutamate transporters in the rat cerebral cortex. J Comp Neurol 435:379–387.

Gras C, Herzog E, Bellenchi GC, Bernard V, Ravassard P, Pohl M, Gasnier B, Giros B, El Mestikawy S (2002) A third vesicular glutamate transporter expressed by cholinergic and serotoninergic neurons. J Neurosci 22:5442–5451.

Hayashi M, Yamada H, Uehara S, Morimoto R, Muroyama A, Yatsushiro S, Takeda J, Yamamoto A, Moriyama Y (2003) Secretory granule-mediated co-secretion of L-glutamate and glucagon triggers glutamatergic signal transmission in islets of Langerhans. J Biol Chem 278:1966–1974.

Herzog E, Bellenchi GC, Gras C, Bernard V, Ravassard P, Bedet C, Gasnier B, Giros B, El Mestikawy S (2001) The existence of a second vesicular glutamate transporter specifies subpopulations of glutamatergic neurons. J Neurosci 21:RC181.

Hofler H, Putz B, Ruhri C, Wirnsberger G, Klimpfinger M, Smolle J (1987) Simultaneous localization of calcitonin mRNA and peptide in a medullary thyroid carcinoma. Virchows Arch B Cell Pathol Incl Mol Pathol 54:144–151.

Hokfelt T (1991) Neuropeptides in perspective: the last ten years. Neuron 7:867–879.

Hrabovszky E, Csapo AK, Kallo I, Wilheim T, Turi GF, Liposits Z (2006) Localization and osmotic regulation of vesicular glutamate transporter-2 in magnocellular neurons of the rat hypothalamus. Neurochem Int 48:753–761.

Hrabovszky E, Halasz J, Meelis W, Kruk MR, Liposits Z, Haller J (2005a) Neurochemical characterization of hypothalamic neurons involved in attack behavior: glutamatergic dominance and co-expression of thyrotropin-releasing hormone in a subset of glutamatergic neurons. Neuroscience 133:657–666.

Hrabovszky E, Turi GF, Liposits Z (2005b) Presence of vesicular glutamate transporter-2 in hypophysiotropic somatostatin but not growth hormone-releasing hormone neurons of the male rat. Eur J Neurosci 21:2120–2126.

Hrabovszky E, Wittmann G, Turi GF, Liposits Z, Fekete C (2005c) Hypophysiotropic thyrotropin-releasing hormone and corticotropin-releasing hormone neurons of the rat contain vesicular glutamate transporter-2. Endocrinology 146:341–347.

Hrabovszky E, Petersen SL (2002) Increased concentrations of radioisotopically-labeled complementary ribonucleic acid probe, dextran sulfate, and dithiothreitol in the hybridization buffer can improve results of in situ hybridization histochemistry. J Histochem Cytochem 50:1389–1400.

Hrabovszky E, Turi GF, Kallo I, Liposits Z (2004) Expression of vesicular glutamate transporter-2 in gonadotropin-releasing hormone neurons of the adult male rat. Endocrinology 145:4018–4021.

Kawakami S (2000) Glial and neuronal localization of ionotropic glutamate receptor subunit-immunoreactivities in the median eminence of female rats: GluR2/3 and GluR6/7 colocalize with vimentin, not with glial fibrillary acidic protein (GFAP). Brain Res 858:198–204.

Kawakami S, Ichikawa M, Murahashi K, Hirunagi K, Tsukamura H, Maeda K (1998a) Excitatory amino acids act on the median eminence nerve terminals to induce gonadotropin-releasing hormone release in female rats. Gen Comp Endocrinol 112:372–382.

Kawakami SI, Hirunagi K, Ichikawa M, Tsukamura H, Maeda KI (1998b) Evidence for terminal regulation of GnRH release by excitatory amino acids in the median eminence in female rats: a dual immunoelectron microscopic study. Endocrinology 139:1458–1461.

Kawasaki A, Hoshi K, Kawano M, Nogami H, Yoshikawa H, Hisano S (2005) Up-regulation of VGLUT2 expression in hypothalamic-neurohypophysial neurons of the rat following osmotic challenge. Eur J Neurosci 22:672–680.

Kiss J, Csaba Z, Csaki A, Halasz B (2005) Glutamatergic innervation of neuropeptide Y and pro-opiomelanocortin-containing neurons in the hypothalamic arcuate nucleus of the rat. Eur J Neurosci 21:2111–2119.

Lennard DE, Eckert WA, Merchenthaler I (1993) Corticotropin-releasing hormone neurons in the paraventricular nucleus project to the external zone of the median eminence: a study combining retrograde labeling with immunocytochemistry. J Neuroendocrinol 5:175–181.

Lin W, McKinney K, Liu L, Lakhlani S, Jennes L (2003) Distribution of vesicular glutamate transporter-2 messenger ribonucleic acid and protein in the septum-hypothalamus of the rat. Endocrinology 144:662–670.

Liposits Z, Merchenthaler I, Reid JJ, Negro-Vilar A (1993) Galanin-immunoreactive axons innervate somatostatin-synthesizing neurons in the anterior periventricular nucleus of the rat. Endocrinology 132:917–923.

Liposits Z, Paull WK (1985) Ultrastructural alterations of the paraventriculo-infundibular corticotropin releasing factor (CRF)-immunoreactive neuronal system in long term adrenalectomized rats. Peptides 6:1021–1036.

Lopez FJ, Donoso AO, Negro-Vilar A (1992) Endogenous excitatory amino acids and glutamate receptor subtypes involved in the control of hypothalamic luteinizing hormone-releasing hormone secretion. Endocrinology 130:1986–1992.

Lopez FJ, Merchenthaler I, Ching M, Wisniewski MG, Negro-Vilar A (1991) Galanin: a hypothalamic-hypophysiotropic hormone modulating reproductive functions. Proc Natl Acad Sci U S A 88: 4508–4512.

Meeker RB, Swanson DJ, Greenwood RS, Hayward JN (1991) Ultrastructural distribution of glutamate immunoreactivity within neurosecretory endings and pituicytes of the rat neurohypophysis. Brain Res 564:181–193.

Meister B, Hokfelt T (1988) Peptide- and transmitter-containing neurons in the mediobasal hypothalamus and their relation to GABAergic systems: possible roles in control of prolactin and growth hormone secretion. Synapse 2:585–605.

Merchenthaler I (1991a) The hypophysiotropic galanin system of the rat brain. Neuroscience 44:643–654.

Merchenthaler I (1991b) Neurons with access to the general circulation in the central nervous system of the rat: a retrograde tracing study with Fluoro-gold. Neuroscience 44:655–662.

Merchenthaler I (1992) Enkephalin-immunoreactive neurons in the parvicellular subdivisions of the paraventricular nucleus project to the external zone of the median eminence. J Comp Neurol 326:112–120.

Merchenthaler I, Csontos C, Kallo I, Arimura A (1986) The hypothalamo-infundibular growth hormone-releasing hormone (GH-RH) system of the rat. Brain Res 378:297–302.

Merchenthaler I, Lennard DE (1991) The hypophysiotropic neurotensin-immunoreactive neuronal system of the rat brain. Endocrinology 129:2875–2880.

Merchenthaler I, Liposits Z (1994) Mapping of thyrotropin-releasing hormone (TRH) neuronal systems of rat forebrain projecting to the median eminence and the OVLT. Immunocytochemistry combined with retrograde labeling at the light and electron microscopic levels. Acta Biol Hung 45:361–374.

Merchenthaler I, Setalo G, Csontos C, Petrusz P, Flerko B, Negro-Vilar A (1989) Combined retrograde tracing and immunocytochemical identification of luteinizing hormone-releasing hormone- and somatostatin-containing neurons projecting to the median eminence of the rat. Endocrinology 125:2812–2821.

Morgan A, Burgoyne RD (1997) Common mechanisms for regulated exocytosis in the chromaffin cell and the synapse. Semin Cell Dev Biol 8:141–149.

Morris JF, Pow DV (1991) Widespread release of peptides in the central nervous system: quantitation of tannic acid-captured exocytoses. Anat Rec 231:437–445.

Sakata-Haga H, Kanemoto M, Maruyama D, Hoshi K, Mogi K, Narita M, Okado N, Ikeda Y, Nogami H, Fukui Y, Kojima I, Takeda J,

Hisano S (2001) Differential localization and colocalization of two neuron-types of sodium-dependent inorganic phosphate cotransporters in rat forebrain. Brain Res 902:143–155.

Schafer MK, Varoqui H, Defamie N, Weihe E, Erickson JD (2002) Molecular cloning and functional identification of mouse vesicular glutamate transporter 3 and its expression in subsets of novel excitatory neurons. J Biol Chem 277:50734–50748.

Schimchowitsch S, Vuillez P, Tappaz ML, Klein MJ, Stoeckel ME (1991) Systematic presence of GABA-immunoreactivity in the tubero-infundibular and tubero-hypophyseal dopaminergic axonal systems: an ultrastructural immunogold study on several mammals. Exp Brain Res 83:575–586.

Schmued LC, Fallon JH (1986) Fluoro-Gold: a new fluorescent retrograde axonal tracer with numerous unique properties. Brain Res 377:147–154.

Setalo G, Merchenthaler I (1990) Translingual approach of the basal surface of the diencephalon of the rat and retrograde labeling from the median eminence. J Neurosci Methods 35:169–173.

van den Pol AN, Wuarin JP, Dudek FE (1990) Glutamate, the dominant excitatory transmitter in neuroendocrine regulation. Science 250:1276–1278.

Walch-Solimena C, Takei K, Marek KL, Midyett K, Sudhof TC, De Camilli P, Jahn R (1993) Synaptotagmin: a membrane constituent of neuropeptide-containing large dense-core vesicles. J Neurosci 13:3895–3903.

Witkin JW (1990) Access of luteinizing hormone-releasing hormone neurons to the vasculature in the rat. Neuroscience 37:501–506.

Zhang L, Volknandt W, Gundelfinger ED, Zimmermann H (2000) A comparison of synaptic protein localization in hippocampal mossy fiber terminals and neurosecretory endings of the neurohypophysis using the cryo-immunogold technique. J Neurocytol 29:19–30.

Zhu PC, Thureson-Klein A, Klein RL (1986) Exocytosis from large dense cored vesicles outside the active synaptic zones of terminals within the trigeminal subnucleus caudalis: a possible mechanism for neuropeptide release. Neuroscience 19:43–54.

Ziegler DR, Cullinan WE, Herman JP (2002) Distribution of vesicular glutamate transporter mRNA in rat hypothalamus. J Comp Neurol 448:217–229.

Zuo Z, Mahesh VB, Zamorano PL, Brann DW (1996) Decreased gonadotropin-releasing hormone neurosecretory response to glutamate agonists in middle-aged female rats on proestrus afternoon: a possible role in reproductive aging? Endocrinology 137:2334–2338.

(Accepted 28 October 2006)
(Available online 18 December 2006)

13. számú melléklet

THE JOURNAL OF COMPARATIVE NEUROLOGY 503:270–279 (2007)

Distribution of Type 1 Cannabinoid Receptor (CB1)-Immunoreactive Axons in the Mouse Hypothalamus

GÁBOR WITTMANN,[1] LEVENTE DELI,[1] IMRE KALLÓ,[1] ERIK HRABOVSZKY,[1] MASAHIKO WATANABE,[2] ZSOLT LIPOSITS,[1,3] AND CSABA FEKETE[1,4]*

[1]Department of Endocrine Neurobiology, Institute of Experimental Medicine, Hungarian Academy of Sciences, Budapest, Hungary 1083

[2]Department of Anatomy, Hokkaido University School of Medicine, Sapporo, Japan 060-8638

[3]Department of Neuroscience, Faculty of Information Technology, Pázmány Péter Catholic University, Budapest, Hungary 1083

[4]Tupper Research Institute and Department of Medicine, Division of Endocrinology, Diabetes, Metabolism and Molecular Medicine, New England Medical Center, Boston, Massachusetts 02111

ABSTRACT

Type 1 cannabinoid receptor (CB1) is the principal receptor for endocannabinoids in the brain; it mainly occurs in preterminal/terminal axons and mediates retrograde neuronal signaling mechanisms. A large body of physiological and electrophysiological evidence indicates the critical role of CB1 in the regulation of hypothalamic functions. Conversely, the distribution of CB1-containing axons in the hypothalamus is essentially unknown. Therefore, we have analyzed the distribution and the ultrastructural characteristics of the CB1-immunoreactive (IR) axons in the mouse hypothalamus by using an antiserum against the C-terminal 31 amino acids of the mouse CB1. We found that CB1-IR axons innervated densely the majority of hypothalamic nuclei, except for the suprachiasmatic and lateral mammillary nuclei, in which only scattered CB1-IR fibers occurred. CB1-IR innervation of the arcuate, ventromedial, dorsomedial, and paraventricular nuclei and the external zone of the median eminence corroborated the important role of CB1 in the regulation of energy homeostasis and neuroendocrine functions. Ultrastructural studies to characterize the phenotype of CB1-IR fibers established that most CB1 immunoreactivity appeared in the preterminal and terminal portions of axons. The CB1-IR boutons formed axospinous, axodendritic, and axosomatic synapses. Analysis of labeled synapses in the paraventricular and arcuate nuclei detected approximately equal numbers of symmetric and asymmetric specializations. In conclusion, the study revealed the dense and differential CB1-IR innervation of most hypothalamic nuclei and the median eminence of the mouse brain. At the ultrastructural level, CB1-IR axons established communication with hypothalamic neurons via symmetric and asymmetric synapses indicating the occurrence of retrograde signaling by endocannabinoids in hypothalamic neuronal networks. J. Comp. Neurol. 503:270–279, 2007.

Indexing terms: hypothalamus; immunocytochemistry; innervation; mouse; type 1 cannabinoid receptor (CB1)

The endocannabinoid signaling system utilizes bioactive lipid mediators including the two most abundant endocannabinoids, anandamide and 2-arachidonoyl-glycerol (2-AG); these arachidonic acid derivatives act via binding to the type 1 (CB1) and type 2 (CB2) cannabinoid receptors (Piomelli, 2003; Pagotto et al., 2006). Both anandamide and 2-AG are synthesized widely in the central nervous system where they act primarily through CB1, the principal cannabinoid receptor of the brain (Pagotto et al., 2006). The subcellular distribution of CB1 protein indicates that the main site of the endocannabinoid actions is on terminal/preterminal axon segments (Nyiri et al., 2005). Endocannabinoids derived from the postsynaptic cell membrane inhibit synaptic neurotransmitter release via retrograde signaling mechanisms. These include depolarization-induced suppression of inhibition and excitation (Freund et al., 2003; Piomelli, 2003; Kawamura et al., 2006)

Grant sponsor: the National Science Foundation of Hungary; Grant numbers: OTKA T046492, T046574, and T043407); Grant sponsor: National Office for Research and Technology; Grant number: 1A/002/2004; Grant sponsor: the Sixth European Union Research Framework Programme; Grant number: LSHM-CT-2003-503041; Grant sponsor: Gedeon Richter Ltd. (Hungary).

The first two authors contributed equally to this work.

*Correspondence to: Csaba Fekete, M. D., Ph. D., Department of Endocrine Neurobiology, Institute of Experimental Medicine, Hungarian Academy of Sciences, 43 Szigony St., Budapest, Hungary 1083. E-mail: feketecs@koki.hu

Received 9 October 2006; Revised 16 January 2007; 16 March 2007

DOI 10.1002/cne.21383

Published online in Wiley InterScience (www.interscience.wiley.com).

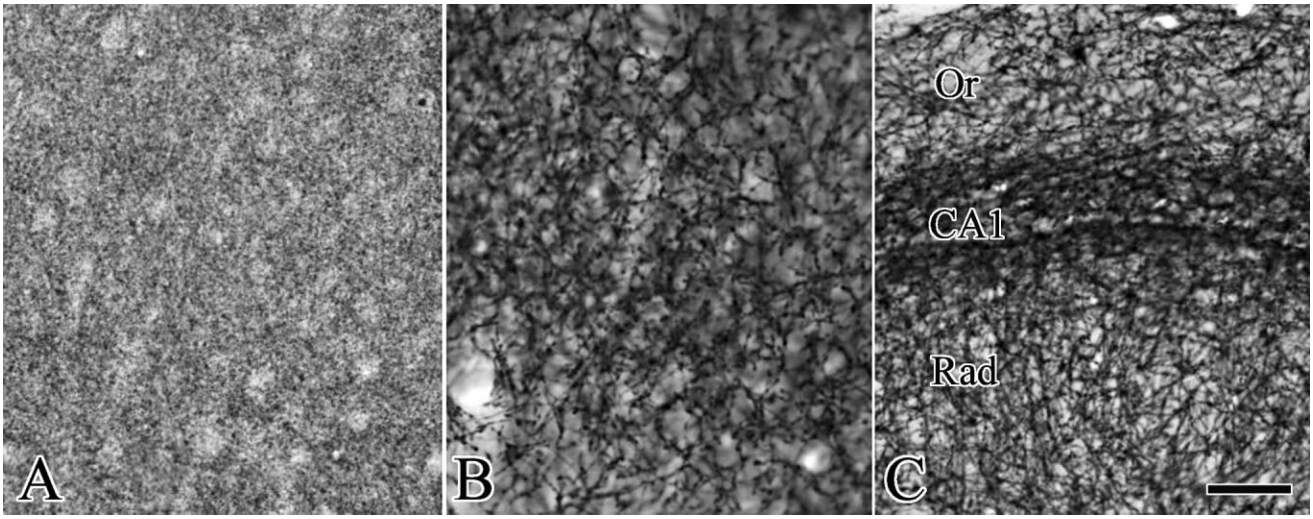

Fig. 1. High-power images illustrate the CB1-immunoreactive (IR) innervation of the hypothalamus (**A**), cortex (**B**), and hippocampus (**C**). Whereas the CB1 immunoreactivity has a punctate appearance in hypothalamic regions, the varicose axons in the cortex and hippocampus are filled with silver-intensified Ni-DAB identifying the CB1 immunoreactivity. Or, stratum oriens; Rad, stratum radiatum; Scale bar = 50 μm in C (applies to A–C).

Endocannabinoid signaling mechanisms have important implications in the normal functioning of hypothalamic neuronal networks (Pagotto et al., 2006), in addition to regulating cortical and hippocampal neuronal circuits (Piomelli, 2003). Exogenous administration of cannabinoids influences neuroendocrine axes, e.g., it stimulates the hypothalamic-pituitary-adrenal (HPA) axis through CB1 (Murphy et al., 1998) and inhibits the hypothalamic-pituitary-thyroid, gonadal, and growth hormone axes (Lomax, 1970; Tyrey, 1978; Rettori et al., 1990; Pagotto et al., 2006). In addition, the endocannabinoid system also plays a critical role in the hypothalamic control of energy homeostasis (Pagotto et al., 2006). Administration of the CB1 antagonist SR141716 reduces food intake (Di Marzo et al., 2001). Furthermore, intrahypothalamic administration of anadamide exerts a significant hyperphagic effect (Kirkham et al., 2002).

Despite growing functional evidence indicating the critical involvement of endocannabinoids in hypothalamic regulation (Pagotto et al., 2006), and the in situ hybridization proof that CB1 is synthesized, albeit at relatively low levels, in the hypothalamus (Marsicano and Lutz, 1999), the intrahypothalamic distribution of axons that may mediate the actions of endocannabinoids on the neuroendocrine axes and the central regulatory machinery of energy homeostasis is entirely unknown.

The aim of the present immunocytochemical study was to describe the regional distribution and ultrastructural characteristics of the hypothalamic CB1-containing neuronal networks and their relationship to hypothalamic target systems, with the aid of a recently generated antiserum against mouse CB1 (Fukudome et al., 2004).

MATERIALS AND METHODS

Animals

The experimental CB1-KO and wild-type (WT) mice were derived from a genotyped stock obtained from IRIBHN, Université Libre de Bruxelles (Ledent et al., 1999) and were bred at the Medical Gene Technology Unit of the Institute of Experimental Medicine. The parent (Belgian) stock was generated from heterozygotes bred for 14 generations on a CD1 (Charles River, L'Arbreole, France) outbred background, with selection for the mutant CB1 gene at each generation. First-generation offspring of these (Belgian) parents were crossbred with wild types for three generations, genotyped, and used as a new parent stock from which the experimental mice of the present study were derived. The animals were genotyped by polymerase chain reaction (PCR) performed on tail DNA by using the following primers: CB1KOD1: CAT CAT CAC AGA TTT CTA TGT AC; CB1WTR1: GAG GTG CCA GGA GGG AAC C; CB1Kor3b: GAT CCA GAA CAT CAG GTA GG; and Neo D/R3: AAG GAA GGG TGA GAA CAG AG. The CB1KOD1-CB1WTR1 and CB1kor3b-Neo D/R3 primer pairs recognized the WT and knockout (KO) allele, respectively.

Adult male WT (n = 6) and CB1-KO mice (n = 3) weighing 30–35 g were used in the experiments. The animals were housed under standard environmental conditions (light between 0600 and 1800 hours, temperature 22 ± 1°C, rodent chow and water ad libitum). All experimental protocols were reviewed and approved by the Animal Welfare Committee at the Institute of Experimental Medicine of the Hungarian Academy of Sciences.

Tissue preparation for light microscopy

Three WT and three CB1-KO mice were deeply anesthetized with sodium pentobarbital (35 mg/kg body weight, ip) and perfused transcardially with 10 ml of 0.01 M phosphate-buffered saline (PBS), pH 7.4, followed by 40 ml of 4% paraformaldehyde in 0.1 M phosphate buffer (PB), pH 7.4. The brains were rapidly removed and cryoprotected in 30% sucrose in 0.01 M PBS, pH. 7.4, overnight at 4°C. Serial 20-μm-thick coronal sections were cut on a freezing microtome (Leica Microsystems, Vienna, Austria). The sections were stored in an antifreeze solu-

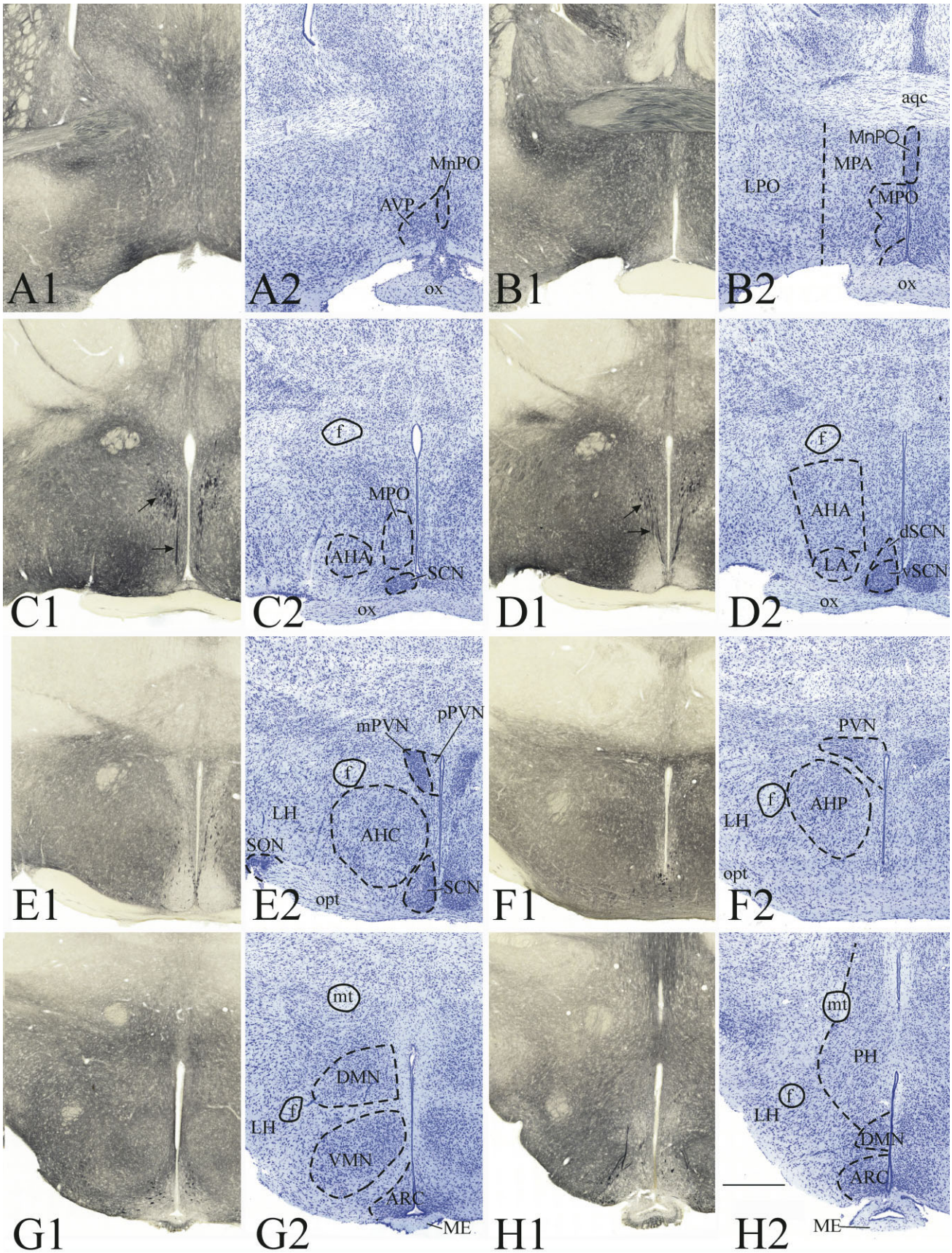
A1
A2
MnPO
AVP
ox
B1
B2
aqc
MnPO
MPA
LPO
MPO
ox
C1
C2
f
MPO
AHA
SCN
ox
D1
D2
f
AHA
dSCN
LA
vSCN
ox
E1
E2
mPVN
pPVN
f
LH
AHC
SON
opt
SCN
F1
F2
PVN
f
AHP
LH
opt
G1
G2
mt
DMN
f
LH
VMN
ARC
ME
H1
H2
mt
PH
f
LH
DMN
ARC
ME

Figure 2

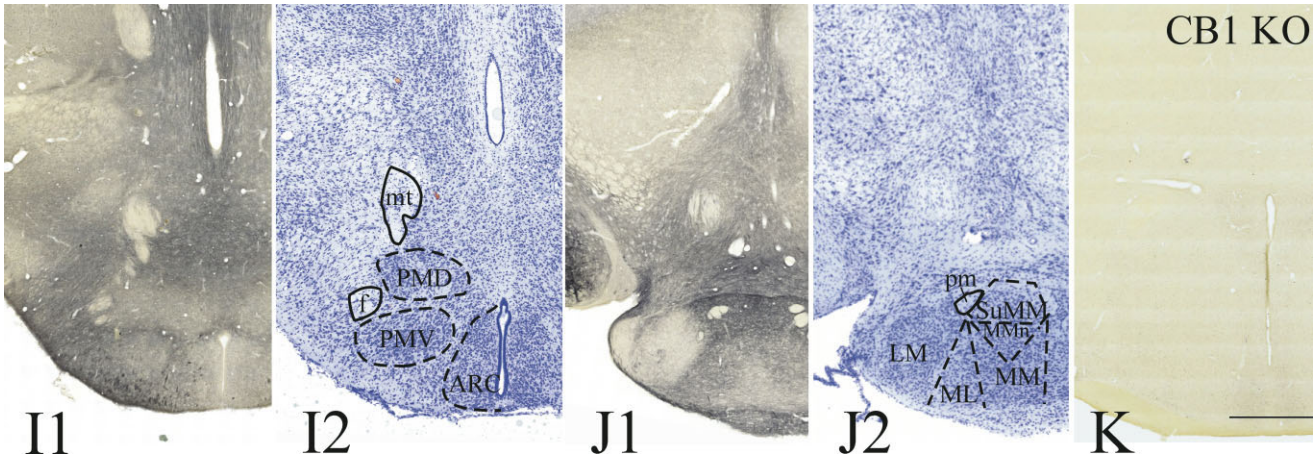

Fig. 2. **A–J:** A series of low-power images illustrates the distribution of CB1-IR axons in the mouse hypothalamus. The brain regions are labeled on a series of Nissl-stained sections corresponding to the regions illustrated in A1–J1. Arrows indicate the medial corticohypothalamic tract (C1,D1). **K:** The lack of CB1 immunoreactivity in the section of CB1 KO mouse hypothalamus illustrates the specificity of the immunostaining. Ac, anterior commissure; AHA, anterior hypothalamic area, anterior part; AHC, anterior hypothalamic area, central part; AHP, anterior hypothalamic area, posterior part; AVP, anterior periventricular nucleus; ARC, hypothalamic arcuate nucleus; DMN, hypothalamic dorsomedial nucleus; f, fornix; LA, lateroanterior hypothalamic nucleus; LH, lateral hypothalamic area; LM, lateral mammillary nucleus; LPO, lateral preoptic area; ME, median eminence; ML, medial mammillary nucleus, lateral part; MM, medial mammillary nucleus, medial part; MMn, medial mammillary nucleus, median part; MnPO, median preoptic nucleus, MPA, medial preoptic area; MPO, medial preoptic nucleus; mt, mammillary tract; mPVN, magnocellular part of the hypothalamic paraventricular nucleus; pPVN, parvocellular part of hypothalamic paraventricular nucleus; PH, posterior hypothalamic area; pm, principal mammillary tract; PMD, dorsal premammillary nucleus; PMV, ventral premammillary nucleus; ox, optic chiasm; opt, optic tract; dSCN, suprachiasmatic nucleus, dorsomedial part; vSCN, suprachiasmatic nucleus, ventrolateral part; SON, supraoptic nucleus; SuMM, supramamillary nucleus; VMN, hypothalamic ventromedial nucleus. Scale bar = 500 μm in H2 and K (applies to A–J).

tion (30% ethylene glycol; 25% glycerol; 0.05 M phosphate buffer) at −20°C until used.

Detection of CB1-immunoreactive neuronal networks in the hypothalamus

Every fifth section through the anteroposterior extent of the hypothalamus were processed for immunocytochemistry from both WT and CB1-KO mice. Sections of WT and CB1-KO mice were processed parallel. They were incubated in a mixture of 0.5% H_2O_2 and 0.5% Triton X-100 in PBS for 15 minutes to increase antibody penetration and reduce endogenous peroxidase activity. To reduce the nonspecific antibody binding, the sections were treated with 2% normal horse serum in PBS for 20 minutes. Then the sections were immersed (for 2 days at 4°C) in a 1:25 dilution (with PBS containing 2% normal horse serum, 0.2% Kodak Photo-Flo [Eastman Kodak, Rochester, NY], and 0.2% sodium azide) of a rabbit antiserum directed against the C-terminal 31 amino acids (443–473;) of mouse CB1 (antibody code number: CB1-2003, bleeding date: July 5, 2003) (Fukudome et al., 2004). Thereafter, the sections were rinsed in PBS and incubated in biotinylated donkey anti-rabbit IgG (1:500; Jackson ImmunoResearch, West Grove, PA) for 2 hours, followed by incubation in biotin-avidin-complex (ABC, 1:1,000; Vector, Burlingame, CA). The immunolabeling was visualized with a peroxidase developer consisting of 0.05% diaminobenzidine, 0.15% nickel ammonium sulfate, and 0.005% H_2O_2 in 0.05 M Tris buffer (pH 7.6).

The resulting reaction product was silver-intensified by using the Gallyas method (Liposits et al., 1984). The immunostained sections were mounted onto glass slides from polyvinyl alcohol (Elvanol, Sigma, Budapest, Hungary), dried, and coverslipped with DPX mounting medium (Fluka, Buchs, Switzerland). A second series of sections neighboring the immunostained specimens described above was mounted on glass slides and counterstained with cresyl violet.

Slides were scanned at constant settings by using an HI-Scope slide scanner (3D Histech, Cellanalysis Lab, Second

TABLE 1. Relative Density of CB1 Immunoreactivity in the Hypothalamic Nuclei of Mouse Brain

Nucleus	Density
Anterior hypothalamic area, anterior part	++++
Anterior hypothalamic area, central part	+++
Anterior hypothalamic area, posterior part	+++
Anterior periventricular nucleus	++
External zone of the median eminence	+++
Hypothalamic arcuate nucleus	+/++
Hypothalamic dorsomedial nucleus	++/+++
Internal zone of the median eminence	+
Lateral hypothalamic area	++/+++
Lateral mammillary nucleus	+
Lateral preoptic area	+++
Lateroanterior hypothalamic nucleus	++++
Magnocellular part of the hypothalamic paraventricular nucleus	++
Medial mammillary nucleus, lateral part	++
Medial mammillary nucleus, medial part	+
Medial mammillary nucleus, median part	++
Medial preoptic area	+++
Medial preoptic nucleus	++/+++
Median preoptic nucleus	+++
Parvocellular part of hypothalamic paraventricular nucleus	++/+++
Periventricular nucleus	++
Posterior hypothalamic area	+++
Premammillary nucleus, ventral	++
Premammillary nucleus, dorsal	++
Suprachiasmatic nucleus dorsomedial part	++
Suprachiasmatic nucleus, ventrolateral part	+
Supramammillary nucleus	+++
Supraoptic nucleus	+
Ventromedial nucleus	+++

Qualitative estimates of CB1 immunoreactivity were made as described in the Results section. The following 5-point density scale was used: +++++, highest density observed in the brain; ++++, high density; +++, intermediate density; ++, moderate density, +, low density above background.

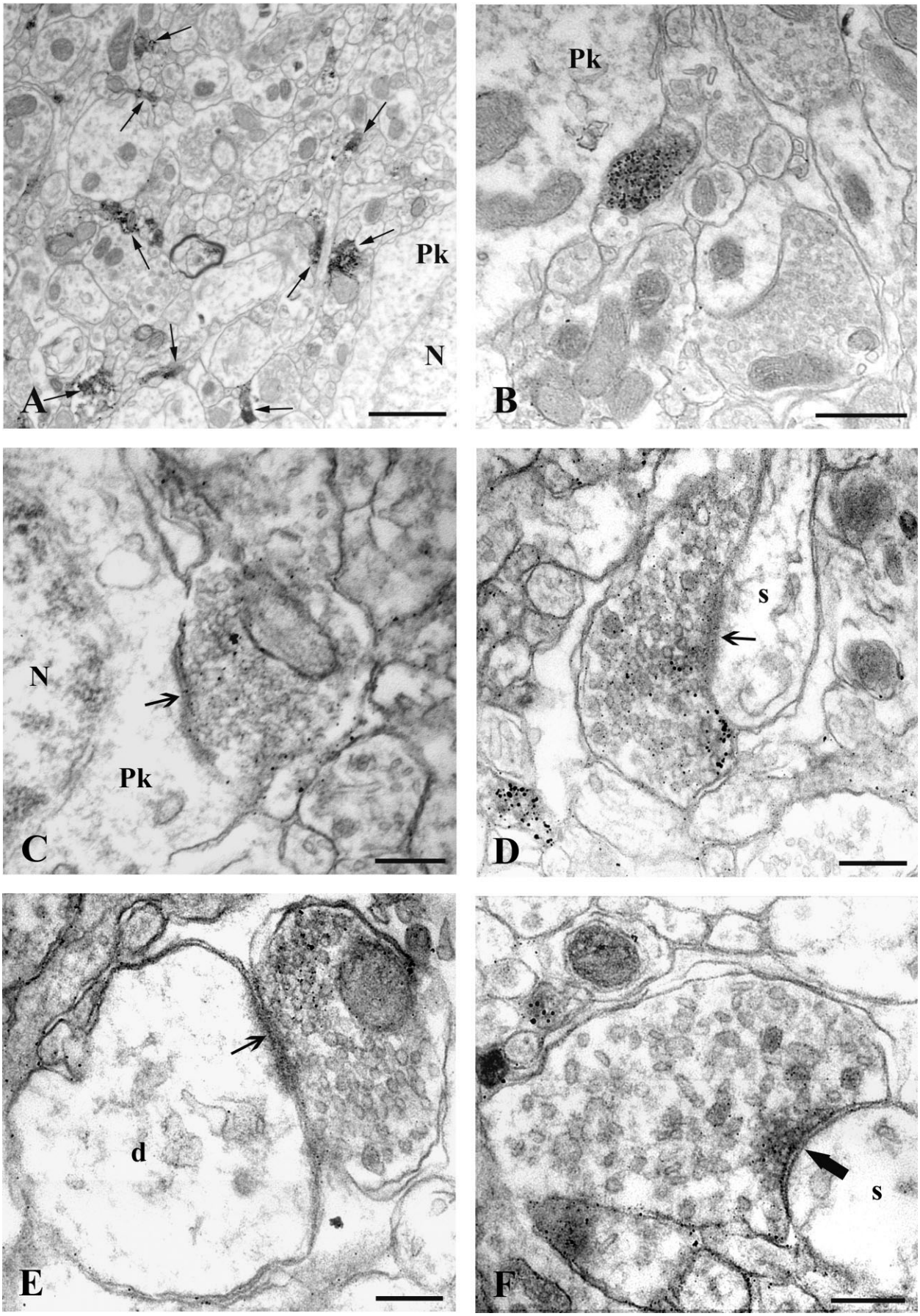

Figure 3

Department of Internal Medicine, Semmelweis University, Budapest, Hungary), which generated high-resolution digitized images of the sections. Regions of interest were selected manually by using the Mirax Viewer software (3D Histech) and saved in TIFF format. Gray-scale values of preoptic/hypothalamic nuclei were determined offline by using Image J image analysis software (in the public domain and available at http://rsb.info.nih.gov/ij/download/src/). Brightness and contrast of the images were modified in Adobe Photoshop 7.0.1 (Adobe Systems, San Jose, CA). The composite figures were prepared by using CorelDRAW Graphics Suite 11 (Corel Corporation, Ottawa, Ontario).

Specificity of antiserum

The specificity of the CB1 antiserum was previously demonstrated by Fukudome and co-workers (2004), who showed by Western blot analyses that the CB1 antiserum recognized a single band in the adult mouse brain. We demonstrate here that CB1 immunoreactivity was completely absent from hypothalamic sections of the CB1-KO mice (Fig. 2K), as well as from other forebrain regions including the hippocampus, cortex, thalamus, and septum.

Tissue preparation for electron microscopy

Three animals were deeply anesthetized with sodium pentobarbital (35 mg/kg body weight, ip) and perfused transcardially first with 10 ml 0.01 M PBS, pH 7.4, followed by 40 ml of 3% paraformaldehyde/1% acrolein in 0.1 M PB, pH 7.4, and then 10 ml of 3% paraformaldehyde in the same buffer. The brains were rapidly removed and stored in PBS for 24 hours at 4°C.

For electron microscopy, 25-μm-thick coronal sections were cut serially from the hypothalami on a Vibratome through the rostrocaudal extent of the hypothalamus, collected in PBS, and stored in antifreeze solution at −20°C until used. Then the sections were treated with 1% sodium borohydride in 0.1 M PB for 30 minutes, followed by 0.5% H_2O_2 in PBS for 15 minutes. To improve antibody penetration, the sections were cryoprotected in 15% sucrose in PBS for 15 minutes (room temperature) and in 30% sucrose in PBS overnight (4°C) and then quickly frozen on liquid nitrogen. To reduce the nonspecific antibody binding, the sections were treated with 2% normal horse serum in PBS for 20 minutes at room temperature.

The sections were incubated in a 1:25 dilution of the rabbit antiserum to CB1 for 4 days at 4°C, then in biotinylated donkey anti-rabbit IgG (1:500; Jackson ImmunoResearch) overnight at 4°C, and finally in ABC Elite working solution (1:1,000; Vector) for 2 hours at room temperature. Immunoreactivity was detected with 0.05% diaminobenzidine, 0.15% nickel ammonium sulfate, and 0.005% H_2O_2 in 0.05 M Tris buffer (pH 7.6). The immunoreaction product was silver-intensified by using the Gallyas method. Sections were then osmicated for 30 minutes in 1% osmium tetroxide, treated with 2% uranyl acetate in 70% ethanol for 30 minutes, dehydrated in an ascending series of ethanol followed by propylene oxide, and flat-embedded in Durcupan ACM epoxy resin (Fluka Chemie) between glass microscope slides precoated with a liquid release agent (Electron Microscopy Sciences, Fort Washington, PA). The resin was allowed to polymerize at 56°C for 2 days. Ultrathin sections (50–60 nm) were cut from a layer of embedded Vibratome sections 2–4 μm below the surface with a Leica ultracut UCT ultramicrotome (Leica Microsystems, Vienna, Austria), collected in ribbons onto Formvar-coated single-slot grids, contrasted with 2% lead citrate, and examined with a Jeol-100C transmission electron microscope.

Ultrastructural examination of CB1-immunoreactive axons in the hypothalamus

Sections at Bregma level −0.82 mm containing the paraventricular and supraoptic nuclei or at −1.94 mm containing the median eminence and arcuate nucleus were selected from all animals studied for electron microscopic examination of CB1 immunoreactivity. The numbers of immunoreactive axon terminals forming either symmetric or asymmetric synapses in the paraventricular or arcuate nuclei were determined from sections in the middle of the ribbons. Via an analysis along a meander scan (to avoid double-counting), the first fifty CB1-IR synaptic connections observed in each nucleus were categorized as symmetric or asymmetric synapses, according to Gray (1959). These morphological characteristics were confirmed on neighboring ultrathin sections.

RESULTS

The hypothalamus received a rich innervation by fine CB1-immunoreactive (IR) fibers, which exhibited a punctate immunostaining (Figs. 1A, 2). Longer axon portions running parallel to the section plane were only seen exceptionally, and they consisted of labeled varicosities and intervaricose segments (data not shown). In contrast with the typical fine axonal immunoreactivity observed in the hypothalamus, the cerebral cortex and the hippocampus contained a dense network of thick and varicose fibers (Fig. 1).

In general, the overall intensity of CB1 immunostaining was much lower in the hypothalamus than in cortical and hippocampal regions. High-power analysis of the immunostained sections revealed that this difference was attributable to the much heavier labeling of individual fibers in the hippocampus and the cortex vs. the hypothalamus (Fig. 1). Although the innervation of the hypothalamus was generally very rich, obvious regional variations were noticed (Fig. 2, Table 1). The density of the CB1-IR innervation of hypothalamic nuclei is summarized in Table 1. Gray-scale values measured in single hypothalamic nuclei are represented on an arbitrary scale of five labeling intensities, from "+," meaning "very low" (slightly above the density measured in sections of CB1-KO animals), to

Fig. 3. Electron micrographs demonstrating CB1-immunoreactive (IR) neuronal profiles labeled with silver/gold-intensified nickel-diaminobenzidine chromogen in the hypothalamic paraventricular nucleus (PVN) of the mouse brain. **A:** Low-power micrograph shows numerous immunoreactive processes (arrows) scattered in the neuropil. **B:** Small-caliber axon labeled intensively by silver-gold grains abuts on the perikaryon of a parvicellular neuron. **C:** CB1-IR axon terminal establishes an asymmetric synapse (thin arrow) on a parvicellular perikaryon. **D,E:** CB1-IR axon terminals form asymmetric synapses (thin arrow) with a dendritic spine (D) and a thin dendritic process (E). Presynaptic profiles contain abundant spherical vesicles. **F:** A symmetric synapse (thick arrow) formed by a CB1-immunopositive axon bouton on a dendritic spine. The labeled terminal possesses many flattened vesicles. Note the silver-gold grains associated with vesicles (B–F) and certain segments of plasma membrane (D, F). d, dendrite; N, cell nucleus; Pk, perikaryon; s, dendritic spine; Scale bar = 1 μm in A; 500 nm in B; 200 nm in C–F.

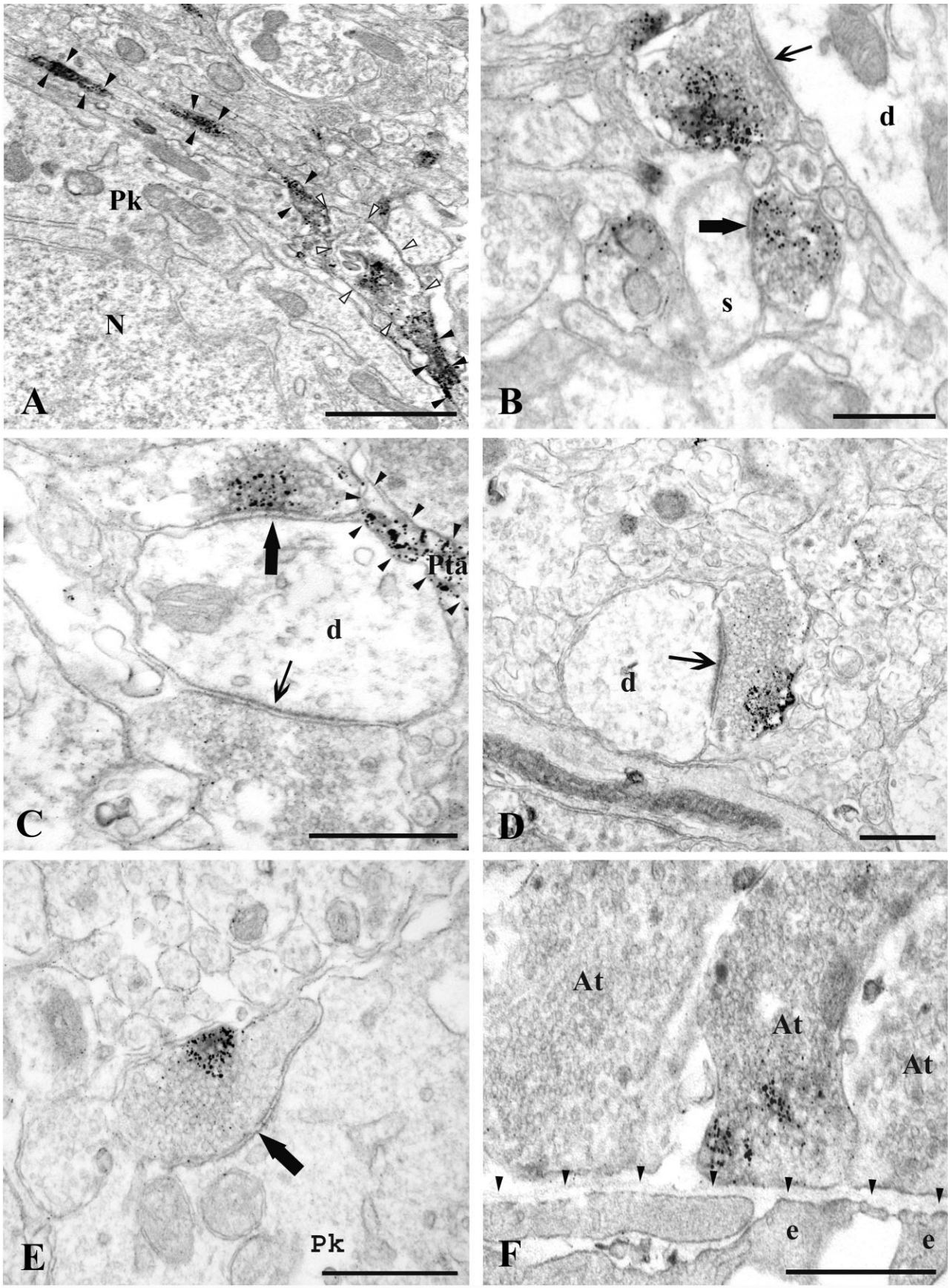

Figure 4

"+++++," meaning "very high" (set according to the highest signal density in the specimen, i.e., the cerebral cortex).

The highest hypothalamic signal intensity was measured in the anterior part of the anterior hypothalamic area and the lateroanterior hypothalamic nucleus (Fig. 2C,D). Lower than average hypothalamic staining intensity was observed in the arcuate nucleus, anteroventral periventricular nucleus, medial preoptic nucleus, periventricular nucleus, dorsolateral part of the suprachiasmatic nucleus, supraoptic nucleus, and regions of the mammillary body. The least dense CB1-IR innervation was revealed in the lateral mammillary nucleus and the ventral part of the suprachiasmatic nucleus, which contained only scattered CB1-IR fibers (Fig. 2). In the median eminence, CB1 immunoreactivity was concentrated in the external zone, but scattered fibers were also observed in the internal zone (Fig. 2G,H). We noted heavy labeling of a CB1-IR fiber tract that projected ventrally from the fornix along the wall of the third ventricle (Fig. 2C,D). This fiber bundle was divided into smaller branches in the retrochiasmatic area and the arcuate nucleus, with a course reminiscent of the medial corticohypothalamic tract (Kishi et al., 2000). CB1 immunoreactivity was not observed in any part of the forebrain, including the hypothalamus, in CB1-KO animals (Fig. 2K).

The ultrastructural analysis of CB1-IR profiles by means of a sensitive pre-embedding technique revealed high numbers of silver/gold-intensified chromogen-labeled CB1-IR processes in the hypothalamus (Figs. 3A, 4A). The silver-gold particles often appeared in clusters within the preterminal and terminal portion of the axons (Figs. 3B, 4B–E). In other cases, they were distributed either among synaptic vesicles or along the plasma membrane (Fig. 3C–F).

CB1-IR axons often formed asymmetric (Figs. 3D,E, 4B,D) and symmetric synapses (Figs. 3F, 4B,C,E) with dendrites, dendritic spines, and neuronal perikarya (Fig. 3C) of the paraventricular, supraoptic, and arcuate nuclei. Quantitative analysis of 50 synapses in the paraventricular and arcuate nuclei revealed 28 asymmetrical and 22 symmetrical synapses in the paraventricular nucleus and 27 asymmetrical and 23 symmetrical synapses in the arcuate nucleus. In the median eminence a subset of axon terminals terminating around the portal vessels were also CB1-IR and showed immunolabeling in association with clear vesicles (Fig. 4F). Processes of tanycytes were CB1 immunonegative.

Fig. 4. Electron micrographs showing communicating CB1-immunoreactive (IR) axons in the supraoptic (A–C) and arcuate (D,E) nuclei and median eminence (F) of the mouse hypothalamus. **A:** Longitudinal section of a CB1-IR axon demonstrates the immunolabel in both the intervaricose segment (black arrowheads) and the dilated axonal bead (white arrowheads). The neighboring magnocellular neuron is immunonegative. **B:** Dendritic spine and shaft receiving innervation from CB1-immunopositive axon terminals via symmetric (thick arrow) and asymmetric (thin arrow) synapses. **C:** Supraoptic dendrite communicates with a heavily (thick arrow) and lightly labeled (thin arrow) axon terminals via symmetric and asymmetric synaptic specializations, respectively. Silver-gold particles are clustered in the preterminal axon (black arrowheads). **D,E:** Dendrite (D) and perikaryon (E) innervated by CB1-immunoreactive axons in the arcuate nucleus via asymmetric (thin arrow) and symmetric (thick arrow) synapses. **F:** CB1 immunoreactivity expressed in one of the three hypophysiotrophic axons terminating on the external limiting membrane (arrowheads) of the median eminence. At, axon terminal; d, dendrite; e, endothelial cell; Pk, perikaryon; Pta, preterminal axon; s, dendritic spine. Scale bar = 1 μm in A; 500 nm in B–F.

DISCUSSION

Although compelling evidence suggests a role of CB1 in the regulation of hypothalamic functions, including regulation of energy homeostasis and neuroendocrine function, little has been known about the distribution of CB1 protein in hypothalamic tissues. Tsou and co-workers (1998) have described CB1-IR in only two regions of the hypothalamus: in the paraventricular nucleus (PVN) and in the lateral hypothalamus.

In contrast, in the current immunocytochemical study, we observed dense CB1-IR innervation in most hypothalamic nuclei, possibly because of the higher sensitivity of the antibody used in our studies. This possibility is further supported by the fact that the antibody used by Tsou et al. (1998) could detect only the CB1 content of γ-aminobutyric acid (GABA)ergic axons in the hippocampus and cortex, whereas the antibody used in our study could also detect the lower concentration of CB1 protein in the glutamatergic terminals in these brain regions (Kawamura et al., 2006).

Paradoxically, the dense innervation of the hypothalamus coincided with a markedly lower intensity of CB1 immunolabeling compared with cortical and hippocampal areas. This relatively lower overall immunostaining is in accordance with the low cannabinoid binding capacity of the hypothalamus (Herkenham et al., 1990) and may indicate that individual hypothalamic axons contain significantly fewer CB1 molecules than do cortical or hippocampal fibers. At the ultrastructural level, the punctuate CB1 immunoreactivity observed in light microscopic specimens was present primarily in axons, many forming either asymmetric or symmetric synapses with the dendritic shafts and/or spines, or perikarya of hypothalamic neurons. The observation of CB1 immunoreactivity in both symmetric and asymmetric synapses of the PVN, supraoptic nucleus (SON), and arcuate nucleus suggests that CB1 modulates inhibitory as well as excitatory synaptic transmission, respectively, in the hypothalamus. In ultrastructural studies of the hypothalamus, we have observed comparable labeling intensities in terminals forming excitatory and inhibitory synapses. This finding is in contrast to the observations made in the hippocampus or the cerebral cortex, where the inhibitory terminals are more heavily labeled for CB1 than the excitatory ones (Kawamura et al., 2006).

Quantitative postembedding studies (Nyiri et al., 2005) on CB1 distribution in the hippocampus revealed immunoreactive loci along the plasma membrane at preterminal and perisynaptic sites. A few immunogold particles have also been reported in vesicles and in association with the synaptic membrane. In our study, hypothalamic CB1 immunoreactivity was strong in preterminal axons, as reported in the hippocampus (Nyiri et al., 2005). Clusters of silver-gold grains also appeared within the terminals in association with vesicles. In addition, short segments of the plasma membrane, including the synaptic membrane, were also weakly labeled. Taken together, these findings indicate a subcellular distribution of the CB1 in the hypothalamus similar to that observed in the hippocampus or

cortex. No explanation is currently available for the high accumulation of CB1 in the preterminal portion of axons.

The fine but very dense CB1-IR axon network likely arises from multiple sources, which may include intrahypothalamic CB1-expressing neurons. The highest levels of hypothalamic CB1 mRNA expression were reported in the ventromedial nucleus and in the anterior hypothalamic area, where most neurons seemed to possess CB1 mRNA (Marsicano and Lutz, 1999). Both regions, indeed, give rise to wide intrahypothalamic projections (Saper et al., 1978; Canteras et al., 1994). It is worth noting that the vast majority of cells in these nuclei have a glutamatergic phenotype (Hrabovszky et al., 2005), indicating that the VMN and the anterior hypothalamic area contribute to the excitatory CB1-IR innervation of the hypothalamus. Additional hypothalamic neurons that synthesize CB1 mRNA and may provide sources for the origin of CB1-IR intrahypothalamic projections are located in the medial and lateral preoptic nuclei, the magnocellular preoptic nucleus, the premammillary nucleus, and the lateral hypothalamus (Marsicano and Lutz, 1999). These authors reported that cells expressing CB1 or GAD65, the biosynthetic enzyme of GABA, form two distinct cell populations within the hypothalamus, suggesting that the inhibitory CB1-IR fibers in the hypothalamus that established symmetric synapses in our electron microscopic study arise mostly from extrahypothalamic neuronal sources.

A large subset of the extrahypothalamic CB1-IR afferents appears to enter the hypothalamus through the medial corticohypothalamic tract, which formed a prominent CB1-IR fiber bundle in the present study. The ventral subiculum, which represents a major source of the fibers in this tract (Kishi et al., 2000), is strongly implicated in the modulation of the hypothalamic-pituitary-adrenal axis (Herman and Mueller, 2006). Lesions in this region increase the synthesis of corticotropin-releasing hormone (CRH) in the PVN and elevate the corticosterone response following restraint stress (Herman and Mueller, 2006). Interestingly, the ventral subiculum does not innervate the hypothalamic paraventricular nucleus (Herman and Mueller, 2006), where the hypophysiotropic CRH neurons reside, indicating that its action on the HPA axis is indirect. Corroborating this concept, glutamatergic neurons of the ventral subiculum innervate GABAergic interneurons in various hypothalamic nuclei that, in turn, project to the PVN (Herman and Mueller, 2006). Because cannabinoids inhibit presynaptic glutamate release via depolarization-induced suppression of excitation (Kawamura et al., 2006), the mechanism whereby endocannabinoids stimulate CRH synthesis may involve reduced glutamate release from fibers of the ventral subiculum upon GABAergic interneurons. This may result in inhibition of GABAergic afferent input to CRH neurons.

Another structure known to contain a large number of CB1-expressing neurons (Marsicano and Lutz, 1999) and to innervate the hypothalamus densely (Canteras et al., 1992, 1995), is the amygdala. A subpopulation of the CB1-synthesizing neurons in the amygdala synthesizes GAD65 (Marsicano and Lutz, 1999), which may designate the amygdala as a putative source of inhibitory CB1-IR projections to the hypothalamus. The possibility exists that excitatory CB1-containing projections also reach the hypothalamus from the amygdala.

The basal ganglia also send prominent projections to the hypothalamus (Haber et al., 1985). Both the caudate putamen and the pallidum contain CB1-expressing neurons in large numbers, and the vast majority of these cells are GABAergic (Marsicano and Lutz, 1999), making it likely that the basal ganglia represent a highly significant source of the inhibitory CB1 innervation of the hypothalamus.

Regional analysis of CB1 immunoreactivity revealed dense networks of endocannabinoid-sensitive fibers in various hypothalamic areas that play crucial roles in neuroendocrine regulation. Magnocellular neurons of the PVN and the SON (which synthesize oxytocin and vasopressin) and parvicellular neurosecretory systems (which include thyrotropin-releasing hormone [TRH] and CRH neurons of the PVN, growth hormone-releasing hormone [GHRH] and tuberoinfundibular dopaminergic neurons of the ARC, somatostatinergic neurons of the Pe, and gonadotropin-releasing hormone [GnRH] neurons of the preoptic area [POA]) may all receive direct synaptic input from CB1-IR afferents. Our ultrastructural observation that both symmetric and asymmetric CB1-IR synapses are present in hypophysiotropic areas indicates that CB1 may modulate inhibitory as well as excitatory neuronal transmission to neuroendocrine cells, respectively. There is electrophysiological evidence that rapid nongenomic glucocorticoid actions on parvicellular neurons of the PVN are partly mediated by decreased glutamatergic synaptic excitation caused by retrograde endocannabinoid signaling through CB1 (Di et al., 2003). These authors also provided proof for the CB1-mediated rapid and opposite actions of glucocorticoids on presynaptic glutamate vs. GABA release onto magnocellular neurons of the PVN and the SON (Di et al., 2005). It is worth noting that although the decreased glutamate release in this in vitro study could be mimicked with the endocannabinoids 2-AG or anandamide, the retrograde signaling molecule(s) that increased GABA release apparently differed from these classical endocannabinoids (Di et al., 2005). It is somewhat difficult to interpret the mechanism of a CB1-mediated increase in GABA release, given that most of the work on the neocortex, hippocampus, and amygdala rather indicates that retrograde signaling via presynaptic CB1 inhibits the release of GABA from presynaptic neurons and reduces the amplitude of inhibitory postsynaptic currents through depolarization-induced suppression of inhibition. (Freund et al., 2003; Piomelli, 2003; Bodor et al., 2005).

The identification of CB1-IR axons in the external zone of the median eminence marks an additional site of endocannabioid actions on neuroendocrine axes. Although the neuropeptide phenotype of CB1-IR neurosecretory axons in the median eminence awaits clarification, the expression of CB1 mRNA in CRH neurons of the PVN (Cota et al., 2003) raises the possibility that some CB1-IR fibers correspond to the neurosecretory terminals of CRH neurons. This adds a further degree of complexity to endocannabinoid actions upon the adrenal axis. Whereas the GnRH-producing GT1-7 cell line also synthesizes CB1 mRNA, in situ hybridization studies were unable to reveal CB1 mRNA in GnRH neurons in vivo (Gammon et al., 2005). As discussed by the authors (Gammon et al., 2005), GnRH neurons may either lack CB1 mRNA or may synthesize the receptor mRNA at levels below the detection threshold of the in situ hybridization method. Future application of the new CB1 antibody to dual-immunofluorescent studies of the median eminence may decide this question and may also determine the neuroendocrine phenotype(s) of parvicellular neurosecretory terminals with CB1 expression.

A second important question arising from the presence of CB1 in the median eminence is the source of the endocannabinoids that act through this receptor. One possibility is that the CB1 ligands originate from the lipid membrane of the neuroendocrine terminal, per se. According to this hypothesis, the presence of CB1 autoreceptors on the same terminals may allow a putative autocrine/paracrine regulatory mechanism to operate in the median eminence whereby an increased endocannabinoid synthesis and binding to this receptor may limit the secretory activity of neuroendocrine terminals. It is tempting to speculate that this putative endocannabinoid feedback signaling may be involved in the synchronized activity of neuroendocrine terminals during secretory pulses. Tanycytes, astrocytes, and vascular endothelial cells of the median eminence should be considered alternative sources of endocannabinoids that bind to CB1 on hypophysiotropic axon terminals.

A large body of evidence suggests a critical role for CB1 in the modulation of food intake and energy balance (Pagotto et al., 2006). According to our results, CB1-IR fibers densely innervate hypothalamic regions that are crucial for feeding regulation, including the dorsomedial, ventromedial, paraventricular, and arcuate nuclei and the lateral hypothalamus and establish synapses with their neuronal assemblies. Clarifying the phenotype of these CB1-IR axons and their target neurons will contribute to the understanding of the circuitry and mechanisms whereby the endocannabinoid system modulates energy balance.

In conclusion, we demonstrated the dense and differential CB1-IR innervation of hypothalamic nuclei and the median eminence. These CB1-IR axons communicate with hypothalamic neurons via symmetric and asymmetric synapses, supporting the view that the retrograde signaling mechanism of endocanabinoids affects both the excitatory and inhibitory inputs of hypothalamic neurons.

LITERATURE CITED

Bodor AL, Katona I, Nyiri G, Mackie K, Ledent C, Hajos N, Freund TF. 2005. Endocannabinoid signaling in rat somatosensory cortex: laminar differences and involvement of specific interneuron types. J Neurosci 25:6845–6856.

Canteras NS, Simerly RB, Swanson LW. 1992. Connections of the posterior nucleus of the amygdala. J Comp Neurol 324:143–179.

Canteras NS, Simerly RB, Swanson LW. 1994. Organization of projections from the ventromedial nucleus of the hypothalamus: a *Phaseolus vulgaris*-leucoagglutinin study in the rat. J Comp Neurol 348:41–79.

Canteras NS, Simerly RB, Swanson LW. 1995. Organization of projections from the medial nucleus of the amygdala: a PHAL study in the rat. J Comp Neurol 360:213–245.

Cota D, Marsicano G, Tschop M, Grubler Y, Flachskamm C, Schubert M, Auer D, Yassouridis A, Thone-Reineke C, Ortmann S, Tomassoni F, Cervino C, Nisoli E, Linthorst AC, Pasquali R, Lutz B, Stalla GK, Pagotto U. 2003. The endogenous cannabinoid system affects energy balance via central orexigenic drive and peripheral lipogenesis. J Clin Invest 112:423–431.

Di S, Malcher-Lopes R, Halmos KC, Tasker JG. 2003. Nongenomic glucocorticoid inhibition via endocannabinoid release in the hypothalamus: a fast feedback mechanism. J Neurosci 23:4850–4857.

Di S, Malcher-Lopes R, Marcheselli VL, Bazan NG, Tasker JG. 2005. Rapid glucocorticoid-mediated endocannabinoid release and opposing regulation of glutamate and gamma-aminobutyric acid inputs to hypothalamic magnocellular neurons. Endocrinology 146:4292–4301.

Di Marzo V, Goparaju SK, Wang L, Liu J, Batkai S, Jarai Z, Fezza F, Miura GI, Palmiter RD, Sugiura T, Kunos G. 2001. Leptin-regulated endocannabinoids are involved in maintaining food intake. Nature 410:822–825.

Freund TF, Katona I, Piomelli D. 2003. Role of endogenous cannabinoids in synaptic signaling. Physiol Rev 83:1017–1066.

Fukudome Y, Ohno-Shosaku T, Matsui M, Omori Y, Fukaya M, Tsubokawa H, Taketo MM, Watanabe M, Manabe T, Kano M. 2004. Two distinct classes of muscarinic action on hippocampal inhibitory synapses: M2-mediated direct suppression and M1/M3-mediated indirect suppression through endocannabinoid signalling. Eur J Neurosci 19: 2682–2692.

Gammon CM, Freeman GM Jr, Xie W, Petersen SL, Wetsel WC. 2005. Regulation of gonadotropin-releasing hormone secretion by cannabinoids. Endocrinology 146:4491–4499.

Gray EG. 1959. Axo-somatic and axo-dendritic synapses of the cerebral cortex: an electron microscope study. J Anat 93:420–433.

Haber SN, Groenewegen HJ, Grove EA, Nauta WJ. 1985. Efferent connections of the ventral pallidum: evidence of a dual striato pallidofugal pathway. J Comp Neurol 235:322–335.

Herkenham M, Lynn AB, Little MD, Johnson MR, Melvin LS, de Costa BR, Rice KC. 1990. Cannabinoid receptor localization in brain. Proc Natl Acad Sci U S A 87:1932–1936.

Herman JP, Mueller NK. 2006. Role of the ventral subiculum in stress integration. Behav Brain Reg 174:215–224.

Hrabovszky E, Halasz J, Meelis W, Kruk MR, Liposits Z, Haller J. 2005. Neurochemical characterization of hypothalamic neurons involved in attack behavior: glutamatergic dominance and co-expression of thyrotropin-releasing hormone in a subset of glutamatergic neurons. Neuroscience 133:657–666.

Kawamura Y, Fukaya M, Maejima T, Yoshida T, Miura E, Watanabe M, Ohno-Shosaku T, Kano M. 2006. The CB1 cannabinoid receptor is the major cannabinoid receptor at excitatory presynaptic sites in the hippocampus and cerebellum. J Neurosci 26:2991–3001.

Kirkham TC, Williams CM, Fezza F, Di Marzo V. 2002. Endocannabinoid levels in rat limbic forebrain and hypothalamus in relation to fasting, feeding and satiation: stimulation of eating by 2-arachidonoyl glycerol. Br J Pharmacol 136:550–557.

Kishi T, Tsumori T, Ono K, Yokota S, Ishino H, Yasui Y. 2000. Topographical organization of projections from the subiculum to the hypothalamus in the rat. J Comp Neurol 419:205–222.

Ledent C, Valverde O, Cossu G, Petitet F, Aubert JF, Beslot F, Bohme GA, Imperato A, Pedrazzini T, Roques BP, Vassart G, Fratta W, Parmentier M. 1999. Unresponsiveness to cannabinoids and reduced addictive effects of opiates in CB1 receptor knockout mice. Science 283:401–404.

Liposits Z, Setalo G, Flerko B. 1984. Application of the silver-gold intensified 3,3′-diaminobenzidine chromogen to the light and electron microscopic detection of the luteinizing hormone-releasing hormone system of the rat brain. Neuroscience 13:513–525.

Lomax P. 1970. The effect of marihuana on pituitary-thyroid activity in the rat. Agents Actions 1:252–257.

Marsicano G, Lutz B. 1999. Expression of the cannabinoid receptor CB1 in distinct neuronal subpopulations in the adult mouse forebrain. Eur J Neurosci 11:4213–4225.

Murphy LL, Munoz RM, Adrian BA, Villanua MA. 1998. Function of cannabinoid receptors in the neuroendocrine regulation of hormone secretion. Neurobiol Dis 5:432–446.

Nyiri G, Cserep C, Szabadits E, Mackie K, Freund TF. 2005. CB1 cannabinoid receptors are enriched in the perisynaptic annulus and on preterminal segments of hippocampal GABAergic axons. Neuroscience 136:811–822.

Pagotto U, Marsicano G, Cota D, Lutz B, Pasquali R. 2006. The emerging role of the endocannabinoid system in endocrine regulation and energy balance. Endocr Rev 27:73–100.

Piomelli D. 2003. The molecular logic of endocannabinoid signalling. Nat Rev 4:873–884.

Rettori V, Aguila MC, Gimeno MF, Franchi AM, McCann SM. 1990. In vitro effect of delta 9-tetrahydrocannabinol to stimulate somatostatin release and block that of luteinizing hormone-releasing hormone by suppression of the release of prostaglandin E2. Proc Natl Acad Sci U S A 87:10063–10066.

Saper CB, Swanson LW, Cowan WM. 1978. The efferent connections of the anterior hypothalamic area of the rat, cat and monkey. J Comp Neurol 182:575–599.

Tsou K, Brown S, Sanudo-Pena MC, Mackie K, Walker JM. 1998. Immunohistochemical distribution of cannabinoid CB1 receptors in the rat central nervous system. Neuroscience 83:393–411.

Tyrey L. 1978. delta-9-Tetrahydrocannabinol suppression of episodic luteinizing hormone secretion in the ovariectomized rat. Endocrinology 102:1808–1814.

14. számú melléklet

dc_27_10

GLUTAMATERGIC PHENOTYPE OF HYPOTHALAMIC NEUROSECRETORY SYSTEMS: A NOVEL ASPECT OF CENTRAL NEUROENDOCRINE REGULATION

Erik Hrabovszky[1], Zsolt Liposits[1, 2]
[1]Laboratory of Endocrine Neurobiology, Institute of Experimental Medicine, Hungarian Academy of Sciences, Budapest
[2]Department of Neuroscience, Faculty of Information Technology, Péter Pázmány Catholic University, Budapest

A HYPOTHALAMICUS NEUROSZEKRETOROS RENDSZEREK GLUTAMÁTERG FENOTÍPUSA: ÚJ SZEMPONT A CENTRÁLIS NEUROENDOKRIN SZABÁLYOZÁSBAN
Hrabovszky E, MD; Liposits Zs, MD
Ideggyogy Sz 2007;60(3–4):182–186.

While three decades ago, the co-existence of classical neurotransmitters and peptide neuromodulators in a single neuronal cell was considered to be rather exceptional, the phenomenon that neurons have a complex transmitter phenotype now appears to be the general rule. Parvicellular and magnocellular neurosecretory systems consist of neuronal cells which are specialized in secreting peptide neurohormones into the blood-stream to regulate hypophyseal functions. This mini-review, dedicated to the memory of Mariann Fodor, summarizes the current knowledge about the classical neurotransmitter content of different hypothalamic neurosecretory systems, with a special focus on the occurrence and putative functions of glutamate in parvicellular and magnocellular neurosecretory cells.

Keywords: *hypothalamic neurosecretory system, glutamate, neuropeptides, in situ hybridization, immunoflourescence*

Míg három évtizede a klasszikus neurotranszmitterek és neuropeptid természetű neuromodulátorok együttes megjelenését egyazon idegsejtben kivételes jelenségként értelmezte a szakirodalom, a neuronalis kemotípus összetettségére ma már általános szabályként tekintünk. A kis- és nagysejtes neuroszekretoros rendszerek olyan idegsejtekből állnak, amelyek a hypophysealis funkciók szabályozásában szerepet játszó, többségükben peptid természetű neurohormonok szekrécióját végzik. Fodor Mariann emlékének szánt összefoglalónkban áttekintést nyújtunk a különböző neuroszekretoros rendszerek klasszikus neurotranszmitter-tartalmáról, különös tekintettel a glutamát előfordulására és lehetséges szerepére a kis- és nagysejtes neuroszekretoros rendszerekben.

Kulcsszavak: *hypothalamicus neuroszekretoros rendszer, glutamát, neuropeptidek, in situ hibridizáció, immunfluoreszcencia*

Corresponding author: Erik Hrabovszky, M.D., Ph.D., Laboratory of Endocrine Neurobiology, Institute of Experimental Medicine, P.O. Box 67, 1450 Budapest, Hungary. E-mail: hrabovszky@koki.hu

Érkezett: 2007. február 5. Elfogadva: 2007. február 14.

www.lam.hu

Neuropeptides are neurohormones as well as non-classic neurotransmitters

Since Guillemin, Schally and their colleagues discovered the peptidergic nature of hypothalamic releasing and release-inhibiting hormones (luteinizing hormone-releasing hormone, LHRH; thyrotropin-releasing hormone, TRH and somatostatin)[1, 2], there has been a growing interest in understanding the role of neuropeptides in the central nervous system. The discovery of these secretory neuropeptides was in coincidence with the isolation and sequencing of other brain peptides including substance P[3] and two endogenous opioid peptides

In memoriam Mariann Fodor

that are ligands for the opioid receptor, methionine- and leucine-enkephalin[4]. These findings and the subsequent discovery of a series of further neuropeptides shaped the view that peptides represent a novel class of chemical transmitters, involved not only in neuroendocrine regulation but also in pain transmission and other important higher functions of the central nervous system (for a review, see Hökfelt et al.[5]).

Neuropeptides coexist with classic neurotransmitters within the same cell

The finding that somatostatin coexists with a classic neurotransmitter molecule noradrenaline in the same neuron[6] was considered initially as an exception. Later evidence for similar cases shaped a consensus opinion that various neuropeptides and classical neurotransmitters virtually always co-exist in neuronal cells which contributes to the biochemical and functional diversity of neurons[5].

Classic neurotransmitters in neuroendocrine cells of the hypothalamus

Tubero-infundibular dopaminergic (TIDA) neurons with cell bodies in the hypothalamic arcuate nucleus represent a particular class of neurosecretory cells in that they release dopamine, and not a peptide neurohormone, into the hypophyseal portal circulation[7]. While dopamine may, indeed, be the major active secretory product of TIDA neurons, these cells also contain and secrete modulator neuropeptides into the hypophyseal portal circulation. These include neurotensin, enkephalins and neuropeptide Y in lactating animals[8]. Hence, the rule that neurons co-contain neuropeptides with classic neurotransmitters pertains to these cells as well. Moreover, dopamine is not the only classic transmitter in TIDA neurons as these cells also express gamma amino butyric acid (GABA) and its marker enzyme, glutamic acid decarboxylase (GAD)[9]. In addition to TIDA neurons, growth hormone-releasing hormone (GHRH) neurons of the arcuate nucleus also exhibit a similar GABA-ergic phenotype[9, 10]. A low percentage of corticotropin-releasing hormone (CRH) cells in the paraventricular nucleus has also been reported to co-contain GABA and GAD with CRH[11]. While the neuropeptide phenotype of the above cells has been cleared, the classic neurotransmitter content of LHRH neurons in the preoptic area, most CRH neurons and TRH neurons in the paraventricular nucleus and somatostatin neurons in the anterior periventricular nucleus has been unknown or doubtful.

Type-2 vesicular glutamate transporter (VGLUT2) is a recently recognized marker for excitatory glutamatergic neurons of the hypothalamus

Glutamate is a major excitatory synaptic transmitter in neuroendocrine regulation[12]. The presence of metabolic glutamate in all living cells makes the visualization of glutamatergic neurons technically difficult. Only the recent discovery of vesicular glutamate transporters (VGLUT1-3), which selectively accumulate glutamic acid into synaptic vesicles, has provided reliable histochemical markers for the identification of glutamatergic neurons. Out of three distinct molecular forms of the transporter, VGLUT2 represents the dominant isoform synthesized by excitatory neurons in the hypothalamus[13, 14]. Whereas VGLUT2 protein occurs and acts in axon terminals[13], VGLUT2 mRNA can serve as a marker for glutamatergic cell bodies of the hypothalamus[13, 14]. The *in situ* hybridization mapping of hypothalamic VGLUT2 mRNA expression revealed excitatory neurons in several hypothalamic regions critically involved in neuroendocrine regulation[13, 14].

Identification of neuroendocrine glutamatergic cells in the hypothalamus

A special feature of neurosecretory neurons is that their axon terminates outside the blood-brain barrier. As a consequence, these neurons can be identified by the uptake of the retrograde fluorescent tract-tracer molecule Fluoro-Gold from the systemic circulation[15]. Results of recent studies combining Fluoro-Gold detection with the *in situ* hybridization detection of VGLUT2 mRNA established that the organum vasculosum of the lamina terminalis (OVLT), the preoptic area (POA), the anterior periventricular nucleus, the supraoptic nucleus and the parvicellular and magnocellular subdivisions of the paraventricular nucleus contain neuroendocrine glutamatergic cells which accumulate the retrograde tracer Fluoro-Gold and also express VGLUT2 mRNA[16]. In accordance with these data, VGLUT2 immunoreactivity has been revealed in neuroendocrine terminals in the palisade zone of the median eminence where parvicel-

lular axons terminate[14] and also in the posterior pituitary[17] where magnocellular neurosecretory axon processes end.

Use of dual-label *in situ* hybridization and dual-immunofluorescent studies to identify the glutamatergic nature of classic neurosecretory systems

The dual-label ISH method adapted from Petersen and McCrone[18] is a powerful technique which enables the simultaneous detection of the neurosecretory peptidergic neurons and the glutamatergic phenotype within the same cells. This technique uses a non-isotopic and a radioisotopic complementary ribonucleic acid hybridization probe in combination, followed by immunocytochemical and autoradiographic signal visualization of the two probes, respectively. A series of recent studies from our laboratory which used this technique established that most LHRH[19], TRH[20], CRH[20] and somatostatin[10] neurons express VGLUT2 mRNA. In addition, magnocellular oxytocin as well as vasopressin neurons in the supraoptic and paraventricular nuclei exhibited VGLUT2 mRNA expression[17]. Dual-immunofluorescent studies of the median eminence and the posterior pituitary were carried out to confirm the presence of VGLUT2 protein in neurosecretory axon endings. Confocal laser microscopic analysis established the presence of VGLUT2 immunoreactivity in most types of neuropeptidergic axon terminals in the external zone of the median eminence and the posterior pituitary. The only exceptions from the glutamatergic (VGLUT2) phenotype were TIDA and GHRH neurons of the arcuate nucleus which were previously reported to be GABA-ergic[9]. The synthesis of growth hormone (GH) and its release from the somatotrophs is under the dual control of the stimulatory GHRH and the inhibitory somatostatin (for a review, see Fodor et al.[21]). Conceptually it is interesting to note that the inhibitory amino acid neurotransmitter GABA is co-localized with the stimulatory peptide GHRH, whereas the stimulatory amino acid neurotransmitter glutamate is co-localized with the inhibitory peptide somatostatin.

Subcellular localization of VGLUT2 in neurosecretory nerve terminals

While secreted neuropeptides are located in dense-core vesicles, pre-embedding immuno-electron microscopic studies have revealed VGLUT2 immunoreactivity in association with small clear synaptic vesicles both in the palisade zone of the median eminence and in the posterior pituitary. Interestingly, small clear vesicles accumulated preferentially in the immediate proximity of the pericapillary space in the terminal portion of neurosecretory axons[16].

Putative role of glutamate in neurosecretory endings

The physiological role of glutamate co-secretion from neuroendocrine terminals remains to be investigated. One possibility is that glutamate released from parvicellular hypophysiotropic terminals reaches the anterior pituitary at high enough concentrations to exert physiological effects. Although this putative hypophyseal site of glutamatergic actions would be compatible with the reported presence of ionotropic as well as metabotropic glutamate receptors in adenohypophyseal cells[22, 23], it seems more likely that the secreted glutamate rather acts locally at the level of the median eminence and the posterior pituitary. Putative target structures for the actions of glutamate include the neurosecretory axon terminal. Accordingly, LHRH terminals in the median eminence exhibit immunoreactivities for the KA2 and NMDAR1 receptor subtypes[24] which may be involved in autocrine/paracrine regulatory mechanisms upon binding glutamate secreted from endogenous sources. While the concept requires experimental support, it is tempting to speculate that the endogenous glutamate content of these systems contributes to common signaling mechanisms that generates the pulsatile patterns of neurohormone output.

In addition to affect directly neurosecretory terminals, secreted glutamate may regulate important glial functions at the sites of release. In support of this concept, tanycytes and astrocytes in the ME were found to contain mRNAs and immunoreactivity for kainate receptors and to express *c-Fos* immunoreactivity upon kainate stimulation[25, 26]. As tanycytic processes regulate the neuro-hemal junction in the ME, it is an intriguing possibility that glutamate induces plastic changes in this cell type to regulate the access of secretion products to the hypophyseal portal vessels. Finally, intrinsic glutamate released by hypophysiotropic terminals may also act on vascular elements though endothelial metabotropic[27, 28] and ionotropic[28] glutamate receptors.

It is interesting to note that the stimulation of NMDA receptors increases nitric oxide production within the median eminence[29] which is considered

to be mostly of endothelial origin in this region[30]. Nitric oxide, in turn, is an important regulator of LHRH and CRH release from the median eminence[30] which is proposed to act via increasing cGMP and/or prostaglandin E2 production in the hypophysiotropic axon terminals[30]. Actions mediated by the soluble nitric oxide may also propagate the glutamatergic signal to a larger group of neurosecretory terminals and to a higher distance from the site of glutamate release.

A final interesting aspect of the glutamatergic phenotype is the recent observation that various endocrine manipulations can alter the expression of VGLUT2 mRNA in endocrine/neuroendocrine cells. Accordingly, salt-loading (2% sodium chloride in the drinking water for 7 days) results in a robust increase of VGLUT2 mRNA expression in vasopressin neurons of the supraoptic nucleus. This is also accompanied by an enhancement of VGLUT2 immunoreactivity in the posterior pituitary where vasopressinergic axons terminate[17]. Anterior pituitary gonadotropes and thyrotropes also exhibit VGLUT2 mRNA and immunoreactivity. Either estrogen substitution to ovariectomized rats or hypothyroidism were found to increases adenohypophyseal VGLUT2 mRNA expression[31]. At present, the functional significance of regulated VGLUT2 synthesis in the above endocrine paradigms is unclear.

ACKNOWLEDGEMENTS

This research was supported by grants from the National Science Foundation of Hungary (OTKA T43407, T46574), NKFP 1A/002/2004, and the European Union FP6 funding (LSHMCT-2003-50304).

REFERENCES

1. *Guillemin R.* Biochemical and physiological correlates of hypothalamic peptides. The new endocrinology of the neuron. Research publications – Association for Research in Nervous and Mental Disease 1978;56:155-94.
2. *Schally AV, Arimura A, Kastin AJ.* Hypothalamic regulatory hormones. Science 1973;179:341-50.
3. *Said SI, Mutt V.* Polypeptide with broad biological activity: isolation from small intestine. Science 1970;169:217-8.
4. *Hughes J, Smith TW, Kosterlitz HW, Fothergill LA, Morgan BA, Morris HR.* Identification of two related pentapeptides from the brain with potent opiate agonist activity. Nature 1975;258:577-80.
5. *Hokfelt T, Broberger C, Xu ZQ, Sergeyev V, Ubink R, Diez M.* Neuropeptides – an overview. Neuropharmacology 2000;39:1337-56.
6. *Hokfelt T, Elfvin LG, Elde R, Schultzberg M, Goldstein M, Luft R.* Occurrence of somatostatin-like immunoreactivity in some peripheral sympathetic noradrenergic neurons. Proc Natl Acad Sci USA 1977;74:3587-91.
7. *Reymond MJ, Porter JC.* Involvement of hypothalamic dopamine in the regulation of prolactin secretion. Horm Res 1985;22:142-52.
8. *Ciofi P, Crowley WR, Pillez A, Schmued LL, Tramu G, Mazzuca M.* Plasticity in expression of immunoreactivity for neuropeptide Y, enkephalins and neurotensin in the hypothalamic tuberoinfundibular dopaminergic system during lactation in mice. J Neuroendocrinol 1993;5:599-602.
9. *Meister B, Hokfelt T.* Peptide- and transmitter-containing neurons in the mediobasal hypothalamus and their relation to GABAergic systems: possible roles in control of prolactin and growth hormone secretion. Synapse 1988;2:585-605.
10. *Hrabovszky E, Turi GF, Liposits Z.* Presence of vesicular glutamate transporter-2 in hypophysiotropic somatostatin but not growth hormone-releasing hormone neurons of the male rat. Eur J Neurosci 2005;21:2120-6.
11. *Meister B, Hokfelt T, Geffard M, Oertel W.* Glutamic acid decarboxylase- and gamma-aminobutyric acid-like immunoreactivities in corticotropin-releasing factor-containing parvocellular neurons of the hypothalamic paraventricular nucleus. Neuroendocrinology 1988;48:516-26.
12. *van den Pol AN, Wuarin JP, Dudek FE.* Glutamate, the dominant excitatory transmitter in neuroendocrine regulation. Science 1990;250:1276-8.
13. *Herzog E, Bellenchi GC, Gras C, et al.* The existence of a second vesicular glutamate transporter specifies subpopulations of glutamatergic neurons. J Neurosci 2001;21: RC181.
14. *Lin W, McKinney K, Liu L, Lakhlani S, Jennes L.* Distribution of vesicular glutamate transporter-2 messenger ribonucleic acid and protein in the septum-hypothalamus of the rat. Endocrinology 2003;144:662-70.
15. *Merchenthaler I.* Neurons with access to the general circulation in the central nervous system of the rat: a retrograde tracing study with fluoro-gold. Neuroscience 1991;44:655-62.
16. *Hrabovszky E, Deli L, Turi GF, Kallo I, Liposits Z.* Glutamatergic innervation of the hypothalamic median eminence and posterior pituitary of the rat. Neuroscience 2007;144: 1383-92.
17. *Hrabovszky E, Csapo AK, Kallo I, Wilheim T, Turi GF, Liposits Z.* Localization and osmotic regulation of vesicular glutamate transporter-2 in magnocellular neurons of the rat hypothalamus. Neurochem Int 2006;48:753-61.
18. *Petersen S, McCrone S.* Characterization of the receptor complement of individual neurons using dual-label in situ hybridization histochemistry. In: *Eberwine JH, Valentino K, Barchas J (eds.). In situ* hybridization in neurobiology. Advances in methodology. New York: Oxford University Press; 1994. p. 78-94.
19. *Hrabovszky E, Turi GF, Kallo I, Liposits Z.* Expression of vesicular glutamate transporter-2 in gonadotropin-releasing hormone neurons of the adult male rat. Endocrinology 2004;145:4018-21.
20. *Hrabovszky E, Wittmann G, Turi GF, Liposits Z, Fekete C.*

Hypophysiotropic thyrotropin-releasing hormone and corticotropin-releasing hormone neurons of the rat contain vesicular glutamate transporter-2. Endocrinology 2005; 146:341-7.
21. *Fodor M, Kordon C, Epelbaum J.* Anatomy of the hypophysiotropic somatostatinergic and growth hormone-releasing hormone system minireview. Neurochem Res 2006;31:137-43.
22. *Bhat GK, Mahesh VB, Chu ZW, Chorich LP, Zamorano PL, Brann DW.* Localization of the N-methyl-D-aspartate R1 receptor subunit in specific anterior pituitary hormone cell types of the female rat. Neuroendocrinology 1995; 62:178-86.
23. *Caruso C, Bottino MC, Pampillo M, et al.* Glutamate induces apoptosis in anterior pituitary cells through group II metabotropic glutamate receptor activation. Endocrinology 2004;145:4677-84.
24. *Kawakami SI, Hirunagi K, Ichikawa M, Tsukamura H, Maeda KI.* Evidence for terminal regulation of GnRH release by excitatory amino acids in the median eminence in female rats: a dual immunoelectron microscopic study. Endocrinology 1998;139:1458-61.
25. *Diano S, Naftolin F, Horvath TL.* Kainate glutamate receptors (GluR5-7) in the rat arcuate nucleus: relationship to tanycytes, astrocytes, neurons and gonadal steroid receptors. J Neuroendocrinol 1998;10:239-47.
26. *Eyigor O, Jennes L.* Identification of kainate-preferring glutamate receptor subunit GluR7 mRNA and protein in the rat median eminence. Brain Res 1998;814:231-5.
27. *Gillard SE, Tzaferis J, Tsui HC, Kingston AE.* Expression of metabotropic glutamate receptors in rat meningeal and brain microvasculature and choroid plexus. J Comp Neurol 2003;461:317-32.
28. *Krizbai IA, Deli MA, Pestenacz A, et al.* Expression of glutamate receptors on cultured cerebral endothelial cells. J Neurosci Res 1998;54:814-9.
29. *Bhat GK, Mahesh VB, Ping L, Chorich L, Wiedmeier VT, Brann DW.* Opioid-glutamate-nitric oxide connection in the regulation of luteinizing hormone secretion in the rat. Endocrinology 1998;139:955-60.
30. *Prevot V, Bouret S, Stefano GB, Beauvillain J.* Median eminence nitric oxide signaling. Brain Res Rev 2000;34: 27-41.
31. *Hrabovszky E, Kallo I, Turi GF, et al.* Expression of vesicular glutamate transporter-2 in gonadotrope and thyrotrope cells of the rat pituitary. Regulation by estrogen and thyroid hormone status. Endocrinology 2006;147:3818-25.

15. számú melléklet

0021-972X/07/$15.00/0
Printed in U.S.A.

The Journal of Clinical Endocrinology & Metabolism 92(7):2827–2830

doi: 10.1210/jc.2006-2819

BRIEF REPORT

Gonadotropin-Releasing Hormone Neurons Express Estrogen Receptor-β

E. Hrabovszky,* I. Kalló,* N. Szlávik, É. Keller, I. Merchenthaler, and Z. Liposits

Laboratory of Endocrine Neurobiology (E.H., I.K., Z.L.), Institute of Experimental Medicine, Hungarian Academy of Sciences; Department of Forensic Medicine (N.S., E.K.), Semmelweis University; and Department of Neuroscience (Z.L.), Faculty of Information Technology, Pázmány Péter Catholic University, Budapest, 1083 Hungary; and Departments of Epidemiology and Preventive Medicine and Anatomy and Neurobiology (I.M.), University of Maryland, Baltimore, Maryland 21201

Context: Recent identification of the second estrogen receptor (ER) isoform (ER-β) within GnRH neurons of the rodent brain has generated much enthusiasm in the field of neuroendocrine research by questioning the dogma that GnRH cells do not directly sense changes in circulating estrogens.

Objective: To address the issue of whether GnRH neurons of the human hypothalamus also contain ER-β, we have performed dual-label immunocytochemical studies.

Design: Tissue sections were prepared from autopsy samples of male human individuals (n = 8; age < 50 yr), with sudden causes of death. Technical efforts were made to minimize postmortem interval (<24 h), optimize tissue fixation (use of a mixture of 2% paraformaldehyde and 4% acrolein for four tissue samples), and sensitize the immunocytochemical detection of ER-β (application of silver-intensified nickel-diaminobenzidine chromogen).

Main Outcome Measure: Distribution and percent ratio of GnRH neurons that also contained ER-β immunoreactivity were analyzed under the light microscope.

Results: With acrolein in tissue fixative, nuclear ER-β immunoreactivity was observed in 10.8–28.0% of GnRH neurons of the four different individuals. ER-β-containing GnRH neurons were widely distributed in the hypothalamus, without showing a noticeable preference in regional location.

Conclusions: The demonstration of ER-β and the previous lack of detection of ER-α in human GnRH cells indicate that estrogens may exert direct actions upon GnRH neurons exclusively through ER-β. In the light of differing ligand-binding characteristics of ER-β from those of ER-α, this discovery offers a potential new approach to influence estrogen feedback to GnRH neurons through ER-β-selective receptor ligands. **(*J Clin Endocrinol Metab* 92: 2827–2830, 2007)**

THE GnRH (ALSO CALLED LHRH) neurosecretory system represents the final common hypothalamic pathway in the neuroendocrine control of reproduction. Changing levels of the ovarian sex steroid hormone 17β-estradiol (E2) tightly regulate the activity of the neuroendocrine reproductive axis through feedback actions to GnRH cells (for review, see Ref. 1). In 1983, Shivers *et al.* (2) reported that GnRH neurons of the rat do not accumulate tritiated E2 *in vivo*. This surprising observation and the coherent results of subsequent immunocytochemical studies that failed to show any estrogen receptors (ERs) in GnRH neurons (3, 4) suggested that estrogen signaling is communicated to the GnRH neuronal system by estrogen-sensitive interneurons and/or glial cells. Shortly after the discovery of a second ER isoform (ER-β), this view was challenged by reports of ER-α immunoreactivity (5), ER-α mRNA (6), ER-β mRNA (6, 7), and [^{125}I]estrogen-binding sites (7) in rodent GnRH neurons. In 2000, our group published the results of dual-label *in situ* hybridization experiments that showed absence of ER-α and presence of ER-β mRNA hybridization signal in GnRH neurons of rats (7). This report was followed by the withdrawal (8) of previous ER-α mRNA detection in mouse GnRH neurons (6). The opinion that rodent GnRH neurons only contain the ER-β isoform started to form. In 2001, two groups detected nuclear ER-β immunoreactivity in 63–73% of GnRH neurons in the rat (9, 10). These immunocytochemical data, together with the previous observation that GnRH neurons of the rat are capable of accumulating a ^{125}I-labeled estrogen compound *in vivo* (7), strengthened the concept that GnRH neurons synthesize functional ER-β.

The recent demonstration of immunoreactive ER-β in a large subset of ovine GnRH neurons (11) that lack ER-α (12) indicates that the selective presence of ER-β in GnRH cells is not restricted to rodent species. The issue of whether or not GnRH neurons of the human also contain ER-β remained unresolved. Therefore, in the present immunocytochemical study, we addressed the putative presence of ER-β in GnRH neurons of the human hypothalamus.

Materials and Methods

Tissue samples

Human hypothalamic samples from eight male individuals with postmortem intervals between 12–14 h were obtained at autopsy from

First Published Online April 24, 2007

* E.H. and I.K. have contributed equally to the studies presented in this manuscript.

Abbreviations: E2, 17β-Estradiol; ER, estrogen receptor.

the Forensic Medicine Department of Semmelweis University (Budapest, Hungary) using protocols reviewed and approved by the Regional Committee of Science and Research Ethics (TUKEB 49/1999). Selection criteria included sudden causes of death, lack of history of neurological and endocrinological disorders, postmortem intervals between 12–24 h and age less than 50 yr. Hypothalamic blocks were dissected out according to guidelines of the optic chiasm (rostrally), mammillary bodies (caudally), the anterior commissure (dorsally), and 2 cm lateral from the midsagittal plane (laterally). The tissue blocks were initially rinsed for 5 min in several changes of 4% paraformaldehyde solution prepared with 0.1 M PBS (pH 7.4) and then transferred for 2 d into a freshly prepared mixture of 4% acrolein and 2% paraformaldehyde (4 C).

Section preparation

Tissue blocks were infiltrated with 30% sucrose for 5 d and cut in half in the midsagittal plane to reduce section size. The hemi-hypothalami were aligned in a freezing mold, surrounded with Jung tissue freezing medium (Leica Microsystems, Nussloch Gmbh, Germany; diluted 1:1 with 0.9% sodium chloride solution), frozen on powdered dry ice, and sectioned serially at 30 μm with a Leica CM 3050 S cryostat (Leica) according to the plane of the lamina terminalis. The sections were stored in antifreeze solution (30% ethylene glycol, 25% glycerol, 0.05 M phosphate buffer) at −20 C until used.

Dual-label immunocytochemical studies

Every 20th section from each block was processed for dual-label immunocytochemistry. Sections were pretreated with 1% sodium borohydride (30 min), a mixture of 0.5% H_2O_2 and Triton X-100 (30 min), 3.7% paraformaldehyde in 30% ethanol (30 min), 8% thioglycolic acid (30 min), and 2% normal horse serum (30 min). The sections were first incubated in a 1:20,000 dilution (in 2% normal horse serum) of primary ER-β antibodies (P3; gift from Dr. P. T. Saunders, Edinburgh, UK) raised in sheep and targeting the A/B region of human ER-β (13), followed by biotinylated secondary antibodies (Jackson ImmunoResearch Europe Ltd., Soham, Cambridgeshire, UK; 1:1,000) and ABC Elite reagent (60 min each). The signal was visualized with nickel-intensified diaminobenzidine and then post-intensified with silver-gold (9, 10). Subsequently, GnRH immunoreactivity was detected with rabbit primary antibodies (LR-1, 1:20,000; gift from Dr. R. A. Benoit, Montreal, Canada) using the biotinylated secondary antibody-ABC technique and nonintensified diaminobenzidine as chromogen. The dual-labeled sections were mounted on microscope slides and coverslipped with DPX mounting medium (Fluka Chemie, Buchs, Switzerland).

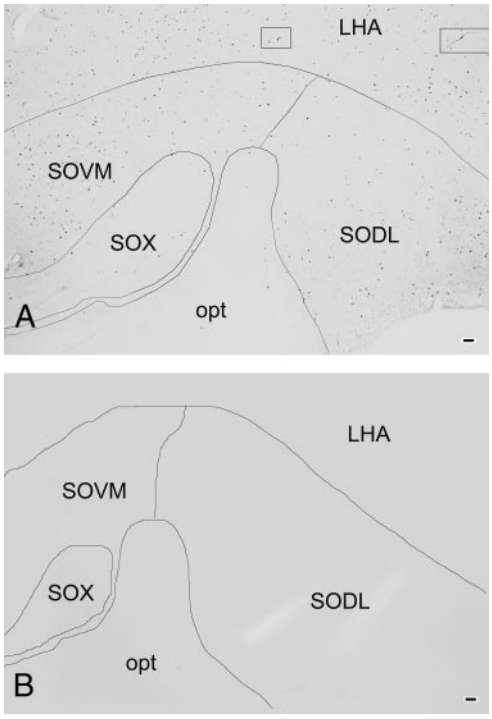

FIG. 1. Detection of ER-β-immunoreactive neurons in the human hypothalamus. The ER-β antigen was visualized with the P3 antibodies using the silver-gold intensification of the nickel-diaminobenzidine peroxidase reaction product (*black*). A, Immunolabeling was localized to the cell nuclei, was abundant in the dorsolateral (SODL) and ventromedial subdivisions (SOVM) of the supraoptic nucleus, but also occurred in high numbers in other hypothalamic regions, including the lateral hypothalamic area (LHA). Note that after the immunolocalization of ER-β, this section also went through the immunocytochemical detection of GnRH using diaminobenzidine chromogen. The two GnRH neurons in *boxed* regions exhibited ER-β labeling in their cell nucleus, as shown at high magnification in Fig. 2, A and B. B, Section showing the lack of any ER-β signal went through the immunocytochemical detection of ER-β using a primary antiserum preabsorbed with 5 μg/ml of the immunization antigen. *Scale bar*, 100 μm.

Results

Distribution of ER-β immunoreactivity in the human hypothalamus

The immunocytochemical detection of ER-β caused nuclear immunolabeling in hypothalamic (Fig. 1A) neurons. The silver-gold intensification step enhanced the staining of labeled nuclei and rendered the nickel-diaminobenzidine chromogen dark and granular (Figs. 1A and 2, A–G). No immunoreactivity was observed if the primary or secondary antibodies were omitted or when the ER-β antibody had been immunoneutralized with 5 μg/ml of the immunization antigen (Fig. 1B). Increasing dilutions of the primary antibody led to a commensurate attenuation of the immunoreactive signal.

The nuclear ER-β signal occurred in common in the hypothalamic sections of the eight individuals. However, the staining intensity varied largely among the brains, suggesting differences in antigen preservation and/or receptor abundance. Clearly, the labeling was heaviest in tissues fixed with the acrolein/paraformaldehyde mixture. ER-β-immunoreactive cell nuclei were widely distributed in the hypothalamus, including the supraoptic nucleus (Fig. 1A) where previous studies have shown its presence in magnocellular oxytocin and vasopressin neurons (14). Considerable variations were noticed in labeling intensity of individual ER-β-containing cell nuclei (Fig. 1A).

Identification of ER-β-immunoreactive GnRH neurons

GnRH neurons occurred in very low numbers within individual hypothalamic sections (Figs. 1A and 2C). Bipolar (Fig. 2B) and multipolar (Fig. 2G) neuronal shapes were distinguishable. High-power microscopic analysis of acrolein/paraformaldehyde-fixed sections revealed ER-β in a subset of GnRH neurons (Fig. 2, B, D, and G), whereas other GnRH cells contained no signal for ER-β (Fig. 2E). Dual-labeled neurons occurred in highest numbers in the lateral and dorsal hypothalamic areas, in the infundibular, lateral tuberal, ventromedial, periventricular, supraoptic, and paraventricular nuclei, without showing a preferential location in any particular hypothalamic region (Fig 2). Their percent ratio in the four individuals was 10.8, 11.1, 21.7, and 28.0%,

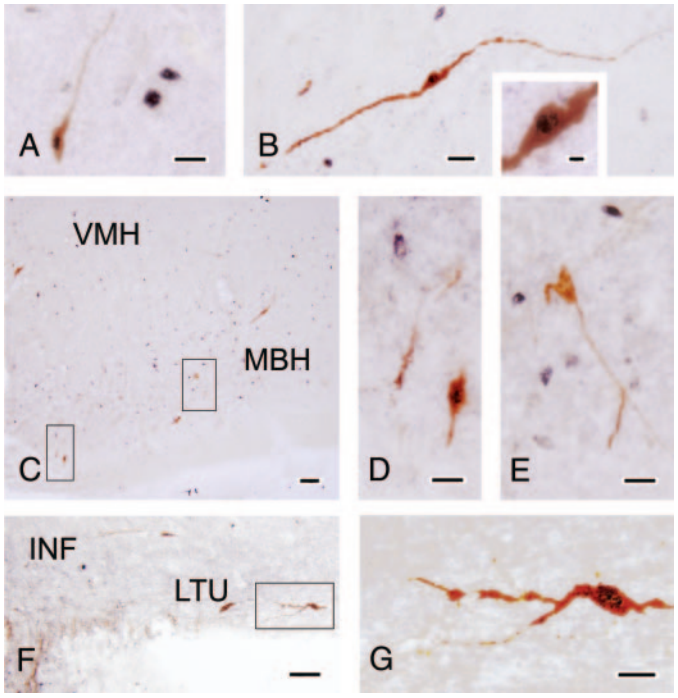

FIG. 2. Demonstration of ER-β immunoreactivity in GnRH neurons of the human hypothalamus. The ER-β antigen was detected using the silver-gold intensification of nickel-diaminobenzidine peroxidase reaction product (*black*), whereas GnRH neurons were stained with the nonintensified diaminobenzidine chromogen (*brown*). Cell nuclei immunoreactive for ER-β occurred in high numbers in the lateral hypothalamic area (LHA) (A and B), ventromedial nucleus (VMH) (C and D), medial basal hypothalamus (MBH) (C and E), infundibular nucleus (INF) (F), and lateral tuberal nucleus (LTU) (F and G). The GnRH neurons were scattered within the same regions and often contained ER-β-immunoreactive nucleus. Note two dual-labeled GnRH neurons in the LHA (A and B; also shown in *boxed* regions of Fig. 1A) that are bipolar in shape. *Inset* in B demonstrates the characteristic nuclear labeling for ER-β. Single-labeled (E) and double-labeled (D and G) GnRH neurons are both found in the MBH (D) and the LTU (G), marked with *boxes* in low-power images C and F. Some GnRH cells exhibit a multipolar morphology (E and G). *Scale bars*, 100 μm (C and F), 25 μm (A, B, D, E, and G), and 5 μm (high-power *inset* in B).

respectively. Paraformaldehyde fixation, in itself, was not sufficient to visualize any ER-β immunoreactivity in GnRH neurons.

Discussion

Results of this dual-label immunocytochemical study provide the first evidence for ER-β in human GnRH neurons. This observation, together with the previously reported lack of ER-α in these cells (15) indicate that E2 may directly regulate human GnRH neurons via the ER-β receptor isoform.

The use of postmortem tissue samples in this study raises the question as to what extent suboptimal tissue processing compromised the sensitivity of ER-β detection. Paraformaldehyde fixation, in itself, was clearly incompatible with the visualization of any ER-β immunoreactivity in the cell nuclei of GnRH cells. Similarly to this observation on human samples, the inclusion of acrolein in the fixative was critically important to maximize the number of ER-β-immunoreactive GnRH neurons in the rat (9, 10). On the other hand, paraformaldehyde-based fixation of human hypothalamic tissue samples clearly ensured sufficient antigen preservation to visualize ER-β immunoreactivity in magnocellular neurosecretory neurons (14). The uncontrolled tissue damage before tissue fixation could interfere further with the visualization of ER-β in GnRH cells of postmortem human tissues. This could account for the variations in the intensity of ER-β staining and in the percentage (10.8–28.0%) of the ER-β-immunoreactive GnRH neurons across the four acrolein/paraformaldehyde-fixed samples. These technical considerations suggest that the ratio of ER-β-expressing GnRH neurons could be significantly underestimated in this study.

A physiological correlate of our present studies is the use of male hypothalami. This has eliminated differences in the ER-β staining of GnRH neurons as an effect of variations in circulating estrogen levels. It is worth noting that our previous immunocytochemical study on rats, indeed, revealed a negative impact of E2 on the percent ratio of ER-β-immunoreactive GnRH neurons (10). Given that only male individuals were included in this study, the potential sexual dimorphism of the colocalization phenomenon will also require future clarification with the parallel use of similarly processed tissue samples from men and women. In this context, it is worth mentioning that previous *in situ* hybridization (9) and immunocytochemical (9) studies failed to detect any significant gender difference in the percent ratio of ER-β-synthesizing GnRH neurons in rats. Although results of preliminary studies also indicate the presence of ER-β in GnRH neurons of the human female, the low sample number has not allowed yet a systematic assessment of potential sex differences (Hrabovszky, E., unpublished observations).

The results of the present immunocytochemical experiments provide strong evidence for the presence of ER-β in human GnRH neurons. In the light of previous studies that showed the lack of ER-α mRNA in human GnRH neurons (15) and the accumulating evidence that only the ER-β isoform occurs in GnRH neurons of rodents (7, 8) and ewes (11), it is reasonable to speculate that direct estrogen actions upon human GnRH neurons may be exerted exclusively via ER-β. With this information, the growing number of ER-β-selective ligands may offer a unique tool to modulate GnRH cell functions and thereby the human reproductive axis. This long-term perspective necessitates a solid knowledge about the direct actions of ER-β on GnRH cell functions. Several studies on rodent GnRH neurons have already identified such ER-β-mediated direct estrogen actions. The fast, nongenomic actions of ligand-bound ER-β include rapid phosphorylation of cAMP-response element-binding protein (16) and stimulation of intracellular calcium oscillations (17) in mouse GnRH neurons. Estrogen also increases excitability of mouse GnRH neurons, partly via mechanisms that include phosphorylation of potassium channels (18). *In vitro* transfection experiments have also established the role of ER-β in a ligand-independent transcriptional activation and a ligand-dependent transcriptional repression of the mouse GnRH promoter (19). Furthermore, *in vivo* studies with newly available ER-β-selective agonist ligands provided evidence for the ER-β-mediated induction of galanin mRNA expression in GnRH neurons of rats (20). Although the precise role of ER-β

in fertility of laboratory animals and humans remains to be determined, one has to remain aware of well-established indirect estrogen actions that involve interneurons expressing the ER-α isoform.

In summary, we have identified ER-β immunoreactivity in GnRH neurons of the human hypothalamus. Because these cells lacked ER-α in previous studies, the new findings indicate that estrogens may exert direct actions upon GnRH cells selectively through the ER-β isoform. The differing ligand-binding characteristics of ER-β from those of the classical ER-α offers a potential new strategy to influence estrogen feedback mechanisms to human GnRH neurons via recently available ER-β-selective ligands.

Acknowledgments

We thank Drs. R. A. Benoit and P. T. Saunders for kindly providing the LR1 (GnRH) and P3 (ER-β) antibodies, respectively, and E. Dobó for helpful technical advice.

Received December 20, 2006. Accepted April 16, 2007.

Address all correspondence and requests for reprints to: Erik Hrabovszky, M.D., Ph.D., Department of Neurobiology, Institute of Experimental Medicine, Hungarian Academy of Sciences, Budapest, 1083 Hungary. E-mail: hrabovszky@koki.hu.

This work was supported by grants from the National Science Foundation of Hungary (OTKA T43407 and T46574), NKFP 1A/002/2004, and the European Union FP6 funding (LSHM-CT-2003-50304).

This publication reflects the authors' views and not necessarily those of the European Union. The information in this document is provided as is, and no guarantee or warranty is given that the information is fit for any particular purpose. The user thereof uses the information at its sole risk and liability.

Disclosure: All of the authors have nothing to declare.

References

1. **Petersen SL, Ottem EN, Carpenter CD** 2003 Direct and indirect regulation of gonadotropin-releasing hormone neurons by estradiol. Biol Reprod 69:1771–1778
2. **Shivers BD, Harlan RE, Morrell JI, Pfaff DW** 1983 Absence of oestradiol concentration in cell nuclei of LHRH-immunoreactive neurones. Nature 304: 345–347
3. **Watson R, Langub M, Landis J** 1992 Further evidence that most luteinizing hormone-releasing hormone neurons are not directly estrogen-responsive: simultaneous localization of luteinizing hormone-releasing hormone and estrogen receptor immunoreactivity in the guinea pig brain. J Neuroendocrinol 4:311–318
4. **Herbison AE, Theodosis DT** 1992 Localization of oestrogen receptors in preoptic neurons containing neurotensin but not tyrosine hydroxylase, cholecystokinin or luteinizing hormone-releasing hormone in the male and female rat. Neuroscience 50:283–298
5. **Butler JA, Sjoberg M, Coen CW** 1999 Evidence for oestrogen receptor α-immunoreactivity in gonadotrophin-releasing hormone-expressing neurones. J Neuroendocrinol 11:331–335
6. **Skynner MJ, Sim JA, Herbison AE** 1999 Detection of estrogen receptor α and β messenger ribonucleic acids in adult gonadotropin-releasing hormone neurons. Endocrinology 140:5195–5201
7. **Hrabovszky E, Shughrue PJ, Merchenthaler I, Hajszan T, Liposits Z, Carpenter CD, Petersen SL** 2000 Detection of estrogen receptor-β messenger ribonucleic acid and ^{125}I-estrogen binding sites in luteinizing hormone-releasing hormone neurons of the rat brain. Endocrinology 141:3506–3509
8. **Herbison A, Skynner M, Sim J** 2001 Lack of detection of estrogen receptor-α transcripts in mouse gonadotropin-releasing hormone neurons. Endocrinology 142:492
9. **Hrabovszky E, Steinhauser A, Barabás K, Shughrue PJ, Petersen SL, Merchenthaler I, Liposits Z** 2001 Estrogen receptor-β immunoreactivity in luteinizing hormone-releasing hormone neurons of the rat brain. Endocrinology 142:3261–3264
10. **Kallo I, Butler JA, Barkovics-Kallo M, Goubillon ML, Coen CW** 2001 Oestrogen receptor β-immunoreactivity in gonadotropin releasing hormone-expressing neurones: regulation by oestrogen. J Neuroendocrinol 13:741–748
11. **Skinner DC, Dufourny L** 2005 Oestrogen receptor β-immunoreactive neurones in the ovine hypothalamus: distribution and colocalisation with gonadotropin-releasing hormone. J Neuroendocrinol 17:29–39
12. **Herbison AE, Robinson JE, Skinner DC** 1993 Distribution of estrogen receptor-immunoreactive cells in the preoptic area of the ewe: co-localization with glutamic acid decarboxylase but not luteinizing hormone-releasing hormone. Neuroendocrinology 57:751–759
13. **Saunders PT, Millar MR, Williams K, Macpherson S, Harkiss D, Anderson RA, Orr B, Groome NP, Scobie G, Fraser HM** 2000 Differential expression of estrogen receptor-α and -β and androgen receptor in the ovaries of marmosets and humans. Biol Reprod 63:1098–1105
14. **Hrabovszky E, Kallo I, Steinhauser A, Merchenthaler I, Coen CW, Petersen SL, Liposits Z** 2004 Estrogen receptor-β in oxytocin and vasopressin neurons of the rat and human hypothalamus: immunocytochemical and in situ hybridization studies. J Comp Neurol 473:315–333
15. **Rance NE, McMullen NT, Smialek JE, Price DL, Young 3rd WS** 1990 Postmenopausal hypertrophy of neurons expressing the estrogen receptor gene in the human hypothalamus. J Clin Endocrinol Metab 71:79–85
16. **Abraham IM, Han SK, Todman MG, Korach KS, Herbison AE** 2003 Estrogen receptor β mediates rapid estrogen actions on gonadotropin-releasing hormone neurons in vivo. J Neurosci 23:5771–5777
17. **Temple JL, Laing E, Sunder A, Wray S** 2004 Direct action of estradiol on gonadotropin-releasing hormone-1 neuronal activity via a transcription-dependent mechanism. J Neurosci 24:6326–6333
18. **DeFazio RA, Moenter SM** 2002 Estradiol feedback alters potassium currents and firing properties of gonadotropin-releasing hormone neurons. Mol Endocrinol 16:2255–2265
19. **Pak TR, Chung WC, Roberts JL, Handa RJ** 2006 Ligand-independent effects of estrogen receptor β on mouse gonadotropin-releasing hormone promoter activity. Endocrinology 147:1924–1931
20. **Merchenthaler I, Hoffman GE, Lane MV** 2005 Estrogen and estrogen receptor-β (ERβ)-selective ligands induce galanin expression within gonadotropin hormone-releasing hormone-immunoreactive neurons in the female rat brain. Endocrinology 146:2760–2765

JCEM is published monthly by The Endocrine Society (http://www.endo-society.org), the foremost professional society serving the endocrine community.

16. számú melléklet

Available online at www.sciencedirect.com
ScienceDirect
Neurochemistry International 52 (2008) 723–728
NEUROCHEMISTRY International
www.elsevier.com/locate/neuint

Cholinergic afferents to gonadotropin-releasing hormone neurons of the rat

Gergely F. Turi [a], Zsolt Liposits [a,b], Erik Hrabovszky [a,*]

[a] Laboratory of Endocrine Neurobiology, Institute of Experimental Medicine, Hungarian Academy of Sciences, H-1083 Budapest, Hungary
[b] Department of Neuroscience, Faculty of Information Technology, Péter Pázmány Catholic University, H-1083 Budapest, Hungary

Received 19 June 2007; received in revised form 31 August 2007; accepted 3 September 2007
Available online 8 September 2007

Abstract

Gonadotropin-releasing hormone-synthesizing neurons represent the final common pathway in the hypothalamic regulation of reproduction and their secretory activity is influenced by a variety of neurotransmitters and neuromodulators acting centrally in synaptic afferents to gonadotropin-releasing hormone neurons. The present study examined the anatomical relationship of cholinergic neuronal pathways and gonadotropin-releasing hormone neurons of the preoptic area. The immunocytochemical detection of choline acetyltransferase or vesicular acetylcholine transporter revealed a fine network of cholinergic fibers in this region. At the light microscopic level, the cholinergic axons formed appositions to the gonadotropin-releasing hormone immunoreactive cell bodies and dendrites. Results of electron microscopic studies confirmed the absence of glial interpositions in many of these neuronal contacts. Classical cholinergic synapses, which belonged to the asymmetric category, were only observed rarely on gonadotropin-releasing hormone neurons. The lack of synaptic density in most contacts corroborates previous observations on the cholinergic system elsewhere in the brain. Further, it suggests a dominantly non-synaptic route also in this cholinergic neuronal communication.

This study provides direct neuromorphological evidence for the involvement of the cholinergic system in the afferent neuronal regulation of gonadotropin-releasing hormone neurons. The sources of cholinergic afferents and the receptorial mechanisms underlying this interaction will require further clarification.

Keywords: Acetylcholine; ChAT; Luteinizing hormone-releasing hormone; Preoptic area; Reproduction; VAChT

1. An introductory statement

The central regulation of the mammalian reproductive axis is carried out by about 1000–1200 gonadotropin-releasing hormone (GnRH) producing neurons (Merchenthaler et al., 1984). In rodents most GnRH neurons are scattered in the medial septum (MS), diagonal band of Broca (DBB) and medial preoptic area (MPOA) (Merchenthaler et al., 1984). Their axons project to the median eminence and release the decapeptide GnRH into the hypophysial portal capillaries (Merchenthaler et al., 1984) in a pulsatile manner (Levine and Duffy, 1988). While the pulsatility appears to be an intrinsic feature of the GnRH neuronal network (Nunemaker et al., 2001), the frequency and amplitude of episodic secretion are modulated by classical neurotransmitters and peptide neuromodulators, which reach GnRH neurons via specific neuronal afferents (Herbison, 1998). Fibers innervating GnRH neurons contain β-endorphin (Leranth et al., 1988b), neuropeptide Y (Tsuruo et al., 1990), GABA (Leranth et al., 1985), glutamate (Kiss et al., 2003), tyrosine-hydroxylase (Leranth et al., 1988a), agouti gene-related peptide (Turi et al., 2003), corticotropin releasing factor (MacLusky et al., 1988), 5-HT (Kiss and Halasz, 1985) the recently discovered kisspeptin (Clarkson and Herbison, 2006) and GnRH itself (Witkin et al., 1995).

A large body of evidence exists to indicate the involvement of acetylcholine (Ach) in the regulation of reproductive events,

Abbreviations: Ach, acetylcholine; ChAT, choline acetyltransferase; DBB, diagonal band of Broca; GABA, gamma-aminobutyric acid; GnRH, gonadotropin-releasing hormone; HDB, horizontal limb of the diagonal band of Broca; 5-HT, serotonin; MPOA, medial preoptic area; MS, medial septum; OVLT, organum vasculosum laminae terminalis; PBS, phosphate buffered saline; VAChT, vesicular acetylcholine transporter.

* Corresponding author at: Department of Neurobiology, Institute of Experimental Medicine, Hungarian Academy of Sciences, 1083 Budapest, Hungary. Tel.: +36 1 210 9400x366; fax: +36 1 210 9944.
E-mail address: hrabovszky@koki.hu (E. Hrabovszky).

0197-0186/$ – see front matter © 2007 Elsevier Ltd. All rights reserved.
doi:10.1016/j.neuint.2007.09.001

including male and female sexual behavior (Bonilla-Jaime et al., 1998; Kow and Pfaff, 1988; Singer, 1968) and gonadotropin secretion (Benedetti et al., 1969; Everett, 1964). The muscarinic acetylcholine receptor antagonist atropine blocks both spontaneous and reflex ovulation (Everett, 1964). In the spontaneously ovulating species rat, atropine implants in the anterior lateral hypothalamus disturb the ovarian cycles and prolong the diestrous phase (Benedetti et al., 1969). While the site(s) and mechanism(s) of the cholinergic actions upon the reproductive axis are not clear, they appear to be exerted, at least in part, at the hypothalamic level. Simonovic and colleagues examined the Ach-stimulated FSH release from halved adenohypophyses of male rats and found enhanced FSH release only if the adenohypophyses were co-incubated with hypothalamic fragments (Simonovic et al., 1974). On the other hand, nanomolar concentrations of Ach could markedly stimulate GnRH release from dissected mediobasal hypothalamic fragments *in vitro* and this effect could be abolished by the nicotinic Ach receptor antagonist hexamethonium (Richardson et al., 1982).

In the light of the evidence for central cholinergic actions on the reproductive axis, we postulated the direct innervation of GnRH neurons by cholinergic afferent pathways. We used dual-labeling immunocytochemistry at the light and electron microscopic levels to address the putative morphological link between central cholinergic axons and the GnRH neurosecretory system of the rat. Cholinergic neuronal elements were visualized by the immunocytochemical detection of the biosynthetic enzyme choline acetyltransferase (ChAT) and the vesicular Ach transporter (VAChT) which carries the newly synthesized Ach into synaptic vesicles for quantal release.

2. Experimental procedures

2.1. Animals

Adult male Wistar rats ($N = 6$; 260–280 g bw) were purchased from the local breeding colony of the Medical Gene Technology Unit of the Institute of Experimental Medicine. The animals were kept under a 12 h day–12 h night schedule (lights on at 07:00 h, lights off at 19:00 h), in a temperature (22 ± 2 °C) and humidity ($60 \pm 10\%$) controlled environment with free access to laboratory rat food (Sniff Spezialdiaeten GmbH, Soest, Germany) and tap water. The experiments were carried out in accordance with the European Communities Council Directive of 24 November 1986 (86/609/EEC) and were reviewed and approved by the Animal Welfare Committee at the Institute of Experimental Medicine.

2.1.1. Tissue preparation for light microscopy

Three rats were anesthetized with pentobarbital (35 mg/kg body weight, i.p.) and perfused transcardially with 20 ml 0.1 M phosphate-buffered saline (PBS; pH 7.4), followed by 150 ml fixative solution containing 4% paraformaldehyde (Sigma Chemical Co., St. Louis, MO) in 0.1 M PBS. Hypothalamic blocks were dissected out and soaked in 25% sucrose overnight for cryoprotection. Then 30-μm-thick free-floating coronal sections were prepared from the preoptic region with a Leica SM 2000R freezing microtome (Leica Microsystems Nussloch Gmbh, Nussloch, Germany).

2.1.2. Tissue preparation for electron microscopic studies

To prepare tissues for ultrastructural studies, three rats were perfused with a mixture of 2% freshly depolymerized paraformaldehyde (Sigma Chemical Co., St. Louis, MO) and 4% acrolein (Sigma) in 0.1 M PBS (pH 7.4). The brains were postfixed in 4% paraformaldehyde for 24 h. Preoptic sections were prepared from the tissue blocks at 50 μm with a Vibratome (Technical Products International, St. Louis, MO, USA).

2.1.3. Immunocytochemical procedures for light microscopy

For light microscopic studies, the sections were rinsed in PBS, incubated in 10% thioglycolic acid for 30 min and then, in 0.5% H_2O_2 and 0.2% Triton X-100 in PBS for 30 min. Non-specific binding of the antibodies was reduced using a 2% normal horse serum blocker in PBS for 10 min. To detect cholinergic neuronal elements, the sections were incubated in polyclonal anti-ChAT antiserum raised in a goat (AB144P; 1:1000; Chemicon, Temecula, CA) for 72 h at 4 °C. The primary antibodies were reacted with donkey, biotin-SP-antigoat IgG (1:1000; Jackson ImmunoResearch Laboratories, West Grove, PA) for 2 h. Alternatively, in a second set of sections the cholinergic system was detected using a rabbit antiserum against vesicular acetylcholine transporter (VAChT) (V5387; 1:10,000; Sigma), followed by biotin-SP-antirabbit secondary antibodies (Jackson). The biotinylated secondary antibodies were reacted with the ABC Elite working solution (Vector Laboratories, Burlingame, CA; 1:1000 dilutions of solutions A and B in 50 mM Tris buffer; pH 7.6) for 1 h. Then the sections were rinsed in Tris buffer and the color reaction visualized with a developer containing 0.05% diaminobenzidine, 0.15% nickel ammonium sulfate and 0.005% H_2O_2 in Tris buffer. Finally, the reaction product was silver intensified according to Liposits et al. (1984) to obtain a final black reaction product. After the detection of cholinergic neuronal elements, the sections were transferred into rabbit LR-1 anti-GnRH antibodies (1:10,000 a gift from Dr. R.A. Benoit, Montreal, Canada) for 2 days at 4 °C. Immunoreactivity for GnRH was also visualized with the ABC method, applying biotin-SP-antirabbit secondary antibody (Jackson) and a developer consisting of 0.025% diaminobenzidine and 0.0036% H_2O_2 in Tris buffer, which yielded a brown reaction product.

Beyond the use of well-characterized primary antibodies in this study against the cholinergic system (Meister et al., 2006; Harkany et al., 2003; Arvidsson et al., 1997), the specificity of labeling was further indicated by the absence of immunocytochemical signal if the primary or the secondary antibodies were omitted from the labeling.

The dual-immunostained sections were mounted on microscope slides, dehydrated with ethanol, cover slipped with DePeX mounting medium (Fluka Chemie, Buchs, Switzerland) and studied with an Axiophot microscope (Zeiss, Göttingen, Germany) equipped with an RT Spot digital camera (Diagnostic Instruments, Sterling Heights, MI).

2.1.4. Immunocytochemical procedures for electron microscopy

Vibratome sections fixed with the acrolein/paraformaldehyde mixture were pretreated with 0.5% sodium borohydride in PBS for 30 min to eliminate residual aldehydes. Then they were infiltrated with sucrose for cryoprotection (15% for 1 h and then, 30% overnight) and permeabilized by three repeated freeze-thaw cycles on liquid nitrogen. Then the immunocytochemical dual-labeling procedures were carried out as described for light microscopy. The dual-labeled sections were treated with 1% osmium tetroxide in 0.1 M PBS for 30 min and dehydrated in an ascending series of ethanol. A 30-min contrasting step using 1% uranyl acetate in 70% ethanol was inserted in this procedure and the fully dehydrated sections were finally infiltrated with propylene oxide and flat embedded in TAAB 812 Embedding resin (TAAB Laboratory Equipments Ltd., Aldermaston, Berks, UK) on liquid release agent (Electron Microscopy Sciences) coated slides. The cover slipped sections were polymerized at 60 °C for 24 h. Ultrathin (50–60 nm) sections were cut with Leica ultracut UCT ultramicrotome (Leica Microsystems, Wetzlar, Germany), collected onto Formvar-coated single-slot grids and contrasted with a stabilized solution of lead citrate. Digital images were captured with a cooled CCD camera.

The light- and electron microscopic digital images were processed with the Adobe Photoshop 7.0 software.

3. Results

The cell bodies of GnRH neurons, immunostained with brown diaminobenzidine, were scattered around the OVLT and

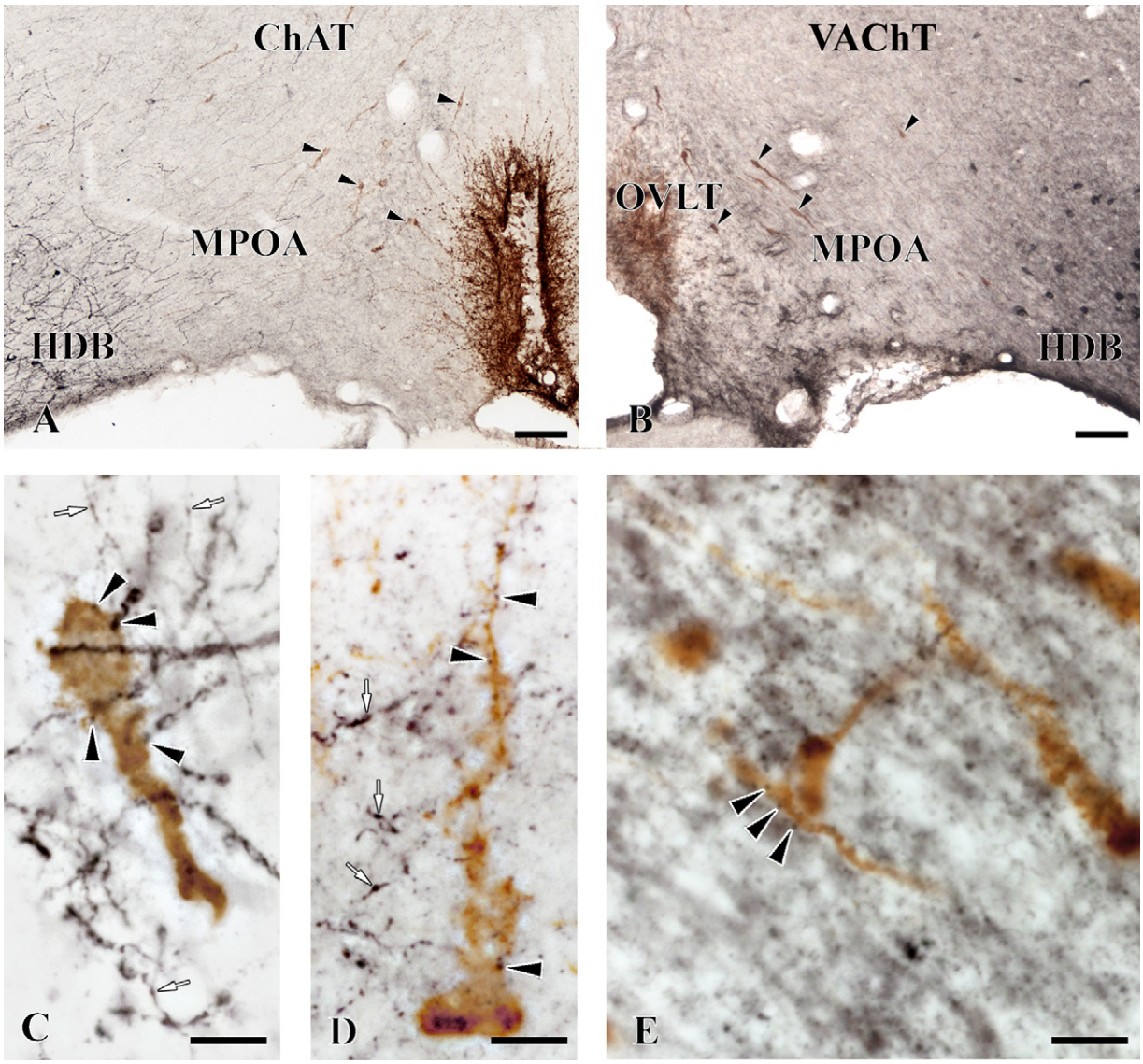

Fig. 1. Cholinergic afferents to gonadotropin-releasing hormone (GnRH) producing neurons in the male rat. (A and B) The cell bodies of gonadotropin-releasing hormone (GnRH) neurons (arrowheads), immunostained with brown diaminobenzidine chromogen, are scattered within the organum vasculosum laminae terminalis (OVLT) and the medial preoptic area (MPOA) and they abundantly innervate the OVLT. Cholinergic neuronal cell bodies (gray-to-black immunostaining with silver-intensified nickel-diaminobenzidine), immunoreactive for choline acetyltransferase (ChAT; A) and vesicular acetylcholine transporter (VAChT; B), are absent in these regions but occur in high numbers in the horizontal limb of the diagonal band of Broca (HDB). (C and D) Thin and varicose cholinergic axons (arrows) immunoreactive for ChAT show an overlapping distribution with that of GnRH neurons and form frequent appositions (arrowheads) to GnRH immunoreactive cell bodies and dendrites. (E) The cholinergic afferent contacts (arrowheads) on GnRH neurons are also detectable using VAChT as the cholinergic marker. Scale bars—A and B: 100 μm; C–E: 15 μm.

in the MPOA (Fig. 1A and B), and their regional distribution followed the characteristic patterns described earlier by others (Merchenthaler et al., 1984). The same regions also contained a fine network of varicose cholinergic fibers that were immunoreactive for ChAT (Fig. 1A) and VAChT (Fig. 1B) and contained gray-to-black silver-intensified nickel-diaminobenzidine chromogen. Immunostaining with the VAChT antiserum resulted in a somewhat higher fiber density compared to that obtained with the ChAT antiserum, corroborating previous observations with the same antisera by others (Meister et al., 2006). High-power analysis of dual-labeled sections established that the cholinergic axons were frequently apposed to GnRH immunoreactive neuronal elements. Cholinergic axons contacted the cell bodies (Fig. 1C) as well as the dendrites (Fig. 1D and E) of GnRH neurons.

At the ultrastructural level, the cholinergic axons exhibited high electron density due to the deposition of silver–gold–intensified nickel–diaminobenzidine. Some of the cholinergic axonal profiles established asymmetric synapses with unlabeled dendrites (Fig. 2A). Gonadotropin-releasing hormone neurons, labeled with electron dense diaminobenzidine, were often contacted by the cholinergic fibers on their somata as well as dendrites (Fig. 2B–D). While the appositions were devoid of glial intercalations (Fig. 2C and D), state-of-the-art synaptic specializations occurred rarely. When present, the synapses showed asymmetric morphology (Fig. 2E and F).

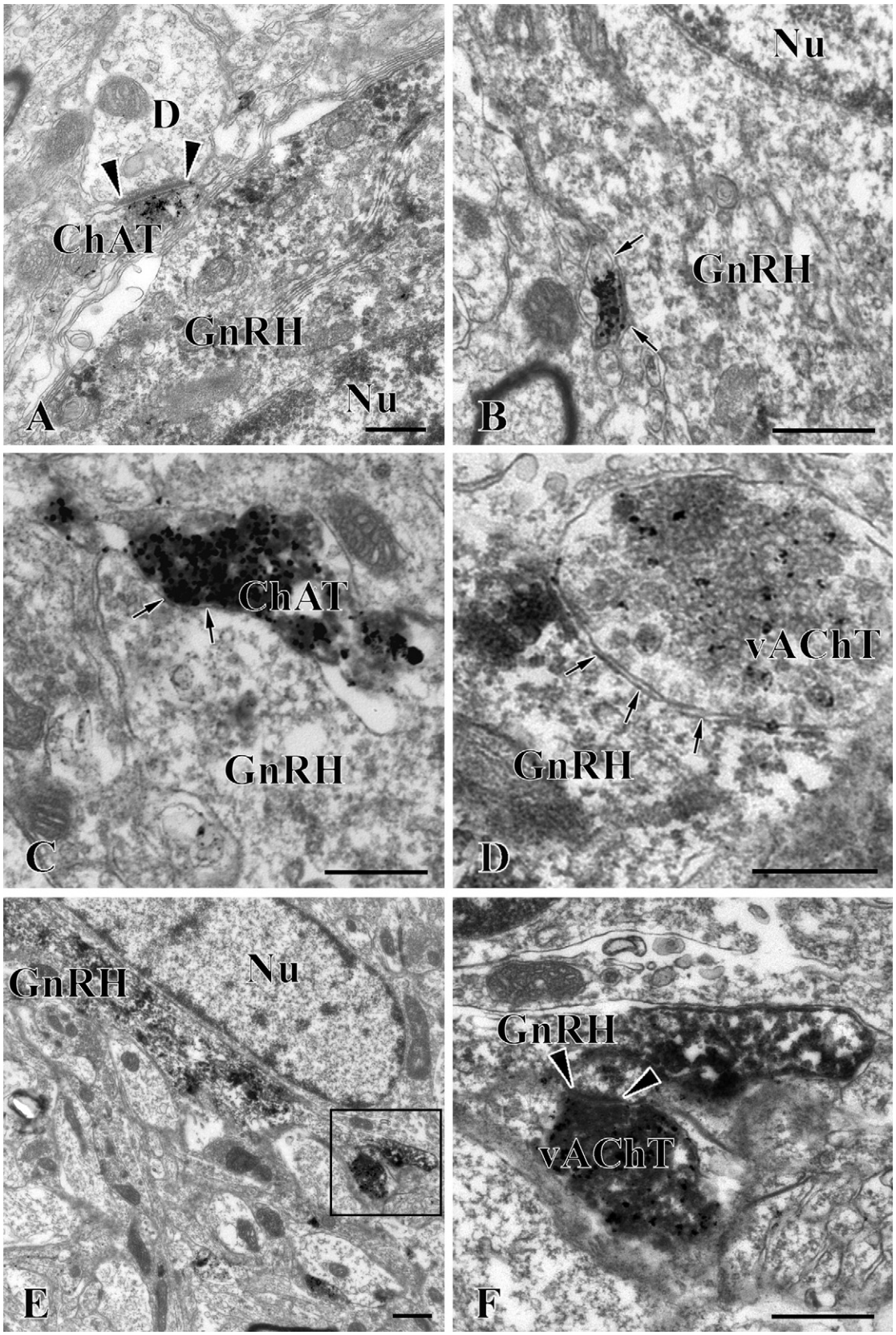

Fig. 2. Ultrastructural evidence for cholinergic innervation of gonadotropin-releasing hormone neurons in the medial preoptic area. (A) Cholinergic axons immunoreactive for choline acetyltransferase (ChAT) exhibit high electron density due to the deposition of silver–gold-intensified diaminobenzidine. Occasionally, they establish asymmetric synapses (arrowheads) with unlabeled dendrites. Gonadotropin-releasing hormone (GnRH) immunoreactive neurons contain dense diaminobenzidine chromogen. (B) The ChAT immunoreactive cholinergic axons are occasionally apposed (arrows) to GnRH immunoreactive neuronal perikarya. (C and D) Intercalation of glial elements is absent at the apposition sites (arrows) between ChAT (C) or vesicular acetylcholine transporter (VAChT; D) immunoreactive

4. Discussion

In this study we present neuromorphological evidence for a direct cholinergic afferent input to the GnRH neuronal system of the rat.

Previous pharmacological experiments analyzing the cholinergic modulation of GnRH release suggested multiple mechanisms of action. Krsmanovic and coworkers studied perifused hypothalamic primary cell cultures and immortalized GnRH producing GT 1–7 cells to conclude a dual receptorial effect of Ach on GnRH neurons: while the cholinergic activation of M2 muscarinic receptors reduced the basal GnRH release via inhibiting G protein-coupled intracellular cAMP elevation, the activation of M1 receptors led to stimulation of phosphoinositide hydrolysis resulting in a rapid and transient increase in GnRH neurosecretion (Krsmanovic et al., 1998). In addition, Ach also increased GnRH secretion via an increased Na^+ and Ca^{2+} influx due to nicotinic receptor activation (Krsmanovic et al., 1998). The Ca^{2+} delivery from intracellular Ca^{2+} stores also forms an important component of cholinergic signaling as shown by Morales and coworkers. The Ach-induced $[Ca^{2+}]_i$ elevation from the endoplasmic reticulum of GT 1–7 cells could be blocked by atropine. Moreover, the cholinergic stimulation of $[Ca^{2+}]_i$ delivery showed a strong modulation by estrogen and was reduced rapidly by 50–60% in the presence of 10 nM 17β-estradiol. The fast onset of this effect and the similar action of a membrane impermeant estradiol conjugate implicated a membrane associated estrogen receptor in this modulatory action (Morales et al., 2003).

The observation that cholinergic axons often formed direct contacts but rarely established classical synapses with the GnRH neurons was highly reminiscent to the previous morphological findings by several other investigators. The observations that out of cholinergic axon varicosities, only 7% in the hippocampus (CA1, stratum radiatum) (Umbriaco et al., 1995), 10% in the neostriatum (Contant et al., 1996) and 14% in the parietal cortex (Umbriaco et al., 1994) were engaged in synapses may indicate non-synaptic mechanisms (Vizi, 1984; Vizi and Kiss, 1998) whereby cholinergic axons influence their target neurons, including GnRH cells. For a review of non-synaptic chemical transmission through nicotinic acetylcholine receptors, see: (Lendvai and Vizi, in press).

Our anatomical observations indicate that GnRH neurons receive cholinergic innervation on their cell bodies as well as dendrites. Worth of note is the recent report by Campbell and colleagues who used biocytin-filled GnRH neurons of mice to detect a surprisingly rich dendritic arborization unknown previously (Campbell et al., 2005). While the number of spines showed a trend to decrease with increasing distance from the cell body, they remained detectable even on the most distal elements of the primary dendrite (Campbell et al., 2005). Considering that cholinergic axons preferentially form contacts and synapses with dendritic branches and spines in other brain regions (Mechawar et al., 2000, 2002; Umbriaco et al., 1995, 1994), our study likely left a significant proportion of cholinergic contacts undetected at the distal dendrites and spines of GnRH neurons which might remain unlabeled for GnRH.

A possible site of origin of the cholinergic afferents to GnRH neurons is the hypothalamic arcuate nucleus. Hahn and coworkers injected the retrograde tract-tracer cholera toxin β subunit around GnRH neurons of the preoptic region and found a moderate number of labeled cells through the rostro-caudal extent of the arcuate nucleus (Hahn and Coen, 2006). Indeed, Meister and colleagues identified a cell group in this region which exhibits a cholinergic/α-melanocyte-stimulating hormone double neurotransmitter phenotype and innervate the medial preoptic area, among other regions (Meister et al., 2006). Cholinergic neurons of the basal forebrain (Zaborszky et al., 1999) may represent a second source for the cholinergic innervation of GnRH neurons. Hahn and coworkers observed retrogradely labeled nerve cells in the horizontal limb of the diagonal band of Broca (Hahn and Coen, 2006), although the chemotype of these neurons has not been determined. The parabrachial complex of the brainstem also contains a major cholinergic cell population (Lauterborn et al., 1993). The idea that these cells may contribute to the cholinergic innervation of the GnRH system gains support from the observation that a large number of neurons in the central and a somewhat lower number of cells in the dorsal and superior lateral parabrachial nuclei could be retrogradely labeled from the preoptic area (Hahn and Coen, 2006; Castaneyra-Perdomo et al., 1992).

In summary, in this study we provide neuroanatomical evidence that cholinergic axons, immunoreactive for ChAT and VAChT, directly innervate GnRH neurons of the rat.

Acknowledgements

The authors are grateful to Mrs. Hajni Bekó for the excellent technical assistance. This work was supported by the National Scientific Research Fund (OTKA T 46574 and K691127), National Research and Development Program (NKFP 1A/002/2004 to ZL) and the European Union FP6 funding (contract no. LSHM-CT-2003-50304). This publication reflects the authors' views and not necessarily those of the European Union. The information in this document is provided as is, and no guarantee or warranty is given that the information is fit for any particular purpose. The user thereof uses the information at its sole risk and liability. The authors wish to thank Dr. R.A. Benoit for kindly providing the LR1 (GnRH) antibodies for these studies.

References

Arvidsson, U., Riedl, M., Elde, R., Meister, B., 1997. Vesicular acetylcholine transporter (VAChT) protein: a novel and unique marker for cholinergic neurons in the central and peripheral nervous systems. J. Comp. Neurol. 378, 454–467.

cholinergic axons and the GnRH immunoreactive neuronal elements. The typical appositions do not exhibit any synaptic specialization. (E and F) State-of-the-art synapses between the cholinergic axons and GnRH neurons are rare. Arrowheads in F (framed region from E) point to the postsynaptic density of an asymmetric axo-dendritic synapse. Nu, cell nucleus. Scale bars—(A) 500 nm; (B and C) 50 nm; (D) 400 nm; (E) 800 nm; (F) 500 nm.

Benedetti, W.L., Lozdziejsky, R., Sala, M.A., Monti, J.M., Grino, E., 1969. Blockade of ovulation after atropine implants in the lateral hypothalamus of the rat. Experientia 25, 1158–1159.

Bonilla-Jaime, H., Retana-Marquez, S., Velazquez-Moctezuma, J., 1998. Pharmacological features of masculine sexual behavior in an animal model of depression. Pharmacol. Biochem. Behav. 60, 39–45.

Campbell, R.E., Han, S.K., Herbison, A.E., 2005. Biocytin filling of adult gonadotropin-releasing hormone neurons in situ reveals extensive, spiny, dendritic processes. Endocrinology 146, 1163–1169.

Castaneyra-Perdomo, A., Perez-Delgado, M.M., Montagnese, C., Coen, C.W., 1992. Brainstem projections to the medial preoptic region containing the luteinizing hormone-releasing hormone perikarya in the rat. An immunohistochemical and retrograde transport study. Neurosci. Lett. 139, 135–139.

Clarkson, J., Herbison, A.E., 2006. Postnatal development of kisspeptin neurons in mouse hypothalamus; sexual dimorphism and projections to gonadotropin-releasing hormone neurons. Endocrinology 147, 5817–5825.

Contant, C., Umbriaco, D., Garcia, S., Watkins, K.C., Descarries, L., 1996. Ultrastructural characterization of the acetylcholine innervation in adult rat neostriatum. Neuroscience 71, 937–947.

Everett, J.W., 1964. Central neural control of reproductive functions of the adenohypophysis. Physiol. Rev. 44, 373–431.

Hahn, J.D., Coen, C.W., 2006. Comparative study of the sources of neuronal projections to the site of gonadotrophin-releasing hormone perikarya and to the anteroventral periventricular nucleus in female rats. J. Comp. Neurol. 494, 190–214.

Harkany, T., Hartig, W., Berghuis, P., Dobszay, M.B., Zilberter, Y., Edwards, R.H., Mackie, K., Ernfors, P., 2003. Complementary distribution of type 1 cannabinoid receptors and vesicular glutamate transporter 3 in basal forebrain suggests input-specific retrograde signalling by cholinergic neurons. Eur. J. Neurosci. 18, 1979–1992.

Herbison, A.E., 1998. Multimodal influence of estrogen upon gonadotropin-releasing hormone neurons. Endocr. Rev. 19, 302–330.

Kiss, J., Halasz, B., 1985. Demonstration of serotoninergic axons terminating on luteinizing hormone-releasing hormone neurons in the preoptic area of the rat using a combination of immunocytochemistry and high resolution autoradiography. Neuroscience 14, 69–78.

Kiss, J., Kocsis, K., Csaki, A., Halasz, B., 2003. Evidence for vesicular glutamate transporter synapses onto gonadotropin-releasing hormone and other neurons in the rat medial preoptic area. Eur. J. Neurosci. 18, 3267–3278.

Kow, L.M., Pfaff, D.W., 1988. Transmitter and peptide actions on hypothalamic neurons in vitro: implications for lordosis. Brain Res. Bull. 20, 857–861.

Krsmanovic, L.Z., Mores, N., Navarro, C.E., Saeed, S.A., Arora, K.K., Catt, K.J., 1998. Muscarinic regulation of intracellular signaling and neurosecretion in gonadotropin-releasing hormone neurons. Endocrinology 139, 4037–4043.

Lauterborn, J.C., Isackson, P.J., Montalvo, R., Gall, C.M., 1993. In situ hybridization localization of choline acetyltransferase mRNA in adult rat brain and spinal cord. Brain Res. Mol. Brain Res. 17, 59–69.

Lendvai, B., Vizi, E.S., in press. Nonsynaptic Chemical transmission through nicotinic acetylcholine receptors. Physiol. Rev.

Leranth, C., MacLusky, N.J., Sakamoto, H., Shanabrough, M., Naftolin, F., 1985. Glutamic acid decarboxylase-containing axons synapse on LHRH neurons in the rat medial preoptic area. Neuroendocrinology 40, 536–539.

Leranth, C., MacLusky, N.J., Shanabrough, M., Naftolin, F., 1988a. Catecholaminergic innervation of luteinizing hormone-releasing hormone and glutamic acid decarboxylase immunopositive neurons in the rat medial preoptic area. An electron-microscopic double immunostaining and degeneration study. Neuroendocrinology 48, 591–602.

Leranth, C., MacLusky, N.J., Shanabrough, M., Naftolin, F., 1988b. Immunohistochemical evidence for synaptic connections between pro-opiomelanocortin-immunoreactive axons and LH-RH neurons in the preoptic area of the rat. Brain Res. 449, 167–176.

Levine, J.E., Duffy, M.T., 1988. Simultaneous measurement of luteinizing hormone (LH)-releasing hormone, LH, and follicle-stimulating hormone release in intact and short-term castrate rats. Endocrinology 122, 2211–2221.

Liposits, Z., Setalo, G., Flerko, B., 1984. Application of the silver-gold intensified 3,3′-diaminobenzidine chromogen to the light and electron microscopic detection of the luteinizing hormone-releasing hormone system of the rat brain. Neuroscience 13, 513–525.

MacLusky, N.J., Naftolin, F., Leranth, C., 1988. Immunocytochemical evidence for direct synaptic connections between corticotrophin-releasing factor (CRF) and gonadotrophin-releasing hormone (GnRH)-containing neurons in the preoptic area of the rat. Brain Res. 439, 391–395.

Mechawar, N., Cozzari, C., Descarries, L., 2000. Cholinergic innervation in adult rat cerebral cortex: a quantitative immunocytochemical description. J. Comp. Neurol. 428, 305–318.

Mechawar, N., Watkins, K.C., Descarries, L., 2002. Ultrastructural features of the acetylcholine innervation in the developing parietal cortex of rat. J. Comp. Neurol. 443, 250–258.

Meister, B., Gomuc, B., Suarez, E., Ishii, Y., Durr, K., Gillberg, L., 2006. Hypothalamic proopiomelanocortin (POMC) neurons have a cholinergic phenotype. Eur. J. Neurosci. 24, 2731–2740.

Merchenthaler, I., Gorcs, T., Setalo, G., Petrusz, P., Flerko, B., 1984. Gonadotropin-releasing hormone (GnRH) neurons and pathways in the rat brain. Cell Tissue Res. 237, 15–29.

Morales, A., Diaz, M., Ropero, A.B., Nadal, A., Alonso, R., 2003. Estradiol modulates acetylcholine-induced Ca^{2+} signals in LHRH-releasing GT1-7 cells through a membrane binding site. Eur. J. Neurosci. 18, 2505–2514.

Nunemaker, C.S., DeFazio, R.A., Geusz, M.E., Herzog, E.D., Pitts, G.R., Moenter, S.M., 2001. Long-term recordings of networks of immortalized GnRH neurons reveal episodic patterns of electrical activity. J. Neurophysiol. 86, 86–93.

Richardson, S.B., Prasad, J.A., Hollander, C.S., 1982. Acetylcholine, melatonin, and potassium depolarization stimulate release of luteinizing hormone-releasing hormone from rat hypothalamus in vitro. Proc. Natl. Acad. Sci. U.S.A. 79, 2686–2689.

Simonovic, I., Motta, M., Martini, L., 1974. Acetylcholine and the release of the follicle-stimulating hormone-releasing factor. Endocrinology 95, 1373–1379.

Singer, J.J., 1968. Hypothalamic control of male and female sexual behavior in female rats. J. Comp. Physiol. Psychol. 66, 738–742.

Tsuruo, Y., Kawano, H., Kagotani, Y., Hisano, S., Daikoku, S., Chihara, K., Zhang, T., Yanaihara, N., 1990. Morphological evidence for neuronal regulation of luteinizing hormone-releasing hormone-containing neurons by neuropeptide Y in the rat septo-preoptic area. Neurosci. Lett. 110, 261–266.

Turi, G.F., Liposits, Z., Moenter, S.M., Fekete, C., Hrabovszky, E., 2003. Origin of neuropeptide Y-containing afferents to gonadotropin-releasing hormone neurons in male mice. Endocrinology 144, 4967–4974.

Umbriaco, D., Garcia, S., Beaulieu, C., Descarries, L., 1995. Relational features of acetylcholine, noradrenaline, serotonin and GABA axon terminals in the stratum radiatum of adult rat hippocampus (CA1). Hippocampus 5, 605–620.

Umbriaco, D., Watkins, K.C., Descarries, L., Cozzari, C., Hartman, B.K., 1994. Ultrastructural and morphometric features of the acetylcholine innervation in adult rat parietal cortex: an electron microscopic study in serial sections. J. Comp. Neurol. 348, 351–373.

Vizi, E.S., Kiss, J.P., 1998. Neurochemistry and pharmacology of the major hippocampal transmitter systems: synaptic and nonsynaptic interactions. Hippocampus 8, 566–607.

Vizi, E.S., 1984. Non-synaptic Interactions Between Neurons: Modulation of Neurochemical Transmission. Pharmacological and Clinical Aspects. John Wiley and Sons, Chichester, New York.

Witkin, J.W., O'Sullivan, H., Silverman, A.J., 1995. Novel associations among gonadotropin-releasing hormone neurons. Endocrinology 136, 4323–4330.

Zaborszky, L., Pang, K., Somogyi, J., Nadasdy, Z., Kallo, I., 1999. The basal forebrain corticopetal system revisited. Ann. NY Acad. Sci. 877, 339–367.

17. számú melléklet

Journal of Neuroendocrinology **20**, 743–751

REVIEW ARTICLE

Novel Aspects of Glutamatergic Signalling in the Neuroendocrine System

E. Hrabovszky* and Z. Liposits*†

**Laboratory of Endocrine Neurobiology, Institute of Experimental Medicine, Hungarian Academy of Sciences, Budapest, Hungary.*

†Department of Neuroscience, Faculty of Information Technology, Péter Pázmány Catholic University, Budapest, Hungary.

Journal of Neuroendocrinology

L-glutamate, the main excitatory neurotransmitter, influences virtually all neurones of the neuroendocrine hypothalamus via synaptic mechanisms. Vesicular glutamate transporters (VGLUT1–3), which selectively accumulate L-glutamate into synaptic vesicles, provide markers with which to visualise glutamatergic neurones in histological preparations; excitatory neurones in the endocrine hypothalamus synthesise the VGLUT2 isoform. Results of recent dual-label *in situ* hybridisation studies indicate that glutamatergic neurones in the preoptic area and the hypothalamic paraventricular, supraoptic and periventricular nuclei include parvocellular and magnocellular neurosecretory neurones which secrete peptide neurohormones into the bloodstream to regulate endocrine functions. Neurosecretory terminals of GnRH, TRH, CRF-, somatostatin-, oxytocin- and vasopressin-secreting neurones contain VGLUT2 immunoreactivity, suggesting the co-release of glutamate with hypophysiotrophic peptides. The presence of VGLUT2 also indicates glutamate secretion from non-neuronal endocrine cells, including gonadotrophs and thyrotrophs of the anterior pituitary. Results of *in vitro* studies show that ionotropic glutamate receptor analogues can elicit hormone secretion at neuroendocrine/endocrine release sites. Structural constituents of the median eminence, adenohypophysis and neurohypophysis contain elements of glutamatergic transmission, including glutamate receptors and enzymes of the glutamate/glutamine cycle. The synthesis of VGLUT2 exhibits robust up-regulation in response to certain endocrine challenges, indicating that altered glutamatergic signalling may represent an important adaptive mechanism. This review article discusses the newly emerged non-synaptic role of glutamate in neuroendocrine and endocrine communication.

Key words: glutamate, neuroendocrine, neurosecretion, paracrine, VGLUT2.

doi: 10.1111/j.1365-2826.2008.01719.x

Correspondence to:
Zsolt Liposits, Laboratory of Endocrine Neurobiology, Institute of Experimental Medicine, P.O. Box 67, 1450 Budapest, Hungary (e-mail: liposits@koki.hu).

Glutamate is the principal neurotransmitter of excitatory synaptic transmission in the neuroendocrine hypothalamus

In addition to participating in normal cell metabolism, L-glutamate acts as the primary mediator of excitatory synaptic transmission in the central nervous system (1, 2). Its major contribution to the synaptic regulation of hypothalamic neuroendocrine systems has been shown by (i) the demonstration of glutamatergic asymmetric synapses on the cell bodies and dendrites of hypothalamic neurosecretory neurones, (ii) the finding of increased intracellular Ca^{2+} in medial hypothalamic neurones grown in monolayer, in response to glutamate and the non-NMDA glutamate receptor agonists kainate and quisqualate, and finally (iii) the observation that the non-NMDA glutamate antagonist CNQX decreased the electrically stimulated and spontaneous excitatory postsynaptic potentials in acute hypothalamic slice preparations (3).

Ionotropic and metabotropic receptors mediate glutamate actions

Glutamate receptors that form cation channels fall into the category of ionotropic receptors. Based on their binding affinities for prototypical ligands, they are further categorised as kainate, AMPA and NMDA receptors (4–7). Metabotropic glutamate receptors (mGluR1–8), in turn, comprise a unique family of G-protein coupled receptors that can be classified into three groups (groups I–III) based on G-protein coupling specificity and sequence similarity (7–10).

Glutamate regulates endocrine functions via binding to hypothalamic and hypophysial glutamate receptors

Glutamate regulates the secretion of various adenohypophysial hormones (11–19); most glutamatergic actions appear to be exerted at the hypothalamic level. Accordingly, intracerebroventricular administration of glutamate receptor agonists is capable of inducing luteinising hormone (19, 20) and ACTH (21) secretion. Further, centrally acting glutamate plays a role in the regulation of TSH (22) and GH (23) secretion from the adenohypophysis and oxytocin and vasopressin release from the magnocellular neurosecretory systems (24).

Results of *in vitro* studies revealed additional direct hypophysial actions of glutamate on luteinising hormone (25), GH (26, 27) and prolactin (28, 29) secretion from the adenohypophysis and on vasopressin release from the neurohypophysis (30).

Vesicular glutamate transporters provide markers for the histochemical detection of glutamatergic neurones

Prior to exocytotic neurotransmitter release, classical non-peptide transmitters are accumulated into synaptic vesicles by vesicular neurotransmitter transporters (31). In 2000, two independent studies (32, 33) demonstrated that the vesicular uptake of L-glutamate (VGLUT1) is carried out by a molecule previously known as the brain-specific Na^+-dependent inorganic phosphate co-transporter (34). Subsequent search for additional VGLUT isoforms identified two new members of the VGLUT family (VGLUT2 and VGLUT3) (35–43). Results of mapping studies with *in situ* hybridisation and immunocytochemistry established that the different VGLUT isoforms tend to occur in distinct classes of glutamatergic neurones (32, 36, 38, 40–42, 44–48).

Type-2 vesicular glutamate transporter (VGLUT2) dominates in the neuroendocrine hypothalamus

Immunocytochemical studies established that axons of the VGLUT2 phenotype account for the bulk of the glutamatergic innervation to hypothalamic neuroendocrine cells (Fig. 1), including parvocellular GnRH (49), growth hormone-releasing hormone (GHRH) (50), TRH (51) and CRF (51) neurones and also neurones of the magnocellular neurosecretory systems (52). VGLUT2 immunoreactivity also occurred in the external zone of the median eminence (48) and in the neurohypophysis (53), which represent the termination fields for the parvo- and magnocellular neurosecretory systems, respectively. This localisation of VGLUT2 strongly suggested that the glutamate-containing synaptic vesicles reside within neurosecretory nerve endings (48, 53).

In situ hybridisation studies to map the expression of distinct VGLUT isoforms established that the hypothalamus synthesises the VGLUT2 transporter isoform. VGLUT2 mRNA occurred in regions critically important in neuroendocrine regulation, including the organum vasculosum laminae terminalis (OVLT) and the medial preoptic area, sites that contain the cell bodies of GnRH neurones, the periventricular nucleus which contains somatostatin neurones, and parvocellular subdivisions of the paraventricular nucleus which

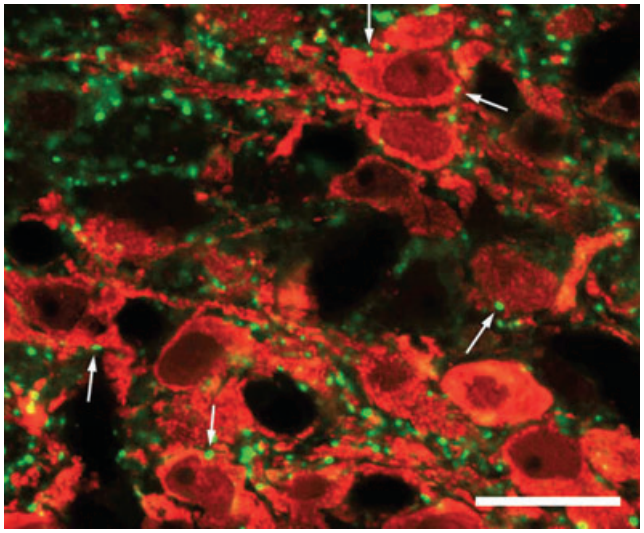

Fig. 1. Immunocytochemical evidence for vesicular glutamate transporter 2 (VGLUT2)-containing glutamatergic axons forming contact with hypophysiotrophic neurones. VGLUT2-immunoreactive axons (green signal) are closely apposed to CRF-immunoreactive neurones (red labelling) in the dorsal part of the medial parvocellular subdivision of the paraventricular nucleus. Arrows indicate putative sites of neuronal communication in the confocal image. Scale bar, 20 μm. [Reproduced with permission from Wittmann *et al.* (51).]

comprise CRF and TRH neurones, among other cell types. In addition, VGLUT2 mRNA was observed in the hypothalamic supraoptic nucleus and magnocellular subdivisions of the paraventricular nucleus where the perikarya of oxytocin- and vasopressin-secreting neurones projecting to the neurohypophysis reside (38, 39, 47, 48, 53, 54).

Glutamatergic phenotype characterises the majority of hypothalamic neurosecretory systems

To address the issue of whether the glutamatergic cell population in the OVLT/medial preoptic area includes GnRH neurones, our laboratory has carried out dual-label *in situ* hybridisation and immunocytochemical experiments. Using a sensitive radioisotopic hybridisation technique (55) to detect VGLUT2 mRNA, we have provided evidence that 98% of GnRH neurones in the male rat express VGLUT2 mRNA (56).

Dual-immunofluorescent labelling of the median eminence, followed by confocal microscopic analysis, established the presence of VGLUT2 immunoreactivity within GnRH axon terminals (56).

The same combined approach of *in situ* hybridisation and immunocytochemistry was used later to demonstrate the presence of VGLUT2 in TRH- (57), CRF- (57) and somatostatin- (58) (Fig. 2) containing parvocellular neurones. Hypophysiotrophic GHRH terminals, in contrast, contained the vesicular GABA transporter, but no VGLUT2 (58), confirming the GABA-ergic phenotype of these neurones established earlier using other GABA-ergic markers (59). Magnocellular neurosecretory neurones in the supraoptic and

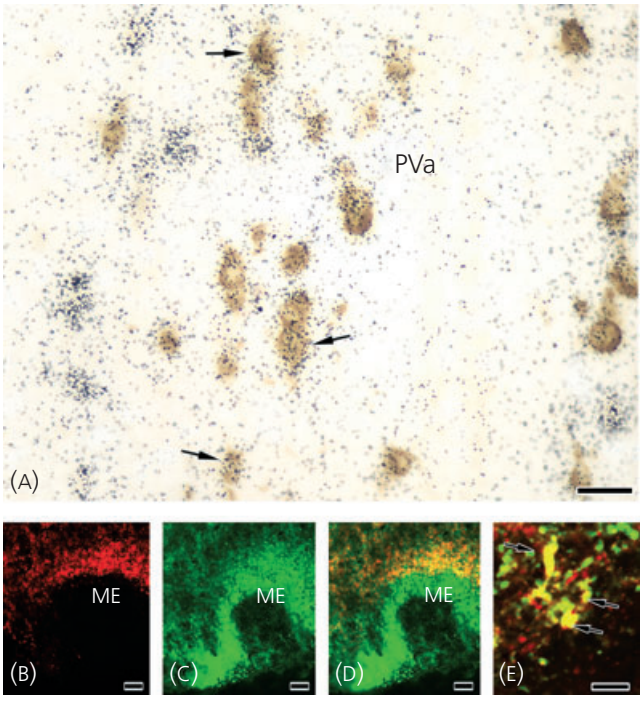

Fig. 2. Morphological evidence for the glutamatergic phenotype of somatostatin neurones. Dual-label *in situ* hybridisation and dual-immunofluorescent studies represent two complementary approaches used in previous studies to reveal the glutamatergic phenotype of various neuroendocrine systems, including somatostatin neurones in the anterior periventricular nucleus (PVa). (A) *In situ* hybridisation studies in the given example used a non-isotopic hybridisation probe labelled with digoxigenin to detect somatostatin mRNA. The final signal was visualised with brown diaminobenzidine chromogen. Expression of type-2 vesicular glutamate transporter (VGLUT2) mRNA was detected with a ^{35}S-labelled radioisotopic probe, followed by autoradiographic signal visualisation. Note that most somatostatin mRNA-expressing neuronal perikarya in the PVa accumulate autoradiographic silver grains, indicative of a VGLUT2 mRNA phenotype. Black arrows point to dual-labelled somatostatin neurones. (B–C) Dual-immunofluorescent studies, followed by confocal laser microscopic analysis of the median eminence (ME), reveal the overlapping distribution of somatostatin immunoreactive (B, red colour) and VGLUT2 immunoreactive (C, green) terminals in the external layer of the ME. Regions where the signals overlap show up as a yellow colour in the merged panel (D). Note that the strongest VGLUT2 signal is present in the outermost layer of the ME which lacks somatostatin immunoreactivity. (E) A high-power confocal image of a 0.45-μm-thick single optical slice in which arrows indicate dual-labelled axons which contain both somatostatin (red) and VGLUT2 (green) immunoreactivities. Scale bars, 25 μm in (A)–(D) and 5 μm in (E). For details of the study that demonstrated VGLUT2 synthesis in hypophysiotrophic somatostatin neurones, see Ref. (58).

paraventricular nuclei also synthesise VGLUT2 mRNA (53, 60, 61) and exhibit VGLUT2 (53, 60–62) and, according to one paper, also VGLUT3 (62) immunoreactivity. The topographical location of classical neuroendocrine systems synthesising VGLUT2 matched well the distribution of VGLUT2 mRNA-expressing hypothalamic neurones that accumulated the retrograde tracer Fluoro-Gold from the systemic circulation (63).

Subsets of adenohypophyseal cells also synthesise VGLUT2

We have revealed that subsets of glandular cells in the adenohypophysis, mostly corresponding to gonadotrophs and thyrotrophs, also synthesise VGLUT2 mRNA and protein (61). A similar VGLUT2 phenotype was previously noted in other non-neuronal endocrine tissues, including alpha and F cells in the pancreatic Langerhans islets (37, 64, 65). Further, melatonin-producing cells of the pineal gland also contain VGLUT1 and VGLUT2 (66) and secrete glutamate (67). Local glutamatergic mechanisms that may act in peripheral endocrine and non-endocrine tissues have been reviewed recently (37, 64, 65, 68). The question needs to be addressed whether or not other VGLUT isoforms also occur in the adenohypophysis.

VGLUT2 is localised to microvesicles in neurosecretory terminals

VGLUT1 and VGLUT2 are associated with synaptic vesicles in the central nervous system (38, 40, 43–45). Accordingly, we established that the VGLUT2 labelling of neurosecretory endings in the median eminence (Fig. 3) and posterior pituitary is also associated with aggregates of synaptic vesicles which preferentially accumulate in the immediate vicinity of the pericapillary space (63). Not surprisingly, in cells of the pineal gland, VGLUT1 and VGLUT2 were also localised to synaptic-like microvesicles (66), the organelles analogous to synaptic vesicles in non-neural cells. The subcellular localisation of VGLUT2 in adenohypophysial gonadotrophs and thyrotrophs awaits clarification. Worthy of note is the finding that in pancreatic Langerhans islets VGLUT2 was observed in glucagon-containing dense-core granules, but not microvesicles (69).

The presence of the glutamate receptors indicates local glutamate actions at hormone secretion sites

Remote effects of glutamate released into the portal and systemic circulations either from nerve terminals of the hypothalamic neurosecretory neurones or from adenohypophysial cells are rather unlikely, suggesting that the target structures of glutamate are local to the neuroendocrine/endocrine release sites.

Indeed, several ionotropic glutamate receptors of the NMDA (NMDAR1), AMPA (GluR1 and GluR2/3) and kainate (GluR6/7 and KA2) types were detected in the median eminence with electron microscopy and some were localised to neuroendocrine terminals (70–72). Tanycytes lining the ventral wall of the third ventricle and astrocytes in the median eminence represent additional target cells for glutamate actions. These cells contain mRNAs and immunoreactivity for AMPA receptors (73) and kainate receptors (73–75) and express c-*fos* immunoreactivity in response to stimulation by kainate (75). Endothelial cells lining portal capillaries may also represent target cells to the released glutamate. There is evidence for the presence of functional metabotropic (76, 77) and ionotropic (76, 78, 79) glutamate receptors on cerebral microvessels, although their functionality has been argued (80).

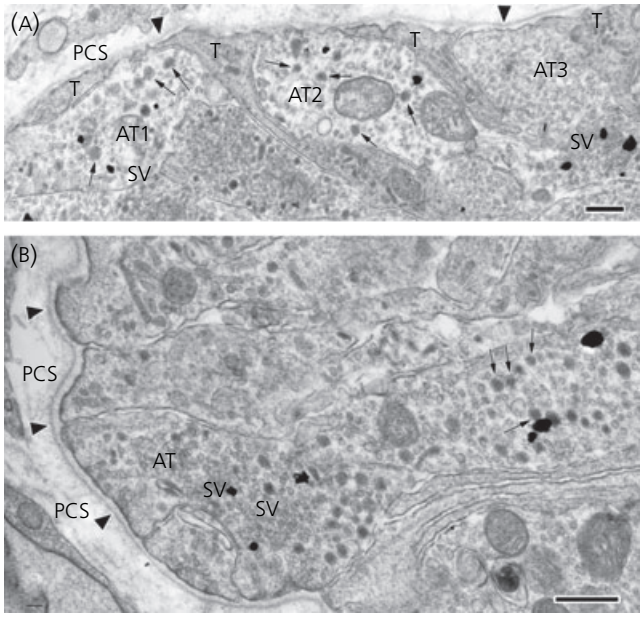

Fig. 3. Ultrastructural localisation of vesicular glutamate transporter 2 (VGLUT2) immunoreactivity in the external zone of the median eminence. (A) Three neuroendocrine axon terminals (AT1–3) freely communicate with the pericapillary space (PCS) of portal blood vessels. Arrowheads delineate the basal lamina. AT1 and AT2 contain both dense-core vesicles (DV; arrows) and small clear vesicles (SV), whereas AT3 comprises SVs only. The silver-intensified gold particles (pre-embedding colloidal gold labelling) identify the VGLUT2 content of the terminals. Note that the immunocytochemical label is preferentially associated with subcellular sites densely populated by SVs, indicating that VGLUT2 is contained in SVs. (B) A glutamatergic axon terminal (AT) terminates on the external limiting membrane (arrowheads) of a portal capillary. Arrowheads delineate the basal lamina. Note the presence of DVs (arrows) as well as SVs in the same terminal profile and the association of the VGLUT2 immune signal with SVs. Scale bars, 0.5 μm. [Reproduced with permission from Hrabovszky *et al.* (63).]

Glutamate receptors also occur in the neurohypophysis. Notably, immunoreactivity for NMDAR1 (81) as well as the GLUR1, GLUR2/3 and GLUR4 AMPA receptor subunits (82) and high-affinity binding sites for kainate (83) were observed in the posterior pituitary.

The adenohypophysis exhibits immunoreactivity for both ionotropic and metabotropic glutamate receptors (82, 84, 85).

Glutamate release from neuroendocrine/endocrine cells is involved in autocrine/paracrine regulatory mechanisms

Ultrastructural studies detected NMDAR1 and KA2 receptor subunits on GnRH immunoreactive axon terminals (70–72). Glutamate and ionotropic glutamate receptor agonists could induce a Ca^{2+}-dependent release of GnRH from superfused median eminence fragments (70). Together with the glutamatergic phenotype of GnRH neurones (56), these data suggest that physiological stimuli eliciting the release of endogenous glutamate from GnRH terminals also enhance GnRH secretion via ionotropic autoreceptors and autocrine/paracrine mechanisms. A recent ultrastructural study with post-embedding colloidal gold labelling established the extensive co-localisation of GnRH and NMDAR1 on the same dense-core vesicles within GnRH terminals (72), suggesting novel mechanisms of signalling to be explained. The chemotype and functionality of glutamate autoreceptors on other types of glutamatergic neurosecretory axons terminating in the median eminence require clarification. It also needs to be addressed whether ionotropic and metabotropic glutamate heteroreceptors are expressed on GABA-ergic hypophysiotrophic terminals (86) which secrete the hypophysiotrophic factors dopamine (58, 59) and GHRH (58, 59). Theoretically, glutamatergic and GABA-ergic heteroreceptors could underlie a paracrine cross-talk between GABA-ergic and glutamatergic terminals, respectively.

In the neurohypophysis, glutamate appears to be derived mostly from neuroendocrine terminals (53, 60–62), as it is in the median eminence. The increased synthesis of VGLUT2 in osmotically stimulated rats (60, 61) suggests an increased release of glutamate from endogenous vesicular pools and enhanced actions on local glutamate receptors (81–83). Glutamate probably acts as an autocrine/paracrine messenger to augment vasopressin secretion, considering the *in vitro* stimulatory action of glutamate on vasopressin release from the neurohypophysis (30). The presence of GLUR2/3 immunoreactivity on pituicytes suggests that these modified glial cells are also responsive to the secreted glutamate (82).

Various AMPA receptor subunits occur in the adenohypophysis (82). NMDAR1 immunoreactivity was also revealed in low percentages of most adenohypophysial cell types (below 12% for each hormonal phenotype) (84). Immunocytochemical studies have also identified group II metabotropic glutamate receptors (mGLUR2/3) on somatotrophs and lactotrophs (85) which do not seem to contain VGLUT2 (87). The different phenotype of cells serving as glutamate sources (gonadotrophs and thyrotrophs) and those carrying glutamatergic receptors, including mGLUR2/3, indicates a paracrine cross-talk between different hormone-secreting cells.

Glutamatergic communication between alpha and beta pancreatic islet cells is an example of paracrine mechanisms that may also act in the adenohypophysis. In Langerhans islets, alpha cells serve as the major source of glutamate (65, 88) and, under low glucose conditions, glutamate is co-secreted with glucagon and triggers GABA secretion from beta cells (65). Glutamate actions on islet cells are mediated by differentially expressed receptors. AMPA receptor subunits are expressed in alpha, beta and pancreatic polypeptide cells, whereas kainate receptors tend to occur in alpha and delta cells (89). The metabotropic receptor mGLUR8 has been detected exclusively in alpha cells, suggesting that it is an autoreceptor (88).

Endocrine challenges modify VGLUT2 synthesis

The issue of whether the increased activity of vasopressin neurones coincides with the regulated synthesis of endogenous VGLUT2 has also been addressed (60, 61). Osmotic challenges, including the application of 2% sodium chloride in the drinking water for 7 days, produced robust increases in VGLUT2 mRNA levels in the supraoptic (60, 61) and paraventricular (60) nuclei. Furthermore, endocrine manipulations of the thyroid and gonadal axes, followed by quantitative *in situ* hybridisation experiments, established the up-regula-

tion of adenohypophysial VGLUT2 mRNA synthesis in response to oestrogen given to ovariectomised female rats or to hypothyroidism induced by the antithyroid drug methimazole in male rats (87). There is evidence that altered VGLUT1 and VGLUT2 synthesis can change quantal size and influence excitatory postsynaptic currents in glutamatergic synapses (90, 91). The functional significance of regulated VGLUT2 synthesis in neuroendocrine/endocrine cells is less clear but probably reflects regulated glutamate release for the proposed autocrine/paracrine communication.

Several elements of the glutamate/glutamine cycle occur at glutamate secretion sites

In the glutamate/glutamine cycle (92–98), glutamate released from excitatory nerve terminals is mostly taken up by surrounding astrocytes via the high-affinity membrane glutamate transporters GLAST and GLT-1 (99) and converted to glutamine by glutamine synthetase. Glutamine is then released from astrocytes via system N transporters into the extracellular fluid to be taken up by neuronal terminals via system A transporters (100, 101). Neuronal terminals then convert glutamine to glutamate via phosphate-activated glutaminase type 1 (102) and glutamate is concentrated into synaptic vesicles by VGLUTs. Although the glutamate/glutamine cycle is crucial to reload excitatory neurones with glutamate, a fraction of glutamate can be directly taken up from the extracellular space by neuronal glutamate transporters, in particular EAAC1 (103, 104). The clearance of glutamate from the extracellular fluid by high-affinity glutamate transporters also represents an important protective mechanism against excitotoxicity (105).

In the median eminence, the mostly likely candidate structures to fulfil glial functions of the glutamate/glutamine cycle are processes of tanycytes. Berger and Hediger (106) demonstrated that different subsets of the tanycytes express GLT-1 and GLAST, with a dominance of the latter in the median eminence.

GLAST synthesis also occurs in the neurohypophysis within pituicyte-like cells (107). This makes it likely that pituicytes also account for the glutamate/glutamine conversion to allow glutamate recycling into magnocellular neurosecretory terminals.

In the adenohypophysis, GLAST occurs in folliculostellate cells (107), the same cell type that was shown to contain glutamine synthetase for converting glutamate to glutamine (108). Glucocorticoids induce glutamine synthetase expression in folliculostellate cells, but the functional consequences for local glutamatergic signalling are yet to be determined (108).

Glutamate overflow may prolong and/or spread glutamatergic receptor stimulation

When glutamate secretion exceeds the regular rate of its local re-uptake by membrane glutamate transporters, glutamatergic effects may be prolonged and/or spread to a higher number of surrounding cells. Excessive release of glutamate may be the consequence of increased VGLUT2 synthesis (61, 87, 108) or a temporary enhancement in the Ca-dependent exocytosis from the secretory cells. However, a reduced glutamate re-uptake may also account for increased glutamatergic signalling. This may occur as a consequence of the biochemical plasticity or structural remodelling of cells responsible for the removal of glutamate from the extracellular space. Plastic remodelling of tanycytes in response to changes in circulating steroids has been reported. At times of increased GnRH secretion, tanycytic end-feet retract and allow GnRH processes to directly contact the pericapillary space (109). Ultrastructural studies indicate that VGLUT2-containing vesicles are most abundant in the immediate vicinity of the pericapillary space (63) and lose glial coverage when GnRH neurones secrete actively (109). Reorganisation of glial elements has also been reported in the neurohypophysis in response to salt loading (110).

Nitric oxide mediates some effects of glutamate

It is interesting to note that the stimulation of NMDA receptors increases nitric oxide production within the median eminence (111), which is considered here to be mostly of endothelial origin (112). Nitric oxide, in turn, is an important regulator of GnRH and CRF release from the median eminence, thought to act via increasing cGMP and/or prostaglandin E2 production in hypophysiotrophic axon terminals (112). Recent evidence indicates the involvement of the kainate receptor in the action of nitric oxide on GnRH release from the median eminence (113). Actions mediated by nitric oxide may propagate the glutamatergic signal to a larger group of neurosecretory terminals and to a greater distance from the site of glutamate release.

The glutamate/nitric oxide interplay may also characterise the adenohypophysis which selectively contains nitric oxide synthase in gonadotroph and folliculostellate cells (114). Administration of the nitric oxide synthase inhibitor L-NAME blunted the GH response to systemic administration of NMDA, kainate or AMPA, actions proposed to occur at the hypophysial level (13).

Secretion of glutamate may contribute to pulsatile hormone secretion

Neurohormone and hormone outputs most often occur in secretory pulses which require co-ordinated activity of the secretory cells. The pulsatile feature of GnRH release is critical to maintain the anterior pituitary sensitivity to GnRH stimulation. Continuous GnRH exposure would otherwise lead to desensitisation of the pituitary (115, 116). There is convincing evidence that an important glutamatergic signalling mechanism which regulates the pulsatile secretion of GnRH exists within the mediobasal hypothalamus (113, 117). *In vitro* use of glutamine is as effective as glutamate in inducing GnRH secretion from retrochiasmatic hypothalamic explants, suggesting local conversion of glutamine to glutamate. Inhibitor of phosphate-activated glutaminase type 1 prevents the action of glutamine and also reduces the frequency of the spontaneous pulsatile secretion of GnRH from the explants, indicating that endogenous glutamate accounts for secretory pulses (118). More recent evidence also indicates that oestradiol increases GnRH secretion from median eminence fragments with an action involving glutamatergic signalling via kainate receptors (113).

It is tempting to speculate that the endogenous glutamate content of GnRH, TRH, CRF and somatostatin axon terminals contributes to the synchronised neurohormone output from individual axon terminals, a prerequisite for pulsatile neurohormone secretion.

Conclusions

Glutamate has long been known as the most important excitatory neurotransmitter in synaptic regulation of neuroendocrine cells. According to recent evidence, it may also act as an autocrine/paracrine messenger released by neuroendocrine/endocrine cells. The presence of VGLUT isoforms, primarily VGLUT2, which accumulates glutamate into synaptic vesicles, was reported in subsets of neurosecretory terminals in the median eminence and in the posterior pituitary. Populations of secretory cells in various endocrine organs, including the adenohypophysis, also express the glutamatergic markers. The presence of ionotropic and metabotropic glutamate receptors as well as enzymes of the glutamate/glutamine cycle provides additional proof for local glutamatergic mechanisms at hormone release sites. The *in vitro* potency of ionotropic glutamate receptor agonists to elicit peptide hormone secretion from neuroendocrine terminals and adenohypophysial cells indicates autocrine/paracrine mechanisms whereby endogenous glutamate modulates endocrine function. The regulated expression of VGLUT2 in neuroendocrine/endocrine cells in response to various endocrine stimuli suggests that the alteration of the proposed autocrine/paracrine glutamatergic signalling underlies crucial adaptive mechanisms.

Elucidation of the role of endogeous glutamate in neuroendocrine/endocrine cells will be a new challenge for neuroendocrine research.

Acknowledgements

This work was supported by grants from the National Science Foundation of Hungary (OTKA K69127, K46574 and K73002) and the European Union FP6 funding (LSHM-CT-2003-503041).

Received: 19 February 2008,
revised 21 March 2008,
accepted 24 March 2008

References

1 Somogyi P, Halasy K, Somogyi J, Storm-Mathisen J, Ottersen OP. Quantification of immunogold labelling reveals enrichment of glutamate in mossy and parallel fibre terminals in cat cerebellum. *Neuroscience* 1986; **19**: 1045–1050.
2 Storm-Mathisen J, Leknes AK, Bore AT, Vaaland JL, Edminson P, Haug FM, Ottersen OP. First visualization of glutamate and GABA in neurones by immunocytochemistry. *Nature* 1983; **301**: 517–520.
3 van den Pol AN, Wuarin JP, Dudek FE. Glutamate, the dominant excitatory transmitter in neuroendocrine regulation. *Science* 1990; **250**: 1276–1278.
4 Oswald RE. Ionotropic glutamate receptor recognition and activation. *Adv Protein Chem* 2004; **68**: 313–349.
5 Barnes GN, Slevin JT. Ionotropic glutamate receptor biology: effect on synaptic connectivity and function in neurological disease. *Curr Med Chem* 2003; **10**: 2059–2072.
6 Koles L, Wirkner K, Illes P. Modulation of ionotropic glutamate receptor channels. *Neurochem Res* 2001; **26**: 925–932.
7 Kew JN, Kemp JA. Ionotropic and metabotropic glutamate receptor structure and pharmacology. *Psychopharmacology* 2005; **179**: 4–29.
8 Schoepp DD, Conn PJ. Metabotropic glutamate receptors. *Pharmacol Biochem Behav* 2002; **74**: 255–256.
9 Pin JP, Duvoisin R. The metabotropic glutamate receptors: structure and functions. *Neuropharmacology* 1995; **34**: 1–26.
10 Nakanishi S. Metabotropic glutamate receptors: synaptic transmission, modulation, and plasticity. *Neuron* 1994; **13**: 1031–1037.
11 Brann DW. Glutamate: a major excitatory transmitter in neuroendocrine regulation. *Neuroendocrinology* 1995; **61**: 213–225.
12 Nagy GM, Bodnar I, Banky Z, Halasz B. Control of prolactin secretion by excitatory amino acids. *Endocrine* 2005; **28**: 303–308.
13 Aguilar E, Tena-Sempere M, Pinilla L. Role of excitatory amino acids in the control of growth hormone secretion. *Endocrine* 2005; **28**: 295–302.
14 Jezova D. Control of ACTH secretion by excitatory amino acids: functional significance and clinical implications. *Endocrine* 2005; **28**: 287–294.
15 Mahesh VB, Brann DW. Regulatory role of excitatory amino acids in reproduction. *Endocrine* 2005; **28**: 271–280.
16 Brann DW, Mahesh VB. Excitatory amino acids: evidence for a role in the control of reproduction and anterior pituitary hormone secretion. *Endocr Rev* 1997; **18**: 678–700.
17 Gore AC. Gonadotropin-releasing hormone neurons, NMDA receptors, and their regulation by steroid hormones across the reproductive life cycle. *Brain Res Brain Res Rev* 2001; **37**: 235–248.
18 Jezova D, Oliver C, Jurcovicova J. Stimulation of adrenocorticotropin but not prolactin and catecholamine release by N-methyl-aspartic acid. *Neuroendocrinology* 1991; **54**: 488–492.
19 Olney JW, Cicero TJ, Meyer ER, de Gubareff T. Acute glutamate-induced elevations in serum testosterone and luteinizing hormone. *Brain Res* 1976; **112**: 420–424.
20 Ondo JG, Pass KA, Baldwin R. The effects of neurally active amino acids on pituitary gonadotropin secretion. *Neuroendocrinology* 1976; **21**: 79–87.
21 Makara GB, Stark E. Effect of intraventricular glutamate on ACTH release. *Neuroendocrinology* 1975; **18**: 213–216.
22 Arufe MC, Duran R, Perez-Vences D, Alfonso M. Endogenous excitatory amino acid neurotransmission regulates thyroid-stimulating hormone and thyroid hormone secretion in conscious freely moving male rats. *Endocrine* 2002; **17**: 193–197.
23 Acs Z, Lonart G, Makara GB. Role of hypothalamic factors (growth-hormone-releasing hormone and gamma-aminobutyric acid) in the regulation of growth hormone secretion in the neonatal and adult rat. *Neuroendocrinology* 1990; **52**: 156–160.
24 Leng G, Brown CH, Russell JA. Physiological pathways regulating the activity of magnocellular neurosecretory cells. *Prog Neurobiol* 1999; **57**: 625–655.
25 Zanisi M, Messi E. Sex steroids and the control of LHRH secretion. *J Steroid Biochem Mol Biol* 1991; **40**: 155–163.
26 Lindstrom P, Ohlsson L. Effect of N-methyl-D,L-aspartate on isolated rat somatotrophs. *Endocrinology* 1992; **131**: 1903–1907.
27 Niimi M, Sato M, Murao K, Takahara J, Kawanishi K. Effect of excitatory amino acid receptor agonists on secretion of growth hormone as assessed by the reverse hemolytic plaque assay. *Neuroendocrinology* 1994; **60**: 173–178.

28 Login IS. Direct stimulation of pituitary prolactin release by glutamate. *Life Sci* 1990; **47**: 2269–2275.
29 D'Aniello G, Tolino A, D'Aniello A, Errico F, Fisher GH, Di Fiore MM. The role of D-aspartic acid and N-methyl-D-aspartic acid in the regulation of prolactin release. *Endocrinology* 2000; **141**: 3862–3870.
30 Berrino l. Participation of glutamatergic mechanisms in vasopressin release from th eisolated rat neurohypophysis. *Pharmacol Res Commun* 1988; **20**(suppl 1): 63–64.
31 Masson J, Sagne C, Hamon M, El Mestikawy S. Neurotransmitter transporters in the central nervous system. *Pharmacol Rev* 1999; **51**: 439–464.
32 Bellocchio EE, Reimer RJ, Fremeau RT Jr, Edwards RH. Uptake of glutamate into synaptic vesicles by an inorganic phosphate transporter. *Science* 2000; **289**: 957–960.
33 Takamori S, Rhee JS, Rosenmund C, Jahn R. Identification of a vesicular glutamate transporter that defines a glutamatergic phenotype in neurons. *Nature* 2000; **407**: 189–194.
34 Ni B, Rosteck PR Jr, Nadi NS, Paul SM. Cloning and expression of a cDNA encoding a brain-specific Na(+)-dependent inorganic phosphate cotransporter. *Proc Natl Acad Sci U S A* 1994; **91**: 5607–5611.
35 Bai L, Xu H, Collins JF, Ghishan FK. Molecular and functional analysis of a novel neuronal vesicular glutamate transporter. *J Biol Chem* 2001; **276**: 36764–36769.
36 Fremeau RT Jr, Troyer MD, Pahner I, Nygaard GO, Tran CH, Reimer RJ, Bellocchio EE, Fortin D, Storm-Mathisen J, Edwards RH. The expression of vesicular glutamate transporters defines two classes of excitatory synapse. *Neuron* 2001; **31**: 247–260.
37 Hayashi M, Otsuka M, Morimoto R, Hirota S, Yatsushiro S, Takeda J, Yamamoto A, Moriyama Y. Differentiation-associated Na^+-dependent inorganic phosphate cotransporter (DNPI) is a vesicular glutamate transporter in endocrine glutamatergic systems. *J Biol Chem* 2001; **276**: 43400–43406.
38 Herzog E, Bellenchi GC, Gras C, Bernard V, Ravassard P, Bedet C, Gasnier B, Giros B, El Mestikawy S. The existence of a second vesicular glutamate transporter specifies subpopulations of glutamatergic neurons. *J Neurosci* 2001; **21**: RC181.
39 Takamori S, Rhee JS, Rosenmund C, Jahn R. Identification of differentiation-associated brain-specific phosphate transporter as a second vesicular glutamate transporter (VGLUT2). *J Neurosci* 2001; **21**: RC182.
40 Fremeau RT Jr, Burman J, Qureshi T, Tran CH, Proctor J, Johnson J, Zhang H, Sulzer D, Copenhagen DR, Storm-Mathisen J, Reimer RJ, Chaudhry FA, Edwards RH. The identification of vesicular glutamate transporter 3 suggests novel modes of signaling by glutamate. *Proc Natl Acad Sci U S A* 2002; **99**: 14488–14493.
41 Gras C, Herzog E, Bellenchi GC, Bernard V, Ravassard P, Pohl M, Gasnier B, Giros B, El Mestikawy S. A third vesicular glutamate transporter expressed by cholinergic and serotoninergic neurons. *J Neurosci* 2002; **22**: 5442–5451.
42 Schafer MK, Varoqui H, Defamie N, Weihe E, Erickson JD. Molecular cloning and functional identification of mouse vesicular glutamate transporter 3 and its expression in subsets of novel excitatory neurons. *J Biol Chem* 2002; **277**: 50734–50748.
43 Varoqui H, Schafer MK, Zhu H, Weihe E, Erickson JD. Identification of the differentiation-associated Na^+/PI transporter as a novel vesicular glutamate transporter expressed in a distinct set of glutamatergic synapses. *J Neurosci* 2002; **22**: 142–155.
44 Bellocchio EE, Hu H, Pohorille A, Chan J, Pickel VM, Edwards RH. The localization of the brain-specific inorganic phosphate transporter suggests a specific presynaptic role in glutamatergic transmission. *J Neurosci* 1998; **18**: 8648–8659.
45 Fujiyama F, Furuta T, Kaneko T. Immunocytochemical localization of candidates for vesicular glutamate transporters in the rat cerebral cortex. *J Comp Neurol* 2001; **435**: 379–387.
46 Sakata-Haga H, Kanemoto M, Maruyama D, Hoshi K, Mogi K, Narita M, Okado N, Ikeda Y, Nogami H, Fukui Y, Kojima I, Takeda J, Hisano S. Differential localization and colocalization of two neuron-types of sodium-dependent inorganic phosphate cotransporters in rat forebrain. *Brain Res* 2001; **902**: 143–155.
47 Ziegler DR, Cullinan WE, Herman JP. Distribution of vesicular glutamate transporter mRNA in rat hypothalamus. *J Comp Neurol* 2002; **448**: 217–229.
48 Lin W, McKinney K, Liu L, Lakhlani S, Jennes L. Distribution of vesicular glutamate transporter-2 messenger ribonucleic Acid and protein in the septum-hypothalamus of the rat. *Endocrinology* 2003; **144**: 662–670.
49 Kiss J, Kocsis K, Csaki A, Halasz B. Evidence for vesicular glutamate transporter synapses onto gonadotropin-releasing hormone and other neurons in the rat medial preoptic area. *Eur J Neurosci* 2003; **18**: 3267–3278.
50 Kiss J, Csaba Z, Csaki A, Halasz B. Glutamatergic innervation of growth hormone-releasing hormone-containing neurons in the hypothalamic arcuate nucleus and somatostatin-containing neurons in the anterior periventricular nucleus of the rat. *Brain Res Bull* 2006; **70**: 278–288.
51 Wittmann G, Lechan RM, Liposits Z, Fekete C. Glutamatergic innervation of corticotropin-releasing hormone- and thyrotropin-releasing hormone-synthesizing neurons in the hypothalamic paraventricular nucleus of the rat. *Brain Res* 2005; **1039**: 53–62.
52 Mueller NK, Di S, Paden CM, Herman JP. Activity-dependent modulation of neurotransmitter innervation to vasopressin neurons of the supraoptic nucleus. *Endocrinology* 2005; **146**: 348–354.
53 Hisano S, Nogami H. Transporters in the neurohypophysial neuroendocrine system, with special reference to vesicular glutamate transporters (BNPI and DNPI): a review. *Microsc Res Tech* 2002; **56**: 122–131.
54 Collin M, Backberg M, Ovesjo ML, Fisone G, Edwards RH, Fujiyama F, Meister B. Plasma membrane and vesicular glutamate transporter mRNAs/proteins in hypothalamic neurons that regulate body weight. *Eur J Neurosci* 2003; **18**: 1265–1278.
55 Hrabovszky E, Petersen SL. Increased concentrations of radioisotopically-labeled complementary ribonucleic acid probe, dextran sulfate, and dithiothreitol in the hybridization buffer can improve results of in situ hybridization histochemistry. *J Histochem Cytochem* 2002; **50**: 1389–1400.
56 Hrabovszky E, Turi GF, Kallo I, Liposits Z. Expression of vesicular glutamate transporter-2 in gonadotropin-releasing hormone neurons of the adult male rat. *Endocrinology* 2004; **145**: 4018–4021.
57 Hrabovszky E, Wittmann G, Turi GF, Liposits Z, Fekete C. Hypophysiotropic thyrotropin-releasing hormone and corticotropin-releasing hormone neurons of the rat contain vesicular glutamate transporter-2. *Endocrinology* 2005; **146**: 341–347.
58 Hrabovszky E, Turi GF, Liposits Z. Presence of vesicular glutamate transporter-2 in hypophysiotropic somatostatin but not growth hormone-releasing hormone neurons of the male rat. *Eur J Neurosci* 2005; **21**: 2120–2126.
59 Meister B, Hokfelt T. Peptide- and transmitter-containing neurons in the mediobasal hypothalamus and their relation to GABAergic systems: possible roles in control of prolactin and growth hormone secretion. *Synapse* 1988; **2**: 585–605.
60 Kawasaki A, Hoshi K, Kawano M, Nogami H, Yoshikawa H, Hisano S. Up-regulation of VGLUT2 expression in hypothalamic-neurohypophysial neurons of the rat following osmotic challenge. *Eur J Neurosci* 2005; **22**: 672–680.
61 Hrabovszky E, Csapo AK, Kallo I, Wilheim T, Turi GF, Liposits Z. Localization and osmotic regulation of vesicular glutamate transporter-2 in magnocellular neurons of the rat hypothalamus. *Neurochem Int* 2006; **48**: 753–761.

62 Ponzio TA, Ni Y, Montana V, Parpura V, Hatton GI. Vesicular glutamate transporter expression in supraoptic neurones suggests a glutamatergic phenotype. *J Neuroendocrinol* 2006; **18**: 253–265.
63 Hrabovszky E, Deli L, Turi GF, Kallo I, Liposits Z. Glutamatergic innervation of the hypothalamic median eminence and posterior pituitary of the rat. *Neuroscience* 2007; **144**: 1383–1392.
64 Hayashi M, Morimoto R, Yamamoto A, Moriyama Y. Expression and localization of vesicular glutamate transporters in pancreatic islets, upper gastrointestinal tract, and testis. *J Histochem Cytochem* 2003; **51**: 1375–1390.
65 Hayashi M, Yamada H, Uehara S, Morimoto R, Muroyama A, Yatsushiro S, Takeda J, Yamamoto A, Moriyama Y. Secretory granule-mediated co-secretion of L-glutamate and glucagon triggers glutamatergic signal transmission in islets of Langerhans. *J Biol Chem* 2003; **278**: 1966–1974.
66 Morimoto R, Hayashi M, Yatsushiro S, Otsuka M, Yamamoto A, Moriyama Y. Co-expression of vesicular glutamate transporters (VGLUT1 and VGLUT2) and their association with synaptic-like microvesicles in rat pinealocytes. *J Neurochem* 2003; **84**: 382–391.
67 Moriyama Y, Hayashi M, Yamada H, Yatsushiro S, Ishio S, Yamamoto A. Synaptic-like microvesicles, synaptic vesicle counterparts in endocrine cells, are involved in a novel regulatory mechanism for the synthesis and secretion of hormones. *J Exp Biol* 2000; **203**: 117–125.
68 Hinoi E, Takarada T, Ueshima T, Tsuchihashi Y, Yoneda Y. Glutamate signaling in peripheral tissues. *Eur J Biochem* 2004; **271**: 1–13.
69 Hayashi M, Otsuka M, Morimoto R, Muroyama A, Uehara S, Yamamoto A, Moriyama Y. Vesicular inhibitory amino acid transporter is present in glucagon-containing secretory granules in alphaTC6 cells, mouse clonal alpha-cells, and alpha-cells of islets of Langerhans. *Diabetes* 2003; **52**: 2066–2074.
70 Kawakami S, Ichikawa M, Murahashi K, Hirunagi K, Tsukamura H, Maeda K. Excitatory amino acids act on the median eminence nerve terminals to induce gonadotropin-releasing hormone release in female rats. *Gen Comp Endocrinol* 1998; **112**: 372–382.
71 Kawakami SI, Hirunagi K, Ichikawa M, Tsukamura H, Maeda KI. Evidence for terminal regulation of GnRH release by excitatory amino acids in the median eminence in female rats: a dual immunoelectron microscopic study. *Endocrinology* 1998; **139**: 1458–1461.
72 Yin W, Mendenhall JM, Bratton SB, Oung T, Janssen WG, Morrison JH, Gore AC. Novel localization of NMDA receptors within neuroendocrine gonadotropin-releasing hormone terminals. *Exp Biol Med (Maywood)* 2007; **232**: 662–673.
73 Kawakami S. Glial and neuronal localization of ionotropic glutamate receptor subunit-immunoreactivities in the median eminence of female rats: GluR2/3 and GluR6/7 colocalize with vimentin, not with glial fibrillary acidic protein (GFAP). *Brain Res* 2000; **858**: 198–204.
74 Diano S, Naftolin F, Horvath TL. Kainate glutamate receptors (GluR5-7) in the rat arcuate nucleus: relationship to tanycytes, astrocytes, neurons and gonadal steroid receptors. *J Neuroendocrinol* 1998; **10**: 239–247.
75 Eyigor O, Jennes L. Identification of kainate-preferring glutamate receptor subunit GluR7 mRNA and protein in the rat median eminence. *Brain Res* 1998; **814**: 231–235.
76 Krizbai IA, Deli MA, Pestenacz A, Siklos L, Szabo CA, Andras I, Joo F. Expression of glutamate receptors on cultured cerebral endothelial cells. *J Neurosci Res* 1998; **54**: 814–819.
77 Gillard SE, Tzaferis J, Tsui HC, Kingston AE. Expression of metabotropic glutamate receptors in rat meningeal and brain microvasculature and choroid plexus. *J Comp Neurol* 2003; **461**: 317–332.
78 Parfenova H, Neff RA III, Alonso JS, Shlopov BV, Jamal CN, Sarkisova SA, Leffler CW. Cerebral vascular endothelial heme oxygenase: expression, localization, and activation by glutamate. *Am J Physiol Cell Physiol* 2001; **281**: C1954–C1963.
79 Parfenova H, Fedinec A, Leffler CW. Ionotropic glutamate receptors in cerebral microvascular endothelium are functionally linked to heme oxygenase. *J Cereb Blood Flow Metab* 2003; **23**: 190–197.
80 Morley P, Small DL, Murray CL, Mealing GA, Poulter MO, Durkin JP, Stanimirovic DB. Evidence that functional glutamate receptors are not expressed on rat or human cerebromicrovascular endothelial cells. *J Cereb Blood Flow Metab* 1998; **18**: 396–406.
81 Petralia RS, Wang YX, Wenthold RJ. Histological and ultrastructural localization of the kainate receptor subunits, KA2 and GluR6/7, in the rat nervous system using selective antipeptide antibodies. *J Comp Neurol* 1994; **349**: 85–110.
82 Kiyama H, Sato K, Tohyama M. Characteristic localization of non-NMDA type glutamate receptor subunits in the rat pituitary gland. *Brain Res Mol Brain Res* 1993; **19**: 262–268.
83 Unnerstall JR, Wamsley JK. Autoradiographic localization of high-affinity [3H]kainic acid binding sites in the rat forebrain. *Eur J Pharmacol* 1983; **86**: 361–371.
84 Bhat GK, Mahesh VB, Chu ZW, Chorich LP, Zamorano PL, Brann DW. Localization of the N-methyl-D-aspartate R1 receptor subunit in specific anterior pituitary hormone cell types of the female rat. *Neuroendocrinology* 1995; **62**: 178–186.
85 Caruso C, Bottino MC, Pampillo M, Pisera D, Jaita G, Duvilanski B, Seilicovich A, Lasaga M. Glutamate induces apoptosis in anterior pituitary cells through group II metabotropic glutamate receptor activation. *Endocrinology* 2004; **145**: 4677–4684.
86 Tappaz ML, Wassef M, Oertel WH, Paut L, Pujol JF. Light- and electron-microscopic immunocytochemistry of glutamic acid decarboxylase (GAD) in the basal hypothalamus: morphological evidence for neuroendocrine gamma-aminobutyrate (GABA). *Neuroscience* 1983; **9**: 271–287.
87 Hrabovszky E, Kallo I, Turi GF, May K, Wittmann G, Fekete C, Liposits Z. Expression of vesicular glutamate transporter-2 in gonadotrope and thyrotrope cells of the rat pituitary. Regulation by estrogen and thyroid hormone status. *Endocrinology* 2006; **147**: 3818–3825.
88 Tong Q, Ouedraogo R, Kirchgessner AL. Localization and function of group III metabotropic glutamate receptors in rat pancreatic islets. *Am J Physiol Endocrinol Metab* 2002; **282**: E1324–E1333.
89 Weaver CD, Yao TL, Powers AC, Verdoorn TA. Differential expression of glutamate receptor subtypes in rat pancreatic islets. *J Biol Chem* 1996; **271**: 12977–12984.
90 Erickson JD, De Gois S, Varoqui H, Schafer MK, Weihe E. Activity-dependent regulation of vesicular glutamate and GABA transporters: a means to scale quantal size. *Neurochem Int* 2006; **48**: 643–649.
91 Wojcik SM, Rhee JS, Herzog E, Sigler A, Jahn R, Takamori S, Brose N, Rosenmund C. An essential role for vesicular glutamate transporter 1 (VGLUT1) in postnatal development and control of quantal size. *Proc Natl Acad Sci U S A* 2004; **101**: 7158–7163.
92 van den Berg CJ, Garfinkel D. A stimulation study of brain compartments. Metabolism of glutamate and related substances in mouse brain. *Biochem J* 1971; **123**: 211–218.
93 Benjamin AM, Quastel JH. Metabolism of amino acids and ammonia in rat brain cortex slices in vitro: a possible role of ammonia in brain function. *J Neurochem* 1975; **25**: 197–206.
94 Martinez-Hernandez A, Bell KP, Norenberg MD. Glutamine synthetase: glial localization in brain. *Science* 1977; **195**: 1356–1358.
95 Hamberger AC, Chiang GH, Nylen ES, Scheff SW, Cotman CW. Glutamate as a CNS transmitter. I. Evaluation of glucose and glutamine as precursors for the synthesis of preferentially released glutamate. *Brain Res* 1979; **168**: 513–530.
96 Hamberger A, Chiang GH, Sandoval E, Cotman CW. Glutamate as a CNS transmitter. II. Regulation of synthesis in the releasable pool. *Brain Res* 1979; **168**: 531–541.

97 Hertz L. Functional interactions between neurons and astrocytes I. Turnover and metabolism of putative amino acid transmitters. *Prog Neurobiol* 1979; **13**: 277–323.
98 Bradford HF, Ward HK, Thomas AJ. Glutamine – a major substrate for nerve endings. *J Neurochem* 1978; **30**: 1453–1459.
99 Shigeri Y, Seal RP, Shimamoto K. Molecular pharmacology of glutamate transporters, EAATs and VGLUTs. *Brain Res Brain Res Rev* 2004; **45**: 250–265.
100 Chaudhry FA, Reimer RJ, Edwards RH. The glutamine commute: take the N line and transfer to the A. *J Cell Biol* 2002; **157**: 349–355.
101 Varoqui H, Zhu H, Yao D, Ming H, Erickson JD. Cloning and functional identification of a neuronal glutamine transporter. *J Biol Chem* 2000; **275**: 4049–4054.
102 Ottersen OP, Zhang N, Walberg F. Metabolic compartmentation of glutamate and glutamine: morphological evidence obtained by quantitative immunocytochemistry in rat cerebellum. *Neuroscience* 1992; **46**: 519–534.
103 Nieoullon A, Canolle B, Masmejean F, Guillet B, Pisano P, Lortet S. The neuronal excitatory amino acid transporter EAAC1/EAAT3: does it represent a major actor at the brain excitatory synapse? *J Neurochem* 2006; **98**: 1007–1018.
104 Beart PM, O'Shea RD. Transporters for L-glutamate: an update on their molecular pharmacology and pathological involvement. *Br J Pharmacol* 2007; **150**: 5–17.
105 McDonald JW, Johnston MV. Pharmacology of N-methyl-D-aspartate-induced brain injury in an in vivo perinatal rat model. *Synapse*. 1990; **6**: 179–188.
106 Berger UV, Hediger MA. Differential distribution of the glutamate transporters GLT-1 and GLAST in tanycytes of the third ventricle. *J Comp Neurol* 2001; **433**: 101–114.
107 Berger UV, Hediger MA. Distribution of the glutamate transporters GLAST and GLT-1 in rat circumventricular organs, meninges, and dorsal root ganglia. *J Comp Neurol* 2000; **421**: 385–399.
108 Shirasawa N, Yamanouchi H. Glucocorticoids induce glutamine synthetase in folliculostellate cells of rat pituitary glands in vivo and in vitro. *J Anat* 1999; **194**: 567–577.
109 King JC, Rubin BS. Dynamic changes in LHRH neurovascular terminals with various endocrine conditions in adults. *Horm Behav* 1994; **28**: 349–356.
110 Miyata S, Takamatsu H, Maekawa S, Matsumoto N, Watanabe K, Kiyohara T, Hatton GI. Plasticity of neurohypophysial terminals with increased hormonal release during dehydration: ultrastructural and biochemical analyses. *J Comp Neurol* 2001; **434**: 413–427.
111 Bhat GK, Mahesh VB, Ping L, Chorich L, Wiedmeier VT, Brann DW. Opioid-glutamate-nitric oxide connection in the regulation of luteinizing hormone secretion in the rat. *Endocrinology* 1998; **139**: 955–960.
112 Prevot V, Bouret S, Stefano GB, Beauvillain J. Median eminence nitric oxide signaling. *Brain Res Brain Res Rev* 2000; **34**: 27–41.
113 Matagne V, Lebrethon MC, Gerard A, Bourguignon JP. Kainate/estrogen receptor involvement in rapid estradiol effects in vitro and intracellular signaling pathways. *Endocrinology* 2005; **146**: 2313–2323.
114 Hokfelt T, Ceccatelli S, Gustafsson L, Hulting AL, Verge V, Villar M, Xu XJ, Xu ZQ, Wiesenfeld-Hallin Z, Zhang X. Plasticity of NO synthase expression in the nervous and endocrine systems. *Neuropharmacology* 1994; **33**: 1221–1227.
115 Johnson ES, Gendrich RL, White WF. Delay of puberty and inhibition of reproductive processes in the rat by a gonadotropin-releasing hormone agonist analog. *Fertil Steril* 1976; **27**: 853–860.
116 Santen RJ, Demers LM, Max DT, Smith J, Stein BS, Glode LM. Long term effects of administration of a gonadotropin-releasing hormone superagonist analog in men with prostatic carcinoma. *J Clin Endocrinol Metab* 1984; **58**: 397–400.
117 Bourguignon JP, Gerard A, Mathieu J, Simons J, Franchimont P. Pulsatile release of gonadotropin-releasing hormone from hypothalamic explants is restrained by blockade of N-methyl-D,L-aspartate receptors. *Endocrinology* 1989; **125**: 1090–1096.
118 Bourguignon JP, Gerard A, Alvarez Gonzalez ML, Purnelle G, Franchimont P. Endogenous glutamate involvement in pulsatile secretion of gonadotropin-releasing hormone: evidence from effect of glutamine and developmental changes. *Endocrinology* 1995; **136**: 911–916.

18. számú melléklet

Neurochemistry International 54 (2009) 119–134

Contents lists available at ScienceDirect

Neurochemistry International

journal homepage: www.elsevier.com/locate/neuint

Temporal profile of estrogen-dependent gene expression in LHRH-producing GT1–7 cells

Patricia Varju [a], Ken C. Chang [b], Erik Hrabovszky [a], István Merchenthaler [c], Zsolt Liposits [a,d,*]

[a] Institute of Experimental Medicine, Hungarian Academy of Sciences, Laboratory of Endocrine Neurobiology, Szigony u. 43, Budapest H-1083, Hungary
[b] Women's Health Research Institute, Wyeth Research, Collegeville, PA, USA
[c] Departments of Epidemiology and Anatomy/Neurobiology University of Maryland, Baltimore, USA
[d] Faculty of Information Technology, Pázmány Péter Catholic University, Budapest H-1083, Hungary

ARTICLE INFO

Article history:
Received 31 October 2008
Accepted 6 November 2008
Available online 25 November 2008

Keywords:
17β-Estradiol
GT1–7
Regulation
Microarray
Expression
Gene

ABSTRACT

The long-term cellular effects of estrogens are mediated by nuclear estrogen receptors which act as transcription factors to regulate gene expression. Hypothalamic targets of estrogen action include luteinizing hormone-releasing hormone-secreting neurons controlling reproduction in vertebrates. Microarray analysis and qRT-PCR studies were performed on GT1–7, immortalized LHRH neurons after 17β-estradiol treatment to reveal the nature of estrogen-regulated genes and the time course of changes in their expression profile. More than 1000 transcripts showed robust responses to estrogen treatment and the majority of responding genes were up-regulated. Early-responding genes showed altered expression 0.5–2 h after estrogen exposure, whereas late-responding genes changed after 24–48 h treatment. Up-regulated genes encoded transcription factors, molecules involved in cellular movement, cell death, immune response, neurotransmitter and neuropeptide receptors, ion channels and transporters. The 17β-estradiol modulation of 12 genes – representing characteristic gene clusters – has been confirmed by qRT-PCR.

Our studies highlighted diverse gene networks, cell regulatory mechanisms and metabolic pathways through which estrogen may alter gene expression in immortalized LHRH neurons. The findings also support the notion that genomic effects of estrogen targeting *in vivo* directly the LHRH neuronal network of mammals play an important role in the central feedback regulation of the reproductive axis by estrogen.

1. Introduction

It has been well established that estrogen hormones operate as feedback signals reporting the functional gonadal status to the brain and play a key role in the control of mammalian reproduction (Herbison et al., 2001). Periodic changes in serum 17β-estradiol (E2) levels across the reproductive cycle of the female in rodents exert both negative and positive feedback actions on the secretion of the two gonadotropins, luteinizing hormone (LH) and follicle stimulating hormone (FSH) from the anterior pituitary. The functions of gonadotropic cells are tightly regulated by the pulsatile release of luteinizing hormone-releasing hormone (LHRH; Burgos-Briceno et al., 1983) into the hypophysial portal circulation from a small group of neurons (~1000–1200 in rodents) scattered in the medial septum (MS), diagonal band of Broca (DBB), and the medial preoptic area (MPOA; Liposits et al., 1984; Merchenthaler et al., 1984). This episodic secretory activity represents an endogenous feature of the LHRH neuronal system which is required to maintain normal reproductive functions (Herbison et al., 2001). Humoral (sexual steroids) and afferent neuronal (norepinephrine, dopamine, acetylcholine, GABA, serotonin, etc.) signals regulate reproduction by modulating the frequency and amplitude of the LHRH secretory pulses (Herbison et al., 2008).

The lack of evidence for estrogen receptors (ER) in LHRH neurons (Langub et al., 1991; Herbison and Theodosis, 1992) formed a long-held view that E2-receptive interneurons are required to communicate E2 signals to the LHRH neuronal system. This opinion has been challenged recently following the detection of ER mRNA transcripts (Skynner et al., 1999; Hrabovszky et al.,

* Corresponding author.
E-mail address: liposits@koki.hu (Z. Liposits).

Abbreviations: ADAM, a disintegrin and matrix metallopeptidase; B2M, beta-2-microglobulin; CAM, cell adhesion molecule; CREBBP, cAMP-response element-binding protein; DMEM, Dulbecco modified Eagle's medium; E2, 17β-estradiol; ECM, extracellular matrix; ER, estrogen receptor; ERE, estrogen response element; FBS, fetal bovine serum; FSH, follicle stimulating hormone; GAD, glutamic acid decarboxylase; HPRT, hypoxanthine guanine phosphoribosyl transferase; HS, horse serum; IgG, immunglobulin; IPA, ingenuity pathway analysis; LH, luteinizing hormone; LHRH, luteinizing hormone-releasing hormone; MMP, matrix metallopeptidase; NO, nitrogen-monoxide; NPY, neuropeptide Y; PBS, phosphate buffered saline; PCA, principal component analysis; PCDH, protocadherin; SG, secretory granule; SR2, serum replacement factor; STP, signal transduction pathway.

0197-0186/$ – see front matter © 2008 Elsevier Ltd. All rights reserved.
doi:10.1016/j.neuint.2008.11.003

2000), ER immunoreactivity (Hrabovszky et al., 2001; Kallo et al., 2001), and ^{125}I-estrogen binding sites (Hrabovszky et al., 2000) in LHRH neurons of various species. Moreover, it now appears that LHRH neurons *in vivo* selectively express the beta (ERβ) estrogen receptor isoform (Hrabovszky et al., 2000). Furthermore, the expression of the beta receptor isoform also characterizes the hypophysiotropic LHRH neurons of the human brain (Hrabovszky et al., 2007b).

Although many of the known effects of E2 upon LHRH neurons, including positive feedback (Wintermantel et al., 2006), still appear to be exerted indirectly through ER-containing interneurons that provide synaptic inputs to LHRH neurons (Herbison, 2007), direct E2 effects also seem to exist. These include the fast, non-genomic actions of ligand-bound ERβ on the rapid phosphorylation of cAMP-response element-binding protein (Abraham et al., 2003), stimulation of intracellular calcium oscillations (Temple et al., 2004), and enhanced excitability of mouse LHRH neurons, partly via mechanisms that include phosphorylation of potassium channels (DeFazio and Moenter, 2002). E2 also exerts direct genomic effects on LHRH neurons, including the induction of galanin mRNA and protein expression (Liposits et al., 1995; Merchenthaler et al., 1993), which is mediated by the ERβ receptor isoform (Merchenthaler, 2005).

The transctiptional effects of E2 are primarily exerted via two ER subtypes (ERα and ERβ) which are encoded by separate genes (Mosselman et al., 1996) and differ in structure, function and anatomical distribution (Green et al., 1986; Shughrue et al., 1997; Milner et al., 2005). Ligand-bound ERs can activate transcription by binding directly to estrogen response elements (ERE) located within the promoter region of a target gene (Paech et al., 1997); or alternatively, they can interact with other transcription factors such as members of the *Fos* and *Jun* families to activate transcription in the absence of direct DNA binding (Kuiper et al., 1997; Paech et al., 1997).

The aim of the present study was to reveal the direct, genomic actions of E2 in immortalized LHRH neurons (Mellon et al., 1991) by the use of a genome-wide expression analysis. GT1–7 cells exhibit neuronal phenotype (Liposits et al., 1991), synthesize LHRH and release LHRH in a pulsatile fashion (Wetsel et al., 1992), and intrinsically express ERs (Butler et al., 1999; Kallo et al., 2001; Wetsel et al., 1992). The exploration of the estrogen-driven regulatory mechanisms in cultured LHRH neurons may serve the proper mapping of genes and basic cellular mechanisms responsible for the processing of estrogen signals *in vivo* within the central regulatory machinery of reproduction, the LHRH neuronal network.

2. Experimental procedures

2.1. Materials

Water-soluble 17β-estradiol (E2), cell culture media, antibiotics, buffers and other cell culture supplements were purchased from Sigma (St. Louis, MO, USA), unless otherwise specified. Real-time PCR reagents and capillaries were obtained from Roche Applied Science (La Roche Ltd., Basel, Switzerland).

2.2. Cell culturing

The GT1–7 cell line was kindly donated by P. Mellon (University of California, San Diego, La Jolla; Mellon et al., 1991). Cells were maintained in Dulbecco modified Eagle's medium (DMEM, Sigma) and Ham's F12 (1:1, Sigma) supplemented with 10% fetal bovine serum (FBS, Invitrogen) and 5% horse serum (HS, Hyclone). All culture media contained 4 mM glutamine, 4500 mg/l glucose, 40 μg/ml gentamicin (Sigma), 100 U/ml penicillin (Sigma) and 0.1 mg/ml streptomycin (Sigma). Cells were incubated at 37 °C in humidified air containing 5% CO_2. Prior to the experiments, the medium was replaced with phenol red-free DMEM (Sigma) containing steroid- and thyroid-free serum replacement factor (SR2, Sigma; at a dilution of 1:50) and cells were cultured in this medium for 48 h. One hour before E2-treatment the medium was changed to fresh one.

Water-soluble E2 (cyclodextrin-encapsulated 17β-estradiol, Sigma) was dissolved in distilled water at a concentration of 10^{-3} M and then diluted further with phenol red-free DMEM to 10^{-5} M (stock solution). This solution was added directly to the culture medium (DMEM-SR2) to obtain a final 10^{-8} M E2 concentration. Cells were treated with E2 for 0.5, 2, 8, 24 and 48 h, respectively. Control cultures were maintained in DMEM-SR2 for 48 h, than the media were replaced with fresh ones for an additional 24 h. For each time-point, the cultures were processed in triplicate and the three equivalent dishes were pooled for further processing. The experiment was replicated four times to provide RNA samples for five parallel arrays for each treatment.

2.3. Gene expression profiling using Affymetrix microarray

Cells were washed two times with phosphate-buffered saline (PBS) and collected by centrifugation. Cell pellets were washed and processed through the RNeasy column (Qiagen's RNeasy Total RNA Isolation Kit) with the application of the total RNA isolation protocol. Biotin-labeled cRNA was generated from total RNA with the first strand and second strand cDNA synthesis kits (Affymetrix, Santa Clara, CA) using procedures recommended by the manufacturer. The resulting cDNAs were than purified and used for *in vitro* transcription with T7 polymerase in the presence of biotin-labeled ribonucleotides (Affymetrix). The resulting cRNAs were purified according to the RNeasy protocol (Qiagen). Labeled cRNAs were hybridized to Affymetrix murine MG-U74Av2 commercial chips and stained according to the protocol recommended by Affymetrix.

2.4. Scanning and data analysis

The chips were scanned using the Hewlett–Packard G2500A Gene Array Scanner. The image data were analyzed using the ArrayAssist (Stratagene, ArrayAssist® Expression Software) program as follows: the mean signal intensities were adjusted for local background by subtracting the median background intensities. Global scaling to 1500 equalized the overall chip fluorescence intensities. Principal component analysis (PCA) was performed on array sets representing different treatment groups and two outliers were excluded from the further analysis. CEL files were converted to CHP files involving the MAS5 normalization algorithm. Statistics-based absolute calls were calculated for each probe set, resulting in present (P), absent (A) or marginally expressed (M) expression categories. Advanced significance analysis (see technical notes on www.stratagene.com) was applied using the ArrayAssist program to determine *p*-values for changes (statistics-based value for differential expression) and signal log ratios representing the binary logarithm of the fold change of each specific probe set.

2.5. Generation of gene lists and functional pathways

Gene expression changes having an absolute signal log ratio of higher than or equal to 1.5 (approximately 2.8-fold) and a *p*-value equal to or lower than 0.05 ($p \leq 0.05$) were sorted and such genes included in further analysis. Thereafter, the genes in each treatment group were assigned to functional groups using the Gene Ontology Tool built in the ArrayAssist program.

Lists of all modulated genes at each time point were further analyzed with the ingenuity pathway analysis (IPA) program (www.ingenuity.com). The IPA suite identifies dynamically generated biological networks, global canonical pathways, and global functions. Candidate gene lists were uploaded in order to identify significantly perturbed biological networks. Applying the IPA pathway BUILD menu, taking into account all types of relationships (activation, inhibition, localization, interaction, etc.) and all types of functional categories (cytokine, enzyme, G-protein coupled receptor, ion channel, etc.), functional links between gene-products were determined at each time point (Fig. 4). Genes without any connections were discarded from the networks. IPA uses a knowledge base derived from the literature to relate gene products with each other based on their interaction and function. Each gene is assigned to a predefined functional category (such as immune response) or sub-functional category (such as cytokine biosynthesis). Highly regulated biological networks are dynamically identified using association rules among focus genes in a particular experiment. Networks of genes at each time point examined were built based on the discovered interaction or regulation links between the gene products.

IPA canonical pathways (built using established information about signaling pathways) were used to overlay the list of genes with altered expression in order to identify pathways that are highly modulated during E2 treatment.

2.6. Quantitative real-time PCR (qRT-PCR)

Total RNA from control and E2-treated GT1–7 cells were isolated with TRIzol LS reagent (Invitrogen) according to the manufacturer's instructions. RNAs from three equivalent cultures were mixed and the RNA solutions were diluted to reach a final concentration of 1 μg/μl. From each treatment group, 1 μg total RNA was used for cDNA synthesis. cDNA reaction mixtures (20 μl) contained dNTPs, 1.25 μM oligo-$dT_{(18)}$, 1.25 ng/μl random hexamers and 5 mM $MgCl_2$. Reverse transcription was performed with the ImProm II Reverse Transcription System (Promega) in a PerkinElmer thermal cycler using the method described by the manufacturer. The reverse transcribed RNA was isolated from samples collected at 0, 0.5, 2, 8, 24 and 48 h after E2-treatment. The resulting cDNA was diluted four times and used for quantitative PCR. cDNA was replaced with H_2O to serve as a no template control.

For each sample tested, reverse transcription efficiency was first evaluated by amplifying one of the reference genes (beta-2-microglobulin, b2m) from cDNA

Table 1
Primer sequences used for the amplification of selected genes by qRT-PCR and the conditions used for each primer pair (for details, see Section 2) during the PCR reaction.

Acc. number	Gene symbol		Sequence	Product length	Tm	PCR conditions		
NM_009497	Vamp2	Forward	CTGCAGCAGACCCAGGC	115 bp	66.2	94 °C	63 °C	72 °C
		Reverse	GGGCATCTGCACGGTTCA		67.6	5 s	10 s	10 s
NM_015738	GALR3	Forward	GCGCTTCCGCCGCCTGT	81 bp	74.5	94 °C	65 °C	72 °C
		Reverse	ACACGACGGAGGGCTCGATGA		73.4	5 s	10 s	10 s
NM_010234	C-FOS	Forward	CTCCAGTCCTCACCTCTTC	102 bp	58.9	94 °C	57 °C	72 °C
		Reverse	CTACCAGCTCTCAGGTGTC		57.4	5 s	10 s	10 s
J 00423	HPRT	Forward	TGTAATGATCAGTCAACGGGG	192 bp	54.9	94 °C	57 °C	72 °C
		Reverse	TGGCCTGTATCCAACACTTCG		52.3	5 s	7 s	10 s
NM_011021	OTP	Forward	CTTCGCCAAGACTCACTACC	179 bp	54.4	94 °C		70 °C
		Reverse	GGCAGCCCCGGCGTGGGCAG		76.5	5 s		20 s
NM_008712	NOS1	Forward	GGTGGGGGAAAAGCAGTCA	133 bp	59.7	94 °C	65 °C	72 °C
		Reverse	AAGACTCGATCATTCTCCCCG		58,1	5 s	10 s	15 s
NM_009963	Cry2	Forward	ACCCCGCGCTGCTAGCTGCCGT	233 bp	74	94 °C	65 °C	72 °C
		Reverse	AACGGGTCACCCCCCATTCC		65.8	5 s	10 s	10 s
NM_008077	GAD1	Forward	CACCACCCACACCAGTTGCT	238 bp	61.9	94 °C	61 °C	72 °C
		Reverse	ACGGGTGCAATTTCATATGTGAACATA		61.4	5 s	10 s	10 s
NM_009735	B2M	Forward	AAAACCCCTCAAATTCAAGTAT	210 bp	55.6	94 °C	57 °C	72 °C
		Reverse	GGGGGTGAATTCAGTGTGAGC		48.6	5 s	7 s	10 s
NM_007420	ADRA2B	Forward	ACGAAGCGTGGGTTGTGGGCAT	331 bp	64.1	94 °C	57 °C	72 °C
		Reverse	GAAGGGCGATGTGATAGCAAC		53.7	5 s	10 s	10 s
NM_011638	Tfrc	Forward	GCCTTGCTCGGCAAGTAGATGGA	252 bp	61.3	94 °C	61 °C	72 °C
		Reverse	TCTGTCTCCTCCGTTTCAGCCAG		59.4	5 s	10 s	10 s
NM_013569	Kcnh2	Forward	ATGGCATCGACATGAACG	80 bp	60.1	94 °C	65 °C	72 °C
		Reverse	CGAGCGGTTCAGGTGTAG		60.5	5 s	10 s	20 s
NM_010849	C-MYC	Forward	TGTCCTCCGAGTCCTCCC	118 bp	61.9	94 °C	60 °C	72 °C
		Reverse	ACATCAATTTCTTCCTCATCTTCTTGC		62.2	5 s	10 s	10 s
NM_007393	beta-Actin	G5740	Promega	240 bp	57	94 °C	57 °C	72 °C
						5 s	10 s	10 s

samples obtained by reverse transcription of RNA dilution series (1, 1:2, 1:4, 1:8, 1:16, 1:32 and 1:64). This allowed the transformation of the RNA concentration to a C_t value (linear relationship), which was essential for evaluating the quantitativness of cDNA synthesis. In the range of 16–25 cycles, the C_t values showed a linear relationship with the concentrations applied (data not shown) indicating that the differences in the initial mRNA template concentrations were maintained during the cDNA synthesis and the following qPCR reaction. In a second step, we tested the efficiency of qPCR via amplifying serial dilutions (1, 1:2, 1:4, 1:8, 1:16 and 1:32) of a selected cDNA template with b2m primers. In the range between 16 and 30 cycles, the starting cDNA amount showed a good correlation with the final qPCR product concentration. In a third test, two potential house-keeping genes (hypoxanthine guanine phosphoribosyl transferase, HPRT; and b2m) were selected and amplified using gene-specific oligonucleotides. Prior to synthesis, the forward and reverse primers were designed using the Probe Design Software (Roche) that also determines the accurate annealing temperature and initiates a BLAST specificity search to confirm the specificity of the primers. If possible, intron-spanning primers were chosen.

Specific PCR products for house-keeping genes and for the genes of interest were purified (QIAquick gel extraction kit, Qiagen). From these, 10-fold serial dilutions were prepared with sterile water to be used in qPCR analysis to prepare standard curves. These dilution series and the sample cDNAs were run simultaneously in PCR experiments to determine the relative concentration of genes in GT1–7 samples. qPCR reactions were carried out in a Light Cycler 2.0 PCR machine (Roche) with the Fast Start DNA Master SYBR Green I mix (Roche). The manufacturer's instructions were followed to compose 10 μl reactions in Light Cycler glass capillaries (Roche). The PCR reactions contained 1 μl DNA Master SYBR Green I (Roche), 1 μl cDNA mix, 2–4 mM $MgCl_2$, 0.3 μM gene-specific primers and were run in triplicates. The differences in the amounts of b2m or HPRT gene products between treatment-groups were used to compensate for any differences in starting total RNA amount of the single samples. Primer sequences used in the PCR reactions and real-time PCR conditions are presented in Table 1. The reactions started with a denaturation step at 95 °C for 5 min, followed by 45 cycles with the indicated conditions. PCR products were elongated at 72 °C for 10 min and cooling the samples to 4 °C ended the assays. The relative amounts of the products were determined from the log phase of the reaction.

To determine the quality of the PCR products, melting curve analysis was performed at the end point of each qPCR reaction. qPCR assays that showed non-specific product or primer dimer at the end point were excluded from further data analysis. PCR product sizes were also verified by agarose gel electrophoresis at the end of the reaction.

3. Results

3.1. Basal expression profile of GT1–7 cells in the absence of estrogen

We found that control, GT1–7 cells not treated with E2 expressed about 6000 mRNA species. They contained the mRNAs encoding for a wide array of receptors including LHRH-, galanin-, ERα- and ERβ receptors (Table 2), transcripts studied extensively by others in GT1–7 cells and LHRH neurons (Butler et al., 1999; Dudas and Merchenthaler, 2004; Hrabovszky et al., 2000, 2007b; Kallo et al., 2001; Liposits et al., 1995). The presence of the ER isoforms predicted the E2-dependence of the gene expression profile. The IPA program (www.ingenuity.com) identified almost 70 active signal transduction pathways (STP) in control cells. Next, we have built up the neurotransmitter-, neuropeptide- and hormone receptor profile of E2-starved cells. We found that "naive" GT1–7 cells expressed several types of dopamine, serotonin, γ-aminobutyric acid (GABA), glutamate, acetylcholine, histamine and adrenergic receptors (Table 2). Among the neuropeptide receptors, somatostatin, galanin, neurotensin, neuromedin, neuropeptide Y (NPY), corticotropin-releasing hormone (CRH), and opioid receptors were expressed (Table 2) at detectable levels. The presence of various hormone and transmitter receptors, many of which have not been observed in GT1–7 cells previously (Table 2), suggests the capability of these cells to respond to a wide scale of bioactive-specific ligands.

dc_27_10

Table 2
Expression of hormone, neurotransmitter and neuropeptide receptor subunits by GT1–7 cells not treated with E2. Microarray analysis of control, non-treated cells strengthened the expression of several types of hormone receptor mRNAs, neuropeptide and neurotransmitter receptor subunit mRNAs. Some of them were previously characterized in GnRH neurons or GT1–7 cells, but numerous mRNAs were found to be expressed for the first time in GT1–7 cells.

Receptors	Subtypes
Progesterone receptor	1
Androgen receptor	1
Estrogen receptor	ERα, β
Luteinizing hormone receptor	1
Glucocorticoid receptor	1
Growth hormone receptor	1
Angiotensin II receptor	1
Prolactin receptor	1
Arginin-vasopressin receptor	1
Parathyroid hormone receptor	1
Thyroid hormone receptor	α1, β2
LHRH receptor	1
GHRH receptor	1
CRH receptor	1, 2
TSH receptor	1
FSH receptor	1
Leptin	1, B
Vasoactive intestinal peptide	VPAC1, VIP2
PACAP	1
Bradykinin	β1, β2
Melanocortin	MC2R, 3R, 5R
Dopamin receptor	D2A, 3, 4
Serotonin (5-HT) receptor	1A, B, C, D, E; 2B; 4L, E; 5A, B
$GABA_A$ receptor	α1, 2, 3, 6; β2, 3; γ1, 2, 3; δ1; ς1, 2
$GABA_B$ receptor	1
Ionotropic glutamate receptor	NR1, NR2A-D AMPA1-4, KA1-5
Metabotrop glutamate receptor	mGluR8
Nicotinic acetylcholine receptor	α6, 7; β2; δ1, ε
Musc. acetylcholine receptor	1,4
Adrenergic receptor	α1a, 1b, 2a, 2b; β1, 2, 3
ATP receptor	P2X4, P2X7, P2U
Glicin receptor	1
Opioid	B3, δ1, κ1, ε1, μ
Galanin	1, 2, 3
Cholecystokinin	A, B
Neurotensin	1
Neuromedin B	1
Neuropeptid Y	Y1, Y2, Y5, Y6
Neurotropin 3	1
Somatostatin	SstR1, 2, 3, 4, 5, 7
Histamin receptor	H1, H2

3.2. Identification of estrogen-regulated genes by cDNA microarray

In these experiments, we compared the expression profile of GT1–7 cells cultured in SR2-containing media either in presence or absence of E2. The ratio of differentially expressed genes in GT1–7 cells (control vs. E2-treated) was determined using the ArrayAssist program (described in Section 2). Different types of analyses were performed to demonstrate gene regulatory patterns within GT1–7 cells. First, scatterplots (Fig. 1) were generated using the ArrayAssist program to illustrate the up- or down-regulated genes at each time point. E2-treatment of GT1–7 cells increased the expression level of the majority of responding genes at each time point examined; the number of down-regulated genes was low.

After filtering the data using the criteria for significant change $p \leq 0.05$ and a $\log_2$ change of equal or more than 1.5, we found that even a short period of E2-treatment (0.5–2 h) induced robust changes in the cellular mRNA pool and activated a high number of genes (Fig. 2). There was an additional elevation in the number of regulated genes at 2 and 24 h following E2-treatment, whereas the application of the hormone for 48 h did not increase further the number of genes with altered expression.

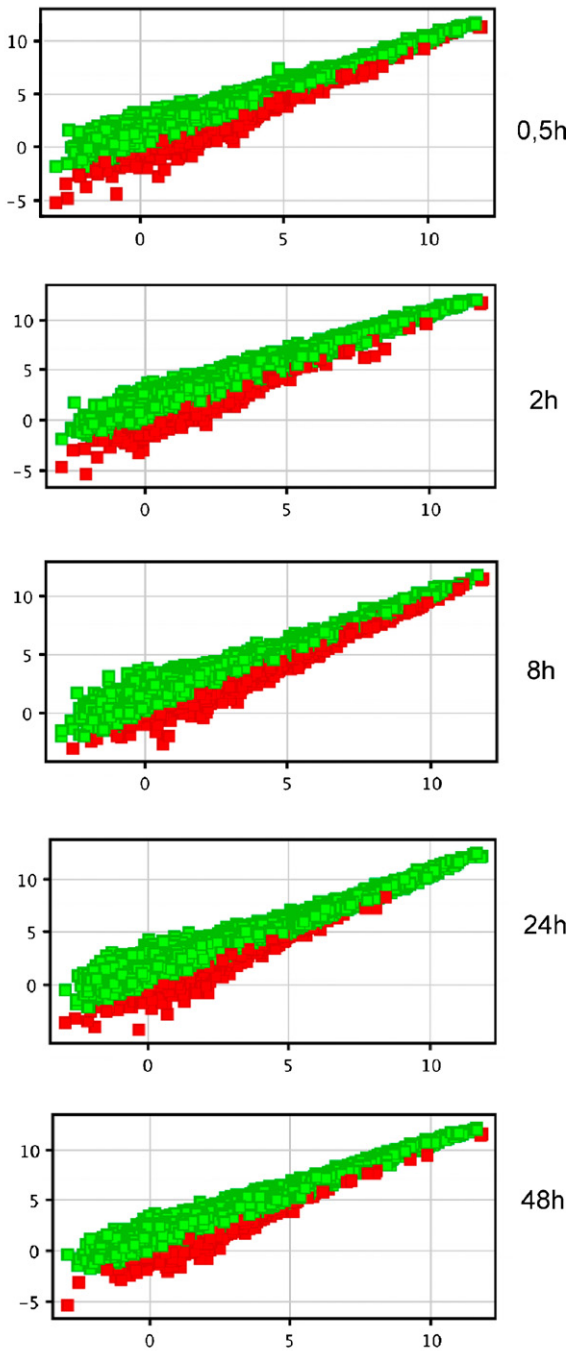

Fig. 1. Scatterplot analysis of estrogen-regulated genes at 0.5, 2, 8, 24 and 48 h of E2 exposure. Scatterplots were produced for each time-point using the average $\log_2$-value for each of the genes at the time of interest, plotted against the control signal for the gene on the *x*-axis. Up-regulated genes are present as green dots while down-regulated genes are red ones. (For interpretation of the references to color in this figure legend, the reader is referred to the web version of the article.)

3.3. Functional categories of differentially expressed genes

At each time point examined, we applied the Gene Ontology (GO) function of the ArrayAssist program to characterize the functional categories of genes affected by E2-treatment. Of the 1200 genes regulated by E2 approximately 90% encoded proteins with a known or an inferred function. For the regulated genes with well-characterized roles, the major functional categories and the number of genes regulated are shown in Table 3. This pattern suggested an initial phase of prominent regulation, which was

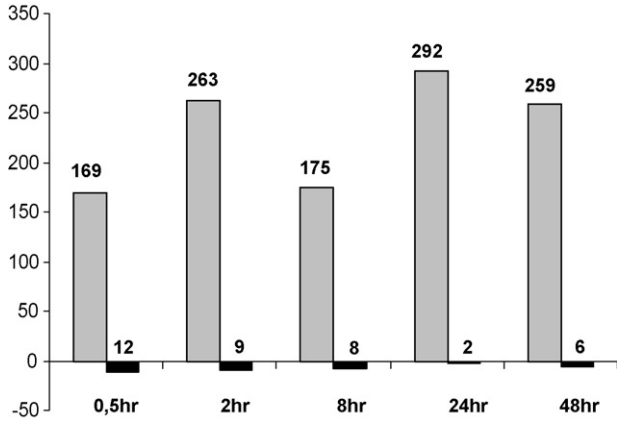

Fig. 2. The number of genes with significant fold changes (+/−1.5) is shown at the indicated time points of estrogen-application. The majority of the genes were up-regulated or induced by E2 (gray columns), whereas only a few genes were detected to be suppressed (black columns) by 10 nM E2 at early and later phases of drug treatment.

slightly reduced at 8 h and a second phase of activity after 24 h, which persisted till the end of the second day of E2-treatment. The analysis of the gene-expression patterns during E2-treatment demonstrated the existence of three types of gene regulatory patterns: (1) early regulated genes (primary responsive genes) showed an induction or inhibition at 0.5–2 h. These genes were mostly transcription factors (Mds1, Tbx3, Rnf20, Rel, Erf) and transporters (Gria1, Gabrb1, Gjb2, Syt4, Sybl1, Aqp1). (2) Genes regulated only at later time points (24–48 h) such as Gja10, Cox6c, Cox6b2, Kcnd2, Cldn6, Col1a1, Fgfr3, Kitl, and Pclo likely represented secondary response genes. (3) Finally, there were genes regulated both at early and late time points (mixed type of regulation). In this third group, we identified genes that were regulated throughout the examined period (Neurog1, Myh11, LOC623195, c-Fos, c-Myc, OTP, Kcna5, Scl12a4, Igfbp4, Myh11), while the expression of others (Hoxb4, Pdx1, Ckmt2, Kifc2, Lama1, Centd3, Fgf2, Ereg, Adm) showed an early phase of regulation at 0.5–2 h, returned to the initial expression level and finally, showed a markedly altered expression again at 24–48 h after treatment. Interestingly, a few of these genes (Esr1, GalR3, c-Myc, Actb) could be stimulated as well as repressed depending upon the time of E2 application.

3.4. Estrogen-regulated genes encoding transcription factors

Numerous transcription factors were markedly regulated by E2 (Table 4). Many of them showed a similar time course of regulation but the fold change of these genes still varied a lot. Well-known transcription factors, including *c-Fos* or *c-Myc*, were found to be highly regulated. Real-time PCR validation of microarray results confirmed that the levels of *c-Fos* and *c-Myc* transcripts were highly affected by E2-treatment (Fig. 3A). The *Jun*-family members *c-Jun* and *JunB* also showed regulation by E2.

We found that various members of the *Fox*-family transcription factors were stimulated by E2 (Table 4), but they exhibited a diversity of regulatory time courses and magnitudes. *Foxa3* and *Foxn1* showed a late response to E2 at 48 h and the latter had a greater magnitude of change. *Foxb1* and *Foxc2* showed an early up-regulation, with *Foxc2* showing a more pronounced change. Finally, *Foxq1* mRNA levels were elevated both in the early and late phases of E2-treatment.

Besides the *Fox*-family, members of the *Hox*-family of transcription factors also responded to E2-treatment with altered gene expression. Among these, only *Hoxb4* was elevated at the initial phases while other *Hox* genes changed their expression

Table 3
Estrogenic modulation of molecular functions, cellular components, biological and physiological processes at 0, 0.5, 2, 8, 24 and 48 h of E2 treatment in GT1–7 cells. Values represent the number of genes regulated at each time point in all categories. Numerical data was obtained with the Gene Ontology Analysis Tool built in the ArrayAssist program.

	0 h	0.5 h	2 h	8 h	24 h	48 h
Molecular function						
Motor activity	47	3	2	2	4	5
Catalytic activity	2224	53	68	54	75	86
Signal transduction	675	39	65	37	75	56
Structural molecule	283	11	13	5	16	14
Transporter activity	562	17	21	20	26	30
Binding	4111	108	156	101	184	162
Antioxidant	34	1	1	0	1	0
Chaperone	5	1	0	1	0	0
Enzyme regulator	260	8	12	6	13	15
Transcription regulation	552	12	27	16	26	28
Translation regulation	93	1	0	0	1	0
Cellular component						
Extracellular Region	569	54	79	47	78	68
Nucleus	1923	18	42	25	43	45
Cytoplasm	2183	42	51	31	55	53
Cytoskeleton	414	14	14	7	24	18
Mitochondrium	144	5	7	8	8	11
Endoplasmatic reticulum	3	8	11	5	8	11
Cytoplasmic vesicle	8	5	3	5	6	8
Presynaptic membrane	536	0	0	0	0	0
Postsynaptic membrane	401	2	0	2	2	2
Biological process						
Reproduction	119	5	2	1	5	4
Aging	17	1	2	0	1	0
Cellular differentiation	340	14	20	10	29	30
Regulation of gene expression	36	1	1	0	2	1
Response to stimulus	695	33	55	38	58	48
Physiological process						
Metabolism	3361	70	119	72	109	120
Death	357	9	18	6	15	13
Homeostatic	125	7	10	7	9	7
Rhythmic process	33	1	1	1	2	1
Membrane fusion	18	0	2	2	1	2
Cell communication	1125	56	77	48	85	77
Cell differentiation	340	14	20	10	29	30

dominantly after 24–48 h of E2-treatment. *Hoxd10* mRNA was exceptional in that it was down-regulated in the presence of E2 for 48 h. *Hoxa11* mRNA showed the highest magnitude of change being up-regulated more than 300-fold after 8 h of treatment. A novel homeobox-containing gene, Orthopedia (*Otp*), was also up-regulated by E2 in GT1–7 cells, mainly in the 0.5 and 24 h treatment groups. qRT-PCR technique, also applied to analyze the expression pattern of *Otp* during E2-treatment, confirmed the strong estrogenic regulation of *Otp* expression (Fig. 3B).

A third group of transcription factors with changing expression was the POU-domain-containing family. Four members were found to be up-regulated (*Pou3f3*, *Pou3f4*, *Pou5f1* and *Pou6f1*) showing elevation in the transcript levels after 2–48 h of E2-application.

Finally, the T-box family members should be mentioned (*Tbx2*, *Tbx3*, *Tbx6*, *Tbr1*, *Tbr2*) which were regulated mainly at early stages of E2-application.

3.5. Estrogen-regulated genes encoding receptors, transporters and ion channels

A significant number of receptors (Table 5), ion channels (Table 6) and transporters (Table 6) were also regulated by E2 in GT1–7 cells. We observed the up-regulation of *Gabrb1* 30 min after E2-application, followed by the elevated expression of the *Gabrg1* subunit, whereas prolonged application of E2 enhanced the level of

Table 4
Regulation of the expression level of several transcription factor mRNAs by E2 at the indicated time points in GT1–7 cells. Besides the c-Fos, c-Jun and JunB mRNAs, the Fox-family, the Hox-family, the POU-domain and T-box containing groups were reacted with an altered expression level to estrogen application. Gray shading indicates changes in gene expression that were validated with qRT-PCR.

Gene	Gene symbol	Public ID	0,5 hr	2 hr	8 hr	24 hr	48 hr
aryl hydrocarbon receptor nuclear translocator	Arnt	NM 009709	-	3.13	4.60	-	4.00
FBJ osteosarcoma oncogene	c-Fos	NM 010234	3.90	-	1.80	2.40	2.50
Jun-B oncogene	JunB	NM 008416	1.75	2.20	5.47	2.55	3.23
Jun oncogene	c-Jun	NM 010591	3.40	2.80	3.00	-	-
myelocytomatosis oncogene	c-Myc	NM 010849	4.80	5.10	-1.80	3.30	-
Early growth response 1	Egr1	NM007913	-	11.30	16.57	-	-
Ets2 repressor factor	Erf	NM 010155	2.25	-	-	-	-
estrogen receptor 1 (alpha)	Esr1	NM 007956	3.52	-2.01	-	-	-
forkhead box A3	Foxa3	NM 008260	-	-	-	-	2.77
forkhead box B1	Foxb1	NM 22378	-	2.27	-	-	-
forkhead box C2	Foxc2	NM013519	-	4.30	-	-	-
forkhead box N1	Foxn1	NM 008238	-	-	-	-	4.62
forkhead box Q1	Foxq1	NM 008239	-	3.18	-	3.05	3.70
homeo box A1	Hoxa1	NM 010449	-	-	-	4.18	-
homeo box A11	Hoxa11	NM 010450	-	4.23	8.72	5.64	-
homeo box B13	Hoxb13	NM 008267	-	-	-	3.67	-
homeo box B4	Hoxb4	NM 010459	3.71	-	-	-	4.36
homeo box D1	Hoxd1	NM 010467	-	-	-	-	3.46
homeo box D10	Hoxd10	NM 013554	-	-	-	-	-2.58
homeo box D8	Hoxd8	NM 008276	-	-	-	4.15	-
neurogenin 1	Neurog1	NM 010896	4.09	2.75	4.71	4.89	-
Ortopedia homolog	OTP	NM 011021	2.94	5.00	1.75	3.66	3.36
POU domain, class 3, transcription factor 3	Pou3f3	NM 008900	-	-	4.73	-	-
POU domain, class 3, transcription factor 4	Pou3f4	NM 009801	-	1.88	-	-	-
POU domain, class 5, transcription factor 1	Pou5f1	NM 013633	-	-	4.36	3.83	-
POU domain, class 6, transcription factor 1	Pou6f1	NM 010127	-	-	2.45	-	-
T-box brain gene 1	Tbr1	NM 009322	-	4.74	4.84	-	-
T-box 2	Tbx2	NM 009324	-	3.91	-	-	-
T-box 3	Tbx3	NM 011535	3.36	-	-	-	-
T-box 6	Tbx6	NM 011538	3.31	-	-	-	4.34
eomesodermin homolog (Xenopus laevis), T-box brain ger	Eomes/Tbr2	NM111136	-	-	-	5.89	3.58

the *Gabra6* subunit mRNA. *Gabrr1*, a $GABA_C$ receptor subunit was also up-regulated in E2-treated cultures (Table 5).

Among the glutamate receptor subunits, the AMPA receptor subunit *Gria1* showed a robust up-regulation shortly after E2-application (Table 5). *Gria2* mRNA started to rise after 24 h stimulation with E2, when *Gria1* subunit levels started to decline.

Regarding the adrenergic receptors, we found that the *Adra1a* subunit mRNA was elevated robustly after 8 h E2-treatment, whereas the *Adra1b* subunit was decreased at the same time-point of E2-application (Table 5). A third subunit, *Adrb2* was also up-regulated in response to a prolonged application of E2. The E2-regulated expression of *Adrb2* was confirmed by real-time qRT-PCR (Fig. 3D). We observed both in microarray and qPCR experiments the initial up-regulation of *Adbr2* expression at 0.5 h, although the change appeared more robust using the previous approach.

Several other neurotransmitter and neuropeptide receptors, such as *Adora2a*, *Drd4*, *Ntsr2*, *Oprd1*, *Tacr2*, *Vipr1* and *GalR3* were also regulated by E2 (Table 5). The E2-regulated expression of *GalR3* receptor mRNA (Fig. 3D) was examined and confirmed by qRT-PCR. The E2-regulated expression of the complement component C5 receptor (*C5aR*) and the function in hypothalamic neurons and GT1–7 cells were recently published (Farkas et al., 2008).

We have to mention the prostaglandin E receptor 3 and 4 (*Ptger3* and *Ptger4*) which also showed a highly regulated expression (Table 5). *Ptger3* was up-regulated at 2 and 24 h, whereas *Ptger4* was expressed at higher levels when *Ptger3* was low at 8 and 48 h. The prostaglandin F receptor (*Ptgfr*) was up-regulated both at earlier and later phases of E2-action.

Microarray analysis revealed the regulated expression of four gap junction membrane channel subunit mRNAs, with distinct patterns (Table 6). Among the *Gja*-family members, *Gja3* was up-regulated in cultures treated for 8 and 48 h, whereas *Gja9*- and *Gja10* levels were elevated in cultures treated for 24 h. In addition, *Gjb2* mRNA levels were decreased at the very beginning of E2-application.

Changes in the levels of voltage-gated potassium channel subunits were also evoked by E2. *Kcna5* (Kv1.5) and the *Kcnd2* (Kv4.2) mRNAs showed inverse regulatory patterns. *Kcna5* mRNA was elevated 0.5 h after E2 administration and declined to basal level at 24 h. qRT-PCR analysis demonstrated that the level of the *Kcnd2* subunit was increased slightly at the early time points and robustly after 24 h of treatment, when *Kcna5* subunit mRNA became undetectable. The expression pattern of the *Kcnh2* subunit was also analyzed by qRT-PCR and showed elevated levels at 2 and 24 h of E2-treatment (Fig. 3A). The presence of the *Kcnd2* subunit on GT1–7 cells and the appearance of A-type currents were further analyzed by patch-clamp electrophysiology (Farkas et al., 2007).

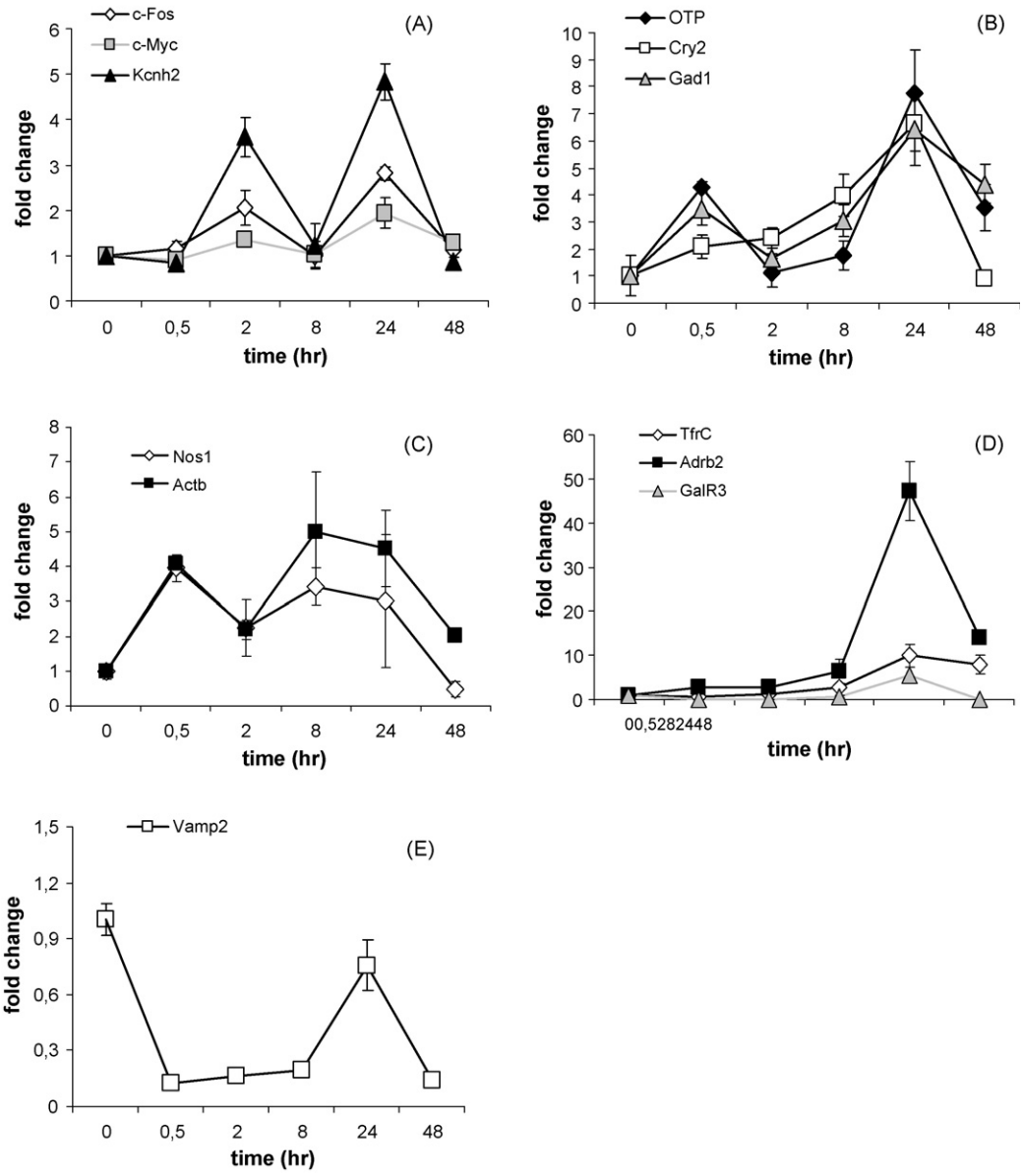

Fig. 3. (A–E) Effects of E2 treatment on mRNA expression in GT1–7 cells. Cultures were treated with 10 nm E2 for 0, 0.5, 2, 8, 24 and 48 h and the mRNA levels were measured by quantitative RT-PCR. The expression was normalized to HPRT mRNA and expressed as a percentage of baseline (0 h group).

The synaptotagmin and synaptobrevin genes encode for synaptic vesicle membrane component proteins. Synaptotagmin II (*Syt2*), *Syt4*, *Syt10* and synaptobrevin like 1 (*Sybl1*) transcripts were up-regulated both at early and later stages of E2-application. The two synaptobrevin transcripts, *Vamp2* and *Vamp4* mRNAs were also found to be regulated. The expression of Vamp2 transcript was also confirmed by qPCR (Fig. 3E).

3.6. Estrogen-regulated genes involved in signaling pathways and in cellular responses

A significant number of receptors and cytoplasmic molecules involved in the detection and transduction of incoming stimuli were found to be regulated by E2 in GT1–7 cells. First, the chemokine receptors (*Ccrl1l*, *Ccr2*) as well as the chemokine ligands (*Cxcl2*, *Cxcl9* and *Cxcl13*) were robustly up-regulated, mainly during the first hours of E2-application. The interleukin signaling was also altered by E2. Receptor mRNA levels were elevated during the first hours, followed by increases in the mRNAs encoding for the IL-family members at later time points (Table 5). Further, several immunoglobulin and Fc receptor transcripts were found regulated in the microarray data, showing the regulation of IgGs at the initial time-points, and the elevation of the Fc receptors (Fcer1g, Fcer2a) after 48 h of E2-treatment. We identified E2-induced changes in the expression levels of several participants of the MAPK-cascade (*Map2k3*, *Map3k12* and *Mapk13*), G-protein signaling (*Rgs2*, *Rgs9*, *Rgs10*, *Gpr4*, *Gpr133*, *Gnat2*, *Gngt2*, *Rab31*, *Ralgds*, *Rasgrf1*), IP_3-signaling (*Prkcb1*, *Prkcm*, *Prkcz*, *Pla2g7*, *Plaa*) and Tnf-signaling (*Tnfrsf8*, *Tnfsf11*, *Traf1*) pathways, suggesting an intracellular adaptation mechanism at the level of signal transducer molecules.

Stimulating the cells with E2 caused an elevated production of genes encoding for hormones and growth factors (*Adm*, *Angpt2*, *Apbb2*, *Apcs*, *Apoe*, *Csf2*, *Ctgf*, *Edn1*, *Ereg*, *Fgf2*, *Ifna4*, *Ifna11*, *Ifnb1*, *Plau*, *Penk1*, *PrlpA*, *Nrg3*, *Thbd*) and receptors for these secreted molecules (*Egfr*, *Fgfr3*, *Ppyr1*, *Trfr2*). The altered expression of *TfrC* was also investigated and confirmed by the qRT-PCR method (Fig. 3D).

dc_27_10

Table 5

Estrogen-dependent regulation of the expression of mRNAs coding for various receptor subunits and intracellular signal transducer proteins. E2 treatment of GT1–7 cells for 0.5, 2, 8, 24 and 48 h affected the expression of several subunits of the adrenergic, GABAergic and glutamatergic receptors and also influenced interleukin, insulin, prostaglandin and G-protein signaling. Gray shading indicates changes in gene expression that were validated with qRT-PCR.

Gene	Gene symbol	Public ID	0,5 hr	2 hr	8 hr	24 hr	48 hr
adenosine A2a receptor	Adora2a	NM 009630	-	-	-	-	2.91
adrenergic receptor, alpha 1a	Adra1a	NM 013461	-	-	5.46	-	-
adrenergic receptor, alpha 1b	Adra1b	NM 007416	-		-5.06	-	-
adrenergic receptor, beta 2	Adrb2	NM 007420	2.39	-	2.32	3.59	1.25
bradykinin receptor, beta 2	Bdkrb2	NM 009747	-	-	4.62	5.35	-
complement component 5a receptor 1	C5ar	NM 007577	-	-	-	4.30	-
chemokine (C-C motif) receptor 1-like 1	Ccr1l1	NM 007718	-	-	6.81	-	-
chemokine (C-C motif) receptor 2	Ccr2	NM 009915	5.76	4.63	-	-	-
chemokine (C-X-C motif) ligand 13	Cxcl13	NM 018866	4.55	-	3.39	-	-
chemokine (C-X-C motif) ligand 2	Cxcl2	NM 009140	4.05	-	-	-	-
Cryptochrome-2	Cry2	NM 009963	-	-	-	1.50	1.56
dopamine receptor 4	Drd4	NM 007878	-	-	-	-	1.97
epidermal growth factor receptor	Egfr	NM 207655	-	-	3.70	3.47	-
fibroblast growth factor 2	Fgf2	NM 008006	-	3.31	-	5.16	4.37
fibroblast growth factor receptor 3	Fgfr3	NM 008010	-	-	-	-	-3.02
GABA-A receptor, subunit alpha 6	Gabra6	NM 008068	-	-	-	3.04	-
GABA-A receptor, subunit beta 1	Gabrb1	NM 008069	2.34	-	-	-	-
GABA-A receptor, subunit gamma 1	Gabrg1	NM 010252	-	-	3.37	-	6.77
GABA-C receptor, subunit rho 1	Gabrr1	NM 008075	-	-	2.70	-	-
glutamic acid decarboxylase 1	Gad1	NM 008077	-	3.52	-	-	-
galanin receptor 3	GalR3	NM 015738	-	-2.30	-	2.00	-1.01
glutamate receptor, ionotropic, AMPA1 (alpha 1)	Gria1	NM 008165	4.60	-	-	-	-
glutamate receptor, ionotropic, AMPA2 (alpha 2)	Gria2	NM 013540	-	-	-	6.58	4.99
insulin-like growth factor binding protein 1	Igfbp1	NM 008341	2.94	4.63	10.68	-	-
insulin-like growth factor binding protein 3	Igfbp3	NM 008343	-	-	-	-	2.62
insulin-like growth factor binding protein 4	Igfbp4	NM 010517	2.52	2.69	4.68	4.11	2.93
interleukin 13 receptor, alpha 2	Il13ra2	NM 008356	-	-	-	5.80	4.82
interleukin 1 receptor accessory protein	Il1rap	NM 134103	-	8.79	-	-	-
interleukin 1 receptor-like 1	Il1rl1	NM 010743	4.91	2.59	-	-	-
interleukin 6 receptor, alpha	Il6ra	NM 010559	-	5.33	-	-	-
interleukin 9 receptor	Il9r	NM 008374	-	1.68	2.12	-	-
mitogen activated protein kinase kinase 3	Map2k3	NM 008928	-	3.75	-	5.96	6.72
mitogen activated protein kinase kinase kinase 12	Map3k12	NM 009582	8.25	-	-	-	-
mitogen activated protein kinase 13	Mapk13	NM 011950	-	6.87	7.69	-	-
MAP/microtubule affinity-regulating kinase 1	Mark1	NM 014551	-	-	4.25	-	-
nitric oxide synthase 1, neuronal	Nos1	NM 008712	1.50	-2.57	-	1.52	-
neuregulin 3	Nrg3	NM 008734	-	-	-	-	2.95
neurotensin receptor 2	Ntsr2	NM 008747	-	-	-	-	4.77
opioid receptor, delta 1	Oprd1	NM 013622	-	-	-	2.58	-
opioid receptor-like 1	Oprl1	NM 011012	2.98	-	-	-	-
phosphodiesterase 6A	Pde6a	NM 146086	-	-	-	4.45	-
phosphodiesterase 6B	Pde6b	NM 008806	-	-	7.34	4.27	-
preproenkephalin 1	Penk1	NM 001002	-	-	-	-	3.58
phospholipase A2, activating protein	Plaa	NM 172695	-	-	-	2.48	-
protein kinase C, beta 1	Prkcb1	NM 008855	-	-	4.68	4.79	-
protein kinase C, mu	Prkcm	NM 008858	-	2.86	-	-	-
protein kinase C, zeta	Prkcz	NM 008860	-	4.23	-	-	-
prostaglandin E receptor 3 (subtype EP3)	Ptger3	NM 011196	-	6.51	-	9.85	-
prostaglandin E receptor 4 (subtype EP4)	Ptger4	NM 008965	-	-	1.72	-	1.76
prostaglandin F receptor	Ptgfr	NM 008966	3.89	3.59	-	-	3.93
RAB31, member RAS oncogene family	Rab31	NM 133685	-	-	-	-	1.90
ral guanine nucleotide dissociation stimulator	Ralgds	NM 009058	3.30	5.12	-	-	-
RAS-specific guanine nucleotide-releasing factor 1	Rasgrf1	NM 011245	12.43	-	-	6.62	11.05
Regulator of G-protein signalling 10	Rgs10	NM 026418	-	-	-	-	4.88
regulator of G-protein signaling 2	Rgs2	NM 009061	-	2.21	-	-	4.63
regulator of G-protein signaling 9	Rgs9	NM 011268	-2.12	-	-	-	-
ras homolog gene family, member J	Rhoj	NM 023275	11.88	6.64	7.56	-	9.40
tachykinin receptor 2	Tacr2	NM 009314	1.78	-	-	-	-
transforming growth factor, beta 3	Tgfb3	NM 009368	-	6.64	-	-	-
tumor necrosis factor receptor superfamily, member 8	Tnfrsf8	NM 009401	-	-	-	-	2.13
Tnf receptor-associated factor 1	Traf1	NM 009421	-	2.99	3.40	-	-
transferrin receptor C	TfrC	NM 015799	-	-	2.39	3.12	4.83
vasoactive intestinal peptide receptor 1	Vipr1	NM 011703	3.15	4.47	4.96	3.99	-

Table 6
Time schedule of the estrogen-regulated expression of mRNAs encoding transporters, ion channels, synaptic proteins and gap junction molecules. Gray shading indicates changes in gene expression that were validated with qRT-PCR.

Gene	Gene symbo	Public ID	0,5 hr	2 hr	8 hr	24 hr	48 hr
aquaporin 1	Aqp1	NM 007472	-	3.61	-	-	-
aquaporin 4	Aqp4	NM 009700	-	-	-	12.11	-
gap junction membrane channel protein alpha 10	Gja10	NM 010289	-	-	-	3.36	-
gap junction membrane channel protein alpha 3	Gja3	NM 016975	-	-	3.76	-	5.51
gap junction membrane channel protein alpha 9	Gja9	NM 0102902	-	5.72	-1.79	-	3.63
gap junction membrane channel protein beta 2	Gjb2	NM 008125	-3.57	-	-	-	-
potassium voltage-gated channel, shaker-related subfamily, member 5	Kcna5	NM 145983	6.64	3.64	2.50	-	4.28
potassium voltage-gated channel, Shal-related family, member 2	Kcnd2	NM 019697	-	-	-	12.72	-
potassium voltage-gated channel, subfamily H (eag-related), member 2	Kcnh2	NM 013569	-	-	-	2.40	-
neurotensin receptor 2	Ntsr2	NM 008747	-	-	-	-	4.77
ryanodine receptor 2, cardiac	Ryr2	NM 023868	-	-	6.53	-	6.21
sodium channel, voltage-gated, type III, alpha	Scn3a	NM 018732	-	-	-	-	3.64
solute carrier family 10 (sodium/bile acid cotransporter family), member 1	Slc10a1	NM 011387	-	-	-	3.58	-
solute carrier family 16 (monocarboxylic acid transporters), member 7	Slc16a7	NM 011391	-	3.05	3.58	4.03	-
K-Cl cotransporter KCC1	Slc12a4	NM 009195	2.06	2.15	1.66	-	-
solute carrier family 22 (organic cation transporter), member 1	Slc22a1	NM 009202	-	-	3.29	-	-
solute carrier family 22 (organic anion transporter), member 6	Slc22a6	NM 008766	-	-	-	5.04	3.36
solute carrier family 23 (nucleobase transporters), member 1	Slc23a1	NM 011397	-	3.71	-	-	-
solute carrier family 29 (nucleoside transporters), member 2	Slc29a2	NM 007854	-	-	-	4.77	-
solute carrier family 2 (facilitated glucose transporter), member 4	Slc2a4	NM 009204	-	-	-	4.11	-
solute carrier family 5 (sodium/glucose cotransporter), member 11	Slc5a11	NM 146198	-	-	-	1.70	-
Solute carrier family 6 (neurotransmitter transporter, creatine), member 8	Slc6a8	NM 133987	1.67	2.04	-	-	-
synaptobrevin like 1	Sybl1	NM 011515	-	3.71	-	-	-
synaptotagmin X	Syt10	NM 018803	-	4.01	6.51	-	4.75
synaptotagmin II	Syt2	NM 009307	2.00	-	4.17	-	4.24
synaptotagmin IV	Syt4	NM 009308	-	3.21	-	-	-
vesicle-associated membrane protein 2	Vamp2	NM 009497	-1.60	-	-2.80	2.50	-2.20

Nitrogen-monoxide (NO), one of the key retrograde signaling molecules is produced partly by the neuronal NO-synthase (*Nos1*) enzyme in the nervous system. Microarray and real-time PCR analysis revealed an early up-regulation of the transcript after 0.5 h of hormone treatment (Fig. 3C) which was followed by a decline later. At the end of the first day of treatment, the level of the enzyme became elevated again. The expression of NOS enzyme by GT1–7 cells and the role of NO in regulating pulsatile LHRH-release were investigated by Lopez and co-workers (Lopez et al., 1997).

Glutamic acid decarboxylases (*Gad1* and *Gad2*) which are the key enzymes in GABA-synthesis, were found to be regulated by E2. Both microarray and real-time PCR detected elevated levels of the mRNA coding for the GAD1 enzyme at the initial stages of hormone treatment, whereas qRT-PCR detected a second phase of induction after 24 h of E2 application (Fig. 3B). *Gad2* mRNA level was elevated only 48 h after E2 application.

Cryptochrome 2 (*Cry2*) mRNA involved in circadian oscillations was also found to be regulated by E2. Both microarray and real-time PCR revealed a marked change in the transcript level after 24–48 h of E2-treatment (Fig. 3B).

3.7. Estrogen-regulated genes encoding cell adhesion molecules and extracellular matrix components

Among the cell adhesion molecules (CAM), cadherins were up-regulated shortly after E2-application. Robust changes were revealed in the expression levels of several transcripts (*Pcdh7*, *Pcdha9*, *Cdh4* and *Cdh15*, *Ctnna2*). Among the integrin-family CAMs, two members were induced by E2. Integrin alpha L (*Itgal*) showed elevated expression throughout the whole treatment period, except at 8 h when integrin alpha E (*Itgae*) mRNA was dominant. The neural CAM (*Ncam1*) was also up-regulated both at the early and late stages of the examined period of E2-treatment. We found elevation in the levels of specific desmocollins and desmogleins (*Dsc2*, *Dsc3*, *Dsg2*) in GT1–7 cells.

E2 also up-regulated the mRNA levels of specific extracellular matrix components (*Col1a1*, *Col4a4*, *Lama1*, *Astn1*, *Eln*, *Matn2*, *Tnc*, *Sntb1*, *Siglec1*). Elevated levels of matrix metallopeptidases (Mmps) were detected in a temporal sequence of *Mmp16*, *Mmp3* and *Mmp7*, finally the *Mmp9*. Besides the Mmps, E2 also elevated the level of the disintegrin and matrix metallopeptidase family members (*Adam12*, *Adam17* and *Adamts1*).

3.8. E2 regulates the expression of genes involved in cytoskeletal remodeling

Numerous genes coding for cytoskeletal proteins were detected by the microarray approach. They included the kinesin motor proteins *Kif9* and *Kifc2*, several keratins and associated proteins (*Krt2*, *4*, *5*, *17*, *19*, *25*, *34*, *81*, *84*, *Krtap3-3*, *5-5*), microtubule-associated proteins (*Mark1*, *Mtap1b*), myosins (*Myo1b*, *1e*, *Myh11*, *Myl2*, *Mybpc3*), and tectins (*Tekt1*, *Tekt2*). Interestingly, most of the genes that were regulated early also had a later phase of induction, and several genes reacted as a secondary response gene being induced only after 1–2 days of drug-treatment. beta-Actin (*Actb*), one of the key components of the actin-cytoskeleton, showed a two-phase induction (Fig. 3C) with an initial peak at 0.5 h and a second peak at 24 h of treatment.

3.9. Ingenuity pathway analysis

Post hoc analysis of the datasets revealed that specific interactive effects exist between genes at different time-points of E2-treatment. At the 0.5 h time point only few relationships could be determined among the regulated transcripts (Fig. 4A), although more than 180 genes (Fig. 1) were found to be regulated

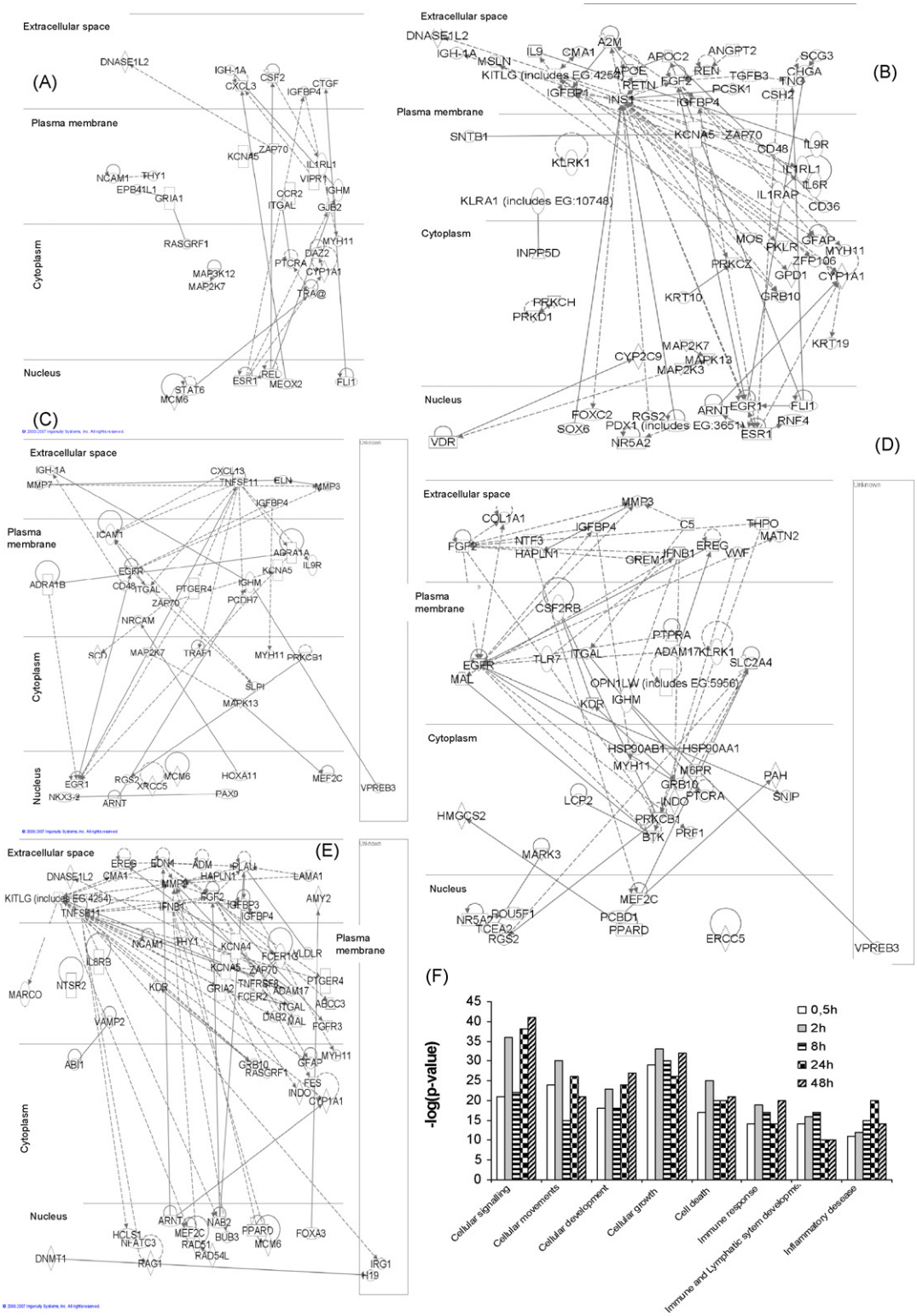

Fig. 4. Ingenuity pathway analysis of estrogen-regulated genes in GT1–7 cells at 0.5, 2, 8, 24 and 48 h (A–E). (F) Significantly regulated cellular functions and disease pathways at different time points of estrogen treatment. Bar charts represent the negative *p*-value of significance associated with the different functions and diseases at each time investigated.

by E2. Only a few canonical pathways could be identified, including axon guidance, Wnt/b-catenin, SAPK/JNK, IGF and calcium signaling. Elevating the time of E2 exposure to 2 h not only increased the number of regulated transcripts but also increased the number of associations among the gene-products and the number of genes involved in the network (Fig. 4B). Interestingly, besides the ER-signaling, insulin, interleukin, integrin, axon guidance, actin cytoskeleton, NF-κB, Arnt, neuregulin, acute phase response signaling, and PPARα/RXRα activation were also affected by E2, showing a preferential regulation of signaling pathways involving secreted molecules at the extracellular space. After 8 h of treatment with E2, we found a decrease in the number of genes

regulated, and in a good accordance with this, fewer transcripts were involved in generating the network (Fig. 4C). Besides the previously detected actin cytoskeleton, axon guidance, NF-κB, integrin signaling; the oxidative stress response, apoptosis, G-protein coupled receptor signaling, and SAPK/JNK signaling were detected to be changed. After E2 application for 1 day, we found an elevation in the number of regulated genes with a highly organized networking of the transcripts (Fig. 4D). The networks involved molecules not only from the extracellular space and plasma membrane but also included cytoplasmic and nuclear participants. The highly regulated canonical pathways were as follows: axonal guidance, NRF2-mediated oxidative stress response, integrin signaling, actin cytoskeleton, acute phase response, NF-κB, neuregulin, calcium signaling, NO signaling, and LPS/IL-1 mediated inhibition of RXR function. Network, built applying the previously described rules demonstrated that extracellular- and plasma membrane-localized gene products are over-represented at this stage of induction, affecting the activation of receptors and transcription factors localized in nuclei (Fig. 4E). The highly regulated canonical pathways are listed in Table 3.

We used IPA to generate and rank functional networks of genes responding to E2 exposure in GT1–7 cell cultures. In the 0.5 h treatment group, the predominant functions associated with the top-ranked networks were 1/Cellular growth and proliferation, 2/Cellular movement, 3/Cell signaling, 4/Tissue morphology, 5/Cellular development, 6/Cell death, 7/Hematological system development and function, 8/Immune response, 9/Immune and lymphatic system development and function and 10/Hematological disease. After 2 h of E2-treatment the first-ranked network was Cell signaling followed by the Cellular growth and proliferation and Cell movement networks. New participants were also detected in the top-ranked category, like cancer and inflammatory disease. After 8 h of E2 application to GT1–7 cells, a marked change in the list of highly-affected networks was revealed. The changes in Cellular growth and proliferation and Cell signaling were followed by changes in the Cell death network. Cell movements became less affected with time. Interestingly, the Immune response, Immune and lymphatic system development and function and also the inflammatory disease networks were substantially perturbed at this time. A 24 h continuous presence of E2 caused extensive changes in the categories of 1/Cell signaling, 2/Cellular growth and proliferation and also in 3/Cellular movements and 4/Cellular development. The Cell death, Immune Response and Inflammatory disease categories were also highly regulated. Prolonged (48 h) application of E2 to LHRH-secreting neuronal cells regulated the previously mentioned networks. However, new participants like the cell-to-cell signaling and interaction and organism survival was also involved in the top 10 networks. Finally, the highly-regulated cellular functions and diseases were ranked by the *p*-value associated with the function. Functions with high *p*-values across all time points are shown in Fig. 4F.

4. Discussion

In this study, we have identified the E2-regulated genes and molecular pathways of immortalized LHRH-producing hypothalamic neurons, the GT1–7 cells. This information may give us an insight to the E2-dependent changes that also characterize the gene expression profile of LHRH neurons *in vivo* across the estrus cycle. Beyond these reproductive aspects, the results also provide a critically important reference database of E2-dependent neuronal genes.

We have used global gene expression profiling by microarray analysis to identify patterns and networks of genes that are either stimulated or inhibited by E2. In representative cases, this was also followed by the quantitative RT-PCR verification of the altered gene expression patterns. We have identified that many E2-regulated genes were associated with specific cellular pathways including cellular signaling, cellular movement, cellular growth and development, immune response, and inflammatory disease.

4.1. Regulation of GT1–7 cells by E2

Of more than 12,000 mRNAs recognized by the array, we identified about 1200 transcripts which showed regulation by E2. At each time point, approximately 90% of the regulated transcripts represented mRNAs with either known or inferred functions, whereas the remaining 10% coded yet unidentified proteins. The known genes were involved in a variety of cellular functions and a group of them was previously reported to be regulated by E2 in the nervous system. These findings are confirmed and supported by our present results. The E2-dependent regulation of a second gene set was reported earlier in tissues different from the brain. Finally, we identified a large number of genes previously not shown to be regulated by E2 at all. Some of these genes may depend on E2 in a variety of cell types whereas others may be E2-dependent in neuronal cells or specifically in LHRH neurons.

4.2. Time-course of regulation: primary vs. secondary responses

The time-course studies we have performed, spanning a wide interval between 0 and 48 h, revealed a diversity of temporal responses to E2. Our first time-point of E2-treatment was at 0.5 h which was short enough to exclude secondary genomic responses. We assume that in such cases the effect of E2 was a rapid primary transcriptional response. Although, we should keep in mind that the actions of E2 may also modulate the half-lives of transcripts. Indeed, substantial evidence indicates that E2 is capable of modulating mRNA levels via affecting mRNA stability through non-genomic mechanisms of action (Ing, 2005). To obtain a secondary response in gene expression, the mRNAs of primary responses have to be translated and the resulting proteins have to initiate a series of secondary transcriptional events. While a 2 h continuous exposure of E2 initiates many primary responses in gene expression, the contribution of secondary responses to the altered gene expression patterns is very likely.

The analysis of functional categories of genes revealed the occurrence of cooperated gene sections at the different time points. The parallel regulation of genes fulfilling diverse functions suggests the involvement of common transcription factors as primary response genes and the divergence of E2 actions.

4.3. Estrogen regulation of transcription factor families

The activity of LHRH neurons could be assessed indirectly by examining the expression pattern of *c-Fos* and *c-Jun* transcription factors. Although not expressed by LHRH neurons under all circumstances of increased LHRH secretion, the presence of *c-Fos* protein within LHRH neurons is often indicative of neuronal activation (Herbison, 1998). Studies in the rat (Hoffman et al., 1993), mouse (Wu et al., 1992), and sheep (Moenter et al., 1993) have shown that many of the LHRH cells express *c-Fos* at the time of the LH surge. E2-application to GT1–7 cells also induced *c-Fos* and *c-Myc* transcription factors and several genes showed similar patterns of expression in response to E2. ERα and *c-Myc* physically interact to stabilize the ERα-coactivator complex, thereby permitting other signal transduction pathways to fine-tune E2-dependent signaling networks (Cheng et al., 2006). The *Jun* family members of transcription factors (*c-Jun*, *Jun-B*) are involved in heterodimer formation with *c-Fos* (Halazonetis et al., 1988) and also partner formation with ERs (Teyssier et al., 2001). *JunB*, which is a member of the AP-1 transcription family, acts as a negative

regulator of transcription through AP-1 binding sites forming heterodimers with *c-Jun* (Teyssier et al., 2001).

Homeobox (*Hox*) genes encode a family of transcription factors which regulate embryonic patterning and organogenesis and a large number of *Hox* genes were found to be regulated by E2 in GT1–7 cells. The functional consequences of these changes are presently unknown. The homeobox-containing gene Orthopedia (*Otp*) is expressed in neurons giving rise to the paraventricular (PVN), supraoptic (SON), anterior periventricular (AVPV), and arcuate nuclei (NA) throughout their development and terminal differentiation (Acampora et al., 2000). The changes in the level of *Otp* mRNA upon E2-treatment suggest a role for this gene in mature neuroendocrine cells. The *in vivo* expression of *Otp* in LHRH neurons and its significance requires further experimental confirmation.

In mammals, the expression profiles of class I, class III, and class IV POU domain transcription factors have roles in the development, maintenance, and function of the neuroendocrine systems (Andersen and Rosenfeld, 2001). Studies on the promoter region of the LHRH gene demonstrated two DNA-binding sites for the POU class of transcription factors (Chandran and DeFranco, 1999), each of which specifically interact with the POU homeodomain proteins *Brn-2* (*Pou3f2*) and *Oct-1* (*Pou2f1*). Functional studies demonstrated that *Brn-2* increased the promoter activity of the human and mouse LHRH genes (Wolfe et al., 2002). In our study, *Brn-4* (*Pou3f4*) transcript, whose expression so far has been seen restricted to the SON and PVN of the hypothalamus (Mathis et al., 1992), was found to be up-regulated by E2. The transcriptional regulator *Brn-5* (*Pou6f1*) which is involved in specifying the mature phenotype of CNS neurons (Cui and Bulleit, 1998)—was also found regulated by E2 in GT1–7 cells. The E2-dependent regulation of POU-domain transcription factors which are required for the proper functioning of neuroendocrine cells may be involved in controlling LHRH secretion in GT1–7 cells.

A large number of Forkhead box (*Fox*) transcription factors were also regulated by E2 in the microarray data set. These data are of particular importance in the light of a functional interplay between the forkhead and the POU-domain transcription (*Foxa3/Pou2f2*) factors on a variety of neuronal gene promoters (Raynal et al., 1998).

T-box transcription factor family (*Tbx2*, *3* and *6*; *Tbr1*, *Eomes/Tbr2*) proteins which also showed altered gene expression in response to E2 play central roles in embryonic development and may also control functions like neural plasticity in differentiated neurons (Miyahara et al., 2004). The *Tbx2/Tbx3* transcriptional factors play important roles in synaptic plasticity and in adaptation of olfactory neurons (Miyahara et al., 2004). *Tbr1*, *NeuroD* and *Eomes/Tbr2* mRNAs are involved in the development of the glutamatergic neuronal phenotype (Hevner et al., 2006). While the precise functional significance of this transcription factor expression is unknown, its common appearance in embryonic and adult neurogenesis and in different brain regions suggests that it is part of a conserved genetic program that specifies general properties of glutamatergic neurons (Hevner et al., 2006). The expression and sequential up-regulation of *Eomes/Tbr2* and *Tbr1* transcription factors by E2 in GT1–7 cells suggests a glutamatergic cell fate (Whitlock, 2005; Hrabovszky et al., 2007a) enhanced by E2 in LHRH neurons.

4.4. E2-dependent regulation of receptors, ion channels, and transporters

LHRH pulsatility can be modulated by exogenous signals such as adrenergic (Herbison, 1997), glutamatergic (van den Pol et al., 1990), and GABAergic inputs (Leranth et al., 1985). Analyzing the receptor profile of control GT1–7 cells clearly established the existence of several subunits of the ionotropic $GABA_A$ receptors, one $GABA_C$ subunit, ionotropic (NMDA-, AMPA- and kainite-type receptor subunits), metabotropic (mGluR8) glutamate receptors, and the adrenergic receptor subunits.

We found an elevation in the level of the ionotropic AMPA receptor subunit *Gria2* mRNA, that could shift the ion selectivity of AMPA receptors towards Ca-ions if mRNA editing occurs (Longone et al., 1998). Besides *Gria2*, the *Gria1* subunit was also found to be elevated after E2-application. The increased levels of AMPA receptor subunits in E2-treated GT1–7 cells might result in enhanced Ca^{2+}-permeability suggesting a regulatory role for these receptors in LHRH neurosecretion (Lopez et al., 1992; Brann and Mahesh, 1994; Spergel et al., 1994).

LHRH neurons in the hypothalamus are surrounded by GABAergic interneurons and GABAergic terminals from other brain regions also reach this area and innervate LHRH neurons (Boehm et al., 2005; Leranth et al., 1985). GABA, acting through $GABA_A$ receptors, was hypothesized to suppress reproduction by inhibiting LHRH secretion (Herbison et al., 1991). Several GABA receptor subunits were detected in E2-untreated GT1–7 cells underlying the importance of GABA signals in LHRH neuronal activity.

During development, GABA was shown to inhibit the rate of LHRH neuronal migration out of the olfactory pit, control the association of LHRH neurons to fibers of guidance, and regulate LHRH fiber extension toward the median eminence (ME; Tobet et al., 2001). GAD1 and GAD2 proteins are responsible for the production of GABA. A subset of LHRH neurons was shown to express GAD proteins during migration from the olfactory placode to the hypothalamus (Heger et al., 2003). The expression and E2-induced up-regulation of *Gad* mRNAs in GT1–7 cells suggests that these cells actively produce GABA but the significance of the finding is not clear.

Noradrenergic mechanisms are also involved in the generation of the LHRH/LH surge (Herbison, 1997), and noradrenaline is a permissive factor in surge generation. Miller and co-workers found direct interactions between DBH-immunoreactive neuronal elements and LHRH dendrites at both light and electron microscopic levels, although the number of synaptic specializations was low (Miller and Zhu, 1995). The expression of adrenergic receptor subunits by GT1–7 cells implies a direct route for noradrenergic/adrenergic actions, although there is also evidence to suggest the involvement of interneurons in the POA/BnST in the mediation of adrenergic effects (Clarke et al., 2006). In GT1–7 cells, E2 induced the up-regulation of the *Adra1a* and *Adrb2* subunits together with the down-regulation of the *Adra1b* subunit. The altered expression of adrenergic receptor subunits by E2 in GT1–7 cells implies different roles for these receptor subunits in LHRH neurons during different stages of the estrus cycle.

Potassium channels play a major role in regulating the secretory and electric oscillatory patterns in cells (Misonou and Trimmer, 2004). Changes in the subunit composition of voltage-gated potassium channels could modulate the voltage-dependency of the channels, the bursting behavior, firing rate, and the interspike intervals, thus playing an important role in regulating rhythmic oscillations in neurons (Li et al., 2006; Jerng et al., 2004). Our results demonstrated that three of the voltage-gated potassium channel subunits were sensitive to E2 showing different expression patterns during E2-application. An inverse relationship was observed in the regulation of the *kcna5* (*Kv1.5*) and the *kcnd2* (*Kv4.2*) subunits. The elevation in the mRNA level of *Kv4.2* subunit of A-type channels and the appearance of A-type potassium currents (Farkas et al., 2007) suggest a role for A-type potassium currents in the negative feedback action of estrogen 24 h after E2-treatment. Expression of a *Kv1.5* subunit – participating in the K-type current – declines at the time of *Kv4.2* up-regulation,

indicating a shift from K- to A-type currents. Down-regulation of the expression of *Kv1.5* subunit by antisense construct in rat superior cervical ganglion neurons increased the excitability of cells by decreasing threshold of the action potential (Malin and Nerbonne, 2001). This converted the firing properties of the neurons from phasic to adapting (Malin and Nerbonne, 2001). The third potassium channel subunit, *kcnh2* (*erg1*) showed induction by E2. The expression of this subunit mRNA was detected in hypothalamic neuronal cells (Papa et al., 2003) characterized by oscillations in their firing behavior suggesting a role for this subunit also in conversion of regular firing to adapting firing (Chiesa et al., 1997).

Galanin and its receptors are widely distributed within the central and peripheral nervous system, especially in the hypothalamus, including the POA, PVN, SON, and ME. Galanin plays an important role in the control of food intake, energy balance, reproduction, water balance, and various neuroendocrine functions. Galanin acts in the brain through galanin receptors (*Galr1*, *2* and *3*). Galanin has been shown to enhance LHRH secretion, but it is not known whether this effect is exerted on the LHRH neuron or is indirect although close juxtapositions between galanin-immunoreactive nerve terminals and LHRH-immunoreactive perikarya and dendrites as they have been reported in the human hypothalamus (Dudas and Merchenthaler, 2004). *Galr1* was shown to be expressed by hypothalamic LHRH neurons (Mitchell et al., 1999; Dufourny and Skinner, 2005) and *Galr2* expression was also detected in several hypothalamic regions with galanin binding affinity (Mitchell et al., 1999) but its expression in LHRH neurons was not detected (Chambers et al., 2007). In a previous study, neither *Galr1* nor *Galr2* could be detected in GT1–7 cells by RT-PCR (Seth et al., 2004), in contrast to the results of our microarray study which revealed the expression of both receptors. The recent cloning of *Galr3* opened a new window in galanin signaling and *in situ* hybridization studies strengthened the presence of this receptor subtype in the hypothalamus (Mennicken et al., 2002). The finding that GT1–7 cells express this new type of galanin receptor suggests that galanin peptide could modulate the function of LHRH cells by each of the three galanin receptor isoforms. *Galr3* mRNA shows a biphasic regulation by E2 in GT1–7 cells, being down-regulated during the early stages of E2-action followed by a marked up-regulation at 24 h. The regulation of *Galr3* by E2 suggests that this receptor might play pivotal roles in galanin signaling during the estrus cycle in rodents.

4.5. E2-regulation of cellular movements, vesicle maturation, trafficking and secretion

Cytoskeletal activity plays an essential role in the maintenance of cellular shape, intracellular transport of membrane vesicles, growth cone formation, filopodial movements, process formation and elongation, axon guidance, and synapse formation. All these events require increased cytoskeletal activity and increased levels of certain cytoskeletal components. In E2-treated GT1–7 cells we found elevated levels of the cytoskeletal tektins and pericentrin (kendrin) that play important roles in the biogenesis of primary cilia (Miyoshi et al., 2004), neuronal filopodium movements (Norrander et al., 1998), and in intraflagellar transport (Miyoshi et al., 2004). The kinesin family member *Kifc2* is present in axons and dendrites of neurons and plays a role in retrograde axonal transport (Yang et al., 2001). The robust and rapid up-regulation of *Kifc2* mRNA we observed in GT1–7 cells suggests an increased retrograde transport along the axonal process. E2-dependent elevation in the level of stathmin (*Stmn1*), a microtubule-associated cytoplasmic protein, plays a permissive role in LHRH cell motility (Mungenast and Ojeda, 2005; Manna et al., 2006, 2007).

Synaptotagmins (Syt) are membrane proteins of secretory vesicles, abundant in neural and some endocrine cells, and they act together to control neurotransmitter release. *Syt4*, activated after 2 h E2 application in GT1–7 cells is involved in reducing neurotransmitter release (Ting et al., 2006). *Syt2*, which was up-regulated by E2 in GT1–7 cells, plays a role in the Ca^{2+} triggering of action potential-induced release and in the restriction of spontaneous release. This is consistent with a general role of synaptotagmins in controlling 'release slots' for synaptic vesicles at the active zone (Pang et al., 2006). The E2-dependent expression of Vamp2 and Vamp4 mRNA suggest that the maturation of secretory granules in LHRH neurons is under the control of E2.

4.6. E2-dependent expression of cell adhesion molecules and extracellular matrix components

Cadherins and protocadherins (PCDHs) are involved in Ca^{2+}-dependent homophilic cell-cell adhesion (adherent junction) and have been suggested to play role in the formation and maintenance of the synaptic connections (Takeichi and Abe, 2005). Previous studies on GT1–7 cell line showed that these cells contain at least one PCDHalpha (CNR-8/PCDHalpha10) mRNA (Mungenast and Ojeda, 2005). Our microarray study demonstrated the expression of numerous cadherin and protocadherin transcripts in GT1–7 cells and the E2-dependent transcription of several family members indicates the active involvement of these proteins in the regulation of LHRH neuronal connections. Alpha N-catenin (*Ctnna2*), a linker between cadherins and the actin cytoskeleton, was shown to be essential for stabilizing dendritic spines in rodent hippocampal neurons in culture (Abe et al., 2004). The E2-dependent up-regulation of *Ctnna2* in GT1–7 cells might function to stabilize the newly formed filopodia and synaptic connections. Novel data demonstrate that canonical tight junction and adherent junction proteins can be recruited to a single junction in which claudins partition into subdomains and form a novel hybrid tight junction with adherens junction organization (Nunes et al., 2006). The expression and up-regulation of claudin mRNAs in GT1–7 cells upon estrogen application could also play important, yet unidentified roles in the regulation of LHRH cellular connections.

Desmosomes are punctate structures comprised of Desmoglein-2 (*Dsg2*) and Desmocollin-2/3 (*Dsc2/3*) that affiliate with the underlying intermediate filaments via linker proteins (catenins) to provide mechanical strength. The sequential up-regulation of desmosomal cadherins by E2 suggests roles for these proteins in modifying cellular connections. Besides this, Dsg2 regulates apoptosis during physiological differentiation and inflammation (Nava et al., 2007). Plakophilin 3 (*Pkp3*) – a unique multiprotein that binds all three *dsg* and *dsc* – was also found to be elevated during the E2-treatment.

An alternative mechanism of interneuronal communication is provided by gap junctions, which allow a rapid, bidirectional exchange of signals. The main protein participants in forming these electric connections are the connexin family members shown to be expressed both by LHRH neurons in the brain (Hosny and Jennes, 1998) and by GT1–7 cells in culture (Hu et al., 1999). In addition, functional gap junction communication among adjacent GT1–7 cells was detected, but only under conditions where pulsatile synchronization was also observed (Hu et al., 1999; Vazquez-Martinez et al., 2001). The estrogenic control of different connexins detected in GT1–7 cells suggests changes in the gap junctional communication between LHRH cells being potentially involved in the pulsatile LHRH release.

Extracellular matrix components secreted by the cells play a key role in cellular movements and also in axon guidance and synapse formation in the nervous system (Gonthier et al., 2007). Changing the composition of the extracellular matrix (ECM)

involves the degradation of matrix proteins by extracellular peptidases (*Mmps*, *Adams*) and the synthesis and secretion of new types of extracellular proteins. The sequential up-regulation of distinct *Mmp* and *Adam* enzymes by E2 in GT1–7 cells might trigger an increased extracellular degrading activity which could be followed by the reformation of the extracellular milieu of the cells. In a good accordance with this, secreted ECM components (*Col4a4*, *Lama1*, *Matr2*, *Fbr2*) were also found to be elevated after E2-application to provide newly synthesized proteins for ECM reorganization.

4.7. Regulation of genes involved in signaling pathways by estrogen

A significant number of receptors involved in the detection of incoming stimuli and also signaling molecules – known to regulate LHRH neurons *in vivo* – were found to be regulated by E2 in GT1–7 cells, both at the early and later stages of E2-treatment. Besides the previously mentioned categories, numerous other signal transduction pathways were activated by E2. E2 treatment affected the MapK-cascade, G-protein and IP3-signalling, suggesting that second messenger systems coupled to transmembrane receptors could also modulate signal-transduction.

In the brain, E2 ameliorates brain performance and has positive effects on selected neural pathologies characterized by a strong inflammatory component (Pozzi et al., 2006). Clinical and experimental studies have established E2 as a neuroprotective hormone in many neurological diseases with inflammatory components, including stroke, Alzheimer's disease, Parkinson's disease, multiple sclerosis, or amyotrophic lateral sclerosis (Sohrabji, 2005). An important role has been suggested for pro-inflammatory cytokines produced by activated glial cells, neurons and immune cells that invade brain tissue (Pozzi et al., 2006; Sohrabji, 2005). Our recent findings that E2 modulates the expression of numerous genes (chemokine receptors and C-X-C ligands, prostaglandin E2 receptors, NO-synthase, TNF-signaling components, interleukin signaling, complement components and receptors, etc.) that are involved in inflammatory pathways and in immune response within the brain further strengthen the idea of hormonal anti-inflammatory treatment strategies for neurodegenerative diseases (Pozzi et al., 2006; Vegeto et al., 2003; Harkonen and Vaananen, 2006). The role of E2 in the regulation of the complement component C5a receptor in neurosecretory cells of the hypothalamus has been recently proposed (Farkas et al., 2008).

The observation that GT1–7 cells *in vitro* exhibit a similar pulsatile secretory pattern to that produced by LHRH neurons *in vivo* (Wetsel et al., 1992) indicates that pulsatility is an intrinsic feature of LHRH neurons. GT1–7 cells express a series of circadian clock genes (Gillespie et al., 2003; Chappell et al., 2003) and both the mRNA and protein products of several clock genes (Per2, Per2, Cry1, Cry2, Bmal1) oscillate in cultured GT1–7 cells with 20–24 h periodicity (Gillespie et al., 2003; Chappell et al., 2003). Results from Chappell and colleagues suggested that the cycling of *Per* and *Cry* mRNA and protein levels in LHRH neurons are required to maintain the pulsatility of LHRH release. Overexpression of Cry1 in GT1–7 cells significantly increased LHRH pulse amplitude without an appreciable difference in mean pulse frequency. In the present study we found that estrogen-treatment significantly up-regulated Cry2 mRNA levels in GT1–7 cells at all time-points investigated. It requires clarification if Cry2 mRNA expression has any effect on LHRH pulse amplitude or pulse frequency on LHRH-secretion. Data from GT1–7 cells indicate that besides estrogen, intracellular cAMP-levels are also involved in the regulation of the endogenous circadian clock machinery, possibly through the opening of cyclic nucleotide gated channels (CNGs) expressed by GnRH neurons, *in vitro* (Blackman et al., 2007).

In summary, the results of our study explored specific gene networks, metabolic and regulatory pathways through which E2 influences the cellular functions of immortalized LHRH cells. Many of the *in vitro* findings fit well previously published regulatory mechanisms obtained from *in vivo* studies. The novel observations are supposed to initiate and give background for further *in vivo* studies elucidating the estrogen-dependent function of the key hypothalamic regulator of reproduction, the LHRH system.

Acknowledgements

This work was supported by the Sixth EU Research Framework Program (contract LSHM-CT-2003-503041), by the NKFP 1A-002-2004 and OTKA K73002 and K69127. The authors highly appreciate the valuable advices of Dr. Balázs Gereben and Dr. William C. Wetsel and the excellent technical assistance of Hajnalka Beko.

References

Abe, K., Chisaka, O., Van Roy, F., Takeichi, M., 2004. Stability of dendritic spines and synaptic contacts is controlled by alpha N-catenin. Nat. Neurosci. 7, 357–363.
Abraham, I.M., Han, S.K., Todman, M.G., Korach, K.S., Herbison, A.E., 2003. Estrogen receptor beta mediates rapid estrogen actions on gonadotropin-releasing hormone neurons in vivo. J. Neurosci. 23, 5771–5777.
Acampora, D., Postiglione, M.P., Avantaggiato, V., Di Bonito, M., Simeone, A., 2000. The role of Otx and Otp genes in brain development. Int. J. Dev. Biol. 44, 669–677.
Andersen, B., Rosenfeld, M.G., 2001. POU domain factors in the neuroendocrine system: lessons from developmental biology provide insights into human disease. Endocr. Rev. 22, 2–35.
Blackman, B.E., Yoshida, H., Paruthiyil, S., Weiner, R.I., 2007. Frequency of intrinsic pulsatile gonadotropin-releasing hormone secretion is regulated by the expression of cyclic nucleotide-gated channels in GT1 cells. Endocrinology 148, 3299–3306.
Boehm, U., Zou, Z., Buck, L.B., 2005. Feedback loops link odor and pheromone signaling with reproduction. Cell 123, 683–695.
Brann, D.W., Mahesh, V.B., 1994. Excitatory amino acids: function and significance in reproduction and neuroendocrine regulation. Front. Neuroendocrinol. 15, 3–49.
Burgos-Briceno, L.A., Smith, C.G., Coy, D.H., Schally, A.V., Asch, R.H., 1983. Dose response inhibition of the circhoral pulsatile secretion of LH and FSH in rhesus monkeys by the administration of a potent inhibitory analogue of LH-RH ([*N*-Ac-D-Trp1, 3, D-*p*-Cl-Phe2, D-Phe6, D-Ala10]-LH-RH). Acta Eur. Fertil. 14, 255–260.
Butler, J.A., Sjoberg, M., Coen, C.W., 1999. Evidence for oestrogen receptor alpha-immunoreactivity in gonadotrophin-releasing hormone-expressing neurones. J. Neuroendocrinol. 11, 331–335.
Chambers, G., Whitelaw, C.M., Robinson, J.E., Evans, N.P., 2007. Distribution of galanin receptor-2 immunoreactive neurones in the ovine hypothalamus: no evidence for involvement in the control of gonadotrophin-releasing hormone secretion. J. Neuroendocrinol. 19, 966–973.
Chandran, U.R., DeFranco, D.B., 1999. Regulation of gonadotropin-releasing hormone gene transcription. Behav. Brain Res. 105, 29–36.
Chappell, P.E., White, R.S., Mellon, P.L., 2003. Circadian gene expression regulates pulsatile gonadotropin-releasing hormone (GnRH) secretory patterns in the hypothalamic GnRH-secreting GT1-7 cell line. J. Neurosci. 23, 11202–11213.
Cheng, A.S., Jin, V.X., Fan, M., Smith, L.T., Liyanarachchi, S., Yan, P.S., Leu, Y.W., Chan, M.W., Plass, C., Nephew, K.P., Davuluri, R.V., Huang, T.H., 2006. Combinatorial analysis of transcription factor partners reveals recruitment of c-MYC to estrogen receptor-alpha responsive promoters. Mol. Cell 21, 393–404.
Chiesa, N., Rosati, B., Arcangeli, A., Olivotto, M., Wanke, E., 1997. A novel role for HERG K^+ channels: spike-frequency adaptation. J. Physiol. 501 (Pt 2), 313–318.
Clarke, I.J., Scott, C.J., Pereira, A., Pompolo, S., 2006. The role of noradrenaline in the generation of the preovulatory LH surge in the ewe. Domest. Anim. Endocrinol. 30, 260–275.
Cui, H., Bulleit, R.F., 1998. Expression of the POU transcription factor Brn-5 is an early event in the terminal differentiation of CNS neurons. J. Neurosci. Res. 52, 625–632.
DeFazio, R.A., Moenter, S.M., 2002. Estradiol feedback alters potassium currents and firing properties of gonadotropin-releasing hormone neurons. Mol. Endocrinol. (Baltimore, MD) 16, 2255–2265.
Dudas, B., Merchenthaler, I., 2004. Bi-directional associations between galanin and luteinizing hormone-releasing hormone neuronal systems in the human diencephalon. Neuroscience 127, 695–707.
Dufourny, L., Skinner, D.C., 2005. Distribution of galanin receptor 1-immunoreactive neurons in the ovine hypothalamus: colocalization with GnRH. Brain Res. 1054, 73–81.
Farkas, I., Varju, P., Liposits, Z., 2007. Estrogen modulates potassium currents and expression of the Kv4.2 subunit in GT1–7 cells. Neurochem. Int. 50, 619–627.

Farkas, I., Varju, P., Szabo, E., Hrabovszky, E., Okada, N., Okada, H., Liposits, Z., 2008. Estrogen enhances expression of the complement C5a receptor and the C5a-agonist evoked calcium influx in hormone secreting neurons of the hypothalamus. Neurochem. Int. 52, 846–856.

Gillespie, J.M., Chan, B.P., Roy, D., Cai, F., Belsham, D.D., 2003. Expression of circadian rhythm genes in gonadotropin-releasing hormone-secreting GT1-7 neurons. Endocrinology 144, 5285–5292.

Gonthier, B., Nasarre, C., Roth, L., Perraut, M., Thomasset, N., Roussel, G., Aunis, D., Bagnard, D., 2007. Functional interaction between matrix metalloproteinase-3 and semaphorin-3C during cortical axonal growth and guidance. Cereb. Cortex (New York, NY) 17, 1712–1721.

Green, S., Kumar, V., Krust, A., Walter, P., Chambon, P., 1986. Structural and functional domains of the estrogen receptor. Cold Spring Harb. Symp. Quant. Biol. 51 (Pt 2), 751–758.

Halazonetis, T.D., Georgopoulos, K., Greenberg, M.E., Leder, P., 1988. c-Jun dimerizes with itself and with c-Fos, forming complexes of different DNA binding affinities. Cell 55, 917–924.

Harkonen, P.L., Vaananen, H.K., 2006. Monocyte-macrophage system as a target for estrogen and selective estrogen receptor modulators. Ann. NY Acad. Sci. 1089, 218–227.

Heger, S., Seney, M., Bless, E., Schwarting, G.A., Bilger, M., Mungenast, A., Ojeda, S.R., Tobet, S.A., 2003. Overexpression of glutamic acid decarboxylase-67 (GAD-67) in gonadotropin-releasing hormone neurons disrupts migratory fate and female reproductive function in mice. Endocrinology 144, 2566–2579.

Herbison, A.E., 1997. Noradrenergic regulation of cyclic GnRH secretion. Rev. Reprod. 2, 1–6.

Herbison, A.E., 1998. Multimodal influence of estrogen upon gonadotropin-releasing hormone neurons. Endocr. Rev. 19, 302–330.

Herbison, A.E., 2007. Estrogen positive feedback to gonadotropin-releasing hormone (GnRH) neurons in the rodent: the case for the rostral periventricular area of the third ventricle (RP3V). Brain Res. Rev. 57, 277–287.

Herbison, A.E., Chapman, C., Dyer, R.G., 1991. Role of medial preoptic GABA neurones in regulating luteinising hormone secretion in the ovariectomised rat. Exp. Brain Res. Exp. Hirnforsch. 87, 345–352.

Herbison, A.E., Pape, J.R., Simonian, S.X., Skynner, M.J., Sim, J.A., 2001. Molecular and cellular properties of GnRH neurons revealed through transgenics in the mouse. Mol. Cell. Endocrinol. 185, 185–194.

Herbison, A.E., Porteous, R., Pape, J.R., Mora, J.M., Hurst, P.R., 2008. Gonadotropin-releasing hormon neuron requirements for puberty, ovulation, and fertility. Endocrinology 149, 597–604.

Herbison, A.E., Theodosis, D.T., 1992. Localization of oestrogen receptors in preoptic neurons containing neurotensin but not tyrosine hydroxylase, cholecystokinin or luteinizing hormone-releasing hormone in the male and female rat. Neuroscience 50, 283–298.

Hevner, R.F., Hodge, R.D., Daza, R.A., Englund, C., 2006. Transcription factors in glutamatergic neurogenesis: conserved programs in neocortex, cerebellum, and adult hippocampus. Neurosci. Res. 55, 223–233.

Hoffman, G.E., Smith, M.S., Verbalis, J.G., 1993. c-Fos and related immediate early gene products as markers of activity in neuroendocrine systems. Front. Neuroendocrinol. 14, 173–213.

Hosny, S., Jennes, L., 1998. Identification of gap junctional connexin-32 mRNA and protein in gonadotropin-releasing hormone neurons of the female rat. Neuroendocrinology 67, 101–108.

Hrabovszky, E., Deli, L., Turi, G.F., Kallo, I., Liposits, Z., 2007a. Glutamatergic innervation of the hypothalamic median eminence and posterior pituitary of the rat. Neuroscience 144, 1383–1392.

Hrabovszky, E., Kallo, I., Szlavik, N., Keller, E., Merchenthaler, I., Liposits, Z., 2007b. Gonadotropin-releasing hormone neurons express estrogen receptor-beta. J. Clin. Endocrinol. Metab. 92, 2827–2830.

Hrabovszky, E., Shughrue, P.J., Merchenthaler, I., Hajszan, T., Carpenter, C.D., Liposits, Z., Petersen, S.L., 2000. Detection of estrogen receptor-beta messenger ribonucleic acid and ^{125}I-estrogen binding sites in luteinizing hormone-releasing hormone neurons of the rat brain. Endocrinology 141, 3506–3509.

Hrabovszky, E., Steinhauser, A., Barabas, K., Shughrue, P.J., Petersen, S.L., Merchenthaler, I., Liposits, Z., 2001. Estrogen receptor-beta immunoreactivity in luteinizing hormone-releasing hormone neurons of the rat brain. Endocrinology 142, 3261–3264.

Hu, L., Olson, A.J., Weiner, R.I., Goldsmith, P.C., 1999. Connexin 26 expression and extensive gap junctional coupling in cultures of GT1–7 cells secreting gonadotropin-releasing hormone. Neuroendocrinology 70, 221–227.

Ing, N.H., 2005. Steroid hormones regulate gene expression posttranscriptionally by altering the stabilities of messenger RNAs. Biol. Reprod. 72, 1290–1296.

Jerng, H.H., Qian, Y., Pfaffinger, P.J., 2004. Modulation of Kv4.2 channel expression and gating by dipeptidyl peptidase 10 (DPP10). Biophys. J. 87, 2380–2396.

Kallo, I., Butler, J.A., Barkovics-Kallo, M., Goubillon, M.L., Coen, C.W., 2001. Oestrogen receptor beta-immunoreactivity in gonadotropin releasing hormone-expressing neurones: regulation by oestrogen. J. Neuroendocrinol. 13, 741–748.

Kuiper, G.G., Carlsson, B., Grandien, K., Enmark, E., Haggblad, J., Nilsson, S., Gustafsson, J.A., 1997. Comparison of the ligand binding specificity and transcript tissue distribution of estrogen receptors alpha and beta. Endocrinology 138, 863–870.

Langub Jr., M.C., Maley, B.E., Watson Jr., R.E., 1991. Ultrastructural evidence for luteinizing hormone-releasing hormone neuronal control of estrogen responsive neurons in the preoptic area. Endocrinology 128, 27–36.

Leranth, C., MacLusky, N.J., Sakamoto, H., Shanabrough, M., Naftolin, F., 1985. Glutamic acid decarboxylase-containing axons synapse on LHRH neurons in the rat medial preoptic area. Neuroendocrinology 40, 536–539.

Li, Y., Um, S.Y., McDonald, T.V., 2006. Voltage-gated potassium channels: regulation by accessory subunits. Neuroscientist 12, 199–210.

Liposits, Z., Merchenthaler, I., Wetsel, W.C., Reid, J.J., Mellon, P.L., Weiner, R.I., Negro-Vilar, A., 1991. Morphological characterization of immortalized hypothalamic neurons synthesizing luteinizing hormone-releasing hormone. Endocrinology 129, 1575–1583.

Liposits, Z., Reid, J.J., Negro-Vilar, A., Merchenthaler, I., 1995. Sexual dimorphism in copackaging of luteinizing hormone-releasing hormone and galanin into neurosecretory vesicles of hypophysiotrophic neurons: estrogen dependency. Endocrinology 136, 1987–1992.

Liposits, Z., Setalo, G., Flerko, B., 1984. Application of the silver-gold intensified 3,3′-diaminobenzidine chromogen to the light and electron microscopic detection of the luteinizing hormone-releasing hormone system of the rat brain. Neuroscience 13, 513–525.

Longone, P., Impagnatiello, F., Mienville, J.M., Costa, E., Guidotti, A., 1998. Changes in AMPA receptor-spliced variant expression and shift in AMPA receptor spontaneous desensitization pharmacology during cerebellar granule cell maturation in vitro. J. Mol. Neurosci. 11, 23–41.

Lopez, F.J., Donoso, A.O., Negro-Vilar, A., 1992. Endogenous excitatory amino acids and glutamate receptor subtypes involved in the control of hypothalamic luteinizing hormone-releasing hormone secretion. Endocrinology 130, 1986–1992.

Lopez, F.J., Moretto, M., Merchenthaler, I., Negro-Vilar, A., 1997. Nitric oxide is involved in the genesis of pulsatile LHRH secretion from immortalized LHRH neurons. J. Neuroendocrinol. 9, 647–654.

Malin, S.A., Nerbonne, J.M., 2001. Molecular heterogeneity of the voltage-gated fast transient outward K^+ current, I(Af), in mammalian neurons. J. Neurosci. 21, 8004–8014.

Manna, T., Grenningloh, G., Miller, H.P., Wilson, L., 2007. Stathmin family protein SCG10 differentially regulates the plus and minus end dynamics of microtubules at steady state in vitro: implications for its role in neurite outgrowth. Biochemistry 46, 3543–3552.

Manna, T., Thrower, D., Miller, H.P., Curmi, P., Wilson, L., 2006. Stathmin strongly increases the minus end catastrophe frequency and induces rapid treadmilling of bovine brain microtubules at steady state in vitro. J. Biol. Chem. 281, 2071–2078.

Mathis, J.M., Simmons, D.M., He, X., Swanson, L.W., Rosenfeld, M.G., 1992. Brain 4: a novel mammalian POU domain transcription factor exhibiting restricted brain-specific expression. EMBO J. 11, 2551–2561.

Mellon, P.L., Windle, J.J., Weiner, R.I., 1991. Immortalization of neuroendocrine cells by targeted oncogenesis. Recent Prog. Horm. Res. 47, 69–93 (discussion 93-66).

Mennicken, F., Hoffert, C., Pelletier, M., Ahmad, S., O'Donnell, D., 2002. Restricted distribution of galanin receptor 3 (GalR3) mRNA in the adult rat central nervous system. J. Chem. Neuroanat. 24, 257–268.

Merchenthaler, I., 2005. Estrogen stimulates galanin expression within luteinizing hormone-releasing hormone-immunoreactive (LHRH-i) neurons via estrogen receptor-beta (ERbeta) in the female rat brain. Neuropeptides 39, 341–343.

Merchenthaler, I., Gorcs, T., Setalo, G., Petrusz, P., Flerko, B., 1984. Gonadotropin-releasing hormone (GnRH) neurons and pathways in the rat brain. Cell Tissue Res. 237, 15–29.

Merchenthaler, I., Lennard, D.E., Lopez, F.J., Negro-Vilar, A., 1993. Neonatal imprinting predetermines the sexually dimorphic, estrogen-dependent expression of galanin in luteinizing hormone-releasing hormone neurons. Proc. Natl. Acad. Sci. U.S.A. 90, 10479–10483.

Miller, M.M., Zhu, L., 1995. Ovariectomy and age alter gonadotropin hormone releasing hormone-noradrenergic interactions. Neurobiol. Aging 16, 613–625.

Milner, T.A., Ayoola, K., Drake, C.T., Herrick, S.P., Tabori, N.E., McEwen, B.S., Warrier, S., Alves, S.E., 2005. Ultrastructural localization of estrogen receptor beta immunoreactivity in the rat hippocampal formation. J. Comp. Neurol. 491, 81–95.

Misonou, H., Trimmer, J.S., 2004. Determinants of voltage-gated potassium channel surface expression and localization in mammalian neurons. Crit. Rev. Biochem. Mol. Biol. 39, 125–145.

Mitchell, V., Bouret, S., Prevot, V., Jennes, L., Beauvillain, J.C., 1999. Evidence for expression of galanin receptor Gal-R1 mRNA in certain gonadotropin releasing hormone neurones of the rostral preoptic area. J. Neuroendocrinol. 11, 805–812.

Miyahara, K., Suzuki, N., Ishihara, T., Tsuchiya, E., Katsura, I., 2004. TBX2/TBX3 transcriptional factor homologue controls olfactory adaptation in *Caenorhabditis elegans*. J. Neurobiol. 58, 392–402.

Miyoshi, K., Asanuma, M., Miyazaki, I., Diaz-Corrales, F.J., Katayama, T., Tohyama, M., Ogawa, N., 2004. DISC1 localizes to the centrosome by binding to kendrin. Biochem. Biophys. Res. Commun. 317, 1195–1199.

Moenter, S.M., Karsch, F.J., Lehman, M.N., 1993. Fos expression during the estradiol-induced gonadotropin-releasing hormone (GnRH) surge of the ewe: induction in GnRH and other neurons. Endocrinology 133, 896–903.

Mosselman, S., Polman, J., Dijkema, R., 1996. ER beta: identification and characterization of a novel human estrogen receptor. FEBS Lett. 392, 49–53.

Mungenast, A.E., Ojeda, S.R., 2005. Expression of three gene families encoding cell–cell communication molecules in the prepubertal nonhuman primate hypothalamus. J. Neuroendocrinol. 17, 208–219.

Nava, P., Laukoetter, M.G., Hopkins, A.M., Laur, O., Gerner-Smidt, K., Green, K.J., Parkos, C.A., Nusrat, A., 2007. Desmoglein-2: a novel regulator of apoptosis in the intestinal epithelium. Mol. Biol. Cell 18, 4565–4578.

Norrander, J., Larsson, M., Stahl, S., Hoog, C., Linck, R., 1998. Expression of ciliary tektins in brain and sensory development. J. Neurosci. 18, 8912–8918.
Nunes, F.D., Lopez, L.N., Lin, H.W., Davies, C., Azevedo, R.B., Gow, A., Kachar, B., 2006. Distinct subdomain organization and molecular composition of a tight junction with adherens junction features. J. Cell Sci. 119, 4819–4827.
Paech, K., Webb, P., Kuiper, G.G., Nilsson, S., Gustafsson, J., Kushner, P.J., Scanlan, T.S., 1997. Differential ligand activation of estrogen receptors ERalpha and ERbeta at AP1 sites. Science (New York, NY) 277, 1508–1510.
Pang, Z.P., Melicoff, E., Padgett, D., Liu, Y., Teich, A.F., Dickey, B.F., Lin, W., Adachi, R., Sudhof, T.C., 2006. Synaptotagmin-2 is essential for survival and contributes to Ca^{2+} triggering of neurotransmitter release in central and neuromuscular synapses. J. Neurosci. 26, 13493–13504.
Papa, M., Boscia, F., Canitano, A., Castaldo, P., Sellitti, S., Annunziato, L., Taglialatela, M., 2003. Expression pattern of the ether-a-gogo-related (ERG) K^+ channel-encoding genes ERG1, ERG2, and ERG3 in the adult rat central nervous system. J. Comp. Neurol. 466, 119–135.
Pozzi, S., Benedusi, V., Maggi, A., Vegeto, E., 2006. Estrogen action in neuroprotection and brain inflammation. Ann. NY Acad. Sci. 1089, 302–323.
Raynal, J.F., Dugast, C., Le Van Thai, A., Weber, M.J., 1998. Winged helix hepatocyte nuclear factor 3 and POU-domain protein brn-2/*N*-oct-3 bind overlapping sites on the neuronal promoter of human aromatic L-amino acid decarboxylase gene. Brain Res. 56, 227–237.
Seth, A., Stanley, S., Jethwa, P., Gardiner, J., Ghatei, M., Bloom, S., 2004. Galanin-like peptide stimulates the release of gonadotropin-releasing hormone in vitro and may mediate the effects of leptin on the hypothalamo-pituitary-gonadal axis. Endocrinology 145, 743–750.
Shughrue, P., Scrimo, P., Lane, M., Askew, R., Merchenthaler, I., 1997. The distribution of estrogen receptor-beta mRNA in forebrain regions of the estrogen receptor-alpha knockout mouse. Endocrinology 138, 5649–5652.
Skynner, M.J., Sim, J.A., Herbison, A.E., 1999. Detection of estrogen receptor alpha and beta messenger ribonucleic acids in adult gonadotropin-releasing hormone neurons. Endocrinology 140, 5195–5201.
Sohrabji, F., 2005. Estrogen: a neuroprotective or proinflammatory hormone? Emerging evidence from reproductive aging models. Ann. NY Acad. Sci. 1052, 75–90.
Spergel, D.J., Krsmanovic, L.Z., Stojilkovic, S.S., Catt, K.J., 1994. Glutamate modulates $[Ca^{2+}]_i$ and gonadotropin-releasing hormone secretion in immortalized hypothalamic GT1–7 neurons. Neuroendocrinology 59, 309–317.
Takeichi, M., Abe, K., 2005. Synaptic contact dynamics controlled by cadherin and catenins. Trends Cell Biol. 15, 216–221.
Temple, J.L., Laing, E., Sunder, A., Wray, S., 2004. Direct action of estradiol on gonadotropin-releasing hormone-1 neuronal activity via a transcription-dependent mechanism. J. Neurosci. 24, 6326–6333.
Teyssier, C., Belguise, K., Galtier, F., Chalbos, D., 2001. Characterization of the physical interaction between estrogen receptor alpha and JUN proteins. J. Biol. Chem. 276, 36361–36369.
Ting, J.T., Kelley, B.G., Sullivan, J.M., 2006. Synaptotagmin IV does not alter excitatory fast synaptic transmission or fusion pore kinetics in mammalian CNS neurons. J. Neurosci. 26, 372–380.
Tobet, S.A., Bless, E.P., Schwarting, G.A., 2001. Developmental aspect of the gonadotropin-releasing hormone system. Mol. Cell. Endocrinol. 185, 173–184.
van den Pol, A.N., Wuarin, J.P., Dudek, F.E., 1990. Glutamate, the dominant excitatory transmitter in neuroendocrine regulation. Science (New York, NY) 250, 1276–1278.
Vazquez-Martinez, R., Shorte, S.L., Boockfor, F.R., Frawley, L.S., 2001. Synchronized exocytotic bursts from gonadotropin-releasing hormone-expressing cells: dual control by intrinsic cellular pulsatility and gap junctional communication. Endocrinology 142, 2095–2101.
Vegeto, E., Belcredito, S., Etteri, S., Ghisletti, S., Brusadelli, A., Meda, C., Krust, A., Dupont, S., Ciana, P., Chambon, P., Maggi, A., 2003. Estrogen receptor-alpha mediates the brain antiinflammatory activity of estradiol. Proc. Natl. Acad. Sci. U.S.A. 100, 9614–9619.
Wetsel, W.C., Valenca, M.M., Merchenthaler, I., Liposits, Z., Lopez, F.J., Weiner, R.I., Mellon, P.L., Negro-Vilar, A., 1992. Intrinsic pulsatile secretory activity of immortalized luteinizing hormone-releasing hormone-secreting neurons. Proc. Natl. Acad. Sci. U.S.A. 89, 4149–4153.
Whitlock, K.E., 2005. Origin and development of GnRH neurons. Trends Endocrinol. Metab. 16, 145–151.
Wintermantel, T.M., Campbell, R.E., Porteous, R., Bock, D., Grone, H.J., Todman, M.G., Korach, K.S., Greiner, E., Perez, C.A., Schutz, G., Herbison, A.E., 2006. Definition of estrogen receptor pathway critical for estrogen positive feedback to gonadotropin-releasing hormone neurons and fertility. Neuron 52, 271–280.
Wolfe, A., Kim, H.H., Tobet, S., Stafford, D.E., Radovick, S., 2002. Identification of a discrete promoter region of the human GnRH gene that is sufficient for directing neuron-specific expression: a role for POU homeodomain transcription factors. Mol. Endocrinol. 16, 435–449.
Wu, T.J., Segal, A.Z., Miller, G.M., Gibson, M.J., Silverman, A.J., 1992. FOS expression in gonadotropin-releasing hormone neurons: enhancement by steroid treatment and mating. Endocrinology 131, 2045–2050.
Yang, Z., Roberts, E.A., Goldstein, L.S., 2001. Functional analysis of mouse C-terminal kinesin motor KifC2. Mol. Cell. Biol. 21, 2463–2466.

dc_27_10

19. számú melléklet

Gene Expression Profiling Identifies Key Estradiol Targets in the Frontal Cortex of the Rat

Miklós Sárvári, Erik Hrabovszky, Imre Kalló, Orsolya Galamb, Norbert Solymosi, István Likó, Béla Molnár, Károly Tihanyi, Zsolt Szombathelyi, and Zsolt Liposits

Laboratory of Endocrine Neurobiology (M.S., E.H., I.K., Z.L.), Institute of Experimental Medicine, and Molecular Medicine Research Unit (O.G., B.M.), Hungarian Academy of Sciences, Budapest H-1083, Hungary; Gedeon Richter Plc. (M.S., I.L., K.T., Z.S.), Budapest H-1103, Hungary; Second Department of Medicine (O.G., N.S., B.M.), Semmelweis University, Budapest H-1089, Hungary; and Faculty of Information Technology (I.K., Z.L.), Pázmány Péter Catholic University, Budapest H-1088, Hungary

Estradiol modulates a wide range of neural functions in the frontal cerebral cortex where subsets of neurons express estrogen receptor-α and -β. Through these receptors, estradiol contributes to the maintenance of normal operation of the frontal cortex. During the decline of gonadal hormones, the frequency of neurological and psychiatric disorders increases. To shed light on the etiology of disorders related to declining levels of estrogens, we studied the genomic responses to estradiol. Ovariectomized rats were treated with a sc injection of estradiol. Twenty-four hours later, samples from the frontal cortices were dissected, and their mRNA content was analyzed. One hundred thirty-six estradiol-regulated transcripts were identified on Rat 230 2.0 Expression Array. Of the 136 estrogen-regulated genes, 26 and 36 genes encoded proteins involved in the regulation of transcription and signal transduction, respectively. Thirteen genes were related to the calcium signaling pathway. They comprised five genes coding for neurotransmitter receptors. Transcription of three neuropeptides, including cocaine- and amphetamine-regulated transcript, were up-regulated. Fifty-two genes were selected for validation, and 12 transcriptional changes were confirmed. These results provided evidence that estradiol evokes broad transcriptional response in the cortex. Modulation of key components of the calcium signaling pathway, dopaminergic, serotonergic, and glutamatergic neurotransmission, may explain the influence of estrogens on cognitive function and behavior. Up-regulation of cocaine- and amphetamine-regulated transcript contributes to the neuroprotective effects of estradiol. Identification of estradiol-regulated genes in the frontal cortex helps to understand the pathomechanism of neurological and psychiatric disorders associated with altered levels of estrogens. **(*Endocrinology* 151: 1161–1176, 2010)**

Besides its well-established effect on reproductive and sexual functions, 17β-estradiol (E2) exerts neuroprotective effects and improves cognitive functions and mood subserved by the frontal cortex (1). During the menopausal transition, a dramatic alteration takes place in the serum level of estrogens. As a result of the falling E2 levels, neurological and psychiatric disorders increase in frequency. The incidence of neurodegenerative disorders is higher in postmenopausal women (2). Although most clinical trials fail to show protection as a result of estrogen replacement therapy (3), the biological plausibility for a neuroprotective E2 effect is overwhelming (4), indicating that estrogens may play a role in the preservation of normal operation of the frontal cortex.

The biological actions of E2 are dependent on two estrogen receptors (ER), ERα (5) and ERβ (6), which belong to the nuclear hormone receptor superfamily. The two ER subtypes are encoded by distinct genes and differ

ISSN Print 0013-7227 ISSN Online 1945-7170
Printed in U.S.A.

doi: 10.1210/en.2009-0911 Received July 31, 2009. Accepted November 23, 2009.
First Published Online January 12, 2010

Abbreviations: CB, Calbindin D-28K; Ct, cycle threshold; DA, dopamine; DAG, diacylglycerol; E2, 17β-estradiol; ER, estrogen receptor; GABA, γ-aminobutyric acid; IP3, inositol-triphosphate; IR, immunoreactive; NiDAB, nickel-enhanced diaminobenzidine; NMDA, *N*-methyl-D-aspartic acid; NT, neurotensin; PKA, protein kinase A; PKC, protein kinase C; PLC, phospholipase C; PP, protein phosphatase; PV, parvalbumin; TLDA, TaqMan low-density array.

in protein structure (7), function (8), and tissue distribution (9). In the classical mechanism of action, E2 enters the cell and binds to ER. Ligand binding induces a conformational change in ER, resulting in the dissociation of accessory proteins and dimerization of ER. In the nucleus, the E2-ER complex binds to estrogen-response elements on target genes and recruits transcriptional coregulators and proteins of the basal transcription initiation machinery to the promoter region of target genes (10). In addition, ER can interact with other transcription factors as well (11). These events converge to produce changes in gene expression that lead to a physiological response hours later.

In addition to genomic effects, E2 induces rapid, nongenomic responses in minutes. Rapid responses include an increase in intracellular calcium ion concentration and activation of intracellular signaling pathways (12, 13). Nongenomic actions are mediated by extranuclear ERα and ERβ (14) and additional membrane ER such as ER-X (15), G protein-coupled plasma membrane ER (16) and G protein-coupled receptor 30 (17). The complexity of estrogen action is further increased by the existence of cross talk between nongenomic and genomic signaling pathways.

Humans have a strikingly diverse and flexible repertoire of sophisticated behaviors. Besides their fixed reactions to external events, humans can devise and implement complex plans to achieve often remote goals. A brain region strongly implicated in this ability is the prefrontal cortex (18, 19). Its damage in humans results in disturbances in a variety of functions including attention, memory, response selection, planning, and inhibitory control. Malfunction of the prefrontal cortex has been implicated in various disorders such as addiction, bipolar disorder, depression, obsessive-compulsive disorder, and schizophrenia. Some of these functions are also disturbed by declining E2 levels. Both ERα and ERβ are expressed in the prefrontal cortex (20). The effects of E2 on cortical synaptic plasticity, spine density, and intracellular signaling pathway activation have been studied extensively (1, 21). In parallel, E2 can also alter gene expression in cortical neurons, but a comprehensive study on the effect of E2 on gene expression governing multiple aspects of cortical function has not been published yet.

Identification of a comprehensive set of E2-regulated genes can provide information about genes through which estrogens maintain the proper functioning of the frontal cortex. In addition, this information is supposed to reveal putative genes, dysregulation of which may contribute to the etiology of neurological and psychiatric disorders related to abrupt changes in E2 levels. To elucidate the cellular and molecular backgrounds of these mechanisms, first ERα and ERβ immunostaining was carried out to confirm the presence and map the distribution of nuclear ER in the frontal cortex. Then, we applied gene expression profiling to elucidate the estrogenic regulation of cortical gene expression in the frontal cortex of young, female, ovariectomized rats after 24 h of a single injection of E2.

Materials and Methods

Animals

Female Harlan-Wistar rats were purchased from Toxicoop (Budapest, Hungary) and housed in groups of four in a temperature-controlled (21 ± 1 C) and humidity-controlled (45–55%) facility at the Institute of Experimental Medicine. Rats were kept on a 12-h light, 12-h dark cycle with lights on at 0700 h, with unrestricted access to phytoestrogen-free food (type 2019S protein-extruded rodent diet; Harlan Teklad Global Diets, Madison, WI) and tap water. All experiments were carried out with the permission of the Animal Welfare Committee of the Institute of Experimental Medicine (No. A5769-01) and in accordance with the legal requirements of the European Community (Decree 86/609/EEC).

Immunocytochemical detection of ER immunoreactivity in the frontal cortex

Rats (n = 5) were ovariectomized bilaterally, allowed to recover for 14 d, and perfused transcardially with 4% acrolein and 2% paraformaldehyde in 0.1 M PBS. Brains were removed and postfixed overnight in 2% paraformaldehyde. Thirty-micrometer-thick sections were prepared in the coronal plane (Bregma +5.20 to +2.20 mm) (22) with a Vibratome (Technical Products International, St. Louis, MO) and collected into a series of six wells. Thus, each well contained consecutive sections that were 150 μm apart rostrocaudally from one another.

Single-labeling immunohistochemistry

ERα and ERβ immunoreactivities were visualized using the ABC method. After pretreatment, sections were incubated for 72 h at 4 C either in C1355 (Upstate Biotechnology, Waltham, MA) or Z8P (Zymed Laboratories, San Francisco, CA) rabbit polyclonal antisera to ERα or ERβ, respectively. Omission of primary or secondary antibodies and use of ERα-knockout tissues as well as preabsorption test by others (23) proved the specificity of ERα immunolabeling with the C1355 antiserum. Similar specificity control approaches were applied in the case of Z8P (Lot 01162852) ERβ antiserum and confirmed labeling specificity as also described elsewhere (24). C1355 was used at the dilution of 1:20,000 and Z8P at the concentration of 0.1 μg/ml. To control specificity of the applied detection methods, two sets of sections were reacted for each receptor subtype. One set was labeled with a fluorescent dye (Alexa 488) and the other series of sections with nickel-enhanced diaminobenzidine (NiDAB), which was further intensified with a silver-gold intensification technique (24, 25).

Double-labeling immunohistochemistry

Double-label immunohistochemistry (26) was carried out to identify the phenotype of ER-immunoreactive (IR) cells by combined application of black nuclear *vs.* brown cytoplasmic chromogens. ER subtype was visualized first using silver-gold-intensified

NiDAB. For subsequent identification of immunoreactivity for parvalbumin (PV), calbindin D-28K (CB), or calretinin, sections were incubated in rabbit anti-PV (1:1000; gift from Dr. Baimbridge), rabbit anti-CB (1:4000; gift from Dr. Baimbridge), or rabbit anti-calretinin (1:5000; gift from Dr. Rogers). DAB alone was used to visualize these calcium-binding proteins.

Neuroanatomical areas analyzed

The analysis of single- and double-labeled cells was undertaken in digital micrographs. The distribution and phenotype of ERα- and β-IR cells were examined in the medial, orbital, and lateral parts of the prefrontal cortex and in the primary motor and somatosensory cortices. The delimitations of regional and laminar boundaries were performed according to Paxinos and Watson (22) and Uylings *et al.* (27).

Animal treatments and preparation of the frontal cortex for microarray studies

Postnatal d-56 rats (n = 24) were deeply anesthetized and ovariectomized bilaterally. After surgery, they were housed individually and 2 wk later divided into control (n = 12) and E2 (Sigma Chemical Co., St. Louis, MO) treatment groups (n = 12). Individual rats received a single sc injection of either the vehicle (mix of 1 vol dimethylsulfoxide and 9 vol sunflower oil) or E2 (50 μg/kg body weight) with 10-min shifts. Twenty-four hours later, animals were deeply anesthetized with pentobarbital (40 mg/kg body weight, ip) and perfused transcardially with ice-cold PBS containing 10% RNA*later* stabilization reagent (QIAGEN, Hilden, Germany) to preserve RNA integrity (28). Brains were removed, and a 3-mm-thick coronal slice was dissected from the forebrain with two blades positioned at bregma 5.2 and 2.2 in a rat brain matrix. The olfactory bulb, the nucleus accumbens, and the striatum were removed from the slice by an inverted V-shaped cut (supplemental Fig. 1, published as supplemental data on The Endocrine Society's Journals Online web site at http://endo.endojournals.org) resulting in a well-defined and reproducible block of the frontal cortex. This frontal cortex sample containing the prefrontal cortex, motor and sensory cortical areas, the rostral tip of the caudate putamen (less than 0.5% vol/vol), and the forceps minor of the corpus callosum (~3.8% vol/vol) was used for subsequent microarray experiments. Tissue samples were immediately immersed into RNA*later* and stored at −80 C. Frontal cortex sections of the right hemisphere were used for RNA isolation, whereas the contralateral sections were used to check the accuracy of dissections by histological analysis.

Isolation of RNA

RNA samples were isolated using the RNeasy lipid tissue mini kit (QIAGEN) according to the manufacturer's instructions. RNA was eluted with 48 μl ribonuclease-free water and divided immediately into three aliquots. One sample was kept on ice for an immediate analysis, whereas the rest was quickly frozen and kept at −80 C. RNA purity and concentration were confirmed from A260-nm/A280-nm readings using Nanodrop spectrophotometer. RNA integrity was determined by capillary electrophoresis using the Agilent 2100 Bioanalyzer (Agilent, Santa Clara, CA). All samples used for microarray experiments displayed RNA integrity numbers above 8.0. To minimize the effect of dissection inconsistencies, cortical RNA samples were pooled from three animals, resulting in four samples for each of the vehicle and E2 treatment groups.

One-cycle target labeling

Eight micrograms of total RNA was used for each labeling reaction. Preparation of poly-A RNA controls (spike-in controls), first-strand and second-strand cDNA synthesis, cleanup of double-stranded cDNA *in vitro* transcription labeling, cleanup of biotin-labeled cRNA and fragmenting the cRNA for target preparation were carried out according to the Affymetrix technical manual of GeneChip expression analysis (https://www.affymetrix.com/support/downloads/manuals/expression_s2_manual.pdf). In brief, first- and second-strand cDNAs were synthesized from 8 μg total RNA using the GeneChip one-cycle cDNA synthesis kit (Affymetrix). The cRNA was synthesized and labeled with biotin-conjugated nucleotide analogs by *in vitro* transcription using the IVT labeling kit (Affymetrix). The cRNA was fragmented by metal-induced hydrolysis at 94 C for 35 min. Before hybridization, the quality of intact and fragmented cRNAs was checked on the Agilent 2100 Bioanalyzer.

Hybridization

Fragmented cRNA was hybridized for 16 h at 45 C to Rat 230 2.0 Expression Array (Affymetrix) containing 31,000 probe sets. Arrays were washed at 25 C with 6× SSPE, followed by a stringent wash at 50 C with 100 mM MES containing 0.1 M Na^+ and 0.01% Tween 20. Then, the arrays were stained with phycoerythrin-conjugated streptavidin (Molecular Probes, Eugene, OR). Fluorescence intensities were determined using the GCS 3000 confocal laser scanner (Affymetrix). Scanned images were analyzed using programs resident in GeneChip operating system version 1.2 (GCOS Affymetrix).

Data analysis

Quality assessment of microarrays was performed using affyQCReport. Raw microarray data were preprocessed for analysis using GCRMA (29). For feature selection, linear models combined with empirical Bayesian methods were used (30). Obtained p-values were adjusted by the FDR-based method (31). All statistical and data mining work was performed in R-environment (http://www.R-project.org) with Bioconductor packages (32).

Real-time PCR

TaqMan low-density array (TLDA) was designed to confirm microarray results by real-time PCR. The TLDA microfluidic card (Applied Biosystems, Santa Clara, CA) was preloaded with selected inventoried gene expression assays for the genes of our interest and four housekeeping genes including 18S rRNA, β-actin (Actb), hypoxanthine guanine phosphoribosyltransferase (Hprt), and peptidyl-prolyl isomerase A (Ppia) by the manufacturer. Each assay consisted of a FAM dye-labeled TaqMan MGB probe and two PCR primers. Every assay had been optimized by the manufacturer to run under universal thermal cycling conditions with a final reaction concentration of 250 nM for the probe and 900 nM for each primer. Total RNA was reverse transcribed by using the high-capacity cDNA reverse transcription kit (Applied Biosystems). Reaction mix was diluted with an equal volume of water, and 10 μl cDNA was used as template in PCR (220 μl). Thermal cycling conditions were 2 min at 50 C and 10 min at 95 C, followed by 40 cycles of 30 sec at 97 C and 1 min at 59.7 C using ABI Prism 7900HT (Applied Biosystems). RealTime StatMiner (Integromics, Granada, Spain) software and relative

quantification against calibrator samples (ΔΔCt) were used for analysis of Applied Biosystems TaqMan gene expression assays. Four housekeeping genes were applied on the TLDA card as potential internal controls. To find the most stable endogenous controls, the nonfinder stability scoring method (33) was used. The analysis showed that three of the four genes, Actb, Hprt, and Ppia, were stable endogenous controls. Therefore, a computed internal control corresponding to the geometric mean of cycle threshold (Ct) values of the three housekeeping genes was used for subsequent ΔCt calculation (34).

In situ hybridization

Twelve-micrometer-thick coronal sections were cut from the prefrontal cortex of ovariectomized rats on a Leica CM 3050 cryostat (Leica Microsystems, Vienna, Austria), thaw-mounted on microscope slides coated with (3-aminopropyl) triethoxysilane (Sigma), and air dried. A pBluescript SK− plasmid vector containing an 866-bp fragment of the rat CART cDNA (35) was kindly provided by Dr. M. Kuhar (Emory University, Atlanta, GA) and used as a transcription template to generate a ^{35}S-labeled cRNA hybridization probe (36). Prehybridization, hybridization, and posthybridization procedures were carried out as detailed elsewhere (37). The signals were first visualized on x-ray film (BioMax MR x-ray film; Kodak, Rochester, NY) and then also on NTB nuclear track emulsion (Kodak; diluted 1:1 with MQ water). The sections were lightly counterstained with 0.05% toluidine blue (Sigma), dehydrated, and coverslipped with DPX. Microscopic images were scanned with an AxioCam MRc 5 digital camera mounted on a Zeiss AxioImager M1 microscope (Carl Zeiss, Göttingen, Germany).

Results

Distribution of nuclear ERα and ERβ immunoreactivity in cortical areas

Immunohistochemical staining revealed that ERα as well as ERβ immunoreactivity is detectable in nearly all cortical areas in the frontal pole of the forebrain (Fig. 1). In accordance with previous findings (38), the immunoreactivity for both ER subtypes appeared primarily in the nucleus of the cells. The regional and laminar distribution of ERα- and ERβ-IR cells showed marked differences. ERα-IR cells were present primarily in the prefrontal cortical areas. Only a few scattered cells appeared in the primary motor and somatosensory cortical regions (Fig. 1, A and C). In contrast, the ERβ-IR cells dominated the primary and secondary motor cortices, and fewer IR cells were present in the prefrontal, especially the orbital cortical areas (Fig. 1, B and D). The dominant layers for both ER subtypes were layers III–V, where the ERβ-IR cells outnumbered the ERα-containing cells (Fig. 1, A and B). Layer I in the primary motor and somatosensory cortical areas contained almost exclusively ERβ-immunopositive cells (Fig. 1, A and B). Subpopulations of cortical γ-aminobutyric acid (GABA) interneurons characterized by the coexpression of calcium-binding proteins have already been shown to express ER (38). In the current study, the most rostral cortical areas were investigated to reveal which calcium-binding protein is present in the cytoplasm of ERα- and ERβ-IR cells. The PV, CB, and calretinin content of ER-IR neurons was analyzed using dual-label immunocytochemistry. Double-labeled calretinin-immunopositive cells were not found in the rostral cortical areas (not shown). Immunoreactivity for PV and CB was extensively colocalized with ERβ (Fig. 1, G and H). In contrast, very few double-labeled cells were found for ERα and either of the Ca-binding proteins (Fig. 1, E and F).

Gene expression profiling of the rat frontal cortex

Data analysis with strict statistical filters (>1.5-fold change; P value < 0.05) revealed 136 genes the transcription of which changed in the rat frontal cortex 24 h after E2 treatment. E2 evoked up-regulation of 46 genes (Table 1) and down-regulation of 90 genes (Table 2). The number of E2-regulated genes was dramatically decreased if more stringent fold change criteria were applied.

The E2-regulated genes were classified according to subcellular localization and biological function of their corresponding protein products (Fig. 2). Among the genes, 42 encoded nuclear, 39 membrane, 22 cytoplasmic, seven cytoskeletal, four extracellular, and three Golgi complex-related proteins. A characteristic feature of genomic E2 effects in the rat frontal cortex was that nearly one third of the genes encoded nuclear proteins. Twenty-six genes (about 20% of E2-regulated genes) encoded proteins involved in the regulation of transcription. This group comprised 12 transcription factors including CCAAT/enhancer binding protein (Cebpg), ets variant gene 1 (Etv1), and Max protein (Max), transcriptional coregulators such as nuclear receptor coactivator 3 (Ncoa3), and histone modification enzymes such as MYST histone acetyltransferase (Myst3).

E2 altered the transcription of 39 genes that encode proteins of intracellular signaling pathways. Of the 39 genes, 13 genes were related to the calcium signaling pathway (Fig. 3). Two genes encoded enzymes, calcineurin (Ppp3ca) and calcium/calmodulin-dependent protein kinase II-α (Camk2a), which were integrators of various pathways and were implicated in learning, memory, and long-term potentiation. The altered expression of these enzymes was likely to result in modulation of calcium signaling lasting for 24 h.

E2 regulated the transcription of five genes coding for neurotransmitter receptors including adenosine A2a receptor (Adora2a), dopamine receptor D1A (Drd1a), metabotropic glutamate receptor 5 (Grm5), 5HT receptor 2c (Htr2c), and ionotropic glutamate receptor NMDA2A (Grin2a). Two GH receptors, epidermal growth factor receptor (Egfr) and IGF-I receptor (Igf1r), were down-reg-

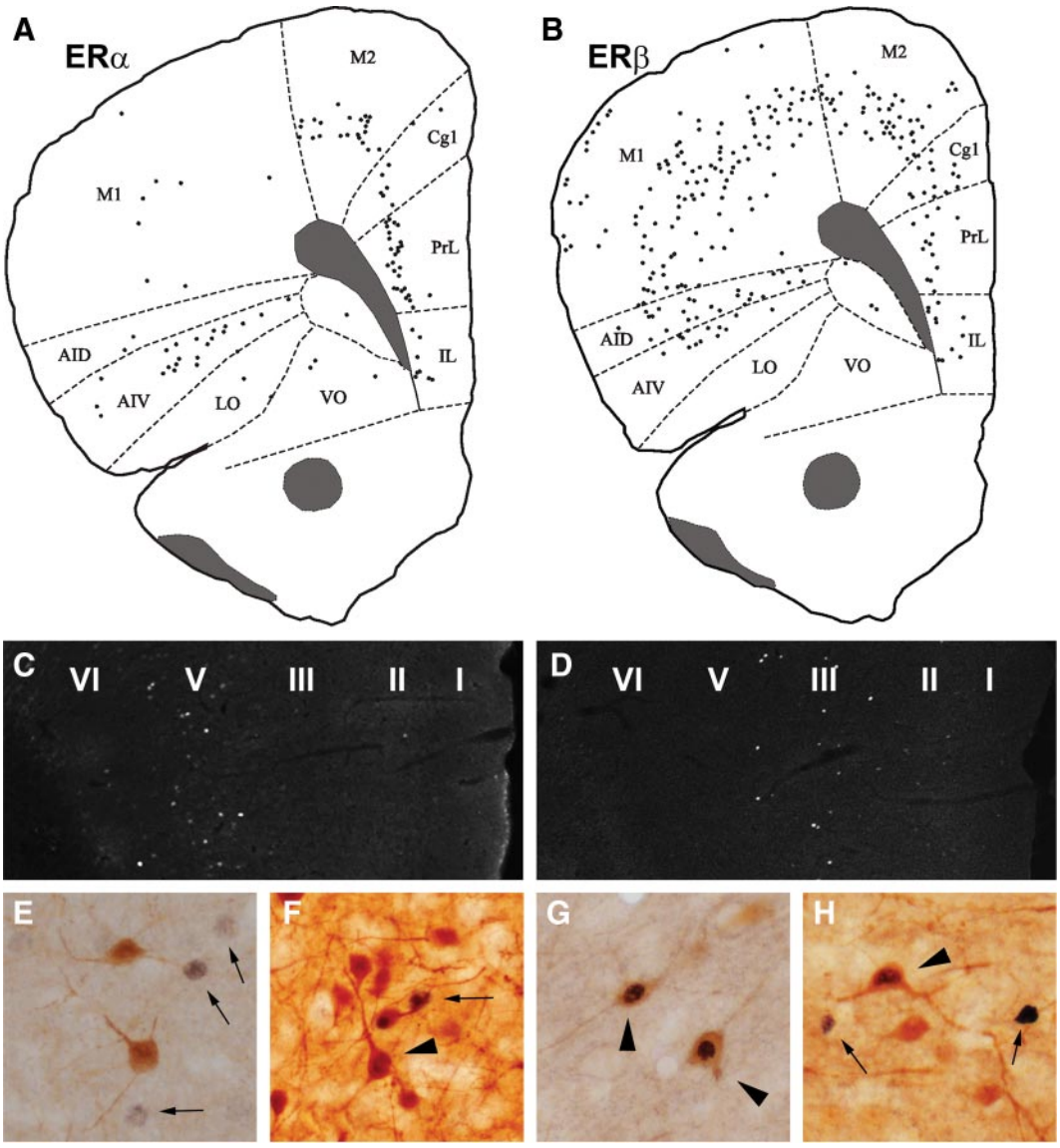

FIG. 1. Immunohistochemical detection of ERα and ERβ in the cortical areas present in the tissue sample used for microarray experiments. Distribution of the stained nuclei is shown separately for ERα (A) and ERβ (B). The ERα-IR cell nuclei occupy mainly layer V (C); the ERβ-IR cell nuclei are also present in layer III of the cingulate cortex (D). Double labeling for the receptors and Ca-binding proteins shows no PV (E) or very few CB (F) cells to express the α-subtype of the receptor. In contrast, PV (G) and CB (H) neurons are immunoreactive for ERβ. *Arrows* point to cell nuclei single labeled for ERs. *Arrowheads* mark the cells double labeled for the receptors and the Ca-binding proteins PV or CB. AID, Agranular insular cortex, dorsal part; AIV, agranular insular cortex, ventral part; Cg1, cingulate cortex; IL, infralimbic cortex; LO, lateral orbital cortex; M1, primary motor cortex; M2, secondary motor cortex; PrL, prelimbic cortex; VO, ventral orbital cortex.

ulated by E2. A voltage-dependent T-type calcium channel, Cacna1g, was up-regulated. Upon ligand binding, these membrane proteins modulate the calcium signaling pathway (Fig. 3).

Validation of microarray results using TaqMan-based real-time PCR

Of the genes the expression of which was altered by E2, 52 (Table 3) were selected for further analysis by quantitative real-time PCR. These 52 genes encoded previously characterized protein products, and most of them were also related to neuronal functions. Based on published data (39–51), they may represent targets for studies with lower throughput methods. Five individual reverse-transcribed samples for each group were run on PCR, and four housekeeping genes were used as potential internal controls for analysis. Data analysis showed that Actb, Hprt, and Ppia were stable endogenous controls whereas 18S rRNA showed expression instability. To determine expression levels accurately, normalization by multiple housekeeping genes instead of one was required (34). As proposed earlier, a normalization factor based on the expression levels (Ct) of Actb, Hprt, and Ppia was calculated using the geometric mean of the three Ct values for determining ΔCt values (34). E2 regulation was confirmed in

TABLE 1. The list of up-regulated genes by E2 in the rat frontal cortex using the selection filters of more than 1.5-fold change and *P* value <0.05

Symbol	Gene	GenBank
Cell adhesion		
Cldn11	Claudin 11	NM 053457
Mcam	Melanoma cell adhesion molecule	AB 035507
Cytoskeleton		
Ank1	Ankyrin 1	AI 172141
Arpc4_pred	Actin-related protein 2/3 complex unit4	AI 411582
Rdx	Radixin	BF 565167
Tpm3	Tropomyosin 3, γ	NM 057208
Ion transport		
Cacna1g	Calcium channel, voltage-dependent, T type, α 1G	NM 031601
Cacng8	Calcium channel, voltage-dependent	AF 361346
Clic4	Chloride intracellular channel 4	NM 031818
Nervous system development		
Mobp	Myelin-associated oligo basic protein	D28110
Six3	Sine oculis homeobox homolog 3	AI 070396
Protein catabolic process		
Fbxl19_pred	F-box and leu-rich repeat protein	BM 390208
Fbxo10_pred	F-box only protein 10	AW 535276
Protein phosphorylation		
Camk2a	CaM-dependent protein kinase Iia	BM 384558
Ppp1r14a	Protein phosphatase 1, regulator 14A	NM 130403
Stk32c_pred	Serine/threonine kinase 32C	BE 097305
Signal transduction		
Adora2a	Adenosine A2a receptor	NM 053294
Cartpt	CART	NM 017110
Cntfr	Ciliary neutrophic factor receptor	BF 562455
Gpcr12	GPCR 12	NM 030831
Nts	Neurotensin	BE 101670
Ppp1r1b	Protein phosphatase 1, regulator 1b	AA 942959
Psd	Pleckstrin and Sec7 domain protein	NM 134370
Rab5c_pred	RAB5C, member RAS family	H35233
Rgs9	Regulator of G-protein signaling 9	NM 019224
Synaptic transmission		
Drd1a	Dopamine receptor D1A	NM 012546
Htr2c	5-HT receptor 2c	U35315
Transcription		
Ascl1	Achaete-scute complex homolog-like 1	NM 022384
Cebpg	CCAAT/enhancer binding protein	X64403
Drg1	Developmentally regulated GTP-binding protein 1	AW 527113
Max	Max protein	NM 022210
Ncoa3	Nuclear receptor coactivator 3	BI 276668
Transport		
Anp32a	Acidic nuclear phosphoprotein 32A	NM 012903
Apba1	APP-binding, family A1, member 1	BF 410366
Hba-a1	Hemoglobin α, adult chain 1	AI 179404
Pafah1b1	PAF acetylhydrolase, isoform Ib	BG 663460
Ttr	transthyretin	NM 012681
Others		
Cdc23	Cell division cycle 23	AI 013729
Ddc	Dopa decarboxylase	U31884
Gpr116	GPCR 116	BF 542425
Hspa4	Heat shock protein 4	AF 077354
Larp6_pred	La ribonucleoprotein domain family	AI 102304
Ngfrap1	NGF receptor-associated protein	BG 381021
Ssr3	Signal sequence receptor 3	NM 031120
Tmem58_pred	Transmembrane protein 58	BG 375421
Vof16	Ischemia-related factor vof-16	BE 107282

E2 evoked up-regulation of 46 genes that were categorized based on function.

the case of 12 genes (Table 4), which correspond to 23% of the genes tested by real-time PCR. The lack of a higher level of validation efficiency can be due to the fact that the majority of changes in mRNA expression after acute E2 treatment falls in the range of fold change between 1.5 and 2.0 in the frontal cortex of the rat.

Of the 12, 11 validated genes including adenosine A2a receptor, cocaine- and amphetamine-regulated transcript,

TABLE 2. The list of down-regulated genes by E2 in the rat frontal cortex using the selection filters of more than 1.5-fold change and *P* value <0.05

Symbol	Gene	GenBank
Cell adhesion		
Clstn2	Calsyntenin 2	BE 109141
Lgals3bp	Lectin, galactoside-binding protein	AF 065438
Negr1	Neuronal growth regulator 1	NM 021682
Pvrl1	Poliovirus receptor-related 1	BI 274299
Cytoskeleton		
Flnb_pred	Filamin β	BI 275447
Myo10_pred	Myosin X	AI 044576
Sgcb_pred	Sarcoglycan, β	NC 005113
Ion transport		
Cacnb4	Calcium channel, voltage-dependent, β 4	BF 404371
Grin2a	Glutamate receptor, ionotropic, NMDA2A	NM 012573
Ryr2	Ryanodine receptor 2	BF 418135
Slc4a4	Sodium bicarbonate cotransporter	AF 210250
Nervous system development		
Crim1_pred	Cysteine-rich motor neuron 1	AI 600057
Enc1	Ectodermal-neural cortex 1	AA 997271
Nrg1	Neuregulin 1	U02323
Tgfb2	Transforming growth factor β 2	AA 963004
Zfhx1b	Zinc finger homeobox 1b	AW 529031
Protein catabolic process		
Fbxo46	F-box only protein 46	
G1p2_pred	Interferon, α-inducible protein	BE 096523
Mdm4	Transformed mouse 3T3 double minute	AI 236886
Ube1dc1	Ubiquitin-activating enzyme E1 domain	AI 408025
Protein phosphorylation		
Bmpr2	Bone morphogenetic protein receptor 2	BE 118651
Egfr	Epidermal growth factor receptor	M37394
Igf1r	Insulin-like growth factor 1 receptor	BE 120747
Ppp3ca	Protein phosphatase 3, catalytic subunit, α	BF 390569
Prkaa2	AMP-activated protein kinase, α 2	NM 023991
Prkcb1	Protein kinase C, β	BF 401586
Signal transduction		
Akap10_pred	A-kinase anchor protein 10	BI 299865
Akap2	A-kinase anchor protein 2	BF 398063
Akap9	A-kinase anchor protein 9	AI 145240
Farp1_pred	FERM, RhoGEF and pleckstrin domain	AI 547942
Gna11	Guanine nucleotide binding protein, α 11	NM 031033
Pik4cb	Phosphatidylinositol 4-kinase	AI 043787
Rgs7	Regulator of G-protein signaling 7	BF 402644
Spred1	Sprouty-protein with EVH1 domain 1	BF 419641
Spred2	Sprouty-protein with EVH1 domain 2	BF 387349
Synaptic transmission		
Grm5	Glutamate receptor, metabotropic 5	AW 526330
Homer1	Homer homolog 1 (Drosophila)	BF 397258
Tmod2	Tropomodulin 2	BE 120185
Transcription		
Aff4_pred	AF4/FMR2 family, member 4	AI 715727
Ash1l_pred	Absent, small or homeotic 1-like	AW 521174
Atrx	α Thalassemia X-linked homolog	BF 393029
Bhlhb2	Basic helic-loop-helix domain, class B2	AW 533010
Ccnt2_pred	Cyclin T2	BE 107044
Crebbp	CREB binding protein	NM 133381
Etv1_pred	ets variant gene 1	AI 112936
Ewsr1	Ewing sarcoma breakpoint region 1	BF 394458
L3mbtl3	l(3)mbt-like 3 (Drosophila)	BF 402723
Maf	v-maf	AA 957811
Mll5	Myeloid/lymphoid leukemia 5	BF 415831
Myst3	MYST histone acetyltransferase	BE 111692
Nr4a1	Nuclear receptor subfam 4a1	NM 024388
Pbx1_pred	Pre-B-cell leukemia transcription factor	BI 281745

(*Continued*)

TABLE 2. Continued

Symbol	Gene	GenBank
Ppargc1b	PPAR γ, coactivator 1 β	BE 113289
Rbm14	RNA binding motif protein 14	BG 670091
Rcor1_pred	REST corepressor 1	BI 281108
Tbl1xr1	Transducin-like 1X-linked receptor 1	AA 859701
Tcf4	Transcription factor 4	BF 548958
Whsc1l1_pred	Wolf-Hirschhorn syndrome candidate 1-like 1	BF 415965
Zfp212	Zinc finger protein 212	
Zfp422	Zinc finger protein 422	AI 232806
Zfp655	Zinc finger protein 655	AI 103040
Transport		
Hdlbp	HDL binding protein	BI 296631
Hook3	Hook homolog 3 (Drosophila)	AI 501458
Kif1a	Kinesin family member 1A	BE 115743
Lin7a	lin-7 homolog A (*C. elegans*)	AF 090134
Tpr	Translocated promoter region	BE 118639
Tram1	Translocation associated protein 1	AA 956421
Others		
Ankrd12_pred	Ankyrin repeat domain 12	XM 237588
Arc	Activity regulated cytoskeletal protein	NM 019361
Auts2_pred	Autism susceptibility candidate 2	AI 070144
Brinp2	BMP/RA-induced neural-specific protein	BF 404835
Cfb	Complement factor B	AI 639117
Cldnd1	Claudin domain containing 1	AI 231223
Coil	Coilin	AI 059075
CPG2	CPG2 protein	BE 102928
Cugbp2	CUG triplet repeat, RNA binding protein	BF 403645
Eif2c2	eu translation initiation factor, 2C2	BF 281131
Galnt1	N-acetylgalactosaminyltransferase 1	AA 963979
Gpt2_pred	Glutamic pyruvate transaminase 2	AA 955605
Hnrpa1	Heterogeneous ribonucleoprotein A1	AA 965147
Kif3c	Kinesin family member 3C	BF 553488
Lpin1	Lipin 1	AI 103917
Maoa	Monoamine oxydase A	BF 414655
Mrlcb	Myosin light chain, regulatory B	BF 401617
Mx2	Myxovirus resistance 2	NM 017028
Pus7_pred	Pseudouridylate synthase 7 homolog (S. cerevisiae)	BM 390168
RT1-Aw2	RT1 class Ib, locus Aw2	M24024
RT1-CE16	RT1 classI, CE16	U50449
Srrm1_pred	Serine/arginine repetitive matrix 1	AI 059437
Zswim6	Zn finger, SWIM domain containing 6	AA 859627

E2 induced down-regulation of 90 genes that were categorized based on function.

dopamine D1A receptor, myelin-associated oligodendrocyte basic protein, neurotensin, preproenkephalin, protein phosphatase 1 regulatory subunit 1b, regulator of G protein signaling 9, and transthyretin were up-regulated (Table 4).

Localization of Cart mRNA in the rat frontal cortex

Cart, implicated in the neuroprotective effects of E2 in the cerebral cortex (52, 53), was selected for neuroanatomical analysis in this study. To localize Cart-expressing cells that responded with altered gene expression to E2 treatment, we carried out radioisotopic *in situ* hybridization experiments. Cart mRNA was ubiquitously expressed in various subregions of the frontal cortex, including the prelimbic cortex (Fig. 4, A, C, and E). A well-patterned signal was observed in the somatosensory cortex (S1; Fig. 4, A and B) where grain clusters were centered in layer IV (Fig. 4, D and F). Results of previous *in situ* hybridization studies by other laboratories also provide us partial information about the cortical distribution of mRNAs coding for validated E2-regulated genes including Adora2a (54), D1A (55), 5HT2c receptor (56), neurotensin (57), Nr4a1 (58), Penk1 (59), and Rgs9 (60).

Discussion

ERα and ERβ immunoreactivity in the rat frontal cortex is present in different cell populations

The current immunohistochemical evidence for the nuclear presence of ERα and ERβ subtypes in frontal cortical areas supports local, direct effects of E2 on gene transcrip-

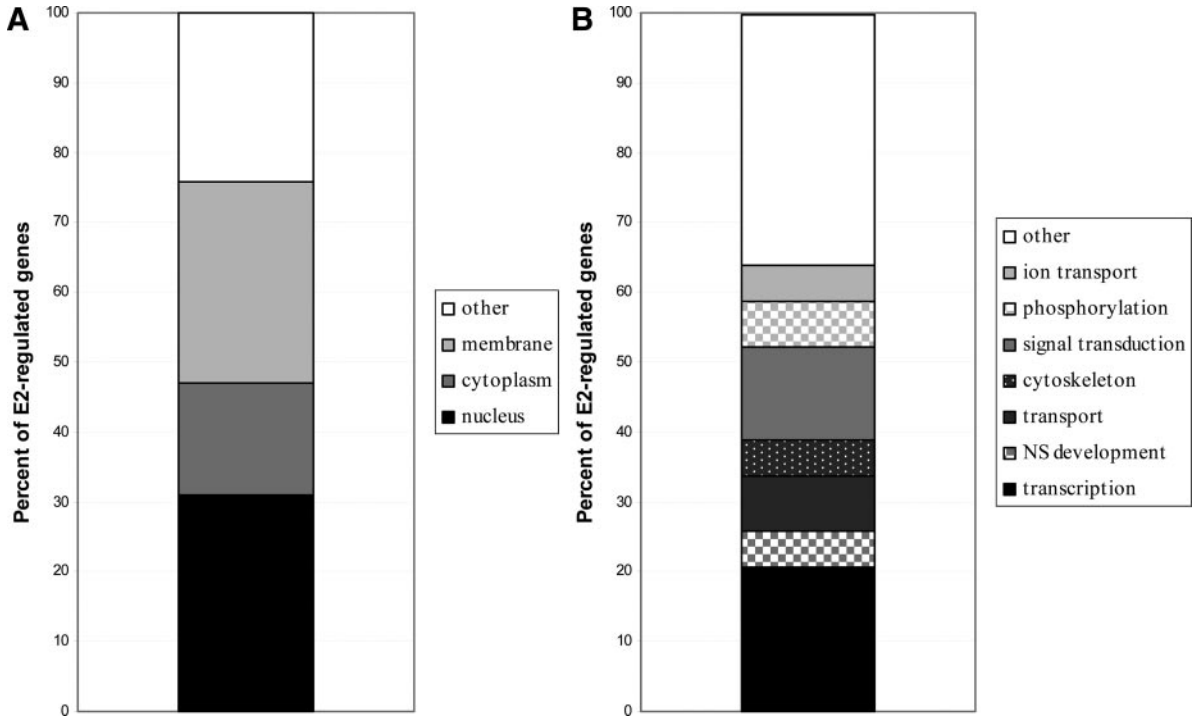

FIG. 2. Classification of E2-regulated genes in the frontal cortex. Classification according to subcellular localization (A) showed that of the 136 E2-regulated genes, 42 (31%) encoded nuclear, 22 (16%) cytoplasmic, 39 (29%) membrane, and 33 (24%) proteins localized to other compartments. Classification according to biological function (B) revealed that among the genes, 28 (21%) were involved in the regulation of transcription, seven (5%) in nervous system development, 11 (8%) in transport, seven (5%) in cytoskeletal organization, 18 (13%) in signal transduction, nine (7%) in protein phosphorylation, seven (5%) in ion transport, and 49 (36%) in other functions.

tion. We found the ERα- and the ERβ-IR cells primarily distributed in layer III–V similarly to their corresponding mRNA hybridization signals described before (60). The double-label immunohistochemical experiments revealed that the ERα- and ERβ-IR cells represent only a small and phenotypically distinct fraction of cortical neurons. Although the ERβ immunoreactivity was found in PV-containing neurons, the ERα immunoreactivity was absent from these cells. In addition, ERβ immunoreactivity was also observed in CB-containing neurons. These colocalization data are in concordance with those demonstrated for other cortical regions (38, 61, 62) and suggest the appearance of ERα either in pyramidal cells or in other types of interneurons. Although calretinin-IR neurons have been reported to show immunoreactivity for ERα in certain cortical areas (61), those in the frontal cortex were found to be ERα immunonegative.

In addition, the 24-h duration of E2 treatment also anticipates indirect effects on gene transcription. Cortical ERβ-IR interneurons (63) as well as other ERα or ERβ-IR subcortical centers and their pathways (64–66) have been suggested to mediate estrogens' remote influence on iso- or allocortical functions, including regulation of gene expression (67). Therefore, it is important to note that the data reported here represent direct as well as indirect transcriptional changes in response to E2 24 h after treatment.

E2 alters the transcription of genes coding for transcription factors and transcriptional coregulators

In these studies to reveal the regulation of cortical gene expression by E2, we have provided evidence for the presence of both ER subtypes in the nuclei of cortical neurons. We have identified changes in the transcription of 136 genes in the frontal cortex of the rat. Classifications show that one third of these genes encode nuclear proteins out of which 26 are involved in the regulation of transcription. This group includes 12 transcription factors and three transcriptional coregulators. Of the 12 transcription factors, Ascl1/Mash1 (68), Etv1, Maf, and Six3 are implicated in neuronal differentiation. Etv1 governs differentiation of dopaminergic neurons in *Caenorhabditis elegans* and mice (69), whereas Nr4a1/Nurr77 plays a role in complex pathways of cell survival and apoptosis (70). The three transcriptional coregulators comprise Ncoa3/SRC3, Ppargc1b, and Rcor1. Two of these coregulators, Ncoa3 and Ppargc1b, directly bind to ER (71, 72). Ncoa3 shows area-specific expression in the rat brain. It is highly expressed in the hippocampus but absent from the hypothalamus (73). Coactivators dramatically enhance the transcriptional activity of nuclear receptors including ERα and ERβ (74). Ncoa3 is the preferred coactivator partner for ER, exhibiting the highest-affinity interaction with ERα (71). Up-

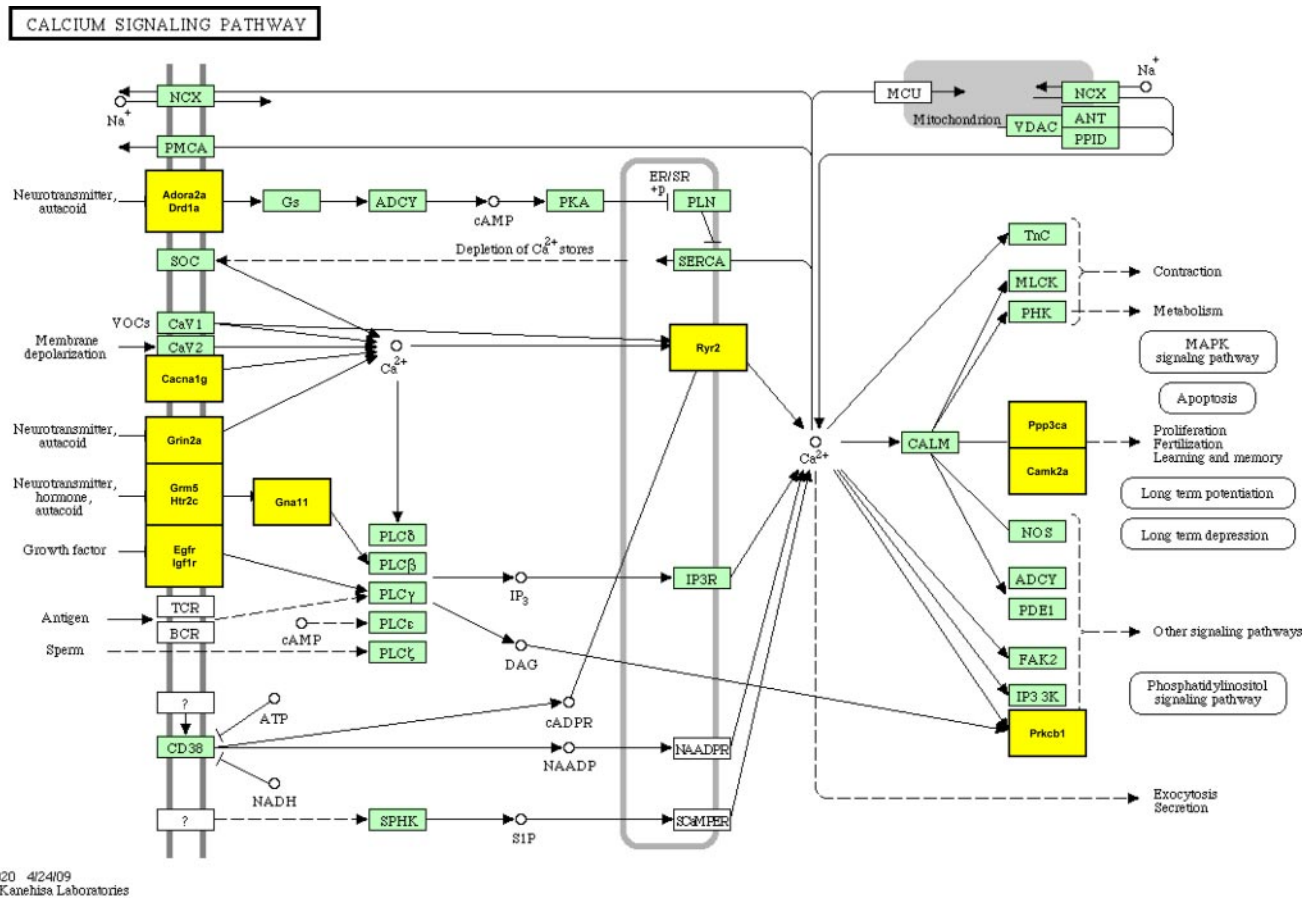

FIG. 3. Transcription of multiple genes coding for elements of the calcium signaling pathway regulated by E2 in the frontal cortex. E2-regulated elements are shown in *yellow*. Among G protein-coupled receptors, Adora2a, Drd1a, Htr2c, and CaV3 Cacna1g were up-regulated, Grm5 was down-regulated. Gq Gna11 was down-regulated. Grin2a and receptor protein tyrosine kinases Egfr and Igf1r were down-regulated. The ER membrane-located ryanodine receptor Ryr2 was down-regulated. The cytoplasm-located CaN Ppp3ca and PKC Prkcb1 were down-regulated, and Camk2a was up-regulated. The KEGG calcium signaling pathway (www.genome.jp) available for the public was used at the drawing of the diagram. CaV3, T-type voltage-dependent calcium channel α1; CaN, calcineurin.

regulation of Ncoa3 may modulate the genomic effect of E2, because coactivators in general are the rate-limiting factors in nuclear receptor-mediated transcription (74).

Protein phosphatases (PP) PP1 and PP2a are the key negative regulators of Ncoa3 activity (39). Our microarray study has shown up-regulation of two inhibitors of PP1, protein kinase C-potentiated inhibitor of PP1 (Ppp1r14a) and DARPP-32, leading to an increased phosphorylation state of Ncoa3. Notably, E2 induces Ncoa3 phosphorylation in an ERα-dependent manner (75). Our results suggest that E2 simultaneously increases the transcription and modulates the phosphorylation state of Ncoa3, resulting in an effective genomic response in the rat frontal cortex after E2 treatment. Additional studies will be required to elucidate the consequences of these alterations.

E2 may affect cognitive functions through the regulation of key elements of the calcium signaling pathway at the level of transcription

The calcium signaling pathway plays a pivotal role in synaptic plasticity (40). Thirteen genes of the Ca signaling pathway show altered expression after E2 treatment. Of the 13 genes, two encode neurotransmitter receptors: adenosine 2A and D1A dopamine receptors. Both receptors activate protein kinase A (PKA) through cAMP, suggesting that the E2-mediated up-regulation of these receptors may result in an enhanced PKA activity. In addition, E2 down-regulates the transcription of three genes encoding PKA anchoring proteins such as Akap2, Akap9, and Akap10. These results indicate that E2 regulates multiple elements of cAMP/PKA signaling. The ryanodine receptor 2 (Ryr2), located at the endoplasmic/sarcoplasmic reticulum membrane, is also a PKA substrate. Ca release is mediated by the PKA-mediated phosphorylation of Ryr2. Therefore, the possibility exists that E2 can rapidly mobilize intracellular Ca from the Ryr2-gated stores (76).

In this study, we have shown that E2 down-regulates epidermal growth factor and IGF receptors (Egfr and Igf1r). These findings are in agreement with multiple studies reporting estrogenic regulation of these growth factor

TABLE 3. The E2-regulated genes selected for validation by TaqMan-based real-time PCR

TaqMan ID	Public RefSeq	Symbol	Gene name
Rn01503265_m1	NM_001102381.1	**Nts**	Neurotensin
Rn01440268_g1	NM_001003929.1	**Cntfr**	Ciliary neurotrophic factor receptor
Rn01449787_m1	XM_215742.4	**Cacnb4**	Ca channel, voltage-dependent, β4 subunit
Rn01766742_m1	NM_001005889.2	**Rdx**	Radixin
Rn00592091_s1	NM_133573.1	Gpr30	G protein-coupled receptor 30[a]
Rn00591291_m1	NM_133381.2	**Crebbp**	CREB binding protein
Hs99999901_s1		*18S*	*18S rRNA*
Rn00589915_m1	NM_080696.2	**Cacng8**	Ca channel, voltage-dependent, γ subunit 8
Rn01422768_m1	NM_001011974.1	**Akap2**	A kinase (PRKA) anchor protein 2
Rn00497196_m1	NM_001033701.1	**Zfhx1b**	Zinc finger homeobox 1b
Rn00561113_m1	NM_012545.3	**Ddc**	Dopa decarboxylase
Rn00576935_m1	NM_023991.1	**Prkaa2**	protein kinase, AMP-activated, α 2 subunit
Rn00589483_m1	NM_057208.2	**Tpm3**	Tropomyosin 3, γ
Rn02533433_s1	NM_053401.1	**Ngfrap1**	NGF receptor associated protein 1
Rn00582341_m1	NM_031779.2	**Apba1**	amyloid β precursor protein-binding, family A
Rn00580917_m1	NM_031588.1	**Nrg1**	Neuregulin 1
Rn00580398_m1	NM_031507.1	**Egfr**	Epidermal growth factor receptor
Rn00577766_m1	NM_024388.1	**Nr4a1**	Nuclear receptor subfamily 4, groUp A, 1
Rn00581785_m1	NM_031707.1	**Homer1**	Homer homolog 1 (Dros)
Rn00582667_m1	NM_031818.1	**Clic4**	Chloride intracellular channel 4
Rn00584481_m1	NM_053369.1	**Tcf4**	Transcription factor 4
Rn00578096_s1	NM_030831.1	**Gpcr12**	G-protein coupled receptor 12
Rn00581051_m1	NM_031601.3	**Cacna1g**	Ca channel, voltage-dependent, T type, α 1G
Rn00583935_m1	NM_053294.3	**Adora2a**	Adenosine A2a receptor
Rn00583837_m1	NM_052807.1	**Igf1r**	Insulin-like growth factor 1 receptor
Rn00572164_m1	NM_021597.1	**Eif2c2**	Eukaryotic translation initiation factor 2C, 2
Rn00577670_m1	NM_024373.1	**Galnt1**	UDP-*N*-acetyl-α-D-galactosamine
Rn00579674_m1	NM_031131.1	**Tgfb2**	Transforming growth factor, β 2
Rn00584747_m1	NM_053424.1	**Slc4a4**	Solute carrier family 4, member 4
Rn00574345_m1	NM_022384.1	**Ascl1**	Achaete-scute complex homolog-like 1 (Dros)
Rn01424654_m1	NM_012573.3	**Grin2a**	Glutamate receptor, ionotropic, NMDA 2A
Rn01437210_m1	XM_217409.4	**Bmpr2**	Bone morphogenic protein receptor, type II
Rn01430446_m1	NM_012689.1	Esr1	Estrogen receptor α[συπι][a]
Rn01645174_m1	NM_017110.1	**Cart**	Cocaine and amphetamine regulated transcript
Rn01412977_g1	NM_031144.2	*Actb*	*actin, β*
Rn00690933_m1	NM_017101.1	*Ppia*	*peptidylprolyl isomerase A*
Rn00592124_s1	NM_001012745.1	**Zfp422**	Zinc finger protein 422
Rn00597468_m1	NM_173115.1	**Brinp2**	BMP/RA-inducible neural-specific protein 2
Rn00597033_m1	NM_172039.2	**Hdlbp**	High density lipoprotein binding protein
Rn01764319_m1	NM_012831.1	**Cebpg**	CCAAT/enhancer binding protein (C/EBP), γ
Rn03062203_s1	NM_012546.2	**Drd1a**	Dopamine receptor D1A
Rn02347501_m1	NM_001009685.1	**Drg1**	Developmentally regulated GTP binding protein 1
Rn00598552_m1	NM_176075.2	**Ppargc1b**	PPAR-γ, coactivator 1 β
Rn00824538_m1	NM_012720.1	**Mobp**	Myelin-associated oligodendrocytic basic protein
Rn00820861_g1	NM_017248.1	**Hnrpa1**	Heterogeneous nuclear ribonucleoprotein A1
Rn01527840_m1	*NM_012583.2*	*Hprt*	*hypoxanthine guanine phosphoribosyl transferase*
Rn01452984_m1	NM_138521.1	**Ppp1r1b**	protein phosphatase 1, regulatory subunit 1B
Rn00443070_m1	NM_031763.3	**Pafah1b1**	PAF acetylhydrolase, isoform Ib
Rn00484802_g1	NM_022210.1	**Max**	Max protein
Rn00567566_m1	NM_017139.1	**Penk1**	Proenkephalin 1
Rn00566628_m1	NM_017012.1	**Grm5**	glutamate receptor, metabotropic 5
Rn00562610_m1	NM_012754.1	Esr2	Estrogen receptor β[a]
Rn00562124_m1	NM_012681.1	**Ttr**	Transthyretin
Rn00563733_g1	NM_012903.1	**Anp32a**	acidic nuclear phosphoprotein 32 family
Rn00562312_m1	NM_012713.2	**Prkcb1**	Protein kinase C, β 1
Rn00562748_m1	NM_012765.3	**Htr2c**	5-Hydroxytryptamine receptor 2C
Rn00563883_m1	NM_012920.1	**Camk2a**	Ca/calmodulin-dependent protein kinase II, α
Rn00570117_m1	NM_019224.1	**Rgs9**	Regulator of G-protein signaling 9
Rn00566855_m1	NM_017041.1	**Ppp3ca**	Protein phosphatase 3, catalytic, α isoform

The symbols of the selected genes are in *bold*. Housekeeping genes are in *italics*. The TaqMan ID gives the product number of Applied Biosystems Gene Expression Assay used for the validation of the corresponding gene.

[a] Genes for ER.

TABLE 4. Confirmation of E2-induced genomic changes by quantitative real-time PCR

	Rat expression array			Real-time PCR		
Genes	**Fold change**	***P***	**Change**	**RQ**	***P***	**Change**
Adora2a	>2.0	<0.01	Up	1.75	0.078	Up
Cart	>1.5	<0.01	Up	2.40	0.053	Up
Drd1a	>1.5	<0.01	Up	1.74	0.012	Up
Htr2c	>1.5	<0.05	Up	1.16	0.291	Up
Max	>2.0	<0.01	Up	1.17	0.215	Up
Mobp	>1.5	<0.05	Up	1.27	0.209	Up
Nr4a1	>1.5	<0.05	Down	1.54	0.317	Down
Nts	>2.0	<0.01	Up	3.83	0.022	Up
Penk1	>1.3	<0.05	Up	1.71	0.010	Up
Ppp1r1b	>1.5	<0.05	Up	1.36	0.075	Up
Rgs9	>1.5	<0.05	Up	1.81	0.041	Up
Ttr	>1.5	<0.05	Up	1.34	0.751	Up

Five samples were measured for each group on TLDA, and results were evaluated by RealTime StatMiner software. In the case of 12 genes, the transcriptional regulation detected by the two methods showed similarity in size and direction. In the case of five genes, the change became statistically significant after five PCR experiments. The table shows comparison of data from microarray and TaqMan-based real-time PCR studies. RQ, Relative quantity.

receptors (41, 77). Igf1r gene transcription is controlled by interactions between ERα and Sp1 (78).

E2 regulates two neurotransmitter receptors (mGluR5 and Htr2c) and two growth factor receptors (Egfr and Igf1r) that activate phospholipase C (PLC). PLC, in turn, hydrolyzes phosphatidylinositol 4,5-bisphosphate to inositol-triphosphate (IP3) and diacylglycerol (DAG). Hence, in addition to regulating Ca and cAMP, E2 also seems to modulate the level of other second messengers, IP3 and DAG. IP3 stimulates Ca release from the smooth endoplasmic reticulum, whereas DAG transiently enhances presynaptic release, which is a central aspect in synaptic plasticity. DAG is also a physiological activator of protein kinase C (PKC), a subunit of which, PKC-β1 (Prkcb1), was down-regulated by E2. These alterations may result in changes in the levels of IP3 and DAG and in the activation of the DAG/PKC signaling pathway.

Up-regulation of Ca/calmodulin-dependent kinase II-α (Camk2a) bears particular importance. It is known that E2 activates Camk2 in a dose- and time-dependent manner (42). Increased intracellular Ca leads to activation of Camk2, which in turn phosphorylates itself. Camk2 may remain active this way even after Ca concentration has fallen back to normal. Up-regulation of Camk2a may result in persistent activation of Camk2 in the frontal cortex. Camk2 is one of the integrators of the Ca signaling pathway and plays a significant role in learning and memory. Any change in the level and/or activity of this molecule may alter cognitive functions. Therefore, our results implicate the Ca signaling pathway in the E2-mediated improvement of cognitive functions.

E2 alters the transcription of neurotransmitter receptor genes

Of the 136 E2-regulated genes, five encode neurotransmitter receptors: 5HT receptor 2c (5HT2cR), dopamine receptor D1A, adenosine A2a receptor, metabotropic glutamate receptor 5, and ionotropic glutamate receptor NR2A. E2 up-regulates 5HT2cR, which has been implicated in a number of psychological disorders such as schizophrenia, anxiety, and depression (79). The receptor is widely expressed throughout the brain. Approximately 50% of 5HT2cR immunoreactivity has been detected in GABA interneurons in the rat prefrontal cortex (43).

A previous *in vitro* study has found that the D1A promoter contains a half-palindrome TGACC for the consensus ERE, and E2 up-regulates D1A gene transcription in a neuroblastoma cell line (44). In the rat cerebral cortex, D1A receptor is expressed in the somata and in the dendritic processes of pyramidal neurons and PV-positive interneurons (45, 80). D1A colocalizes with the NR1 and NR2A *N*-methyl-D-aspartic acid (NMDA) receptor subunits in the cortex (81). It is known that dopamine (DA) acts mainly through D1 to modulate glutamatergic neuronal activity. D1 receptors and activation of the cAMP/PKA pathway result in the phosphorylation of NMDA receptor subunits and through this mechanism they can modulate synaptic strength (46). Up-regulation of D1A may lead to an enhanced potentiating effect of DA on NMDA-dependent processes.

The effects of glutamate are mediated by activation of ionotropic and metabotropic receptors. Ionotropic glutamate receptors mediate fast excitatory neurotransmission, whereas metabotropic glutamate receptors including mGluR5 mediate slower responses. mGluR5 is particularly abundant in the cerebral cortex (47). The highest density of the receptor was localized outside the synaptic membrane specialization, and it appeared to be restricted to postsynaptic elements. Slow excitatory transmission through mGluR5 has gained attention owing to its role in controlling prefrontal cortical activity, working memory

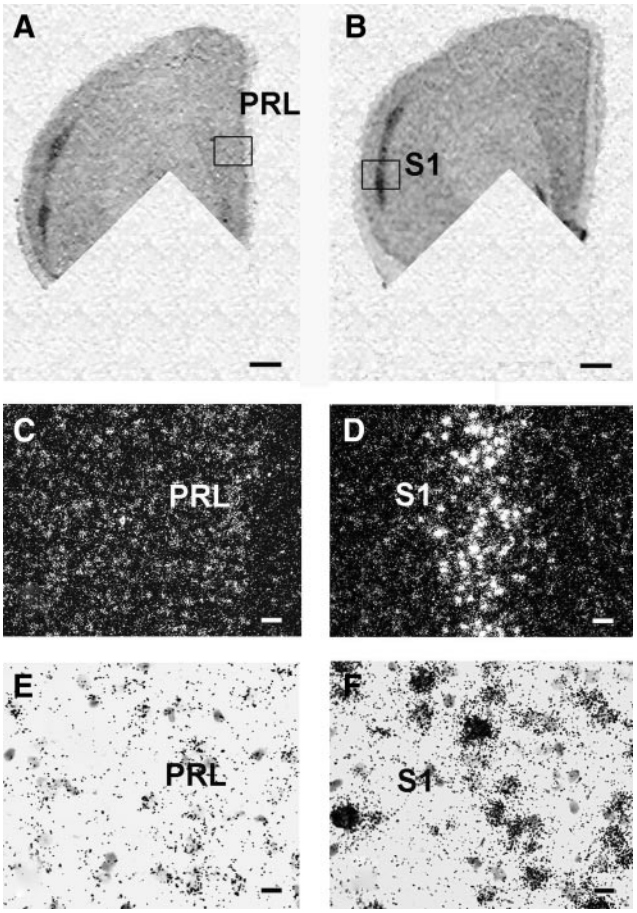

FIG. 4. Detection of CART mRNA using *in situ* hybridization on x-ray film (A and B) and nuclear-track emulsion (C–F). The *black boxes* in A and B correspond to the areas in C and D, respectively. E and F, High-power bright-field images of toluidine blue-counterstained specimens. Clusters of silver grains correspond to individual CART-expressing neurons. PRL, Prelimbic cortex; S1, primary somatosensory cortex. *Scale bars*, 1 mm (A and B), 50 μm (C and D), and 10 μm (E and F).

processes, reward, and synaptic plasticity. A recent paper has shown that DA modulates an mGluR5-mediated depolarization underlying prefrontal persistent activity (82). E2 may modulate cortical activity via down-regulation of mGluR5 transcription.

Adenosine plays a unique role to integrate and fine-tune dopaminergic and glutamatergic neurotransmission. Adenosine exerts its neuromodulatory effects by signaling through specific G protein-coupled receptors (83) including adenosine A2A receptor, which is up-regulated by E2 in the frontal cortex. In the rat brain, dense A2A immunoreactivity was found in the striatum, and light perikaryal labeling was found in various areas including the cerebral cortex (48). A2A stimulates adenylate cyclase and produces excitatory effects in the central nervous system. Activation of central A2A receptors enhances the release of acetylcholine, glutamate, GABA, and DA and opposes the actions of dopamine D2 receptor stimulation (83). Up-regulation of A2A may contribute to the effect of estrogens on dopaminergic neurotransmission.

E2 modulates dopaminergic neurotransmission in the frontal cortex via pre- and postsynaptic mechanisms

Up-regulation of D1A and A2A suggests that E2 modulates dopaminergic neurotransmission in the frontal cortex. In addition, we have found that DARPP-32, one of the major downstream targets of D1 signaling (84), is also up-regulated. Up-regulation of D1 and its downstream target DARPP-32 indicates that E2 may enhance D1-mediated signaling in the rat frontal cortex.

Our study has shown that E2 up-regulates three neuropeptides including neurotensin (NT). NT acts in the central nervous system as a primary neurotransmitter or neuromodulator of classical neurotransmitters. Local administration of NT in the prefrontal cortex produces a significant, long-lasting, and concentration-dependent increase in the extracellular DA and other neurotransmitters such as 5-hydroxytryptamine (49). Up-regulation of NT in the frontal cortex may lead to enhanced extracellular DA level.

Up-regulation of regulators of G protein signaling 9 (Rgs9) also affects dopaminergic neurotransmission. RGS9-2 protein negatively modulates signal transduction, thus playing a key role in brain function and resultant behavioral responses. In particular, there is evidence of important interactions with μ-opioid and dopamine D2 receptor signaling pathways (85).

Based on the validated transcriptional up-regulation of D1A, A2A, NT, and Rgs9, it is likely that E2 affects dopaminergic neurotransmission in the frontal cortex. This conclusion is in agreement with many publications showing E2 effects in other brain regions on the DA system (86).

Up-regulation of CART may contribute to the neuroprotective effects of estradiol in the cortex

CART peptides are widely distributed in the central nervous system and involved in the regulation of many physiological processes (87). The Cart promoter harbors the cAMP response element (CRE) consensus sequence (88), and it drives the expression of Cart in several neuronal cell lines. In the rat cortex, CART is mainly localized in barrel field neurons of the somatosensory cortex (50, 51). We have confirmed this result but observed an additional, weaker Cart expression in many neurons at all layers throughout the female rat frontal cortex.

In the rat frontal cortex, CART is implicated in at least two functions, *i.e.* neuroprotection and behavior. CART peptides show neuroprotective activity *in vivo* and *in vitro* (52). Enhanced CART expression may contribute to E2-mediated neuroprotection in the ischemic cortex. CART-mediated neuroprotection may be linked to preservation of mitochondrial function (53). We have found an E2-

evoked up-regulation of Cart, indicating that E2 induces an important neuroprotective mechanism in the frontal cortex.

There is evidence that CART peptides may be involved in anxiety-like behavior as well. Intracerebroventricular administration of $CART_{55–102}$ increases anxiety-like behavior in rodents, as measured in elevated plus maze and in social interaction tests (89). Cart is down-regulated in the cortex of anhedonic rats (90). Moreover, adolescents carrying a missense mutation in the Cart gene exhibit higher anxiety and depression scores (91).

In summary, we identified 136 transcriptional changes in the rat frontal cortex 24 h after an acute E2 regimen. Of the 136 genes, we found several genes that may be implicated in the beneficial effects of estrogens on cortical function. Modulation of multiple elements of the Ca signaling pathway and dopaminergic neurotransmission as well the regulation of serotonergic and glutamatergic signal processing at the level of transcription may play a role in the cognitive and behavioral effects of estrogens. Up-regulation of CART indicates that E2 induces an important neuroprotective mechanism in the frontal cortex. Our results highlight the importance of genomic responses to E2 in the cerebral cortex.

Acknowledgments

We thank Hajni Bekó and Barna László for their excellent technical work.

Address all correspondence and requests for reprints to: Zsolt Liposits, M.D., Ph.D., D.Sc., Laboratory of Endocrine Neurobiology, Institute of Experimental Medicine, Hungarian Academy of Sciences, Szigony utca 43, Budapest H-1083, Hungary. E-mail:liposits@koki.hu.

This work was supported by grants from the EU FP6 funding (LSHM-CT-2003-503041) and the National Science Foundation of Hungary (OTKA K69127 and T73002).

Disclosure Summary: The authors have nothing to declare.

References

1. **McEwen B** 2002 Estrogen actions throughout the brain. Recent Prog Horm Res 57:357–384
2. **Craig MC, Murphy DG** 2007 Estrogen: Effects on normal brain function and neuro-psychiatric disorders. Climacteric 10(Suppl 2): 97–104
3. **Henderson VW** 2006 Estrogen-containing hormone therapy and Alzheimer's disease risk: understanding discrepant inferences from observational and experimental research. Neuroscience 138:1031–1039
4. **Wise PM, Dubal DB, Rau SW, Brown CM, Suzuki S** 2005 Are estrogens protective or risk factors in brain injury and neurodegeneration? Reevaluation after the Women's Health Initiative. Endocr Rev 26:308–312
5. **Green S, Walter P, Kumar V, Krust A, Bornert JM, Argos P, Chambon P** 1986 Human oestrogen receptor cDNA: sequence, expression and homology to v-erb-A. Nature 320:134–139
6. **Kuiper GG, Enmark E, Pelto-Huikko M, Nilsson S, Gustafsson JA** 1996 Cloning of a novel receptor expressed in rat prostate and ovary. Proc Natl Acad Sci USA 93:5925–5930
7. **Pike AC, Brzozowski AM, Walton J, Hubbard RE, Thorsell AG, Li YL, Gustafsson JA, Carlquist M** 2001 Structural insights into the mode of action of a pure antiestrogen. Structure 9:145–153
8. **Nilsson S, Mäkelä S, Treuter E, Tujague M, Thomsen J, Andersson G, Enmark E, Pettersson K, Warner M, Gustafsson JA** 2001 Mechanisms of estrogen action. Physiol Rev 81:1535–1565
9. **Kuiper GG, Shughrue PJ, Merchenthaler I, Gustafsson JA** 1998 The estrogen receptor β subtype: a novel mediator of estrogen action in neuroendocrine systems. Front Neuroendocrinol 19:253–286
10. **Gronemeyer H, Gustafsson JA, Laudet V** 2004 Principles for modulation of the nuclear receptor superfamily. Nat Rev Drug Discov 3:950–964
11. **Safe S, Kim K, Kim K** 2008 Non-classical genomic estrogen receptor (ER)/specificity protein and ER/activating protein-1 signaling pathways. J Mol Endocrinol 41:263–275
12. **Graber R, Sumida C, Vallette G, Nunez EA** 1993 Rapid and long-term effects of 17β-estradiol on PIP2-phospholipase C-specific activity of MCF-7cells. Cell Signal 5:181–186
13. **Mermelstein PG, Becker JB, Surmeier DJ** 1996 Estradiol reduces calcium currents in rat neostriatal neurons via a membrane receptor. J Neurosci 16:595–604
14. **Abrahám IM, Todman MG, Korach KS, Herbison AE** 2004 Critical in vivo roles for classical estrogen receptors in rapid estrogen actions on intracellular signaling in mouse brain. Endocrinology 145:3055–3061
15. **Toran-Allerand CD, Guan X, MacLusky NJ, Horvath TL, Diano S, Singh M, Conolly Jr ES, Nethrapalli IS, Tinnikov AA** 2002 ER-X: a novel, plasma membrane-associated, putative estrogen receptor that is regulated during development and after ischemic brain injury. J Neurosci 22:8391–8401
16. **Lagrange AH, Ronnekleiv OK, Kelly MJ** 1997 Modulation of G protein-coupled receptors by an estrogen receptor that activates protein kinase A. Mol Pharmacol 51:605–612
17. **Revankar CM, Cimino DF, Sklar LA, Arterburn JB, Prossnitz ER** 2005 A transmembrane intracellular estrogen receptor mediates rapid cell signaling. Science 307:1625–1630
18. **Miller EK, Cohen JD** 2001 An integrative theory of prefrontal cortex function. Annu Rev Neurosci 24:167–202
19. **Arnsten AF** 2009 Stress signaling pathways that impair prefrontal cortex structure and function. Nat Rev Neurosci 10:410–422
20. **Shughrue PJ, Merchenthaler I** 2000 Estrogen is more than just a "sex hormone": novel sites for estrogen action in the hippocampus and cerebral cortex. Front Neuroendocrinol 21:95–101
21. **Tang Y, Janssen WG, Hao J, Roberts JA, McKay H, Lasley B, Allen PB, Greengard P, Rapp PR, Kordower JH, Hof PR, Morrison JH** 2004 Estrogen replacement increases spinophilin-immunoreactive spine number in the prefrontal cortex of female rhesus monkeys. Cerebral Cortex 14:215–223
22. **Paxinos G, Watson C** 1998 The rat brain. New York: Academic Press
23. **Moffatt CA, Rissman EF, Shupnik MA, Blaustein JD** 1998 Induction of progestin receptors by estradiol in the forebrain of estrogen receptor-α gene-disrupted mice. J Neurosci 18:9556–9563
24. **Kalló I, Butler JA, Barkovics-Kalló M, Goubillon ML, Coen CW** 2001 Oestrogen receptor β-immunoreactivity in gonadotropin releasing hormone-expressing neurons: regulation by oestrogen. J Neuroendocrinol 13:741–748
25. **Liposits Z, Sétáló G, Flerkó B** 1984 Application of the silver-gold intensified 3,3′-diamino-benzidine chromogen to the light and electronmicroscopic detection of the luteinizing hormone-releasing hormone system of the rat brain. Neuroscience 13:513–525
26. **Liposits Z, Sherman D, Phelix C, Paull WK** 1986 A combined light

and electron microscopic immunocytochemical method for the simultaneous localization of multiple tissue antigens. Tyrosine hydroxylase immunoreactive innervation of corticotropin releasing factor synthesizing neurons in the paraventricular nucleus of the rat. Histochemistry 85:95–106

27. **Uylings HB, Groenewegen HJ, Kolb B** 2003 Do rats have a prefrontal cortex? Behav Brain Res 146:3–17
28. **Sanna PP, King AR, van der Stap LD, Repunte-Canonigo V** 2005 Gene profiling of laser-microdissected brain regions and sub-regions. Brain Res Protoc 15:66–74
29. **Wu Z, Irizarry RA, Gentleman R, Martinez-Murillo F, Spencer F** 2004 A model-based background adjustment for oligonucleotide expression arrays. J Am Stat Assoc 99:909–917
30. **Smyth G** 2004 Linear models and empirical Bayes methods for assessing differential expression in microarray experiments. Stat Appl Genet Mol Biol 3:Article 3
31. **Benjamini Y, Hochberg Y** 1995 Controlling the false discovery rate: a practical and powerful approach to multiple testing. J Royal Stat Soc Ser B 57:289–300
32. **Gentleman RC, Carey VJ, Bates DM, Bolstad B, Dettling M, Dudoit S, Ellis B, Gautier L, Ge Y, Gentry J, Hornik K, Hothorn T, Huber W, Iacus S, Irizarry R, Leisch F, Li C, Maechler M, Rossini AJ, Sawitzki G, Smith C, Smyth G, Tierney L, Yang JY, Zhang J** 2004 Bioconductor: open software development for computational biology and bioinformatics. Genome Biol 5:R80
33. **Andersen CL, Jensen JL, Ørntoft TF** 2004 Normalization of real-time quantitative reverse transcription-PCR data: a model-based variance estimation approach to identify genes suited for normalization, applied to bladder and colon cancer data sets. Cancer Res 64:5245–5250
34. **Vandesompele J, De Preter K, Pattyn F, Poppe B, Van Roy N, De Paepe A, Speleman F** 2002 Accurate normalization of real-time quantitative RT-PCR data by geometric averaging of multiple internal control genes. Genome Biol 3:RESEARCH0034.1–0034.11
35. **Douglass J, McKinzie AA, Couceyro P** 1995 PCR differential display identifies a rat brain mRNA that is transcriptionally regulated by cocaine and amphetamine. J Neurosci 15:2471–2481
36. **Hrabovszky E, Kalló I, Steinhauser A, Merchenthaler I, Coen CW, Petersen SL, Liposits Z** 2004 Estrogen receptor-β in oxytocin and vasopressin neurons of the rat and human hypothalamus: immunocytochemical and in situ hybridization studies. J Comp Neurol 473: 315–333
37. **Hrabovszky E, Petersen SL** 2002 Increased concentrations of radioisotopically-labeled complementary ribonucleic acid probe, dextran sulfate, and dithiothreitol in the hybridization buffer can improve results of in situ hybridization histochemistry. J Histochem Cytochem 50:1389–1400
38. **Kritzer MF** 2002 Regional, laminar, and cellular distribution of immunoreactivity for ERα and ERβ in the cerebral cortex of hormonally intact, adult male and female rats. Cereb Cortex 12: 116–128
39. **Li C, Liang YY, Feng XH, Tsai SY, Tsai MJ, O'Malley BW** 2008 Essential phosphatases and a phosphor-degron are critical for regulation of SRC-3/AIB1 coactivator function and turnover. Mol Cell 31:835–849
40. **West AE, Chen WG, Dalva MB, Dolmetsch RE, Kornhauser JM, Shaywitz AJ, Takasu MA, Tao X, Greenberg ME** 2001 Calcium regulation of neuronal gene expression. Proc Natl Acad Sci USA 98:11024–11031
41. **Scheidegger KJ, Cenni B, Picard D, Delafontaine P** 2000 Estradiol decreases IGF-1 and IGF-1 receptor expression in rat aortic smooth muscle cells. J Biol Chem 275:38921–38928
42. **Sawai T, Bernier F, Fukushima T, Hashimoto T, Ogura H, Nishizawa Y** 2002 Estrogen induces a rapid increase of calcium-calmodulin-dependent protein kinase II activity in the hippocampus. Brain Res 950:308–311
43. **Liu S, Bubar MJ, Lanfranco MF, Hillman GR, Cunningham KA** 2007 Serotonin2c receptor localization in GABA neurons of the rat medial prefrontal cortex: implications for understanding the neurobiology of addiction. Neuroscience 148:1677–1688
44. **Lee SH, Mouradian MM** 1999 Up-regulation of D1A dopamine receptor gene transcription by estrogen. Mol Cell Endocrinol 156: 151–157
45. **Gaspar P, Bloch B, Le Moine C** 1995 D1 and D2 receptor gene expression in the rat frontal cortex: cellular localization in different classes of efferent neurons. Eur J Neurosci 7:1050–1063
46. **Snyder GL, Fienberg AA, Huganir RL, Greengard P** 1998 A dopamine/D1 receptor/protein kinase A/dopamine- and cAMP-regulated phosphoprotein (Mr 32kDa)/protein phosphatase-1 pathway regulates dephosphorylation of the NMDA receptor. J Neurosci 18: 10297–10303
47. **Shigemoto R, Nomura S, Ohishi H, Sugihara H, Nakanishi S, Mizuno N** 1993 Immunohistochemical localization of a metabotropic glutamate receptor, mGluR5, in the rat brain. Neurosci Lett 163:53–57
48. **Rosin DL, Robeva A, Woodard RL, Guyenet PG, Linden J** 1998 Immunohistochemical localization of adenosine A2A receptors in the rat central nervous system. J Comp Neurol 401:163–186
49. **Petkova-Kirova P, Rakovska A, Zaekova G, Ballini C, Corte LD, Radomirov R, Vágvölgyi A** 2008 Stimulation by neurotensin of dopamine and 5-hydroxytryptamine (5-HT) release from rat prefrontal cortex: possible role of NTR1 receptors in neuropsychiatric disorders. Neurochem Int 53:355–361
50. **Couceyro PR, Koylu EO, Kuhar MJ** 1997 Further studies on the anatomical distribution of CART by in situ hybridization. J Chem Neuroanat 12:229–241
51. **Koylu EO, Couceyro PR, Lambert PD, Kuhar MJ** 1998 Cocaine- and amphetamine-regulated transcript peptide immunohistochemical localization in the rat brain. J Comp Neurol 391:115–132
52. **Xu Y, Zhang W, Klaus J, Young J, Koerner I, Sheldahl LC, Hurn PD, Martínez-Murillo F, Alkayed NJ** 2006 Role of cocaine- and amphetamine-regulated transcript in estradiol-mediated neuroprotection. Proc Natl Acad Sci USA 103:14489–14494
53. **Mao P, Ardeshiri A, Jacks R, Yang S, Hurn PD, Alkayed NJ** 2007 Mitochondrial mechanism of neuroprotection by CART. Eur J Neurosci 26:624–632
54. **Cunha RA, Johansson B, van der Ploeg I, Sebastião AM, Ribeiro JA, Fredholm BB** 1994 Evidence for functionally important adenosine A2a receptors in the rat hippocampus. Brain Res 649:208–216
55. **Pandey GN, Dwivedi Y, Ren X, Rizavi HS, Faludi G, Sarosi A, Palkovits M** 2006 Regional distribution and relative abundance of serotonin(2c) receptors in human brain: effect of suicide. Neurochem Res 31:167–176
56. **Alexander MJ, Miller MA, Dorsa DM, Bullock BP, Melloni Jr RH, Dobner PR, Leeman SE** 1989 Distribution of neurotensin/neuromedin N mRNA in rat forebrain: unexpected abundance in hippocampus and subiculum. Proc Natl Acad Sci USA 86:5202–5206
57. **Belluardo N, Olsson PA, Mudo G, Sommer WH, Amato G, Fuxe K** 2005 Transcription factor gene expression profiling after acute intermittent nicotine treatment in the rat cerebral cortex. Neuroscience 133:787–796
58. **Harlan RE, Shivers BD, Romano GJ, Howells RD, Pfaff DW** 1987 Localization of prepro-enkephalin mRNA in the rat brain and spinal cord by in situ hybridization. J Comp Neurol 258:159–184
59. **Gold SJ, Ni YG, Dohlman HG, Nestler EJ** 1997 Regulators of G-protein signaling (RGS) proteins: region-specific expression of nine subtypes in rat brain. J Neurosci 17:8024–8037
60. **Shughrue PJ, Lane MV, Merchenthaler I** 1997 Comparative distribution of estrogen receptor-α and -β mRNA in the rat central nervous system. J Comp Neurol 388:507–525
61. **Kritzer MF** 2006 Regional, laminar and cellular distribution of immunoreactivity for ERβ in the cerebral cortex of hormonally intact, postnatally developing male and female rats. Cereb Cortex 16:1181–1192
62. **Blurton-Jones M, Tuszynski MH** 2002 Estrogen receptor-β colocalizes extensively with parvalbumin-labeled inhibitory neurons

in the cortex, amygdala, basal forebrain, and hippocampal formation of intact and ovariectomized adult rats. J Comp Neurol 452:276–287
63. **Blurton-Jones M, Kuan PN, Tuszynski MH** 2004 Anatomical evidence for transsynaptic influences of estrogen on brain-derived neurotrophic factor expression. J Comp Neurol 468:347–360
64. **Prange-Kiel J, Rune GM, Leranth C** 2004 Median raphe mediates estrogenic effects to the hippocampus in female rats. Eur J Neurosci 19:309–317
65. **Lâm TT, Leranth C** 2003 Role of the medial septum diagonal band of Broca cholinergic neurons in oestrogen-induced spine synapse formation on hippocampal CA1 pyramidal cells of female rats. Eur J Neurosci 17:1997–2005
66. **Leranth C, Shanabrough M** 2001 Supramammillary area mediates subcortical estrogenic action on hippocampal synaptic plasticity. Exp Neurol 167:445–450
67. **Blurton-Jones M, Tuszynski MH** 2006 Estradiol-induced modulation of estrogen receptor-β and GABA within the adult neocortex: a potential transsynaptic mechanism for estrogen modulation of BDNF. J Comp Neurol 499:603–612
68. **Battiste J, Helms AW, Kim EJ, Savage TK, Lagace DC, Mandyam CD, Eisch AJ, Miyoshi G, Johnson JE** 2007 Ascl1 defines sequentially generated lineage-restricted neuronal and oligodendrocyte precursor cells in the spinal cord. Development 134:285–293
69. **Flames N, Hobert O** 2009 Gene regulatory logic of dopamine neuron differentiation. Nature 458:885–889
70. **Li QX, Ke N, Sundaram R, Wong-Staal F** 2006 NR4A1,2,3: an orphan nuclear hormone receptor family involved in cell apoptosis and carcinogenesis. Histol Histopathol 21:533–540
71. **Wong CW, Komm B, Cheskis BJ** 2001 Structure-function evaluation of ERα and β interplay with SRC family coactivators. ERselective ligands. Biochemistry 40:6756–6765
72. **Kressler D, Schreiber SN, Knutti D, Kralli A** 2002 The PGC-1-related protein PERC is a selective coactivator of estrogen receptor α. J Biol Chem 277:13918–13925
73. **Apostolakis EM, Ramamurphy M, Zhou D, Oñate S, O'Malley BW** 2002 Acute disruption of select steroid receptor coactivators prevents reproductive behavior in rats and unmasks genetic adaptation in knockout ice. Mol Endocrinol 16:1511–1523
74. **O'Malley BW** 2006 Little molecules with big goals. Science 313: 1749–1750
75. **Zheng FF, Wu RC, Smith CL, O'Malley BW** 2005 Rapid estrogen-induced phosphorylation of the SRC-3 coactivator occurs in an extranuclear complex containing estrogen receptor. Mol Cell Biol 25: 8273–8284
76. **Muchekehu RW, Harvey BJ** 2008 17β-Estradiol rapidly mobilizes intracellular calcium from ryanodine receptor-gated stores via a PKC-PKA-Erk-dependent pathway in the human eccrine sweat gland cell line NCL-SG3. Cell Calcium 44:276–288
77. **Wilson MA, Chrysogelos SA** 2002 Identification and characterization of a negative regulatory element within the epidermal growth factor receptor gene first intron in hormone-dependent breast cancer cells. J Cell Biochem 85:601–614
78. **Maor S, Mayer D, Yarden RI, Lee AV, Sarfstein R, Werner H, Papa MZ** 2006 Estrogen receptor regulates insulin-like growth factor-I receptor gene expression in breast tumor cells: involvement of transcription factor Sp1. J Endocrinol 191:605–612
79. **Niswender CM, Herrick-Davis K, Dilley GE, Meltzer HY, Overholser JC, Stockmeier CA, Emeson RB, Sanders-Bush E** 2001 RNA editing of the human serotonin 5-HT2C receptor: alterations in suicide and implications for serotonergic pharmacotherapy. Neuropsychopharmacology 24:478–491
80. **Ariano MA, Sibley DR** 1994 Dopamine receptor distribution in the rat CNS: elucidation using anti-peptide antisera directed against D1A and D3 subtypes. Brain Res 649:95–110
81. **Kruse MS, Prémont J, Krebs MO, Jay TM** 2009 Interaction of dopamine D1 with NMDA NR1 receptors in rat prefrontal cortex. Eur Neuropsychopharmacol 19:296–304
82. **Sidiropoulou K, Lu FM, Fowler MA, Xiao R, Phillips C, Ozkan ED, Zhu MX, White FJ, Cooper DC** 2009 Dopamine modulates an mGluR5-mediated depolarization underlying prefrontal persistent activity. Nat Neurosci 12:190–199
83. **Olah ME, Stiles GL** 1995 Adenosine receptor subtypes: characterization and therapeutic regulation. Ann Rev Pharmacol Toxicol 35: 581–606
84. **Bateup HS, Svenningsson P, Kuroiwa M, Gong S, Nishi A, Heintz N, Greengard P** 2008 Cell type-specific regulation of DARPP-32 phosphorylation by psychostimulant and antipsychotic drugs. Nat Neurosci 11:932–939
85. **Traynor JR, Terzi D, Caldarone BJ, Zachariou V** 2009 RGS9-2: probing an intracellular modulator of behavior as a drug target. Trends Pharmacol Sci 30:105–111
86. **Morissette M, Le Saux M, D'Astous M, Jourdain S, Al Sweidi S, Morin N, Estrada-Camarena E, Mendez P, Garcia-Segura LM, Di Paolo T** 2008 Contribution of estrogen receptors α and β to the effects of estradiol in the brain. J Steroid Biochem Mol Biol 108: 327–338
87. **Rogge G, Jones D, Hubert GW, Lin Y, Kuhar MJ** 2008 CART peptides: regulators of body weight, reward and other functions. Nat Rev Neurosci 9:747–758
88. **Barrett P, Davidson J, Morgan P** 2002 CART gene promoter transcription is regulated by a cyclic adenosine monophosphate response element. Obes Res 10:1291–1298
89. **Chaki S, Kawashima N, Suzuki Y, Shimazaki T, Okuyama S** 2003 Cocaine- and dopamine-regulated transcript peptide produces anxiety-like behavior in rodents. Eur J Pharmacol 464:49–54
90. **Orsetti M, Di Brisco F, Canonico PL, Genazzani AA, Ghi P** 2008 Gene regulation in the frontal cortex of rats exposed to the chronic mild stress paradigm, an animal model of human depression. Eur J Neurosci 27:2156–2164
91. **Miraglia del Giudice E, Santoro N, Fiumani P, Dominguez G, Kuhar MJ, Perrone L** 2006 Adolescents carrying a missense mutation in the CART gene exhibit increased anxiety and depression. Depress Anxiety 23:90–92

20. számú melléklet

Neurochemistry International 56 (2010) 479–486

Contents lists available at ScienceDirect

Neurochemistry International

journal homepage: www.elsevier.com/locate/neuint

Demonstration of vesicular glutamate transporter-1 in corticotroph cells in the anterior pituitary of the rat

Zsuzsa S. Kocsis [a], Csilla S. Molnár [a], Masahiko Watanabe [b], Guy Daneels [c], Dieder Moechars [c], Zsolt Liposits [a,d], Erik Hrabovszky [a,*]

[a] Laboratory of Endocrine Neurobiology, Institute of Experimental Medicine, Hungarian Academy of Sciences, Budapest 1083, Hungary
[b] Department of Anatomy, Hokkaido University School of Medicine, Sapporo, Japan
[c] Johnson & Johnson Pharmaceutical Research and Development, B-2340 Beerse, Belgium
[d] Department of Neuroscience, Faculty of Information Technology (ZL), Pázmány Péter Catholic University, Budapest 1083, Hungary

ARTICLE INFO

Article history:
Received 8 December 2009
Accepted 11 December 2009
Available online 16 December 2009

Keywords:
ACTH
Adenohypophysis
Anterior lobe
Glutamate
VGLUT1

ABSTRACT

Recent immunohistochemical studies of the rat adenohypophysis identified type-2 vesicular glutamate transporter (VGLUT2), a marker for glutamatergic neuronal phenotype, in high percentages of adenohypophysial gonadotrophs and thyrotrophs. The presence and molecular identity of amino acid neurotransmitters in the remaining hormone producing cell types are unknown. In the present study we addressed the putative synthesis of another glutamatergic marker, VGLUT1 by adenohypophysial cells. Immunohistochemical studies revealed VGLUT1 immunoreactivity in a small subset of polygonal medium-sized cells in the anterior lobe. Western blot analysis revealed a single major 60 kDa protein band in the adenohypophysis. Furthermore, the expression of VGLUT1 mRNA was confirmed by reverse transcription-polymerase chain reaction followed by sequence analysis of the amplicon. In contrast with rats which only showed VGLUT1 signal in the anterior lobe of the pituitary, mice contained high levels of VGLUT1 immunoreactivity in the intermediate, in addition to the anterior lobe. No signal was present in VGLUT1-knockout mice, providing evidence for specificity. In rats, results of colocalization studies with dual-immunofluorescent labeling provided evidence for VGLUT1 immunoreactivity in 45.9% of corticotrophs and 7.7% of luteinizing hormone β-immunopositive gonadotrophs. Cells of the other peptide hormone phenotypes were devoid of VGLUT1 signal. A few cells in the adenohypophysis expressed both VGLUT1 and VGLUT2 immunoreactivities. The presence of the glutamate markers VGLUT1 and VGLUT2 in distinct populations of peptide hormone-secreting hypophysial cells highly indicates the involvement of endogenous glutamate release in autocrine/paracrine regulatory mechanisms. The biological function of adenohypophysial glutamate will require clarification.

1. Introduction

L-Glutamate acts as the primary mediator of excitatory synaptic transmission in the central nervous system (Somogyi et al., 1986; Storm-Mathisen et al., 1983), including the endocrine hypothalamus (van den Pol et al., 1990). The recently discovered vesicular glutamate transporter isoforms (VGLUT1-3) selectively accumulate L-glutamate into synaptic vesicles in distinct subsets of excitatory axon terminals (Bellocchio et al., 2000; Fremeau et al., 2001, 2002; Fujiyama et al., 2001; Gras et al., 2002; Hackett and de la Mothe, 2009; Herzog et al., 2001; Lin et al., 2003; Sakata-Haga et al., 2001; Schafer et al., 2002; Zeng et al., 2009; Ziegler et al., 2002), thus serving also as immunohistochemical markers for glutamatergic neurons. Glutamate contributes to non-synaptic mechanisms, in addition to regulating synaptic neurotransmission (Vizi and Mike, 2006). Synthesis of the VGLUT2 transporter isoform has been observed in various neuroendocrine systems of the hypothalamus, raising the possibility of glutamate secretion at neurohemal junctions in the median eminence and the posterior lobe of the hypophysis (Hrabovszky et al., 2004, 2005a, 2005b, 2006a; Kawasaki et al., 2005; Lin et al., 2003; Ziegler et al., 2002). For reviews of putative functions that glutamate may play as a neuroendocrine secretion product, see Hrabovszky and Liposits (2007, 2008).

The occurrence of the VGLUT isoforms is not confined to neuronal cells but also characterizes secretory cells in various endocrine glands (Moriyama and Yamamoto, 2004). Among others, these include alpha and F cells of the pancreatic Langerhans islets, intestinal L cells (Hayashi et al., 2001, 2003) and pinealocytes of the pineal gland (Hayashi et al., 2001; Morimoto et al., 2003).

* Corresponding author at: Laboratory of Endocrine Neurobiology, Institute of Experimental Medicine, P.O. Box 67, 1450 Budapest, Hungary.
Tel.: +36 1 210 9400/366; fax: +36 1 210 9944.
E-mail address: hrabovszky@koki.hu (E. Hrabovszky).

0197-0186/$ – see front matter © 2009 Elsevier Ltd. All rights reserved.
doi:10.1016/j.neuint.2009.12.007

While studying VGLUT2 immunoreactivity in magnocellular neurosecretory terminals of the posterior hypophysial lobe (Hrabovszky et al., 2006a), we have observed a cell group in the anterior pituitary which exhibited VGLUT2 immunoreactivity (Hrabovszky et al., 2006b). Specificity of the VGLUT2 immunolabeling was confirmed using different VGLUT2 antibodies for dual-label immunohistochemistry and the *in situ* hybridization detection of VGLUT2 mRNA expression in the adenohypophysis. The synthesis of VGLUT2 was confined to subsets of gonadotroph and thyrotroph cells and regulated in different endocrine paradigms. Notable, VGLUT2 mRNA expression of the adenohypophysis was increased in response to estrogen treatment of ovariectomized female rats as well as to hypothyroidism induced by chemical ablation of the thyroid gland in male rats (Hrabovszky et al., 2006b).

Because VGLUT2 was only present in gonadotrophs and thyrotrophs (Hrabovszky et al., 2006b) and the presence and molecular identity of amino acid neurotransmitters in the remaining hormone producing cell types of the anterior pituitary remained unknown, in the present studies we raised the possibility that VGLUT1, instead of VGLUT2, confers a glutamatergic phenotype to other cell types of the adenohypophysis, including somatotroph, lactotroph and corticotroph cells. The presence of VGLUT1 in the adenohypophysis of the rat was studied first with immunohistochemistry. Labeling specificity was confirmed with Western blot analysis, reverse transcription-polymerase chain reaction (RT-PCR) and the use of VGLUT1-knockout tissues as a negative control in immunohistochemistry. Finally, the phenotype of VGLUT1 containing anterior lobe cells was determined using immunofluorescent approaches.

2. Experimental procedures

2.1. Immunohistochemistry on rat tissues

2.1.1. Tissue preparation

Adult male Wistar rats ($N = 4$; 200–225 g bw) were purchased from the local breeding colony of the Medical Gene Technology Unit of the Institute of Experimental Medicine and maintained under a 12:12 h day–night schedule (lights on 0700–1900; 22 °C), in a temperature (22 ± 2 °C) and humidity (60 ± 10%) controlled environment with free access to laboratory rat food (Sniff Spezialdiaeten GmbH, Soest, Germany) and tap water. All experiments were carried out in accordance with the Council Directive of 24 November 1986 of the European Communities (86/609/EEC) and were reviewed and approved by the Animal Welfare Committee of the Institute of Experimental Medicine (47/003/2005).

To collect pituitaries for immunohistochemical experiments, three rats were deeply anaesthesized with pentobarbital (35 mg/kg bw, ip) and perfused transcardially, first with 20 ml of 0.1 M phosphate buffered saline (PBS; pH 7.4), and then with 150 ml fixative solution containing 4% paraformaldehyde (Sigma Chemical Company, St. Louis, MO, USA) in PBS. The glands were immersed into 20% sucrose for 36 h than surrounded with egg-yolk and exposed to formalin fume for 48 h as recommended for the processing of soft histological specimens (Martin et al., 1983). The hardened pituitary blocks were snap-frozen on powdered dry ice and sectioned at 20 μm with a Leica SM 2000R freezing microtome (Leica Microsystems, Nussloch GmbH, Nussloch, Germany). Endogenous peroxidase activity was eliminated and sections were permeabilized by a 30-min incubation in 1% H_2O_2 and 0.4% Triton X-100 in PBS. Then the tissues were treated with 2% normal horse serum (NHS) in Tris buffered saline (TBS; 0.1 M Tris–HCl with 0.9% NaCl; pH 7.8) to prevent non-specific binding of the antibodies.

2.1.2. Demonstration of VGLUT1 and VGLUT2-immunoreactive adenohypophysial cells with peroxidase immunohistochemistry

Floated sections were incubated in either a goat polyclonal VGLUT1 antiserum (Brumovsky et al., 2007) (used at 1:2000) or a commercial rabbit polyclonal VGLUT1 antiserum (#135302; SYnaptic SYstems, Göttingen, Germany; 1:2000) for 72 h (4 °C). VGLUT2 cells were visualized using rabbit polyclonal antibodies from SYnaptic SYstems (#135402; 1:2000). The primary antibody step was followed by sequential treatments with species-specific biotinylated secondary antibodies (Jackson ImmunoResearch Laboratories, West Grove, PA, USA; 1:1,000) for 2 h and ABC Elite working solution (1:1000; Vector Laboratories, Burlingame, CA, USA) for 1 h at room temperature. Finally, the peroxidase signal was visualized with a 3,3′-diaminobenzidine tetrahydrochloride (DAB) containing developer, in the presence of nickel ions. Negative control experiments included omission of the primary or the secondary antibodies from the labeling procedure. In addition, control experiments were carried out with the working solutions of the SYnaptic SYstems VGLUT1 and VGLUT2 antibodies that had been preabsorbed overnight with 5 μg/ml of fusion proteins used for immunizations (135-3P and 135-4P, respectively; SYnaptic SYstems). Following chromogen deposition, the immunostained pituitary sections were mounted on microscope slides from Elvanol, air-dried, dehydrated with 95% (5 min), followed by 100% (2× 5 min) ethanol, cleared with xylene (2× 5 min), coverslipped with DPX mounting medium (Fluka Chemie, Buchs, Switzerland) and studied with an Axiophot microscope (Zeiss, Göttingen, Germany) equipped with an RT Spot digital camera (Diagnostic Instrument, Sterling Heights, MI).

2.1.3. Characterization of VGLUT1-immunoreactive adenohypophysial cells using dual-immunofluorescent labeling

Positive control experiments to address further the specificity of VGLUT1 immunoreactivity applied the mixture of the goat and the rabbit VGLUT1 primary antibodies to the same tissue sections for dual-labeling, similarly to recently used strategies to establish the specificity of hypothalamic (Hrabovszky et al., 2004, 2005b) and adenohypophysial (Hrabovszky et al., 2006b) VGLUT2 signals. The cocktail of goat (1:2000) and rabbit (1:1000) VGLUT1 primary antibodies was applied for 3 days (4 °C), which was followed by a 12-h incubation (4 °C) of sections in a cocktail of Cy3-conjugated anti-goat IgG and FITC-conjugated anti-rabbit IgG (Jackson ImmunoResearch; 1:250 ea).

To determine the functional phenotype of adenohypophysial cells synthesizing VGLUT1, dual-immunofluorescent experiments were carried out. The immunofluorescent visualization of VGLUT1 was followed by the labeling of adenohypophysial hormone markers. Sections were first incubated in the goat VGLUT1 antibodies (1:2000) for 72 h (4 °C), then in biotinylated secondary antibodies (Jackson ImmunoResearch; 1:1000) for 2 h and Cy3-conjugated streptavidin (Jackson ImmunoResearch; 1:250) for 12 h. Subsequently, the sections were incubated in one of the following polyclonal antisera: rabbit anti-rat adrenocorticotropic hormone (ACTH), guinea pig anti-rat prolactin (PRL), guinea pig anti-rat luteinizing hormone β (LHβ), guinea pig anti-rat thyroid stimulating hormone β (TSHβ), guinea pig anti-rat follicle-stimulating hormone β (FSHβ; each from the National Hormone and Peptide Program, NHPP, NIDDK; 1:2000) or rabbit anti-rat growth hormone (GH; Accurate, Westbury, NY, USA; 1:1000). The incubations in anti-hormone primary antibodies were followed by FITC-conjugated secondary antibodies (Jackson ImmunoResearch; 1:250) for 12 h (4 °C).

To also address the issue of whether or not, VGLUT1 and VGLUT2 are co-contained in the same anterior lobe cells, the goat VGLUT1 and the rabbit VGLUT2 antisera were applied to the sections in a cocktail for 72 h (4 °C), then reacted with a mixture of anti-goat FITC and anti-rabbit-Cy3 for 12 h (4 °C).

The immunofluorescent specimens were mounted on glass slides from 0.05 M Tris/HCl solution (pH 7.8), dried and coverslipped with Vectashield mounting medium (Vector Laboratories). Dual-immunofluorescent specimens were analyzed with a Radiance 2100 confocal microscope (Bio-Rad Laboratories, Hemel Hempstead, UK) using laser excitation lines 488 nm for FITC and 543 nm for Cy3 and dichroic/emission filters 560 nm/500–530 nm for FITC and 560–610 nm for Cy3. To eliminate emission cross-talk, single optical slices (<0.7 μm) were collected in "lambda strobing" mode so that only one excitation laser and the corresponding emission detector were active during a line scan (Hrabovszky et al., 2005a). The digital images were processed with the Adobe PhotoShop 7.0 software at 300 dpi resolution.

2.1.4. Quantitative analysis to determine the percent ratios of different adenohypophysial cell types with VGLUT1

From each of three rats and for each dual-labeling experiment, digital photographs were analyzed quantitatively to estimate the percent ratios of the distinct cell types with VGLUT1. The results were expressed as the mean of 3 rats ± SEM.

2.1.5. Western blot analysis

The Western blot analysis was carried out using the BM Chemiluminescence Western Blotting Kit from Roche Molecular Biochemicals (Indianapolis, IN), as described (Curcio-Morelli et al., 2003). In brief, tissue extracts were prepared from the anterior pituitary lobes (pooled from four adult male rats) as well as from a piece of the prefrontal cerebral cortex of an adult male rat. 80 μg of tissue homogenate was separated in each lane by sodium dodecyl sulfate-polyacrylamide gel electrophoresis (SDS-PAGE) using a 10% polyacrylamide gel and blotted onto polyvinylidene difluoride (PVDF) membranes (Millipore). The blots were probed with the rabbit and the goat primary antisera (1:1000), reacted with peroxidase-labeled secondary antibodies (Jackson ImmunoResearch; 1:1000) and visualized using chemiluminescence.

2.2. Demonstration of adenohypophysial VGLUT1 synthesis using reverse transcription-polymerase chain reaction

To demonstrate adenohypophysialVGLUT1 mRNA synthesis, one rat was decapitated and its skull opened. The pituitary and a tissue piece from the frontal cortex where VGLUT1 is expressed were removed and immersed into RNAlater (Ambion, Inc, Austin, TX). Twenty-four hours later the adenohypophysis was isolated from the intermediate and posterior lobes under a preparation microscope. Total RNA was isolated from the adenohypophysial block as well as from the cortical block with TRIzol reagent (Invitrogen, Carlsbad, CA). Three μg of total RNA

was reverse transcribed from each sample using oligo-dT primers and the SuperScript III reverse transcriptase (Invitrogen) in a 20 μl reaction volume. One μl of the first-strand cDNA was used for polymerase chain reaction (PCR). Intron-spanning primers (forward: CCTGGTACAGTATTCAGGATG; reverse: GGTGAGG-CAGTGCCGACA) were designed for exon-to-exon PCR reactions so that the expected 365-bp final amplicon corresponded to bases 766–1130 of the rat VGLUT1 mRNA (EU253553). Cortical cDNA was used as a positive control for VGLUT1 amplification, whereas the cDNA was replaced with H_2O for use as a no-template PCR control. The PCR reactions included an initial denaturation at 94 °C for 2 min, 35 amplification cycles (denaturation at 94 °C for 40 s, primer annealing at 56 °C for 60 s, extension at 72 °C for 60 s) and a final extension at 72 °C for 7 min. The PCR products were size-fractionated by electrophoresis in 1% agarose gels in the presence of ethidium bromide. The product amplified from the adenohypophysial sample was excised from the gel, purified with the QIAquick gel Extraction Kit (Qiagen, Valencia, CA) and custom-sequenced (BIOMI Ltd., Godollo, Hungary) with the VGLUT1 forward primer.

2.3. Immunohistochemical control experiments using mouse hypophyses

Adult male CD1 mice ($N = 3$) from the Medical Gene Technology Unit of the Institute of Experimental were used in experiments to study the normal distribution of VGLUT1 immunoreactivity in the mouse hypophysis. The mice were anaesthesized with pentobarbital, perfused with 4% paraformaldehyde through the ascending aorta and their hypophyses were processed for the immunohistochemical detection of VGLUT1 with the goat VGLUT1 primary antiserum, as described for rat sections. In addition, the hypophyses of 3-week old homozygous ($N = 3$; VGLUT1$^{-/-}$) and heterozygous ($N = 3$; VGLUT1$^{+/-}$) VGLUT1-knockout mice were used in control experiments to verify the specificity of hypophysial VGLUT1 immunolabeling. The experiments were carried out in accordance with the European Communities Council Directives (86/609/EEC) and were approved by the local ethical committee at Johnson & Johnson Pharmaceutical Research and Development. The generation and phenotypic characterization of these mice have been detailed elsewhere (Balschun et al., 2009; Leo et al., 2009). The animals were killed by decapitation. Their hypophyses were immersion-fixed in 4% paraformaldehyde overnight and then infiltrated with 20% sucrose for 36 h. Section preparation and immunohistochemical processing of VGLUT1$^{+/-}$ and VGLUT1$^{-/-}$ with the goat anti-VGLUT1 antiserum and peroxidase-based immunohistochemistry was carried out as for sections from normal adult rats and mice.

3. Results

3.1. Immunohistochemical detection of type-1 vesicular glutamate transporter (VGLUT1) in the adenohypophysis

When used for peroxidase-based immunohistochemistry, the rabbit (Fig. 1A) as well as the goat (Fig. 1B) VGLUT1 antibodies labeled the cytoplasm of a small subset of medium-sized adenohypophysial cells. The immunopositive cells exhibited irregular or polygonal shapes. Dual-immunofluorescent detection of VGLUT1 with the two primary antibodies showed that the two antisera labeled identical cells (Fig. 1C and D). Omission of the primary or secondary antibodies from the labeling procedure resulted in the absence of immunolabeling in all cases. The VGLUT1 signals were absent following the use of the rabbit (Fig. 1E) and the goat (Fig. 1F) primary antibody solutions that had been pre-absorbed overnight with the VGLUT1 immunization antigen from SYnaptic SYstems (135-3P). When the peroxidase reaction was used for the detection of VGLUT2, large cells with rounded contours were labeled (Fig. 1G). The different morphology of VGLUT1- and VGLUT2-immunoreactive elements highly indicated

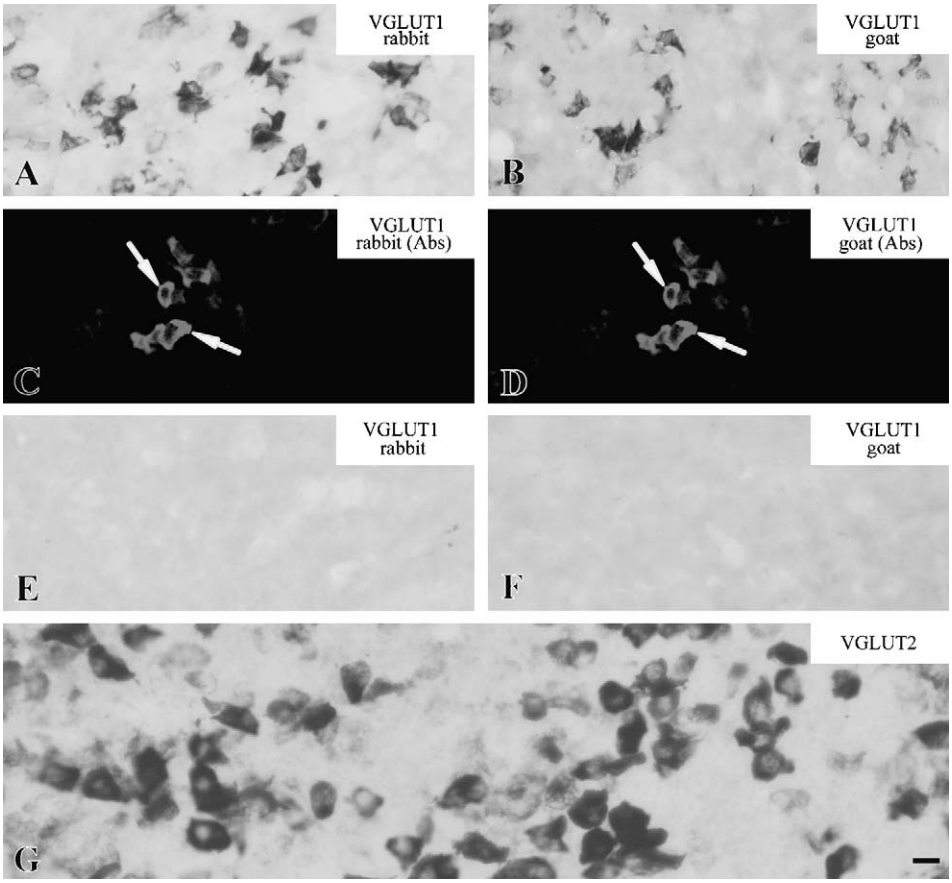

Fig. 1. Immunohistochemical detection of type-1 vesicular glutamate transporter (VGLUT1) in the adenohypophysis of the male rat. (A and B) High-power digital photomicrographs of hypophysial sections immunostained for VGLUT1 with rabbit (A) and goat (B) polyclonal antibodies and peroxidase immunohistochemistry (Ni-DAB chromogen) reveal a small subset of adenohypophysial cells which exhibit cytoplasmic VGLUT1 immunoreactivity. The immunostained cells have polygonal shape and medium size. (C and D) Dual-immunofluorescent detection of VGLUT1 with the rabbit and goat primary antibodies and secondary antibody-conjugated Cy3 and FITC fluorochromes, respectively, show dual-fluorescent labeling of the same cells (arrows), highly indicating that labeling is specific to VGLUT1. (E and F) Similarly, lack of immunolabeling with primary antisera preabsorbed with the immunization antigen supports specificity of labeling. (G) The immunohistochemical detection of VGLUT2 with peroxidase immunohistochemistry and Ni-DAB chromogen reveals large round cells. This morphology of VGLUT2 cells is distinct from those of VGLUT1 cells in A–D. Scale bar = 10 μm.

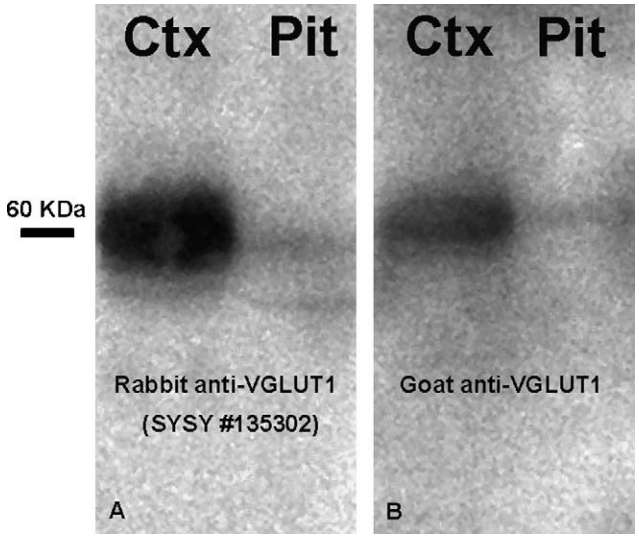

Fig. 2. Western blot on cortical and adenohypophysial homogenates using two different polyclonal antibodies against VGLUT1. In the cerebral cortex (Ctx) a dominant band of ~60 kDa was detected using both the rabbit (A) and goat (B) polyclonal VGLUT1 antibodies. The same band is detectable in anterior pituitary lobe (Pit) homogenates. Note that a weaker band of lower molecular weight could be seen with the rabbit antiserum in cortical and hypophysial samples in (A). This band was absent when using the goat antiserum in (B). This highly specific goat antiserum was used in dual-label immunofluorescent experiments to determine the endocrine phenotype of VGLUT1-immunoreactive cells.

that the two transporter isoforms occur in distinct classes of adenohypophysial cells.

3.2. Visualization of VGLUT1 with Western blot analysis

The rabbit as well as the goat VGLUT1 antisera revealed a major band of the expected 60 kDa size in the cerebral cortex. The same band was observed in adenohypophysial homogenates using both antisera (Fig. 2).

3.3. Demonstration of adenohypophysial VGLUT1 mRNA expression with reverse transcription-polymerase chain reaction

The amplification of cortical and adenohypophysial cDNA samples with PCR resulted in a single amplicon in both the cortical and the adenohypophysial samples. The product exhibited the predicted size (about 365 bp) and was absent if the cDNA was omitted from the reaction (Fig. 3). The adenohypophysial amplicon was excised and purified from the gel. Its base sequence analysis verified that the product corresponded to the expected VGLUT1 fragment. The detection of the authentic VGLUT1 mRNA in the adenohypophysis supports further the concept that the immunohistochemical signal for VGLUT1 is specific.

3.4. Visualization of VGLUT1 in the hypophysis of wild-type and knockout mice

An interesting species difference was noticed in that VGLUT1 immunolabeling in rats was confined to the anterior lobe (Fig. 4A), whereas adult male mice exhibited a relatively strong VGLUT1 immunolabeling in the intermediate, in addition to the anterior lobe of the pituitary (Fig. 4B). A similar labeling pattern was also noticed in the anterior and intermediate lobes of 3-week-old heterozygous VGLUT1-knockout mice ($VGLUT1^{+/-}$). As expected, no immunohistochemical labeling was observed in hypophysial sections of the age-matched homozygous knockout mice ($VGLUT1^{-/-}$), indicating labeling specificity for the authentic VGLUT1 in both the anterior and the intermediate lobes.

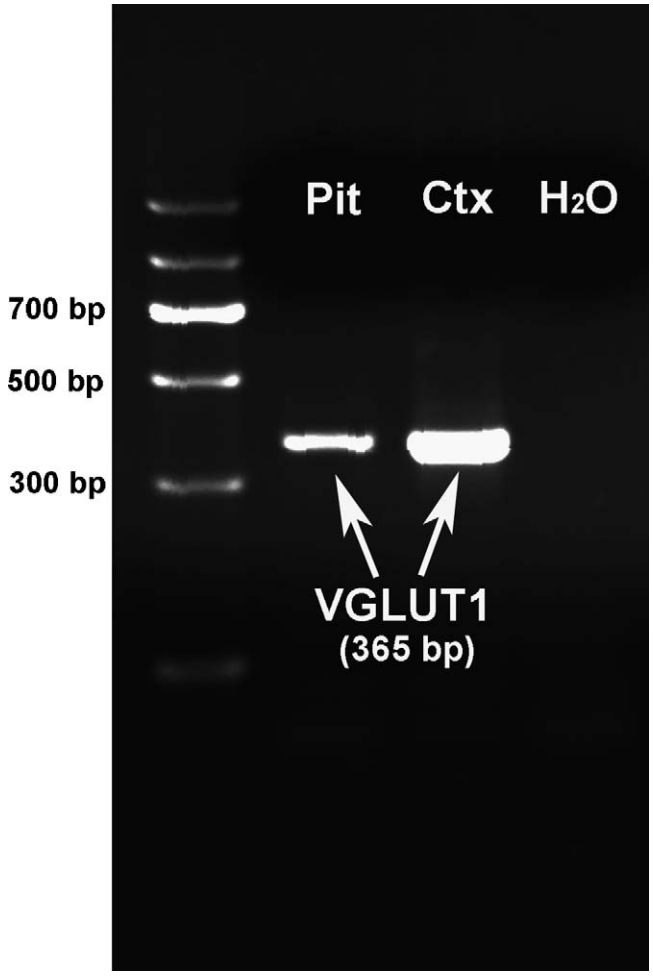

Fig. 3. Demonstration of VGLUT1 mRNA expression in the adenohypophysis using reverse transcription-polymerase chain reaction. Amplification of a 365-bp fragment of VGLUT1 cDNA was carried out from anterior pituitary (Pit) and cortical (Ctx) cDNAs using intron-spanning primers. Control lane (H_2O) shows absence of the specific reaction product if template cDNA is replaced with H_2O. The band containing the 365-bp PCR amplicon from the adenohypophysis was excised and purified from the gel and its nucleotide sequence was confirmed.

3.5. Immunofluorescent experiments in rats to determine the functional phenotype of VGLUT2 expressing adenohypophysial cells

The analysis of a series of sections dual-labeled for VGLUT1 and one of the hypophysial peptide hormones, established that VGLUT1 immunoreactivity occurred in a relatively large subset of ACTH-immunoreactive corticotroph cells (Fig. 5A–C) and a small subset of LHβ-immunoreactive gonadotrophs (Fig. 5F). In contrast, VGLUT1 was absent from the FSHβ-immunoreactive gonadotrophs as well as from GH- (Fig. 5D), TSHβ- (Fig. 5G) and PRL-immunoreactive cells (Fig. 5H). A quantitative analysis showed the presence of VGLUT1 in 45.9 ± 1.8% of corticotrophs and 7.7 ± 0.9% of LHβ-immunoreactive gonadotrophs (Fig. 6). The simultaneous detection of VGLUT1 and VGLUT2 confirmed that the two transporters were expressed by distinct cell types, although a low percentage of labeled cells contained both VGLUT1 and VGLUT2 (Fig. 5I).

4. Discussion

The results of this study provided immunohistochemical evidence that the glutamatergic phenotype marker VGLUT1 is present in 45.9% of adenohypophysial corticotrophs and 7.7% of LHβ synthesizing gonadotrophs in rats. Support for the specificity

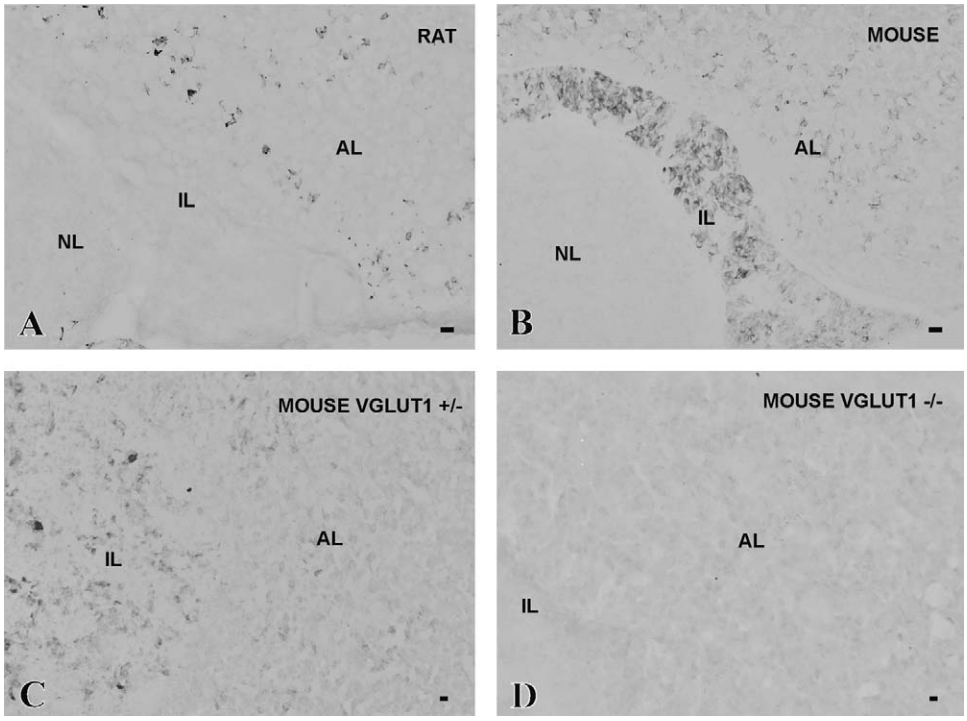

Fig. 4. Immunohistochemical studies of VGLUT1 in the pituitary of wild-type and VGLUT1-knockout mice. Whereas adult male rats (A) exhibit VGLUT1 immunoreactivity in the anterior lobe (AL) but not in the intermediate (IL) and the neural (NL) lobes, adult male mice (B) contain VGLUT1-immunoreactive cells in both the AL and IL. The distinct labeling pattern of rat and mouse sections with the goat VGLUT1 antibodies reveals a species difference. (C and D) Control studies to demonstrate the specificity of VGLUT1 immunolabeling provide evidence for VGLUT1-immunoreactive cells in the AL and the IL of 3-week-old heterozygous VGLUT1-knockout ($VGLUT1^{+/-}$) mice. The lack of any immunolabeling in 3-week-old homozygous knockouts (D; $VGLUT1^{-/-}$) provides evidence for the synthesis of the authentic VGLUT1 protein in the AL and the IL of mice. Scale bars = 20 μm.

of VGLUT1 detection was presented using multiple approaches. These included the application of two distinct primary antisera with identical results for immunofluorescence, the identification of a protein band of the appropriate size on Western blots, the demonstration of VGLUT1 mRNA expression in the anterior pituitary with RT-PCR followed by nucleotide sequence analysis, and finally, the absence of immunohistochemical labeling in the hypophyses of the $VGLUT1^{-/-}$ mice.

The different VGLUT isoforms occur in distinct classes of glutamatergic neurons in the nervous system (Bellocchio et al., 1998, 2000; Fremeau et al., 2001, 2002; Fujiyama et al., 2001; Gras et al., 2002; Hackett and de la Mothe, 2009; Herzog et al., 2001; Lin et al., 2003; Sakata-Haga et al., 2001; Schafer et al., 2002; Zeng et al., 2009; Ziegler et al., 2002). The functional significance of this segregation is presently unclear. Interestingly, in this study we found the VGLUT1 and VGLUT2 isoforms together in a very small subset of adenohypophysial cells. Although we have not carried out triple-labeling experiments to identify the hormonal phenotype of these VGLUT1/VGLUT2 cells, some of them likely belong to LH-secreting gonadotrophs. Notably, 93% of LHβ cells contained VGLUT2 immunoreactivity in our previous study (Hrabovszky et al., 2006b) and 7.7% contained VGLUT1 in the present study. Together with the previous observation of the VGLUT2 transporter isoform in thyrotroph and gonadotroph cells, our present findings delineate three adenohypophysial cell populations (gonadotrophs, thyrotrophs and corticotrophs) which are likely capable of accumulating glutamate into secretory vesicles for a regulated secretion upon need. It needs to be established whether somatotroph and lactotroph cells, which contain neither VGLUT2 nor VGLUT1, contain any amino acid transmitter, in addition to peptide hormones. While we were processing the hypophyses of VGLUT1-knockout mice for control experiments, we have noticed an interesting species difference between rats and mice in that VGLUT1 was present at high relative levels in the intermediate lobe of the mouse, but not the rat, pituitary. A biosynthetic feature shared by anterior lobe corticotrophs and intermediate lobe melanotrophs is the synthesis of the same preproopiomelanocortin peptide precursor.

Future studies need to establish, whether or not, VGLUT1 synthesis in corticotrophs is regulated under endocrine conditions when ACTH secretion is altered. Kawasaki et al. as well as our laboratory (Hrabovszky et al., 2006a; Kawasaki et al., 2005) have found that hyperosmotic stimulation of magnocellular vasopressin neurons in the hypothalamus increases their VGLUT2 mRNA synthesis. The expression of VGLUT2 mRNA also appears to be strongly regulated in the adenohypophysis. In previous studies we carried out endocrine manipulations of the thyroid and gonadal axes, followed by the quantitative *in situ* hybridization analysis of adenohypophysial VGLUT2 mRNA expression (Hrabovszky et al., 2006b). The results of these studies established the upregulation of adenohypophysial VGLUT2 mRNA synthesis in response to estrogen given to ovariectomized female rats or to hypothyroidism induced by methimazole in male rats (Hrabovszky et al., 2006b). A putative regulatory response of VGLUT1 synthesis in ACTH cells to specific stimulation by stress, needs to be addressed. Also, if enhanced VGLUT synthesis is accompanied by increased glutamate release requiring clarification. In the nervous tissue, altered VGLUT1 and VGLUT2 synthesis can change quantal size and influence excitatory postsynaptic currents in glutamatergic synapses (Erickson et al., 2006; Wojcik et al., 2004). It has to be noted that glutamate released into the extracellular space also acts via binding to non-synaptic glutamate receptors (Vizi and Mike, 2006). In the absence of synapses at release sites, glutamate secretion from neuroendocrine/endocrine cells also acts via non-synaptic glutamate receptors and putative autocrine/paracrine mechanisms. The regulated synthesis of VGLUT in these cells likely

dc_27_10

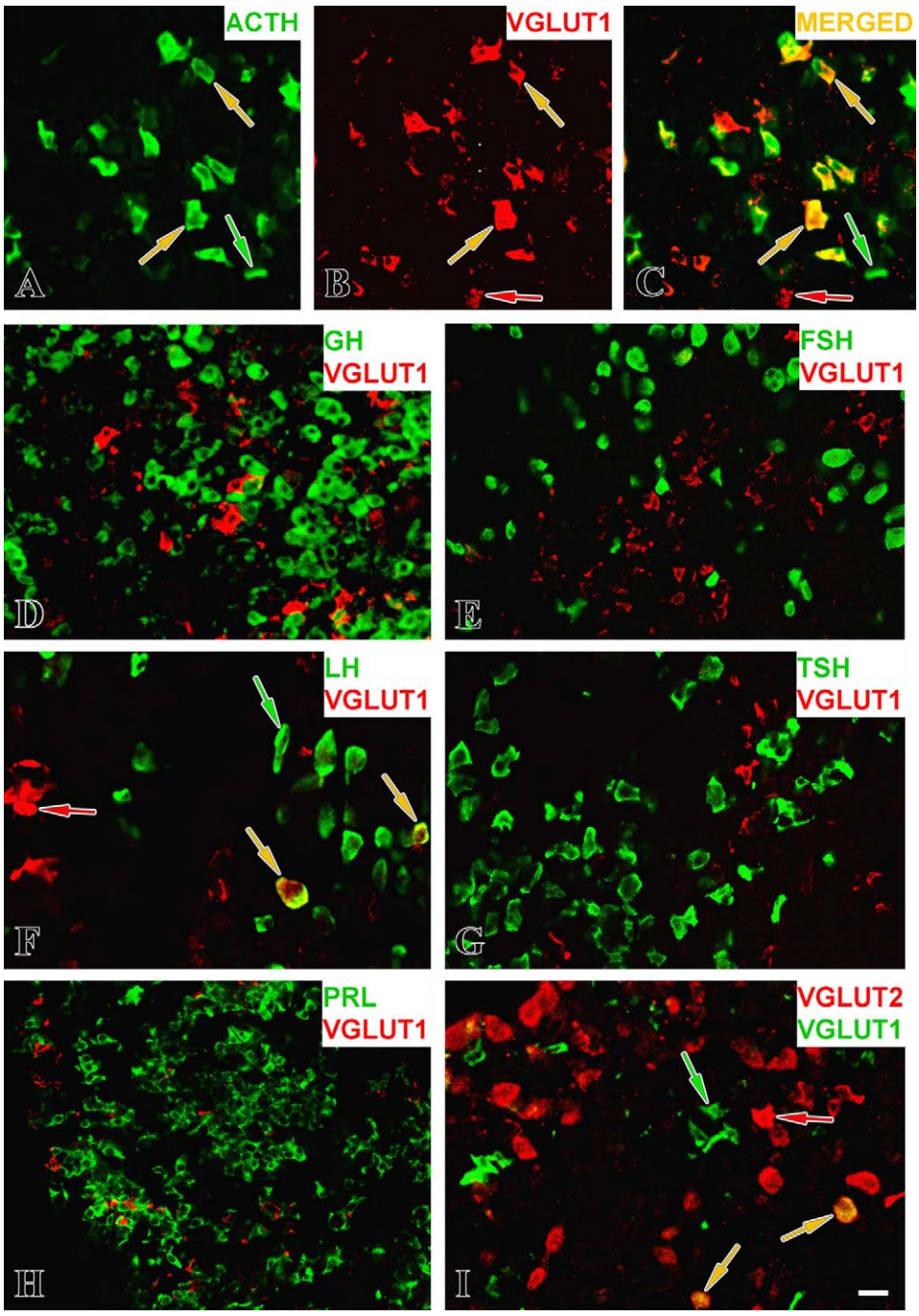

Fig. 5. Results of dual-immunofluorescent studies with confocal microscopy to determine the endocrine phenotype of VGLUT1-expressing adenohypophysial cells. (A–C) Yellow arrows point to a large subset of adrenocorticotropin (ACTH)-immunoreactive (green) cells (yellow cells in merged figure; C) which show co-labeling with the VGLUT1 antiserum (red color). Results of these dual-immunofluorescent studies reveal VGLUT1 in 46% of the corticotrophs. Note that cases of single-labeling for both ACTH and VGLUT1 exist. These are indicated by the red and green arrows, respectively. (D–H) The simultaneous detection of VGLUT1 and growth hormone (GH; D), VGLUT1 and follicle-stimulating hormone β (FSH; E), VGLUT1 and luteinizing hormone β (LH; F), VGLUT1 and thyroid stimulating hormone β (TSH; G), VGLUT1 and prolactin (PRL; H) result in the absence of double-labeled cells (lack of yellow color in merged figures), except for a small population (8%) of LH cells which are VGLUT1-immunoreactive (yellow arrows in panel F). (I) The simultaneous detection of VGLUT1 and VGLUT2 mostly reveal distinct cell populations with different sizes and morphological features. Note that a small subset of the cells contains both transporters (yellow arrows). Scale bar = 20 μm.

reflects a regulated release of glutamate for a local autocrine/paracrine communication.

In order to understand the functional consequences of glutamate release from anterior lobe cells, the identification of glutamate target cells and the pharmacological/molecular characterization of glutamate receptors will be of prime importance. Glutamate likely acts locally within the hypophysis. Accordingly, various AMPA receptor subunits (Kiyama et al., 1993), NMDAR1 (Bhat et al., 1995) and group II metabotropic glutamate receptors (mGLUR2/3) (Caruso et al., 2004) have been revealed in the gland. Interestingly, mGLUR2/3 was identified on somatotrophs and lactotrophs (Caruso et al., 2004) which contain neither VGLUT2 (Hrabovszky et al., 2006b) nor VGLUT1 (present studies). The different phenotype of cells serving as glutamate sources (gonadotrophs and thyrotrophs) and those carrying glutamatergic receptors, including mGLUR2/3, raises the possibility of a

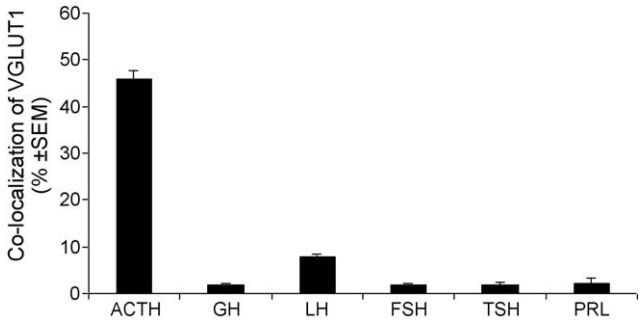

Fig. 6. Percent ratios of VGLUT1-immunoreactive adenohypophysial cell types in the rat. Results represent the mean percentage ± SEM of 3 animals from each double-labeling experiment. VGLUT1 signal was detected in 45.9 ± 1.8% of adrenocorticotropin (ACTH)-immunoreactive cells, 1.7 ± 0.3% of growth hormone (GH)-immunoreactive cells, 7.7 ± 0.9% of luteinizing hormone β immunoreactive LH cells, 1.7 ± 0.3% of follicle-stimulating hormone β immunoreactive FSH cells, 1.7 ± 0.7% of thyroid stimulating hormone β immunoreactive TSH cells and 2.0 ± 1.2% of prolactin (PRL)-immunoreactive cells.

glutamatergic paracrine cross-talk between different hormone-secreting cells. Glutamatergic communication between alpha and beta pancreatic islet cells is an example of such a paracrine communication. Alpha cells serve as the major source of glutamate (Hayashi et al., 2003). Under low glucose conditions they co-secrete glutamate with glucagon and glutamate triggers GABA secretion from neighboring beta cells (Hayashi et al., 2003).

If glutamate is, indeed, released from adenohypophysial cells, a further interesting question is how glutamate stores are refilled. It is unknown if thyrotrophs, gonadotrophs and corticotrophs possess membrane glutamate transporters for a direct glutamate uptake. In the central nervous system, glutamate reuptake mostly uses the glutamate/glutamine cycle in which glutamate released from excitatory nerve terminals is taken up by astrocytes via the high-affinity membrane glutamate transporters GLAST and GLT-1 (Shigeri and Shimamoto, 2003) and converted to glutamine by glutamine synthetase. Glutamine released from astrocytes via system N transporters into the extracellular fluid is taken up by neuronal terminals via system A transporters (Chaudhry et al., 2002; Varoqui et al., 2000) and converted to glutamate via phosphate-activated glutaminase type 1 (Ottersen et al., 1992). Glutamate is finally concentrated into synaptic vesicles by VGLUTs. In the adenohypophysis, GLAST has been detected in folliculostellate cells (Berger and Hediger, 2000), the same cell type that was shown to contain glutamine synthetase for converting glutamate to glutamine (Shirasawa and Yamanouchi, 1999). Glucocorticoids induce glutamine synthetase expression in folliculostellate cells, but the functional consequences for local glutamatergic signalling are yet to be determined (Shirasawa and Yamanouchi, 1999). It is an interesting question if GLAST and glutamine synthetase of folliculostellate cells are involved in recycling glutamate or they play a different role which is unrelated to the VGLUT content and putative glutamate release from the adenohypophysial cells.

The ultrastructural distribution of VGLUT1 in the adenohypophysis requires clarification. While electron microscopic studies in our laboratory localized VGLUT2 immunoreactivity to small clear vesicles within parvicellular and magnocellular neurosecretory terminals (Hrabovszky et al., 2007), our unpublished observations indicate that VGLUT2 is localized to dense-core vesicles, and not microvesicles, in gonadotroph and thyrotroph cells of the anterior lobe. A similar subcellular distribution of VGLUT2 has been observed by Hayashi and colleagues in dense-core granules, but not microvesicles, in alpha cells of the pancreatic Langerhans islets which secrete stoichiometric amounts of glucagone and glutamate under low glucose conditions (Shirasawa and Yamanouchi, 1999).

To summarize these findings, we have established the presence of VGLUT1 in a large subset of corticotroph and a low percentage of gonadotroph cells in the adenohypophysis of male rats. The functional significance of adenohypophysial VGLUT1 and VGLUT2 synthesis and the physiological role of endogenous glutamate stores in peptide hormone-secreting adenohypophysial cells will require clarification.

Acknowledgments

This research was supported by the National Science Foundation of Hungary (OTKA K69127 and T73002). The technical assistance of Hajni Bekó is highly appreciated. Several antibodies used in these studies were provided by the National Hormone and Peptide Program (NHPP), NIDKDK, and Dr. Parlow.

References

Balschun, D., Moechars, D., Callaerts-Vegh, Z., Vermaercke, B., Van Acker, N., Andries, L., D'Hooge, R., 2009. Vesicular glutamate transporter VGLUT1 has a role in hippocampal long-term potentiation and spatial reversal learning. Cereb. Cortex, doi:10.1093/cercor/bhp133.

Bellocchio, E.E., Hu, H., Pohorille, A., Chan, J., Pickel, V.M., Edwards, R.H., 1998. The localization of the brain-specific inorganic phosphate transporter suggests a specific presynaptic role in glutamatergic transmission. J. Neurosci. 18, 8648–8659.

Bellocchio, E.E., Reimer, R.J., Fremeau Jr., R.T., Edwards, R.H., 2000. Uptake of glutamate into synaptic vesicles by an inorganic phosphate transporter. Science 289, 957–960.

Berger, U.V., Hediger, M.A., 2000. Distribution of the glutamate transporters GLAST and GLT-1 in rat circumventricular organs, meninges, and dorsal root ganglia. J. Comp. Neurol. 421, 385–399.

Bhat, G.K., Mahesh, V.B., Chu, Z.W., Chorich, L.P., Zamorano, P.L., Brann, D.W., 1995. Localization of the *N*-methyl-D-aspartate R1 receptor subunit in specific anterior pituitary hormone cell types of the female rat. Neuroendocrinology 62, 178–186.

Brumovsky, P., Watanabe, M., Hokfelt, T., 2007. Expression of the vesicular glutamate transporters-1 and -2 in adult mouse dorsal root ganglia and spinal cord and their regulation by nerve injury. Neuroscience 147, 469–490.

Caruso, C., Bottino, M.C., Pampillo, M., Pisera, D., Jaita, G., Duvilanski, B., Seilicovich, A., Lasaga, M., 2004. Glutamate induces apoptosis in anterior pituitary cells through group II metabotropic glutamate receptor activation. Endocrinology 145, 4677–4684.

Chaudhry, F.A., Reimer, R.J., Edwards, R.H., 2002. The glutamine commute: take the N line and transfer to the A. J. Cell Biol. 157, 349–355.

Curcio-Morelli, C., Gereben, B., Zavacki, A.M., Kim, B.W., Huang, S., Harney, J.W., Larsen, P.R., Bianco, A.C., 2003. In vivo dimerization of types 1, 2, and 3 iodothyronine selenodeiodinases. Endocrinology 144, 937–946.

Erickson, J.D., De Gois, S., Varoqui, H., Schafer, M.K., Weihe, E., 2006. Activity-dependent regulation of vesicular glutamate and GABA transporters: a means to scale quantal size. Neurochem. Int. 48, 643–649.

Fremeau Jr., R.T., Burman, J., Qureshi, T., Tran, C.H., Proctor, J., Johnson, J., Zhang, H., Sulzer, D., Copenhagen, D.R., Storm-Mathisen, J., Reimer, R.J., Chaudhry, F.A., Edwards, R.H., 2002. The identification of vesicular glutamate transporter 3 suggests novel modes of signaling by glutamate. Proc. Natl. Acad. Sci. U.S.A. 99, 14488–14493.

Fremeau Jr., R.T., Troyer, M.D., Pahner, I., Nygaard, G.O., Tran, C.H., Reimer, R.J., Bellocchio, E.E., Fortin, D., Storm-Mathisen, J., Edwards, R.H., 2001. The expression of vesicular glutamate transporters defines two classes of excitatory synapse. Neuron 31, 247–260.

Fujiyama, F., Furuta, T., Kaneko, T., 2001. Immunocytochemical localization of candidates for vesicular glutamate transporters in the rat cerebral cortex. J. Comp. Neurol. 435, 379–387.

Gras, C., Herzog, E., Bellenchi, G.C., Bernard, V., Ravassard, P., Pohl, M., Gasnier, B., Giros, B., El Mestikawy, S., 2002. A third vesicular glutamate transporter expressed by cholinergic and serotoninergic neurons. J. Neurosci. 22, 5442–5451.

Hackett, T.A., de la Mothe, L.A., 2009. Regional and laminar distribution of the vesicular glutamate transporter, VGluT2, in the macaque monkey auditory cortex. J. Chem. Neuroanat. 38, 106–116.

Hayashi, M., Otsuka, M., Morimoto, R., Hirota, S., Yatsushiro, S., Takeda, J., Yamamoto, A., Moriyama, Y., 2001. Differentiation-associated Na^+-dependent inorganic phosphate cotransporter (DNPI) is a vesicular glutamate transporter in endocrine glutamatergic systems. J. Biol. Chem. 276, 43400–43406.

Hayashi, M., Yamada, H., Uehara, S., Morimoto, R., Muroyama, A., Yatsushiro, S., Takeda, J., Yamamoto, A., Moriyama, Y., 2003. Secretory granule-mediated co-secretion of L-glutamate and glucagon triggers glutamatergic signal transmission in islets of Langerhans. J. Biol. Chem. 278, 1966–1974.

Herzog, E., Bellenchi, G.C., Gras, C., Bernard, V., Ravassard, P., Bedet, C., Gasnier, B., Giros, B., El Mestikawy, S., 2001. The existence of a second vesicular glutamate

transporter specifies subpopulations of glutamatergic neurons. J. Neurosci. 21, RC181.
Hrabovszky, E., Csapo, A.K., Kallo, I., Wilheim, T., Turi, G.F., Liposits, Z., 2006a. Localization and osmotic regulation of vesicular glutamate transporter-2 in magnocellular neurons of the rat hypothalamus. Neurochem. Int. 48, 753–761.
Hrabovszky, E., Deli, L., Turi, G.F., Kallo, I., Liposits, Z., 2007. Glutamatergic innervation of the hypothalamic median eminence and posterior pituitary of the rat. Neuroscience 144, 1383–1392.
Hrabovszky, E., Kallo, I., Turi, G.F., May, K., Wittmann, G., Fekete, C., Liposits, Z., 2006b. Expression of vesicular glutamate transporter-2 in gonadotrope and thyrotrope cells of the rat pituitary. Regulation by estrogen and thyroid hormone status. Endocrinology 147, 3818–3825.
Hrabovszky, E., Liposits, Z., 2007. Glutamatergic phenotype of hypothalamic neurosecretory systems: a novel aspect of central neuroendocrine regulation. Ideggyogy Sz 60, 182–186.
Hrabovszky, E., Liposits, Z., 2008. Novel aspects of glutamatergic signalling in the neuroendocrine system. J. Neuroendocrinol. 20, 743–751.
Hrabovszky, E., Turi, G.F., Kallo, I., Liposits, Z., 2004. Expression of vesicular glutamate transporter-2 in gonadotropin-releasing hormone neurons of the adult male rat. Endocrinology 145, 4018–4021.
Hrabovszky, E., Turi, G.F., Liposits, Z., 2005a. Presence of vesicular glutamate transporter-2 in hypophysiotropic somatostatin but not growth hormone-releasing hormone neurons of the male rat. Eur. J. Neurosci. 21, 2120–2126.
Hrabovszky, E., Wittmann, G., Turi, G.F., Liposits, Z., Fekete, C., 2005b. Hypophysiotropic thyrotropin-releasing hormone and corticotropin-releasing hormone neurons of the rat contain vesicular glutamate transporter-2. Endocrinology 146, 341–347.
Kawasaki, A., Hoshi, K., Kawano, M., Nogami, H., Yoshikawa, H., Hisano, S., 2005. Up-regulation of VGLUT2 expression in hypothalamic-neurohypophysial neurons of the rat following osmotic challenge. Eur. J. Neurosci. 22, 672–680.
Kiyama, H., Sato, K., Tohyama, M., 1993. Characteristic localization of non-NMDA type glutamate receptor subunits in the rat pituitary gland. Brain Res. Mol. Brain Res. 19, 262–268.
Leo, S., Moechars, D., Callaerts-Vegh, Z., D'Hooge, R., Meert, T., 2009. Impairment of VGLUT2 but not VGLUT1 signaling reduces neuropathy-induced hypersensitivity. Eur. J. Pain 13, 1008–1017.
Lin, W., McKinney, K., Liu, L., Lakhlani, S., Jennes, L., 2003. Distribution of vesicular glutamate transporter-2 messenger ribonucleic acid and protein in the septum-hypothalamus of the rat. Endocrinology 144, 662–670.
Martin, G.K., Wise, R.P., Lonsbury-Martin, B.L., 1983. Frozen-section autoradiography of the cochlea: evidence for differential distribution of amino acids. Ann. Otol. Rhinol. Laryngol. 92, 254–258.
Morimoto, R., Hayashi, M., Yatsushiro, S., Otsuka, M., Yamamoto, A., Moriyama, Y., 2003. Co-expression of vesicular glutamate transporters (VGLUT1 and VGLUT2) and their association with synaptic-like microvesicles in rat pinealocytes. J. Neurochem. 84, 382–391.
Moriyama, Y., Yamamoto, A., 2004. Glutamatergic chemical transmission: look! Here, there, and anywhere J. Biochem. (Tokyo) 135, 155–163.
Ottersen, O.P., Zhang, N., Walberg, F., 1992. Metabolic compartmentation of glutamate and glutamine: morphological evidence obtained by quantitative immunocytochemistry in rat cerebellum. Neuroscience 46, 519–534.
Sakata-Haga, H., Kanemoto, M., Maruyama, D., Hoshi, K., Mogi, K., Narita, M., Okado, N., Ikeda, Y., Nogami, H., Fukui, Y., Kojima, I., Takeda, J., Hisano, S., 2001. Differential localization and colocalization of two neuron-types of sodium-dependent inorganic phosphate cotransporters in rat forebrain. Brain Res. 902, 143–155.
Schafer, M.K., Varoqui, H., Defamie, N., Weihe, E., Erickson, J.D., 2002. Molecular cloning and functional identification of mouse vesicular glutamate transporter 3 and its expression in subsets of novel excitatory neurons. J. Biol. Chem. 277, 50734–50748.
Shigeri, Y., Shimamoto, K., 2003. Pharmacology of excitatory amino acid transporters (EAATs and VGLUTs). Nippon Yakurigaku Zasshi 122, 253–264.
Shirasawa, N., Yamanouchi, H., 1999. Glucocorticoids induce glutamine synthetase in folliculostellate cells of rat pituitary glands in vivo and in vitro. J. Anat. 194 (Pt 4), 567–577.
Somogyi, P., Halasy, K., Somogyi, J., Storm-Mathisen, J., Ottersen, O.P., 1986. Quantification of immunogold labelling reveals enrichment of glutamate in mossy and parallel fibre terminals in cat cerebellum. Neuroscience 19, 1045–1050.
Storm-Mathisen, J., Leknes, A.K., Bore, A.T., Vaaland, J.L., Edminson, P., Haug, F.M., Ottersen, O.P., 1983. First visualization of glutamate and GABA in neurones by immunocytochemistry. Nature 301, 517–520.
van den Pol, A.N., Wuarin, J.P., Dudek, F.E., 1990. Glutamate, the dominant excitatory transmitter in neuroendocrine regulation. Science 250, 1276–1278.
Varoqui, H., Zhu, H., Yao, D., Ming, H., Erickson, J.D., 2000. Cloning and functional identification of a neuronal glutamine transporter. J. Biol. Chem. 275, 4049–4054.
Vizi, E.S., Mike, A., 2006. Nonsynaptic receptors for GABA and glutamate. Curr. Top. Med. Chem. 6, 941–948.
Wojcik, S.M., Rhee, J.S., Herzog, E., Sigler, A., Jahn, R., Takamori, S., Brose, N., Rosenmund, C., 2004. An essential role for vesicular glutamate transporter 1 (VGLUT1) in postnatal development and control of quantal size. Proc. Natl. Acad. Sci. U.S.A. 101, 7158–7163.
Zeng, C., Nannapaneni, N., Zhou, J., Hughes, L.F., Shore, S., 2009. Cochlear damage changes the distribution of vesicular glutamate transporters associated with auditory and nonauditory inputs to the cochlear nucleus. J. Neurosci. 29, 4210–4217.
Ziegler, D.R., Cullinan, W.E., Herman, J.P., 2002. Distribution of vesicular glutamate transporter mRNA in rat hypothalamus. J. Comp. Neurol. 448, 217–229.

dc_27_10

21. számú melléklet

EJN fens European Journal of Neuroscience
dc_27_10
European Journal of Neuroscience, Vol. 31, pp. 1984–1998, 2010 doi:10.1111/j.1460-9568.2010.07239.x

NEUROSYSTEMS

The kisspeptin system of the human hypothalamus: sexual dimorphism and relationship with gonadotropin-releasing hormone and neurokinin B neurons

E. Hrabovszky,[1] P. Ciofi,[2] B. Vida,[1] M. C. Horvath,[3] E. Keller,[3] A. Caraty,[4] S. R. Bloom,[5] M. A. Ghatei,[5] W. S. Dhillo,[5] Z. Liposits[1,6] and I. Kallo[1,6]
[1]Laboratory of Endocrine Neurobiology, Institute of Experimental Medicine, Hungarian Academy of Sciences, Budapest, 1083 Hungary
[2]INSERM U862, Neurocentre Magendie, Bordeaux, France
[3]Department of Forensic Medicine, Semmelweis University, Budapest, Hungary
[4]INRA/CNRS/University Tours/Haras Nationaux, Nouzilly, France
[5]Department of Investigative Medicine, Hammersmith Hospital, Imperial College London, London, UK
[6]Department of Neuroscience, Faculty of Information Technology, Pázmány Péter Catholic University, Budapest, Hungary

Keywords: immunohistochemistry, infundibulum, luteinizing hormone-releasing hormone, reproduction

Abstract

Kisspeptin signaling via the kisspeptin receptor G-protein-coupled receptor-54 plays a fundamental role in the onset of puberty and the regulation of mammalian reproduction. In this immunocytochemical study we addressed the (i) topography, (ii) sexual dimorphism, (iii) relationship to gonadotropin-releasing hormone (GnRH) neurons and (iv) neurokinin B content of kisspeptin-immunoreactive hypothalamic neurons in human autopsy samples. In females, kisspeptin-immunoreactive axons formed a dense periventricular plexus and profusely innervated capillary vessels in the infundibular stalk. Most immunolabeled somata occurred in the infundibular nucleus. Many cells were also embedded in the periventricular fiber plexus. Rostrally, they formed a prominent periventricular cell mass (magnocellular paraventricular nucleus). Robust sex differences were noticed in that fibers and somata were significantly less numerous in male individuals. In dual-immunolabeled specimens, fine kisspeptin-immunoreactive axon varicosities formed axo-somatic, axo-dendritic and axo-axonal contacts with GnRH neurons. Dual-immunofluorescent studies established that 77% of kisspeptin-immunoreactive cells in the infundibular nucleus synthesize the tachykinin peptide neurokinin B, which is known to play crucial role in human fertility; 56 and 17% of kisspeptin fibers in the infundibular and periventricular nuclei, respectively, contained neurokinin B immunoreactivity. Site-specific co-localization patterns implied that kisspeptin neurons in the infundibular nucleus and elsewhere contributed differentially to these plexuses. This study describes the distribution and robust sexual dimorphism of kisspeptin-immunoreactive elements in human hypothalami, reveals neuronal contacts between kisspeptin-immunoreactive fibers and GnRH cells, and demonstrates co-synthesis of kisspeptins and neurokinin B in the infundibular nucleus. The neuroanatomical information will contribute to our understanding of central mechanisms whereby kisspeptins regulate human fertility.

Introduction

The clinical observations that loss-of-function mutations of the G-protein-coupled receptor-54 (*GPR54*) gene cause autosomal recessive hypogonadotropic hypogonadism (de Roux *et al.*, 2003; Seminara *et al.*, 2003; Semple *et al.*, 2005) generated much interest in reproductive endocrinology. The *GPR54* gene codes for the receptor of kisspeptins (Kotani *et al.*, 2001; Muir *et al.*, 2001; Ohtaki *et al.*, 2001) that are derived from the metastasis suppressor gene *KISS1*. Kisspeptins stimulate gonadotropin secretion (Gottsch *et al.*, 2004; Irwig *et al.*, 2004; Matsui *et al.*, 2004; Dhillo *et al.*, 2005, 2007; Shahab *et al.*, 2005), which is prevented by gonadotropin-releasing hormone (GnRH) antagonists (Gottsch *et al.*, 2004; Shahab *et al.*, 2005), indicating that the action is mediated by hypothalamic GnRH-synthesizing neurons. In accordance with the concept that kisspeptins influence the GnRH neuronal system directly, kisspeptin-immunoreactive fibers establish contacts with GnRH neurons (Kinoshita *et al.*, 2005; Clarkson & Herbison, 2006; Ramaswamy *et al.*, 2008; Smith *et al.*, 2008a), GnRH neurons express GPR54 mRNA (Irwig *et al.*, 2004; Han *et al.*, 2005; Messager *et al.*, 2005), kisspeptins induce cFos expression in GnRH neurons (Irwig *et al.*, 2004; Matsui *et al.*, 2004; Kauffman *et al.*, 2007b), and kisspeptins directly depolarize GnRH neurons in acute slice preparations (Han *et al.*, 2005; Dumalska *et al.*, 2008; Pielecka-Fortuna *et al.*, 2008). In the present study we have addressed several neuromorphological aspects of central kisspeptin signaling in the human hypothalamus.

Correspondence: Dr Erik Hrabovszky, as above.
E-mail: hrabovszky@koki.hu

Received 14 December 2009, revised 2 March 2010, accepted 25 March 2010

We first carried out immunocytochemical experiments with two well-characterized kisspeptin antisera to map the distribution of kisspeptin-immunoreactive neuronal fibers and cell bodies in the hypothalamus of female and male human individuals.

Kisspeptin immunoreactivity exhibits sexual dimorphism in rodents in that the number of kisspeptin-synthesizing neurons is higher in females vs. males (Clarkson & Herbison, 2006; Kauffman *et al.*, 2007a). In the second part of our study we investigated putative sex differences of the human kisspeptin system by comparing the immunocytochemical labeling of hypothalamic samples from female vs. male individuals.

In rodents, kisspeptin-containing axons innervate the dendrites and cell bodies of GnRH cells (Clarkson & Herbison, 2006), whereas in an agonadal male rhesus monkey model (Ramaswamy *et al.*, 2008), axo-axonal contacts in the median eminence were proposed to represent the primary route of communication between the kisspeptin and GnRH systems. The third goal of this study was to visualize the site(s) of the putative neuronal interaction between kisspeptin- and GnRH-immunoreactive neurons in humans.

Very recently, the critical neuroendocrine significance of the tachykinin peptide neurokinin B (NKB) in human reproduction has been established by case reports of familial hypogonadotropic hypogonadism caused by loss-of-function mutations of genes encoding either NKB or its receptor (neurokinin-3 receptor) (Guran *et al.*, 2009; Topaloglu *et al.*, 2009). Remarkably, kisspeptins, NKB and dynorphin were previously co-localized in the same neurons of the arcuate nucleus (ARC) in ewes (Goodman *et al.*, 2007) and mice (Navarro *et al.*, 2009). In the final part of our study, we addressed the co-expression of preproNKB and kisspeptin immunoreactivities within the same human hypothalamic neurons and their fiber projections.

Materials and methods

Tissue samples

Human hypothalamic samples from seven male and five female individuals were obtained at autopsy from the Forensic Medicine Department of Semmelweis University (Budapest, Hungary) using protocols reviewed and approved by the Regional Committee of Science and Research Ethics (TUKEB 49/1999). As in our previous immunocytochemical studies on human hypothalami (Hrabovszky *et al.*, 2007), the selection criteria included sudden causes of death and lack of history of neurological and endocrine disorders. Postmortem intervals were kept below 24 h. The ages of the individuals were 26, 28, 28, 31, 52, 53 and 66 years in the case of males and 27, 32, 46, 49 and 74 years in the case of females. Hypothalamic tissue blocks were dissected from the samples to include the optic chiasma rostrally, the mammillary bodies caudally and the anterior commissure dorsally. A bilateral cut was made 2 cm lateral from the mid-sagittal plane. The dissected tissues were initially rinsed for 5 min in 4% paraformaldehyde solution prepared with 0.1 M phosphate-buffered saline (pH 7.4). Five blocks were immersed for 2 days in a freshly prepared mixture of 4% acrolein and 2% paraformaldehyde (4°C). Seven samples were fixed for 7 days in 4% paraformaldehyde (4°C).

Section preparation and pretreatments

Following fixation, the tissue blocks were trimmed further and cut in half in the mid-sagittal plane to obtain section surfaces that fitted regular microscope slides. These blocks were infiltrated with 20% sucrose for 5 days at 4°C. The right hemihypothalami were placed in a freezing mold, surrounded with Jung tissue freezing medium (diluted 1 : 1 with 0.9% sodium chloride solution; Leica Microsystems, Nussloch Gmbh, Germany), snap-frozen on powdered dry ice and sectioned coronally at 30 μm with an SM 2000R freezing microtome (Leica Microsystems). Sections fixed with the mixture of 4% acrolein and 2% paraformaldehyde were treated with 0.5% sodium borohydride for 30 min and rinsed in phosphate-buffered saline copiously. All sections were stored permanently in antifreeze solution (30% ethylene glycol, 25% glycerol and 0.05 M phosphate buffer; pH 7.4) at −20°C. Prior to immunocytochemical experiments, the sections were rinsed in phosphate-buffered saline and pretreated with a mixture of 0.5% H_2O_2 and 0.4% Triton X-100 for 30 min.

Mapping the distribution of kisspeptin-immunoreactive neuronal elements

To detect kisspeptin immunoreactivity, every 20th section from each block was incubated in one of the following two primary antisera. A rabbit antiserum (#566; diluted at 1 : 25 000 with 2% normal horse serum) was directed against peptide YNWNSFGLRY-NH2, which is common to all forms of mouse (and rat) kisspeptins (Franceschini *et al.*, 2006) and 90% identical to the corresponding human sequence (YNWNSFGLRF). Although this kisspeptin-10 antiserum has not yet been validated for the immunocytochemical labeling of human tissue sections, it has been characterized and used extensively in previous immunocytochemical experiments in rodents (Clarkson & Herbison, 2006; Clarkson *et al.*, 2009) and sheep (Franceschini *et al.*, 2006), and reported not to bind to brain sections from kisspeptin-knockout mice (Clarkson *et al.*, 2009). A second polyclonal antiserum (GQ2) was raised in sheep against the full-length human kisspeptin-54 peptide sequence. It was diluted 1 : 200 000 for sections fixed with acrolein/paraformaldehye and 1 : 100 000 for sections fixed with paraformaldehyde alone, when using peroxidase-based immunohistochemistry. The GQ2 antiserum was found to react 100% with the human kisspeptin-54, kisspeptin-14 and kisspeptin-10 forms (Dhillo *et al.*, 2005). It showed virtually no cross-reactivity (< 0.01%) with any other related human RF amide peptide, including prolactin-releasing peptide, neuropeptide FF, neuropeptide AF and RF amide-related peptides (RFRP1, RFRP2 and RFRP3) (Dhillo *et al.*, 2005). Furthermore, the same kisspeptin antiserum has been used successfully in previous immunofluorescence experiments by others to study the distribution and connectivity to GnRH neurons of the rhesus monkey kisspeptin system (Ramaswamy *et al.*, 2008).

Incubation of two separate series of sections in each one of these primary antisera for 48 h at 4°C was followed by biotinylated secondary antibodies (biotin-SP anti-rabbit IgG or biotin-SP anti-sheep IgG; Jackson ImmunoResearch Laboratories, West Grove, PA, USA; 1 : 500) and the ABC Elite reagent (1 : 1000; Vector, Burlingame, CA, USA) for 60 min each. The peroxidase signal was visualized with nickel-intensified diaminobenzidine chromogen and then postintensified with silver–gold (Liposits *et al.*, 1984). The immunostained sections were mounted on microscope slides from Elvanol and air-dried. A third series of sections adjacent to the immunolabeled specimens was Nissl-stained with cresyl violet to facilitate anatomical analysis. Finally, all sections were dehydrated with 95% (5 min) followed by 100% (2 × 5 min) ethanol, cleared with xylene (2 × 5 min) and coverslipped with DPX mounting medium (Fluka Chemie, Buchs, Switzerland). The microscopic images of the Nissl-stained sections were scanned with an AxioCam MRc 5 digital camera mounted on a Zeiss AxioImager M1 micro-

scope using the AxioVision 4.6 software (Carl Zeiss, Göttingen, Germany). Digital images of representative sections were used to draw schematic plates with the CorelDRAW11 software. The immunocytochemical results were illustrated in schematic plates from different rostro-caudal levels. The anatomical nomenclature and abbreviations were based on the human brain atlas of Mai *et al.* (1997).

Analysis of sexual dimorphism

Initial screening of kisspeptin immunolabeling revealed more fibers in hypothalamic samples from female vs. male individuals using both the rabbit and sheep kisspeptin antibodies. Sex differences obtained with the sheep kisspeptin-54 antibodies were quantitatively evaluated in hypothalamic sections of female and male individuals. Counting of kisspeptin-immunoreactive fibers in the periventricular nucleus (Pe) (from the plane represented in Fig. 1G) and the infundibular nucleus (Inf) was carried out using a 5 × 5 ocular grid at 200 × magnification. Immunoreactive fiber profiles that exhibited continuous immunolabeling were considered as one, independently of their length or thickness and quantified in 25 separate fields. The number was summarized for a final 0.0625 mm^2 counting area. Cell bodies were counted similarly in the Inf at 100 × magnification (in a 0.25 mm^2 area). For consistency, each human individual was characterized by the maximal fiber and soma counts obtained from several (two to six) sections and counting was carried out by an investigator who was blind to the identity of the experimental samples. Statistical analyses were carried out with the Statistica 8.0 software package (StatSoft, Inc., Tulsa, USA). Two-way ANOVA was used to reveal the effects of sex and tissue fixative on fiber and cell body counts. Age effects on counts were addressed in a general regression model separately in the two sexes.

Studying the relationship of kisspeptin- and gonadotropin-releasing hormone-immunoreactive neurons

The detection of kisspeptin immunoreactivity was carried out as described for single-label mapping studies. Subsequently, GnRH immunoreactivity was detected with a rabbit primary antiserum against GnRH (LR1; 1 : 20 000; kind gift from Dr R.A. Benoit, Montreal, Canada), followed by biotinylated secondary antibodies and ABC. The signal was visualized with the non-intensified brown diaminobenzidine as a chromogen and, finally, the dual-labeled sections were mounted, coverslipped and photographed. Neuronal contacts of kisspeptin-immunoreactive fibers with GnRH neurons were counted using an immersion oil lens at 630 × magnification. Sex effects on the number of neuronal contacts and the percentage of GnRH neurons receiving kisspeptin-immunoreactive axon contacts were addressed by one-way ANOVA.

Co-localization of preproneurokinin B with kisspeptins

The immunocytochemical detection of preproNKB in the human hypothalamus was carried out with newly developed polyclonal antisera against a 28-amino-acid-long segment from the C-terminal of human preproNKB. The synthetic peptide (NH2-SVQPDSPTD-VNQENVPSFGILKYPPRAE-OH) was coupled to bovine thyroglobulin with glutaraldehyde and the conjugate was used to immunize two rabbits with standard procedures. Immunocytochemical labeling specificity with the resulting polyclonal antibodies (codes IS-681 and IS-682) was addressed using control sections. Some sections were incubated with the preimmune sera (used at 1 : 30 000–1 : 100 000) and others with preproNKB antisera preabsorbed overnight with 5 μg/mL of the immunization antigen. Test sections from rats and mice, which do not contain similar peptide sequences to the C-terminal human preproNKB, were also processed as negative controls.

Two parallel series of human hypothalamic sections were first processed for peroxidase immunolabeling to obtain an overview of preproNKB immunoreactivity in the human hypothalamus. The IS-681 and IS-682 primary antisera were diluted at 1 : 100 000 and reacted with biotinylated secondary antibodies (1 : 500; Jackson ImmunoResearch Laboratories) and ABC for 1 h each. The signal was visualized with silver–gold-intensified Ni-diaminobenzidine.

Subsequently, dual-immunofluorescence experiments were carried out to address the co-localization of kisspeptins and preproNKB. To reduce tissue autofluorescence due to neuronal lipofuscin deposits, the sections were pretreated with Sudan black as described previously (Mihaly *et al.*, 2002). A cocktail of sheep anti-kisspeptin-54 (1 : 10 000) and rabbit anti-preproNKB (IS-681; 1 : 1000) primary antisera was applied to the sections for 48 h at 4°C. The sections were then incubated in a mixture of fluorochrome-conjugated secondary antibodies (donkey anti-sheep-FITC and donkey anti-rabbit-Cy3; Jackson ImmunoResearch Laboratories, 1 : 300 each) for 5 h, mounted, coverslipped with Vectashield (Vector) and analyzed at high magnifications with a Radiance 2100 confocal microscope (Bio-Rad Laboratories, Hemel Hempstead, UK) using laser excitation lines of 488 nm for FITC and 543 nm for Cy3, and dichroic/emission filters of 560 nm/500–530 nm for FITC and 560–610 nm for Cy3. To eliminate emission cross-talk, single optical slices (< 0.7 μm) were collected in 'lambda strobing' mode so that only one excitation laser and the corresponding emission detector were active during a line scan. The digital images were processed with the Adobe Photoshop CS software at 300 dpi resolution. The degree of co-localization

FIG. 1. Topographic distribution of kisspeptin-10-immunoreactive fibers in representative rostral hypothalamic sections of the human. Kisspeptin immunoreactivity was detected using the rabbit kisspeptin-10 antiserum and the silver–gold intensification of the Ni-diaminobenzidine peroxidase reaction product in tissue sections from a 27-year-old human female fixed with the mixture of 4% paraformaldehyde and 2% acrolein. Diagrams on the left were generated with CorelDRAW using Nissl-stained section templates from different rostro-caudal levels. Shaded circles indicate regions illustrated in A–I. The rabbit kisspeptin-10 antiserum mostly revealed axonal profiles, although a few kisspeptin-immunoreactive cell bodies were also faintly immunostained (arrow in H). The labeled preoptic/hypothalamic fibers were most numerous in the proximity of the third ventricle, in an area including the organum vasculosum of the lamina terminalis (OVLT in C), Pa [PaMc as well as the anterior parvocellular part of the paraventricular hypothalamic nucleus (PaAP); A, D, G and H] and VPe (B). Note the dense fiber labeling within and lateral to the PaMc (D), which contains kisspeptin-immunoreactive axonal varicosities as well as thicker immunolabeled dendrites (compare with Fig. 3B). Lateral hypothalamic sites including the ventromedial nucleus (VMH in I) contained only a few scattered fibers. The InfS received a particularly dense kisspeptin-immunoreactive innervation; labeled fibers formed plexuses around capillary vessels (CV) (arrows in F). Note that extrahypothalamic kisspeptin-immunoreactive projections were also observed in the ventrolateral septal nucleus (LSV) (E). Scale bars: 2.5 mm in schematic drawings and 50 μm in photomicrographs. 3V, third cerebral ventricle; Ac, anterior commissure; BST, bed nucleus of the stria terminalis; Fx, fornix; HDB, horizontal limb of the diagonal band; LHA, lateral hypothalamic area; Mfb, medial forebrain bundle; Opt, optic tract; OX, optic chiasm; SO, supraoptic nucleus; SOVM, ventromedial part of the supraoptic nucleus; SODL, dorsolateral part of the supraoptic nucleus.

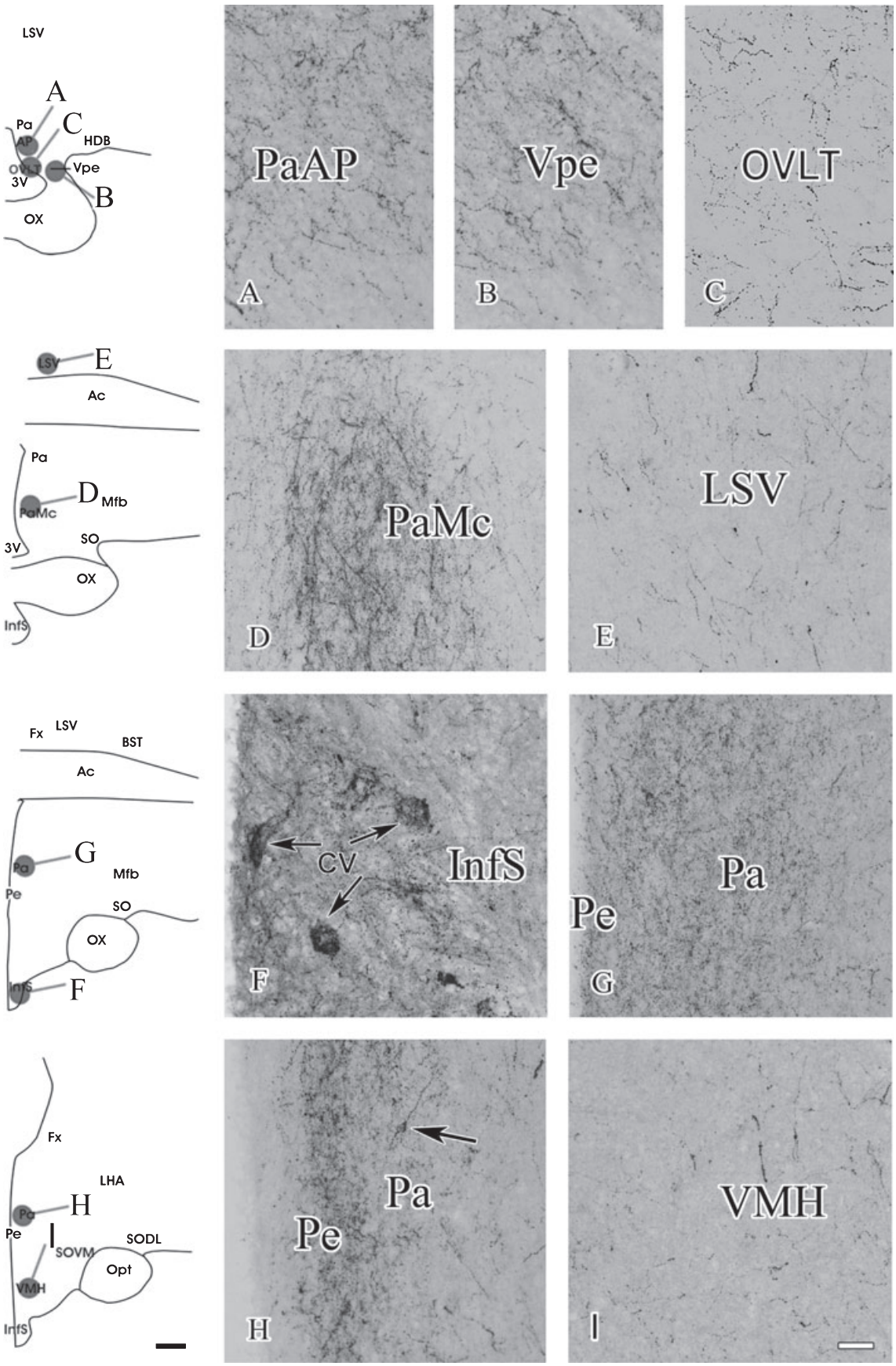

between kisspeptin-54 and preproNKB immunoreactivities was determined in digital photomicrographs from three individuals whose sections showed low autofluorescence and sufficient kisspeptin immunolabeling. Co-localization percentages in kisspeptin fibers of the Pe (from a similar plane as shown in Fig. 1G) vs. the Inf were compared by one-way ANOVA.

Results

Distribution of kisspeptin-immunoreactive axons in the hypothalamus of female individuals

The immunoperoxidase-based detection of kisspeptins using the rabbit kisspeptin-10 antibodies visualized a dense network of immunoreactive axons in the medial hypothalamus (Figs 1 and 2). The fibers were varicose and exhibited highly varying calibers. Sections fixed with the acrolein/paraformaldehyde mixture and those fixed with paraformaldehyde alone produced identical results, except that higher primary antiserum dilutions could be used on the former. Regional analysis revealed the highest fiber densities around the third ventricle, including the organum vasculosum of the lamina terminalis (Fig. 1C), ventral Pe (VPe) (Fig. 1B), Pe (Figs 1G and H, and 2C and G), anteromedial and anterolateral preoptic nuclei, paraventricular nucleus (Pa) [magnocellular (PaMc) and parvocellular subdivisions; Figs 1A, D, G and H, and 2A], Inf (Fig. 2E), dorsomedial hypothalamic nucleus (Fig. 2C and F) and the dorsal hypothalamic area (Fig. 2H) received an abundant innervation, and dense pericapillary plexuses were labeled in the infundibular stalk (InfS) (Fig. 1F). Overall, the density of immunoreactive fibers decreased with distance from the third ventricle and labeled axons became scarce in the ventromedial hypothalamic nucleus (Figs 1I and 2B) and the lateral hypothalamic area (Fig. 2D). The ventrolateral septal nucleus, a part of which was included in the tissue blocks, contained extrahypothalamic kisspeptin projections (Fig. 1E).

Distribution of kisspeptin-immunoreactive cell bodies in the hypothalamus of female individuals

Although relatively few neuronal cell bodies were labeled with the rabbit antiserum to mouse kisspeptin-10 (Fig. 2A and C), the sheep antiserum to human kisspeptin-54 visualized numerous perikarya in the female hypothalami. This finding was in accordance with the better performance of this sheep kisspeptin-54 antiserum on monkey hypothalami, in comparison with kisspeptin-10 antisera (Ramaswamy *et al.*, 2008). The highest numbers of kisspeptin-54-immunoreactive cell bodies were observed in the Inf (Fig. 3D, left panel) and the proximal portion of the InfS (Fig. 3C). Intensely labeled cell bodies were also scattered periventricularly throughout the rostro-caudal extent of the hypothalamus. A compact although less intensely immunostained cell group was observed in the rostral periventricular area, overlapping with the VPe (Fig. 3A), anterior parvocellular Pa (Fig. 3A), parvocellular and, in particular, magnocellular (PaMc) (Fig. 3B) subdivisions of the Pa. Immunoreactive cells in the PaMc occurred just medial and ventral to a prominent kisspeptin-54-immunoreactive fiber bundle (Fig. 3B).

Sexual dimorphism of the human kisspeptin system

The immunocytochemical detection of kisspeptins yielded strikingly different results in female vs. male hypothalami.

Both the rabbit kisspeptin-10 and sheep kisspeptin-54 primary antibodies revealed consistently many fewer immunoreactive fibers in the hypothalamic sections of male individuals, compared with the patterns found in female brains (right and left panels in Fig. 3D, respectively). Fiber numbers in 0.0625 mm^2 counting areas of the Inf (212.1 ± 58.2 in females vs. 29.6 ± 7.1 in males, mean ± SEM) and Pe (114.0 ± 17.9 in females vs. 29.0 ± 7.6 in males) showed robust sex differences (main effect of sex: in the Inf, $F_{1,7} = 9.42$, $P = 0.018$ and in the Pe, $F_{1,8} = 14.87$, $P = 0.005$), whereas the type of fixative had no effect ($F_{1,7} = 0.52$, $P = 0.49$ in the Inf and $F_{1,8} = 0.004$, $P = 0.95$ in the Pe) by two-way ANOVA. The age of individuals did not exert detectable effects on fiber counts in either males ($r_5 = 0.10$, $P = 0.83$ for the Inf and $r_5 = 0.20$, $P = 0.67$ for the Pe) or females ($r_2 = 0.11$, $P = 0.89$ for the Inf and $r_3 = 0.57$, $P = 0.32$ for the Pe) in the general regression model. For raw data from individual samples, see Fig. 3E.

The numbers of immunoreactive somata also showed striking sex differences. Whereas kisspeptin-immunoreactive cell bodies were consistently observed in the rostral periventricular zone (including the VPe and PaMc) of the female samples (Fig. 3A and B), the seven male samples were devoid of labeled perikarya at this site. A further obvious sex difference was that the Inf contained very few, if any, faintly-labeled neuronal perikarya in males, compared with many heavily labeled somata in the Inf of females (two panels in Fig. 3D). This sex difference in the number of somata in 0.25 mm^2 counting areas (49.3 ± 4.6 in females vs. 7.7 ± 7.6 in males; mean ± SEM) was statistically significant ($F_{1,7} = 35.72$, $P = 0.0006$). Similarly to fiber counts, the number of counted cells was not influenced by the type of fixative (ANOVA: $F_{1,7} = 3.05$, $P = 0.12$) or the age of individuals (general regression model: $r_5 = 0.18$, $P = 0.70$ for males and $r_2 = 0.78$, $P = 0.22$ for females). For data from individual samples, see Fig. 3E.

Innervation of gonadotropin-releasing hormone neurons

The analysis of dual-labeled sections revealed many kisspeptin-immunoreactive fibers in close proximity to GnRH neuronal cell bodies and dendrites (Fig. 4). Although kisspeptin-immunoreactive axons were often thick with conspicuous swellings, most of their contacts with GnRH neurons involved fine or medium-sized varicosities, which were apposed to both the cell bodies (Fig. 4A and B) and dendrites (Fig. 4C and D) of GnRH-immunoreactive neurons. The contacts obtained with the kisspeptin-10 rabbit antiserum (Fig. 4A–D) were readily reproducible with the sheep kisspeptin-54 antiserum (Fig. 4E–G). The number of neuronal contacts varied robustly among individual samples. In female individuals (Fig. 4F), GnRH-immunoreactive somata received 0.7 ± 0.5 contacts (mean ± SEM), whereas 0.12 ± 0.05 contacts were counted on GnRH-immunoreactive cell bodies in samples from male individuals (Fig. 4G); 25.8 ± 15.0% (mean ± SEM) of GnRH-immunoreactive somata in females and 8.3 ± 3.6% of GnRH-immunoreactive somata in males received at least one axo-somatic apposition. None of these parameters differed statistically (number of contacts: $F_{1,7} = 0.37$, $P = 0.56$; percentage of neurons with kisspeptin contacts: $F_{1,7} = 1.52$, $P = 0.26$) by one-way ANOVA.

The InfS contained kisspeptin- and GnRH-immunoreactive projections in partly overlapping regions. The two types of axon often surrounded the same capillary vessels in the internal zone of the median eminence (Fig. 4H). At high magnification, the frequent juxtaposition of fine-caliber kisspeptin-immunoreactive axons to thick GnRH-immunoreactive varicosities suggested that kisspeptin and

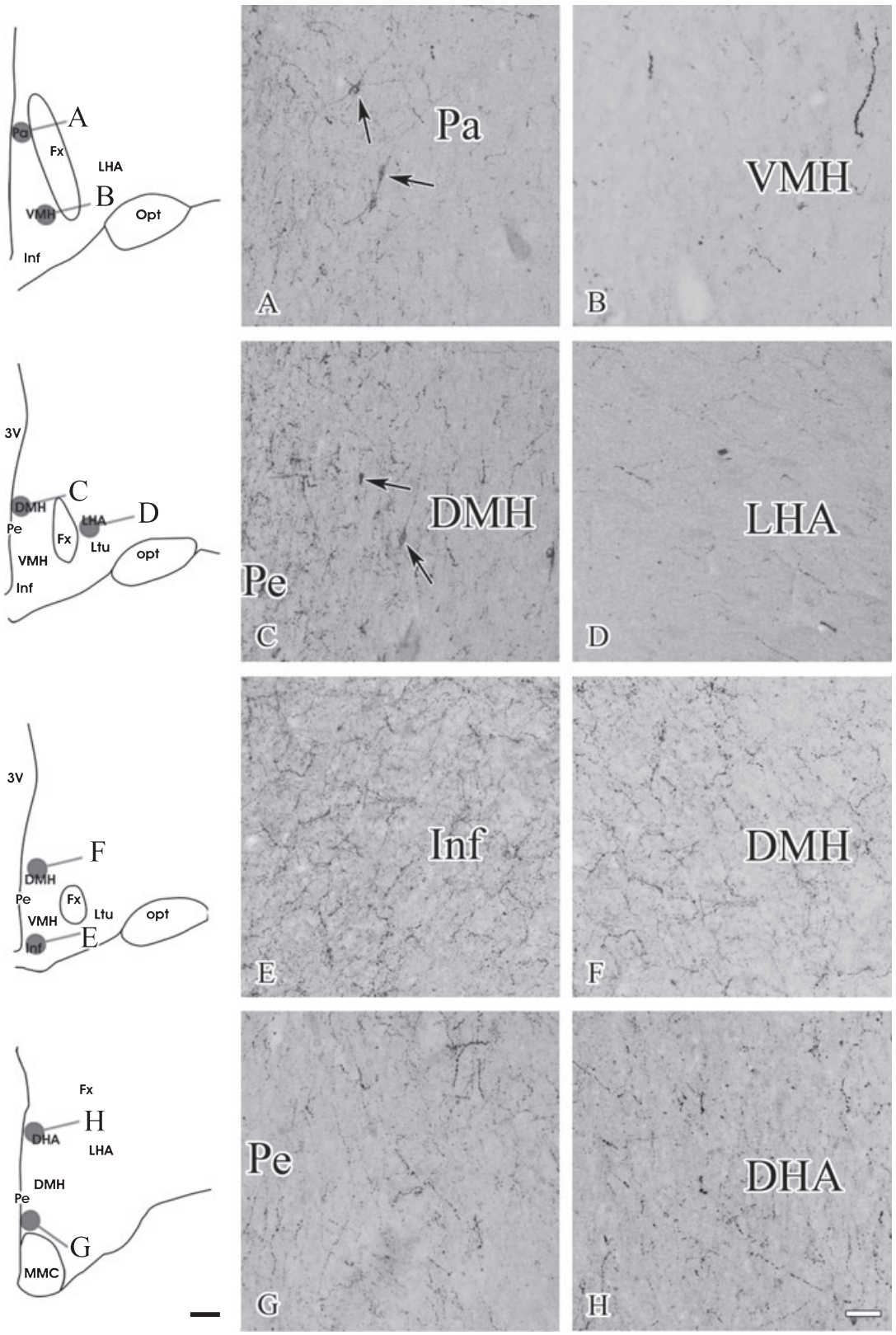

FIG. 2. Distribution of kisspeptin-10-immunoreactive fibers in representative caudal hypothalamic sections of the human. Similarly to findings at rostral hypothalamic levels in Fig. 1, kisspeptin-immunoreactive fibers continued to accumulate in the proximity of the third cerebral ventricle (3V) at more caudal levels of the hypothalamus. Accordingly, the paraventricular (Pa) (A), dorsomedial hypothalamic nucleus (DMH) (C and F) and periventricular (Pe; G) and infundibular (Inf) (E) hypothalamic nuclei and the dorsal hypothalamic area (DHA) (H) were innervated densely, whereas immunoreactive fibers were scarce in the ventromedial nucleus [ventromedial hypothalamic nucleus (VMH)] (B) and the lateral hypothalamic area (LHA) (D). Note a few immunoreactive cell bodies (arrows) in A and C. Scale bars: 2.5 mm in schematic drawings and 50 μm in photomicrographs. Fx, fornix; Ltu, lateral tuberal nucleus; MMC, magnocellular part of the mammillary nucleus; Opt, optic tract.

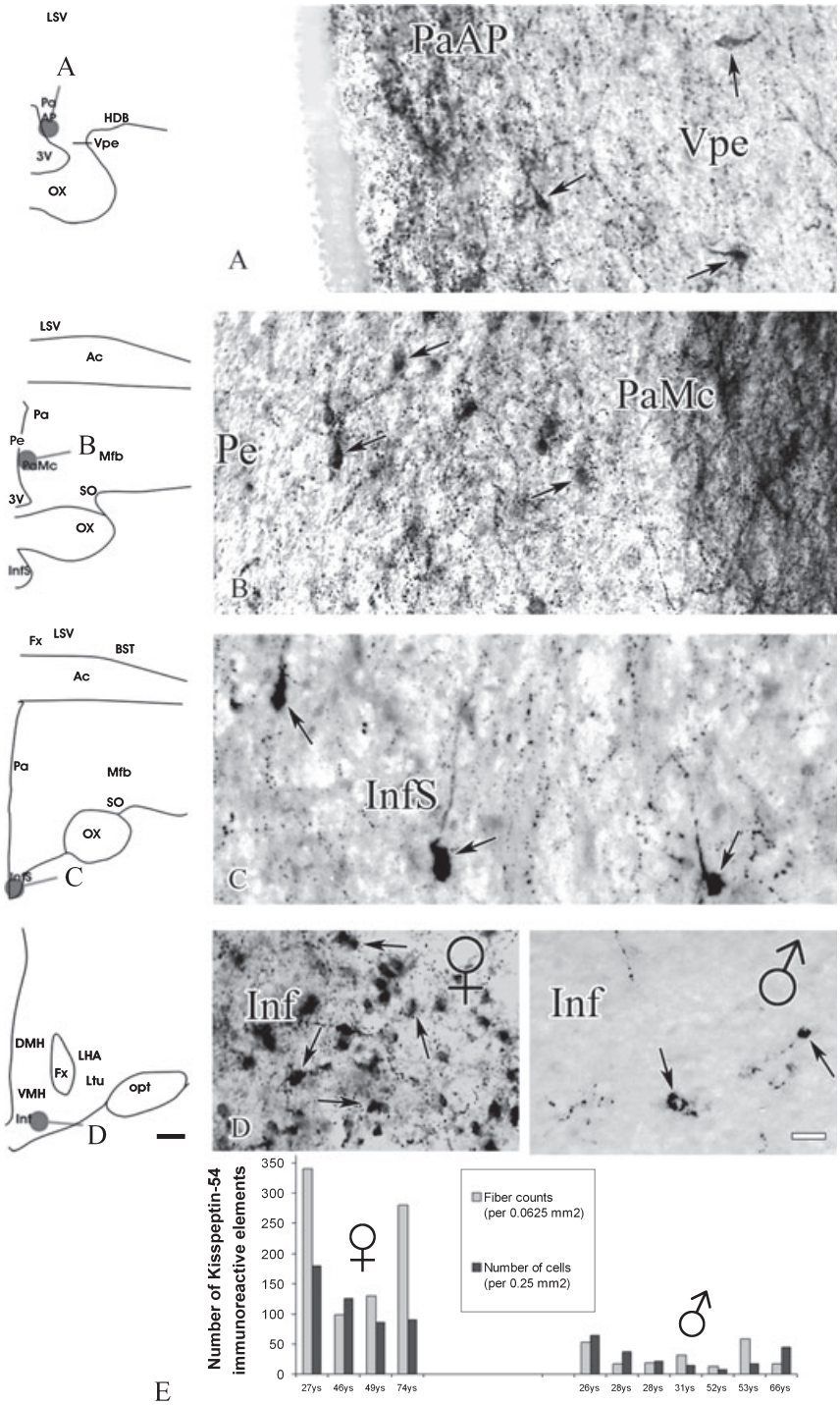

FIG. 3. Distribution and sexual dimorphism of kisspeptin-54-immunoreactive neuronal cell bodies and fibers in the human hypothalamus. Using the same female tissue samples as for Figs 1 and 2, the sheep kisspeptin-54 antiserum revealed an immunoreactive fiber distribution in the medial hypothalamus similar to that obtained with the rabbit kisspeptin-10 antiserum. In addition, a more intense labeling and a higher number of neuronal cell bodies were observed with this sheep antiserum. The immunolabeled somata were scattered periventricularly. Rostrally, a prominent group of faintly-stained neurons occurred in the VPe (A) and in the anterior parvocellular subdivision of the Pa (PaAP) (A). More caudally, cell bodies accumulated in the PaMc (B). Although scattered neurons occurred throughout the rostro-caudal extent of the periventricular region, the highest number of kisspeptin-54-immunoreactive cell bodies was detected in the Inf (D) and within the proximal portion of the InfS (C). The left panel in D illustrates a typical signal pattern in the female Inf. The corresponding photomicrograph on the right was taken from the hypothalamus of a 31-year-old male and reveals much lower kisspeptin cell numbers as well as fiber densities. Arrows in A–D point to kisspeptin-54-immunoreactive neuronal perikarya. Scale bars: 2.5 mm in schematic drawings and 25 μm in photomicrographs. (E) High variabilities in the kisspeptin fiber and cell body counts among different individuals. Although a sex difference is obvious (higher number of kisspeptin-54-immunoreactive fibers and cell bodies in the Inf of females vs. males), no age effect is detectable. See Results for detailed statistics. 3V, third cerebral ventricle; Ac, anterior commissure; BST, bed nucleus of the stria terminalis; DMH, dorsomedial hypothalamic nucleus; Fx, fornix; HDB, horizontal limb of the diagonal band; LHA, lateral hypothalamic area; LSV, ventrolateral septal nucleus; Ltu, lateral tuberal nucleus; Mfb, medial forebrain bundle; Opt, optic tract; OX, optic chiasm; SO, supraoptic nucleus; VMH, ventromedial hypothalamic nucleus.

GnRH neurons may communicate via non-synaptic mechanism at the level of their terminals (Fig. 4I).

Comparative distribution of preproneurokinin B and kisspeptin immunoreactivities

The immunoperoxidase-based detection of preproNKB provided evidence for an abundant NKB innervation of the human hypothalamus (Fig. 5). The new polyclonal antibodies from the two rabbits (IS-681 and IS-682) performed similarly. The specificity of the immunocytochemical labeling for preproNKB was indicated by the absence of labeling in sections incubated in preimmune sera of the two rabbits (#681 and #682). A further indication for labeling specificity was the complete absence of immunostaining in sections incubated with the working solutions of antisera that were preabsorbed overnight with 5 μg/mL of the immunization antigen. Finally, sections from rodent hypothalami were unlabeled, according to the expected lack of antiserum cross-reactions with the rodent preproNKB or related sequences. The distribution of preproNKB-immunoreactive fibers in hypothalami of female humans extended to the lateral hypothalamus (Fig. 5D), in contrast with the medially restricted distribution of kisspeptin-immunoreactive fibers. The InfS, where fibers surrounded capillary vessels, received a particularly dense innervation (Fig. 5B). In addition to an abundant innervation of the internal zone of the median eminence (Fig. 5B), many preproNKB-immunoreactive axons were seen in an unusual perivascular position in the outermost periphery of the external zone, lining the ventral surface of the InfS (Fig. 5C); here kisspeptin-immunoreactive fibers were relatively rare. PreproNKB-immunoreactive cell bodies were present in high numbers in the bed nucleus of the stria terminalis (Fig. 5A), along the diagonal band of Broca (not shown) and, notably, in the proximal portion of the InfS (Fig. 5E) and Inf (Fig. 5F) where large subsets of kisspeptin-immunoreactive cell bodies were also observed (Fig. 3C and D). The periventricular region also contained scattered preproNKB-immunoreactive somata (not shown). Overall, preproNKB labeling was more abundant in the hypothalamus compared with kisspeptin labeling and no obvious sex differences, similar to those seen with kisspeptin immunolabeling, were noticed.

Co-localization of preproneurokinin B and kisspeptin immunoreactivities in cell bodies and axons

In sections of the Inf, 77.0 ± 13.8% of kisspeptin-54-immunoreactive neuronal perikarya also exhibited preproNKB immunoreactivity and 95 ± 3.1% of the preproNKB-immunoreactive somata were labeled for kisspeptin-54 (Fig. 6A–C). Double-labeled axon varicosities were found frequently in various hypothalamic regions, including the Inf (Fig. 6D–F) and InfS (Fig. 6G–I). The preproNKB-immunoreactive fraction of kisspeptin-immunopositive axons changed from region to region. It represented 56.5 ± 7.8% of the kisspeptin-immunoreactive axons in the Inf and 13.6 ± 7.9% in the Pe. This regional difference was significant by one-way ANOVA ($F_{1,4} = 2.8$, $P = 0.02$). Extrahypothalamic kisspeptin-immunoreactive projections to the ventrolateral septal nucleus were devoid of preproNKB signal (< 0.5%). These area-specific differences (Fig. 6J) implicated neurochemically distinct cell sources for kisspeptin projections. The high representation of preproNKB-negative kisspeptin-54-immunoreactive fibers in several regions (PaMc, ventrolateral septal nucleus and Pe) provided indirect evidence for significant sources of kisspeptin fiber projections from outside the Inf. These sources probably include the rostral periventricular region (VPe and PaMc).

Discussion

The results of this study reveal the topography of kisspeptin-immunoreactive neurons and their fiber projections in the human hypothalamus, demonstrate a robust sexual dimorphism of this system, provide light microscopic evidence for kisspeptin-immunoreactive contacts on the soma, dendrites and axon terminals of GnRH neurons, and reveal the occurrence of preproNKB in a large population of kisspeptin-immunoreactive neurons in the Inf and their projections throughout the medial hypothalamus.

Kisspeptin signaling through GPR54 (Kiss1R) is critically important in mammalian reproduction (for recent reviews, see Herbison, 2008; Popa *et al.*, 2008; Castano *et al.*, 2009; Colledge, 2009; Gottsch *et al.*, 2009; Plant & Ramaswamy, 2009; Roseweir & Millar, 2009). In humans, the loss-of-function mutations of the *Kiss1R* gene cause autosomal recessive hypogonadotropic hypogonadism (de Roux *et al.*, 2003; Seminara *et al.*, 2003; Semple *et al.*, 2005), whereas activating mutation of *Kiss1R* results in central precocious puberty (Teles *et al.*, 2008). In mice, disruption of either the *Kiss1* (d'Anglemont de Tassigny *et al.*, 2007; Lapatto *et al.*, 2007) or *Kiss1R* gene (Seminara *et al.*, 2003; Lapatto *et al.*, 2007) causes hypogonadotropic hypogonadism. Kisspeptins regulate reproduction via influencing adenohypophysial gonadotropin secretion. Central or systemic administration of kisspeptins strongly stimulates luteinizing hormone release in various mammals (Gottsch *et al.*, 2004; Irwig *et al.*, 2004; Matsui *et al.*, 2004; Dhillo *et al.*, 2005, 2007). Although Kiss1R is detectable in the adenohypophysis (Richard *et al.*, 2009) and kisspeptins in the portal blood (Smith *et al.*, 2008b), the actions of kisspeptin appear to be mediated primarily by hypothalamic GnRH neurons, given that they can be prevented by a GnRH antagonist in rodents and monkeys (Gottsch *et al.*, 2004; Shahab *et al.*, 2005). Indeed, kisspeptin-immunoreactive fibers establish direct neuronal contacts with GnRH-immunoreactive cell bodies and dendrites in rats, mice and sheep (Kinoshita *et al.*, 2005; Clarkson & Herbison, 2006; Smith *et al.*, 2008a) and with the axon terminals of GnRH neurons in agonadal male rhesus monkeys (Ramaswamy *et al.*, 2008). Furthermore, Kiss1R mRNA is expressed in GnRH neurons in rats, mice and sheep (Irwig *et al.*, 2004; Han *et al.*, 2005; Messager *et al.*, 2005), central administration of kisspeptins induces cFos expression in GnRH neurons of rodents (Irwig *et al.*, 2004; Matsui *et al.*, 2004; Kauffman *et al.*, 2007b), and kisspeptins directly depolarize GnRH neurons in acute slice preparations from mice (Han *et al.*, 2005; Dumalska *et al.*, 2008; Pielecka-Fortuna *et al.*, 2008).

In view of the critical importance of kisspeptin/Kiss1R signaling in human reproduction, in the present immunocytochemical study we investigated various neuroanatomical aspects of central kisspeptin signaling in the human hypothalamus.

Distribution of kisspeptin immunoreactivity in the female hypothalamus

Mapping experiments used a previously characterized rabbit anti-mouse kisspeptin-10 antiserum (Clarkson & Herbison, 2006; Franceschini *et al.*, 2006; Clarkson *et al.*, 2009) and a sheep anti-human kisspeptin-54 antiserum (Dhillo *et al.*, 2007; Ramaswamy *et al.*, 2008). The identical distribution of kisspeptin-immunoreactive fibers with the two different kisspeptin antisera served as a strong argument for the specificity of labeling in our human samples. The better performance of the kisspeptin-54 antiserum in visualizing kisspeptin-synthesizing cell bodies was in accordance with similar immunocytochemical observations by others using kisspeptin-54 and kisspeptin-

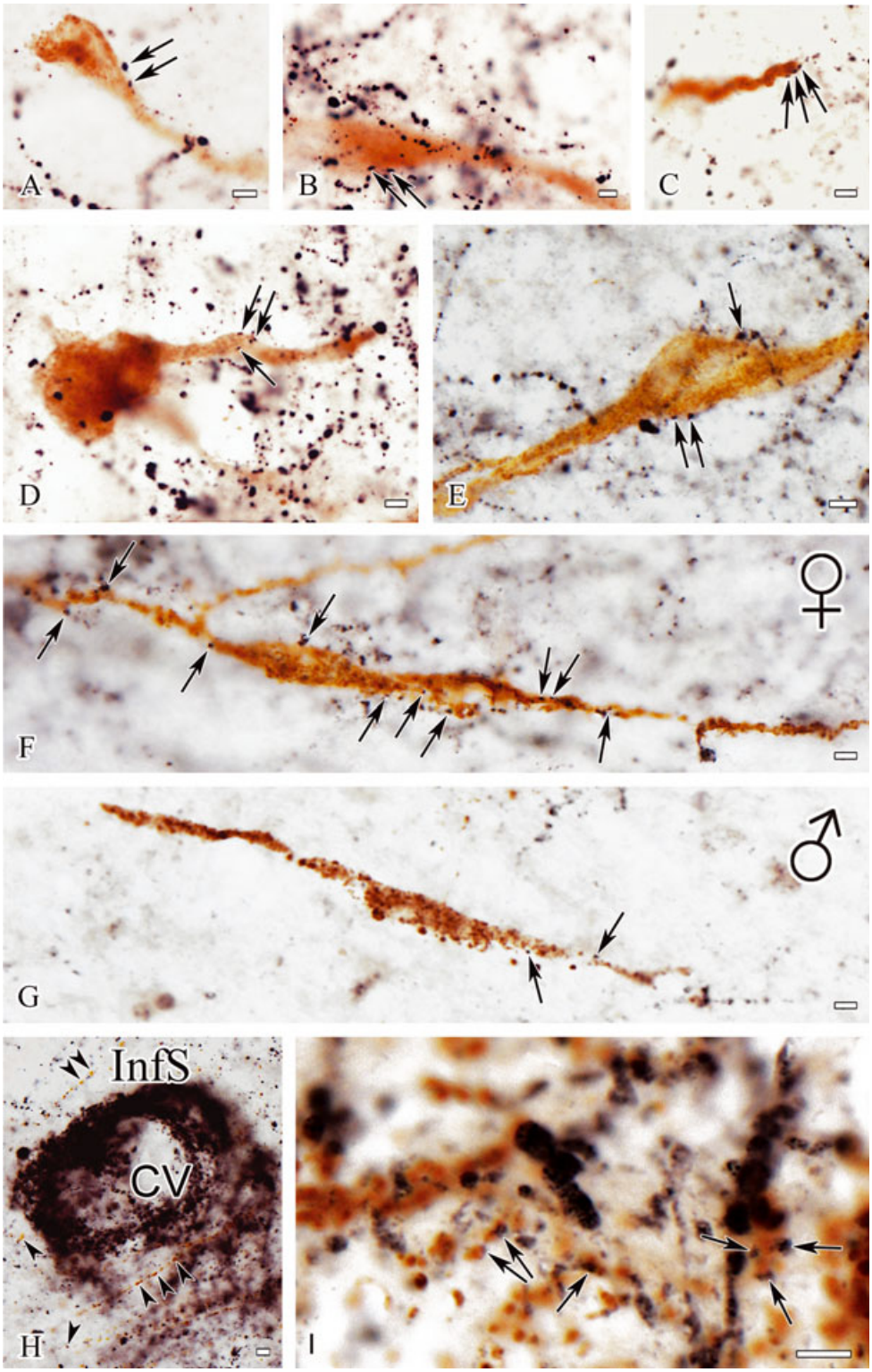

FIG. 4. Innervation of GnRH neurons by kisspeptin-immunoreactive fibers in the human. The dual-label immunocytochemical detection of kisspeptin fibers and GnRH neurons with the silver-intensified Ni-diaminobenzidine and diaminobenzidine chromogens, respectively, resulted in contrasting colors. Kisspeptin-immunoreactive axons identified with the rabbit kisspeptin-10 antiserum established neuronal appositions (arrows) to the cell bodies (A and B) and, more frequently, the dendrites (C and D) of GnRH-immunoreactive neurons in female hypothalami. Typical kisspeptin fibers in such appositions had a fine caliber. The application of the sheep kisspeptin-54 antiserum to detect kisspeptin fibers (E and F) resulted in the identification of similar juxtapositions. Contacts could also be revealed in specimens from male individuals (28-year-old male) (G). The InfS (H) contained many capillary vessels (CV), which were surrounded by kisspeptin-immunoreactive fibers. Arrowheads point to GnRH-immunoreactive axon varicosities. Kisspeptin- and GnRH-immunopositive fibers largely intermingled in the internal zone of the median eminence and high-power microscopic analysis revealed their frequent axo-axonal juxtapositions (shown by arrows in I). Scale bars: 5 μm.

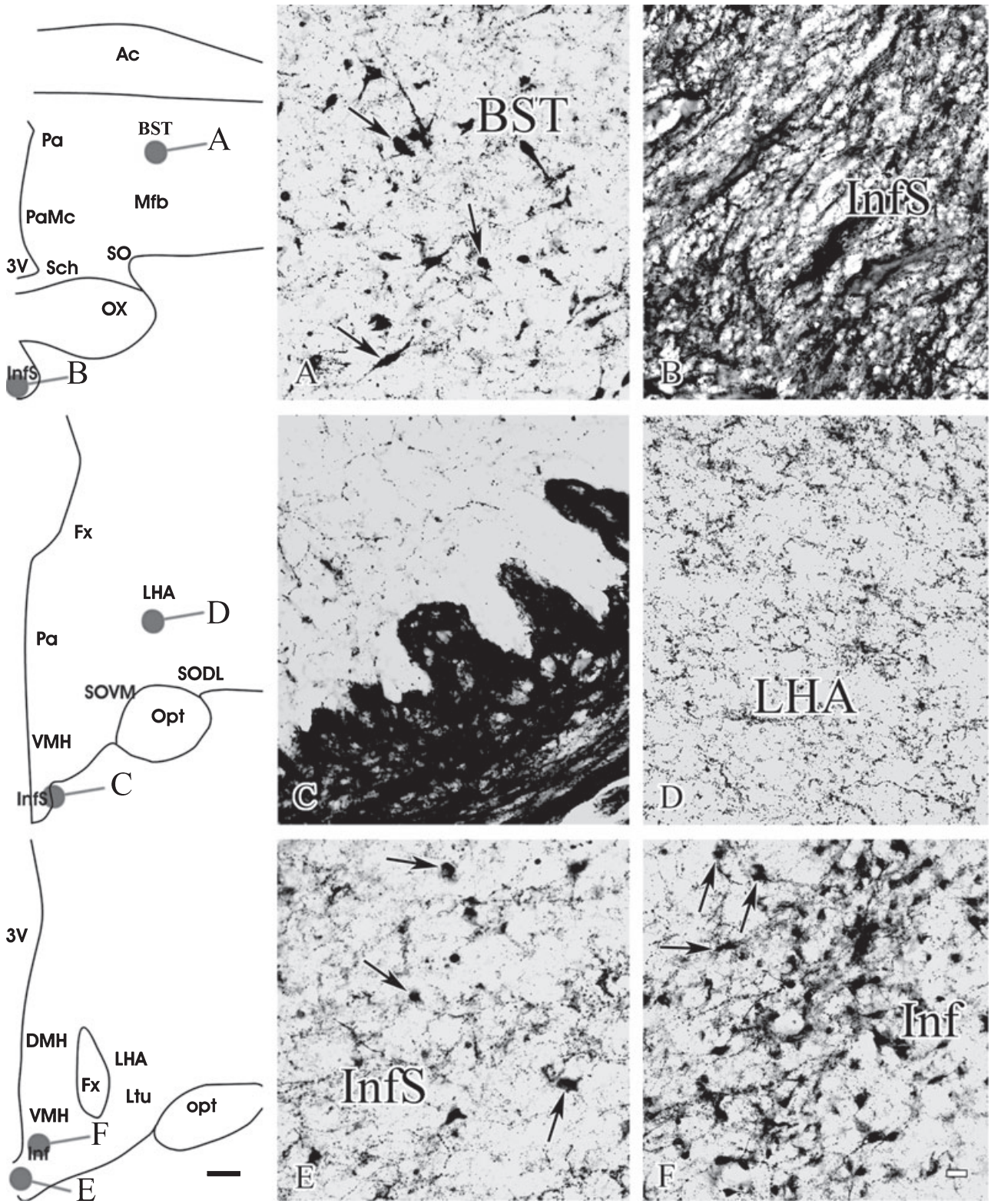

FIG. 5. Immunocytochemical detection of preproNKB in the human hypothalamus. The immunocyochemical detection of preproNKB (27-year-old female individual) resulted in the occurrence of dense hypothalamic and extrahypothalamic networks. In contrast with kisspeptin fibers, which occurred mostly in the medial hypothalamus, preproNKB-immunoreactive fibers were also highly abundant in the lateral hypothalamus, including the lateral hypothalamic area (LHA) (D). The innervation of the InfS (B) was particularly heavy, especially in its outermost periphery lining the ventral surface of the InfS (C). Several sites contained preproNKB-immunoreactive neuronal cell bodies, including a prominent cell group in the bed nucleus of the stria terminalis (BST) (A). The Inf (F) and the proximal portion of the InfS (E) contained preproNKB-immunoreactive perikarya with a distribution reminiscent of the labeling pattern of kisspeptin-immunoreactive somata. Scale bars: 2.5 mm in schematic drawings and 25 μm in photomicrographs. 3V, third cerebral ventricle; Ac, anterior commissure; DMH, dorsomedial hypothalamic nucleus; Fx, fornix; LHA, lateral hypothalamic area; Ltu, lateral tuberal nucleus; Mfb, medial forebrain bundle; Opt, optic tract; OX, optic chiasm; Sch, suprachiasmatic nucleus; SO, supraoptic nucleus; SOVM, ventromedial part of the supraoptic nucleus; SODL, dorsolateral part of the supraoptic nucleus; VMH, ventromedial hypothalamic nucleus.

10 antisera on tissue sections of monkey hypothalami (Ramaswamy *et al.*, 2008). The difference may be partly attributed to the presence of more epitopes on the longer peptide form. In addition, the kisspeptin-54 antiserum may recognize not only the fully processed but also the immature kisspeptin peptide precursor. Finally, the rabbit antiserum that we used in the present study was raised against the mouse (and rat) kisspeptin-10 sequence. Its relatively low (1%) cross-reactivity with the human kisspeptin-10 peptide sequence in radioimmunoassay, which was attributed to a single amino acid difference at the C-terminus between the mouse and human kisspeptin-10 (Franceschini *et al.*, 2006), could decrease further the labeling of neuronal cell bodies in our human study.

The highest density of kisspeptin-immunoreactive fibers was observed periventricularly throughout the rostro-caudal extent of the medial hypothalamus. Fibers were particularly abundant in the VPe, Pe, anteromedial and anterolateral preoptic nuclei, PaMc and parvocellular subdivisions of the Pa, Inf, DMN, dorsal hypothalamic area and InfS. There was a particularly strong fiber bundle just lateral to the PaMc where a large population of kisspeptin-immunoreactive cell bodies was found. The wide distribution of kisspeptin-immunoreactive fibers suggests multiple functions of the central kisspeptin system, in addition to providing an afferent input to GnRH neurons (present study). Of particular interest was the abundant innervation of the InfS where kisspeptin fibers surrounded capillary blood vessels, similarly to the terminals of GnRH neurons and other parvocellular neurosecretory systems. This finding raised the possibility of kisspeptin secretion into the hypophysial portal circulation. Kisspeptins were, indeed, detected in the ovine portal blood, albeit only at low levels (Smith *et al.*, 2008b). Kisspeptin axons in the median eminence may also exert local actions on other types of neuroendocrine terminals. Appositions between kisspeptin- and GnRH-immunoreactive fibers have been reported recently in the InfS of the agonadal male rhesus monkey model and proposed to underlie an axo-axonal neuronal communication (Ramaswamy *et al.*, 2008). In the present study we confirm that similar axo-axonal contacts also exist in the InfS of the human hypothalamus.

The largest groups of kisspeptin-immunoreactive cell bodies in our study were identified in the proximal portion of the InfS and in the Inf, which agreed well with the distribution of kisspeptin mRNA-expressing cells in the Inf of postmenopausal women (Rometo *et al.*, 2007) and of kisspeptin-immunoreactive neurons in the ARC of the agonadal male rhesus monkey model (Ramaswamy *et al.*, 2008). We have also observed significant additional groups of kisspeptin-immunoreactive neurons in the human female. Many scattered cell bodies were embedded in the kisspeptin-immunoreactive periventricular plexus. Particularly interesting was a relatively compact kisspeptin-immunoreactive cell population in the VPe and PaMc of the female hypothalamus. Although rostral periventricular kisspeptin neurons have been described in the sheep (Pompolo *et al.*, 2006) and rodent (Gottsch *et al.*, 2004) hypothalami, previous *in-situ* hybridization studies in the human (Rometo *et al.*, 2007) and immunocytochemical (Ramaswamy *et al.*, 2008) and *in-situ* hybridization studies in the monkey (Ramaswamy *et al.*, 2008) did not find significant numbers of kisspeptin-synthesizing neurons outside the Inf/ARC, except for rare, sparsely labeled neurons that were scattered within the human hypothalamic sections including the medial preoptic area (Rometo *et al.*, 2007). We propose that the kisspeptin-immunoreactive cells that we observed in the rostral periventricular zone (mostly lying within the PaMc and VPe) may be anatomically analogous to kisspeptin neurons of the rostral periventricular area of the third ventricle (RP3V) in rodents, which appears to mediate the positive estrogen feedback to GnRH neurons (Herbison, 2008). It is worth noting that this relatively compact cell group was only observed in the female hypothalami. Its neurochemical properties, including the expression of steroid hormone receptors, require clarification. Functional analysis of the rostral periventricular kisspeptin neurons will rely strongly on studies of non-human primates, provided that an analogous cell group in monkeys can be identified.

Sexual dimorphism of the human kisspeptin system

One aspect of the sexual dimorphism of the rodent kisspeptin neuronal system is that more kisspeptin-synthesizing neurons can be found in the RP3V of female vs. male mice (Clarkson & Herbison, 2006) and rats (Kauffman *et al.*, 2007a). Our observation that a putative primate equivalent of the RP3V (largely overlapping with the PaMc and VPe) also contained a prominent kisspeptin-immunoreactive cell group in the female but not the male hypothalamus, indicates that a similar sex difference also exists in the human. From a functional point of view, we have to note that, although the RP3V of the rodent hypothalamus has been strongly implicated in the positive estrogen feedback regulation of GnRH neurons, the current consensus regarding primates rather supports an exclusive role of the ARC/Inf in steroid feedback mechanisms (Knobil, 1980), leaving the functional significance of kisspeptin-immunoreactive neurons in the human RP3V unresolved.

The second important sex difference that we identified was in the number of kisspeptin-immunopositive cell bodies in the Inf. Whereas the male Inf contained only few, if any, lightly stained kisspeptin-immunoreactive neurons, about sevenfold more cell bodies could be visualized in the female Inf. This sex difference does not seem to be unique in humans as lower kisspeptin cell numbers have been reported very recently in the ARC of the male vs. female sheep (Cheng *et al.*, 2010).

The most prominent sex difference was in the density of kisspeptin-immunoreactive fibers throughout the medial hypothalamus. Fiber counting confirmed that the differences were significant and robust and showed about sevenfold more fibers in the Inf and fourfold more fibers in the Pe of females vs. males.

Sexual dimorphism of the kisspeptin system partly develops perinatally in rats as a result of testosterone exposure in the male (Kauffman *et al.*, 2007a). This also addresses the vulnerability of this important regulatory circuitry to environmental endocrine disruptors

FIG. 6. Co-localization of neuokinin and kisspeptin in cell bodies of the infundibular nucleus and in neuronal fibers of the medial hypothalamus in human females. The immunofluorescent detection of kisspeptins (green fluorochrom in A, D, G) and preproNKB (red fluorochrom in B, E, H) in hypothalamic sections of a 46-year-old human female revealed numerous immunoreactive cell bodies within the infundibular nucleus (Inf; A – C). Many of these neurons (indicated by double arrows) exhibited kisspeptin as well as preproNKB immunolabeling, whereas smaller subsets were single-labeled (arrows). Hypothalamic kisspeptin fibers in the Inf (D), infundibular stalk (InfS; G), and also elsewhere in the medial hypothalamus often contained preproNKB immunolabeling (E and H). Double arrows indicate dual-labeled axons, whereas additional fiber populations that are single-labeled are shown by arrows. Panels C, F and I represent merged images from A – B, D – E, and G – H, respectively. Scale bars = 50 μm in A – C and 10 μm in D – I. Lower diagram (J) illustrates the results of a quantitative analysis to determine the percentages of kisspeptin-54-immunoreactive fibers that also contain preproNKB signal in the Inf (56.5 ± 7.8%), the periventricular nucleus (Pe; 16.8 ± 7.9%) and ventrolateral septal nucleus (LSV) (< 0.5%). *Significantly different from the Inf ($F_{1,4}$ = 2.8, P = 0.02).

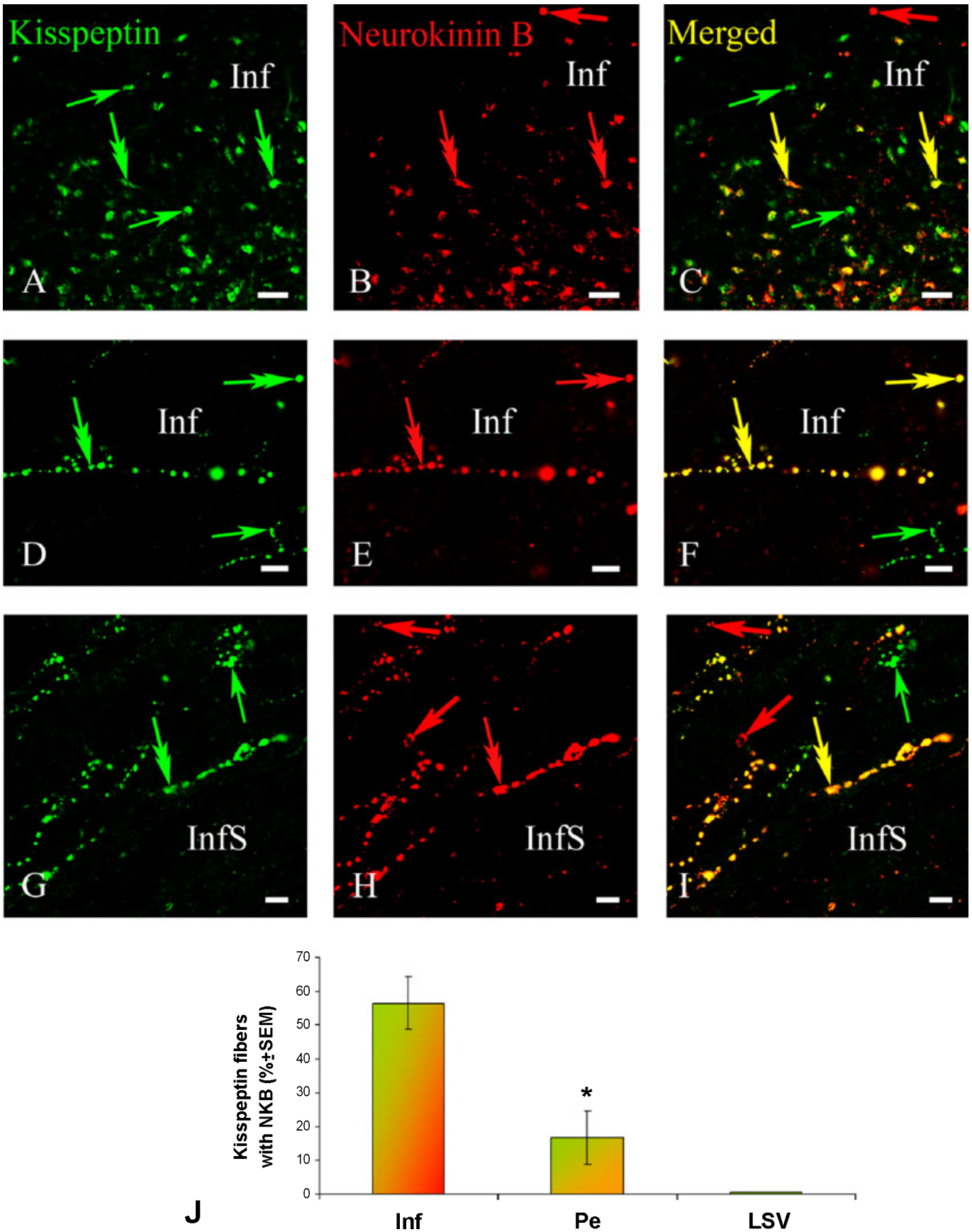

during the critical period of sexual differentiation, as reviewed recently (Tena-Sempere, 2009).

Sites of interaction between central kisspeptin and gonadotropin-releasing hormone neurons

The kisspeptin-immunoreactive fiber appositions to the dendrites and cell bodies of GnRH neurons in the present study indicate axo-dendritic and axo-somatic neuronal communications. Similar neuronal contacts have been observed in rodents (Kinoshita *et al.*, 2005; Clarkson & Herbison, 2006). About 10% of GnRH neurons in adult male and 40% of GnRH neurons in adult female mice, most in the rostral preoptic area, were reported to receive kisspeptin-immunoreactive fiber appositions (Kinoshita *et al.*, 2005; Clarkson & Herbison, 2006). The concept that kisspeptins can, indeed, act on the somatic/dendritic compartments of GnRH cells gains strong functional support from the direct depolarization of GnRH neurons in acute preoptic slice preparations of mice (Han *et al.*, 2005; Dumalska *et al.*, 2008; Pielecka-Fortuna *et al.*, 2008). Although similar axo-somatic and axo-dendritic contacts were reported to occur only rarely in the agonadal male rhesus monkey model, some 25–50% of GnRH perikarya in that study did receive kisspeptin-immunoreactive fiber contacts, with an average frequency of 0.3–0.5 contacts/GnRH soma (Ramaswamy *et al.*, 2008). In the present study we observed kisspeptin-immunoreactive neuronal contacts on highly variable percentages of the GnRH-immunoreactive cell bodies in gonadally intact female (25.8 ± 15.0%) and male (8.3 ± 3.6%) human individuals. GnRH neurons received 0.7 ± 0.5 contacts in female specimens and 0.12 ± 0.05% contacts in samples from male individuals (mean ± SEM). A previous detailed analysis of the female sheep revealed regional as well as breeding-season-dependent variations in the number of contacts onto GnRH neurons and in the percentage of the innervated GnRH neurons (Smith *et al.*, 2008a). Whereas the above published numbers indicate some species differences, it has to be noted that all species examined so far show similarities with our present human data in that not all GnRH neurons receive kisspeptin-immunoreactive fiber contacts (Clarkson & Herbison, 2006; Ramaswamy *et al.*, 2008; Smith *et al.*, 2008a) and the incidence of neuronal contacts is low (about 0.1–3.5 contacts/GnRH neuron) (Ramaswamy *et al.*, 2008; Smith *et al.*, 2008a).

In addition to axo-somatic and axo-dendritic appositions, axo-axonal contacts were also found between kisspeptin- and GnRH-immunoreactive axons in the InfS, in accordance with similar observations made recently in the median eminence of agonadal male rhesus monkeys (Ramaswamy *et al.*, 2008). These axo-axonal contacts suggest that GnRH secretion may also be regulated by kisspeptins in the InfS. Functional support for the concept that an important site of kisspeptin action lies outside the blood–brain barrier in the median eminence/InfS is provided by observations from rodent species that peripheral kisspeptin administration increases luteininzing hormone release (Matsui *et al.*, 2004) without inducing c-fos immunoreactivity in GnRH neurons (Mikkelsen *et al.*, 2009) and that kisspeptins can elicit GnRH release from mediobasal hypothalamic explants via Kiss1R, in the absence of GnRH neuronal cell bodies (d'Anglemont de Tassigny *et al.*, 2008). Appositions between kisspeptin-immunoreactive axons and GnRH terminals have not yet been reported in the rodent median eminence. The contacts between NKB-immunoreactive axons and GnRH terminals (Krajewski *et al.*, 2005; Ciofi *et al.*, 2006) serve as indirect evidence that these appositions may exist, in view of the fact that the NKB axons involved probably originate from the kisspeptin/NKB/dynorphin-positive cell group of the ARC (Navarro *et al.*, 2009).

The immunocytochemical localization of Kiss1R will be critically important to assess the relative importance of kisspeptin actions exerted at the level of GnRH neuronal cell bodies, dendrites and terminals. None of the available data exclude that kisspeptins may act upon multiple cellular compartments of the GnRH neuron.

Demonstration of neurokinin B in kisspeptin neurons

Our study to assess the presence of preproNKB in kisspeptin-immunoreactive neurons of the Inf was motivated by (i) the presence of immunoreactivities for preproNKB and dynorphin in kisspeptin neurons of the arcuate nucleus in sheep (Goodman *et al.*, 2007) and mice (Navarro *et al.*, 2009), (ii) the observations that kisspeptin (Rometo *et al.*, 2007) and NKB (Rance, 2009) neurons exhibit postmenopausal hypertrophy at similar locations of the human Inf and (iii) the results of recent studies that have demonstrated reproductive failure in humans due to mutation of either the NKB or the NKB receptor (neurokinin-3 receptor) gene (Guran *et al.*, 2009; Topaloglu *et al.*, 2009). Our dual-immunofluorescent experiments revealed that a high proportion (77%) of kisspeptin neurons in the Inf also synthesize preproNKB in the human female. Furthermore, the analysis of neuronal fibers established that varying subsets of kisspeptin axons in different hypothalamic nuclei also exhibit immunoreactivity for preproNKB. Although dual-labeled kisspeptin fibers probably arise in the Inf where we detected numerous dual-labeled perikarya, multiple sources of the single-labeled kisspeptin fibers may exist. It is possible that large subsets of such fibers arise from the kisspeptin-immunoreactive perikarya that we observed in the Pa, Pe and other hypothalamic regions along the third ventricle, in particular the VPe and PaMc, which contained a large population of kisspeptin neurons but no preproNKB-immunoreactive cells. Alternatively, some single-labeled kisspeptin fibers may also arise from those kisspeptin-immunoreactive somata in the Inf that do not synthesize detectable amounts of preproNKB. Based on our observation that preproNKB was present in 56.5% of the kisspeptin-immunoreactive axons in the Inf and in only 13.6% of kisspeptin-immunoreactive fibers in the Pe, and was absent from kisspeptin projections in the ventrolateral septal nucleus, we conclude that kisspeptin-synthesizing neurons within and outside the Inf contribute differentially to the innervation of different hypothalamic and extrahypothalamic sites. Furthermore, the preproNKB-negative fibers that predominated in the rostral hypothalamus also indicated that significant cellular sources for kisspeptin fibers exist outside the Inf. The receptorial mechanisms and sites of action whereby NKB influences human reproduction are not entirely understood. In the rat, at least some actions of NKB may occur at the level of terminals. Accordingly, GnRH terminals in the external zone of the median eminence express immunoreactivity for neurokinin-3 receptor (Krajewski *et al.*, 2005) and establish contacts with NKB-immunoreactive endings (Ciofi *et al.*, 2006).

Technical limitations

As also noted in previous human studies (Hrabovszky *et al.*, 2007), our limited access to human tissue samples prevented us from answering some otherwise important questions in this study. The low labeling intensity of kisspeptin-immunoreactive neuronal cell bodies limited the analysis of dual-labeled perikarya to the Inf where kisspeptin immunoreactivity was strongest. The immunocytochemical staining of the different tissue samples also showed considerable variability. This could result from the combined effect of different age,

hormonal status, circumstances of death and postmortem delay. Although correlation analysis showed no effect of age on the kisspeptin fiber or cell counts in the present study, this negative finding could be largely due to the high variation among individual specimens in view of the fact that *in-situ* hybridization studies by others managed to detect increased kisspeptin mRNA levels and kisspeptin cell numbers in the Inf of postmenopausal vs. premenopausal women (Rometo *et al.*, 2007).

In summary, in this study we have mapped the kisspeptin-immunoreactive fibers and neuronal cell bodies in the hypothalamus of human males and females. We have shown that the female hypothalamus contains significantly more kisspeptin-immunoreactive neurons and axons than the male. We have demonstrated that kisspeptin-immunopositive fibers are directly apposed to the dendrites and the cell bodies of GnRH neurons and they also form contacts with GnRH fibers in the InfS. Finally, we have demonstrated that a large subset of kisspeptin neurons in the Inf and varying subsets of kisspeptin fibers throughout the medial hypothalamus exhibit prepro-NKB immunoreactivity.

Acknowledgements

This research was supported by the National Science Foundation of Hungary (OTKA K69127 and T73002) and the Medical Research Council (ETT 122-09/2009). We thank Dr R. A. Benoit for the kind donation of the LR1 GnRH antibodies and Hajni Bekó for technical assistance.

Abbreviations

ARC, arcuate hypothalamic nucleus; GnRH, gonadotropin-releasing hormone; GPR54, G-protein-coupled receptor-54; Inf, infundibular nucleus; InfS, infundibular stalk; NKB, neurokinin B; Pa, paraventricular hypothalamic nucleus; PaMc, magnocellular part of the paraventricular hypothalamic nucleus; Pe, periventricular hypothalamic nucleus; RP3V, rostral periventricular area of the third ventricle; VPe, ventral periventricular hypothalamic nucleus.

References

d'Anglemont de Tassigny, X., Fagg, L.A., Dixon, J.P., Day, K., Leitch, H.G., Hendrick, A.G., Zahn, D., Franceschini, I., Caraty, A., Carlton, M.B., Aparicio, S.A. & Colledge, W.H. (2007) Hypogonadotropic hypogonadism in mice lacking a functional Kiss1 gene. *Proc. Natl Acad. Sci. USA*, **104**, 10714–10719.

d'Anglemont de Tassigny, X., Fagg, L.A., Carlton, M.B. & Colledge, W.H. (2008) Kisspeptin can stimulate gonadotropin-releasing hormone (GnRH) release by a direct action at GnRH nerve terminals. *Endocrinology*, **149**, 3926–3932.

Castano, J.P., Martinez-Fuentes, A.J., Gutierrez-Pascual, E., Vaudry, H., Tena-Sempere, M. & Malagon, M.M. (2009) Intracellular signaling pathways activated by kisspeptins through GPR54: do multiple signals underlie function diversity? *Peptides*, **30**, 10–15.

Cheng, G., Coolen, L.M., Padmanabhan, V., Goodman, R.L. & Lehman, M.N. (2010) The kisspeptin/neurokinin B/dynorphin (KNDy) cell population of the arcuate nucleus: sex differences and effects of prenatal testosterone in the sheep. *Endocrinology*, **151**, 301–311.

Ciofi, P., Leroy, D. & Tramu, G. (2006) Sexual dimorphism in the organization of the rat hypothalamic infundibular area. *Neuroscience*, **141**, 1731–1745.

Clarkson, J. & Herbison, A.E. (2006) Postnatal development of kisspeptin neurons in mouse hypothalamus; sexual dimorphism and projections to gonadotropin-releasing hormone neurons. *Endocrinology*, **147**, 5817–5825.

Clarkson, J., d'Anglemont de Tassigny, X., Colledge, W.H., Caraty, A. & Herbison, A.E. (2009) Distribution of kisspeptin neurones in the adult female mouse brain. *J. Neuroendocrinol.*, **21**, 673–682.

Colledge, W.H. (2009) Kisspeptins and GnRH neuronal signalling. *Trends Endocrinol. Metab.*, **20**, 115–121.

Dhillo, W.S., Chaudhri, O.B., Patterson, M., Thompson, E.L., Murphy, K.G., Badman, M.K., McGowan, B.M., Amber, V., Patel, S., Ghatei, M.A. & Bloom, S.R. (2005) Kisspeptin-54 stimulates the hypothalamic-pituitary gonadal axis in human males. *J. Clin. Endocrinol. Metab.*, **90**, 6609–6615.

Dhillo, W.S., Chaudhri, O.B., Thompson, E.L., Murphy, K.G., Patterson, M., Ramachandran, R., Nijher, G.K., Amber, V., Kokkinos, A., Donaldson, M., Ghatei, M.A. & Bloom, S.R. (2007) Kisspeptin-54 stimulates gonadotropin release most potently during the preovulatory phase of the menstrual cycle in women. *J. Clin. Endocrinol. Metab.*, **92**, 3958–3966.

Dumalska, I., Wu, M., Morozova, E., Liu, R., van den Pol, A. & Alreja, M. (2008) Excitatory effects of the puberty-initiating peptide kisspeptin and group I metabotropic glutamate receptor agonists differentiate two distinct subpopulations of gonadotropin-releasing hormone neurons. *J. Neurosci.*, **28**, 8003–8013.

Franceschini, I., Lomet, D., Cateau, M., Delsol, G., Tillet, Y. & Caraty, A. (2006) Kisspeptin immunoreactive cells of the ovine preoptic area and arcuate nucleus co-express estrogen receptor alpha. *Neurosci. Lett.*, **401**, 225–230.

Goodman, R.L., Lehman, M.N., Smith, J.T., Coolen, L.M., de Oliveira, C.V., Jafarzadehshirazi, M.R., Pereira, A., Iqbal, J., Caraty, A., Ciofi, P. & Clarke, I.J. (2007) Kisspeptin neurons in the arcuate nucleus of the ewe express both dynorphin A and neurokinin B. *Endocrinology*, **148**, 5752–5760.

Gottsch, M.L., Cunningham, M.J., Smith, J.T., Popa, S.M., Acohido, B.V., Crowley, W.F., Seminara, S., Clifton, D.K. & Steiner, R.A. (2004) A role for kisspeptins in the regulation of gonadotropin secretion in the mouse. *Endocrinology*, **145**, 4073–4077.

Gottsch, M.L., Clifton, D.K. & Steiner, R.A. (2009) From KISS1 to kisspeptins: an historical perspective and suggested nomenclature. *Peptides*, **30**, 4–9.

Guran, T., Tolhurst, G., Bereket, A., Rocha, N., Porter, K., Turan, S., Gribble, F.M., Kotan, L.D., Akcay, T., Atay, Z., Canan, H., Serin, A., O'Rahilly, S., Reimann, F., Semple, R.K. & Topaloglu, A.K. (2009) Hypogonadotropic hypogonadism due to a novel missense mutation in the first extracellular loop of the neurokinin B receptor. *J. Clin. Endocrinol. Metab.*, **94**, 3633–3639.

Han, S.K., Gottsch, M.L., Lee, K.J., Popa, S.M., Smith, J.T., Jakawich, S.K., Clifton, D.K., Steiner, R.A. & Herbison, A.E. (2005) Activation of gonadotropin-releasing hormone neurons by kisspeptin as a neuroendocrine switch for the onset of puberty. *J. Neurosci.*, **25**, 11349–11356.

Herbison, A.E. (2008) Estrogen positive feedback to gonadotropin-releasing hormone (GnRH) neurons in the rodent: the case for the rostral periventricular area of the third ventricle (RP3V). *Brain Res. Rev.*, **57**, 277–287.

Hrabovszky, E., Kallo, I., Szlavik, N., Keller, E., Merchenthaler, I. & Liposits, Z. (2007) Gonadotropin-releasing hormone neurons express estrogen receptor-beta. *J. Clin. Endocrinol. Metab.*, **92**, 2827–2830.

Irwig, M.S., Fraley, G.S., Smith, J.T., Acohido, B.V., Popa, S.M., Cunningham, M.J., Gottsch, M.L., Clifton, D.K. & Steiner, R.A. (2004) Kisspeptin activation of gonadotropin releasing hormone neurons and regulation of KiSS-1 mRNA in the male rat. *Neuroendocrinology*, **80**, 264–272.

Kauffman, A.S., Gottsch, M.L., Roa, J., Byquist, A.C., Crown, A., Clifton, D.K., Hoffman, G.E., Steiner, R.A. & Tena-Sempere, M. (2007a) Sexual differentiation of Kiss1 gene expression in the brain of the rat. *Endocrinology*, **148**, 1774–1783.

Kauffman, A.S., Park, J.H., McPhie-Lalmansingh, A.A., Gottsch, M.L., Bodo, C., Hohmann, J.G., Pavlova, M.N., Rohde, A.D., Clifton, D.K., Steiner, R.A. & Rissman, E.F. (2007b) The kisspeptin receptor GPR54 is required for sexual differentiation of the brain and behavior. *J. Neurosci.*, **27**, 8826–8835.

Kinoshita, M., Tsukamura, H., Adachi, S., Matsui, H., Uenoyama, Y., Iwata, K., Yamada, S., Inoue, K., Ohtaki, T., Matsumoto, H. & Maeda, K. (2005) Involvement of central metastin in the regulation of preovulatory luteinizing hormone surge and estrous cyclicity in female rats. *Endocrinology*, **146**, 4431–4436.

Knobil, E. (1980) The neuroendocrine control of the menstrual cycle. *Recent Prog. Horm. Res.*, **36**, 53–88.

Kotani, M., Detheux, M., Vandenbogaerde, A., Communi, D., Vanderwinden, J.M., Le Poul, E., Brezillon, S., Tyldesley, R., Suarez-Huerta, N., Vandeput, F., Blanpain, C., Schiffmann, S.N., Vassart, G. & Parmentier, M. (2001) The metastasis suppressor gene KiSS-1 encodes kisspeptins, the natural ligands of the orphan G protein-coupled receptor GPR54. *J. Biol. Chem.*, **276**, 34631–34636.

Krajewski, S.J., Anderson, M.J., Iles-Shih, L., Chen, K.J., Urbanski, H.F. & Rance, N.E. (2005) Morphologic evidence that neurokinin B modulates gonadotropin-releasing hormone secretion via neurokinin 3 receptors in the rat median eminence. *J. Comp. Neurol.*, **489**, 372–386.

Lapatto, R., Pallais, J.C., Zhang, D., Chan, Y.M., Mahan, A., Cerrato, F., Le, W.W., Hoffman, G.E. & Seminara, S.B. (2007) Kiss1$^{-/-}$ mice exhibit more variable hypogonadism than Gpr54$^{-/-}$ mice. *Endocrinology*, **148**, 4927–4936.

Liposits, Z., Setalo, G. & Flerko, B. (1984) Application of the silver-gold intensified 3,3′-diaminobenzidine chromogen to the light and electron microscopic detection of the luteinizing hormone-releasing hormone system of the rat brain. *Neuroscience*, **13**, 513–525.

Mai, J., Assheuer, J. & Paxinos, G. (Eds) (1997) *Atlas of the Human Brain*. Academic Press, San Diego.

Matsui, H., Takatsu, Y., Kumano, S., Matsumoto, H. & Ohtaki, T. (2004) Peripheral administration of metastin induces marked gonadotropin release and ovulation in the rat. *Biochem. Biophys. Res. Commun.*, **320**, 383–388.

Messager, S., Chatzidaki, E.E., Ma, D., Hendrick, A.G., Zahn, D., Dixon, J., Thresher, R.R., Malinge, I., Lomet, D., Carlton, M.B., Colledge, W.H., Caraty, A. & Aparicio, S.A. (2005) Kisspeptin directly stimulates gonadotropin-releasing hormone release via G protein-coupled receptor 54. *Proc. Natl Acad. Sci. USA*, **102**, 1761–1766.

Mihaly, E., Fekete, C., Lechan, R.M. & Liposits, Z. (2002) Corticotropin-releasing hormone-synthesizing neurons of the human hypothalamus receive neuropeptide Y-immunoreactive innervation from neurons residing primarily outside the infundibular nucleus. *J. Comp. Neurol.*, **446**, 235–243.

Mikkelsen, J.D., Bentsen, A.H., Ansel, L., Simonneaux, V. & Juul, A. (2009) Comparison of the effects of peripherally administered kisspeptins. *Regul. Pept.*, **152**, 95–100.

Muir, A.I., Chamberlain, L., Elshourbagy, N.A., Michalovich, D., Moore, D.J., Calamari, A., Szekeres, P.G., Sarau, H.M., Chambers, J.K., Murdock, P., Steplewski, K., Shabon, U., Miller, J.E., Middleton, S.E., Darker, J.G., Larminie, C.G., Wilson, S., Bergsma, D.J., Emson, P., Faull, R., Philpott, K.L. & Harrison, D.C. (2001) AXOR12, a novel human G protein-coupled receptor, activated by the peptide KiSS-1. *J. Biol. Chem.*, **276**, 28969–28975.

Navarro, V.M., Gottsch, M.L., Chavkin, C., Okamura, H., Clifton, D.K. & Steiner, R.A. (2009) Regulation of gonadotropin-releasing hormone secretion by kisspeptin/dynorphin/neurokinin B neurons in the arcuate nucleus of the mouse. *J. Neurosci.*, **29**, 11859–11866.

Ohtaki, T., Shintani, Y., Honda, S., Matsumoto, H., Hori, A., Kanehashi, K., Terao, Y., Kumano, S., Takatsu, Y., Masuda, Y., Ishibashi, Y., Watanabe, T., Asada, M., Yamada, T., Suenaga, M., Kitada, C., Usuki, S., Kurokawa, T., Onda, H., Nishimura, O. & Fujino, M. (2001) Metastasis suppressor gene KiSS-1 encodes peptide ligand of a G-protein-coupled receptor. *Nature*, **411**, 613–617.

Pielecka-Fortuna, J., Chu, Z. & Moenter, S.M. (2008) Kisspeptin acts directly and indirectly to increase gonadotropin-releasing hormone neuron activity and its effects are modulated by estradiol. *Endocrinology*, **149**, 1979–1986.

Plant, T.M. & Ramaswamy, S. (2009) Kisspeptin and the regulation of the hypothalamic-pituitary-gonadal axis in the rhesus monkey (Macaca mulatta). *Peptides*, **30**, 67–75.

Pompolo, S., Pereira, A., Estrada, K.M. & Clarke, I.J. (2006) Colocalization of kisspeptin and gonadotropin-releasing hormone in the ovine brain. *Endocrinology*, **147**, 804–810.

Popa, S.M., Clifton, D.K. & Steiner, R.A. (2008) The role of kisspeptins and GPR54 in the neuroendocrine regulation of reproduction. *Annu. Rev. Physiol.*, **70**, 213–238.

Ramaswamy, S., Guerriero, K.A., Gibbs, R.B. & Plant, T.M. (2008) Structural interactions between kisspeptin and GnRH neurons in the mediobasal hypothalamus of the male rhesus monkey (Macaca mulatta) as revealed by double immunofluorescence and confocal microscopy. *Endocrinology*, **149**, 4387–4395.

Rance, N.E. (2009) Menopause and the human hypothalamus: evidence for the role of kisspeptin/neurokinin B neurons in the regulation of estrogen negative feedback. *Peptides*, **30**, 111–122.

Richard, N., Corvaisier, S., Camacho, E. & Kottler, M.L. (2009) KiSS-1 and GPR54 at the pituitary level: overview and recent insights. *Peptides*, **30**, 123–129.

Rometo, A.M., Krajewski, S.J., Voytko, M.L. & Rance, N.E. (2007) Hypertrophy and increased kisspeptin gene expression in the hypothalamic infundibular nucleus of postmenopausal women and ovariectomized monkeys. *J. Clin. Endocrinol. Metab.*, **92**, 2744–2750.

Roseweir, A.K. & Millar, R.P. (2009) The role of kisspeptin in the control of gonadotrophin secretion. *Hum. Reprod. Update*, **15**, 203–212.

de Roux, N., Genin, E., Carel, J.C., Matsuda, F., Chaussain, J.L. & Milgrom, E. (2003) Hypogonadotropic hypogonadism due to loss of function of the KiSS1-derived peptide receptor GPR54. *Proc. Natl Acad. Sci. USA*, **100**, 10972–10976.

Seminara, S.B., Messager, S., Chatzidaki, E.E., Thresher, R.R., Acierno, J.S. Jr, Shagoury, J.K., Bo-Abbas, Y., Kuohung, W., Schwinof, K.M., Hendrick, A.G., Zahn, D., Dixon, J., Kaiser, U.B., Slaugenhaupt, S.A., Gusella, J.F., O'Rahilly, S., Carlton, M.B., Crowley, W.F. Jr, Aparicio, S.A. & Colledge, W.H. (2003) The GPR54 gene as a regulator of puberty. *N. Engl. J. Med.*, **349**, 1614–1627.

Semple, R.K., Achermann, J.C., Ellery, J., Farooqi, I.S., Karet, F.E., Stanhope, R.G., O'Rahilly, S. & Aparicio, S.A. (2005) Two novel missense mutations in g protein-coupled receptor 54 in a patient with hypogonadotropic hypogonadism. *J. Clin. Endocrinol. Metab.*, **90**, 1849–1855.

Shahab, M., Mastronardi, C., Seminara, S.B., Crowley, W.F., Ojeda, S.R. & Plant, T.M. (2005) Increased hypothalamic GPR54 signaling: a potential mechanism for initiation of puberty in primates. *Proc. Natl Acad. Sci. USA*, **102**, 2129–2134.

Smith, J.T., Coolen, L.M., Kriegsfeld, L.J., Sari, I.P., Jaafarzadehshirazi, M.R., Maltby, M., Bateman, K., Goodman, R.L., Tilbrook, A.J., Ubuka, T., Bentley, G.E., Clarke, I.J. & Lehman, M.N. (2008a) Variation in kisspeptin and RFamide-related peptide (RFRP) expression and terminal connections to gonadotropin-releasing hormone neurons in the brain: a novel medium for seasonal breeding in the sheep. *Endocrinology*, **149**, 5770–5782.

Smith, J.T., Rao, A., Pereira, A., Caraty, A., Millar, R.P. & Clarke, I.J. (2008b) Kisspeptin is present in ovine hypophysial portal blood but does not increase during the preovulatory luteinizing hormone surge: evidence that gonadotropes are not direct targets of kisspeptin in vivo. *Endocrinology*, **149**, 1951–1959.

Teles, M.G., Bianco, S.D., Brito, V.N., Trarbach, E.B., Kuohung, W., Xu, S., Seminara, S.B., Mendonca, B.B., Kaiser, U.B. & Latronico, A.C. (2008) A GPR54-activating mutation in a patient with central precocious puberty. *N. Engl. J. Med.*, **358**, 709–715.

Tena-Sempere, M. (2009) Kisspeptin/GPR54 system as potential target for endocrine disruption of reproductive development and function. *Int. J. Androl.*, **33**, 360–368.

Topaloglu, A.K., Reimann, F., Guclu, M., Yalin, A.S., Kotan, L.D., Porter, K.M., Serin, A., Mungan, N.O., Cook, J.R., Ozbek, M.N., Imamoglu, S., Akalin, N.S., Yuksel, B., O'Rahilly, S. & Semple, R.K. (2009) TAC3 and TACR3 mutations in familial hypogonadotropic hypogonadism reveal a key role for Neurokinin B in the central control of reproduction. *Nat. Genet.*, **41**, 354–358.

dc_27_10

22. számú melléklet

Endocrinology dc_27_10

Estradiol Replacement Alters Expression of Genes Related to Neurotransmission and Immune Surveillance in the Frontal Cortex of Middle-Aged, Ovariectomized Rats

Miklós Sárvári, Imre Kalló, Erik Hrabovszky, Norbert Solymosi, Kinga Tóth, István Likó, Béla Molnár, Károly Tihanyi and Zsolt Liposits

Endocrinology 2010 151:3847-3862 originally published online Jun 9, 2010; , doi: 10.1210/en.2010-0375

Estradiol Replacement Alters Expression of Genes Related to Neurotransmission and Immune Surveillance in the Frontal Cortex of Middle-Aged, Ovariectomized Rats

Miklós Sárvári, Imre Kalló, Erik Hrabovszky, Norbert Solymosi, Kinga Tóth, István Likó, Béla Molnár, Károly Tihanyi, and Zsolt Liposits

Laboratory of Endocrine Neurobiology (M.S., I.K., E.H., Z.L.), Institute of Experimental Medicine, and Molecular Medicine Research Unit (B.M.), Hungarian Academy of Sciences, H-1083 Budapest, Hungary; Gedeon Richter Plc. (M.S., I.L., K.Ti.), H-1103 Budapest, Hungary; Faculty of Information Technology (I.K., Z.L.), Pázmány Péter Catholic University, H-1088 Budapest, Hungary; Department of the Physics of Complex Systems (N.S.), Eötvös Loránd University, H-1117 Budapest, Hungary; and Second Department of Medicine (K.To., B.M.), Semmelweis University, H-1089 Budapest, Hungary

Estradiol (E2) modulates a wide range of functions of the frontal cerebral cortex. From the onset of menopause, declining levels of E2 can cause cognitive disturbances and changes in behavior that can be counterbalanced by hormone replacement. To study the effect of E2 replacement on the cortical transcriptome in a rodent model with low serum E2 level, we treated middle-aged, ovariectomized rats with E2 or vehicle using osmotic minipumps for 4 wk. Six animals for each group were selected, and samples of their frontal cortex were subjected to expression profiling using oligonucleotide microarrays. The explored E2-regulated genes were related to neurotransmission (*Adora2a*, *Cartpt*, *Drd1a*, *Drd2*, *Gjb2*, *Nts*, and *Tac1*), immunity (*C3*, *C4b*, *Cd74*, *Fcgr2b*, *Mpeg1*, and *RT1-Aw2*), signal transduction (*Igf2*, *Igfbp2*, *Igfbp6*, *Rgs9*, and *Sncg*), transport (*Abca1*, *Hba-a2*, *Slc13a3*, and *Slc22a8*), extracellular matrix (*Col1a2*, *Col3a1*, *Fmod*, and *Lum*), and transcription (*Irf7* and *Nupr1*). Seventy-four percent of the transcriptional changes identified by microarray were confirmed by quantitative real-time PCR. The genes identified by expression profiling indicated that chronic E2 replacement significantly altered the transcriptome of the frontal cortex. The genomic effects of E2 influenced dopaminergic and peptidergic neurotransmission, immune surveillance, adenosine and insulin-like growth factor signaling and transport processes, among other functions. Identification of these novel E2-regulated mechanisms highlights the wide range of genomic responses of the aging female frontal cerebral cortex subjected to hormone replacement. Some of the genomic effects identified in this study may underlie the beneficial effects of E2 on cognition, behavior, and neuroprotection. **(*Endocrinology* 151: 3847–3862, 2010)**

The prefrontal cortex (PFC) plays an indispensable role in cognitive and executive processes including emotion, motivation, learning and memory (1, 2). The PFC receives and integrates inputs from cortical and subcortical regions. Activity of the PFC is shaped by various neurotransmitters/neuromodulators such as dopamine (3), norepinephrine (4), serotonin (5), histamine (6), orexin (7), and steroid hormones including corticosterone (8) and 17β-estradiol (E2) (9). The rat frontal cortex consists of the prefrontal, motor, and sensory cortices, among other areas (10). Its functions are strongly modulated by the actions of E2 on the two estrogen receptor (ER) isoforms, ERα and ERβ (11, 12). Various cell types of the rat frontal cortex express ERα and/or ERβ (13, 14). Immunohisto-

ISSN Print 0013-7227 ISSN Online 1945-7170
Printed in U.S.A.

doi: 10.1210/en.2010-0375 Received March 31, 2010. Accepted May 14, 2010.
First Published Online June 9, 2010

Abbreviations: ABC, ATP-binding cassette; CART, cocaine- and amphetamine-regulated transcript; Ct, cycle threshold; E2, 17β-estradiol; ER, estrogen receptor; GABA, γ-aminobutyric acid; IFN, interferon; IGFBP, IGF-binding protein; KEGG, Kyoto Encyclopedia of Genes and Genomes; MHC, major histocompatibility complex; MIF, migration-inhibitory factor; NMDA, *N*-methyl-D-aspartate; NT, neurotensin; PFC, prefrontal cortex; RGS, regulator of G-protein signaling; SP, substance P; TLDA, TaqMan low-density array.

chemical studies have localized the ERα- and the ERβ-immunoreactive cells primarily in layers III–V (14–16), in agreement with *in situ* hybridization studies (17). These two receptors are members of the nuclear receptor superfamily of ligand-activated transcription factors (18). Via a classic mode of action, ERs can induce transcription upon binding to estrogen-responsive elements in target gene promoters. They can also modulate gene transcription via interfering with other promoter-bound transcription factors or via influencing a variety of intracellular signaling pathways (18). In the frontal cortex, E2 may alter gene transcription directly via ERs in inhibitory interneurons (14, 16), astrocytes (19), and microglia (20). E2 can also affect transcription in cortical neurons indirectly via influencing subcortical centers and their cortical projections (21). Whatever the underlying regulatory mechanism is, we have recently identified a large number of E2-regulated genes in the frontal cortex of young, ovariectomized rats 24 h after a single sc E2 injection (16).

Despite controversies (22), numerous clinical studies have proved the beneficial effects of estrogen hormone therapy on cognition (23–26). Studies in animal models have also shown that E2 can facilitate certain aspects of learning and memory (27–29) and release anxiety (30). We hypothesized that alterations of cortical functions by E2 are reflected in the altered gene expression profile of the frontal cortex. To reveal the genomic effects of chronic E2 replacement, we used ovariectomized, middle-aged rats as a rodent model to mimic the low E2 level found in postmenopause. Using this animal model, we studied the genomic response in the frontal cortex after a 4-wk E2 replacement.

Materials and Methods

Experimental animals

Female, middle-aged (31) retired breeder Harlan-Wistar rats (n = 12) were originally purchased from Toxicoop (Budapest, Hungary) and then housed in a temperature- and humidity-controlled room in the laboratory animal care facility of the Institute of Experimental Medicine. They were caged with their litters until the last weaning, and individually for the subsequent month, on a 12-h light, 12-h dark cycle (lights on at 1900 h) and with unrestricted access to type 2019S phytoestrogen-free rodent diet (Harlan Teklad Global Diets, Madison, WI) and tap water. Protocols were reviewed and approved by the Animal Welfare Committee of the Institute of Experimental Medicine (A5769-01), and the experiments were carried out in accordance with the legal requirements of the European Community (Decree 86/609/EEC). Before ovariectomy, estrous cycle patterns were determined via the microscopic examination of vaginal smears taken daily at 0800 h.

Surgery and treatment

At the age of 13 months, the rats were deeply anesthetized ip with a mixture of xylazine (12 mg/kg) and ketamine (60 mg/kg) and were ovariectomized bilaterally to minimize the levels of endogenous estrogens. Ten days later, Alzet 2004 osmotic minipumps (DURECT Corp., Cupertino, CA) filled with either E2 (0.33 mg/ml in propylene-glycol, n = 6, E2 group) or the vehicle only (n = 6, control group) were implanted sc for 4 wk. Concentration of E2 was calculated to produce a release rate of 2 μg/d. On the day of sample preparation, animals were deeply anesthetized with pentobarbital (35 mg/kg body weight, ip) and perfused transcardially at a rate of 18 ml/min with 100 ml of fixative solution containing 10% RNAlater (QIAGEN, Hilden, Germany) in 0.1 M PBS (pH 7.4).

Measurement of serum estradiol levels

A blood sample was collected from the tail vein of each animal at the time of ovariectomy. A second sample was taken from the right atrium of the heart immediately before perfusion. E2 levels were determined according to the manual provided with the Ultrasensitive Estradiol RIA kit (DSL-4800; Diagnostic Systems Laboratories, Webster, TX).

Total RNA isolation from the frontal cortex

After RNAlater perfusion, brains were removed and the frontal cortex was dissected from the forebrain and sampled as described earlier (16). The dissected frontal cortex sample consisted of the PFC, motor and sensory cortical areas, the rostral tip of the caudate putamen (less than 0.5% vol/vol), and the forceps minor of the corpus callosum (approximately 3.8% vol/vol). From this sample, total RNA was isolated using the RNeasy Lipid Tissue Mini Kit (QIAGEN, Valencia, CA). RNA analytics included A260 nm/A280 nm readings using a Nanodrop spectrophotometer and capillary electrophoresis using 2100 Bioanalyzer (Agilent, Santa Clara, CA). All samples used for microarray experiments displayed RNA integrity numbers above 8.2.

Expression profiling using Rat 230 2.0 Expression Array

One-cycle target labeling, hybridization, staining, and scanning were carried out as described earlier (16). In brief, preparation of poly-A RNA controls (spike-in controls), first-strand and second-strand cDNA synthesis, cleanup of double-stranded cDNA, *in vitro* transcription labeling, cleanup of biotin-labeled cRNA, and fragmenting the cRNA for target preparation were carried out according to the Affymetrix (Santa Clara, CA) technical manual. Fragmented cRNA was hybridized for 16 h to Rat 230 2.0 Expression Array (Affymetrix). Arrays were washed and stained with phycoerythrin-conjugated streptavidin (Molecular Probes, Eugene, OR). Fluorescence intensities were determined using the GCS 3000 confocal laser scanner (Affymetrix). Scanned images were analyzed using programs resident in GeneChip Operating System version 1.2 (Affymetrix).

Data analysis

For quality assessment of microarrays, the selected parameters and their corresponding quantities recommended by Affymetrix were controlled using the affyQCReport package (QC report generation for affyBatch objects, R package version 1.16.0). Raw microarray data were preprocessed for analysis by

TABLE 1. Mean values (±SEM) of serum E2 levels in samples taken at the time of ovariectomy (OVX) and 40 d later at the time of killing

	At the time of OVX	At the time of killing	
		OVX + vehicle	OVX + E2
Number of animals (n)	12	6	6
Serum E2 level (pg/ml)	11.26 ± 2.99	2.36 ± 0.82	29.49 ± 3.26[a]
Change in body weight (g)		59.5 ± 4.15	10.5 ± 7.94[a]
Uterus weight (mg)		204.87 ± 15.26	592.87 ± 30.42[a]

Chronic E2 treatment of ovariectomized animals significantly elevated serum E2 levels compared with both the pre-ovariectomy values ($P < 0.001$; one-way ANOVA, *post hoc* test Tukey) and values measured in the vehicle-treated animals ($P < 0.001$). Significant reduction in body weight gain ($P < 0.001$; paired, two-tailed *t* test) and a significant increase in the uterus weight ($P < 0.0001$; paired, two-tailed *t* test) were observed in the OVX + E2 group compared with the control group.

[a] Significant changes.

GC robust multi-array average (32). Outlier identification was carried out using a recently developed approach (33). To select differentially expressed genes, the raw fold change values were used (34) and linear models combined with empirical Bayesian methods were applied (35). In the latter case, obtained *P* values were adjusted by the false discovery rate-based method (36). In all statistical and data mining work, Bioconductor packages (37) in R-environment (38) were used.

Gene set enrichment analysis was performed as well. In gene set enrichment analysis, Kyoto Encyclopedia of Genes and Genomes (KEGG) pathways (39) were used as collaborator gene sets, analyzed by the method developed by Tian and co-workers (40). In brief, in this approach, two null hypotheses (Q_1 and Q_2) tested whether the gene sets have association with the phenotype. For testing Q_1 and Q_2, two statistics, T_k and E_k, were calculated, respectively. The gene sets were ranked by NT_k and NE_k standardized statistics. Ordering by the average rank of the two statistics was a useful heuristic in ranking KEGG pathways (40).

Quantitative real-time PCR

TaqMan low-density array (TLDA) was designed to confirm microarray results by real-time PCR. The TLDA microfluidic card (Applied Biosystems, Foster City, CA) was preloaded by the manufacturer with selected inventoried gene expression assays for the genes of our interest and six potential housekeeping genes including 18S rRNA, β-actin (*Actb*), glyceraldehyde-3-phosphate dehydrogenase (*Gapdh*), glucuronidase-β (*Gusb*), hypoxanthine guanine phosphoribosyltransferase (*Hprt*), and peptidyl-prolyl isomerase A (*Ppia*). Each assay consisted of a FAM dye-labeled TaqMan MGB probe and two PCR primers. Every assay had been optimized by the manufacturer to run under universal thermal cycling conditions with a final reaction concentration of 250 nM for the probe and 900 nM for each primer. Reverse transcription and real-time PCR were run as described earlier (16). RealTime StatMiner (Integromics, Granada, Spain) software and relative quantification against calibrator samples [ΔΔ cycle threshold (Ct)] were used for analysis of Applied Biosystems (Foster City, CA) TaqMan gene expression assays. Six housekeeping genes were applied on the TLDA card as potential internal controls. To find the most stable endogenous controls, the nonfinder stability scoring method (41) was used. A computed internal control corresponding to the geometric mean of Ct values of selected housekeeping genes was used for subsequent ΔCt calculation (42).

Results

Characterization of the hormonal status of the animals

Before surgery, the middle-aged female rats showed irregular ovarian function reflected by prolonged diestrus and persistent estrus vaginal smears. Serum E2 levels were at 11.25 ± 2.99 pg/ml (mean ± SD). The efficacy of chronic E2 treatment was estimated by comparing serum E2 levels and body and uterus weights of the E2-treated animals with those of vehicle-treated controls (Table 1). Serum E2 levels (29.49 ± 3.26 pg/ml) in ovariectomized, E2-treated rats were significantly higher than in ovariectomized, vehicle-treated animals (2.35 ± 0.81 pg/ml). Differences between E2- and vehicle-treated animals in the change of body weight (10.5 ± 7.93 *vs.* 59.5 ± 4.15 g/animal) and uterus weight (592.9 ± 30.41 *vs.* 204.9 ± 15.26 mg) reached statistical significance in both cases.

Oligonucleotide microarray revealed alterations of gene transcription in the frontal cortex of middle-aged, ovariectomized rats after E2 replacement

The Rat 230 2.0 Expression Array used in this study provides information on over 31,000 probe sets. The top 100 transcripts, *i.e.* transcripts with the highest fold change, were determined and listed with the corresponding probe set ID, fold change, and *P* value (Table 2). Expression values of these transcripts across samples were also visualized on a heat map (Fig. 1). The top 100 probe sets identified 86 genes that were listed and categorized based on function (Fig. 2). Classification revealed that a large number of E2-regulated genes encoded proteins that were related to extracellular matrix (*Col1a1*, *Col1a2*, *Col3a1*, *Fmod*, *Hapln2*, *Lum*, and *Ogn*), immunity (*A2m*, *C3*, *C4b*, *Cd74*, *Fcgr2a*, *Fcgr2b*, *H2-T23*, *Lrrc8a*, *Mpeg1*, *RT1-Aw2*, and *Ythdf2*), metabolism (*Acer2*, *Clybl*, *Dguok*, *Echdc2*, *Osbpl3*, and *Pxmp4*), neurotransmission

TABLE 2. The list of the top 100 E2-regulated transcripts that were categorized based on function

Symbol	Gene	Probe set	Log FC	*P* value
Extracellular matrix				
Col1a1	Collagen, type 1, α1	1388116_at	−1.14	0.04
Col1a2	Collagen, type 1, α2	1370155_at	−1.91	0.14
		1387854_at	−1.08	0.17
Col3a1	Collagen, type 3, α1	1370959_at	−1.34	0.08
Fmod	Fibromodulin	1367700_at	−0.98	0.14
Lum	Lumican	1367749_at	−0.81	0.07
Ogn	Osteoglycin	1390450_a_at	−1.22	0.14
		1385248_a_at	−1.21	0.12
		1376749_at	−1.01	0.41
		1383263_at	−0.82	0.43
Immunity				
A2m	**α2-Macroglobulin**	**1367794_at**	**0.59**	**0.16**
C3	Complement C3	1368000_at	−1.39	0.00
C4b	Complement C4b	1370892_at	−0.66	0.01
Cd74	CD74	1367679_at	−1.19	0.10
Fcgr2a	Fcγ receptor 2a	1367850_at	−0.60	0.03
Fcgr2b	Fcγ receptor 2b	1371079_at	−0.97	0.01
H2-T23	RT1 class1b, locus S3	1388213_a_at	−0.70	0.19
Lrrc8a	**Leucine rich repeat containing**	**1382920_at**	**0.90**	**0.12**
Mpeg1	Macrophage expressed 1	1369427_at	−0.68	0.02
RT1-Aw2	RT1 class1b, locus EC2	1388202_at	−1.33	0.47
	RT1 class1b, locus EC2	1370428_x_at	−0.76	0.03
	RT1 class1b, locus EC2	1388203_x_at	−0.66	0.48
	RT1 class1b, locus EC2	1369110_x_at	−0.60	0.02
Ythdf2	**YTH domain family**	**1371960_at**	**0.84**	**0.54**
Metabolism				
Acer2	**Alkaline ceramidase 2**	**1373302_at**	**0.65**	**0.03**
Clybl	**Citrate lyase, β-like**	**1374190_at**	**0.67**	**0.00**
Dguok	**Deoxyguanosine kinase**	**1379435_at**	**0.93**	**0.33**
Echdc2	**Enoyl coenzyme A hydratase**	**1374527_at**	**0.77**	**0.00**
Osbpl3	**Oxysterol-binding protein-like 3**	**1384136_at**	**0.63**	**0.12**
Pxmp4	Peroxisomal membrane protein 4	1383117_at	−1.44	0.15
		1393421_at	−0.84	0.22
Neurotransmission				
Adora2a	**Adenosine A2a receptor**	**1368300_at**	**1.37**	**0.10**
Cartpt	**Cocaine, amphetamine-regulated transcript**	**1368585_at**	**0.88**	**0.04**
Chrm3	Cholinergic receptor, muscarinic 3	1369112_at	−0.87	0.27
Drd1a	**Dopamine D1a receptor**	**1368479_at**	**0.87**	**0.15**
	Dopamine D1a receptor	**1368478_at**	**0.77**	**0.09**
Drd2	**Dopamine D2 receptor**	**1368708_a_at**	**1.52**	**0.09**
Gjb2	Gap junction protein, β	1373386_at	−1.00	0.11
Nts	**Neurotensin**	**1380967_at**	**0.78**	**0.09**
Tac1	**Tachykinin, precursor 1**	**1369309_a_at**	**0.84**	**0.06**
Other				
Cacna1g	**Calcium channel, T-type, α1g**	**1368398_at**	**0.66**	**0.27**
Cpxm1	Carboxypeptidase X	1390420_at	−1.02	0.03
Cyp4f4	**Cytochrome P450, family 4, subfamily f**	**1387973_at**	**0.66**	**0.02**
Eml2	Echinoderm microtubule-associated protein	1370544_at	−1.37	0.27
Gart	Phosphoribosylglycinamide formyltransferase	1390787_at	−0.62	0.05
Hapln2	**Hyaluronan and proteoglycan link protein**	**1394952_at**	**0.73**	**0.08**
	Hyaluronan and proteoglycan link protein	**1370849_at**	**0.70**	**0.03**
Lmo7	**LIM domain 7**	**1381798_at**	**0.61**	**0.01**
Senp5	**SUMO/sentrin/SMT3-specific peptidase 5**	**1391262_at**	**1.54**	**0.01**
Siglec5	**Sialic acid-binding, IgG-like lectin 5**	**1385465_at**	**0.63**	**0.28**
Sned1	Sushi, nidogen and EGF-like domain 1	1380250_at	−0.63	0.13
Tjp1	Tight junction protein 1	1395337_at	−0.62	0.10

(*Continued*)

(*Adora2a*, *Cartpt*, *Chrm3*, *Drd1a*, *Drd2*, *Gjb2*, *Nts*, and *Tac1*), signal transduction (*Asb1*, *Camk4*, *Crlf1*, *Gnb1*, *Gpr88*, *Igf2*, *Igfbp2*, *Igfbp6*, *Psd*, *Rasgrp2*, *RGD1309362*, *Rgs9*, *Sgk1*, and *Sncg*), transcription (*Aebp1*, *Bhlhe40*, *Brd4*, *Ccdc49*, *Etv4*, *Ilf3*, *Irf7*, *Jund*, *Klf2*, *Nrip3*, *Nupr1*, *Rarb*, and *Zbtb20*), and transport

TABLE 2. Continued

Symbol	Gene	Probe set	Log FC	*P* value
Signal transduction				
Asb1	Ankyrin repeat and SOCS box-containing	1381002_at	−0.63	0.04
Camk4	Calcium/calmodulin kinase 4	1369753_at	−0.66	0.17
Crlf1	**Cytokine receptor-like factor 1**	**1376799_a_at**	**0.90**	**0.00**
	Cytokine receptor-like factor 1	**1395512_at**	**0.71**	**0.03**
Gnb1	**G-protein, β-polypeptide 1**	**1367732_at**	**0.91**	**0.01**
	G-protein, β-polypeptide 1	**1367731_at**	**0.80**	**0.00**
Gpr88	**G protein-coupled receptor 88**	**1387241_at**	**0.63**	**0.08**
Igf2	IGF-II	1367571_a_at	−0.86	0.16
Igfbp2	IGFBP	1367648_at	−0.65	0.33
Igfbp6	IGFBP	1387625_at	−0.80	0.07
Psd	Pleckstrin sec7 domain containing	1387572_at	−0.75	0.34
Rasgrp2	**RAS guanyl releasing protein 2**	**1374619_at**	**0.67**	**0.04**
RGD1309362	Similar to IFN-inducible GTPase	1377950_at	−0.89	0.05
Rgs9	**Regulator of G-protein signaling**	**1368500_a_at**	**0.78**	**0.13**
Sgk1	**Serum glucocorticoid kinase**	**1367802_at**	**0.61**	**0.00**
Sncg	**Synuclein γ**	**1398245_at**	**2.21**	**0.10**
Transcription				
Aebp1	Adipocyte enhancer-binding protein 1	1395695_at	−0.72	0.14
Bhlhe40	Basic helix-loop-helix e40	1369415_at	−0.87	0.05
Brd4	**Bromodomain containing 4**	**1380392_at**	**0.75**	**0.06**
Ccdc49	**Coiled-coil domain containing 49**	**1374888_at**	**0.87**	**0.08**
Etv4	**Ets variant 4**	**1380168_at**	**0.78**	**0.01**
Ilf3	IL enhancer-binding factor 3	1387366_at	−0.83	0.34
Irf7	IFN regulatory factor 7	1383564_at	−0.85	0.02
Jund	**junD protooncogene**	**1387762_s_at**	**1.76**	**0.16**
Klf2	Kruppel-like factor 2	1386041_a_at	−0.72	0.15
Nrip3	Nuclear receptor interacting protein 3	1396173_at	−0.60	0.04
Nupr1	Nuclear protein 1	1367847_at	−0.67	0.25
Rarb	**Retinoic acid receptor, β**	**1376755_at**	**0.90**	**0.07**
Zbtb20	Zn finger and BTB domain containing 20	1382524_at	−0.60	0.20
Transport				
Abca1	**ABC, subfamily A**	**1394490_at**	**1.03**	**0.22**
Alb	**Albumin**	**1367556_s_at**	**1.76**	**0.04**
	Albumin	**1367555_at**	**1.37**	**0.08**
Hba-a2	**Hemoglobin, α, adult chain 2**	**1370240_x_at**	**0.77**	**0.37**
	Hemoglobin, α, adult chain 2	**1370239_at**	**0.68**	**0.47**
Hbb	**Hemoglobin, β**	**1367553_x_at**	**0.94**	**0.26**
Pitpnm2	Phosphatidylinositol transfer protein	1379924_at	−0.74	0.04
Rtp4	Receptor (chemosensory) transporter protein	1379285_at	−0.83	0.14
Slc13a3	NA-dependent dicarboxylate transporter	1368047_at	−0.72	0.18
Slc22a8	Organic anion transporter	1368461_at	−0.71	0.17
Slc35d3	**Solute carrier family 35, d3**	**1378899_at**	**0.62**	**0.17**
Slco2b1	Solute carrier organic anion transporter	1368296_at	−0.72	0.04
Unclassified				
Fam111a	**Family with sequence similarity 111**	**1371970_at**	**1.16**	**0.60**
Fam134c	Family with sequence similarity 134	1376087_at	−0.65	0.38
Klhl26	Kelch-like 26	1383142_at	−0.67	0.03
LOC497860		**1378220_at**	**0.73**	**0.22**
LOC503175		1395556_at	−0.82	0.09
Pcp4l1	**Purkinje cell protein 4-like 1**	**1390227_at**	**0.76**	**0.08**
RGD1563862	**Similar to RIKEN cDNA 4930555G01**	**1391152_at**	**0.63**	**0.21**

Data were filtered according to fold change (FC). Genes are listed in alphabetical order. Up-regulated genes are shown in *bold*. In the case of several genes, multiple probe sets detected changes of mRNA levels resulting in 86 E2-regulated genes. Affymetrix probe set IDs are also presented. *P* values are the raw, uncorrected values obtained from linear models combined with empirical Bayesian method (35).

(*Abca1*, *Alb*, *Hba-a2*, *Hbb*, *Pitpnm2*, *Rtp4*, *Slc13a3*, *Slc22a8*, *Slc35d3*, and *Slco2b1*). The lists included several miscellaneous (*Cacna1g*, *Cpxm1*, *Cyp4f4*, *Eml2*, *Gart*, *Hapln2*, *Lmo7*, *Senp5*, *Siglec5*, *Sned1*, and *Tjp1*) and unclassified (*Fam111a*, *Fam134c*, *Klhl26*, *LOC497860*, *LOC503175*, *Pcp4l1*, and *RGD1563862*) genes as well. E2 replacement down-regulated most of the genes related to extracellular matrix and immunity and up-

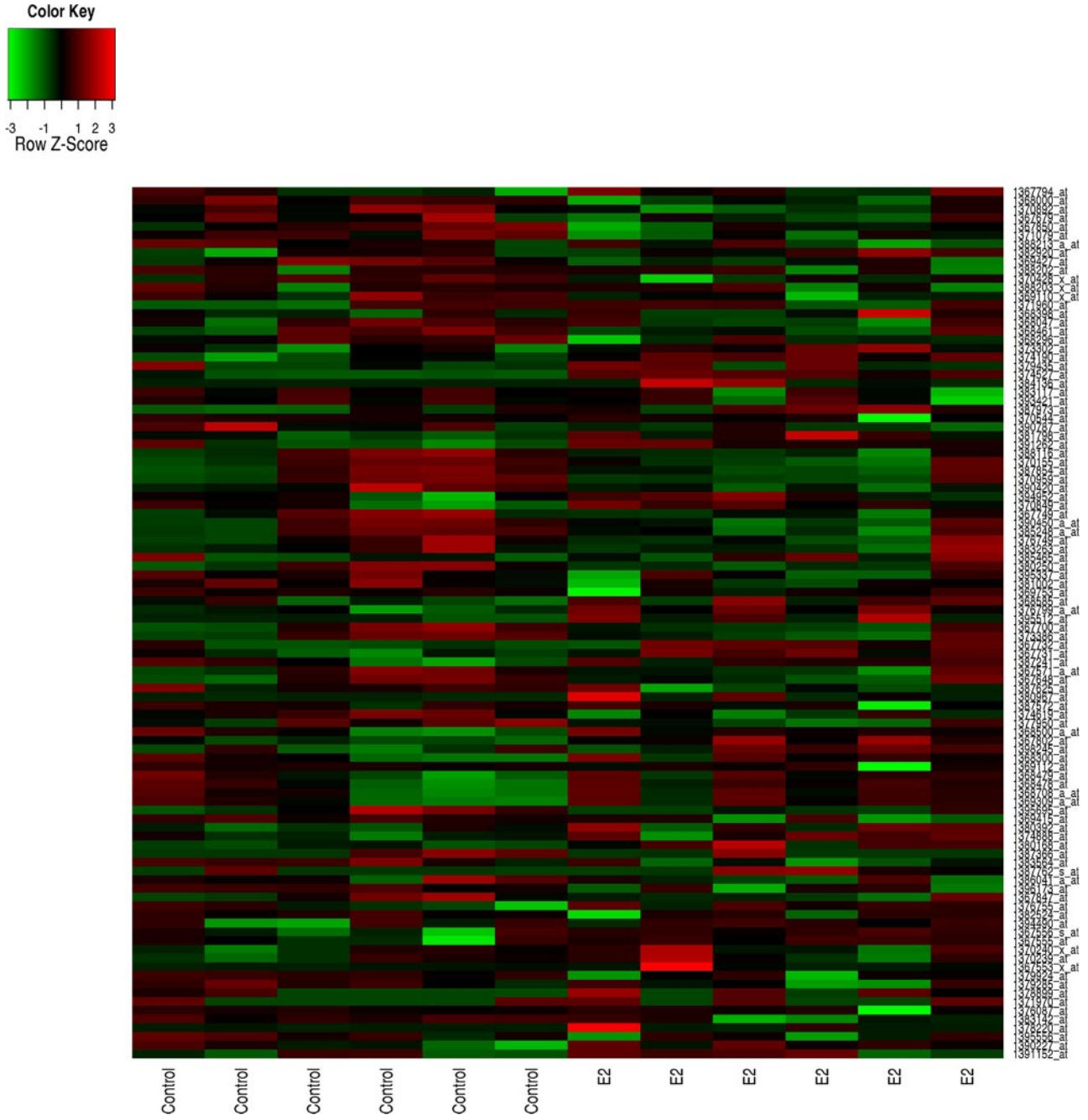

FIG. 1. Heat map. Expression levels for the top 100 E2-regulated transcripts are visualized on a heat map. Probe sets occur in the same order in the *rows* as listed in Table 2. *Columns* represent individual samples. *Red* intensities correspond to increased expression levels, whereas *green shades* label reduced levels of expression.

regulated genes related to metabolism and neurotransmission. E2 regulated in both directions several genes that are associated with signal transduction and transport. Among the genes associated with signal transduction, elements of IGF signaling were down-regulated, whereas components of other G protein-coupled receptor signaling pathways were up-regulated. In the case of transport-related genes *Abca1*, *Alb*, *Hba-a2*, *Hbb*, and Slc35d3 were up-regulated, whereas *Pitpnm2*, *Rtp4*, *Slc13a3*, *Slc22a8*, and *Slco2b1* were down-regulated.

Down-regulation of several components of immunity, transport machinery, IGF signaling, and extracellular matrix

Of 11 immunity-related genes, eight were down-regulated by E2 replacement. These genes included complement components *C3* and *C4b*, Fcγ receptors *Fcgr2a* and *Fcgr2b*, major histocompatibility complex (MHC) class I antigens *H2-T23* and *RT1-Aw2*, macrophage marker *Mpeg1*, and invariant chain *CD74*. Among the transcriptional regulators, IL enhancer-binding factor 3 (*Ilf3*) and

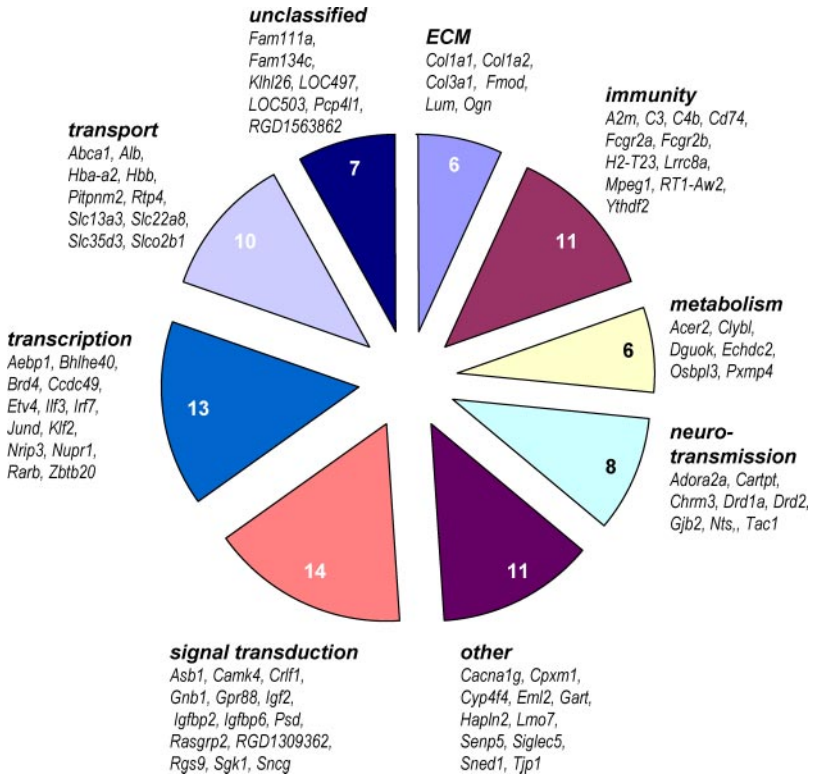

FIG. 2. E2-regulated genes categorized based on function shown in a pie diagram. E2 replacement altered a large number of genes that are related to extracellular matrix, immunity, metabolism, neurotransmission, signal transduction, transcription, and transport. The 86 E2-regulated genes are listed under the relevant function. ECM, Extracellular matrix.

interferon (IFN) regulatory factor 7 (*Irf7*) were associated with the immune response. Both transcriptional regulators were down-regulated.

Of 10 transport genes, phosphatidylinositol transfer protein (*Pitpnm2*), receptor transporter protein (*Rtp4*), sodium-dependent dicarboxylate transporter (*Slc13a3*), organic anion transporter (*Slc22a8*), and solute carrier organic anion transporter (*Slco2b1*) were down-regulated.

E2 regulated the transcription of 14 genes coding for proteins involved in signal transduction, and half of them, including ankyrin repeat and SOCS box-containing 1 (*Asb1*), calcium/calmodulin-dependent kinase IV (*Camk4*), IGF-2 (*Igf2*), IGF-binding protein 2 (*Igfbp2*), IGF-binding protein 6 (*Igfbp6*), pleckstrin and sec7 domain-containing (*Psd*), and *RGD1309362* were down-regulated.

All of the six extracellular matrix-related genes, including type 1 (Col1a1, Col1a2) and type 3 (Col3a1) collagens, fibromodulin (Fmod), osteoglycin (Ogn) and lumican (Lum) were down-regulated.

Up-regulation of genes related to neurotransmission, metabolism, and transport

The eight genes related to neurotransmission were adenosine A2A receptor (*Adora2a*), cocaine- and amphetamine-regulated transcript (*Cartpt*), cholinergic muscarine 3 receptor (*Chrm3*), dopamine D1A (*Drd1a*) and D2 receptors (*Drd2*), gap junction protein-β (*Gjb2*), neurotensin (*Nts*), and tachykinin 1 (Tac1). All of the eight genes but *Chrm3* and *Gjb2* were up-regulated by E2. All of the three neuropeptide genes, *Cartpt*, *Nts*, and *Tac1* were up-regulated. Both *Cartpt* and *Tac1* promoters harbor the cAMP response element consensus sequence (21, 22). Adenosine A2A and dopamine D1A and D2 receptors were up-regulated. Several G protein signaling-related genes, including *Gpr88*, G protein β (*Gnb1*), and regulator of G protein signaling 9 (*Rgs9*), were also up-regulated.

Ten transcriptional regulators were regulated by E2. These included four up-regulated transcription factors: *Jund*, *Rarb*, *Irf7*, and *Etv4*. *Jund* codes for a component of activator protein 1 transcription factor complex; *Rarb* for retinoic acid receptor-β, a member of the nuclear hormone receptor superfamily; *Irf7* for IFN regulatory factor 7; and *Etv4* for E26 transformation specific translocation variant 4.

Of six differentially expressed genes encoding proteins associated with metabolism, the following five were up-regulated: alkaline ceramidase 2, citrate lyase β-like, deoxyguanosine kinase, enoyl coenzyme A hydratase domain containing, and oxysterol-binding protein-like 3. Up-regulation of Golgi alkaline ceramidase could result in decreased level of ceramide and elevated levels of sphingosine and sphingosine-1-phosphate.

Of seven transport protein genes five were up-regulated by E2 replacement. These genes included Abca1 (ATP-binding cassette, subfamily A), albumin, adult chain 2 of hemoglobin α, hemoglobin β, and solute carrier family 35, d3 (Slc35d3). Abca1, albumin and hemoglobin are involved in cholesterol, steroid and oxygen transport, respectively.

The group of genes with miscellaneous functions included *Cacna1g*, which codes for the pore-forming α-subunit of low-voltage-activated Cav3.1/α1G T-type calcium ion channel.

Validation of microarray results by quantitative real-time PCR using custom TaqMan low-density array

Custom TaqMan low-density array was designed to confirm a large number of changes of the top 100 transcript list. In the selection, we focused on genes involved in neurotransmission, immunity, signal transduction, transport, and extracellular matrix formation. Thirty-nine E2-

TABLE 3. The list of selected genes and the corresponding TaqMan assays for PCR validation

Gene	Gene name	TaqMan assay	RefSeq	Amplicon
Abca1	**ABC, subfamily A**	**Rn00710172_m1**	**NM_178095.2**	**76**
Actb[a]	β-Actin	Rn00667869_m1	NM_031144.2	91
Adora2a	**Adenosine A2a receptor**	**Rn00583935_m1**	**NM_053294.3**	**58**
Alb	Albumin	Rn00592480_m1	NM_134326.2	96
C3	**Complement C3**	**Rn00566466_m1**	**NM_016994.2**	**72**
C4b	**Complement C4b**	**Rn00709527_m1**	**NM_031504.2**	**70**
Camk4	CA/calmodulin-dependent protein kinase IV	Rn00562394_m1	NM_012727.3	102
Cartpt	**CART prepropeptide**	**Rn01645174_m1**	**NM_017110.1**	**77**
Cd74	**CD74, MHC class II invariant chain**	**Rn00565062_m1**	**NM_013069.2**	**68**
Chrm3	Cholinergic receptor, muscarinic 3	Rn00560986_s1	NM_012527.1	129
Col1a1	**Collagen, type 1, α1**	**Rn01463848_m1**	**NM_053304.1**	**115**
Col1a2	Collagen, type 1, α2	Rn00584426_m1	NM_053356.1	130
Col3a1	**Collagen, type 3, α1**	**Rn01437681_m1**	**NM_032085.1**	**71**
Cyp4f4	**Cytochrome P450, family 4, subfamily f**	**Rn00597513_m1**	**NM_173123.1**	**75**
Drd1a	**Dopamine D1A receptor**	**Rn03062203_s1**	**NM_012546.2**	**83**
Drd2	**Dopamine D2 receptor**	**Rn01418275_m1**	**NM_012547.1**	**85**
Fcgr2b	**Fc fragment of IgG, low affinity IIb receptor**	**Rn00598391_m1**	**NM_175756.1**	**142**
Fmod	**Fibromodulin**	**Rn00589918_m1**	**NM_080698.1**	**99**
Gapdh[a]	Glyceraldehide-3-phosphate dehydrogenase	Rn99999916_s1	NM_017008.3	87
Gjb2	**Gap junction protein, β2**	**Rn02376786_s1**	**NM_001004099.1**	**109**
Gnb1	Guanine nucleotide-binding protein, β1	Rn00821225_g1	NM_030987.2	64
Gusb[a]	β-Glucuronidase	Rn00566655_m1	NM_017015.2	63
Hapln2	Hyaluronan and proteoglycan-link protein 2	Rn01459065_g1	NM_022285.1	59
Hba-a2	**Hemoglobin α, adult chain 2**	**Rn00820725_g1**	**NM_013096.1**	**129**
Hprt[a]	hypoxanthine phosphoribosyltransferase	Rn01527840_m1	NM_012583.2	64
Igf2	**IGF-II**	**Rn01454518_m1**	**NM_031511.1**	**74**
Igfbp2	**IGFBP-2**	**Rn00565473_m1**	**NM_013122.2**	**93**
Igfbp6	**IGFBP-6**	**Rn00565371_m1**	**NM_013104.2**	**106**
Ilf3	IL enhancer-binding factor 3	Rn00584682_m1	NM_053412.1	85
Irf7	**IFN regulatory factor 7**	**Rn01450778_g1**	**NM_001033691.1**	**66**
Jund	junD protooncogene	Rn00824678_s1	NM_138875.3	77
Lum	**Lumican**	**Rn00579127_m1**	**NM_031050.1**	**130**
Mpeg1	**Macrophage expressed gene 1**	**Rn02769865_s1**	**NM_022617.1**	**113**
Nts	**Neurotensin**	**Rn01503265_m1**	**NM_001102381.1**	**123**
Nupr1	**Nuclear protein, transcriptional regulator 1**	**Rn00586046_m1**	**NM_053611.1**	**112**
Ppia[a]	Peptidyl-prolyl-isomerase (cyclophilin A)	Rn00690933_m1	NM_017101.1	149
Pxmp4	Peroxisomal membrane protein 4	Rn00597183_m1	NM_172223.2	61
Rgs9	**Regulator of G-protein signaling 9**	**Rn00570117_m1**	**NM_019224.1**	**80**
RT1-Aw2	**RT1 classIb, locus EC2**	**Rn03034964_u1**	**NM_012645.1**	**98**
Sgk1	Serum/glucocorticoid-regulated kinase	Rn00570285_m1	NM_019232.2	79
Slc13a3	**Solute carrier family 13, member 3**	**Rn00575872_m1**	**NM_022866.2**	**70**
Slc22a8	**Solute carrier family 22, member 8**	**Rn00580082_m1**	**NM_031332.1**	**64**
Sncg	**γ-Synuclein**	**Rn00581652_m1**	**NM_031688.1**	**100**
Tac1	**Tachykinin 1**	**Rn00562002_m1**	**NM_001124768.1**	**64**

TaqMan-based real-time PCR were used on microfluidic card to confirm selected transcriptional changes. The applied inventoried TaqMan assays with the public reference sequence and the amplicon's length are listed. Successfully confirmed genes are in *bold*.

[a] Housekeeping genes.

regulated genes and six potential housekeeping genes were selected for further analysis by quantitative real-time PCR (Table 3). Of 39 selected genes, regulation of 29 was confirmed corresponding to 74.4% validation efficiency. The 29 confirmed genes were listed with the corresponding microarray and real-time PCR results (Table 4).

Pathway analysis highlighted novel biological pathways affected by chronic E2 treatment in the frontal cortex

In the analysis, we used KEGG pathways (39) and the method proposed by Tian *et al.* (40). Differentially expressed gene sets were identified, and the top 30 pathways, with the size of the pathway, percentage of up-regulated genes, NT_k, NE_k, and average ranks, were listed (Table 5). In all cases, the difference was statistically significant ($P < 0.05$). Ordering by the average rank of NT_k and NE_k was a reliable heuristic in ranking KEGG pathways (40). Highly ranked pathways involved allograft rejection, graft-*vs*.-host disease, cell adhesion molecules, autoimmune thyroid disease, type I diabetes mellitus, and neuroactive ligand-receptor interaction. These pathways highlighted those biological processes that were most probably modulated by E2. It is noteworthy that among

TABLE 4. Summary of the results of microarray and real-time PCR studies

Gene	Gene name	Microarray, FC	Real-time PCR, RQ
Abca1	ABC, subfamily A	2.04	1.49
Adora2a	Adenosine A2a receptor	2.58	2.60
C3	Complement C3	0.38	0.62
C4b	complement C4b	0.63	0.67
Cartpt	CART prepropeptide	1.84	2.34
Cd74	CD74, MHC class II invariant chain	0.44	0.67
Col1a1	Collagen, type 1, α1	0.27	0.72
Col3a1	Collagen, type 3, α1	0.40	0.16
Cyp4f4	cytochrome P450, family 4, subfamily f	1.58	1.46
Drd1a	Dopamine D1A receptor	1.83	1.68
Drd2	Dopamine D2 receptor	2.87	2.34
Fcgr2b	Fc fragment of IgG, low affinity IIb receptor	0.51	0.63
Fmod	Fibromodulin	0.51	0.77
Gjb2	Gap junction protein, β2	0.50	0.71
Hba-a2	Hemoglobin α, adult chain 2	1.71	2.47
Igf2	IGF-II	0.55	0.54
Igfbp2	IGFBP-2	0.64	0.70
Igfbp6	IGFBP-6	0.57	0.59
Irf7	IFN regulatory factor 7	0.55	0.56
Lum	Lumican	0.57	0.60
Mpeg1	Macrophage expressed gene 1	0.62	0.61
Nts	Neurotensin	1.72	1.36
Nupr1	Nuclear protein, transcriptional regulator 1	0.63	0.68
Rgs9	Regulator of G-protein signaling 9	1.72	1.84
RT1-Aw2	RT1 classIb, locus EC2	0.40	0.53
Slc13a3	Solute carrier family 13, member 3	0.61	0.53
Slc22a8	Solute carrier family 22, member 8	0.61	0.62
Sncg	γ-Synuclein	4.63	2.06
Tac1	Tachykinin 1	1.79	1.48

The 29 genes show similar alterations with the two independent methodologies. FC, Fold change; RQ, relative quantity.

the top 30 pathways, 12 pathways including allograft rejection, graft-*vs*.-host disease, autoimmune thyroid disease, cytokine-cytokine receptor interaction, hematopoietic cell lineage, complement and coagulation cascades, primary immunodeficiency, natural killer cell-mediated cytotoxicity, Jak-signal transducer and activator of transcription signaling pathway, antigen processing and presentation, systemic lupus erythematosus, and asthma were related to immunity.

Discussion

In this work, we have demonstrated that in middle-aged, ovariectomized rats, chronic E2 replacement significantly alters the gene expression profile of the frontal cortex. This result is in accordance with our hypothesis that cortical functions influenced by E2 are reflected in the altered transcriptome of the frontal cortex. The identified changes of the expression profile suggest that E2 replacement modifies both neuronal and glial functions.

Up-regulation of genes related to dopaminergic neurotransmission

The rat PFC receives glutamatergic inputs from the thalamus (1, 43), the hippocampus (44), and other cortical areas as well as dopaminergic projections from the ventral tegmental area (45). In the PFC, dopamine has a unique role in the modulation of network activity via G protein-coupled receptors and recruitment of multiple signaling pathways (46). In the rat frontal cortex, D1 receptors are far more abundant than D2 receptors (47, 48). D1 and D2 mRNA-containing neurons are present in the medial prefrontal, insular, and cingulate cortices and, at a lower expression level, also in the motor and parietal cortices (47). D1 is expressed in layers V and VI of all cortical areas and in layer II of the medial prefrontal, insular, and cingulate areas. D2 expression is restricted to layer V. D1 and D2 receptors are found on pyramidal and γ-aminobutyric acid (GABA)ergic neurons of the rat PFC (48–50). Among the various subpopulations of cortical interneurons, primarily parvalbumin-containing inhibitory neurons express D1 and D2 receptors (51).

Here, we found that chronic E2 replacement activates the transcription of *Drd1a* and *Drd2* in the frontal cortex. These findings are in agreement with the results of our previous study that showed that acute E2 treatment increases the level of *Drd1a* and *Drd2* mRNAs in young, ovariectomized rats (16). Estrogenic regulation of D2 receptors in the rat striatum has also been reported (52). Cells of the rat frontal cortex express ERα and ERβ (15,

TABLE 5. Pathway analysis

Rank	KEGG pathway	Size	% up	NT_k rank	NE_k rank	Average
1	Allograft rejection	68	9	8.0	6.0	7.0
2	Graft-*vs.*-host disease	67	9	9.0	6.0	7.5
3	Cell adhesion molecules	189	23	10.0	6.0	8.0
4	Autoimmune thyroid disease	73	8	6.0	10.0	8.0
5	Type I diabetes mellitus	77	16	17.0	6.0	11.5
6	neuroactive ligand-receptor interaction	335	19	1.0	23.5	12.2
7	Cytokine-cytokine receptor interaction	210	13	2.0	30.0	16.0
8	Hematopoietic cell lineage	101	10	3.0	30.0	16.5
9	Complement and coagulation cascades	92	12	4.0	30.0	17.0
10	Primary immunodeficiency	33	6	18.0	17.0	17.5
11	Glycosphingolipid biosynthesis	35	17	31.0	6.0	18.5
12	Natural killer cell-mediated cytotoxicity	136	26	27.0	10.0	18.5
13	Jak-STAT signaling pathway	172	24	14.0	23.5	18.7
14	Antigen processing and presentation	103	21	29.0	13.5	21.2
15	Androgen and estrogen metabolism	33	18	28.0	23.5	25.8
16	Retinol metabolism	64	19	11.0	44.0	27.5
17	Systemic lupus erythematosus	92	26	26.0	30.0	28.0
18	Drug metabolism, cytochrome P450	63	22	13.0	44.0	28.5
19	Focal adhesion	272	28	33.5	23.5	28.5
20	Hedgehog signaling pathway	73	25	47.5	10.0	28.7
21	Basal cell carcinoma	68	25	44.0	13.5	28.7
22	Calcium signaling pathway	276	29	19.0	44.0	31.5
23	Regulation of actin cytoskeleton	272	29	44.0	19.5	31.7
24	Asthma	25	8	21.0	44.0	32.5
25	ECM-receptor interaction	101	20	25.0	44.0	34.5
26	Caffeine metabolism	10	20	33.5	36.5	35.0
27	Metabolism of xenobiotics, cytochrome P450	48	21	16.0	57.0	36.5
28	Keratan sulfate biosynthesis	27	30	72.0	1.5	36.7
29	Drug metabolism, other enzymes	38	21	30.0	44.0	37.0
30	Fatty acid biosynthesis	10	20	75.0	1.5	38.2

Tian's method identified KEGG pathways affected by E2 replacement in the frontal cortex. All of the alterations were statistically significant ($P < 0.05$). Rank corresponds to the rank of the pathway analysis. Size indicates the number of elements/genes of the given pathway. Percent up shows the percentage of up-regulated genes in the given pathway. NT_k and NE_k are the standardized test statistics for the evaluation of the two null hypotheses (Q_1 and Q_2). Average corresponds to the average of the NT_k and NE_k ranks. ECM, Extracellular matrix; STAT, signal transducer and activator of transcription.

16). The dominant layers for both ER subtypes are layers III–V. The localization of both dopamine and ERs in parvalbumin-positive neurons suggests that E2 may directly regulate the transcription of *Drd1a* and *Drd2* in this subtype of cortical interneurons. This idea is supported further by promoter studies showing that regulatory regions of *Drd1a* and *Drd2* contain a half-palindrome TGACC for the consensus estrogen-responsive elements (53) and multiple Sp1 sites (54), respectively.

There is a substantial decline in D1 and D2 receptors during a lifetime (55–57). This finding is in agreement with animal studies showing age-related reductions in dopamine release and dopamine markers in the cerebral cortex (58). We propose that in aged female animals, the expression of D1A and D2 receptors is suppressed due to the low levels of E2, and these alterations can contribute to the reduction of dopaminergic neurotransmission and impairments of cognitive and motor functions (56).

Regulator of G-protein signaling (RGS) proteins are ubiquitous regulators of signal duration in G protein signaling pathways (59). The RGS homology domain, present in all members of the RGS family, accelerates the GTPase activity of G protein α-subunits. RGS9 is one of the best-studied members of the family because of its regulatory role in such fundamental functions as vision and behavior. Via alternative splicing, *Rgs9* gives rise to two products, *RGS9-1* and *RGS9-2* (59). The short splice variant of *RGS9*, *RGS9-1* is localized primarily to the retina, whereas the long one, *RGS9-2* has been identified in the brain, mainly in striatal regions including the caudate putamen, nucleus accumbens, and olfactory tubercle (59, 60). Moderate *RGS9-2* expression has been detected in the rat frontal cortex (60, 61). *RGS9-2* colocalizes with dopamine D2 receptor and accelerates the termination of D2 signals (62). Estrogenic regulation of *Rgs9* has been described in the shell of the nucleus accumbens (63). Here, we showed that chronic E2 treatment activates the transcription of *Rgs9* in the frontal cortex. This finding is in agreement with our previous result that acute E2 treatment up-regulates *Rgs9* (16).

Adenosine A2A receptor is a G protein-coupled receptor that mediates the role of extracellular adenosine in many physiological processes in the brain (64), including cerebral blood flow, the activity of brainstem respiratory

networks, and sleep. A2A receptors are highly expressed in the striatum, and a lower expression level has been observed in the frontal cortex (65). A2A is coupled to the cAMP second messenger system, and upon activation, the intracellular levels of cAMP increase. Adenosine also exerts a neuromodulatory role by participating in the integration and fine tuning of glutamatergic and dopaminergic neurotransmission. Activation of A2A enhances the release of acetylcholine, GABA, glutamate, and dopamine (66). Adenosine via A2A antagonizes dopaminergic signaling at D2 receptors (67). Based on these data, we suggest that up-regulation of *Adora2a* by E2 can modulate dopaminergic and glutamatergic neurotransmission in the frontal cortex.

It is known that dopamine acts mainly through D1 to modulate glutamatergic neuronal activity as well (68). D1A receptor is expressed in pyramidal neurons and parvalbumin-positive interneurons (47, 51). D1A colocalizes with NR1 and NR2A *N*-methyl-D-aspartate (NMDA) receptor subunits in the cortex (68). Activation of the cAMP/protein kinase A pathway through D1A results in the phosphorylation of NMDA receptor subunits, and through this mechanism, glutamate receptors can modulate synaptic strength (69). Activation of D1 by receptor agonists leads to elevated surface expression of NR1 and NR2B on pyramidal neurons of the PFC via tyrosine phosphorylation of NR2B (70). Up-regulation of *Drd1a* may potentiate the effect of dopamine on NR2B expression and NMDA-dependent processes.

Up-regulation of genes associated with peptidergic neurotransmission

In addition to *bona fide* neurotransmitters, neuropeptides synthesized in neurons of the cerebral cortex also take part in neuromodulation and interneuronal communication (71, 72). Increased levels of mRNAs for three neuropeptides including cocaine- and amphetamine-regulated transcript (CART), neurotensin (NT), and tachykinin 1 (TAC1) were identified in the frontal cortex of E2-treated animals compared with controls.

CART peptides are widely distributed in the central nervous system (CNS) and involved in the regulation of many physiological processes (73). In the rat frontal cortex, CART is mainly localized to barrel field neurons of the somatosensory cortex (16, 74, 75) and implicated in neuroprotection (76) and behavior (77, 78). In the ischemic cortex, enhanced CART expression may contribute to E2-mediated neuroprotection (76), which is partially linked to preservation of mitochondrial function (79). We found up-regulation of *Cartpt*, indicating that E2 induces an important and long-lasting neuroprotective mechanism in the frontal cortex after E2 replacement.

Nts encodes a precursor protein containing the tridecapeptide NT and the hexapeptide neuromedin. The promoter region of rat Nts harbors two near-consensus cAMP response element sites. In neurons, NT is stored in dense-core vesicles and released in a Ca^{2+}-dependent manner. In the rat PFC, NT is localized to dopamine axons. NT activates GABAergic interneurons via the high-affinity NT receptor NTR1, which is localized primarily to parvalbumin-containing neurons (72). Local administration of NT in the PFC produces significant, long-lasting, and concentration-dependent increase in extracellular dopamine and other neurotransmitters such as 5-hydroxytryptamine (81). Estrogenic regulation of NT may lead to enhanced levels of extracellular dopamine in the frontal cortex. In addition, NT acts as a neuromodulator in the brain, and one of its actions is to modulate dopaminergic neurotransmission (82).

Tac1 encodes four peptide hormones of the tachykinin family including substance P (SP), neurokinin A, neuropeptide-γ, and neuropeptide K. In the cerebral cortex, SP and its receptor, NK1 are thought to modulate the communication between GABAergic interneurons (83). SP immunoreactivity is localized to a subset of parvalbumin-positive interneurons, whereas its receptor, NK1, is also found in a subset of somatostatin-containing interneurons (84). This distribution pattern suggests that SP acts predominantly as a paracrine neuromodulator of GABAergic neurotransmission in the frontal cortex. SP acts through G protein-coupled receptors to evoke a slow excitation of neurons that can be attributed to opening a cation channel complex that contains sodium leak channel, non-selective (NALCN) and NALCN channel-associated protein (UNC-80) (85).

Gap junctions, which allow direct intercellular exchange of small molecules and ions, are formed by two connexin hexamers (86). One of the connexins, Cx26/Gjb2, was regulated by E2. Cx26/Gjb2 is implicated in the genesis and synchronization of cortical electrical activity (87) as well as in the final stages of neuronal migration in the neocortex (88).

The frontal cortex is one of the terminal regions of the mesocorticolimbic dopamine system where complex interactions take place between various neurotransmitters such as dopamine, 5-hydroxytryptamine, GABA, glutamate, and neuropeptides. Here, we demonstrated that E2 replacement in middle-aged, ovariectomized rats modulates several neurotransmitter systems, especially dopaminergic neurotransmission. The frontal cortex has been implicated in various types of behavior such as cognitive processes, reward-oriented behavior, and stress response (1). We propose that in females, in the absence of endogenous estrogens, E2 replacement alters frontal cortex-de-

pendent behavior in part via the genomic effects identified in this study.

Down-regulation of immunity-related genes including *Cd74* and complement *C3*

Microglia, the resident macrophages of the brain, continually survey the local environment and rapidly change their phenotype in response to any disturbance of brain homeostasis (89, 90). Steroid hormones are well-known regulators of microglia (91). Estrogens regulate the function of microglia mainly through ERα (20). We found down-regulation of genes such as classical complement pathway components *C3* and *C4b*, Fc receptors *Fcgr2a* and *Fcgr2b*, MHC class I antigens, and *Cd74*. This regulation indicates that E2 has a major impact on the function of microglia via genomic effects in the frontal cerebral cortex.

CD74, a type II integral membrane protein, acts as a chaperone for MHC class II molecules by blocking the peptide-binding groove during transportation (92). In addition, CD74 binds macrophage migration-inhibitory factor (MIF) and is required for MIF-mediated signaling (93). Beyond its key role in MHCII trafficking and MIF signaling, CD74 associates with myosin II and CD44, two actin-interacting proteins that regulate cell locomotion (94). These data indicate that E2 may elevate the threshold for microglia activation through down-regulation of key regulatory molecules.

Microglia survey the signals released by neurons and astrocytes via receptors for chemokines (95) and complement activation fragments (96). Therefore, the extracellular level of early complement components along with activators of the classical complement pathway can regulate microglial function. We have found that the central component of complement activation pathways, C3 (97), is down-regulated by E2 replacement in the frontal cortex. Complement is a powerful activator of inflammation, and the level of complement components increases with age (98). This may help to eliminate neurotoxic protein oligomers/polymers and injured axons, but the elevated proinflammatory potential is a double-edged sword. Ample evidence implicates the involvement of the complement system in the pathology of age-related dementia including Alzheimer's disease (99). Amyloid β-protein exerts enhanced neurotoxicity in the presence of complement on primary hippocampal cells, and toxicity is significantly suppressed by C1-Inh and C1q antagonists *in vitro* (100). A recent study has provided evidence that absence of C1q leads to decreased neuropathology in APP and APP/PS1 transgenic mice (101). These data provide evidence that activation of the classical complement pathway contributes significantly to the neuronal loss in various Alzheimer's disease models. Although the mechanisms of neuronal loss are poorly understood, the microglial involvement is likely because these cells express early complement components and receptors for complement activation fragments (99).

In aggregate, these results highlight microglia as one of the cellular targets of chronic E2 treatment in the frontal cortex. We suggest that the described alterations in microglial gene expression result in a decreased proinflammatory potential that may attenuate the progression of age-related neurodegenerative diseases.

Estrogenic regulation of genes related to transport in the frontal cortex

Four transport-related genes including *Abca1*, *Hba-a2*, *Slc13a3*, and *Slc22a8* have been regulated by E2. ATP-binding cassette (ABC) transporters play an important role in lipid transport across membranes. *Abca1* encodes the member 1 of the A subfamily of ABC transporters that promotes efflux of cholesterol and phospholipids from intracellular compartments to lipid-free apolipoprotein A-I and apolipoprotein E. In the brain, cholesterol is required for myelination, dendrite differentiation, and synaptic activity (102). In the murine brain, ABCA1 is highly expressed in pyramidal neurons and glial cells (103). Here, we found that *Abca1* is up-regulated by E2 replacement. The role of CNS cholesterol in synaptic function and neurodegenerative disorders has recently been appreciated, but the mechanisms regulating its transport and homeostasis are only partially understood. Therefore, the functional consequences of *Abca1* up-regulation in the frontal cortex are not clear yet.

Hemoglobin-α, adult chain 2 (*Hba-a2*) and hemoglobin-β are expressed in the mammalian brain (104–106), indicating that hemoglobin chains are not restricted to the erythroid lineage of cells, as previously assumed. *Hba-a2* is also expressed in cortical pyramidal neurons (104). We demonstrated up-regulation of *Hba-a2* by E2 in the frontal cortex. Although the function of hemoglobin remains elusive in the brain, a recent study has provided clues that hemoglobin acts on the main elements of oxygen homeostasis (105). In addition, it has been proposed that neuronal expression of hemoglobin is connected to facilitated oxygen uptake and that hemoglobin serves as an oxygen capacitator molecule (106).

Slc13a3 encodes for sodium-dependent dicarboxylate transporter 3, which mediates the uptake of Krebs cycle intermediates in various tissues, including the brain (107). Neurons are dependent on extracellular sources of Krebs cycle intermediates to replenish intracellular neurotransmitter pools (108) because pyruvate carboxylase, the major enzyme for the synthesis of Krebs cycle intermediates,

is specifically located in astrocytes but not in neurons (109). Sodium-dependent dicarboxylate transporter 3 shows high affinity for succinate (and other dicarboxylates) and lower affinity for citrate.

Cacna1g, which codes for the pore-forming α-subunit of low-voltage-activated Cav3.1/α1G T-type calcium ion channel, was up-regulated by chronic E2 replacement. *Cacna1g* has been up-regulated in the acute E2 treatment paradigm as well (16). In addition, estrogens up-regulate T-type calcium channels also in the hypothalamus (110). These steady results suggest that up-regulation of Cav3.1/α1G by E2 takes place in various brain regions including the frontal cortex. T-type calcium channels can be opened by the small depolarization of the plasma membrane, resulting in low-threshold spikes, which in turn trigger a burst of action potentials through sodium channels (111). In addition, calcium entry through *Cacna1g* regulates intracellular calcium ion concentration, which is an important second messenger for a wide range of cellular processes (112, 113).

Down-regulation of *Igf2*, *Igfbp2*, and *Igfbp6* associated with IGF signaling

IGFs are mitogens that share structural homology with preinsulin and are involved in the growth and development of many organs, including the brain (114–117). In the CNS, endothelial cells produce several trophic factors for neurons including IGF2 (118). We found that E2 replacement down-regulated *Igf2*. Regulation of IGF-II action depends not only on the expression of IGF-II and its receptor, the cation-independent mannose-6-phosphate receptor, but also on the modulation of IGF-II activity by IGF-binding proteins (IGFBPs). Six IGFBPs have been cloned and characterized so far (119, 120). We showed that E2 down-regulated *Igfbp2* and *Igfbp6* in the frontal cortex. IGF-II bioavailability is modulated mainly by IGFBP2, which sequestrates the trophic factor and prevents its interaction with IGF-II receptor (121). IGFBP6 has a selective affinity for IGF-II over IGF-I. These data suggest that E2 regulates the activity of IGF-II at multiple levels. In accordance with our results, a recent study has identified *Igf2* and *Igfbp2* as estrogen-responsive genes in the rat hippocampus (80).

In a previous work, we examined changes of the cortical transcriptome of young ovariectomized rats 24 h after a single injection of E2 (16). Of 136 genes identified in that work, seven can be found in the top 100 list of the present study showing similar regulation in the two models. The seven genes include *Cacna1g*, *Adora2a*, *Cartpt*, *Nts*, *Rgs9*, *Drd1a*, and *RT1-Aw2*. The overlapping genes indicate that activation of the genes related to dopaminergic and peptidergic neurotransmission is a characteristic feature of the genomic effects of E2 in the rat frontal cortex, and it is independent of age (between 2 and 13 months) and mode of treatment.

In summary, we described a large number of transcriptional changes in the frontal cortex of middle-aged, ovariectomized rats after a 4-wk chronic E2 replacement. Transcriptional regulation affected multiple elements of dopaminergic and peptidergic neurotransmission, immunity, adenosine and IGF signaling, and transport processes. The frontal cortex has been implicated in various types of behavior such as cognitive processes, reward-oriented behavior, and stress response. We propose that in females in the absence of endogenous estrogens, E2 hormone replacement alters frontal cortex-dependent behavior and various neuroprotective mechanisms in part via the genomic effects identified in this study.

Acknowledgments

We are indebted to the Laboratory of Prof. G. M. Nagy (Semmelweis University, Budapest, Hungary) for the measurements of serum E2. We thank Hajni Bekó and Barna László for their excellent technical work.

Address all correspondence and requests for reprints to: Zsolt Liposits, M.D., Ph.D., D.Sc., Laboratory of Endocrine Neurobiology, Institute of Experimental Medicine, Hungarian Academy of Sciences, Szigony utca 43, H-1083 Budapest, Hungary. E-mail:liposits@koki.hu.

This work was supported by grants from the Hungarian Scientific Research Fund (OTKA K69127 and T73002).

Disclosure Summary: The authors have nothing to disclose.

References

1. **Fuster JM** 2001 The prefrontal cortex—an update: time is of the essence. Neuron 30:319–333
2. **Miller EK, Cohen JD** 2001 An integrative theory of prefrontal cortex function. Annu Rev Neurosci 24:167–202
3. **Brozoski TJ, Brown RM, Rosvold HE, Goldman PS** 1979 Cognitive deficit caused by regional depletion of dopamine in prefrontal cortex of rhesus monkey. Science 205:929–932
4. **Cole BJ, Robbins TW** 1992 Forebrain norepinephrine: Role in controlled information processing in the rat. Neuropsychopharmacology 7:129–142
5. **Jakab RL, Goldman-Rakic PS** 1998 5-Hydroxytryptamine2A serotonin receptors in the primate cerebral cortex: possible site of action of hallucinogenic and antipsychotic drugs in pyramidal cell apical dendrites. Proc Natl Acad Sci USA 95:735–740
6. **Jin CY, Panula P** 2005 The laminar histamine receptor system in human prefrontal cortex suggests multiple levels of histaminergic regulation. Neuroscience 132:137–149
7. **Lambe EK, Olausson P, Horst NK, Taylor JR, Aghajanian GK** 2005 Hypocretin and nicotine excite the same thalamocortical synapses in the prefrontal cortex: correlation with improved attention in rat. J Neurosci 25:5225–5229
8. **Lin Y, Westenbroek C, Bakker P, Termeer J, Liu A, Li X, Ter Horst**

GJ 2008 Effects of long-term stress and recovery of the prefrontal cortex and dentate gyrus in male and female rats. Cereb Cortex 18:2762–2774

9. **Hao J, Rapp PR, Janssen WG, Lou W, Lasley BL, Hof PR, Morrison JH** 2007 Interactive effects of age and estrogen on cognition and pyramidal neurons in monkey prefrontal cortex. Proc Natl Acad Sci USA 104:11465–11470
10. **Paxinos G, Watson C** 1998 The rat brain. New York: Academic Press
11. **Sanz A, Carrero P, Pernía O, Garcia-Segura LM** 2008 Pubertal maturation modifies the regulation of insulin-like growth factor-I receptor signaling by estradiol in the rat prefrontal cortex. Dev Neurobiol 68:1018–1028
12. **Meyers B, D'Agostino A, Walker J, Kritzer MF** 2010 Gonadectomy and hormone replacement exert region- and enzyme isoform-specific effects on monoamine oxidase and catechol-*O*-methyltransferase activity in prefrontal cortex and neostriatum of adult male rats. Neuroscience 165:850–862
13. **Shughrue PJ, Merchenthaler I** 2000 Estrogen is more than just a "sex hormone": novel sites for estrogen action in the hippocampus and cerebral cortex. Front Neuroendocrinol 21:95–101
14. **Kritzer MF** 2002 Regional, laminar, and cellular distribution of immunoreactivity for ERα and ERβ in the cerebral cortex of hormonally intact, adult male and female rats. Cereb Cortex 12:116–128
15. **Kritzer MF** 2006 Regional, laminar and cellular distribution of immunoreactivity for ER-β in the cerebral cortex of hormonally intact, postnatally developing male and female rats. Cereb Cortex 16:1181–1192
16. **Sárvári M, Hrabovszky E, Kalló I, Galamb O, Solymosi N, Likó I, Molnár B, Tihanyi K, Szombathelyi Z, Liposits Z** 2010 Gene expression profiling identifies key estradiol targets in the frontal cortex of the rat. Endocrinology 151:1161–1176
17. **Shughrue PJ, Lane MV, Merchenthaler I** 1997 Comparative distribution of estrogen receptor-α and -β mRNA in the rat central nervous system. J Comp Neurol 388:507–525
18. **Gronemeyer H, Gustafsson JA, Laudet V** 2004 Principles for modulation of the nuclear receptor superfamily. Nat Rev Drug Discov 3:950–964
19. **Barreto G, Santos-Galindo M, Diz-Chavez Y, Pernía O, Carrero P, Azcoitia I, Garcia-Segura LM** 2009 Selective estrogen receptor modulators decrease reactive astrogliosis in the injured brain: effects of aging and prolonged depletion of ovarian hormones. Endocrinology 150:5010–5015
20. **Sierra A, Gottfried-Blackmore A, Milner TA, McEwen BS, Bulloch K** 2008 Steroid hormone receptor expression and function in microglia. Glia 56:659–674
21. **Blurton-Jones M, Tuszynski MH** 2006 Estradiol-induced modulation of estrogen receptor-β and GABA within the adult neocortex: a potential transsynaptic mechanism for estrogen modulation of BDNF. J Comp Neurol 499:603–612
22. **Morrison JH, Brinton RD, Schmidt PJ, Gore AC** 2006 Estrogen, menopause, and the aging brain: How basic neuroscience can inform hormone therapy in women. J Neurosci 26:10332–10348
23. **Zandi PP, Carlson MC, Plassman BL, Welsh-Bohmer KA, Mayer LS, Steffens DC, Breitner JC** 2002 Hormone replacement therapy and incidence of Alzheimer disease in older women. JAMA 288: 2123–2129
24. **Sherwin BB** 2006 Estrogen and cognitive aging in women. Neuroscience 138:1021–1026
25. **Joffe H, Hall JE, Gruber S, Sarmiento IA, Cohen LS, Yurgelun-Todd D, Martin KA** 2006 Estrogen therapy selectively enhances prefrontal cognitive processes: a randomized, double-blind, placebo-controlled study with functional magnetic resonance imaging in perimenopausal and recently postmenopausal women. Menopause 13:411–422
26. **Henderson VW** 12 November 2009 Action of estrogens in the aging brain: Dementia and cognitive aging. Biochim Biophys Acta 10.1016/j.bbagen.2009.11.005
27. **Rapp PR, Morrison JH, Roberts JA** 2003 Cyclic estrogen replacement improves cognitive function in aged ovariectomized rhesus monkeys. J Neurosci 23:5708–5714
28. **Luine VN, Jacome LF, Maclusky NJ** 2003 Rapid enhancement of visual and place memory by estrogens in rats. Endocrinology 144: 2836–2844
29. **Rodgers SP, Bohacek J, Daniel JM** 2010 Transient estradiol exposure during middle age in ovariectomized rats exerts lasting effects on cognitive function and the hippocampus. Endocrinology 151: 1194–1203
30. **Walf AA, Frye CA** 2006 A review and update of mechanisms of estrogen in the hippocampus and amygdale for anxiety and depression behavior. Neuropsychopharmacology 31:1097–1111
31. **Wise PM, Dueker E, WuttkeW** 1988 Age-related alterations in pulsatile luteinizing hormone release: effects of long-term ovariectomy, repeated pregnancies and naloxone. Biol Reprod 39:1060–1066
32. **Wu Z, Irizarry RA, Gentleman R, Martinez-Murillo F, Spencer F** 2004 A model-based background adjustment for oligonucleotide expression arrays. J Am Stat Assoc 99:909–917
33. **Kauffmann A, Gentleman R, Huber W** 2009 Array quality metrics: a bioconductor package for quality assessment of microarray data. Bioinformatics 25:415–416
34. **MAQC Consortium, Shi L, Reid LH, Jones WD, Shippy R, Warrington JA, Baker SC, Collins PJ, de Longueville F, Kawasaki ES, Lee KY, Luo Y, Sun YA, Willey JC, Setterquist RA, Fischer GM, Tong W, Dragan YP, Dix DJ, Frueh FW, Goodsaid FM, Herman D, Jensen RV, Johnson CD, Lobenhofer EK, *et al.*** 2006 The Microarray Quality Control (MAQC) project shows inter- and intraplatform reproducibility of gene expression measurements. Nat Biotechnol 24:1151–1161
35. **Smyth G** 2004 Linear models and empirical Bayes methods for assessing differential expression in microarray experiments. Stat Appl Genet Mol Biol 3:Article 3
36. **Benjamini Y, Hochberg Y** 1995 Controlling the false discovery rate: a practical and powerful approach to multiple testing. J R Stat Soc Ser B 57:289–300
37. **Gentleman RC, Carey VJ, Bates DM, Bolstad B, Dettling M, Dudoit S, Ellis B, Gautier L, Ge Y, Gentry J, Hornik K, Hothorn T, Huber W, Iacus S, Irizarry R, Leisch F, Li C, Maechler M, Rossini AJ, Sawitzki G, Smith C, Smyth G, Tierney L, Yang JY, Zhang J** 2004 Bioconductor: open software development for computational biology and bioinformatics. Genome Biol 5:R80
38. **R Development Core Team** 2009 A language and environment for statistical computing. Vienna: R Foundation for Statistical Computing
39. **Kanehisa M, Bork P** 2003 Bioinformatics in the post-sequence era. Nat Genet 33:305–310
40. **Tian L, Greenberg SA, Kong SW, Altschuler J, Kohane IS, Park PJ** 2005 Discovering statistically significant pathways in expression profiling studies. Proc Natl Acad Sci USA 102:13544–13549
41. **Andersen CL, Jensen JL, Ørntoft TF** 2004 Normalization of real-time quantitative reverse transcription-PCR data: a model-based variance estimation approach to identify genes suited for normalization, applied to bladder and colon cancer data sets. Cancer Res 64:5245–5250
42. **Vandesompele J, De Preter K, Pattyn F, Poppe B, Van Roy N, De Paepe A, Speleman F** 2002 Accurate normalization of real-time quantitative RT-PCR data by geometric averaging of multiple internal control genes. Genome Biol 3:RESEARCH0034.1–0034.11
43. **Barroso-Chinea P, Castle M, Aymerich MS, Pérez-Manso M, Erro E, Tuñon T, Lanciego JL** 2007 Expression of the mRNAs encoding for the glutamate transporters 1 and 2. J Comp Neurol 501:703–715
44. **Parent MA, Wang L, Su J, Netoff T, Yuan LL** 2010 Identification of the hippocampal input to medial prefrontal cortex in vitro. Cereb Cortex 20:393–403
45. **Thierry AM, Blanc G, Sobel A, Stinus L, Golwinski J** 1973 Dopaminergic terminals in the rat cortex. Science 182:499–501

46. **Robbins TW, Arnsten AFT** 2009 The neuropsychopharmacology of fronto-executive function: monoaminergic modulation. Annu Rev Neurosci 32:267–287
47. **Gaspar P, Bloch B, Le Moine C** 1995 D1 and D2 receptor gene expression in the rat frontal cortex: cellular localization in different classes of efferent neurons. Eur J Neurosci 7:1050–1063
48. **Santana N, Mengod G, Artigas F** 2009 Quantitative analysis of the expression of dopamine D1 and D2 receptors in pyramidal and GABAergic neurons of the rat prefrontal cortex. Cereb Cortex 19:849–860
49. **Vincent SL, Khan Y, Benes FM** 1995 Cellular colocalization of dopamine D1 and D2 receptors in rat medial prefrontal cortex. Synapse 19:112–120
50. **Ariano MA, Sibley DR** 1994 Dopamine receptor distribution in the rat CNS: elucidation using anti-peptide antisera directed against D1A and D3 subtypes. Brain Res 649:95–110
51. **Le Moine C, Gaspar P** 1998 Subpopulations of cortical GABAergic interneurons differ by their expression of D1 and D2 dopamine receptor subtypes. Mol Brain Res 58:231–236
52. **Le Saux M, Morissette M, Di Paolo T** 2006 ERβ mediates the estradiol increase of D2 receptors in rat striatum and nucleus accumbens. Neuropharmacology 50:451–457
53. **Lee SH, Mouradian MM** 1999 Up-regulation of D1A dopamine receptor gene transcription by estrogen. Mol Cell Endocrinol 156: 151–157
54. **Minowa T, Minowa MT, Mouradian MM** 1992 Analysis of the promoter region of the rat D2 dopamine receptor gene. Biochemistry 31:8389–8396
55. **Wang Y, Chan GL, Holden JE, Dobko T, Mak E, Schulzer M, Huser JM, Snow BJ, Ruth TJ, Calne DB, Stoessl AJ** 1998 Age-dependent decline of dopamine D1 receptors in human brain: a PET study. Synapse 30:56–61
56. **Volkow ND, Gur RC, Wang GJ, Fowler JS, Moberg PJ, Ding YS, Hitzemann R, Smith G, Logan J** 1998 Association between decline in brain dopamine activity with age and cognitive and motor impairment in healthy individuals. Am J Psychiatry 155:344–349
57. **Bäckman L, Ginovart N, Dixon RA, Wahlin TB, Wahlin A, Halldin C, Farde L** 2000 Age-related cognitive deficits mediated by changes in the striatal dopamine system. Am J Psychiatry 157:635–637
58. **Mizoguchi K, Shoji H, Tanaka Y, Maruyama W, Tabira T** 2009 Age-related spatial working memory impairment is caused by prefrontal cortical dopaminergic dysfunction in rats. Neuroscience 162:1192–1201
59. **Rahman Z, Gold SJ, Potenza MN, Cowan CW, Ni YG, He W, Wensel TG, Nestler EJ** 1999 Cloning and characterization of RGS9-2: a striatal-enriched alternatively spliced product of the RGS9 gene. J Neurosci 19:2016–2026
60. **Gold SJ, Ni YG, Dohlman HG, Nestler EJ** 1997 Regulators of G protein signaling (RGS) proteins: region-specific expression of nine subtypes in rat brain. J Neurosci 17:8024–8037
61. **Maple AM, Perna MK, Parlaman JP, Stanwood GD, Brown RW** 2007 Ontogenetic quinpirole treatment produces long-lasting decreases in the expression of Rgs9, but increases Rgs17 in the striatum, nucleus accumbens and frontal cortex. Eur J Neurosci 26: 2532–2538
62. **Kovoor A, Seyffarth P, Ebert J, Barghshoon S, Chen CK, Schwarz S, Axelrod JD, Cheyette BN, Simon MI, Lester HA, Schwarz J** 2005 D2 dopamine receptors colocalize regulator of G protein signaling 9-2 (RGS9-2) via the RGS9 DEP domain, and RGS9 knock-out mice develop dyskinesias associated with dopamine pathways. J Neurosci 25:2157–2165
63. **Sharifi JL, Brady DL, Koenig JI** 2004 Estrogen modulates RGS9 expression in the nucleus accumbens. Neuroreport 15:2433–2436
64. **Jacobson KA, Gao ZG** 2006 Adenosine receptors as therapeutic targets. Nat Rev Drug Discov 5:247–264
65. **Svenningsson P, Le Moine C, Fisone G, Fredholm BB** 1999 Distribution, biochemistry and function of striatal adenosine A2A receptors. Prog Neurobiol 59:355–396
66. **Quarta D, Borycz J, Solinas M, Patkar K, Hockemeyer J, Ciruela F, Lluis C, Franco R, Woods AS, Goldberg SR, Ferré S** 2004 Adenosine receptor-mediated modulation of dopamine release in the nucleus accumbens depends on glutamate neurotransmission and *N*-methyl-D-aspartate receptor stimulation. J Neurochem 91:873–880
67. **Schwarzschild MA, Agnati L, Fuxe K, Chen JF, Morelli M** 2006 Targeting adenosine A2A receptors in Parkinson's disease. Trends Neurosci 29:647–654
68. **Kruse MS, Prémont J, Krebs MO, Jay TM** 2009 Interaction of dopamine D1 with NMDA NR1 receptors in rat prefrontal cortex. Eur Neuropsychopharmacol 19:296–304
69. **Snyder GL, Fienberg AA, Huganir RL, Greengard P** 1998 A dopamine/D1 receptor/protein kinase A/dopamine- and cAMP-regulated phosphoprotein (Mr 32kDa)/protein phosphatase-1 pathway regulates dephosphorylation of the NMDA receptor. J Neurosci 18:10297–10303
70. **Gao C, Wolf ME** 2008 Dopamine receptors regulate NMDA receptor surface expression in prefrontal cortex neurons. J Neurochem 106:2489–2501
71. **Markram H, Toledo-Rodriguez M, Wang Y, Gupta A, Silberberg G, Wu C** 2004 Interneurons of the neocortical inhibitory system. Nat Rev Neurosci 5:793–807
72. **Petrie KA, Schmidt D, Bubser M, Fadel J, Carraway RE, Deutch AY** 2005 Neurotensin activates GABAergic interneurons in the prefrontal cortex. J Neurosci 25:1629–1636
73. **Rogge G, Jones D, Hubert GW, Lin Y, Kuhar MJ** 2008 CART peptides: regulators of body weight, reward and other functions. Nat Rev Neurosci 9:747–758
74. **Couceyro PR, Koylu EO, Kuhar MJ** 1997 Further studies on the anatomical distribution of CART by in situ hybridization. J Chem Neuroanat 12:229–241
75. **Koylu EO, Couceyro PR, Lambert PD, Kuhar MJ** 1998 Cocaine- and amphetamine-regulated transcript peptide immunohistochemical localization in the rat brain. J Comp Neurol 391:115–132
76. **Xu Y, Zhang W, Klaus J, Young J, Koerner I, Sheldahl LC, Hurn PD, Martínez-Murillo F, Alkayed NJ** 2006 Role of cocaine- and amphetamine-regulated transcript in estradiol-mediated neuroprotection. Proc Natl Acad Sci USA 103:14489–14494
77. **Chaki S, Kawashima N, Suzuki Y, Shimazaki T, Okuyama S** 2003 Cocaine- and dopamine-regulated transcript peptide produces anxiety-like behavior in rodents. Eur J Pharmacol 464:49–54
78. **Orsetti M, Di Brisco F, Canonico PL, Genazzani AA, Ghi P** 2008 Gene regulation in the frontal cortex of rats exposed to the chronic mild stress paradigm, an animal model of human depression. Eur J Neurosci 27:2156–2164
79. **Mao P, Ardeshiri A, Jacks R, Yang S, Hurn PD, Alkayed NJ** 2007 Mitochondrial mechanism of neuroprotection by CART. Eur J Neurosci 26:624–632
80. **Takeo C, Ikeda K, Horie-Inoue K, Inoue S** 2009 Identification of Igf2, Igfbp2 and Enpp2 as estrogen-responsive genes in rat hippocampus. Endocr J 56:113–120
81. **Petkova-Kirova P, Rakovska A, Zaekova G, Ballini C, Corte LD, Radomirov R, Vágvölgyi A** 2008 Stimulation by neurotensin of dopamine and 5-HT release from the rat prefrontal cortex. Neurochem Int 53:355–361
82. **Fawaz CS, Martel P, Leo D, Trudeau LE** 2009 Presynaptic action of neurotensin on dopamine release through inhibition of D2 receptor function. BMC Neurosci 10:96
83. **Kaneko T, Murashima M, Lee T, Mizuno N** 1998 Characterization of neocortical non-pyramidal neurons expressing preprotachykinins A and B: a double immunofluorescence study in the rat. Neuroscience 86:765–781
84. **Vruwink M, Schmidt HH, Weinberg RJ, Burette A** 2001 Substance P and nitric oxide signaling in cerebral cortex: anatomical evidence for reciprocal signaling between two classes of interneurons. J Comp Neurol 441:288–301
85. **Lu B, Su Y, Das S, Wang H, Wang Y, Liu J, Ren D** 2009 Peptide

neurotransmitters activate a cation channel complex of NALCN and UNC-80. Nature 457:741–744
86. **Spray DC, Ye ZC, Ransom BR** 2006 Functional connexin "hemichannels": a critical appraisal. Glia 54:758–773
87. **Gajda Z, Hermesz E, Gyengési E, Szupera Z, Szente M** 2006 The functional significance of gap junction channels in the epileptogenicity and seizure susceptibility of juvenile rats. Epilepsia 47:1009–1022
88. **Elias LA, Wang DD, Kriegstein AR** 2007 Gap junction adhesion is necessary for radial migration in the neocortex. Nature 448:901–907
89. **Ransohoff RM, Perry VH** 2009 Microglial physiology: unique stimuli, specialized responses. Annu Rev Immunol 27:119–145
90. **Barres BA** 2008 The mystery and magic of glia: a perspective on their roles in health and disease. Neuron 60:430–440
91. **Vegeto E, Bonincontro C, Pollio G, Sala A, Viappiani S, Nardi F, Brusadelli A, Viviani B, Ciana P, Maggi A** 2001 Estrogen prevents the lipopolysaccharide-induced inflammatory response in microglia. J Neurosci 21:1809–1818
92. **Moldenhauer G, Henne C, Karhausen J, Möller P** 1999 Surface-expressed invariant chain (CD74) is required for internalization of human leukocyte antigen-DR molecules to early endosomal compartments. Immunology 96:473–484
93. **Leng L, Metz CN, Fang Y, Xu J, Donnelly S, Baugh J, Delohery T, Chen Y, Mitchell RA, Bucala R** 2003 MIF signal transduction initiated by binding to CD74. J Exp Med 197:1467–1476
94. **Faure-André G, Vargas P, Yuseff MI, Heuzé M, Diaz J, Lankar D, Steri V, Manry J, Hugues S, Vascotto F, Boulanger J, Raposo G, Bono MR, Rosemblatt M, Piel M, Lennon-Duménil AM** 2008 Regulation of dendritic cell migration by CD74, the MHC class II-associated invariant chain. Science 322:1705–1710
95. **Cardona AE, Pioro EP, Sasse ME, Kostenko V, Cardona SM, Dijkstra IM, Huang D, Kidd G, Dombrowski S, Dutta R, Lee JC, Cook DN, Jung S, Lira SA, Littman DR, Ransohoff RM** 2006 Control of microglial cytotoxicity by the fractalkine receptor. Nat Neurosci 9:917–924
96. **Reid DM, Perry VH, Andersson PB, Gordon S** 1993 Mitosis and apoptosis of microglia in vivo induced by an anti-CR3 antibody which crosses the blood-brain barrier. Neuroscience 56:529–533
97. **Gros P, Milder FJ, Janssen BJC** 2008 Complement driven by conformational changes. Nat Rev Immunol 8:48–58
98. **Müller-Eberhard HJ** 1988 Molecular organization and function of the complement system. Annu Rev Biochem 57:321–347
99. **Schwab C, Klegeris A, McGeer PL** 31 October 2009 Inflammation in transgenic mouse models of neurodegenerative disorders. Biochim Biophys Acta 10.1016/j.bbadis.2009.10.013
100. **Sárvári M, Vágó I, Wéber CS, Nagy J, Gál P, Mák M, Kósa JP, Závodszky P, Pázmány T** 2003 Inhibition of C1q-beta-amyloid binding protects hippocampal cells against complement mediated cytotoxicity. J Neuroimmunol 137:12–18
101. **Fonseca MI, Zhou J, Botto M, Tenner AJ** 2004 Absence of C1q leads to less neuropathology in transgenic mouse models of Alzheimer's disease. J Neurosci 24:6457–6465
102. **Mauch DH, Nägler K, Schumacher S, Göritz C, Müller EC, Otto A, Pfrieger FW** 2001 CNS synaptogenesis promoted by glia-derived cholesterol. Science 294:1354–1357
103. **Wellington CL, Walker EK, Suarez A, Kwok A, Bissada N, Singaraja R, Yang YZ, Zhang LH, James E, Wilson JE, Francone O, McManus BM, Hayden MR** 2002 ABCA1 mRNA and protein distribution patterns predict multiple different roles and levels of regulation. Lab Invest 82:273–283
104. **Richter F, Meurers BH, Zhu C, Medvedeva VP, Chesselet MF** 2009 Neurons express hemoglobin α- and β-chains in rat and human brains. J Comp Neurol 515:538–547
105. **Biagioli M, Pinto M, Cesselli D, Zaninello M, Lazarevic D, Roncaglia P, Simone R, Vlachouli C, Plessy C, Bertin N, Beltrami A, Kobayashi K, Gallo V, Santoro C, Ferrer I, Rivella S, Beltrami CA, Carninci P, Raviola E, Gustincich S** 2009 Unexpected expression of α- and β-globin in mesencephalic dopaminergic neurons and glial cells. Proc Natl Acad Sci USA 106:15454–15459
106. **Schelshorn DW, Schneider A, Kuschinsky W, Weber D, Krüger C, Dittgen T, Bürgers HF, Sabouri F, Gassler N, Bach A, Maurer MH** 2009 Expression of hemoglobin in rodent neurons. J Cereb Blood Flow Metab 29:585–595
107. **Pajor AM, Gangula R, Yao X** 2001 Cloning and functional characterization of a high-affinity Na^+/dicarboxylate cotransporter from mouse brain. Am J Physiol Cell Physiol 280:C1215–1223
108. **Schousboe A, Westergaard N, Waagepetersen HS, Larsson OM, Bakken IJ, Sonnewald U** 1997 Trafficking between glia and neurons of TCA cycle intermediates and related metabolites. Glia 21:99–105
109. **Cesar M, Hamprecht B** 1995 Immunocytochemical examination of neural rat and mouse primary cultures using monoclonal antibodies raised against pyruvate carboxylase. J Neurochem 64:2312–2318
110. **Qiu J, Bosch MA, Jamali K, Xue C, Kelly MJ, Rønnekleiv OK** 2006 Estrogen upregulates T-type calcium channels in the hypothalamus and pituitary. J Neurosci 26:11072–11082
111. **Perez-Reyes E** 2003 Molecular physiology of low-voltage-activated T-type calcium channels. Physiol Rev 83:117–161
112. **Neher E, Sakaba T** 2008 Multiple roles of calcium ions in the regulation of neurotransmitter release. Neuron 59:861–872
113. **Greer PL, Greenberg ME** 2008 From synapse to nucleus: calcium-dependent gene transcription in the control of synapse development and function. Neuron 59:846–860
114. **Mayack SR, Shadrach JL, Kim FS, Wagers AJ** 2010 Systemic signals regulate ageing and rejuvenation of blood stem cell niches. Nature 463:495–500
115. **Echave P, Machado-da-Silva G, Arkell RS, Duchen MR, Jacobson J, Mitter R, Lloyd AC** 2009 Extracellular growth factors and mitogens cooperate to drive mitochondrial biogenesis. J Cell Sci 122:4516–4525
116. **Bitoun E, Finelli MJ, Oliver PL, Lee S, Davies KE** 2009 AF4 is a critical regulator of the IGF-1 signaling pathway during Purkinje cell development. J Neurosci 29:15366–15374
117. **Liang L, Guo WH, Esquiliano DR, Asai M, Rodriguez S, Giraud J, Kushner JA, White MF, Lopez MF** 2010 Insulin-like growth factor 2 and the insulin receptor, but not insulin, regulate fetal hepatic glycogen synthesis. Endocrinology 151:741–747
118. **Dugas JC, Mandemakers W, Rogers M, Ibrahim A, Daneman R, Barres BA** 2008 A novel purification method for CNS projection neurons lead to the identification of brain vascular cells as a source of trophic support for corticospinal motor neurons. J Neurosci 28:8294–8305
119. **Brinkman A, Groffen C, Kortleve DJ, Geurts van Kessel A, Drop SL** 1988 Isolation and characterization of a cDNA encoding the low molecular weight insulin-like growth factor binding protein (IBP-1). EMBO J 7:2417–2423
120. **Binkert C, Landwehr J, Mary JL, Schwander J, Heinrich G** 1989 Cloning, sequence analysis and expression of a cDNA encoding a novel insulin-like growth factor binding protein (IGFBP-2). EMBO J 8:2497–2502
121. **Firth SM, Baxter RC** 2002 Cellular actions of the insulin-like growth factor binding proteins. Endocr Rev 23:824–854

23. számú melléklet

Retrograde Endocannabinoid Signaling Reduces GABA-ergic Synaptic Transmission to Gonadotropin-Releasing Hormone Neurons

Imre Farkas[1], Imre Kalló[1], Levente Deli[1], Barbara Vida[1], Erik Hrabovszky[1], Csaba Fekete[1], Suzanne M. Moenter[2], Masahiko Watanabe[3], and Zsolt Liposits[1,4]

[1]Department of Endocrine Neurobiology, Institute of Experimental Medicine, Hungarian Academy of Sciences, Budapest, Hungary

[2]Departments of Medicine and Cell Biology, University of Virginia, Charlottesville, Virginia, USA

[3]Department of Anatomy, Hokkaido University School of Medicine, Sapporo, Japan

[4]Department of Neuroscience, Faculty of Information Technology, Pázmány Péter Catholic University, Budapest, Hungary

Abbreviated title: Cannabinoids affect GABA to GnRH cells

Keywords: type-1 cannabinoid receptor; retrograde cannabinoid signaling; GnRH neurons; GABA; hypothalamus

Précis: Endocannabinoids synthesized in GnRH neurons decrease GnRH neuron firing rate via inhibiting GABA-ergic afferents.

Disclosure summary: All of the authors have nothing to declare.

Financial support: This research was supported by the National Science Foundation of Hungary (OTKA K69127 and T73002).

Corresponding author and to whom reprint requests should be addressed:

Zsolt Liposits MD, PhD, DSc

Laboratory of Endocrine Neurobiology, Institute of Experimental Medicine, Hungarian Academy of Sciences, Szigony. u. 43., H-1083 Budapest, Hungary

Tel.: 36-1-210-9943

Fax: 36-1-210-9944

Email: liposits@koki.hu

Abstract

Cannabinoids suppress fertility via reducing hypothalamic GnRH output. $GABA_A$ receptor ($GABA_A$-R)-mediated transmission is a major input to GnRH cells that can be excitatory. We hypothesized that cannabinoids act via inhibiting GABAergic input. We performed loose-patch electrophysiological studies of acute slices from adult male GnRH-GFP transgenic mice. Bath application of type-1 cannabinoid receptor (CB1) agonist WIN55,212 decreased GnRH neuron firing rate. This action was detectable in presence of the glutamate receptor antagonist kynurenic acid, but disappeared when bicuculline was also present, indicating $GABA_A$-R involvement. In immunocytochemical experiments, CB1-immunoreactive axons formed contacts with GnRH neurons and a subset established symmetric synapses characteristic of GABA-ergic neurotransmission. Functional studies were continued with whole-cell patch-clamp electrophysiology in presence of tetrodotoxin. WIN55,212 decreased the frequency of $GABA_A$-R-mediated miniature postsynaptic currents (mPSCs, reflecting spontaneous vesicle fusion), which was prevented with the CB1 antagonist AM251, indicating collectively that activation of presynaptic CB1 inhibits GABA release. AM251 alone increased mPSC frequency, providing evidence that endocannabinoids tonically inhibit $GABA_A$-R drive onto GnRH neurons. Increased mPSC frequency was absent when diacylglycerol lipase was blocked intracellularly with tetrahydrolipstatin, showing that tonic inhibition is caused by 2-arachidonoylglycerol production of GnRH neurons. $CdCl_2$ in extracellular solution can maintain both action potentials and spontaneous vesicle fusion. Under these conditions, when endocannabinoid-mediated blockade of spontaneous vesicle fusion was blocked with AM251, GnRH neuron firing increased, revealing an endogenous endocannabinoid brake on GnRH neuron firing.

Retrograde endocannabinoid signaling may represent an important mechanism under physiological and pathological conditions whereby GnRH neurons regulate their excitatory GABA-ergic inputs.

Introduction

Δ-9-tetrahydro-cannabinol (THC), the main psychoactive substance of the cannabis sativa plant, modulates a wide array of endocrine functions that operate under hypothalamic control (1). THC influences various aspects of reproductive physiology by inhibiting luteinizing hormone (LH) secretion from the adenohypophysis (2-5). A consensus opinion exists that cannabinoids suppress gonadotropin release via reducing the neurosecretory output from hypothalamic GnRH neurons. Accordingly, i) THC does not inhibit adenohypophysial LH secretion *in vitro* (6, 7), ii) GnRH prevents the inhibitory effects of cannabinoids on ovulation and LH secretion (3, 6, 8) and iii) the decreased serum LH following intracerebroventricular injection of THC coincides with an increased mediobasal hypothalamic GnRH content (6).

In the central nervous system the actions of THC are primarily exerted via the type 1 cannabinoid receptor (CB1), which has been localized to axon terminals (1, 9). CB1 activation by either exogenous THC or the main endogenous cannabinoid ligands (endocannabinoids) 2-arachidonylglycerol (2-AG) and anandamide (AEA) inhibits the presynaptic release of neurotransmitters including γ-aminobutyric acid (GABA) (9-12) and glutamate (13, 14). The importance of CB1 receptors in central inhibitory regulation of the reproductive axis has been demonstrated by the ability of 2-AG to suppress LH secretion in wild-type but not in CB1 receptor knockout mice (15).

The pulsatile secretory activity of GnRH neurons is influenced by physiological or pathological alterations in the synaptic input (16). The amino acid neurotransmitter GABA plays a pivotal role in this afferent regulation. GnRH neurons receive GABA-ergic synapses (17) and express functional $GABA_A$-Rs (18-22) and $GABA_B$ (23) receptors. Whereas GABA acts as the major inhibitory neurotransmitter in the adult hypothalamus (24), mature GnRH neurons maintain high intracellular chloride concentrations, which can result in excitatory responses to $GABA_A$-R activation in adult mice (18, 21) and rats (25, 26). Modulation of GABA-ergic drive onto GnRH neurons has been commonly implicated in metabolic (27), sex steroid (28) and circadian (29) signaling to GnRH neurons.

In the present studies we hypothesized that cannabinoids inhibit GABA-ergic neurotransmission to GnRH neurons. The decreased $GABA_A$-R mediated drive, in turn, decreases GnRH neuron activity. To test this hypothesis, we have carried out a series of

electrophysiological and neuroanatomical studies.

Materials and methods

Animals

Adult gonadally intact male mice were used from local colonies bred at the Medical Gene Technology Unit of the Institute of Experimental Medicine (IEM). They were housed in light (12:12 light-dark cycle, lights on at 07:00h)- and temperature (22 ± 2°C) controlled environment, with free access to standard food and tap water. All studies were carried out with permissions from the Animal Welfare Committee of the IEM (No.: A5769-01) and in accordance with legal requirements of the European Community (Decree 86/609/EEC). GnRH-green-fluorescent protein (GnRH-GFP) transgenic mice (n=70) bred on a C57Bl/6J genetic background were used for electrophysiological experiments. In this animal model a GnRH promoter segment drives selective GFP expression in the majority of GnRH neurons (30). For immunohistochemistry, GnRH-GFP mice (n=5) and homozygous CB1 knockout mice (CB1-KO; n=12) and their wild-type littermates (CB1-WT; n=12) were used. The parent stock of the CB1-KO animals was obtained from IRIBHN, Université Libre de Bruxelles (31) and transferred earlier onto a CD1 (Charles River, L'Arbreole, France) genetic background at IEM.

Brain slice preparation and recording

Mice were killed by cervical dislocation between 1100-1200 h. The brain was removed rapidly and immersed in ice cold aCSF which had been bubbled with a mixture of 95% O_2 and 5% CO_2. The solution contained the following (in mM): NaCl 135, KCl 3.5, $NaHCO_3$ 26, $MgSO_4$ 1.2, NaH_2PO_4 1.25, $CaCl_2$ 2.5, glucose 10. Hypothalamic blocks were dissected and 250µm-thick coronal slices were prepared from the medial septum/preoptic area with a VT-1000S vibratome (Leica GmBH, Germany) in ice-cold oxygenated aCSF. The slices containing the preoptic area were bisected along the midline and equilibrated in aCSF saturated with O_2/CO_2 at room temperature for 1 h. During recording (between 1400-1800 h at 33 ^oC) the brain slices were oxygenated by bubbling the aCSF with O_2/CO_2 gas. Axopatch 200B patch-clamp amplifier, Digidata-1322A data acquisition system, and pCLAMP 9.2 software (Molecular Devices Co., USA) were used for recording. Cells were visualized with a BX51WI IR-DIC microscope (Olympus Co. Japan). The patch electrodes (OD=1.5mm, thin wall, Garner Co., USA) were pulled with a Flaming-Brown P-97 puller (Sutter Instrument Co., USA) and polished with an MF-830 microforge (Narishige).

GnRH-GFP neurons were identified by brief illumination at 470 nm using an epifluorescent filter set, based on their green fluorescence, typical fusiform shape and topographic location in the preoptic area (30). After control recording the slices were treated with various drugs for 10 min and the recording repeated for 250 sec. Each neuron served as its own control when drug effects were evaluated.

Loose-patch-clamp experiments

Recording of action current firing of GnRH neurons was carried out at 33^{o}C. Pipette potential was 0 mV, pipette resistance 1-2 MOhm, resistance of loose-patch seal 7-40 MOhm. The pipette solution contained (in mM): NaCl 150, KCl 3.5, $CaCl_2$ 2.5, $MgCl_2$ 1.3, HEPES 10, glucose 10 (pH=7.3 with NaOH).

After recording basal action currents, the CB1 agonist WIN55,212 was added at 1 µM for 10 min and the recording was repeated. In experiments to investigate involvement of $GABA_A$-R activation in WIN55,212 actions, ionotropic glutamate receptors were first blocked with 2 mM kynurenic acid for 10 min and then, $GABA_A$-Rs with 20 µM bicuculline-methiodide for 10 min. Subsequently, WIN55,212 was added to the extracellular solution. Use of the ionotropic glutamate receptor blocker together with bicuculline was an important part of the strategy to prevent an unbalanced excitatory tone in the slices (21, 32, 33).

The putative effect of tonic endocannabinoid release on GnRH neuron firing was addressed in the presence of the non-selective Ca^{++} channel inhibitor cadmium ($CdCl_2$, 200 µM; 10 min). $CdCl_2$ in the aCSF allows actions potentials and neurotransmitter release due to spontaneous vesicle fusion to continue but blocks action potential-dependent neurotransmitter release (34). A putative endocannabinoid blockade of spontaneous vesicle fusion was addressed by studying changes in GnRH neuron firing after the

addition of the CB1 antagonist AM251 (1μM, Tocris) to the aCSF for 10 min, in the presence of $CdCl_2$. NaH_2PO_4 was omitted from the aCSF in this experiment, to avoid precipitation.

Whole-cell patch-clamp experiments

The cells were voltage-clamped at holding potential –70mV. Pipette offset potential, series resistance and capacitance were compensated before recording. Only cells with low holding current (<50pA) and stable baseline were used. R_{in}, R_s and C_m were also measured before each recording by using 5 mV hyperpolarizing pulses. To ensure consistent recording qualities, only cells with Rs<20 MΩ, Rin>500 MΩ and Cm>10 pF were accepted; further if these values changed by more than 20% during measurements, the recordings were discarded (35). The pipette solution contained (in mM): HEPES 10, KCl 140, EGTA 5, $CaCl_2$ 0.1, Mg-ATP 4, Na-GTP 0.4 (pH=7.3 with NaOH). The resistance of the patch electrodes was 2-3 MΩ. Spike-mediated transmitter release was blocked in all experiments by adding the voltage-sensitive Na-channel inhibitor tetrodotoxin (TTX, 750nM, Tocris) to the aCSF 10min before control miniature postsynaptic currents (mPSCs) were recorded. Picrotoxin (100μM, Sigma) was used in the aCSF to verify that mPSCs were related to $GABA_A$-R activation. In subsequent experiments, modulation of mPSCs by CB1 was addressed by treating slices with the CB1 agonist WIN55,212 (1μM, Tocris) for 10 min. In other experiments, slices were incubated with the CB1 antagonist AM251 (1μM, Tocris) for 10 min and recorded. Then WIN55,212 (1μM) was added and recording repeated after 10 min. Finally, the source of endogenous cannabinoids that regulate GABA-ergic afferents to GnRH neurons was investigated: the diacylglycerol (DAG) lipase inhibitor tetrahydrolipstatin (THL) was added to the intracellular solution at 10 μM to block 2-AG synthesis. To minimize THL spill, the GnRH cells were approached rapidly (<1 min) and the flow rate of aCSF was increased from 5-6 to 8-9 ml/min. Just before release of the positive pressure in the pipette, the flow rate was restored to 5-6 ml/min to avoid any mechanical movement of the slice. The pipette solution containing THL was allowed to equilibrate with the intracellular milieu of the cell for 25min before control recording. Then AM251 was added for 10 min and recording repeated.

Statistical analysis

Each experimental group contained 8-10 recorded cells from 6-7 animals. Recordings (250 sec) were stored and analyzed off-line. Baseline correction of the action current and mPSC recordings was carried out using the Corrector software developed in our laboratory (L. Tatai, G. Lőcsei, B. Wittner, Judit Bálintné Farkas). In brief, background current fluctuations were smoothed by the running averages of a 300-point window, which was shifted point-by-point. At the sampling rate applied (4 kHz) this width caused no distortion of the mPSCs and action currents. Event detection was performed using the Clampfit module of the PClamp 9.2 software (Molecular Devices). Group data were expressed as mean ± standard error (SEM). Statistical significance was analyzed using the Student's t-test or ANOVA followed, by Newman-Keuls (NK) test (GraphPad Software Inc., USA), and considered at $p<0.05$.

Preparation of sections for immunohistochemistry

Mice were deeply anesthetized with a cocktail of ketamine (25 mg/kg), xylavet (5 mg/kg) and pipolphen (2.5 mg/kg) in saline and perfused through the ascending aorta first with 10 ml phosphate buffered saline (0.1 M, pH 7.4; PBS) and then with 40 ml of fixative in PBS. The fixative contained 4% paraformaldehyde (PFA) for brightfield and fluorescent microscopy and 4% PFA and 0.2% glutaraldehyde (GA) for electron microscopy. The solution containing GA was rinsed out from the vasculature immediately with 10 ml 4% PFA to prevent excessive cross-linking of tissues and antigens. The perfused brains were postfixed overnight in 2% PFA at 4°C. Serial 30μm-thick coronal sections were cut on a Vibratome from the rostro-caudal extent of the preoptic area/anterior hypothalamus.

Confocal microscopic analysis of CB1-immunoreactive fibers apposed to GnRH neurons

Every third section of the preoptic area (POA) and anterior hypothalamus (AH) was pre-treated with 0.5% Triton X-100 (20 min),

0.5% hydrogen peroxide (H_2O_2, 10 min) and 2% normal horse serum (NHS; 20 min) before antibody incubations. All treatments and rinses with PBS (3x5 min) in between were carried out at room temperature, except for primary antibody and fluorochrom incubations performed at 4 °C. The primary antibodies were applied in cocktails for 72h; a goat anti-CB1 (1:100, raised against the C-terminal 31 amino acids of mouse CB1) (36) antiserum was mixed either with a rabbit antiserum to GnRH (1:10,000; LR1, from Dr. R. Benoit, McGill University, Montreal, Canada) or, as an alternative, with a rabbit antiserum to GFP (1:5,000; ab3080, Millipore, USA) in studies of transgenic mice. The rabbit primary antibodies were visualised by sequential applications of biotinylated donkey anti-rabbit immunoglobulins (IgG, 1:500; 2h, Jackson Immunoresearch Laboratories, USA), peroxidase-conjugated avidin-biotin complex (ABC, 1:1,000, 1h, Vector Laboratories, USA), biotinylated tyramide (1:200; 0.5h) and Alexa Fluor 488-conjugated streptavidin (1:500, 24h, Molecular Probes, USA). The CB1 immunoreactive sites were reacted with carbocyanine (Cy)3-conjugated donkey anti-goat IgG (1:500; 12h, Jackson Immunoresearch Laboratories). Finally, sections were mounted onto glass slides and coverslipped with Vectashield mounting medium (Vector Laboratories).

The fluorescent signals were studied with a Radiance 2100 confocal microscope (Bio-Rad Laboratories, Hemel Hempstead, UK) using the following laser lines and filters: 488 nm for Alexa Fluor 488 and EGFP; 543 nm for Alexa Fluor 594 and CY3 and dichroic/emission filters 560 nm/500–540 nm for Alexa Fluor 488 and EGFP, 650 nm/560-610 nm for Alexa 594. A series of optical sections was prepared using a 60x oil immersion objective. The sequentially scanned red and green channels were merged and displayed with the Laser Vox software (Bio-Rad) and an IBM-compatible personal computer. Appositions were only considered if a gap could not be recognized between the CB1 and GnRH immunoreactive profiles in optical slices below 0.7 µm. The specificity of CB1 receptor immunolabeling was verified by the absence of immunoreactivity in sections of CB1-KO mice processed in parallel with tissues of the CB1-WT animals.

Light- and electron microscopic analysis of CB1-immunoreactive input to GnRH neurons

A set of sections from brains fixed with the PFA-GA mixture was pretreated with 1% sodium borohydride for 30 min, and with 0.5% H_2O_2 for 15 min. Then they were cryoprotected with 15% (15 min), followed by 30% sucrose (12h) in PBS. Sequential freeze-thaw cycles were carried out three times on liquid nitrogen to permeabilize sections. Finally, 2% NHS was applied (20 min) to prevent non-specific antibody binding. The pretreated sections were double-immunostained for CB1 and GnRH in two consecutive steps. First, the sections were incubated in goat anti-CB1 (1:900; 4 days), biotinylated donkey anti-goat IgG (1:500; 1 day, Jackson ImmunoResearch), and ABC Elite solution (1:1,000; 1.5 h). The signal was visualized with silver-gold intensified nickel-diaminobenzidine (SGI-NiDAB) with modifications detailed elsewhere (37). Next, the sections were transferred into rabbit anti-GnRH antibodies (1:5,000; 2 days), biotinylated donkey anti-rabbit IgG (1:500; 1 day), and ABC Elite solution (1:1,000; 1.5 h). The GnRH signal was detected with DAB. The double-labeled sections were treated with 1% osmium tetroxide for 60 min and 2% uranyl acetate (prepared in 70% ethanol) for 40 min, then dehydrated in an ascending series of ethanol and propylene oxide. Flat-embedding in TAAB 812 medium epoxy resin was carried out between a pair of glass microscope slides pre-coated with liquid release agent (Electron Microscopy Sciences, USA). The resin was allowed to polymerize at 56°C for 2 days. Ultrathin sections (50-60 nm) were collected with a Leica Ultracut UCT ultramicrotome (Leica Microsystems, Austria) onto Formvar-coated single-slot grids, contrasted with 2% lead citrate and examined with a Jeol-100C transmission electron microscope.

Results

Activation of CB1 receptors decreases the activity of GnRH neurons

To test the hypothesis that cannabinoid signaling inhibits the electric activity of GnRH

neurons, action currents were recorded from GnRH neurons of adult male GnRH-GFP transgenic mice using the loose-patch approach (38). Administration of the CB1 agonist WIN55,212 (1μM) reduced the frequency of action currents to 49±15% of the control (control: 0.6±0.07 Hz; WIN55,212: 0.3±0.08 Hz; Fig. 1A; p=0.0136 by paired Student's test). This finding served as support for the hypothesis that CB1 signaling in the preoptic area results in a net decrease in the electric activity of GnRH neurons. The amplitude did not change (107±6.5 % of control).

The average number of spikes within a burst (S/B: 4.2±0.2 in control cells) decreased by 8±2.5 % (p=0.043) in response to WIN55,212 treatment. The interburst interval (IBI: 34±11.2 s in control cells) increased by 47±11 % (p=0.022), whereas the interspike interval (ISI, time between spikes within a burst: 0.2±0.03 s in control cells) did not change.

WIN55,212 decreases GnRH neuron activity via modulating $GABA_A$-R signaling

In their classic mode of action, endocannabinoids bind to presynaptic CB1 receptors to reduce neurotransmitter release (9). Because GABA acting through $GABA_A$-R is the major neurotransmitter in the afferent regulation of GnRH neurons (16), we analyzed the effect of WIN55,212 in the presence of the $GABA_A$-R blocker bicuculline (20μM). Because correct interpretation of experimental results would not be possible in this paradigm due to an unbalanced excitatory tone (21, 32, 33), the extracellular solution also contained the ionotropic glutamate receptor blocker kynurenic acid (2mM).

Kynurenic acid increased the firing rate of GnRH neurons by 95±20.8 % (control: 0.48±0.07 Hz; p=0.0022 by paired Student's test). The S/B increased by 14+3.1 % (p=0.021; control: 4.2±0.2) and IBI decreased by 48±9 % (p=0.017; control: 34±11.2 s). In response to the subsequent administration of 1μM WIN55,212, the frequency was reduced by 33±2.4% (p=0.015 by paired Student's test) (Figs. 1B, D). The S/B parameter decreased by 13±4 % (p=0.037), and IBI increased by 57+13 % (p=0.029). The amplitude of the action currents did not change throughout the treatments. Results of the above study established that 1μM WIN55,212 can decrease the firing activity of GnRH neurons independently of ionotropic glutamate receptors. To show that the underlying mechanisms include $GABA_A$-R-dependent neurotransmission, we tested if WIN55,212 can also reduce the firing activity of GnRH neurons in the presence of the $GABA_A$-R antagonist bicuculline (20μM). Similarly to findings in the previous study, the firing rate of GnRH neurons (0.55±0.07 Hz; 100 %) was increased in response to 2 mM kynurenic acid, reaching 181±24.4% of the control frequency (p=0.037 by paired Student's test; Figs. 1C, E). The S/B increased by 14+3.1 % (control: 4.2±0.2; p=0.037) and IBI decreased by 48±9 % (control: 34±11.2 s; p=0.025). After bicuculline was also added for 10 min, firing rate decreased by 57±10.3% (ANOVA: p=0.0143 and Newman-Keuls test: p=0.012; Kyn+Bic *vs.* Kyn, Figs. 1C, E). The S/B decreased by 23+4.2 % (p=0.033) and IBI increased by 63±18 % (p=0.021). Subsequent addition of 1μM WIN55,212 was unable to decrease further the firing rate, providing evidence that CB1 receptor activation reduces the activity of GnRH neurons via interfering with $GABA_A$-R-mediated signaling. Interestingly, the firing rate of GnRH neurons tended to increase, rather than decrease, (by 70.5±21.9%), although this effect did not reach statistical significance (Newman-Keuls test: p=0.071, Kyn+Bic+WIN *vs.* Kyn+Bic; Figs. 1C, E). The S/B and IBI did not change further. The amplitude of the action currents and ISI remained unchanged throughout the treatments.

GABA-ergic afferents to GnRH neurons express CB1 receptors

The above findings established that the inhibitory effect of WIN55,212 on GnRH cell activity is mediated by a neuronal circuitry that includes GABA-ergic interneurons and uses $GABA_A$-Rs. The complexity of this circuitry remained unclear. Because GABA is the major neurotransmitter in the afferent regulation of GnRH neurons (16), further, $GABA_A$-R activation excites GnRH neurons (18, 21, 25, 26, 39), we hypothesized that WIN55,212 directly inhibits the GABA-ergic input to GnRH neurons in its action to reduce GnRH neuron activity. To begin to examine this mechanism, we addressed the presence of CB1 receptors on synaptic afferents to GnRH neurons. CB1-immunoreactive axons were first examined with confocal microscopy. These

studies revealed the frequent apposition of CB1-IR fibers to the perikaryon and dendrites of GnRH neurons (Figs. 2A-D). Neuronal contacts were studied further with dual-label pre-embedding immunohistochemistry. When studied at light microscopic level, individual CB1 immunoreactive (CB1-IR) fibers stained with SGI-NiDAB chromogen showed moderate labeling intensity and formed a dense network in the preoptic area/anterior hypothalamus where GnRH neurons (stained with brown DAB chromogen) reside (Figs. 3A and B). At the electron microscopic level GnRH neurons exhibited medium electron density (Fig. 3C). CB1 immunoreactivity, detected by the highly electron dense silver-gold grains, was observed in axonal profiles (Figs. 3D-E). The CB1-IR axon terminals formed synaptic contacts with GnRH-IR dendrites (Fig. 3D) and perikarya (Figs. 3 E and F). The synapses belonged to both asymmetric (Figs. 3D and E) and symmetric (Fig. 3F) categories, suggesting a functional diversity of the CB1-IR input to GnRH neurons. Photographic panels illustrate immunocytochemical results obtained from 5 mice in each of the light-, confocal- and electron microscopic experiments.

Cannabinoid signaling via presynaptic CB1 receptors reduces GABA-ergic mPSCs in GnRH neurons

All inward miniature postsynaptic currents (mPSCs) were abolished by the extracellular application of 100 μM picrotoxin (n=8 cells, Fig. 4A) demonstrating that they were evoked by $GABA_A$-R activation.

The CB1 receptor agonist WIN55,212 (1 μM) reduced the frequency of mPSCs (Figs. 4B and D) in GnRH neurons by 52±8 % (control: 0.4±0.03 Hz, Student's t-test, p=0.0035). The amplitude of mPSCs showed no significant change (Fig. 4E; control: -49±6 pA, WIN55,212: -54±104 pA). In the presence of AM251, WIN55,212 was not able to change either the frequency or the amplitude of mPSCs (Figs. 4C, D and E; AM251-control: 0.6±0.08 Hz, AM251+WIN55,212: 0.7±0.05 Hz; AM251-control: -50±8 pA; AM251+WIN55,212: -50±8 pA), confirming that CB1 receptors mediate presynaptic inhibition of spontaneous vesicle fusion in GABA-ergic afferents of GnRH neurons.

Vesicular GABA release onto GnRH neurons is inhibited by endocannabinoids

The application of the CB1 antagonist AM251 (1μM) alone increased the frequency of mPSCs by 63±15 % (control: 0.4±0.03 Hz, AM251: 0.6±0.08 Hz) (Figs. 5A and D; Student's paired t-test, p=0.0489). The increased mPSC frequency suggested that AM251 can suspend an endogenous inhibitory endocannabinoid action on GABAergic terminals. The amplitude of mPSCs remained unaltered (control: -49±6 pA, AM251: -50±8 pA) (Figs. 5E).

Endocannabinoids act as an endogenous brake on GnRH neuron spiking

AM251 increased the frequency of mPSCs by suspending an endogenous blockade of random GABA vesicle fusion. To test if this blockade also acts as a brake on GnRH neuron spiking, loose patch measurements were carried out in the presence of the non-selective Ca^{++} channel inhibitor cadmium ($CdCl_2$, 200 μM). $CdCl_2$ maintains actions potentials and blocks the action potential-dependent neurotransmitter release. Because it spares neurotransmitter release due to random, spontaneous vesicle fusion, it has been used successfully in earlier studies of GABAergic mPSCs in cerebellar Purkinje cells and their suppression by the CB1 agonist WIN55,212 (34)

$CdCl_2$ application for 10 min decreased the firing rate of GnRH cells by 33±12 % (control: 0.6±0.04 Hz, p=0.030, Student's test) which could reflect the absence of action potential-dependent neurotransmitter release from GABA inputs or loss of low-voltage-activated calcium channel initiated spiking (40, 41) (Figs. 5B and F). After AM251 was also added, the firing rate increased by 210±22 % (p=0.012) (Figs. 5B and F). $CdCl_2$ decreased S/B by 10±2 % (control: 4.2±0.2; p=0.043), whereas AM251 increased S/B to 17±6.5.2 % (p=0.046). $CdCl_2$ increased IBI by 82±23 % (control=34±11.2 s, p=0.028), whereas AM251 decreased it by 63±17 % (p=0.034). These data suggest that GnRH neuron excitability is under an inhibitory endocannabinoid tone.

2-AG production by GnRH neurons tonically inhibits GABAergic drive to GnRH neurons.

In a classic mode of retrograde endocannabinoid signaling, presynaptic neurotransmitter release is inhibited by endocannabinoids from postsynaptic sources (9). The most abundant endocannabinoid in the brain is 2-AG (11). We therefore, hypothesized that GnRH neurons generate 2-AG, which then accounts for the presynaptic inhibition of GABA release. The DAG lipase inhibitor THL was added to the intracellular solution at 10 μM to block 2-AG synthesis in GnRH cells. THL significantly increased the frequency of mPSCs *vs.* controls (control: 0.4±0.03 Hz, THL: 148±12 % of the control, Figs. 5C *vs.* 5A; intergroup analyses /ANOVA followed by *post hoc* Newman-Keuls test/ : ANOVA: p=0.00008, F=8.481; NK: p=0.0235). In addition, THL prevented the effect of AM251 on the frequency of mPSCs (Figs. 5C and D; THL-control: 0.6±0.07 Hz, THL+AM251: 0.6±0.05 Hz). The amplitude of mPSCs was unaffected (THL-control: -48±5 pA, THL+AM251: -49±2 pA)(Figs.5 C and E). These data provided evidence that tonic inhibition is caused by 2-AG production in GnRH neurons.

Discussion

This study provides electrophysiological and morphological evidence that retrograde endocannabinoid signaling reduces GABA-ergic afferent drive onto GnRH neurons via the activation of presynaptic CB1 receptors. The reduced $GABA_A$-R signaling, in turn, inhibits GnRH neuron firing activity. This mechanism is represented schematically in Fig. 6.

Although somewhat controversial (19, 20), a growing body of evidence suggests that GABA can act as an excitatory neurotransmitter on postsynaptic $GABA_A$-R channels of adult GnRH neurons of rodents and fish (18, 21, 25, 26, 39). The findings of the present study that WIN55,212 reduces the firing rate of GnRH neurons via $GABA_A$-R dependent mechanisms and CB1 receptor activation on GABA-ergic afferents decreases the $GABA_A$-R mediated mPSCs in GnRH neurons, provide circumstantial evidence to support an excitatory role of GABA on GnRH neuron activity.

While reduced GnRH neuron electric activity in the presence of WIN55,212 could result from cannabinoid actions on a complex multineuronal circuit impinging on GnRH neurons, results of morphological experiments showed that GnRH neurons receive a direct cannabinoid-sensitive neuronal input. Symmetric morphology of a subset of CB1 immunoreactive synapses was also indicative of GABA-ergic neurotransmission (17). GABA is the major neurotransmitter in the afferent regulation of GnRH neurons (16).

To study further the cannabinoid-dependent modulation of GABA release from these synapses, mPSCs were recorded from GnRH neurons in the presence of TTX to exclude activity-dependent effects. We found that the CB1 agonist WIN55,212 decreased GABA release onto GnRH neurons, as revealed by the reduced frequency of $GABA_A$-R mediated mPSCs. This finding was in accordance with the concept that cannabinoids modulate neurotransmitter release via action potential-independent mechanisms (1, 9). The observation that the frequency, but not the amplitude, of mPSCs was altered was in keeping with the presynaptic effect of WIN55,212 treatment on GABA release (42).

We propose that inhibition of GABA-ergic afferent input to GnRH neurons by presynaptic CB1 may represents the primary mechanism whereby cannabis drugs act to inhibit LH release (2-6, 8). In the physiological context, reduced mPSC frequency in GnRH neurons following the intracellular application of THL indicated that GnRH neurons produce 2-AG to tonically inhibit their GABA-ergic input. Because GABA plays a crucial role in the regulation of GnRH neuronal activity (29, 43-45), any alteration of this retrograde signaling results in functional consequences on GnRH neuronal activity. Accordingly, modulation of GABA-ergic drive onto GnRH neurons has been commonly implicated in metabolic (27, 45)-, estrogen (29)- and circadian (29)- signaling to GnRH neurons. It will require clarification if GABA-ergic pathways communicating these afferent modalities are modulated by retrograde endocannabinoid signaling from the GnRH neuron.

The observation that AM251 on its own increased the frequency of GABA-ergic mPSCs in GnRH neurons suggested the tonic production and retrograde action of

endocannabinoids. Furthermore, results of the loose patch experiments carried out in the presence of CdCl2 provide evidence that endocannabinoids act as an endogenous brake to inhibit GnRH neuron spiking, which could be suspended with AM251.

The absence of tonic inhibition after the intracellular blockade of DAG lipase in GnRH cells designated the GnRH neuron as the source of the acting endocannabinoid, 2-AG. This inhibitory tone may be particularly important in view of the excitatory role of GABA in the afferent regulation of GnRH neurons (18, 21, 25, 26, 39). As GnRH neuron activity is driven by two excitatory neurotransmitters, GABA and glutamate, other control systems are required to stabilize the GnRH network activity. There is evidence to show that activation of GnRH neurons represses the GABA-ergic afferent drive to these cells (46). We propose that retrograde endocannabinoid signaling may play a critically important role in this phenomenon. Similarly to other types of neurons (9), GnRH cells likely respond to activation with an enhanced endocannabinoid production, which, in turn, reduces or switches off GABA release onto GnRH neurons. A similarly strong control of GABA-driven activity by endocannabinoids has been proposed to act in developing cortical networks, in the same specific context of depolarizing GABA (47).

It remains to be established if cannabinoids also inhibit the glutamatergic input to GnRH neurons. The present immuno-electron microscopic studies found morphological evidence for CB1-immunoreactive asymmetric, in addition to symmetric, synapses on GnRH neurons, suggesting that some cannabinoid-sensitive afferents may be glutamatergic. Alternatively, such synapses can also belong to atypical GABA-ergic terminals that have been observed in the hypothalamus (48, 49). It is worth noting that a group of neurons in the anteroventral periventricular nucleus of female rats exhibits a dual GABA/glutamate phenotype (50) and their synaptic morphology may be atypical. Nevertheless, whereas GABA-ergic PSCs were detectable in all GnRH neurons in the present and previous studies (19, 20, 27, 28), optimized recording conditions failed to detect glutamatergic excitatory PSCs in 20-35% of GnRH neuron somata (51). This can only be partly attributed to the technical issue that excitatory input is often received by distal dendrites, which exert lower impact on the recordings from cell bodies (51). It is worth of note that in loose patch experiments, WIN55,212 showed a tendency to increase the firing rate of GnRH neurons when ionotropic glutamate- and $GABA_A$-R-mediated neurotransmissions were both suspended. Although this effect did not reach statistical significance ($p= 0.07$), the trend suggests that additional cannabinoid sensitive mechanisms also contribute to the regulation of the GnRH neuronal network. The increased activity of GnRH neurons in this experiment could be due to the reduced presynaptic release of GABA, which could withdraw the postsynaptic $GABA_B$ receptor-mediated inhibition of GnRH neurons (23). Alternatively, WIN55,212 could reduce the release of an unknown inhibitory neurotransmitter/neuromodulator directly upon GnRH neurons or influence a multisynaptic pathway impinging on GnRH neurons.

The present evidence for retrograde endocannabinoid signaling that inhibits the GABA-ergic afferent drive onto GnRH neurons does not exclude the possibility that cannabinoid ligands also influence GnRH release via additional mechanisms and sites of action. It has been demonstrated that AEA reduces GnRH secretion from mediabasal hypothalamic explants that contain the GnRH neurosecretory terminals (52). This finding, together with the previous observations of CB1 immunoreactivity on unidentified neurosecretory axon terminals in the median eminence of mice (53) and on GnRH axon terminals of the frog (54), raise the possibility that cannabinoids also influence GnRH release directly from the GnRH neurosecretory terminals. *In vitro,* GT1-7 neurons are not only cannabinoid source but also target cells. They synthesize, transport and degrade cannabinoids and possess cannabinoid receptors whose activation suppresses the pulsatile secretion of GnRH (55). Because mouse GnRH neurons did not contain detectable CB1 mRNA levels in dual-label *in situ* hybridization experiments (55), the physiological relevance of these data to the mouse hypothalamus will require clarification.

The retrograde endocannabinoid signaling may be used widely by other neuronal systems in the neuroendocrine hypothalamus. Our previous

immunocytochemical experiments revealed a dense innervation of the preoptic area and the hypothalamus by CB1-immunoreactive fibers (53, 56) and demonstrated CB1-immunoreactive synaptic terminals in the arcuate, supraoptic and paraventricular nuclei (53, 56). Functional observations by others indicate that endocannabinoid signaling modulates GABA-ergic and/or glutamatergic synaptic transmission to proopiomelanocortin neurons of the arcuate nucleus (42, 57), and to parvo- (58, 59) and magnocellular neurons (60) of the paraventricular nucleus. Further evidence indicates that endocannabinoid signaling strongly contributes to the mechanisms whereby ghrelin (59) and glucocorticoids (61) modulate the glutamatergic synaptic input to parvocellular neurons of the paraventricular nucleus.

Tonic production and retrograde action of endocannabinoids is not a unique phenomenon to GnRH neurons. Accordingly, an increased frequency of mPSCs after CB1 inhibition has also been demonstrated in hypothalamic proopiomelanocortin (42, 57) and oxytocin neurons (62, 63) and in hippocampal pyramidal cells (64). In the hippocampus, tonic release of endocannabinoids by CA3 pyramidal cells results in a persistent activation of presynaptic cannabinoid receptors and provides a state-dependent switch in cortical networks (64). A similar silencing of GABA-ergic inputs to GnRH cells by endocannabinoids may underlie an important gating mechanism for the transmission of metabolic-, circadian-, stress-, emotional- and steroid signals to the GnRH network. The driving force behind the production of endocannabinoids by GnRH neurons, as well as the functional characteristics of the regulated cannabinoid-sensitive GABA-ergic afferents to GnRH cells, remain to be determined. Estrogen might be one critically important modulator of endocannabinoid synthesis as higher levels of endocannabinoids were detected in the hypothalamus of the ovariectomized and estrogen-substituted female *vs.* the ovariectomized and vehicle-treated female or intact male rat (52). In our patch-clamp study, tonic 2-AG release was detected in the presence of TTX, suggesting that the phenomenon is, at least partly, activity-independent. The underlying mechanism may be related to the function of currently unknown constitutively active receptors in GnRH neurons. For example, metabotropic glutamate receptors (mGluRs) can show such constitutive activity in the hippocampus (65) and mGluR activation can, indeed, result in elevated synthesis of 2-AG in hippocampal, cerebellar and corticostriatal neurons, for a review see (11). MGluRs are also present in GnRH neurons (66). The putative involvement of mGluR and/or other constitutively active receptors in tonic endocannabinoid release from GnRH cells requires clarification.

Retrograde endocannabinoid signaling we report in this study may represent an important regulatory mechanism whereby GnRH neurons decrease their excitatory GABA-ergic input under physiological and pathological conditions.

Acknowledgements:
We thank Dr. R.A. Benoit for the kind donation of the LR1 GnRH antibodies, Drs. Norbert Hájos and János Szabadics for their invaluable comments and Hajni Bekó and Barna László for the technical assistance.

References

1. **Pagotto U, Marsicano G, Cota D, Lutz B, Pasquali R** 2006 The emerging role of the endocannabinoid system in endocrine regulation and energy balance. Endocrine Rev 27:73-100
2. **Asch RH, Smith CG, Siler-Khodr TM, Pauerstein CJ** 1981 Effects of delta 9-tetrahydrocannabinol during the follicular phase of the rhesus monkey (Macaca mulatta). J Clin Endocrinol Metab 52:50-55
3. **Smith CG, Smith MT, Besch NF, Smith RG, Asch RH** 1978 Effect of delta 9-tetrahydrocannabinol (THC) on female reproductive function. Adv Biosci 22-23:449-467
4. **Mendelson JH, Mello NK, Ellingboe J, Skupny AS, Lex BW, Griffin M** 1986 Marihuana smoking suppresses luteinizing hormone in women. J Pharmacol Exp Ther 237:862-866
5. **Tyrey L** 1978 delta-9-Tetrahydrocannabinol suppression of episodic luteinizing hormone secretion in the ovariectomized rat. Endocrinology 102:1808-1814
6. **Wenger T, Rettori V, Snyder GD, Dalterio S, McCann SM** 1987 Effects of

delta-9-tetrahydrocannabinol on the hypothalamic-pituitary control of luteinizing hormone and follicle-stimulating hormone secretion in adult male rats. Neuroendocrinology 46:488-493

7. **Dalterio S, Steger R, Peluso J, de Paolo L** 1987 Acute delta 9-tetrahydrocannabinol exposure: effects on hypothalamic-pituitary-testicular activity in mice. Pharmacol Biochem Behav 26:533-537
8. **Ayalon D, Nir I, Cordova T, Bauminger S, Puder M, Naor Z, Kashi R, Zor U, Harell A, Lindner HR** 1977 Acute effect of delta1-tetrahydrocannabinol on the hypothalamo-pituitary-ovarian axis in the rat. Neuroendocrinology 23:31-42
9. **Piomelli T** 2003 The molecular logic of endocannabinoid signallig. Nat Rev Neurosci 4:873-884
10. **Hoffman AF, Lupica CR** 2000 Mechanisms of cannabinoid inhibition of GABA(A) synaptic transmission in the hippocampus. J Neurosci 20:2470-2479
11. **Kano M, Ohno-Shosaku T, Hashimotodani Y, Uchigashima M, Watanabe M** 2009 Endocannabinoid-mediated control of synaptic transmission. Physiol Rev 89:309-380
12. **Katona I, Freund TF** 2008 Endocannabinoid signaling as a synaptic circuit breaker in neurological disease. Nat Med 14:923-930
13. **Gerdeman G, Lovinger DM** 2001 CB1 cannabinoid receptor inhibits synaptic release of glutamate in rat dorsolateral striatum. J Neurophysiol 85:468-471
14. **Huang CC, Lo SW, Hsu KS** 2001 Presynaptic mechanisms underlying cannabinoid inhibition of excitatory synaptic transmission in rat striatal neurons. J Physiol 532:731-748
15. **Olah M, Milloh H, Wenger T** 2008 The role of endocannabinoids in the regulation of luteinizing hormone and prolactin release. Differences between the effects of AEA and 2AG. Mol Cell Endocrinol 286:S36-40
16. **Herbison AE** 1998 Multimodal influence of estrogen upon gonadotropin-releasing hormone neurons. Endocr Rev 19:302-330
17. **Leranth C, MacLusky NJ, Sakamoto H, Shanabrough M, Naftolin F** 1985 Glutamic acid decarboxylase-containing axons synapse on LHRH neurons in the rat medial preoptic area. Neuroendocrinology 40:536-539
18. **Defazio RA, Heger S, Ojeda SR, Moenter SM** 2002 Activation of A-type gamma-aminobutyric acid receptors excites gonadotropin-releasing hormone neurons. Mol Endocrinology 16:2872-2891
19. **Han SK, Abraham IM, Herbison AE** 2002 Effect of GABA on GnRH neurons switches from depolarization to hyperpolarization at puberty in the female mouse. Endocrinology 143:1459-1466
20. **Han SK, Todman MG, Herbison AE** 2004 Endogenous GABA release inhibits the firing of adult gonadotropin-releasing hormone neurons. Endocrinology 145:495-499
21. **Moenter SM, Defazio RA** 2005 Endogenous gamma-aminobutyric acid can excite gonadotropin-releasing hormone neurons. Endocrinology 146:5374-5379
22. **Spergel DJ, Kruth U, Hanley DF, Sprengel R, Seeburg PH** 1999 GABA- and glutamate-activated channels in green fluorescent protein-tagged gonadotropin-releasing hormone neurons in transgenic mice. J Neurosci 19:2037-2050
23. **Zhang C, Bosch MA, Ronnekleiv OK, Kelly MJ** 2009 Gamma-aminobutyric acid B receptor mediated inhibition of gonadotropin-releasing hormone neurons is suppressed by kisspeptin-G protein-coupled receptor 54 signaling. Endocrinology 150:2388-2394
24. **Tasker JG, Dudek FE** 1993 Local inhibitory synaptic inputs to neurones of the paraventricular nucleus in slices of rat hypothalamus. J Physiol 469:179-192
25. **Watanabe M, Sakuma Y, Kato M** 2009 GABAA receptors mediate excitation in adult rat GnRH neurons. Biol Reprod 81:327-332
26. **Yin C, Ishii H, Tanaka N, Sakuma Y, Kato M** 2008 Activation of A-type gamma-amino butyric acid receptors excites gonadotrophin-releasing hormone neurones isolated from adult rats. J Neuroendocrinol 20:566-575
27. **Sullivan SD, DeFazio RA, Moenter SM** 2003 Metabolic regulation of fertility through presynaptic and postsynaptic signaling to gonadotropin-releasing hormone neurons. J Neurosci 23:8578-8585

28. **Sullivan SD, Moenter SM** 2005 GABAergic integration of progesterone and androgen feedback to gonadotropin-releasing hormone neurons. Biol Reprod 72:33-41
29. **Christian CA, Moenter SM** 2007 Estradiol induces diurnal shifts in GABA transmission to gonadotropin-releasing hormone neurons to provide a neural signal for ovulation. J Neurosci 27:1913-1921
30. **Suter KJ, Song WJ, Sampson TL, Wuarin JP, Saunders JT, Dudek FE, Moenter SM** 2000 Genetic targeting of green fluorescent protein to gonadotropin-releasing hormone neurons: characterization of whole-cell electrophysiological properties and morphology. Endocrinology 141:412-419
31. **Ledent C, Valverde O, Cossu G, Petitet F, Aubert JF, Beslot F, Bohme GA, Imperato A, Pedrazzini T, Roques BP, Vassart G, Fratta W, Parmentier M** 1999 Unresponsiveness to cannabinoids and reduced addictive effects of opiates in CB1 receptor knockout mice. Science 283:401-404
32. **Laschet JJ, Kurcewicz I, Minier F, Trottier S, Khallou-Laschet J, Louvel J, Gigout S, Turak B, Biraben A, Scarabin JM, Devaux B, Chauvel P, Pumain R** 2007 Dysfunction of GABAA receptor glycolysis-dependent modulation in human partial epilepsy. Proc Natl Acad Sci U S A 104:3472-3477
33. **Meurs A, Clinckers R, Ebinger G, Michotte Y, Smolders I** 2008 Seizure activity and changes in hippocampal extracellular glutamate, GABA, dopamine and serotonin. Epilepsy Res 78:50-59
34. **Takahashi KA, Linden DJ** 2000 Cannabinoid receptor modulation of synapses received by cerebellar Purkinje cells. J Neurophysiol 83:1167-1180
35. **Defazio RA, Moenter SM** 2002 Estradiol feedback alters potassium currents and firing properties of gonadotropin-releasing hormone neurons. Mol Endocrinology 16:2255-2265
36. **Makara J, Katona I, Nyiri G, Nemeth B, Ledent C, Watanabe M, de Vente J, Freund T, Hajos N** 2007 Involvement of nitric oxide in depolarization-induced suppression of inhibition in hippocampal pyramidal cells during activation of cholinergic receptors. J Neurosci 27:10211-10222
37. **Kallo I, Butler JA, Barkovics-Kallo M, Goubillon ML, Coen CW** 2001 Oestrogen receptor alpha-immunoreactivity in gonadotropin-releasing hormone-expressing neurons: regulation by oestrogen. J Neuroendocrinol 13:741-748
38. **Nunemaker CS, DeFazio RA, Moenter SM** 2003 A targeted extracellular approach for recording long-term firing patterns of excitable cells: a practical guide. Biol Proced Online 5:53-62
39. **Nakane R, Oka Y** 2010 Excitatory action of GABA in the terminal nerve gonadotropin-releasing hormone neurons. J Neurophysiol 103:1375-1384
40. **Sun J, Chu Z, Moenter SM** 2010 Diurnal in vivo and rapid in vitro effects of estradiol on voltage-gated calcium channels in gonadotropin-releasing hormone neurons. J Neurosci 30:3912-3923
41. **Zhang C, Bosch MA, Rick EA, Kelly MJ, Ronnekleiv OK** 2009 17Beta-estradiol regulation of T-type calcium channels in gonadotropin-releasing hormone neurons. J Neurosci 29:10552-10562
42. **Nguyen QH, Wagner EJ** 2006 Estrogen differentially modulates the cannabinoid-induced presynaptic inhibition of amino acid neurotransmission in proopiomelanocortin neurons of the arcuate nucleus. Neuroendocrinology 84:123-137
43. **Christian CA, Moenter SM** 2008 Critical roles for fast synaptic transmission in mediating estradiol negative and positive feedback in the neural control of ovulation. Endocrinology 149:5500-5508
44. **Chu Z, Andrade J, Shupnik MA, Moenter SM** 2009 Differential regulation of gonadotropin-releasing hormone neuron activity and membrane properties by acutely applied estradiol: dependence on dose and estrogen receptor subtype. J Neurosci 29:5616-5627
45. **Sullivan SD, Moenter SM** 2004 Gamma-aminobutyric acid neurons integrate and rapidly transmit permissive and inhibitory metabolic cues to gonadotropin-releasing hormone neurons. Endocrinology 145:1194-1202

46. **Chu Z, Moenter SM** 2005 Endogenous activation of metabotropic glutamate receptors modulates GABAergic transmission to gonadotropin-releasing hormone neurons and alters their firing rate: a possible local feedback circuit. J Neurosci 25:5740-5749
47. **Bernard C, Milh M, Morozov YM, Ben-Ari Y, Freund TF, Gozlan H** 2005 Altering cannabinoid signaling during development disrupts neuronal activity. Proc Natl Acad Sci U S A 102:9388-9393
48. **Belenky MA, Yarom Y, Pickard GE** 2008 Heterogeneous expression of gamma-aminobutyric acid and gamma-aminobutyric acid-associated receptors and transporters in the rat suprachiasmatic nucleus. J Comp Neurol 506:708-732
49. **Miklos IH, Kovacs KJ** 2002 GABAergic innervation of corticotropin-releasing hormone (CRH)-secreting parvocellular neurons and its plasticity as demonstrated by quantitative immunoelectron microscopy. Neuroscience 113:581-592
50. **Ottem EN, Godwin JG, Krishnan S, Petersen SL** 2004 Dual-phenotype GABA/glutamate neurons in adult preoptic area: sexual dimorphism and function. J Neurosci 24:8097-8105
51. **Christian CA, Pielecka-Fortuna J, Moenter SM** 2009 Estradiol suppresses glutamatergic transmission to gonadotropin-releasing hormone neurons in a model of negative feedback in mice. Biol Reprod 80:1128-1135
52. **Scorticati C, Fernandez-Solari J, DeLaurentiis A, Mohn C, Prestifilippo JP, Lasaga M, Seilicovich A, Billi S, McCann SM, Rettori V** 2004 The inhibitory effect of anandamide on luteinizing hormone-releasing hormone secretion is reversed by estrogen. Proc Natl Acad Sci U S A 101:11891-11896
53. **Wittmann G, Deli L, Kallo I, Hrabovszky E, Watanabe M, Liposits Z, Fekete C** 2007 Distribution of type 1 cannabinoid receptor (CB1)-immunoreactive axons in the mouse hypothalamus. J Comp Neurology 503:270-279
54. **Meccariello R, Franzoni MF, Chianese R, Cottone E, Scarpa D, Donna D, Cobellis G, Guastalla A, Pierantoni R, Fasano S** 2008 Interplay between the endocannabinoid system and GnRH-I in the forebrain of the anuran amphibian Rana esculenta Endocrinology 149:2149-2158
55. **Gammon CM, Freeman GM, Xie W, Petersen SL, Wetsel WC** 2005 Regulation of gonadotropin-releasing hormone secretion by cannabinoids. Endocrinology 146:4491-4499
56. **Deli L, Wittmann G, Kallo I, Lechan RM, Watanabe M, Liposits Z, Fekete C** 2009 Type 1 cannabinoid receptor-containing axons innervate hypophysiotropic thyrotropin-releasing hormone-synthesizing neurons. Endocrinology 150:98-103
57. **Hentges ST, Low MJ, Williams JT** 2005 Differential regulation of synaptic inputs by constitutively released endocannabinoids and exogenous cannabinoids. J Neurosci 25:9746-9751
58. **Di S, Malcher-Lopes R, Halmos K, Tasker JG** 2003 Nongenomic glucocorticoid inhibition via endocannabinoid release in the hypothalamus: a fast feedback mechanism. J Neurosci 23:4850-4857
59. **Kola B, Farkas I, Christ-Crain M, Wittmann G, Lolli F, Amin F, Harvey-White J, Liposits Z, Kunos G, Gross AB, Fekete C, Korbonits M** 2008 The orexigenic effect of ghrelin Is mediated through central activation of the endogenous cannabinoid system. PLoS One 3:e1797.-doi:1710.1371/journal.pone.0001797
60. **Di S, Boudaba C, Popescu IR, Weng FJ, Harris C, Marcheselli VL, Bazan NG, Tasker JG** 2005 Activity-dependent release and actions of endocannabinoids in the rat hypothalamic supraoptic nucleus. J Physiol 569:751-760
61. **Di S, Maxson MM, Franco A, Tasker JG** 2009 Glucocorticoids regulate glutamate and GABA synapse-specific retrograde transmission via divergent nongenomic signaling pathways. J Neurosci 29:393-401
62. **Oliet SH, Baimoukhametova DV, Piet R, Bains JS** 2007 Retrograde regulation of GABA transmission by the tonic release of oxytocin and endocannabinoids governs postsynaptic firing. J Neurosci 27:1325-1333
63. **Di S, Malcher-Lopes R, Marcheselli VL, Bazan NG, Tasker JG** 2009 Rapid

glucocorticoid-mediated endocannabinoid release and opposing regulation of glutamate and gamma -aminobutyric acid inputs to hypothalamic magnocellular neurons. Endocrinology 145:4292-4301

64. **Losonczy A, Biro AA, Nusser Z** 2004 Persistently active cannabinoid receptors mute a subpopulation of hippocampal interneurons. Proc Natl Acad Sci U S A 101:1362-1367
65. **Losonczy A, Somogyi P, Nusser Z** 2003 Reduction of excitatory postsynaptic responses by persistently active metabotropic glutamate receptors in the hippocampus. J Neurophysiol 89:1910-1919
66. **Dumalska I, Wu M, Morozova E, Liu R, van den Pol A, Alreja M** 2008 Excitatory effects of the puberty-initiating peptide kisspeptin and group I metabotropic glutamate receptor agonists differentiate two distinct subpopulations of gonadotropin-releasing hormone neurons. J Neurosci 28:8003-8013

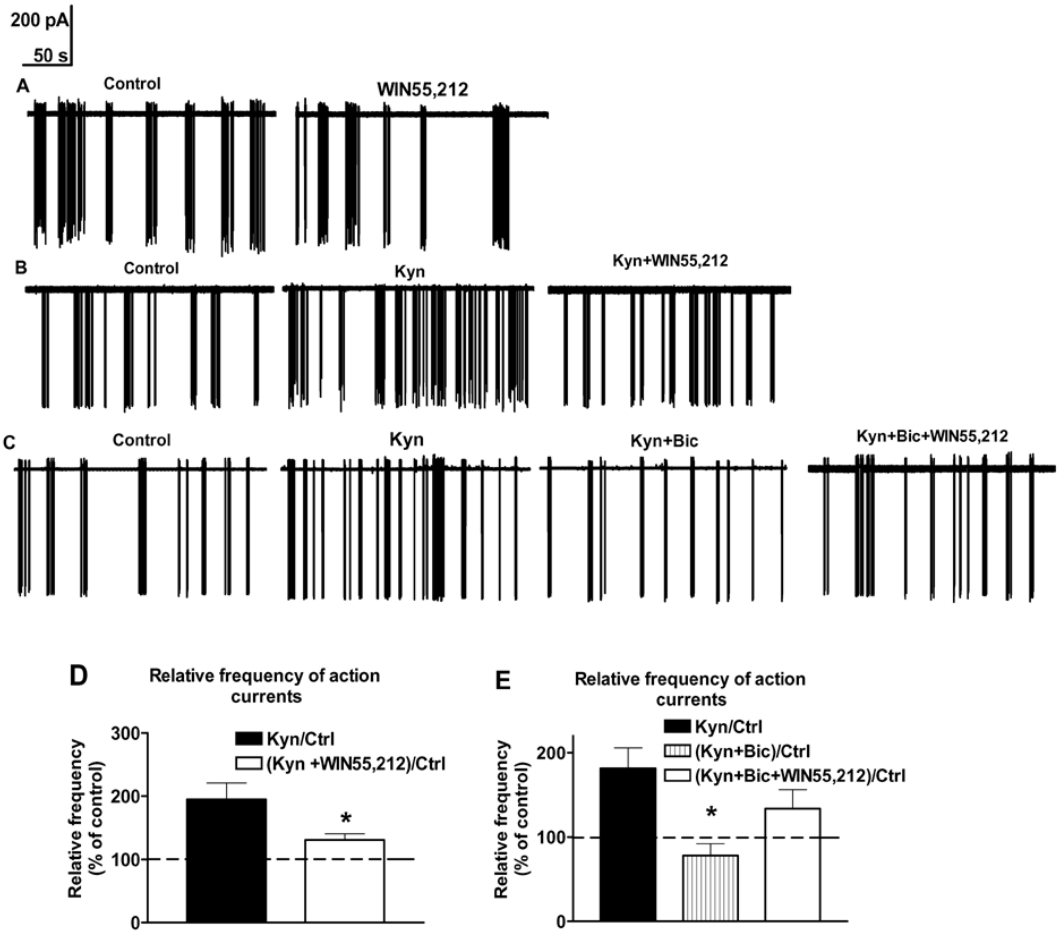

Figure 1. The CB1 receptor agonist WIN55,212 inhibits GnRH neuron firing via a $GABA_A$-R dependent mechanism. When applied to acute slice preparations of the preoptic area, WIN55,212 (1 μM) reduces the action current frequency of a representative GnRH neuron, compared to its control firing rate before treatment (A). The control firing rate of a representative GnRH neuron is increased in the presence of the ionotropic glutamate receptor blocker kynurenic acid (2 mM). The subsequent application of WIN55,212 results in a decrease of this firing rate, indicating that WIN55,212 can act via non-glutamatergic mechanisms (B). Histograms show the relative percentages of action current frequencies from 8 recorded cells (D). When the $GABA_A$-R blocker bicuculline (20 μM) is applied in the presence of kynurenic acid, the firing rate of GnRH neurons decrease. In this paradigm WIN55,212 is not capable of reducing the action current frequency of GnRH neurons (C). This finding provides evidence that WIN55,212 reduces the firing of GnRH neurons via a $GABA_A$–R dependent mechanisms. Histograms of loose patch recordings show the relative percentages of action current frequencies from 8 recorded cells (mean±SEM; E). Kyn=Kynurenic acid; Bic=Bicuculline. *$p<0.05$ *vs.* Kyn.

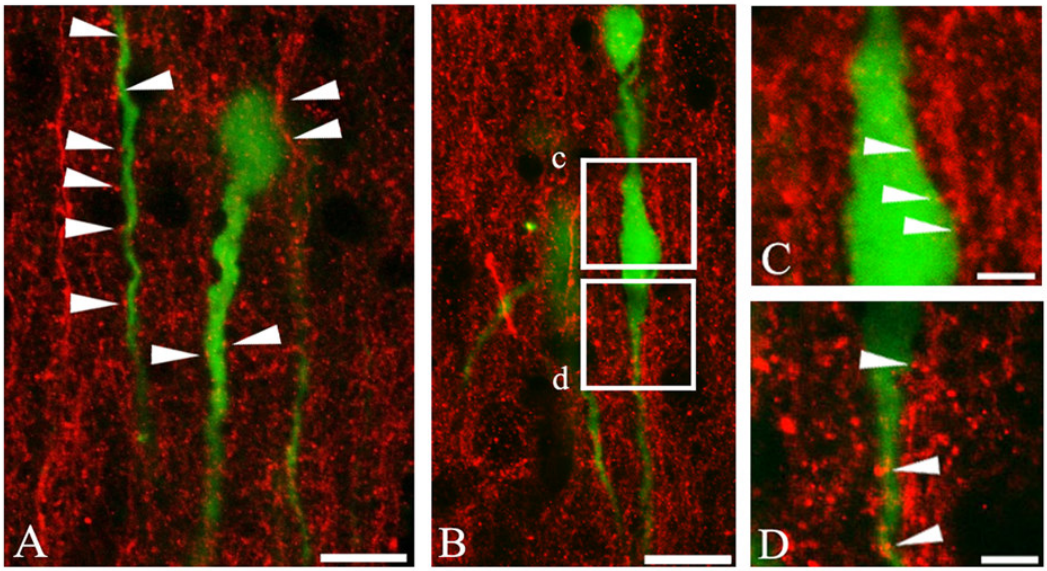

Figure 2. Confocal analysis of CB1-immunoreactive fibers and GnRH-GFP neurons provides evidence for CB1 immunoreactive neuronal input to GnRH neurons.
GnRH neurons (green) occur embedded in a dense field of CB1 immunoreactive axons (red) in the preoptic area. Arrowheads in A, C and D indicate CB1 containing axons that form contacts with the perikaryon and dendrites of GnRH neurons. Boxed areas in B correspond to panels C and D at higher power. Scale bars=15 μm in A and B, and 5 μm in C and D.

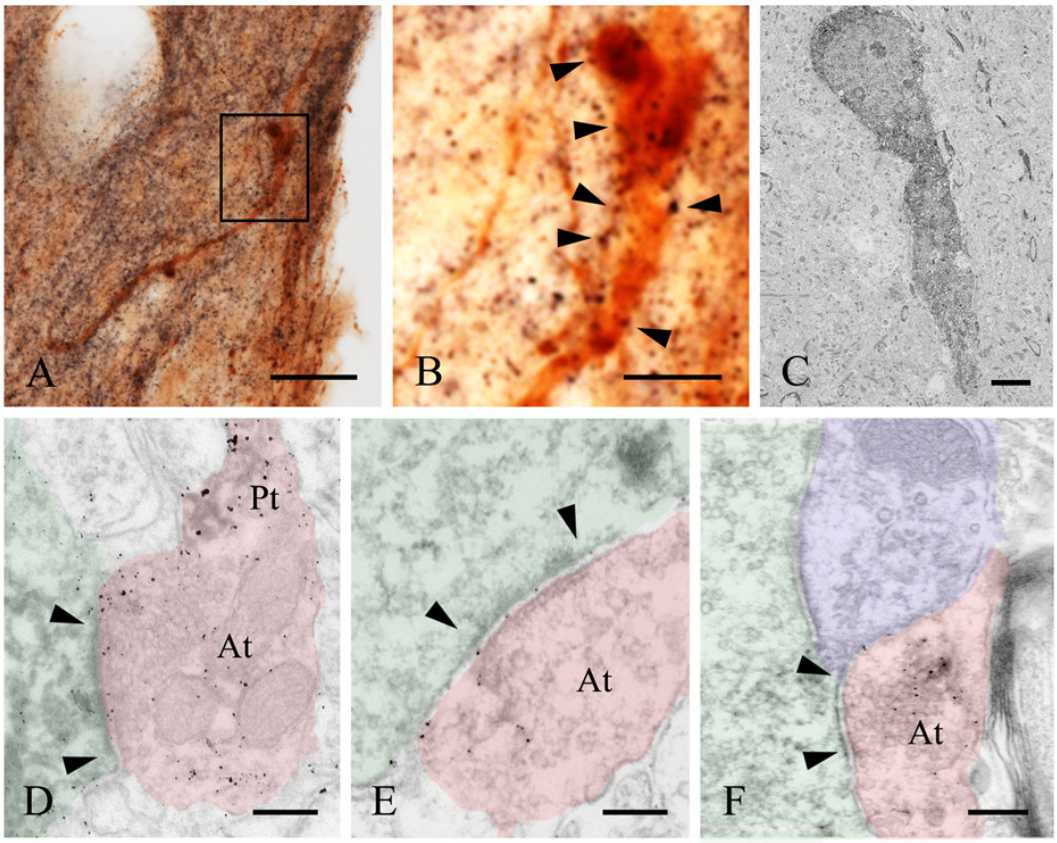

Figure 3. Pre-embedding immunocytochemical studies reveal CB1-immunoreactive synaptic afferents to GnRH neurons.
Simultaneous detection of CB1-immunoreactive fibers with silver-gold grains (black color in light microscopy and electron dense metallic deposits in electron micrographs) and GnRH-immunoreactive neurons with diaminobenzidine (brown color in light microscopy and medium electron density in electron micrographs) enables the ultrastructural analysis of CB1-immunoreactive contacts on GnRH neurons. Boxed area in low-power light micrograph A is enlarged in B. Arrowheads indicate appositions of CB1-immunoreactive fibers to a GnRH-immunoreactive neuron. Low power electron micrograph in C illustrates a GnRH-synthesizing neuron (electron dense profile) from the OVLT region. A CB1-immunoreactive axon terminal (At; pink shading in D) establishes an asymmetric synapse (arrowheads) with a GnRH-immunoreactive dendrite (light green shading). Arrowheads point to an asymmetric axo-somatic synapse in E and a symmetric axo-somatic synapse in F. Note the accumulation of silver particles in the pre-terminal (Pt) segments of the CB1 immunoreactive axon (pink shading) in D, E and F. Blue shading in F labels a CB-negative synaptic terminal. .Scale bars=50 μm in A, 15 μm in B, 4 μm in C, and 200 nm in D, E and F.

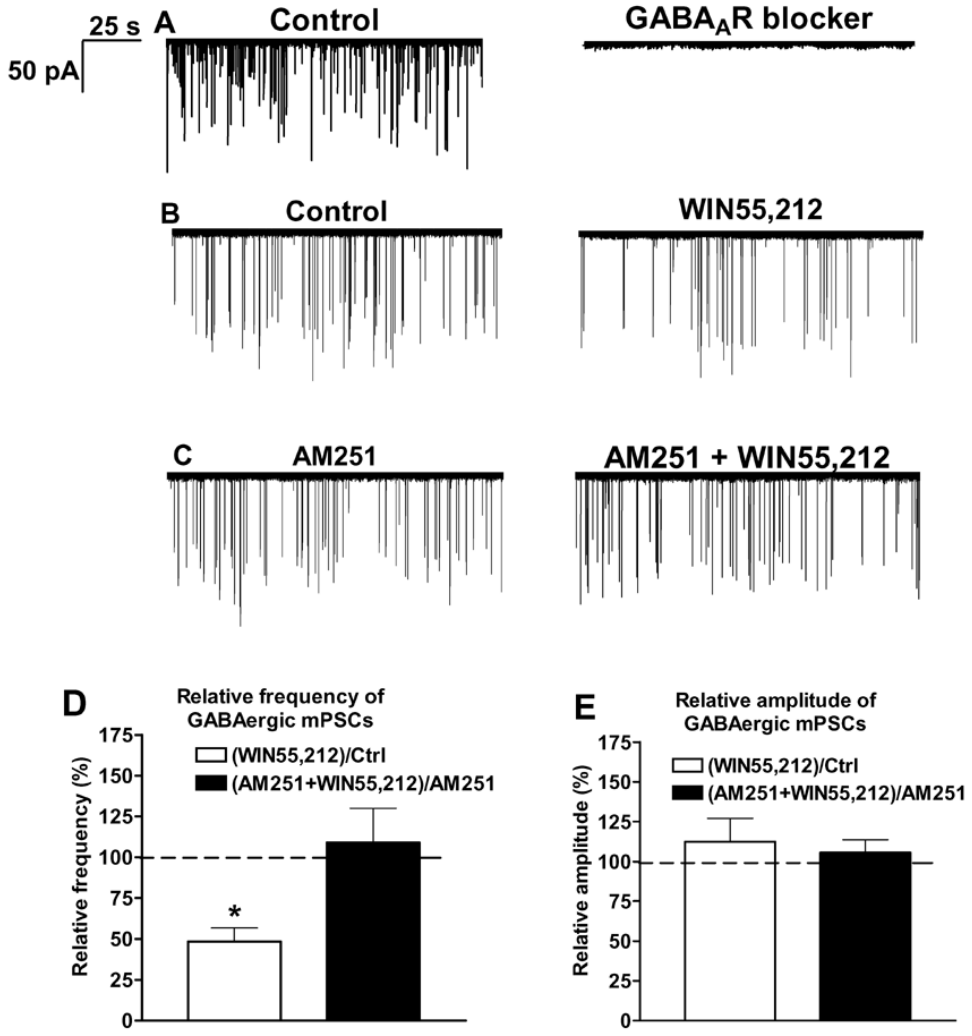

Figure 4. Whole-cell patch-clamp recordings of mPSCs reveal that CB1 receptor activation inhibits the GABA-ergic afferent drive onto GnRH neurons. All recorded mPSCs in a representative GnRH neuron can be eliminated with 100 μM picrotoxin showing that they are related to $GABA_A$–R activation (A). The frequency of GABA-ergic mPSCs from a representative GnRH neuron is reduced by the synthetic endocannabinoid agonist WIN55,212 (1 μM) (B). GnRH neurons preincubated with the CB1 antagonist AM251 (1 μM) fail to respond with reduced mPSCs to the WIN55,212 challenge (C). Histograms of whole-cell patch-clamp recordings show the relative percentages of mPSC frequencies (D) and amplitudes (E). Bars correspond to the mean±SEM of 10 recorded cells for each treatment. *$p<0.05$ *vs.* Ctrl. Note that all changes detected in these experiments affect the frequency, but not the amplitude, of mPSCs.

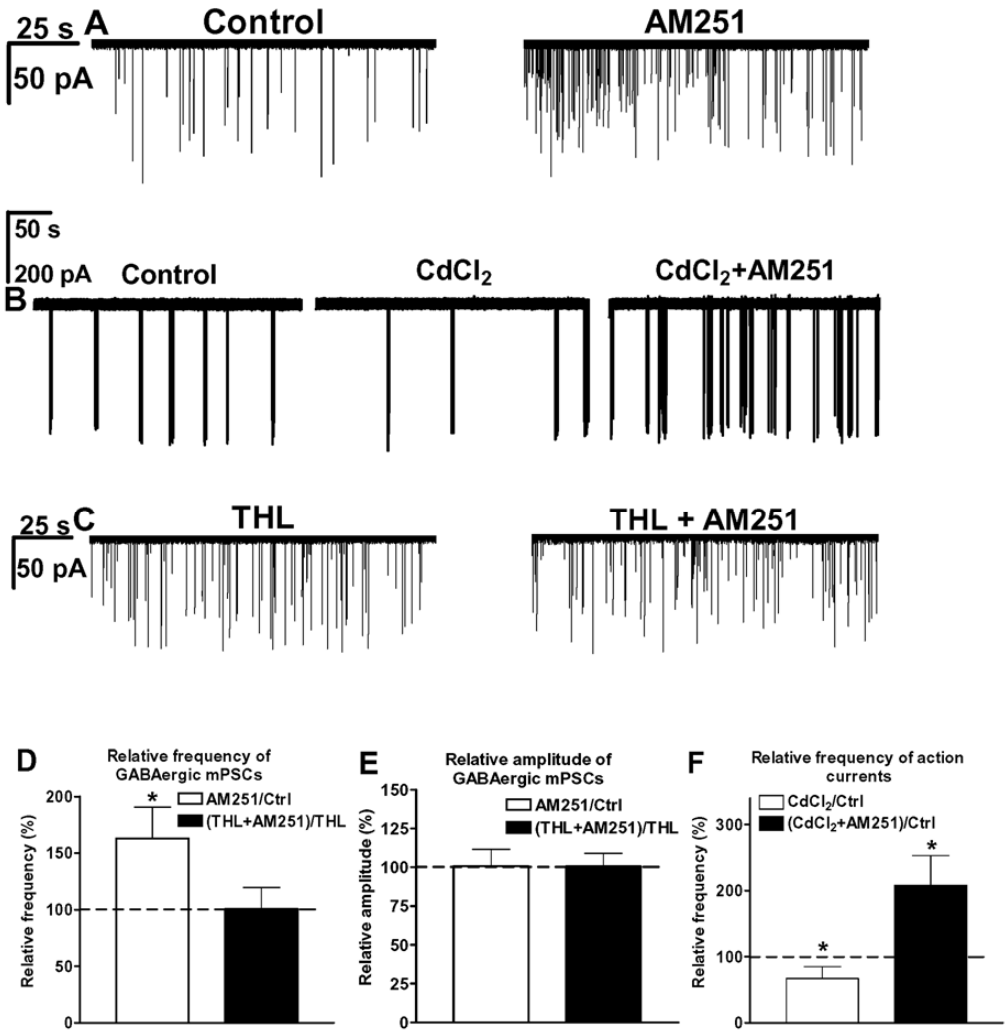

Figure 5. Results of whole-cell patch-clamp and loose patch recordings provide evidence for tonic 2-AG release from GnRH neurons that inhibits GnRH neuron excitability. Bath application of the CB1 antagonist AM251 alone enhances the control frequency of mPSCs in a representative GnRH neuron (A). Firing rate decreases in response to $CdCl_2$ treatment, and increases when AM251 is subsequently applied to suspend a tonic endocannabinoid blockade of spontaneous vesicle fusion-related neurotransmitter release (B). Application of the 2-AG synthesis inhibitor THL (10 μM) in the patch electrode prevents any subsequent effect of AM251 on the mPSC frequency of a representative GnRH cell (C). Histograms of whole-cell patch-clamp and loose patch recordings show the relative percentages of mPSC frequencies (D), amplitudes (E), and firing rate (F)**.** The bars correspond to the mean ±SEM of 10 recorded cells for each treatment, except for loose patch experiments (n=8). *p<0.05.

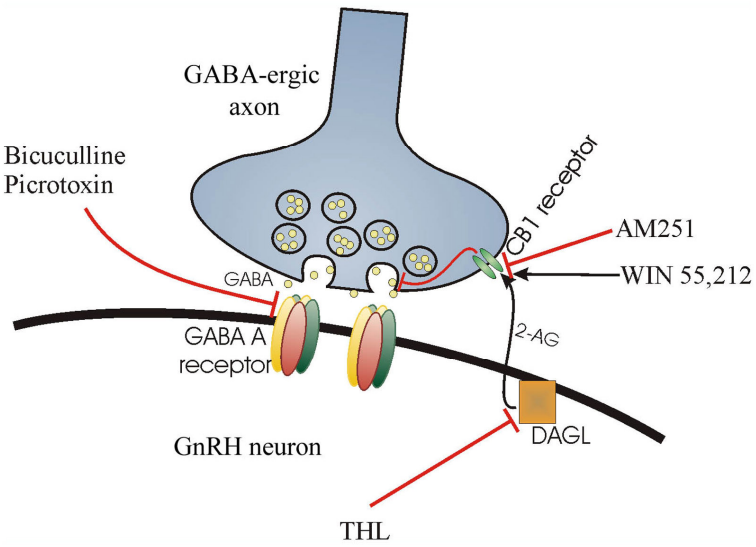

Figure 6. Schematic illustration of the retrograde endocannabinoid signaling mechanism that regulates $GABA_A$-R-mediated drive onto GnRH neurons. 2-AG is synthesized by the GnRH neuron via the diacylglycerol-lipase (DAGL) pathway. This process can be blocked by the intracellular application of the DAGL inhibitor tetrahydrolipstatin (THL). 2-AG is released tonically and binds to CB1 receptors located on GABA-ergic synaptic afferents. The activation of CB1 inhibits spontaneous GABA release, an effect mimicked by the synthetic CB1 agonist WIN55,212. The CB1 antagonist AM251 can block agonist binding to CB1 which results in increased GABA release. GABA binds preferentially to postsynaptic $GABA_A$-Rs, which can be antagonized by bicuculline or picrotoxin.